Université de Montréal

Modulation of HIV-specific T cell responses during standard antiretroviral treatment and immunotherapy

par

Julia Niessl

Département de microbiologie, infectiologie et immunologie

Faculté de médecine

Thèse présentée en vue de l'obtention du grade de

Philosophiae Doctor (Ph.D.)

en Virologie et Immunologie

Mai, 2020

Université de Montréal

Faculté des études supérieures et postdoctorales

Département de microbiologie, infectiologie et immunologie, Faculté de médecine

Cette thèse intitulée

Modulation of HIV-specific T cell responses during standard antiretroviral treatment and immunotherapy

Présentée par

Julia Niessl

A été évaluée par un jury composé des personnes suivantes

Dr. Nathalie Arbour

Présidente-rapportrice

Dr. Daniel E. Kaufmann

Directeur de recherche

Dr. Marika Sarfati

Membre du jury

Dr. Alain Lamarre

Examinateur externe

Dr. Sophie Petropoulos

Représente du doyen

Résumé

Seule une minorité des individus infectés par le virus de l'immunodéficience humaine (VIH) développe une réponse immunitaire capable de contrôler le virus. Chez la plupart des individus, on observe un échappement virologique et un épuisement des lymphocytes T $CD8^+$ spécifiques du VIH. L'infection chronique non-traitée altère également les lymphocytes T $CD4^+$ spécifiques du VIH caractérisé par l'expression accrue des récepteurs co-inhibiteurs et une signature des cellules auxiliaires T folliculaires (Tfh). La thérapie antirétrovirale (TAR) est très efficace pour supprimer durablement la charge virale dans le plasma. Néanmoins, elle ne permet pas une éradication complète du VIH car le virus persiste, intégré dans le génome des cellules réservoirs, desquelles le virus réapparaît lors de l'interruption de la thérapie. Cela démontre que l'immunité adaptive spécifiques du VIH n'est pas restaurée.

Les anticorps neutralisants à large spectre (bNAbs) représentent une alternative potentielle à la TAR. En plus de la neutralisation du virus – et contrairement à la TAR – les bNAbs ne limitent pas la disponibilité de l'antigène et peuvent engager le système immunitaire. L'administration de bNAbs à des macaques rhésus induit des réponses immunitaires adaptatives associées à un contrôle prolongé de la virémie, mais cela n'a pas été établi chez l'Homme.

Dans cette thèse, nous avons donc exploré la modulation des réponses des lymphocytes T spécifiques du VIH lors d'une TAR standard et d'une immunothérapie utilisant des bNAbs.

Dans un premier objectif nous avons analysé la modulation persistante des réponses des lymphocytes T $CD4^+$ spécifiques du VIH chez les individus sous TAR. Nous avons pu démontrer l'expansion persistante des Tfh spécifiques au VIH avec des caractéristiques phénotypiques et fonctionnelles les distinguant des Tfh spécifiques d'antigènes viraux comparatifs (cytomégalovirus, virus de l'hépatite B). Ces caractéristiques ont été induites au cours de l'infection chronique non-traitée, persistaient pendant la TAR et étaient associées au réservoir du VIH compétent pour la traduction. Ces données suggèrent qu'une stimulation antigénique persistante, malgré une TAR efficace, maintient des modifications immunologiques notamment au niveau des Tfh.

Dans un second objectif, nous avons caractérisé les réponses T spécifiques du VIH à la suite d'un traitement utilisant des bNAbs et une interruption structurée de la TAR (IST). Des individus inclus dans une étude clinique de phase Ib ont reçu une perfusion d'une combinaison des bNAbs 10-

1074 et 3BNC117 et ont démontré une suppression virale prolongée après l'IST. Chez ces participants, nous avons observé une augmentation des réponses immunitaires des lymphocytes T $CD8^+$ et $CD4^+$ spécifiques du VIH due à l'expansion des réponses immunitaires préexistantes et au développement de réponses ciblant de nouveaux épitopes. Cela suggère que la combinaison d'un traitement par bNAbs avec l'IST est associée au maintien de la charge virale plasmatique indétectable et à une intensification de la réponse immunitaire des lymphocytes T spécifiques du VIH.

Nos travaux permettent une meilleure compréhension des réponses des lymphocytes T spécifiques du VIH au cours de la TAR et lors d'une immunothérapie. Ils peuvent contribuer au développement de stratégies thérapeutiques plus efficaces visant à contrôler la réplication virale sans la TAR.

Mots-clés: VIH, cellules T spécifiques du VIH, thérapie antirétrovirale, anticorps neutralisants à large spectre, cellules T auxiliaires folliculaires

Abstract

Only a small fraction of individuals infected with the human immunodeficiency virus (HIV) develops effective immune responses able to control the virus. In most individuals, the virus escapes the antiviral immune response and HIV-specific $CD8^+$ T cell responses become exhausted. Untreated progressive HIV infection also leads to alterations in HIV-specific $CD4^+$ T cells. This includes increased expression of co-inhibitory receptors and skewing towards a T follicular helper cell (Tfh) signature. Antiretroviral therapy (ART) is highly effective in controlling the HIV viral load at undetectable levels in the plasma. However, ART does not represent a cure as the virus integrates into the genome of infected cells from where the virus rebounds once ART is stopped. This demonstrates that the HIV-specific T cell immunity is not restored. However, the changes that are introduced during progressive infection and that are maintained after viral suppression with ART are poorly known.

Broadly neutralizing antibodies (bNAbs) represent a potential alternative to ART. In addition to virus neutralization and unlike ART, bNAbs to do not limit HIV antigen availability and can engage the immune system. bNAb administration elicited adaptive immune responses that were associated with long-lasting viral control in a simian animal model, but this has not been established in HIV-infected individuals.

In this thesis, we therefore proceeded to study the modulation of HIV-specific T cell responses during standard ART and after an immunotherapeutic intervention using bNAbs.

The first objective was to better understand persistent modulation of HIV-specific $CD4^+$ T cell responses in ART-treated individuals. Our results demonstrated the persistent expansion of HIV-specific Tfh cell responses with multiple phenotypic and functional features that differed from Tfh cells specific for comparative viral antigens (cytomegalovirus, hepatitis B virus). These features were induced during chronic untreated HIV infection, persisted during ART and correlated with the translation-competent HIV reservoir. This suggests that persistent HIV antigen expression, despite effective ART, maintains these altered immunological features specifically for Tfh responses.

For the second objective, we characterized changes in the HIV-specific $CD8^+$ and $CD4^+$ T cell immunity after bNAb treatment and analytical treatment interruption (ATI). For this, we used samples obtained from participants enrolled in a clinical phase Ib study that received combined infusion of bNAbs 10-1074 and 3BNC117 and demonstrated prolonged viral suppression after ATI. In these individuals, we detected an increase of HIV-specific $CD8^+$ and $CD4^+$ T cell responses during ART interruption when compared to baseline. Increased T cell responses were due to both

expansion of pre-existing responses and the emergence of responses to new epitopes. In contrast, HIV-specific T cell responses remained unchanged in ART-treated individuals who did not receive bNAb infusions. This suggests that bNAb treatment and ATI is associated with increased HIV-specific T cell immunity while viral suppression is maintained.

Together our results contribute to a better understanding of HIV-specific T cell responses during ART and immunotherapy treatment. Our findings may help to develop more effective HIV treatment strategies to improve the host's immune system so that HIV can be controlled without the need for ART.

Keywords: HIV, HIV-specific T cells, antiretroviral therapy, broadly neutralizing antibodies, T follicular helper cells

Table of contents

List of tables

List of figures

Abbreviations

ADCC	Antibody-dependent cellular cytotoxicity
ADCVI	Antibody-dependent cell-mediated viral inhibition
AIDS	Acquired immunodeficiency syndrome
AIM	Activation-induced marker
APC	Allophycocyanin or antigen-presenting cell
APOBEC	Apolipoprotein B mRNA editing enzyme, catalytic polypeptide-like
ART	Antiretroviral therapy
ATI	Analytical treatment interruption
BB	Brilliant blue
Bcl6	B-cell lymphoma 6 protein
BCR	B cell receptor
bNAb	Broadly neutralizing antibody
BSA	Bovine serum albumin
BSL	Biosafety level
BUV	Brilliant Ultraviolet
BV	Brilliant Violet
CA	Capsid
CCR	Chemokine (C-C motif) receptor
CD	Cluster of differentiation
CD4bs	CD4-binding site
CMV	Cytomegalovirus
CRF	Circulating recombinant forms
CSR	Class-switch recombination

CTL	Cytotoxic T lymphocyte
CTLA-4	Cytotoxic T lymphocyte-associated protein 4
CXCL	Chemokine (C-X-C motif) ligand
CXCR	Chemokine (C-X-C motif) receptor
Cy	Cyanine
DC	Dendritic cell
DE	Delayed early
DMSO	Dimethyl sulfoxide
DNA	Deoxyribonucleid acid
DZ	Dark zone
EBV	Epstein-Barr virus
EC	Elite controller
ELISA	Enzyme-linked immunosorbent assay
ELISpot	Enzyme-linked immune absorbent spot
Env	Envelope
EOMES	Eomesodermin
FACS	Fluorescence activated cell sorting
FBS	Fetal bovine serum
Fc(R)	crystallizable fragment (receptor)
FDC	Follicular dendritic cell
FISH	Fluorescence in situ hybridization
FITC	Fluorescein isothiocyanate
FMO	Fluorescence minus one
FNA	Fine needle aspiration

FP	Fusion peptide
FSC(-A,-H,-W)	Forward scatter (area, height, width)
Gag	Group-specific antigen
gB	Glycoprotein B
GC	Germinal center
gp	Glycoprotein
HBsAg	Hepatitis B surface antigen
HBV	Hepatitis B virus
HCV	Hepatitis C virus
HEPES	4-(2-hydroxyethyl)-1-piperazineethanesulfonic acid
HIV	Human immunodeficiency virus
HLA	Human leukocyte antigen
ICB	Immune checkpoint blockade
ICOS	Inducible T cell costimulatory
ICS	Intracellular cytokine staining
IE	Immediate early
IFN	Interferon
Ig	Immunoglobulin
IL	Interleukin
ILC	Innate lymphoid cell
IN	Integrase
IR	Co-inhibitory receptor
ISG	Interferon-stimulated gene
L	Late

LCMV	Lymphocytic choriomeningitis virus
LN	Lymph node
LOD	Limit of detection
LRA	Latency reversing agent
LTR	Long terminal repeat
LZ	Light zone
MA	Matrix
MFI	Mean fluorescence intensity
MHC	Major histocompatibility complex
MIP	Macrophage inflammatory protein
MPER	Membrane-proximal external region
NC	Nucleocapsid
Nef	Negative regulatory factor
NHP	Non-human primate
NK	Natural killer
NNRTI	Non-nucleoside reverse transcriptase inhibitor
NPC	Nuclear pore complex
NRTI	Nucleoside reverse transcriptase inhibitor
PAMP	Pathogen-associated molecular pattern
PBMC	Peripheral blood mononuclear cell
PBS	Phosphate buffered saline
PCR	Polymerase chain reaction
PD-1	Programmed cell death 1
PE	Phycoerythrin

PerCP	Peridinin chlorophyll
PFA	Paraformaldehyde
PHA	Phytohemmagglutinin
PIC	Pre-integration complex
PMA	Phorbol 12-myristate 13-acetate
Pol	Polymerase
pp65	phosphoprotein with 65 kDa
PRR	Pattern recognition receptor
qVOA	Quantitative viral outgrowth assay
Rev	Regulator of expression of virion proteins
RLR	RIG-I-like receptor
(m)RNA	(messenger) ribonucleic acid
ROR	Retinoic acid receptor-related orphan receptor
RPMI	Roswell Park Memorial Institute
RT(C)	Reverse transcription (complex)
SEB	Staphylococcal enterotoxin B
s.f.u.	Spot forming unit
SHIV	Simian-Human Immunodeficiency Virus
SHM	Somatic hypermutation
SIV	Simian Immunodeficiency Virus
SLAM	Signaling lymphocytic activation molecule
SSC (-A, -H, -W)	Side scatter (area, height, width)
STAT	Signal transducers and activators of transcription
Tat	Trans-activating protein

T_{CM}	Central memory T cell
TCR	T cell receptor
T_{EM}	Effector memory T cell
T/F	Transmitter/Founder
Tfh/cTfh	T follicular helper/circulating T follicular helper cell
Tfr	regulatory follicular T cell
Th	T helper
TIGIT	T cell immunoreceptor with immunoglobulin and ITIM domains
Tim-3	T cell immunoglobulin- and mucin domain-containing molecule 3
TLR	Toll-like receptor
TNF	Tumor necrosis factor
T_{RM}	Tissue-resident memory T cell
T_{SCM}	Stem-cell memory T cell
T_{TM}	Transitional memory T cell
V2/V3	Second/Third variable loop
Vif	Virion infectivity factor
Vpu	Viral protein u
Vpr	Viral protein r

Acknowledgements

A PhD thesis should have an author list like scientific publications to highlight the fact that this work was not done by one single person but that it is rather the result of a group effort of numerous people. So many colleagues, friends and my family have contributed to this amazing, not always easy, experience during the past five years, and I will not be able to thank them enough for that.

First, I want to thank my mentor and supervisor *Daniel Kaufmann* for his immense support, his confidence in me and his generosity throughout the entire time. Thank you, Daniel, for the liberty you gave me to pursue my own ideas, your always open door, for giving me the opportunity to present my work at so many conferences and to meet incredible scientists from all over the world, and thank you for your guidance to become a better scientist.

I want to thank all past and current members of the Kaufmann lab, for the many discussions, their technical help and support and the special team spirit that made it such a great experience to be in this group. In particular, I want to thank *Amy* for her support and friendship during her time in the Kaufmann lab and after. She has taught me so much and has shown me, through her example, what a great researcher should be. A special thanks to *Elsa,* who has been with me almost all the way and who was just the best desk neighbor ever*, Antigoni, Gérémy, Nathalie, Gloria, Mathieu, Roxanne and Manon*. It was a pleasure to work with all of you.

Thanks to all the scientists and students at the CRCHUM for the discussions and interactions during and after work hours and for making the institute such a great research environment. Thanks to all the collaborators who contributed to the two research articles included in this thesis and to the people that supported me during this PhD, in particular the members of my predoctoral exam committee, *Dr. Irah King, Dr. Nathalie Labrecque* and *Dr. John Stagg*, as well as my thesis defense committee *Dr. Nathalie Arbour, Dr. Alain Lamarre, Dr. Marika Sarfati* and *Dr. Sophie Petropoulus.*

I would also like to take the opportunity to thank the organizations that funded my doctorate studies: The Bavarian Research Alliance (BayFor), the Département de Microbiologie, Infectiologie et Immunologie de l'Université de Montréal and the Fonds de la recherche en santé du Québec (FRQS).

Lastly, I would like to thank my family and friends in Germany and Canada. Thank you, *Mum, Dad* and *Fabian* for always supporting me from afar, keeping up my spirits and believing in me. Thank you, *Mathieu*, for your patience, your endless encouragements and for being there for me every day. Thanks to all the members of the Catafard clan, in particular to *Serge* and *Marielle*, for being my second family here in Montreal.

A special thanks goes to my friends *Saipriya, Jérémie, Amélie, Thomas, Sabine, Ursi*, *Julia, Julien, Alain, Marie,* all the other old friends that kept in touch and the new friends that I made along the way all over the world.

Thank you all, I could not have done it without you.

Chapter 1 Introduction

Parts of this introduction were used in the review articles

"Niessl *et al.,* Harnessing T Follicular Helper Cell Responses for HIV Vaccine Development, *Viruses*, 2018"

and

"Niessl *et al.*, Tools for Visualizing HIV in Cure Research, *Current HIV/AIDS Reports*, 2018".

Both articles are included in Chapter 9 – Appendices

A complete understanding of the modulations of HIV-specific T cell responses during chronic HIV infection, the persistence of these modulations during antiretroviral therapy, and how effective antiviral responses could be restored is still missing to date.

Here, we studied alterations of the HIV-specific $CD4^+$ T cell response in chronically infected individuals that are maintained during antiretroviral therapy (ART), with a specific focus on T follicular helper cells. We compared the phenotypic and functional profile of HIV-specific $CD4^+$ T cells to responses elicited by other viruses within the same individual. These included responses that were generated during an acute infection that became subsequently resolved or via vaccination (hepatitis B virus), and a chronic infection that is usually controlled by the host's own immune system (cytomegalovirus).
In a second study, we investigated the effect of anti-HIV antibody therapy and interruption of ART on the HIV-specific $CD8^+$ and $CD4^+$ T cell response.

This introduction, therefore, discusses what is known about immune responses directed against acute viral infections or generated after vaccination and responses against chronic viral infections with a specific focus on HIV and CMV. Furthermore, it discusses examples of current strategies to improve the anti-HIV T cell immunity, the development of anti-HIV antibodies in infected individuals and their use for HIV prevention and treatment.

1.1 Immunity against acute viral infections or after vaccination

The immune system consists of two arms to fight invading pathogens or developing tumors: the innate and the adaptive immune system. While the innate immune system is non-specific and senses pathogen-associated molecular patterns (PAMPs) by pattern recognition receptors (PRRs), the adaptive immune system develops specifically to pathogen-specific antigens and forms a long-term memory response that is able to respond faster upon a secondary infection with the same pathogen.

1.1.1 Innate antiviral immunity

All cells have intrinsic systems to recognize and inhibit viral infections. In mammalian cells, PRRs include Toll-like receptors (TLRs), RIG-I-like receptors (RLRs), NOD-like receptors and C-type receptors [1]. Binding of viral PAMPs, such as viral nucleic acids, to these surface or intracellular PRRs, activates an intracellular signalling cascade to induce antiviral type-I interferons (IFNs), cell death or inflammatory cytokines. Autocrine or paracrine type I IFN signalling leads to the expression of IFN-stimulated genes (ISGs) that can directly inhibit viral replication through various mechanisms [1]. Several innate immune responses form the first line of cellular-mediated defense against viral infections. Tissue-resident myeloid cells such as dendritic cells (DCs) and macrophages secrete type I IFNs and other pro-inflammatory cytokines after PAMP recognition. Group 1 innate lymphoid cells (ILCs) such as tissue-resident ILC1s and natural killer (NK) cells express high levels of IFN-γ. In addition, NK cells can directly kill virally infected cells via perforin or granzyme B secretion, which induce cell lysis [2].

PAMP recognition via PRRs on antigen-presenting cells (APCs) leads to their activation and local expression of inflammatory cytokines [3]. Additionally, APCs internalize the PAMP, migrate to secondary lymphoid organs, where they present the processed antigen in the context of major histocompatibility (MHC) class I and class II molecules to naïve T cells [3]. Antigen can also reach secondary lymphoid organs through the lymphatic system, where it is captured by lymph node (LN)-resident DCs [4].

1.1.2 Adaptive antiviral immunity

1.1.2.1 T cell responses

Adaptive immune responses are generated a few days after infection and peak around one to two weeks [5]. T cells undergo three different phases during a primary viral infection: Expansion, contraction and maintenance (Figure 1).

During the expansion phase, naïve cluster of differentiation (CD)4^+ or $CD8^+$ T cells are activated or primed by T cell receptor (TCR)-dependent recognition of the antigen presented by MHC-I for $CD8^+$ T cells or MHC-II on APCs for $CD4^+$ T cells in secondary lymphoid organs. In addition, costimulatory signals and cytokines are necessary to induce their massive proliferation and differentiation into effector T cells. Effector T cells lose the expression of lymphoid homing molecules (e.g. chemokine (C-C motif) receptor (CCR) 7, CD62L), enter the circulation and acquire homing markers to migrate to sites of inflammation [6].

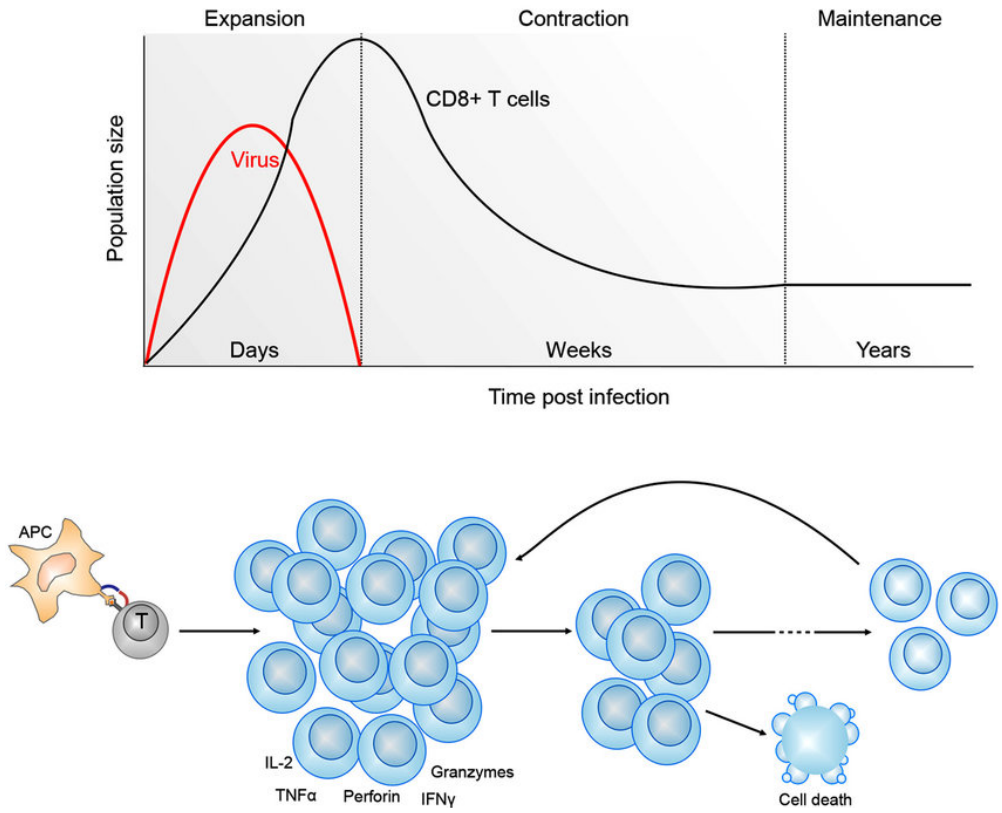

Figure 1 – **Kinetics of T cell responses following an acute viral infection**

Priming of naïve T cells via APCs leads to clonal expansion and differentiation into effector T cells. Effector functions for CD8$^+$ T cells include secretion of cytokines and cytotoxic molecules, CD4$^+$ Thelper cells support antiviral responses by cytokine secretion and cell-cell interactions. After the antigen is cleared, T cells undergo a massive contraction and undergo apoptosis. The remaining T cell pool persists as memory cells for years and can mount a rapid antiviral response upon secondary infection. This figure is licensed under an open-access Creative Commons Attribution License (CC BY) and was obtained from [7].

Antiviral CD8$^+$ T cell responses (also called cytotoxic T lymphocytes (CTLs)) recognize virally infected cells through the binding of the TCRs to foreign antigens presented on the MHC-I. They kill infected cells by secreting granules that contain perforin or granzymes. These cytolytic molecules create pores in the lipid bilayer of the target cells or induce cell death by activating intracellular apoptotic signalling cascades [8]. In addition, CD8$^+$ T cells kill target cells via a Fas-FasL-dependent induction of apoptosis, and they release the antiviral and pro-inflammatory cytokines IFN-γ, tumor necrosis factor (TNF)-α and others [8].

Naïve CD4$^+$ T cells can differentiate into distinct Thelper (Th) subsets with specific immunological functions. Each subset is characterized by its transcriptional program that is governed by a so-called master regulator transcription factor, which regulates functional and phenotypic properties. Th1 CD4$^+$ T cells express the transcription factors T-bet and/or eomesodermin (EOMES), secrete

IFN-γ, interleukin (IL)-2 and TNF-α are important for the immunity against intracellular pathogens including viruses [9]. A subset of Th1 $CD4^+$ T cells expressing both T-bet and EOMES have been shown to have cytolytic functions similar to CTL cells and kills target cells by the secretion of perforin or granzyme B [10]. Th2 cells are important to resist extracellular pathogens such as helminths and nematodes, secrete for example IL-4, IL-5 and IL-13 and express the master regulator GATA3 [9]. Th17 or Th22 cells are able to migrate to mucosal tissues via the expression of CCR6 or gut-homing integrins. Here, they secrete IL-17, IL-22 and other cytokines and chemokines to induce an anti-bacterial and anti-fungal immune response. At the transcriptional level, this is coordinated by the lineage-specific transcription factors retinoic acid receptor-related orphan receptor γ t and α (RORγt and RORα) [11, 12]. Finally, T follicular helper (Tfh) cells express the transcription factor B-cell lymphoma 6 protein (Bcl6) and others and give help to B cells in the germinal center (GC) or secondary lymphoid organs to produce high-affinity antibody responses, for example via the secretion of IL-21 and IL-4 [9] (Tfh cells will be discussed more in detail below). $CD4^+$ T cell differentiation into the various subsets is dependent on the signals received by the primed naïve T cell such as cytokines, co-stimulatory signals, or the type of DC that presents the antigen [7].

After successful clearance, about 90-95% of the effector T cell population undergoes apoptosis [13]. During this contraction phase, the surviving T cells form a pool of long-lived memory cells, which persist during the maintenance phase even in the absence of antigen. Memory T cell survival is dependent on the cytokines IL-7 and IL-15, which induce a homeostatic turnover of T cells to keep the number at a constant size [14]. Originally, two memory T cell subsets have been identified: central memory T cells (T_{CM}) homing to secondary lymphoid organs and effector memory T cells (T_{EM}) circulating through non-lymphoid tissues [15]. However, it has become clear that during the acute phase of infection, effector cells infiltrate the tissue to mediate pathogen clearance and differentiate to tissue-resident memory T cells (T_{RM}) without re-entering the blood stream for circulation [16]. After formation, T_{RM} cells demonstrate a long-term persistence and provide a first-line defense against tissue-invading pathogens upon secondary infection. A commonly used marker for the identification of $CD4^+$ and $CD8^+$ T_{RM} cells is the C-type lectin protein CD69. Although CD69 can also be expressed by circulating T cell populations shortly after activation, it remains persistently upregulated on T_{RM} cells [17]. Once established, T_{RM} cells can persist for long periods of time after formation. Some studies suggest that, similar to circulating memory T cells, T_{RM} cells require IL-15 and IL-7 for their long-term maintenance and survival in the skin. However, IL-15 was dispensable for T_{RM} cell persistence in the lung suggesting that signals for T_{RM} cell development and maintenance might be tissue dependent [18].

Independent of the location, in the tissue or in circulation, long-lived memory T cells differentiate into functional effector cells upon re-encounter with the pathogen, they are specific for. This allows the immune system to rapidly mount an effective recall immune response to prevent a secondary infection or to limit disease severity [7].

The antiviral $CD4^+$ T cell response is typically characterized by cells with a Th1 or Tfh phenotype [19, 20]. However, while antigen-specific Th1 responses have been well characterized in mice and humans, less is known about Tfh responses in the context of viral infections or vaccinations. As Tfh cells produce low levels of cytokines that are difficult to detect by cytokine-dependent assays such as intracellular cytokine staining (ICS) or ELISpot, they have been missed in previous analyses [21, 22]. However, the recent development of cytokine-independent assays to study antigen-specificity [21-23], now allows to phenotypically and functionally characterize this population. As Tfh responses will be a major focus of the manuscript included in Chapter 3, they are introduced here in detail.

1.1.2.2 T follicular helper cells and humoral responses

Tfh cells are a specialized $CD4^+$ T helper subset, characterized by the expression of the chemokine (C-X-C motif) receptor (CXCR)5, the ligand for the chemokine (C-X-C motif) ligand (CXCL)13, which allows their migration into the GC of secondary lymphoid organs [24, 25]. There, they provide B cell help for the generation of high affinity antibody responses. Further phenotypic and functional markers include Bcl6, programmed cell death 1 (PD-1), inducible T cell costimulator (ICOS), CD40L and IL-21, which are important for differentiation and function of Tfh cells and can be expressed at different levels depending on the differentiation status.

1.1.2.2.1 Tfh Differentiation

Tfh differentiation is a multifactorial and multistep process (see Overview, Figure 2). Initially, naïve $CD4^+$ T cells are primed by antigen-presenting DCs in the T cell zone of secondary lymphoid organs. Early expression of the transcription factors Lef-1 and Tcf-1 primes naïve $CD4^+$ T cells for further Tfh-promoting signals and leads to the upregulation of the transcriptional repressor Bcl6 [26, 27], which is absolutely required for Tfh development [28-30]. Bcl6 acts together with other Tfh-related transcription factors (e.g., Maf and Ascl2) to repress non-Tfh related signature genes and induce key Tfh-associated genes such as PD-1 and CXCR5 [28, 31, 32]. In contrast to non-Tfh cells that leave secondary lymphoid organs, the expression of CXCR5 and concomitant downregulation of CCR7 on the cell surface allows early Tfh cells to migrate to the T-B border [33]. There, Tfh cells interact with antigen-presenting B cells via ICOS-ICOSL [34], which leads to

the reinforcement and persistence of the Tfh signature, and migration into the B cell follicle for the formation of GCs [35]. Further interactions between Tfh and antigen-presenting B cells in the GC are necessary to sustain Tfh commitment, demonstrating that continuous antigenic activation is important for their maintenance [36].

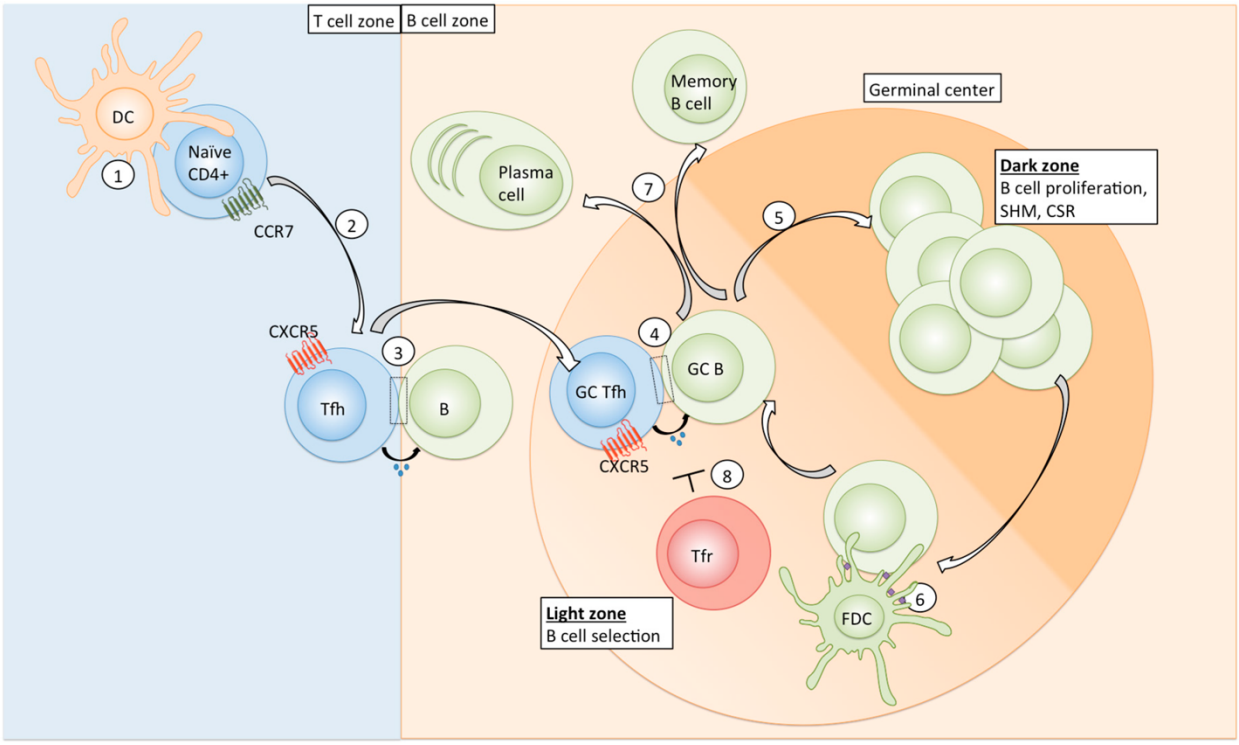

Figure 2 – **Overview of Tfh differentiation and function**

Naïve CD4⁺ T cells are primed by antigen-presenting dendritic cells (DCs) in the T cell zone of secondary lymphoid organs (1); Specific cytokines, co-signalling surface receptor molecules (see Table 1) and a prolonged DC-naïve CD4 interaction favour Tfh commitment. Tfh-polarized cells downregulate CCR7 and express CXCR5, the CXCL13 ligand, which allows their migration to the T-B-border (2); where first interaction with B cells occurs (3); Tfh cells then migrate into the germinal center, where further interaction with GC B cells sustains the GC Tfh polarization (4); In the dark zone of the GC, B cells undergo proliferation, affinity maturation via SHM, and CSR (5); B cells migrate to the light zone to receive survival and selection signals. They take up and process antigen (purple) from FDCs (6) and subsequently present it to GC Tfh cells (4). High affinity B cells are able to capture and present more antigen and therefore receive more Tfh cell help. Repeated circulation of B cells between DZ and LZ results in the acquisition of high levels of SHM and selection of high affinity clones. B cells eventually differentiate into antibody-producing plasma cells or memory B cells and enter the blood circulation (7); Tfr cells can inhibit GC Tfh and B cell responses via multiple mechanisms (8); DC: dendritic cell, Tfh: T follicular helper cell, SHM: somatic hypermutation, CSR: class switch recombination, FDC: follicular dendritic cell, DZ: dark zone; LZ: light zone; Tfr: follicular T regulatory cell. Figure obtained with permission from [37].

Signalling molecules involved in the positive or negative regulation of Tfh differentiation present some notable differences between mice and humans and are shown in Table 1. In addition, quantitative signals related to strong and prolonged interaction between the T cell receptor and the MHC-II molecule favours Tfh vs. non-Tfh commitment [38].

Table 1 – **Signalling molecules regulating Tfh differentiation in mice and humans**

Table modified with permission from [37].

Signalling Molecule/Receptor Pair	Species	Role in Tfh Differentiation	Source/Interacting Cell Type
IL-6/IL-6R	Mouse	Promotion	DCs, B cells
IL-12/IL-12R	Mouse, human	Promotion	DCs
IL-21/Il-21R	Mouse	Promotion	T cells
IL-23/IL-23R	Human	Promotion	DCs
IL-27/IL-27R	Mouse	Promotion	DCs
IFN-γ/IFN-γR	Mouse	Promotion	T cells
TGF-β/TGF-βR	Mouse, human	Inhibition (mouse), Promotion (human)	DCs
Activin A/Activin-R	Human	Promotion	DCs
Ox40L/Ox40	Mouse, human	Promotion	DCs, B cells
ICOSL/ICOS	Mouse, human	Promotion	B cells
B7/CD28	Mouse	Promotion	DCs, B cells
SLAM family members	Mouse, human	Promotion	B cells
IL-2/IL-2R	Mouse, human	Inhibition	T cells
IL-7/IL-7R	Mouse	Inhibition	DCs
B7/CTLA-4	Mouse	Inhibition	-

1.1.2.2.2 Tfh-dependent B cell responses

B cell differentiation and isotype switch can occur after initial T-B interaction and outside of the GC. This extrafollicular response emerges early after immunization or infection and provides a first line of protective antibodies upon infection [39]. However, plasma cells generated following this type of interaction are usually short-lived and of low affinity due to only minimal affinity maturation [39]. For the efficient neutralization of viruses and other pathogens, high affinity antibodies are required. In addition, induction of long-lived memory B cell responses after infection or vaccination is desired to ensure long-term immunity. Both can be achieved in the GC reaction.

GC Tfh cells play a central role as they regulate multiple aspects of this process: B cell survival, proliferation, somatic hypermutation (SHM), class-switch recombination (CSR), and differentiation. Tfh cells reside in the light zone of a mature GC. There, B cells take up antigen from follicular dendritic cells (FDCs), process it and present it to GC Tfh via MHC-II. During this process, B cells compete for limited Tfh help: High affinity B cells, which were able to capture and therefore present more antigen compared to B cells with lower affinity, are more likely to receive Tfh signals [40, 41]. Selected B cells enter the dark zone (DZ), where they proliferate and undergo SHM of the B cell receptor (BCR) V-region genes, the rate of which directly correlates with the Tfh help received in the light zone (LZ) [42]. During this process, mainly single nucleotide exchanges are introduced, resulting in a random modification of the BCR binding-affinity. GC B cell clones return to the LZ and are further selected by Tfh based on their antigen binding capacity. Repeated circulation between the LZ for selection for high-affinity and DZ for proliferation and affinity maturation results in the acquisition of elevated rates of somatic mutations and ensures the dominance of high-affinity B cell clones. Eventually, B cells differentiate into long-lived plasma cells or memory B cells and enter the circulation, thus allowing seeding of other anatomic locations.

Tfh help in the GC occurs via direct cell-cell interactions with B cells and secretion of cytokines. Some important mediators for B cell survival, proliferation, and differentiation are summarized in Table 2. In addition, B cell functions and differentiation can be complemented and modulated by a variety of other cytokines that regulate alone or in combination CSR and differentiation and thus outcome of antibody responses (reviewed in [43]). Signals regulating GC B cell differentiation to plasma cell vs. memory B cells are not well understood but recent studies suggested that high affinity B cell antigen interaction and IL-21 produced by Tfh cells favour plasma cell differentiation [44, 45].

Table 2 –**Tfh mediators for B cell activation, differentiation and affinity maturation**

Table modified with permission from [37].

Tfh Functional Molecule	Effect on B Cells
IL-21	CSR, activation, proliferation, SHM, plasma cell differentiation
IL-4	Proliferation, CSR, SHM
IL-10	Proliferation, CSR, plasma cell differentiation
CD40L	Activation, proliferation, CSR

Virus-specific antibodies can bind viral surface proteins via the variable antigen-binding fragment (Fab) and neutralize it by inhibiting viral entry into target cells. In addition, the crystallizable fragment (Fc) can bind to Fc-receptors (FcRs) expressed on multiple immune effector cells to mediate antibody-dependent cell-mediated viral inhibition (ADCVI). ADCVI includes the killing of infected cells via antibody-dependent cellular cytotoxicity (ADCC) by NK cells, antibody-dependent phagocytosis by monocytes, the antibody-dependent complement-mediated lysis, or induction of the release of soluble viral inhibitors. Together with cell intrinsic and innate immune systems, adaptive T and B cell responses contribute to the resistance against invading pathogens (reviewed in [46]).

1.1.2.2.3 Memory and Circulating Tfh Cells

GC Tfh cells have been shown to form a pool of memory cells upon antigen clearance in both mice and humans. Memory Tfh cells localize together with antigen-specific memory B cells in the draining LN for the rapid induction of humoral responses upon re-exposure to antigen [47]. A subset of $CD4^+$ T cells in peripheral blood, termed circulating Tfh (cTfh) or peripheral Tfh (pTfh), shares several features with tissue Tfh [48]. cTfh cells have a memory phenotype and express CXCR5, although at lower levels compared to their GC counterparts [49]. In addition, certain phenotypic markers of GC Tfh, e.g., BCL6, are lost or downregulated [50]. Studies in mice showed that cTfh cells originate from GC Tfh cells that left the GC into the blood. Upon activation cTfh cells can migrate to the GC secondary lymphoid organs for the interaction with B cells [51]. In humans, matched samples from blood and tonsils revealed that after vaccination clonal relatives of GC Tfh enter the circulation [52]. Despite the phenotypic differences, functional properties of cTfh cells are partially preserved when compared to their tissue counterparts: cTfh cells express higher levels of Tfh-related cytokines such as IL-21 and CXCL13 and show a superior capacity for B cell help in *in vitro* co-culture assays when compared to $CXCR5^-$ non-cTfh cells [48]. Of note, all cells identified by a given set of markers as cTfh in blood may not have the same potential to home to lymphoid tissue and become activated GC Tfh. While a better understanding of the relationships between quantitative and qualitative characteristics of cTfh responses and GC activity is thus necessary, monitoring of cTfh and antigen-specific cTfh responses in blood can represent an alternative investigational tool during infection or in vaccine trials when access to lymphoid tissue is limited or not possible.

cTfh represent a heterogeneous population that can be classified into multiple subsets based on polarization and activation status. Differential expression of the chemokine receptors CXCR3 and CCR6 allows the distinction of Th1-like ($CXCR3^+CCR6^-$), Th1Th17-like ($CXCR3^+CCR6^+$), Th17-

like ($CXCR3^{-}CCR6^{+}$), and Th2-like ($CXCR3^{-}CCR6^{-}$) cTfh subsets. These cTfh subsets express transcription factors and can produce cytokines upon stimulation that are typically associated with Th1, Th2, Th17, and Th1Th17 $CD4^{+}$ subsets [48]. Using these surface markers, several groups have identified a differential B cell helper capacity of cTfh subsets in *in vitro* culture assays: $CXCR3^{-}$ populations were able to provide help for naïve and memory B cells and induced proliferation, differentiation, and class-switched antibody production after stimulation with Staphylococcal enterotoxin B (SEB) [48, 49, 53]. In contrast, $CXCR3^{+}$ cTfh cells were able to provide help to memory B cells *in vitro* [53], suggesting a role in promoting recall responses instead of priming primary antibody responses.

Tfh subsets based on the expression of CXCR3 and CCR6 can also be identified in the LN of macaques [54]. However, it remains to be determined whether the helper potential of different cTfh subsets can be translated into GC Tfh cells in tissues.

Given the important role of Tfh cells for the generation of high-affinity antibody responses, it is not surprising that absence of or impaired Tfh responses hampered the generation of protective antibodies after infection or vaccination [55]. However, on the other hand, excessive accumulation of an overactive GC Tfh response correlated with the development of antibody-mediated autoimmunity or the generation of low affinity antibody responses by allowing the survival of B cells with self-reactivity or low binding capacity [56, 57]. This shows that Tfh number and function in the GC needs to be regulated to ensure an efficient and targeted B cell help. Indeed, Tfh cells are only a minor population in the GC to allow competition of B cells for limited help and selection of only high-affinity clones. Tfh number can be regulated at the stage of differentiation as mentioned above. In addition, several mechanisms control Tfh number and function in the GC.

Tfh cells are characterized by the high expression of multiple co-inhibitory receptors (IRs) including PD-1, T cell immunoreceptor with immunoglobulin and ITIM domains (TIGIT) or CD200 [49, 58, 59]. While PD-1 and likely other of these molecules are required for interaction with B cells and additional cell types, Tfh positioning and function to ensure proper humoral responses [60, 61], they might also be involved in the regulation of Tfh expansion and function in the context of chronic antigen exposure in the GC environment. For example, knockout or blocking of the immune checkpoints cytotoxic T-lymphocyte-associated protein (CTLA)-4 or PD-1, alone or in combination with Lag-3, induced Tfh proliferation and enhanced cytokine production [62-64].

In addition, GC responses are controlled by the recently identified T follicular regulatory cells (Tfr) [65-67]. Tfr cells express similar phenotypic markers compared to Tfh cells including CXCR5, PD-

1, Bcl6, and ICOS [59, 65-67]. In contrast to Tfh cells, Tfr cells differentiate from natural Tregs and express Foxp3 and Helios [67]. The mechanism of Tfr-mediated GC regulation is – especially in humans – not well understood. Studies in mice demonstrated that Tfr cells inhibit proliferation and cytokine expression in Tfh cells as well as CSR and antibody production in B cells [51, 68]. These effects were mediated via Tfr-induced changes in the cellular metabolism of Tfh and B cells that were long lasting but reversible and partially due to epigenetic modifications [68]. Additional Tfr-mediated suppressor mechanisms may include the physical inhibition of Tfh-B-interaction, induction of cell death via granzyme B, and the expression of inhibitory cytokines (reviewed in [68]).

1.1.3 Adaptive immunity after vaccination

Generating a long-lived memory response is the goal of immunization. Passive immunization refers to the injection with pathogen-specific antibodies. Although this form of vaccination is protective, it is only temporal because of a relatively short half-live of antibodies [69].

Active immunization follows similar principles and mimics a primary infection with pathogens without causing the disease. The host's immune system is primed with a pathogenic agent in combination with an adjuvant. Adjuvants are used to promote or shape immune responses during vaccination as the vaccine antigen alone is in most cases of low immunogenicity [70]. They can enhance immune cell infiltration and antigen uptake into APCs as well as activate innate immune cells via binding to specific receptors (e.g. TLR agonists) to prime and generate a long-lived protective T and B cell response [70].

Although vaccines are an important tool for public health and have shown a tremendous success against multiple infections, e.g. against hepatitis B, yellow fever, smallpox, mumps, and pertussis, it is not well understood, how the protective immunity is generated and why some vaccines induce a longer lasting immunity than others [71].

Most successful vaccines (e.g., against hepatitis B, yellow fever, and smallpox) work by inducing long-lasting neutralizing antibody responses that prevent infection of target cells, and vaccine-induced antibody titers above a certain threshold correlate with protection [72]. Given the important role of Tfh responses for the development of high-affinity and long-lived B cells, recent studies focus on understanding the role of this $CD4^+$ T cell subset in the context of vaccination. In humans, the Tfh response is best studied in the context of influenza vaccination, which in most individuals induces a recall memory response due to prior exposure [73]. Activated influenza-specific cTfh responses peaked at around one week after vaccination and preferentially had a Th1-like $CXCR3^+$

phenotype [53]. As mentioned above, this phenotype is associated with a lower B cell helper capacity *in vitro* compared to CXCR3$^-$ Tfh cells, and might therefore explain the low efficacy of the flu vaccine (discussed in [74]). Indeed, Th1-cytokine IL-2 and TNF-α expression in influenza-specific cTfh responses was associated with a poor response to the vaccine [75]. Future studies investigating Tfh biology during infection and vaccination and how to induce Tfh subsets with the capacity to generate protective and long-lived B cell responses will be of importance for the development of vaccine regimens against multiple pathogens.

1.2 Immunity against chronic viral infections

In contrast to acute viral infections, during which the pathogen is completely cleared, chronic viral infections cause a persistent, often lifelong infection in specific cells in the infected individual. Chronic viral infections can be either characterized by a continuous productive infection (e.g. hepatitis B or C virus (HBV, HCV) in some individuals), the establishment of a latently infected pool, from which the virus can be reactivated (e.g. Herpesviruses such as Epstein-Barr virus (EBV) or cytomegalovirus (CMV)), or both (e.g. HIV) [76]. Each of these types of chronic viral infections has different implications on the host's immune system.

One aim of this thesis was the characterization of persistent alterations of the HIV-specific $CD4^+$ T cell response induced during uncontrolled HIV infection. In the manuscript included in Chapter 3 of this thesis, we compared phenotypic and functional characteristics of HIV-specific responses to T cells specific for CMV, as an example of a chronic viral infection that is controlled by potent antiviral T cell responses. Therefore, this introduction gives a brief account of different aspects of CMV in addition to HIV.

1.2.1 Cytomegalovirus (CMV)

CMV is a member of the *Herpesviridae* family and was first discovered in 1881 [77]. Cells infected with CMV grow in size and have large nuclei, an observation which has given the virus its name [78]. CMV infection is usually controlled by a strong adaptive immune response in immunocompetent individuals [79]. Although CMV persists for life in infected individuals, the immune system does not show signs of typical exhaustion as can be seen for other chronic viral infections [80].

1.2.1.1 CMV epidemiology

CMV infection is usually acquired during early childhood and adolescence, and generally causes an asymptomatic infection [80]. Regional differences regarding the CMV prevalence exists with the highest seroprevalence in Eastern Mediterranean countries (~90%) and the lowest in European countries and Canada (~66%) [81]. Independent of the region, the HIV-infected population shows a higher seroprevalence compared to HIV-negative individuals, e.g. around 82% in Canada [82].

1.2.1.2 CMV particle

The virus with a diameter of about 150-200 nm is enveloped by a host-cell derived double-lipid membrane that has eight different viral glycoproteins embedded (Figure 3). The envelope

encloses the viral icosahedral capsid that contains the linear, double-stranded DNA genome with a size of 236 kbp and over 200 open reading frames to encode functional proteins [83, 84]. CMV therefore has the largest known human virus genome [85]. The tegument layer lies between envelope and capsid and contains several viral proteins that are important for viral replication and immune evasion [83].

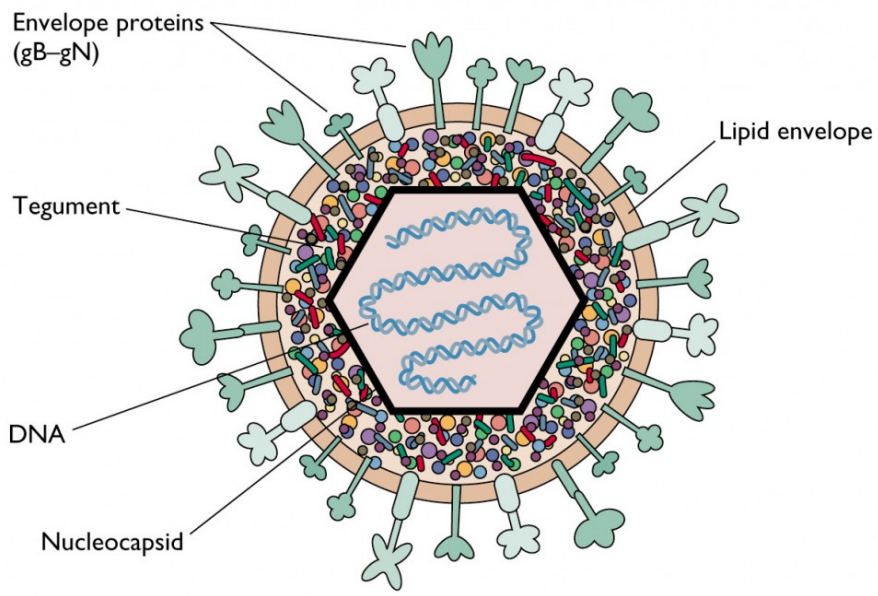

Figure 3 – **CMV particle structure**

The CMV DNA genome is enclosed by an icosahedral nucleocapsid, which is surrounded by a lipid envelope. The viral tegument layer defines the space between nucleocapsid and envelope and contains a large number of viral and cellular proteins and RNAs. Viral glycoproteins (gB-gN) in the envelope mediate viral entry into target cells. This figure is licensed under a Creative Commons Attribution 3.0 Unported License and was obtained from http://www.twiv.tv/virus-structure/.

1.2.1.3 CMV genome and life cycle

CMV infects multiple different immune cells (macrophages, DCs) and non-immune cell types (epithelial cells, smooth muscle cells, fibroblasts, hepatocytes, endothelial cells) and therefore spreads throughout the human body [86]. Upon binding of the viral surface glycoproteins to the host cell receptors, CMV enters the cell via endocytosis of membrane fusion [83]. The capsid is transported to the nucleus membrane by tegument proteins that bind to the cellular microtubule network [83]. The viral genome is released into the nucleus, where it circularizes [87]. During the lytic phase, viral protein classes are expressed in three closely regulated temporal phases: immediate early (IE), delayed early (DE) and late (L) [87]. IE proteins together with tegument

proteins regulate the host immune and stress response, DE proteins initiate viral genome replication and L proteins regulate the assembly of new viral particles that are released from the host cell [87]. However, CMV can undergo latency and persist in hematopoietic progenitor cells in the bone marrow, thus causing a lifelong infection in humans [87]. During this period, CMV viral load remains undetectable in immunocompetent individuals but virus reactivation has been associated with the activation and differentiation of persistently infected myeloid cells into macrophages and DCs [88].

1.2.1.4 CMV-specific immunity

Primary CMV infection and reactivation remain asymptomatic in immunocompetent individuals due to a strong CMV-specific immunity [80]. Although studies suggest that NK cells and humoral responses contribute to the control of the virus [89], CMV-specific $CD8^+$ and $CD4^+$ T cell responses are the best studied correlates for protection in animal models and humans [90]. These cells can be found at very high frequencies of around 10% of the memory $CD4^+$ or $CD8^+$ T cell population in the blood of CMV^+ individuals [90]. The large responses develop during the first year of infection [91]. However, in contrast to primary viral infections, for which a contraction of the T cell pool can be observed after viral clearance, CMV-specific $CD8^+$ and $CD4^+$ T cell responses are maintained at very high frequencies and can even increase over time [92, 93]. This is thought to be due to the repeated stimulation with antigens from reactivated viruses. Multiple CMV proteins induce potent T cell responses. High frequency responses in CMV^+ individuals can be observed against CMV IE-1 and the tegument phosphoprotein with 65 kDa (pp65) for $CD8^+$ and against pp65 and glycoprotein B (gB) for $CD4^+$ T cell responses [90]. The continuous antigen stimulation keeps the CMV-specific T cell pool in an effector-like state and the rapid expression of effector cytokines such as IFN-γ, TNF-α and cytolytic markers such as CD107A, perforin or granzyme B after *in vitro* activation of CMV-specific $CD8^+$ T cells is typical [94]. In addition, $CD4^+$ T cells targeting CMV exhibit potent cytolytic and Th1-like functions that contribute to the antiviral response *in vivo* [95].

Despite the chronic exposure to viral antigens, CMV-specific T cell responses do not show signs of T cell exhaustion. $CD8^+$ T cells retain their functional capacity and IR expression, e.g. PD-1, is lower when compared to T cells specific for other chronic viral infections or T cells exposed to chronic stimulation in the tumor microenvironment [94]. This is likely associated with a low amount of antigen and a low-level inflammatory environment during CMV re-exposure. Low-level lifelong reactivation induces, however, an enhanced terminal differentiation profile of CMV-specific responses and immune senescence [94].

As mentioned above, humoral responses against several CMV structural and non-structural proteins can be detected that increase during primary infection or after reactivation. Antibodies directed against the glycoproteins on the viral surface neutralize the virus and contribute to the inhibition of virus dissemination, but alone are not sufficient to control the infection [96]. CMV-specific cTfh responses are less well understood. However, activated CMV-specific cTfh and non-cTfh can be detected in CMV-infected individuals after primary infection that decrease in frequency during later time points [97].

Although CMV is usually controlled by a functional immune system, it can cause serious complications in immunocompromised individuals such as newborns, transplant patients or viremic HIV-infected individuals [98]. Uncontrolled CMV replication can cause end-organ damage and death. In HIV-infected individuals, this is associated with very low $CD4^+$ T cell count (<50 cells/µl) [99], and a loss of the CMV-specific T cell response [100]. With the induction of antiretroviral therapy (ART) and the recovery of $CD4^+$ T cells, HIV-infected individuals regain control of the CMV infection and CMV DNA levels are generally undetectable in the blood of successfully ART-treated HIV^+ individuals [101].

1.2.2 HIV

HIV is a retrovirus, belongs to the subgroup of lentiviruses and is the cause for the Acquired Immune Deficiency Syndrome (AIDS). HIV first became evident in the 1980s when several cases of opportunistic infections (CMV infections, mucosal candidiasis, and others) were reported in the USA that usually only occurred in state of severe immune suppression [102, 103]. More cases were reported subsequently worldwide, and many died quickly from the opportunistic infections. In 1982, the Center for Disease Control in the United States published a first case definition of what they termed AIDS [104]. In 1983, the group of Dr. Luc Montagnier at the Pasteur-Institute in Paris, France [105], and soon after the group of Dr. Robert Gallo at the National Institutes of Health in Bethesda, USA [106], discovered the HI-Virus as cause for the disease. However, its origin goes back to the beginning of the 20th century when cross-species transmission events from non-human primates (NHPs) infected with simian immunodeficiency virus (SIV) to humans initiated today's pandemic. While HIV-2, which today affects 1 to 2 million people mainly in West Africa [107], has been shown to be transmitted from sooty mangabeys to humans in the 1940s [108], HIV-1 the major form of HIV with higher pathogenicity is of chimpanzee and gorilla origin [109, 110]. HIV-1 is composed of four distinct phylogenetic lineages (groups M, N, O, and P), which were caused by four different cross-species transmission events. Groups N (transmitted from chimpanzees, [111]), O, and P (both transmitted from gorillas, [110]) are largely restricted to West African countries and together account for less than 1% of all HIV-1 infections.

Related to the extensive genetic diversity of HIV-1, today, group M (M for "major") can be classified into nine subtypes or clades (A-D, F-H, J, K) and more than 70 circulating recombinant forms (CRFs) that were generated by recombination events in individuals infected with multiple clades at the same time [112]. Different HIV strains demonstrate distinct geographical distributions with a subtype B predominance in the Americas, Western Europe and Australia [113]. However, more than 50% of all current HIV-infections belong to subtype C, which can be mainly found in Southern Africa and Southeast Asia. However, newest findings demonstrate the increase of HIV genetic diversity and prevalence of CRFs in recent years [113].

1.2.2.1 HIV epidemiology

Although the number of new HIV infections has decreased by 40% since its peak in 1997 [114], HIV still represents a major global health problem. During its 40 years history, around 78 million people have been infected with HIV and 39 million people died so far due to diseases related to AIDS caused by the infection. Currently, 37.9 million people are infected with HIV worldwide, which represents about 0.8% of the worldwide adult population [114]. However, the HIV burden varies

greatly between countries. In Western and Central Europe and North America, an estimated number of around 2.2 million people are living with HIV, while in eastern and southern Africa around 20.6 million people are HIV$^+$ [114].

1.2.2.2 HIV particle structure

The virus with a diameter of about 100nm is enveloped by a double-lipid membrane derived by the host cell covered with trimeric spikes that consist of the non-covalent bound surface glycoprotein (gp) gp120 and the transmembrane glycoprotein gp41 (Figure 4). The tail of gp41 is connected to the HIV matrix (MA) built by the MA protein p17. The core of the HIV particle is encased by the cone-shaped virus capsid (CA) made up by p24 molecules. It surrounds the two positive strand copies of HIV RNA that is covered by nucleocapsid (NC) proteins, the viral enzymes reverse transcriptase (RT) and integrase (IN), other viral proteins, and host cellular factors from the producer cells [115].

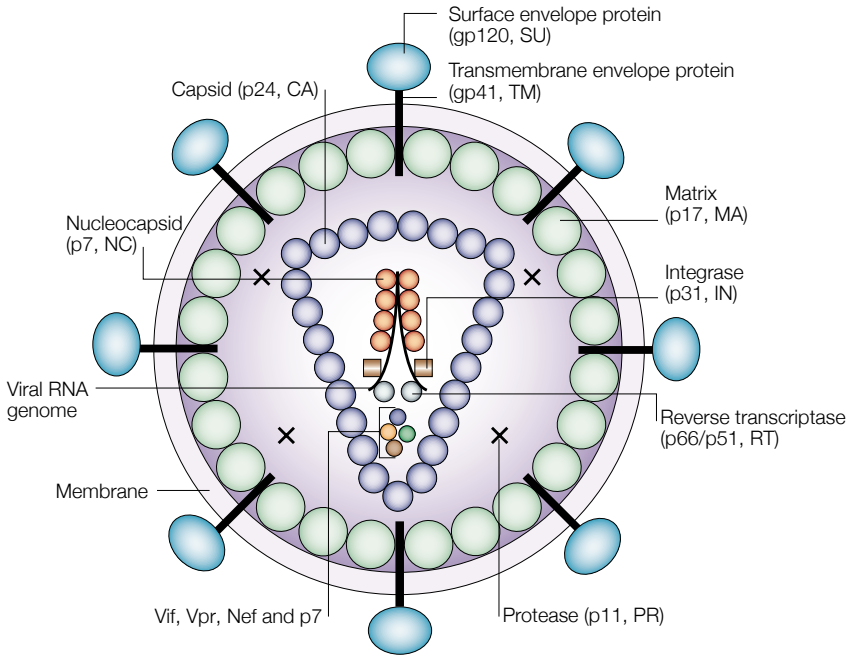

Figure 4 – **HIV particle structure**

The HIV polyprotein Gag is processed into several structural proteins: MA proteins surround the inner layer of the double-lipid membrane, CA proteins form the cone-shaped viral capsid that contains two positive strand HIV RNA copies that is covered by NC proteins. In addition, the HIV capsid contains viral enzymes (reverse transcriptase, integrase) and other viral and cellular proteins. The polyprotein Env gives rise to the glycoproteins gp120 and gp41, which form trimeric structures on the surface of the HIV particle. MA: matrix, CA: capsid, NC: nucleocapsid, Env: envelope. Figure adapted from [116] with permission from *Springer Nature.*

1.2.2.3 HIV genome and proteins

The HIV genome consists of two identical single-strand RNA copies (9.2 kb each). After reverse transcription of the HIV genome after infection, the double-stranded HIV DNA is integrated into the human genome of the infected cell [115]. Viral DNA integration is dependent on the long terminal repeats (LTR) at the 3'- and 5'-end of the HIV DNA, which are formed by combining the two regions RU5 and UR3 at the end of the HIV RNA during reverse transcription (Figure 5) [117]. In addition, the 5'-LTR contains the HIV promoter [115].

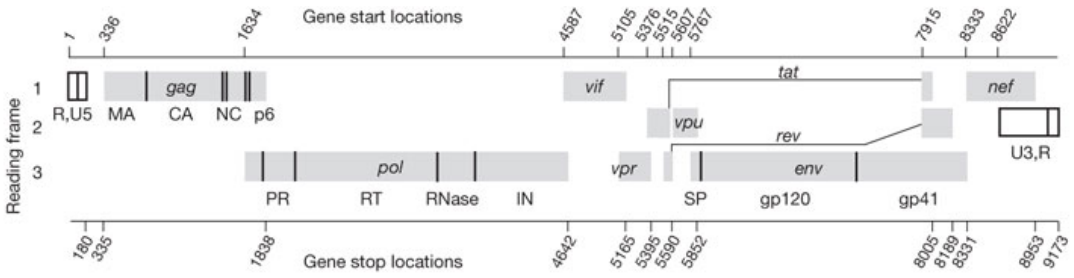

Figure 5 – **HIV-1 genome organization**

The HIV-RNA strand (9.2 kb) encodes for nine genes and 15 proteins. The genome includes *gag*, *pol* and *env*, coding for structural proteins and enzymes, *tat* and *rev*, coding for regulator proteins, and *vif, vpr, vpu, nef*, coding for accessory proteins. CA: capsid; env: envelope; gag: group-specific antigen; gp: glycoprotein; IN: integrase; MA: matrix; NC: nucleocapsid; nef: negative regulatory factor; pol: polymerase, PR: protease; RT: reverse transcriptase; vif: virion infectivity factor; vpr/vpu: viral protein r/u. Figure adapted from [118] with authorization from *Springer Nature.*

The HIV genome consist of nine genes encoding for 15 viral proteins. *Gag* (group-specific antigen), *env* (envelope) and *pol* (polymerase) are first transcribed into large polyprotein complexes, which are later cleaved into single proteins [115]. *Gag* encodes for the proteins of the MA (p17), CA (p24), and nucleocapsid (NC, p7). *Env* encodes for the protein gp150, which is proteolyzed to gp120 and gp41. Both genes together give rise to all structural proteins of the HIV particle. In addition, the Pol protein is cleaved into the viral enzymes protease (PR), RT, RNase and IN [115].

In addition to the structural and enzymatic proteins common to all retrovirus, the HIV genome encodes for virus-specific proteins with variable functions. While the regulatory proteins Rev (regulator of expression of virion proteins) and Tat (HIV trans-activating protein) have important functions during HIV replication, the accessory proteins Nef (negative regulatory factor), Vpu (viral protein u), Vpr (viral protein r), and Vif (virion infectivity factor) are involved in viral replication and distinct mechanisms to antagonize the host's viral defense mechanisms to enhance HIV infectivity

and pathogenesis [115]. Several structural and non-structural HIV proteins have multiple functions during the replication process, some of which will be discussed below. Together, viral proteins ensure the formation of a functional and pathogenic virus particle that is able to cause the severe infection of $CD4^+$ T cells and other cell types.

1.2.2.4 HIV replication

HIV preferentially infects $CD4^+$ T cells and macrophages as these cell types express the primary HIV receptor CD4 that can be bound by HIV Env trimer [119]. Receptor binding induces a conformational change in the HIV gp120 molecule to expose a second binding site for the engagement of the HIV-coreceptor expressed on the surface of the target cell (CCR5 for R5-tropic or CXCR4 for X4-tropic HIV strains) [120]. This interaction leads to the exposure of the hydrophobic fusion protein on the gp41 molecule, which enters into the plasma membrane of the cells. Further conformational changes in the gp41 protein brings viral and cell membranes into close proximity and leads to their fusion [120]. The viral core is subsequently released into the cellular cytoplasm (Figure 6) [120].

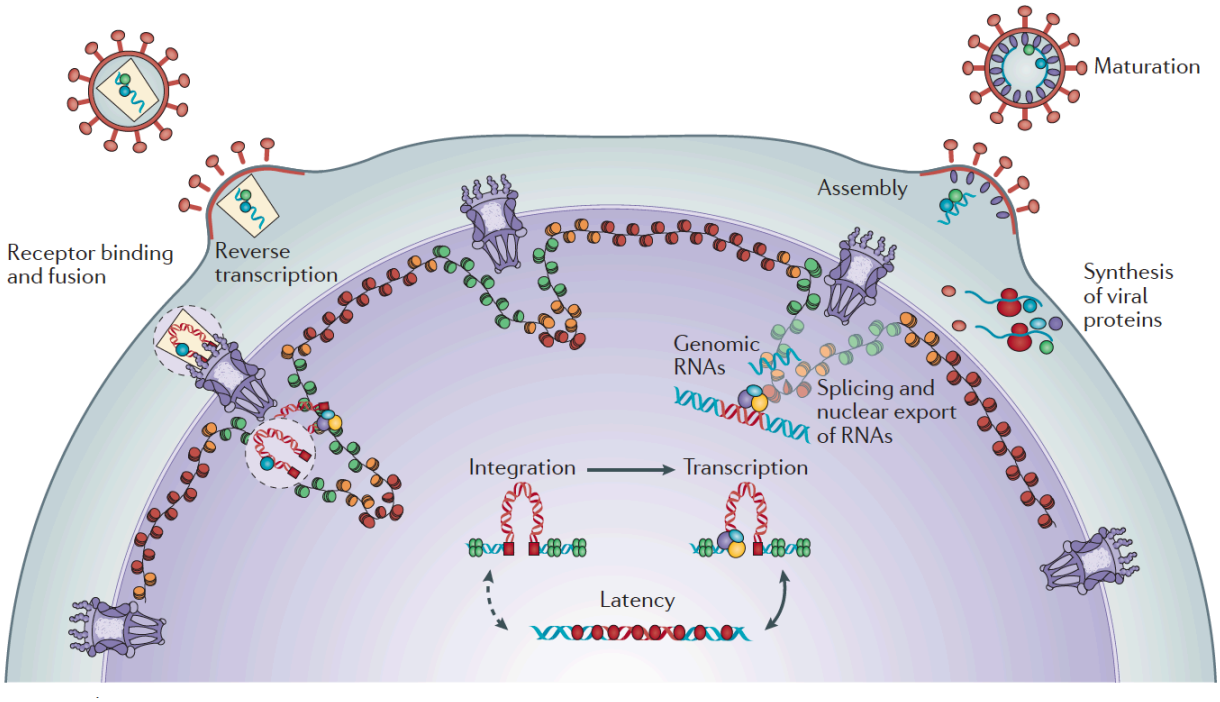

Figure 6 – **HIV life cycle**

HIV enters the target cell through binding of the HIV Env with cellular receptors and fusion of viral and cellular plasma membranes. After uncoating and reverse transcription, the viral DNA is transported into the nucleus, where it integrates into the host genome. Integrated HIV DNA can enter latency and stay transcriptionally silent. During viral replication, HIV DNA is transcribed, and transported to the cytoplasm, where production of viral proteins allows the assembly of new viral particles. After maturation, these particles are able to infect new cells. Figure from [121] with authorization from *Nature Springer.*

The process of uncoating, which describes the disassembly of the CA proteins, begins in the cytoplasm early after viral entry. The HIV RT enzyme is sufficient for reverse transcription, however, other viral proteins such as MA, CA, NC, IN and Vpr, and cellular proteins aid during the process by forming the reverse transcription complex (RTC) [122]. HIV is characterized by its extremely high mutation rate, which is due to several mechanisms. First, like other retroviruses, the HIV RT has no proofreading activity and spontaneously introduces mutational errors (nucleotide exchanges and indels) at a rate of about 3.0×10^{-5} substitutions per nucleotide per cell infection [123]. The mutational rate of HIV is further increased by cellular enzymes of the apolipoprotein B mRNA editing enzyme, catalytic polypeptide-like 3 (APOBEC3) family. APOBEC3 proteins from infected cells can be packaged into the virion and edit cytidine to uracil in the HIV DNA strand in newly infected cells. At the HIV RNA level, this results in G→A substitutions [124]. Although these processes lead to the accumulation of defective, replication-

incompetent genomes, they allow also the quick acquisition of antiretroviral drug resistance and immune escape mutations.

Viral and cellular proteins attached as RTC will stay in close proximity to the newly generated HIV DNA and will also serve as pre-integration complex (PIC) [125]. Once the PIC arrives at the nucleus after trafficking along the cellular cytoskeleton network, due to its size, it has to be actively transported across the nuclear membrane via nuclear pore complexes (NPC). This explains why also non-dividing cells with intact nuclear membranes can be infected efficiently [126].

During integration, the viral IN binds to the viral DNA and removes two nucleotides at the 3'-ends to create reactive hydroxyl groups. After attaching to the cellular DNA, the IN then uses these hydroxyl ends to join phosphates of the cellular DNA. This creates gaps in the cellular DNA at the joints, which are closed by the host cell's own repair machinery [127]. HIV integration is not a random process. It occurs more frequently in regions with high transcriptional activity because of the accessibility of the open chromatin for the PIC [127]. In addition, specific targeting of these active sites is regulated by the integrase itself and/or cellular host proteins that are part of the PIC [128].

HIV transcription is characterized by the interplay of viral and cellular factors that act as repressors or activators on the viral promoter, enhancer, and modulatory regions in the 5'-LTR [129]. During the early phase of transcription, only multiply spliced mRNAs (< 2kb) are transported into the cytoplasm, where they are translated into the regulatory proteins Tat and Rev and the accessory protein Nef. Tat re-enters the nucleus to enhance viral gene expression via several mechanisms [130]. Tat recruits chromatin modifying enzymes like histone acetyltransferases to the HIV promoter, which causes its release from former repression [131]. In addition, Tat acts by binding to the hairpin-like structure on the end of the newly generated HIV RNA called TAR. The complex then recruits cellular elongation factors allowing the phosphorylation of the RNA polymerase to enhance its processivity [130, 131]. Incompletely spliced and full-length unspliced HIV mRNAs are usually degraded in the nucleus and require Rev for their export into the cytoplasm. Rev binds to the RNA binding site for Rev on incompletely spliced or non-spliced HIV mRNAs and mediates their nuclear export via NPCs [132]. This allows translation of incompletely spliced mRNAs that encode for Vif, Vpr, Vpu and Env and unspliced mRNAs that encode for the Gag-Pol polyprotein. The full-length unspliced mRNA transcript also serves as the genome for new viral particles.

The late phase of the viral life cycle, which includes assembly of virus particle contents, budding from the host cell, and maturation of the particle, is mainly coordinated by the unprocessed poly-

protein Gag [133, 134]. This is achieved by different functional domains of the Gag protein: MA, CA, NC and p6. While the MA domain is responsible for the binding of the Gag protein to the plasma membrane and the concentration of Env proteins, NC binds the full-length HIV genome to include it in the virus particle. Gag-Gag interactions are mediated *via* the CA domain, thus, creating a lattice of radially oriented Gag proteins forming the immature virion [134]. Finally, virus particle release from the cell is mediated *via* the p6 domain that recruits cellular factors for the scission event [135].

The final step – transforming the immature virus particle into an infectious virus – involves the PR-dependent cleavage of the Gag and Gag-Pol poly-protein complexes during and right after the viral budding. This will create the single structural particles necessary to form capsid, matrix and nucleocapsid as well as the viral enzymes [136].

1.2.2.5 Stages of HIV infection

The clinical course of HIV infection can be described in three stages: acute/early phase, chronic phase, and finally the progression to AIDS (Figure 7). The acute/early phase only lasts a few weeks, while the asymptomatic chronic phase in HIV-infected individuals without treatment can last around 7 to 10 years. However, cases of rapid disease progression (3-5 years) or slow disease progression (10-20 years) have been reported [137]. AIDS is associated with the development of opportunistic infections due to the final break-down of the immune system leading to the death of HIV-infected individuals.

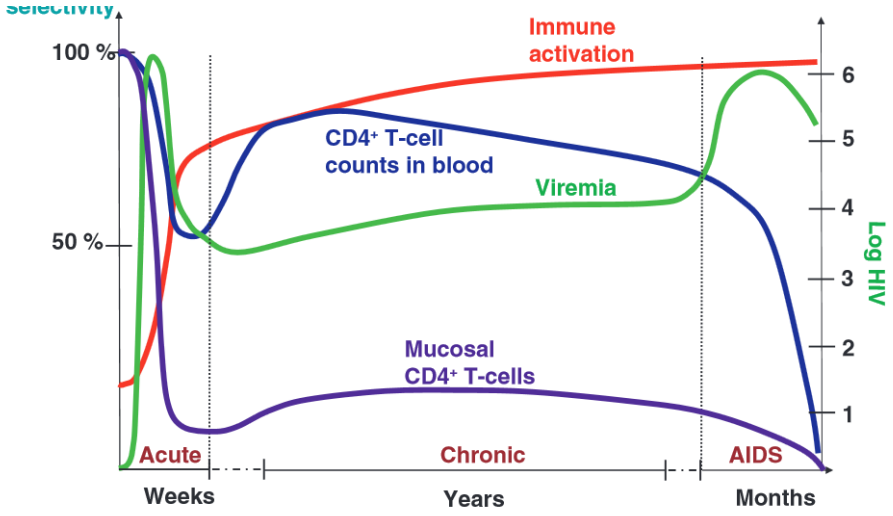

Figure 7 – **Stages of HIV infection**

HIV infection can be described in three clinical phases: Acute/early, chronic and AIDS. During the acute/early phase, HIV viremia peaks in the blood and a massive loss of $CD4^+$ T cells in the blood, but especially in the gut mucosa, can be observed. HIV viral load decreases to a viral set point that remains relatively stable during the chronic phase, which can last years. This is accompanied by a rise in general immune activation. $CD4^+$ T cells recover partially in the blood but decline slowly. In contrast, $CD4^+$ T cells do not recover in the mucosa and immune activation increases. Lastly, HIV-infected individuals progress to AIDS without treatment, which is characterized by the accelerated loss of $CD4^+$ T cells and increase in viremia. Figure adapted from [138] with authorization by the *Nature Publishing Group.*

1.2.2.5.1 Early phase

Cellular and humoral responses during this period and the establishment of the HIV reservoir are major determinants for disease progression. Most findings related to transmission events have been done in SIV-infected monkey models or *ex vivo* organ models because these processes are impossible to study in humans. The majority of people are infected with HIV during sexual contact with infected individuals and the virus is transmitted through the genital tract or rectal mucosa [139]. Other forms of transmission include sharing needles/syringes among people who inject drugs, mother-to-child transmission during pregnancy, labour and breastfeeding, and blood transfusion. Although the inoculum (semen, cervicovaginal secretion, blood) contains a mixture of genetically diverse HIV quasi-species, only a minority of viruses called transmitter/founder (T/F) viruses are able to establish an infection [140]. When compared to viruses isolated during chronic HIV infection, T/F viruses demonstrate a preferential CCR5 utilization, increased infectivity and replication capacity, type I IFN resistance and Env glycosylation [140]. Once the T/F passes the mucus layer and reaches the mucosal epithelium, it comes into contact with resident immune cells. Foci of infected $CD4^+$ T can be detected two to four days post infection in the female genital tract of SIV-infected monkeys [141]. Local inflammation induces recruitment of additional target cells to

the site of infection [142]. In addition, HIV binds to DCs and myeloid cells via interactions between HIV gp120 and C-type lectin receptors or sialylated gangliosides anchored in the viral membrane and the sialic acid binding immunoglobulin-like lectin-1 (Siglec-1/CD169) [143]. HIV is subsequently transported by infected $CD4^+$ T cells and APCs to the draining LNs, where the virus spreads to more $CD4^+$ T cells. During this so called “eclipse phase” that lasts around seven to 21 days, no viral RNA can be detected in the blood and the infected individuals experience no clinical symptoms [144].

From the mucosa-draining LNs, HIV disseminates throughout the body to secondary lymphoid organs such as spleen and especially the gut-associated lymphoid tissue (GALT). During this time, the plasma RNA level reaches a peak of several million copies per ml while the loss of $CD4^+$ T-cells in the blood and lymphoid tissues due to viral induced cell death or bystander effects is dramatic [145]. Important driver of the HIV progression is the general immune activation during early infection causing an enhanced, burst-like T cell turnover and subsequent cell death of most effector cells [146]. Although its cause is not completely understood, the systemic immune activation is thought to be induced *via* several mechanisms. HIV itself triggers an adaptive immune response as well as the release of proinflammatory cytokines from a variety of immune cells. Sustained immune activation is supported by the massive depletion of Th17 cells in the mucosal gut and the subsequent microbial translocation of commensal bacteria in the blood [147]. Clinically, HIV-infected individuals suffer from the acute HIV syndrome with unspecific flu-like manifestations.

The phase of acute/early HIV infection can be further subdivided into Fiebig stages (named after Dr. E. W. Fiebig) based on the detection of HIV using different clinical diagnostic assays (Figure 8).

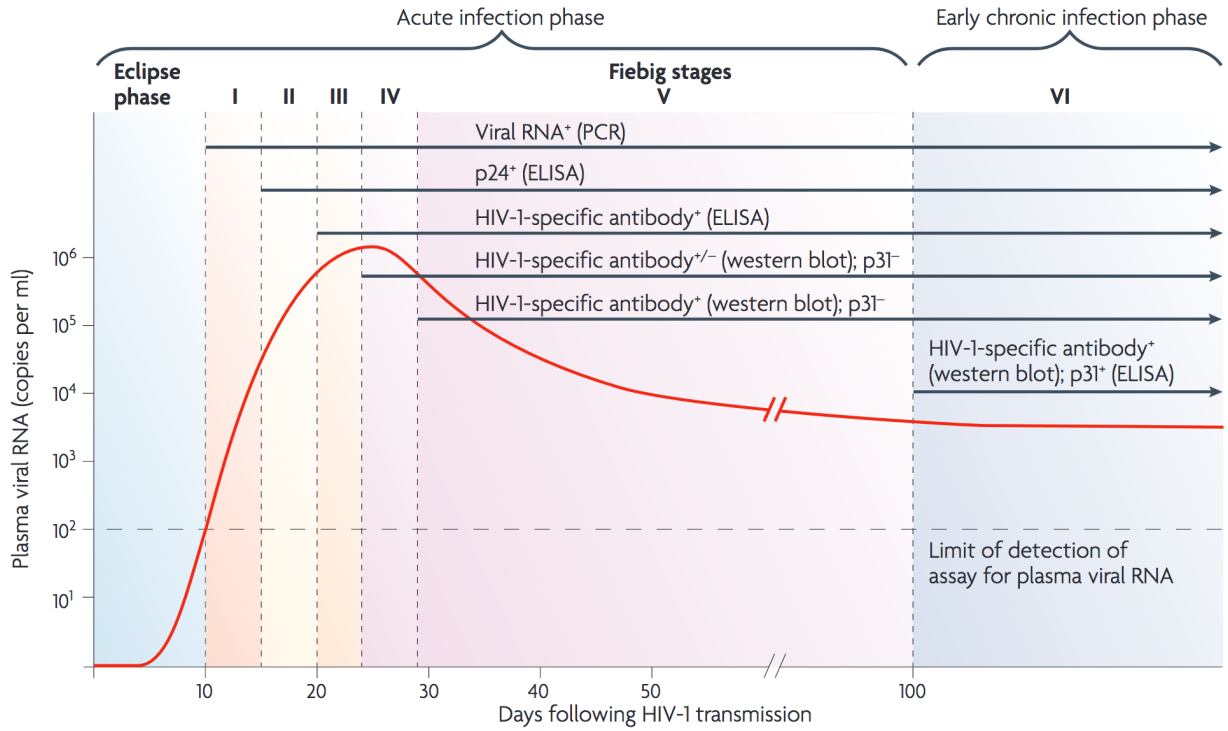

Figure 8 – **Subclassification of acute and early chronic HIV infection into Fiebig stages.**

HIV-infected individuals progress through different Fiebig stages during the early phase of the infection. Fiebig stages I to VI are based on the sequential gain in different clinical diagnostic tests able to detect HIV infection (PCR for viral RNA, ELISA for HIV p24 antigens, ELISA for HIV-specific antibodies, western blot for HIV-specific antibodies, ELISA for HIV p31 antigen). Fiebig stage VI corresponds to the early chronic phase of HIV infection and is also characterized by the establishment of a stable HIV plasma viremia (red line). Figure from [145] with permission from *Nature Springer.*

Even in the absence of antiretroviral therapy, the high plasma HIV RNA peak decreases to a constant steady-state level during the chronic phase of infection. This is accompanied by the partial recovery of the $CD4^+$ T cell count. Several studies demonstrated that the decline of plasma viremia and the magnitude of the viral set point is associated with HIV-specific T cell responses [148], which will be further discussed below.

1.2.2.5.2 Chronic phase

The chronic phase of HIV infection is characterized by a relatively stable HIV plasma viremia. However, the constantly high $CD4^+$ T cell turnover leads to the continuous decline of their regenerative potential. Although this phase is generally asymptomatic, the gradual loss of $CD4^+$ T cells results in the failure of the immune system and the progression to AIDS within seven to ten years after infection [138]. The steady depletion of $CD4^+$ T cells is mediated by several mechanisms. Productively infected $CD4^+$ T cells might either undergo apoptosis via a HIV PR-

dependent activation of caspase-3 [149], or might be killed by NK cells or HIV-specific $CD8^+$ T cells. However, cell death is not only restricted to HIV-infected cells. Accumulation of incomplete HIV reverse transcripts in non-permissive cells has been shown to induce cell death via caspase-1-dependent pyroptosis [150]. In addition, HIV proteins gp120, Tat, Vpr, Vpu and Nef are released into circulation and induce apoptosis in non-infected bystander cells through surface-receptor binding or intracellular mechanisms upon uptake [151]. $CD4^+$ T cell depletion is further caused by activation-induced cell death mediated by reactivation of other latent viral infections and microbial translocation from the gut [151].

1.2.2.5.3 AIDS

During the last stage of the infection, the regenerative capacity of the immune system is ultimately lost. The $CD4^+$ T cell count in the peripheral blood declines to a minimum level and the immune system is not able to control opportunistic infections. Clinically, an HIV-infected individual has AIDS when the $CD4^+$ T cell count is lower than 200 cells/µl or if AIDS-defining conditions occur. These conditions include for example candidiasis, cytomegalovirus retinitis, HIV-related encephalopathy, Kaposi's sarcoma, pneumocystis jiroveci pneumonia and cause the death of HIV-infected individuals [152].

1.2.2.6 Antiretroviral therapy (ART)

Only a few years after the identification of HIV as the cause of AIDS, a first antiretroviral drug, zidovudine, which inhibits the RT was correlated with decreased mortality and frequency of opportunistic infections in AIDS and therefore approved for the treatment of HIV in 1987 [153]. However, the beneficial effect of this monotherapy could not be maintained due to the development of resistant HIV strains [154]. This led to the introduction of a dual and later a triple drug combination from at least two different drug classes as gold standard for the antiretroviral treatment of HIV-infected individuals [155].

In 2019, about 65% of HIV-infected individuals worldwide have access to ART [114]. However, this varies largely depending on the region with the highest percentage in Western and central Europe and North America (79%) and the lowest in Middle East and North Africa (32%) [114]. ART suppresses viral replication to undetectable levels in the plasma (<20-50 copies of HIV RNA/ml) by current standard clinical assays within a few weeks after initiation and prevents the progression to AIDS. Thus, ART has transformed HIV infection from a deadly to a chronic disease.

Current ART regimens can be categorized according to their antiretroviral effect acting on different steps of the viral replication cycle and their mechanism: Nucleoside-analog reverse transcriptase

inhibitors (NRTIs), non-nucleoside reverse transcriptase inhibitors (NNRTIs), IN inhibitors, PR inhibitors (PIs), and entry inhibitors (Figure 9). The majority of triple-therapy combinations consist of two NRTIs with a NNRTI, PI or IN inhibitor.

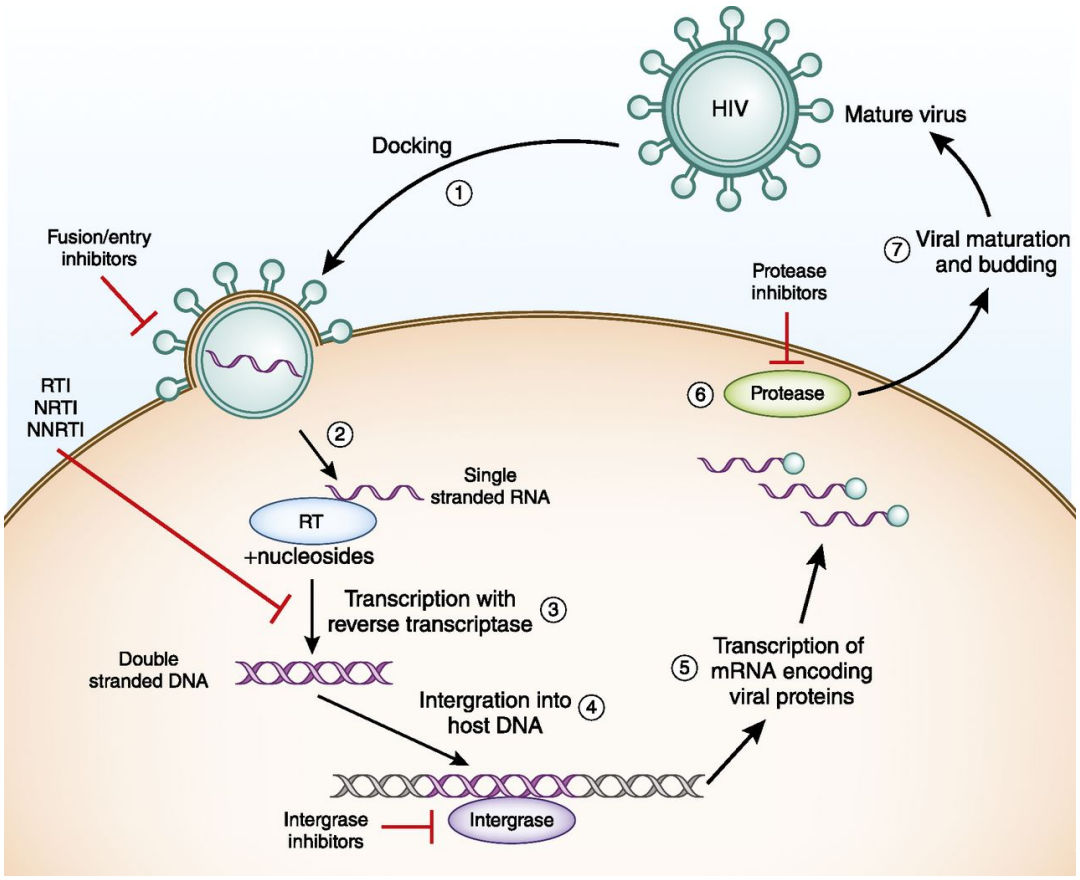

Figure 9 – **Classes of current ART regimens and mechanisms of action**

HIV replication can be inhibited at multiple steps by different classes of antiretrovirals (red lines). NNRTI: non-nucleoside reverse transcription inhibitor; NRTI: nucleoside reverse transcription inhibitor; RT: reverse transcription; RTI: reverse transcription inhibitor. Figure from [156] with authorization from the *American Society of Nephrology.*

NRTIs and NNRTIs are both inhibitors of the HIV RT and account together for almost half of all approved antiretroviral drugs. NRTIs are phosphorylated by intracellular phosphotransferases and compete with endogenous nucleoside triphosphates as analogs for their incorporation in the generated HIV DNA strand. However, due to the lack of a 3'-hydroxyl group or its replacement, they serve as chain terminators of DNA elongation [157]. NNRTIs on the other hand bind to the RT causing a conformational change in the enzyme thus reducing its catalytic activity [158].

HIV IN is involved in HIV DNA processing and strand transfer. The three currently FDA-approved PIs (Raltegravir, Elvitegravir, and Dolutegravir) only target the strand transfer capacity of the enzyme by removing the 3'-processed DNA from the active site.

PIs block the cleavage of the poly-protein complexes Gag and Pol and therefore the maturation of the generated virus particle [159].

Entry inhibitors inhibit the first step of the viral life cycle and currently include three FDA-approved drugs with distinct mechanisms. The fusion inhibitor Enfuvirtide binds to the gp41 protein at the surface of the virus particle and keeps the molecule in a pre-fusion conformation [158]. This prevents the structural changes necessary to bring virus and cell membrane into close proximity for viral entry. The CCR5 antagonist Maraviroc binds the HIV coreceptor and prevents its interaction with HIV gp120 [158]. CXCR4 antagonist were similarly developed but failed in clinical trials [159]. Finally, the post-attachment inhibitor Ibalizumab, a humanized monoclonal antibody, binds to CD4 and prevents the – for viral entry essential – conformational change in the CD4-gp120 complex [160]. This drug was only recently approved by the FDA in March 2018 and is currently in use for the treatment of HIV-infected individuals with multi-drug resistant infections [161].

Combining three ART regimens from different classes that target multiple steps of the viral life cycle has been proven to be very effective in preventing the emergence of drug-resistance mutations. However, in recent years a rise in the prevalence of HIV drug resistance in people reinitiating ART with previous ART exposure but also in treatment-naïve individuals has been observed [162]. In addition, even newer generation ART show some side effects and need to be taken daily. These findings highlight the need for the development of new antiretroviral drugs and/or alternative treatment strategies.

Although ART has dramatically improved the life expectancy of HIV-infected individuals, it does not represent a cure since it does not fully eradicate the virus. Lifelong treatment is necessary as ART cessation leads to the rebound of HIV viremia within a few weeks in most cases [163]. This is due to a very stable and long-lived pool of persistently infected $CD4^+$ T cells that form the HIV reservoir.

1.2.2.7 HIV reservoir

As discussed above, reverse transcribed HIV DNA integrates into the cellular genome, where it can be transcribed for the production of new viral particles. However, a small fraction of infected $CD4^+$ T cells harbors integrated replication-competent HIV DNA that remains transcriptionally silent. These latently infected cells cannot be detected by the immune system and survive for years. Lifelong ART is necessary, as treatment interruption would allow virus to rebound from this pool of reservoir cells and plasma viral load to return to pre-ART levels [163].

In the "Mississippi-baby" which was born to a HIV-positive mother, ART was introduced within 30 hours after birth. After stopping the treatment, the viral load stayed undetectable for 27 months in the plasma and then reoccurred accompanied by a drop of the $CD4^+$ T cell counts [164]. Studies by Whitney *et al.* revealed further that in SIV-infected rhesus monkeys the seeding of the viral reservoir occurred before viremia was detectable and that proviral DNA was already integrated in cells of the LNs and the gastrointestinal tract within three days after infection [165]. These findings strongly indicate the very early seeding of the viral reservoir after infection, mainly in sites with primary viral replication.

The majority of latently infected $CD4^+$ T cells during ART demonstrate a resting memory phenotype, in which viral transcription is limited by epigenetic gene silencing mechanisms such as histone deacetylation and methylation of the HIV promoter region, the restricted availability of cellular transcription factors important for viral reactivation and the presence of transcriptional repressors [166]. However, how this pool of resting HIV reservoir cells is generated is not fully understood. Resting $CD4^+$ T cells can be directly infected by HIV *in vitro* but the process is slow and likely does not represent the main mechanisms of infection. The infection of activated $CD4^+$ T cells that later reverts to a quiescent state is unlikely due to the cytopathic effect of active viral replication. Instead, the widely accepted model of reservoir establishment suggests the infection of a $CD4^+$ T cell during its transition from an activated to a resting state [166]. During this phase, cellular machineries necessary for reverse transcription, nuclear import, and integration are likely still efficient, while viral gene expression is limited [166]. Although this has model has been confirmed *in vitro*, experimental evidence *in vivo* is lacking.

At the cellular level, transitional memory (T_{TM}), T_{CM}, stem-cell memory (T_{SCM}), T_{EM} and even naïve $CD4^+$ T cells harbor integrated HIV DNA [167]. $CD4^+$ T cells obtained from the blood are the most studied HIV reservoir, yet these only account for around 2% of the total number of $CD4^+$ T cells in a human body [168]. Major anatomical sites of the reservoir include lymphoid organs (LNs, spleen, thymus, bone marrow) as well as the gut, but $CD4^+$ T cells with integrated HIV DNA have been

detected in ART-treated individuals throughout the entire body [169]. Lymphoid and gut tissues are major sites of viral replication during untreated infection, and GC Tfh cells as well as Th17 cells are highly permissive to HIV or SIV infection [170-173]. In addition, cytotoxic $CD8^+$ T cells are excluded from the GC [174]. It is therefore not surprising to find a high level of HIV DNA at these sites during ART [175].

HIV RNA and in some studies also HIV protein can be detected in GCs of LNs of long-term treated individuals [175-177]. This has been associated with a limited ART penetration [175], but the limited immune surveillance of GC by $CD8^+$ T cells could also play a role during ART. However, whether this reflects HIV transcription and translation of some viral proteins or full viral replication including the infection of new $CD4^+$ T cells remains controversial. Several studies were unable to find proof of genetic evolution of HIV during ART [178, 179], but these studies were mainly focused on the blood reservoir. A recent study using LN samples from ART-treated individuals demonstrated ongoing viral evolution in the tissue [180]. However, samples were taken after only six months of therapy, and the results might not reflect the situation in long-term treated individuals. Therefore, further studies using tissue samples are necessary to decipher whether there is ongoing viral replication in ART-treated individuals.

One widely accepted concept is that the viral reservoir is maintained through homeostatic proliferation of infected $CD4^+$ T cells during ART. This can be demonstrated by the very high frequency of clusters with identical, clonally expanded sequences within the pool of infected $CD4^+$ T cells [181]. This proliferation could be induced through antigenic T cell stimulation or TCR-independent mechanisms and keeps the HIV reservoir at highly stable levels during ART. Estimates assume that the HIV reservoir would only be eradicated after about 70 years of continuous ART without further intervention [182, 183].

Multiple techniques have been developed to quantify and characterize the HIV reservoir. Polymerase chain reaction (PCR)-based approaches represent simple and rapid methods to measure, for example, the total and integrated forms of HIV DNA [184-187], and have been widely used to study both circulating cellular populations and also disrupted tissue biopsies [188, 189]. However, although a substantial fraction of $CD4^+$ T cells of HIV-infected subjects on ART harbor integrated HIV DNA (~ 600 copies/million resting $CD4^+$ T cells [190]), the majority of integrated proviral sequences (~ 90–95%) are defective and not able to produce infectious viral particles (defined as replication-competent virus) [191, 192]. In contrast to measures of integrated DNA, inducible infectious virus was detected after reactivation from the T_{CM}, but rarely the T_{TM}, by the quantitative viral outgrowth assay (qVOA) [193]. While further studies are necessary, these

apparent discrepancies may be explained by the nature of the reservoir measured by these different techniques. Assays quantifying HIV DNA, such as PCR, cannot discriminate between intact or defective proviral sequences and, therefore, may vastly overestimate the size of the replication-competent reservoir in these populations [194]. At the other end of the scale, results obtained using qVOA represents a minimal estimate, as multiple rounds of stimulations might be needed for reactivation [8] and replication-competent viruses *in vivo* may not be able to spread *in vitro*. Our group recently developed an alternative flow cytometry-based approach measuring the frequency of $CD4^+$ T cells that are able to produce viral RNA and Gag protein and are therefore translation-competent [195, 196] (see also Chapter 9 – Appendices). Using this technique, we were able to narrow down estimates of the true size of the reservoir to around 4.7 cells/million $CD4^+$ T cells [195].

1.2.2.8 Innate immunity during HIV infection

Like other viruses, PAMPs in HIV products are sensed by multiple PRRs, including TLRs, RLRs and cytosolic DNA sensors triggering downstream intracellular signalling pathways (reviewed in [197]). This results in a variety of cell-intrinsic antiviral innate immune responses. The expression of intracellular HIV restriction factors such as SAMHD1, APOBECs or TRIM5α, BST-2/Tetherin and others inhibit different steps of the HIV replication cycle [197]. In addition, soluble factors such as type I and type III IFNs and other proinflammatory cytokines and chemokines are secreted. These increase the abundant of PRRs and amplifies their signaling actions. In addition, they mediate a danger signal to neighboring uninfected bystander cells, and induce the recruitment and activation of immune cells such as DCs, macrophages, NK cells [197]. Together, these mechanisms generate an antiviral state to limit HIV replication and spread of infection. HIV has adopted strategies to counteract this variety of antiviral immune mechanisms. For example, accessory HIV proteins inhibit the function of HIV restriction factors [198, 199], or induce the downregulation of surface receptors that limit the recognition and killing of infected cells by NK cells [200].

However, in addition to their beneficial role, a sustained proinflammatory response during chronic viremic HIV has detrimental effects on the innate and adaptive immune responses. This proinflammatory state is not only directly related to immune responses against HIV, but – as mentioned earlier – also caused by opportunistic infections and enhanced microbial translocation of gut bacteria into the circulation due to the depletion of $CD4^+$ T cells especially in the gut [201]. High levels of type I IFNs can impair the development of DCs, limit $CD4^+$ T cell proliferation and promote the apoptosis of non-infected $CD4^+$ T cells [202]. In addition, IFN and other

proinflammatory cytokines such as common γ-chain cytokines contribute to immune exhaustion of the T cell response by inducing the expression of IRs and their ligands [203-206]. Proinflammatory cytokines and chemokines do not only impact cells of the immune system but are also associated with the development of non-AIDS co-morbidities like neurological disorders, cardiovascular diseases or metabolic syndrome [207]. Importantly, ART does not lead to a normalization of the inflammatory state and its effects in all HIV-infected individuals [208]. Therefore, chronic immune activation is generally associated with a poor prognosis of HIV-infected individuals.

1.2.2.9 HIV-specific T cell immunity during HIV infection

A robust antiviral T cell response is mounted in nearly all HIV-infected individuals during the early phase of the infection. These responses become apparent in the blood at around the time of peak viremia [209]. However, T cell responses might be detectable in lymphoid tissues already at earlier time points [210]. Early HIV-specific $CD8^+$ T cell responses are directed against a low number of epitopes in the Env and Nef proteins of the T/F variant and contribute to the initial decline in HIV viremia [211]. At the same time, viral diversification and evolution at the targeted epitope sites following peak viremia indicates the immune pressure the CTL response applies to the virus [211]. In addition, the early HIV-specific $CD8^+$ and $CD4^+$ T cell response plays a major role for the outcome of HIV infection. Individuals, who later developed a low viral set point during the chronic phase of the infection showed high-avidity $CD8^+$ or potent cytolytic HIV-specific $CD4^+$ T cell responses during early HIV infection [212, 213], whereas progressive disease was associated with an exhaustion or dysfunction of the HIV-specific T cell immunity (Figure 10).

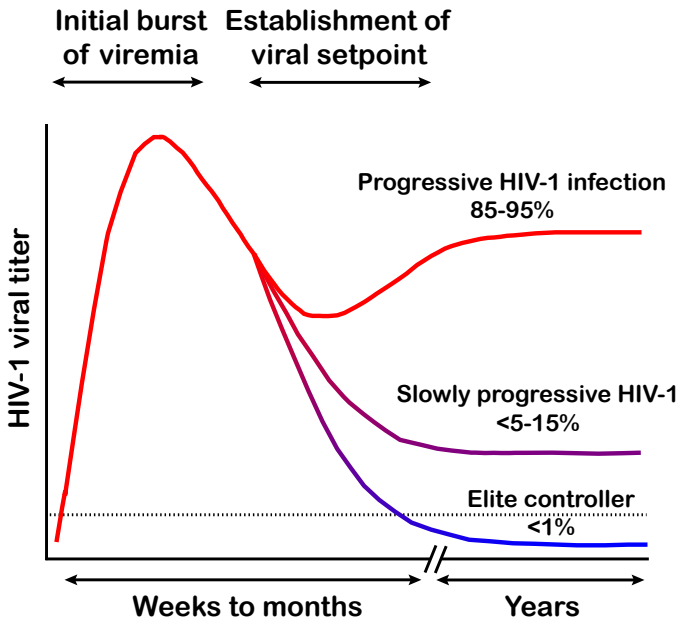

Figure 10 – **Schematic representation of outcomes of HIV infection**

After the initial burst of viremia in the weeks after HIV infection, the viral load decreases and a viral setpoint is established during chronic infection. The decrease of the viral load and the magnitude of the viral setpoint is associated with the HIV-specific T cell response. In the majority of individuals, the viral set point remains high in individuals with progressive disease as the T cell response is inefficient or exhausted. In a minority of individuals, very potent and broad HIV-specific T cell responses can partially or completely control the infection causing a state of slow HIV progression or elite control with low or undetectable viral load in the plasma respectively. Figure modified from [214] with authorization from *Elsevier.*

During the chronic phase of infection, HIV-specific T cell responses broaden and target additional HIV antigens. A minority of HIV-infected individuals (<1%) are able to suppress viremia in the blood to undetectable levels by clinical assays, preserve the plasma $CD4^+$ T cell count and do not progress to AIDS for sometimes decades without ART [214]. These so-called elite controllers (ECs) and other individuals with low viral set points during chronic infection more often express the human leukocyte antigen (HLA)-B57 or HLA-B27 allele [215, 216]. HLA-B57 or B27-restricted CTL responses target multiple conserved epitopes, especially in HIV Gag, to which escape mutations were associated with a cost in viral fitness [217, 218]. In addition, HIV-specific $CD8^+$ T cells with enhanced cytotoxicity, proliferative capacity, polyfunctionality and breadth have been correlated with slower disease progression (Figure 11) [219]. In addition to cytolytic functions, $CD8^+$ T cells from individuals with slow disease progression demonstrated a superior capacity to control HIV by nonlytic mechanisms that involved soluble molecules such as the chemokines RANTES and macrophage inflammatory protein (MIP)1-β and MIP1-α [220]. These chemokines can bind to their receptor CCR5, which either causes receptor downregulation from the surface or the binding blocks the interaction of HIV Env and CCR5, and therefore limits HIV infection [221].

ECs demonstrated a similar frequency of HIV specific $CD4^+$ T cell responses but functional differences when compared to viremic individuals with progressive disease (chronic progressors, CPs) [222]. HIV-specific $CD4^+$ T cell responses from ECs were enriched in Th1 and Th17 signatures at the transcriptional level that functionally correlated with elevated expression of granzymes, IFN-γ as well as IL-17 [222]. In addition, HIV-specific $CD4^+$ T cells from ECs demonstrated a higher proliferative capacity and expression of IL-2 (Figure 11) [223]. However, some of these findings might be rather a consequence than cause of viral control [223]. Not all ECs carry protective HLA alleles and other mechanisms such as potent innate immune cell responses might contribute to viral control in some individuals [219].

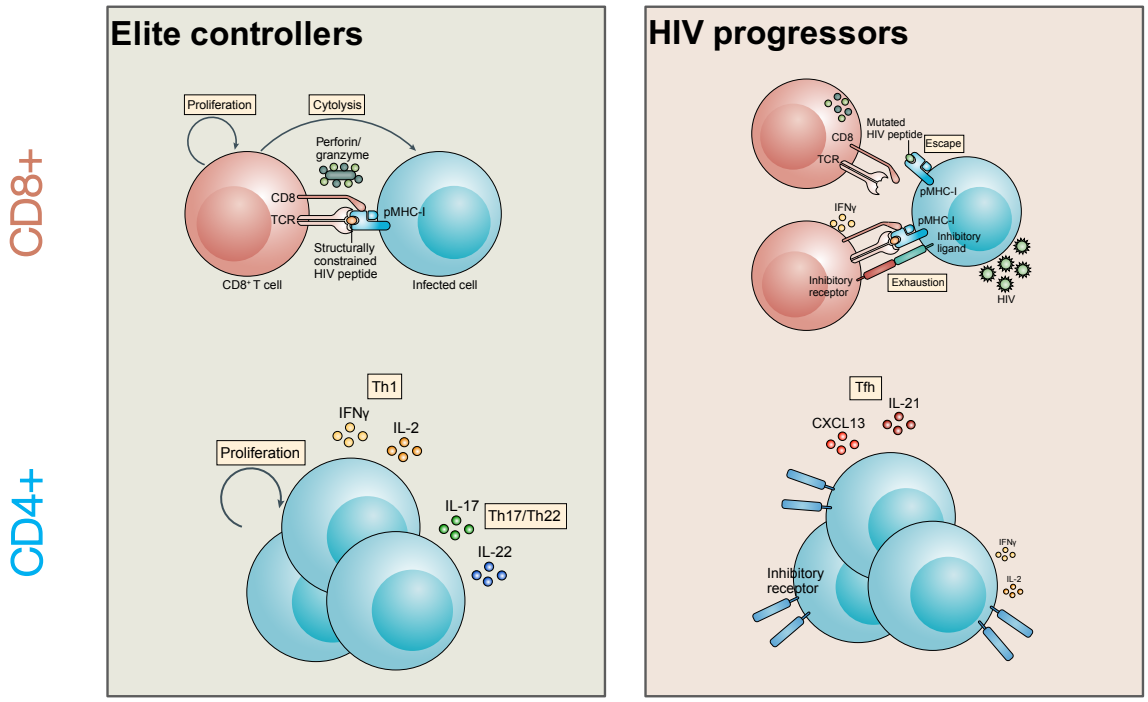

Figure 11 – **Differential HIV-specific $CD8^+$ and $CD4^+$ T cell responses in ECs and chronic HIV progressors**

HIV-specific $CD8^+$ T cell responses in ECs are characterized by the recognition of infected CD4+ T cells and a preserved proliferative capacity and cytotoxic functions. In contrast, immune escape and exhaustion are hallmarks of the HIV-specific CTL response in chronic progressors. Altered differentiation is central to differences in the HIV-specific $CD4^+$ T cell response with high levels of antiviral Th1- and mucosal Th17-related functions in ECs and a differentiation towards a Tfh profile in chronic progressors. Graphs related to HIV-specific $CD8^+$ responses from [224] with authorization from *Springer Nature.* Graphs related to HIV-specific $CD4^+$ responses were generated based on findings in [222].

Most studies, which investigated correlates of HIV control, analyzed peripheral blood because the access to tissue samples is limited in humans. However, recent analyses of lymphoid tissue samples from animal models of chronic Lymphocytic choriomeningitis virus (LCMV)-infection highlighted the importance of virus-specific $CD8^+$ T cells that express CXCR5 and are therefore

able to migrate into B cell follicles, in the viral control [225, 226]. These CXCR5$^+$ CD8$^+$ T cells demonstrated stem-like properties and elevated proliferation potential and longevity [227]. Increased proliferation and differentiation of this population after immune checkpoint blockade in chronically LCMV infected mice was associated with viral control [228]. Virus-specific CXCR5$^+$ CD8$^+$ T cells with some cytolytic functions could also be found in LNs of chronically HIV-infected subjects [174, 226, 229], and SIV-infected NHPs [230, 231]. They did not, however, colocalize with sites of viral replication but were rather attracted by the inflammatory environment and expression of the CXCR5-ligand CXCL13 [174]. Nevertheless, an inverse correlation between the frequency of CXCR5$^+$ CD8$^+$ T cells in the LN and blood viral load was observed, suggesting their contribution in the control of viral replication [229]. Current efforts therefore focus on the induction of HIV-specific CXCR5-expressing CD8$^+$ T cells and their migration into LN GCs to achieve HIV control in infected individuals.

Although these findings demonstrate that the host immune system is able to suppress HIV viremia, this only occurs in a minority of individuals [214]. In most cases, the HIV-specific immune response is not able to control the infection, the plasma viral load remains high, and the disease progresses to AIDS over the course of years. This is associated with the capacity of HIV to escape from the CTL response through mutations at its T cell epitopes. This becomes already evident during the early phases of infection but continuous even during the chronic phase [232]. In addition, a pronounced immune exhaustion or dysfunction of the HIV-specific T cell immunity can be observed in viremic individuals [233].

T cell exhaustion is mediated by the persistent exposure to high levels of antigen and inflammatory milieu, which is a hallmark of HIV infection. High level HIV replication at various sites throughout the body but especially in lymphoid organs and gut mucosa promote a massive cytokine release from innate and adaptive immune cells. The depletion of gut Th17 cells disrupts the gut barrier and leads to microbial translocation and systemic immune activation by microbial products. In addition, CD4$^+$ T cell depletion can lead to the unchecked reactivation of persistent viruses such as EBV or CMV that further contribute to immune activation (reviewed in [234]).

Similar to other models of chronic viral infections in animals and humans, and cancer [234], several studies demonstrated that HIV-specific CD8$^+$ T cells in individuals with progressive disease upregulate multiple IRs and lose their cytolytic and non-cytolytic functions, polyfunctionality and proliferative capacity, and show decreased survival [235]. These exhausted CD8$^+$ T cells persistently upregulate PD-1, T cell immunoglobulin- and mucin domain-containing molecule (Tim)-3, TIGIT and others that attenuate T cell functions [234]. Importantly, T cell

functions are highly restricted in HIV-specific $CD8^+$ T cell responses co-expressing multiple IRs [233, 234].

Similar to $CD8^+$ T cells, HIV-specific $CD4^+$ T cell responses show signs of exhaustion. PD-1 or CTLA-4 were upregulated on HIV-specific $CD4^+$ T cells from CPs, which limited their proliferation, but were absent or lowly expressed in ECs [236, 237]. Blockade of PD-1 or CTLA-4 interaction with their respective ligands led to enhanced proliferation and cytokine production [236, 237]. However, $CD4^+$ T cell dysfunction is more complex than a mere loss of function. HIV-specific $CD4^+$ T cells with a Tfh phenotype were expanded in lymphoid tissues of chronically HIV-infected individuals [238, 239]. This was driven by clonal expansion of chronically stimulated HIV-specific GC Tfh cells [239]. In addition, there seems to be a Tfh-favourable cytokine milieu, as a general increase in number and frequency of non-HIV-specific Tfh could be observed [170, 171, 238]. This observation is not limited to HIV; virus-specific Tfh expansion occurs in the context of other chronic viral infections such as HCV in humans or LCMV in mice [240, 241]. However, in LCMV infection, this Tfh skewing ultimately results in virus clearance [240], whereas it does not in HIV infection, perhaps due to the capacity of HIV to escape the autologous antibody response. Our group recently demonstrated that HIV-specific $CD4^+$ T cell responses in the blood of CPs also show a preferential differentiation towards a Tfh cell signature [222]. Although a substantial fraction of the HIV-specific $CD4^+$ T cell response demonstrated a Tfh-phenotype and expressed CXCR5, the cTfh frequency was comparable in progressors and ECs. Instead, $CXCR5^-$ non-cTfh cells from HIV-progressors exhibited a Tfh-like phenotype and function, characterized by CXCL13 and IL-21 production [222]. Indeed, a Tfh-like subset that does not express CXCR5 can be found in the LN of HIV-infected individuals [242]. These cells have a B cell helper capacity *in vitro,* express IL-21, are clonally related to $CXCR5^+$ Tfh cells and show an open chromatin state of the CXCR5 promoter, suggesting that these cells are functionally Tfh cells but have downregulated CXCR5 possibly due to chronic inflammation [242]. Aberrant expansion, function and or localization of HIV-specific Tfh responses could therefore contribute to the observed dysregulated B cell responses during chronic HIV infection [243].

As described above, ART has substantially increased the life expectancy of HIV-infected individuals by inhibiting viral replication to undetectable levels in the plasma and restoring the $CD4^+$ T cell count. ART initiation reduces the size of the total HIV-specific $CD8^+$ T cell response, but it remains detectable at stable frequencies even in long-term treated individuals [233]. Prolonged ART increases the cytokine expression and polyfunctionality of CTL responses [244], but this did not reach levels observed in ECs. Accordingly, the level of IR expression decreases

with ART but remains higher than what can be observed for ECs, despite undetectable viremia in the blood [233]. This could be related to the establishment of a stable epigenetic program after chronic antigen stimulation as has been seen for the PD-1 promoter in HIV-specific CTLs [245]. In addition, low level antigen stimulation in the tissue and residual immune activation in ART-treated individuals likely contribute to the persistent dysfunction of the immune response. Less is known about the stability of induced changes in the HIV-specific $CD4^+$ T cell response during ART. At the transcriptional level, certain functions were restored to levels seen in ECs, however, others remained dysregulated [222]. Although ART initiation leads to a dramatic improvement of the immune system against opportunistic infections and some changes in the HIV-specific T cell response, it does not restore an effective HIV-specific T cell response capable of suppressing virus. Consequently, ART interruption generally leads to a rapid viral rebound from a reservoir of latently infected cells [163]. Understanding the persistent dysregulation of HIV-specific T cell responses during ART will be important for the development of therapeutic interventions that involve boosting antiviral immunity.

1.2.2.10 Humoral response and broadly neutralizing antibodies

HIV-specific antibodies become first detectable in the plasma during the first two to three weeks after HIV infection (early acute phase). The initial responses are immunoglobulin (Ig)M antibodies directed against the envelope protein gp41 of the transmitted variant and likely arise from short-lived plasmablasts that developed outside of the GC and independent of Tfh help [246]. During the weeks after, class-switched IgA and IgG responses can be detected, which are also directed against additional HIV proteins such as Gag or gp120 [246]. However, these antibodies neither neutralize the virus nor bind to NK cells to induce ADCC and do not impact the HIV plasma viral load [246]. Neutralizing antibody responses with low potency against the autologous virus can be first detected after two to three months post-infection [247]. These are directed against variable regions of the HIV Env protein, which leads to the selection of viral variants with antibody-escape mutations [248, 249]. In chronically infected individuals, elevated numbers of GC B cells and plasma cells, accompanied by hypergammaglobulinemia can be observed, which correlate with GC Tfh expansion [238]. In contrast, memory B cells are decreased. These abnormalities are not restricted to HIV-specific responses but affect the general humoral immune response and are due to the systemic immune activation, dysfunction in Tfh response and enhanced exposure to non-HIV antigens [250].

However, in a subset of HIV-infected individuals, antibodies are developed that target Env epitopes that are conserved between multiple HIV variants, called broadly neutralizing antibodies

(bNAbs). BNAbs against HIV target relatively conserved epitopes on the glycosylated HIV Env trimer, the only target on the virus surface, and are able to neutralize multiple HIV strains and therefore prevent viral entry into HIV target cells [251, 252]. Although the HIV Env trimer represents a difficult protein to target due to its dynamic conformation, extreme sequence variability and glycan shield covering the protein surface [253], different bNAbs targeting multiple epitopes have so far been isolated from HIV-infected humans, demonstrating that these can be generated naturally. Although about 10-50% of individuals are able to generate broad HIV-neutralizing antibody responses [254], bNAbs with very high breadth and potency can only be found in about 1-2% of the HIV-infected population, also called elite neutralizers [255]. Longitudinal plasma sampling early after and throughout HIV infection revealed that these bNAbs develop gradually over a time course of two to four years in untreated individuals [256, 257]. Initially, unmutated naïve B cells recognize epitopes of the T/F or early autologous viral strains to induce an antibody response (Figure 12). Subsequent viral diversification related to the selection of antibody-escape mutations forces the humoral response to adapt to these newly emerged diverse strains. Over time, this repeated evolution and co-evolution process of virus and B cells leads to the development an increased breadth: high level of antigen exposure leads to repeated B cell editing in the GC with an accumulation of unusually high levels of SHM, insertions and deletions, common features of multiple bNAb lineages [251].

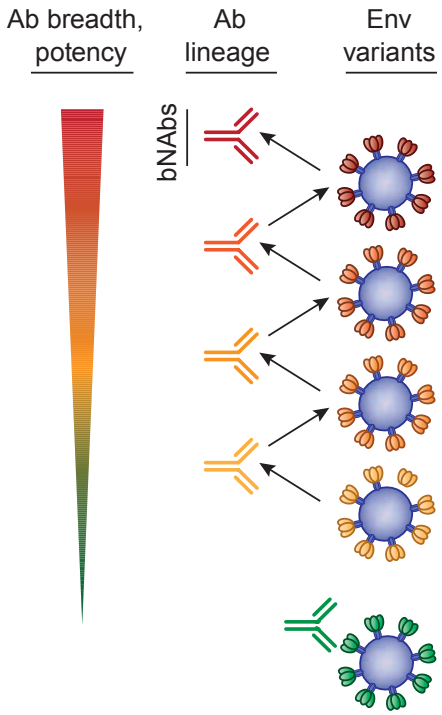

Figure 12 – **Development of bNAbs in HIV-infected individuals**

Through antibody cloning, next-generation sequencing and computational analysis of longitudinal samples from individuals, development of bNAbs and co-evolution of HIV Env can be reconstructed. Figure adapted from [258] with permission from *Springer Nature*.

The first monoclonal HIV-neutralizing antibodies were isolated in 1993 and 1994 and demonstrated some breadth but limited potency [259, 260]. Technical advances including large scale screening neutralization assays, which allowed the testing of sera from large cohorts of HIV-infected individuals, and the *in vitro* isolation and cloning of monoclonal antibodies in the following years, resulted in the discovery of a new generation of bNAbs with higher potency and breadth [261]. As of 2019, around 40 different bNAbs have been identified that can be classified based on the six distinct epitopes targeted on the Env trimer: The glycan-dependent second variable loop (V2) apex, CD4 binding site (CD4bs), V3-glycan region, interface/fusion peptide (FP), silent face, and the gp41 membrane-proximal external region (MPER) [251] (Figure 13). Depending on the site targeted, bNAbs show distinct mechanisms of neutralization. CD4bs-bNAbs and V3-glycan region-binding bNAbs hinder the interaction between the HIV Env trimer and cell surface CD4 or CCR5 molecule, respectively [262, 263]. BnAbs against the V2 apex, interface/FP region, the silent face or MPER bind the trimer in different states and prevent conformational changes, which are important for the viral entry process [264-267]. It is likely that in the next years additional bNAbs and epitopes will be identified.

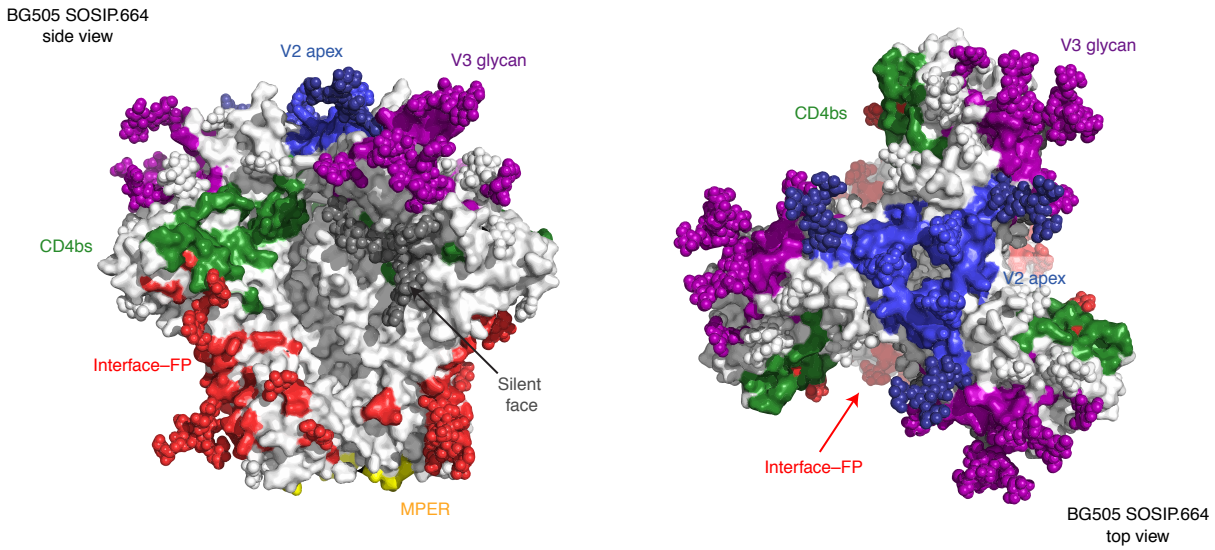

Figure 13 – **The bNAb epitopes on the Env trimer**

Electron microscope reconstruction and model of the HIV Env trimer shown as side view (left) and top view (right). Model shows amino acid residues and glycans of the stabilized SOSIP.664 gp140 trimer of the HIV isolate BG505. Distinct epitopes targeted by currently identified bNAbs are highlighted in color: V2 apex (blue), V3 glycan (purple), CD4bs (green), silent face (dark gray), interface/FP (red), MPER (yellow).V: variable loop, bs: binding site, FP: fusion peptide, MPER: membrane-proximal external region. Figure adapted from [251] with authorization from *Nature Springer.*

Despite the generation of bNAbs in elite neutralizers, these individuals usually do not benefit from the very potent antibody responses. Continuous evolution of viral sequences leads to a persistent adaption of the antibody response and the bNAb loses its breadth and increases the specificity against the autologous strain [268]. Instead, bNAbs have shown potential as strategies to prevent or treat HIV infection.

1.2.2.11 Strategies for HIV prevention

Most successful vaccines (e.g., against hepatitis B, yellow fever, and smallpox) work by inducing long-lasting neutralizing antibody responses that prevent infection of target cells [72]. Current HIV prevention strategies, including public awareness campaigns, condom use, and post-exposure prophylaxis, led to a decline of the annual number of new HIV infections to 1.8 million worldwide. In addition, full suppression of viral replication by ART in HIV-infected individuals strongly reduces transmission rates. However, ending the pandemic without an effective vaccine seems unlikely [269].

Studies using NHP and humanized mouse models demonstrated that passive administration of very potent bNAbs can protect from high-dose or repeated simian-human immunodeficiency virus (SHIV) or HIV challenges [270]. Ongoing placebo-controlled clinical trials will test the impact of

bNAb treatment on protection from HIV acquisition in high risk populations: VRC01, a CD4bs-specific bNAb, is given to women in Sub-Saharan Africa (ClinicalTrials.gov identifier: NCT02568215), or to men or transgender who have sex with men in North America, South America, and Switzerland (ClinicalTrials.gov identifier: NCT02716675). These studies will decipher whether and at what concentrations bNAbs can also protect from a wide range of HIV strains that circulate in the human population in contrast to the limited number of viral strains selected for the challenges in the animal models. As bNAbs have to be present at high concentrations to elicit protection [271], the study participants receive 10 or 30 mg/kg every 8 weeks. Modifications of the Fc domain of antibodies to extend their half-life [272], or the delivery of bNAbs via adeno-associated virus vectors [273], are currently tested possibilities to limit the number of administrations and antibody production costs.

Studies using passive administration of bNAbs suggest that vaccine-induced protective antibody responses could also serve as a strategy for an HIV vaccine. However, the induction of long-lasting bNAb responses remains a major challenge and has been unsuccessful in human HIV vaccine trials [274]. As mentioned above, bNAbs are characterised by high levels of SHM of up to 25% [251]. In addition, several bNAbs have relatively long heavy chain complementarity determining region 3 (HCDR3), which can only be found in at a very low frequency in the naïve B cell repertoire (~0.4%) [251]. CD4bs-, V3-glycan and especially MPER-specific bNabs show some degree of autoreactivity [275]. In addition, the unusual high rate of SHM shows that HIV-bNAbs must have undergone multiple rounds of affinity maturation in the GC [276]. Together, these uncommon characteristics likely explain why potent bNAbs only develop in a minority of HIV-infected individuals and why they may be difficult to elicit via vaccination. Indeed, administration of designed Env trimer immunogens that express bNAb epitopes and hide non-neutralizing epitopes, only generated autologous antibody responses or responses with limited breadth in NHP vaccine studies [277, 278]. This was likely due to the lacking exposure of the immune system to different HIV variants over time as can be seen for the development of bNAbs during natural infection. Therefore, new vaccine strategies include the repeated immunization with a cocktail of diverse Env trimer immunogens. Alternatively, sequential immunization strategies with multiple designed immunogens aim to guide the B cell response towards the development of bNAbs by mimicking the natural exposure to different HIV Env variants over time necessary for bNAb induction during the infection [251].

In addition to efforts to improve the design and administration of HIV immunogens, vaccine strategies aim to recreate immunological parameters that have been associated with bNAb

development in HIV-infected individuals, including the stimulation of Tfh cells. As mentioned above, in untreated HIV infection, bNAbs typically develop after a few years of chronic antigen exposure. Because of immune escape of the autologous strain, these humoral responses are not associated with viral control [279]. These findings show that in a subset of HIV^+ individuals, the immunological environment allows acquisition of the extensive hypermutations necessary for bNAb generation. Several groups subsequently investigated Tfh responses in subjects with good versus poor neutralization to find correlates of efficient help. Studies in SHIV-infected rhesus macaques demonstrated a positive correlation between $IL\text{-}4^+$ Env-specific LN Tfh and the frequency of Env-specific IgG^+ GC B cells as well as neutralization breadth [280]. Further transcriptional analysis of these Env-specific Tfh cells revealed that animals with greater neutralization activity showed a higher expression of Tfh-related (Bcl6, MAF, CXCL13, and IL-21) and Th2-related genes (GATA3), whereas Th1- and Treg-related signatures (TBX21, IFNγ, or FoxP3) were reduced [280].

Correlates between Tfh responses and development of bNAbs in humans have been largely restricted to the analysis of blood as access to lymphoid tissue is limited. Differences in the cTfh response between HIV^+ subjects with high or low levels of neutralizing antibody activity were detected with a high frequency of $CXCR3^-PD\text{-}1^+$ cTfh being associated with the development of bNAbs [49, 281]. Individuals who later developed broad neutralization already showed superior Tfh and B cell responses during the early phase of infection when compared to study participants who remained low neutralizers [282-284]. They demonstrated an enhanced ability of cTfh cells to induce antibody class-switching *in vitro*, a preserved B cell activation profile comparable to uninfected controls, and elevated levels of plasma CXCL13, which is a marker of GC activity. Furthermore, HIV-infected donors with bNAbs showed a higher level of plasma autoantibodies and less functional regulatory $CD4^+$ T cells with elevated PD-1 expression, which limited their suppressive capacity [281]. Together, these results demonstrated that a high GC activity and Tfh quality seems to be important for the development of high-affinity antibody responses. Therefore, further studies on how to induce efficient Tfh responses are necessary for HIV vaccine strategies.

1.2.2.12 Alternative HIV treatment or cure strategies

Despite the tremendous success of ART, HIV persists in infected subjects predominantly in rare latently infected $CD4^+$ T cells [285-287]. Therefore, life-long therapy is needed to avoid the rebound of the virus from its reservoir but is associated with the necessity for strict adherence, side-effects of the drugs, and a high economic burden.

Broadly, a cure may be achieved by either complete eradication of the HIV reservoir from the body (known as a sterilizing cure) or a long-term control of HIV replication without ART (functional cure) [288]. To date only two individuals have been cured from HIV, the so-called “Berlin patient” and “London patient” [289, 290]. Both individuals were HIV^+, developed acute myeloid leukaemia and were treated with allogeneic haematopoietic stem-cell transplantation using donors with a homozygous mutation in the HIV coreceptor CCR5 (CCR5Δ32/Δ32). ART was interrupted months after the transplantation and both individuals have since been in HIV remission with undetectable plasma viral load and undetectable reservoir in blood $CD4^+$ T cells [289, 290]. This treatment, however, will not be suitable for HIV-infected individuals without leukemia given the high risk of fatal complications.

Recent cure strategies have mainly focused on the “shock/kick and kill” strategy whereby HIV is reactivated from its latent state using latency-reversing agents (LRAs). This is followed by the death of the infected cell, due to the cytopathic effects of HIV itself or killing by the host’s own immune system. However, despite initial promise, LRA-based strategies have shown limited success in clinical trials to reactivate the virus and reduce the viral reservoir [291], suggesting that additional information regarding the HIV reservoir and alternative approaches are required to help rationally design effective cure strategies. In the context of a functional cure, in addition to the reduction of the reservoir, an effective HIV-specific T cell response might be needed to ensure a durable control of the virus. However, ART alone is not sufficient to restore the antiviral T cell immunity. Instead, current efforts pursue the idea to either boost the existing T cell response or generate *de novo* responses, so that the host’s immune system can control the viral infection once ART is stopped (Figure 14). Several studies demonstrated that although the HIV-specific T cell response increases after ART interruption due to the release of viral antigens and particles [292, 293], it is not able to control the infection in most individuals. Instead, it might be necessary to generate an effective antiviral response in a setting without detectable viremia and reduced inflammation (with or without reducing the HIV reservoir).

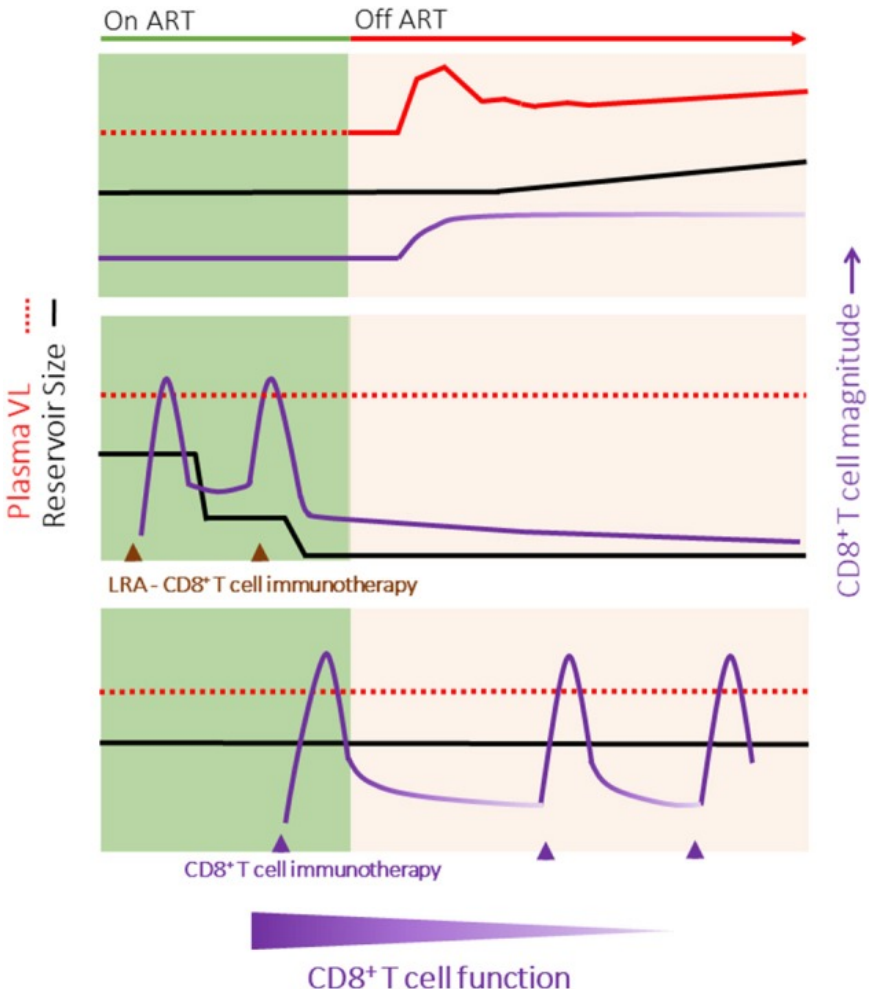

Figure 14 – **Strategies to improve the HIV-specific T cell response to achieve a functional cure**

Top: Typical rebound of HIV once ART is interrupted. Although the increased release of antigen primes HIV-specific T cell responses, these are not able to control the virus. **Middle:** Combination of LRA and immunotherapy treatment to reduce the size of the HIV reservoir and increase the virus-specific immunity. The generated T cell response is then able to suppress viremia after ART is stopped. **Bottom:** Repeated boosting of the HIV-specific T cell immunity (e.g. via immunization strategies) to ensure a persistently high immune response capable to control the virus. Dotted line indicates undetectable plasma viremia. This figure is licensed under a Creative Commons Attribution License and was obtained from [294].

1.2.2.12.1 Therapeutic approaches to directly improve T cell immunity

Several different strategies are currently being developed to boost the HIV-specific T cell response in HIV-infected individuals on ART to achieve a functional cure, but none have demonstrated a major impact on the rebound of viremia after ART interruption.

Randomized controlled clinical trials immunized HIV-infected ART-treated study participants with various vaccine vectors encoding for HIV Gag that led to a minor increase in Gag-specific T cell responses [295, 296]. ART interruption was either not attempted [295], or did not show a delay in

viral rebound in the vaccine group when compared to the placebo-control group [296]. In contrast, administration of DCs pulsed with multiple HIV antigens induced HIV-specific T cell responses against Gag, Nef and Env, which correlated with a lower viral load after ART interruption [297]. This suggests that, similar to what can be found in ECs with natural HIV control, the induction of broad and potent HIV-specific T cell responses might be important to achieve HIV control through vaccination.

There are several potential caveats with vaccine strategies that use full length HIV proteins for immunization. For example, these immunogens might drive immunodominant responses directed against non-protective or escaped epitopes or might favor the expansion of pre-existing HIV-specific responses that may be dysfunctional or exhausted rather than induce new functional responses. In addition, designed HIV immunogens might induce responses that are not able to target the HIV-infected individual's own virus due to the high sequence variability. Instead, individualized vaccines might be necessary to induce responses against the autologous virus.

Some recent vaccine studies tried to overcome these limitations, for example by aiming to refocus T cell responses towards epitopes associated with protection or to restore pre-existing dysfunctional HIV-specific T cell responses.

During a recent clinical study by Mothe *et al*., ART-treated HIV-infected individuals were immunized with a HIV protein immunogen variant that only included regions that are highly conserved across different HIV clades [298]. This vaccination strategy was able to shift the HIV-specific T cell response towards conserved epitopes that were previously associated with protection, but failed to improve the *in vitro* HIV-suppressive capacity of $CD8^+$ T cells [298]. However, in this study it could not be deciphered whether the vaccine induced *de novo* responses against the conserved epitopes or whether it merely propagated the expansion of low-level immunogen-specific responses that existed prior to vaccination [298]. Nevertheless, it demonstrated the plasticity of epitopes targeted by the HIV-specific T cell response.

Instead of inducing new responses, other strategies aim to restore the dysfunctional HIV-specific T cell response that is boosted via vaccination by combining it with cytokine treatment or immune checkpoint blockade (ICB).

IL-15 administration alone improved NK cell proliferation and enhanced virus-specific $CD8^+$ T cell functions in blood and LNs in NHPs [299]. Similarly, treatment with N-803, a IL-15 superagonist, induced SIV-specific $CD8^+$ T cell recruitment in the B cell follicles, which was associated with lower

SIV-RNA and SIV-DNA levels [300]. IL-15 is currently investigated in a clinical trial in combination with a HIV vaccine vector (ClinicalTrials.gov identifier: NCT00775424).

Given the high expression of IRs on HIV-specific T cell responses and based on the success in the cancer field, ICB is currently being investigated as an HIV treatment option. As IRs are also important mediators of HIV persistence, ICB acts in addition as an LRA to possibly reduce the HIV reservoir in treated individuals [301]. ICB treatment of cancer patients that were also HIV^+ was associated with a decrease in the HIV reservoir, reduction of T cells with an exhausted phenotype, and an increase in HIV-specific $CD8^+$ T cell functions [302, 303]. As PD-1 blockade in combination with therapeutic vaccination enhanced the antiviral $CD8^+$ T cell response against LCMV in mice [304], ICB is also discussed for the use of enhancing anti-HIV vaccine responses [305].

As can be seen by the examples mentioned above, no single vaccine strategy was yet able to induce potent HIV-specific T cell responses able to control the infection without the need for ART. However, this field remains a highly researched topic with the goal to better understand the effect of different vaccines on the *de novo* generation or expansion of pre-existing responses and how these can be improved to generate an immune system able to control HIV.

1.2.2.12.2 Therapeutic bNAb therapy

In addition to HIV prevention, bNAbs have been used in animal models and clinical trials as therapeutic HIV treatment during chronic untreated infection or after ART interruption.

First studies using neutralizing antibodies for HIV-treatment in clinical trials showed no significant effect on viral suppression [306, 307]. However, antibody-monotherapy in mice and NHPs using new generation bNAbs with higher breadth and potency resulted in a transient reduction of the plasma viral load for about two weeks before the viremia returned to initial levels due to viral escape [308-310]. After initial safety and pharmacokinetics studies in HIV-uninfected individuals, clinical trials evaluated the antiviral functions of 3BNC117, VRC01 and 10-1074 bNAb-monotherapy in viremic individuals. Infusion of these bNAbs to the study participants led to a rapid decrease of the plasma viral load in people infected with bNAb-sensitive viruses [311-313]. However, full viral suppression was only observed in a minority of study participants, and the plasma viral load rebounded after a few weeks, mainly due to the development of escape mutations as was seen for humanized mice and NHPs [311-313].

Similar to the concept that escape can be avoided by combining multiple ART regimens targeting different steps of the viral replication cycle, a combination of multiple bNAbs targeting non-overlapping epitopes on the Env trimer, was associated with prolonged viral suppression in animal

models when compared to monotherapy [308]. This finding could be translated into a phase Ib clinical trial (ClinicalTrials.gov identifier: NCT02825797): The administration of 3BNC117 and 10-1074 to viremic individuals infected with viruses sensitive to both bNAbs resulted in a reduction of viral load that was longer when compared to single bNAb-treatment [314]. However, despite the decrease, viral load remained detectable in some individuals.

Instead treating viremic HIV-infected animals, some animals that first received ART to decrease the HIV viral load and were then treated with single bNAbs, were able to control viremia after ART interruption at undetectable levels until antibody levels decreased [315]. This suggests that a combination of ART and bNAb therapy might be more effective for viral control than bNAb administration alone.

Based on these results, during a phase Ib clinical study, a combination of bNAbs (3BNC117+10-1074) was used to treat HIV-infected individuals who were already successfully treated with ART [316]. The study participants received three bNAb-infusions and stopped ART after the first treatment. All nine individuals with sensitive virus to both bNAbs kept the HIV viral load at undetectable levels in the blood for at least 15 weeks before HIV rebound [316]. Of note, two individuals did not rebound until the end of the observation period of 30 weeks [316]. Due to the shorter half-live of 3BNC117, the study participants were only exposed to 10-1074 during the later phase of the studies. Escape mutations to the 10-1074 binding site could therefore be found in rebound viruses of some of the study participants [316]. This treatment strategy of bNAb infusion and ART interruption could also affect the size of the HIV reservoir as bNAbs do not inhibit viral reactivation. A decreased replication-competent reservoir was detected in some individuals after combination bNAb treatment, but the difference was minor [316]. More infusions and a longer period off ART might be necessary to allow more latently infected cells to become reactivated and die.

In several studies and in both contexts, animal models and human trials, it was demonstrated that bNAbs in addition to their neutralizing capacity, interact with the immune system. In viremic humanized mice that were treated with 10-1074, 3BNC117 or PG16, the suppression of viremia was not only dependent on the neutralizing capacity of the bNAbs but also on their ability to interact with immune cell receptors that bind the antibody Fc region [317, 318]. Mice that received bNAbs unable to bind the FcR demonstrated a shorter time of viral suppression compared to wildtype bNAbs [319]. Conversely, bNAbs with a modified FcR domain corresponding to a higher affinity for activating FcRs suppressed viral load faster and more prolonged [317]. However, in NHP studies using the PGT121 antibody, the Fc-dependent function was redundant [320], suggesting

that the mechanism of protection might differ between certain bNAbs. A contribution of these additional functions was indirectly shown in human trials, when mathematic modelling suggested that the 3BNC117-mediated decrease of the viral load in treated study participants can not only be explained by viral neutralization and inhibition of new infection. Enhanced clearance of infected cells, possibly via FcR-dependent mechanisms such as ADCC, as seen in the animal models, likely played a role as well [318]. Another known Fc-dependent effect of antibodies is the binding to FcRs expressed on APCs. In the context of cancer antigen-specific antibodies or antibodies against influenza, APCs internalized the antigen-antibody complexes for processing and (cross-) presentation to generate antigen-specific T cell responses in mouse models [321, 322]. An interaction between antibody treatment and the adaptive immune system could also be observed in the context of bNAb treatment. A subset of NHPs that were treated with 10-1074 and 3BNC117 shortly after SHIV-infection were able to control the infection even after clearance of the antibodies, which was dependent on $CD8^+$ T cell responses [323]. In addition, 3BNC117-treated study participants developed an improved humoral immunity against HIV [324].

These studies demonstrated that combination bNAb-therapy can act as an alternative to ART and suppress HIV viremia as long as both bNAbs are present at sufficiently high concentrations. In addition, bNAbs might act on the adaptive immune system. However, whether bNAb treatment and ART interruption in humans increases HIV-specific T cell immunity remained unknown.

Chapter 2 Hypotheses and objectives

The HIV-specific T cell response is characterized by an exhaustion or dysfunction in HIV-infected individuals with progressive disease that shows similarities with other settings of chronic viral antigen exposure such as other chronic viral infections or cancer. $CD8^+$ T cells and $CD4^+$ T cells persistently upregulate inhibitory receptors. While the $CD8^+$ T cell response and its exhaustion and loss of functional capacity during progressive disease has been well studied, less was known about HIV-specific $CD4^+$ T cell responses, especially Tfh cells. This analysis was hampered by the lack of assays to study the antigen-specificity of this T cell subset. Most assays are dependent on functional analyses, but Tfh cells do produce very little amounts of the classical Th1-cytokines, which are the readout for most assays. With the development of recent cytokine-independent activation-induced marker (AIM) assays [21-23], we and others were able to close this gap. Our group recently demonstrated that in contrast to $CD8^+$ T cells, HIV-specific $CD4^+$ T cell responses show no loss but an alteration of function characterized by the increase in the Tfh signature during progressive disease [222]. Matched samples obtained from HIV-infected individuals before and after ART initiation demonstrated that some transcriptional features returned to levels seen in EC, while others did not change with the initiation of therapy [222].
Similar to ART, bNAbs suppress HIV viremia and preserve the $CD4^+$ T cell count. However, in contrast to ART, they do not inhibit the production of viral particles and can engage the immune system through the Fc portion. Previous studies demonstrated that antibodies can bind to FcR-expressing APCs to generate antigen-specific T cell responses, e.g. in animal models of cancer or influenza [321, 322]. Also, bNAb-treatment of NPHs early after SHIV infection induced a control of the infection in a subset of the animals that was $CD8^+$ T cell-dependent [323], but this has not been established in humans.

Based on these previous results, **we hypothesized** that i) irrespective of ART, HIV-specific $CD4^+$ T cells differ phenotypically and functionally from those targeting other viruses; and ii) while ART alone does not enhance HIV-specific T cell responses, immunotherapy with bNAb combined with ART interruption is associated with enhanced virus-specific immunity.

For the first project, our objective was therefore to define characteristics of the HIV-specific $CD4^+$ T, and especially cTfh, response in a large cohort of ART-treated individuals in comparison to responses elicited against HBV or CMV within the same individual. We studied; i) the frequency of cells with a cTfh phenotype within antigen-specific $CD4^+$ T cell responses, ii) the phenotype and function of antigen-specific cTfh and non-cTfh responses; and iii) the association between HIV-specific cTfh and non-cTfh responses, antibody responses, and the magnitude of the persistent HIV reservoir in ART-treated individuals.

For the second project included in this work, we collaborated with Dr. Michel C. Nussenzweig from the Rockefeller University and Dr. Florian Klein from the University of Cologne, who conducted a phase Ib clinical trial [316]. HIV-infected individuals on ART received three infusions with two different bNAbs and were able to maintain viral suppression after ART interruption in presence of antibodies. **Our objective was** to investigate the effect of combination bNAb-therapy and ART interruption on the HIV-specific $CD8^+$ and $CD4^+$ T cell response in the study participants [316]. We studied i) the magnitude and polyfunctionality of HIV-specific $CD8^+$ and $CD4^+$ responses longitudinally after bNAb therapy and ART interruption compared to baseline; ii) the change of breadth of HIV-specific T cells against multiple HIV antigens; and iii) the expansion of pre-existing responses and generation of responses against new epitopes.

Chapter 3 Manuscript 1: Persistent expansion and Th1-like skewing of HIV-specific circulating T follicular helper cells during antiretroviral therapy

Status: This research article was published in *EBioMedicine,* April 5, 2020; https://doi.org/10.1016/j.ebiom.2020.102727

Author contribution: Julia Niessl, Amy E. Baxter and Daniel E. Kaufmann designed the immunological studies. Antigoni Morou developed and optimized the AIM assay protocol. Julia Niessl performed the majority of AIM assay experiments and developed and performed the delayed ICS assays. Elsa Brunet-Ratnasingham performed some AIM assays on HIV-infected untreated individuals. Gérémy Sannier performed the RNA flow FISH assay for the detection of HIV-translation competent reservoir cells. Gabrielle Gendron-Lepage measured p24-specific antibodies using ELISA. Jonathan Richard used a FACS-based assay to measure gp120-specific antibodies. Gloria-Gabrielle Delgado assisted with the AIM assay. Nathalie Brassard performed the standard IFNγ-ICS assay and tetramer staining. Isabelle Turcotte and Rémi Fromentin measured total and integrated HIV DNA by PCR. Julia Niessl analyzed the data and prepared the figures with Amy E. Baxter's assistance. Mathieu Dubé provided input on manuscript content and data representation. Jean-Pierre Routy contributed to recruitment and clinical assessments. Nicole F. Bernard, Nicolas Chomont, Andrés Finzi contributed to data analysis. Julia Niessl, Amy E. Baxter. and Daniel E. Kaufmann interpreted the data and Julia Niessl wrote the initial draft of the manuscript with edits from Amy E. Baxter and Daniel E. Kaufmann. All co-authors reviewed and edited the manuscript and Daniel E. Kaufmann provided supervision.

Persistent expansion and Th1-like skewing of HIV-specific circulating T follicular helper cells during antiretroviral therapy

Julia Niessl[ab], Amy E. Baxter[ab1], Antigoni Morou[a2], Elsa Brunet-Ratnasingham[a], Gérémy Sannier[a], Gabrielle Gendron-Lepage[a], Jonathan Richard[a], Gloria-Gabrielle Delgado[a], Nathalie Brassard[a], Isabelle Turcotte[a], Rémi Fromentin[a], Nicole F. Bernard[c], Nicolas Chomont[a], Jean-Pierre Routy[cd], Mathieu Dubé[a], Andrés Finzi[a], Daniel E. Kaufmann[ab*]

[a]Research Centre of the Centre Hospitalier de l'Université de Montréal (CRCHUM) and Université de Montréal, Montreal, Qc, Canada.

[b]Consortium for HIV/AIDS Vaccine Development (CHAVD), La Jolla, CA, USA.

[c]Chronic Viral Illnesses Service and Division of Hematology, McGill University Health Centre, Montreal, Qc, Canada.

[d]Research Institute of the McGill University Health Centre, Montreal, Qc, Canada

[1]Current affiliation: Perelman School of Medicine, University of Pennsylvania, Philadelphia, USA.

[2]Current affiliation: Roche Diagnostics GmbH, Penzberg, Germany.

* Address correspondence to Daniel E. Kaufmann, CRCHUM, 900 rue St-Denis, room 09-456, Montreal, (Quebec) H2X 0A9, Canada. Phone: +1 514 890 8000, ext. 35261;

E-mail: daniel.kaufmann@umontreal.ca

Abstract

Background: Untreated HIV infection leads to alterations in HIV-specific $CD4^+$ T cells including increased expression of co-inhibitory receptors (IRs) and skewing toward a T follicular helper cell (Tfh) signature. However, which changes are maintained after suppression of viral replication with antiretroviral therapy (ART) is poorly known.

Methods: We analyzed blood $CD4^+$ T cells specific to HIV and comparative viral antigens in ART-treated people using a cytokine-independent activation-induced marker assay alone or in combination with functional readouts.

Findings: In intra-individual comparisons, HIV-specific $CD4^+$ T cells were characterized by a larger fraction of circulating Tfh (cTfh) cells than CMV- and HBV-specific cells and preferentially expressed multiple IRs and showed elevated production of the Tfh cytokines CXCL13 and IL-21. In addition, HIV-specific cTfh exhibited a predominant Th1-like phenotype and function when compared to cTfh of other specificities, contrasting with a reduction in Th1-functions in HIV-specific non-cTfh. Using longitudinal samples, we demonstrate that this distinct HIV-specific cTfh profile was induced during chronic untreated HIV infection, persisted on ART and correlated with the translation-competent HIV reservoir but not with the total HIV DNA reservoir.

Interpretation: Expansion and altered features of HIV-specific cTfh cells are maintained during ART and may be driven by persistent HIV antigen expression.

Funding: This work was supported by the National Institutes of Health (NIH), the Canadian Institutes of Health Research (CIHR) and the FRQS AIDS and Infectious Diseases Network.

Keywords: HIV, T follicular helper T cells, HIV-specific $CD4^+$ T cells, Antiretroviral therapy (ART)

Research in context

Evidence before this study

Combination antiretroviral therapy (ART) is highly effective in controlling HIV but requires life-long medication due to the existence of a latent viral reservoir, and to the fact that, with rare exceptions, ART alone does not restore immune responses capable of suppressing HIV. T follicular helper cells (Tfh) are of high interest both as HIV reservoirs and for their critical role in enabling the development of potent broadly neutralizing antibodies (bNAbs). The identification of a circulating Tfh (cTfh) population in peripheral blood with strong similarities with lymphoid tissue Tfh has attracted much attention over the past few years. However, investigations of cTfh at the antigen (Ag)-specific level have been hampered by the lack of sensitive assays to detect them. We recently overcame this hurdle by using new experimental, cytokine-independent approaches to evaluate HIV-specific $CD4^+$ T cell responses. We found an elevated Tfh signature in HIV-specific $CD4^+$ T cells of chronically infected, untreated individuals that correlated with blood HIV viremia. Although this Tfh signature decreased after ART initiation at the transcriptional level, detailed phenotypic and functional analyses of the HIV-specific $CD4^+$ T cell responses during ART are lacking.

Added value of this study

Here, we evaluated HIV-specific $CD4^+$ T cells, and in particular cTfh, in a cohort of ART-treated individuals. Comparative phenotypic and functional analyses with antigen (Ag)-specific responses (CMV, HBV) in the same study participant revealed that HIV-specific cTfh cells are abundant in ART-treated humans and represent a much larger fraction of the virus-specific $CD4^+$ T cell response compared to their CMV- and HBV-specific counterparts. HIV-specific cTfh also differ from CMV-specific and HBV-specific cTfh by multiple phenotypic and functional features that are established during chronic viremic infection, which persist on ART and appear less responsive to viral suppression than in non-cTfh HIV-specific $CD4^+$ T cells. This distinctive HIV-specific cTfh profile correlates with the translation-competent HIV reservoir, but not the total HIV DNA reservoir, suggesting that persistent HIV antigen expression maintains these altered features during ART.

Implications of all the available evidence

Increasing evidence suggest that cTfh are ontogenically related to lymphoid tissue Tfh. As animal models suggest that overabundant, qualitatively impaired Ag-specific Tfh may be detrimental and lead to low affinity Ab responses, it will be important to determine if priming of new, effective Tfh

responses may be hampered in therapeutic vaccine trials by competition with such large pre-existing HIV-specific Tfh populations during ART.

1. Introduction

Virus-specific $CD4^+$ T cell help is critical for pathogen control in chronic infections [1,2]. High-level antigen (Ag) exposure and inflammatory signals induce virus-specific $CD8^+$ T cell exhaustion, a state characterized by decreased proliferative potential and loss of effector function [3]. While dysfunctional pathogen-specific $CD4^+$ T cells share some characteristics with their $CD8^+$ counterparts during chronic infections, such as increased co-inhibitory receptor (IR) expression, they also present distinct characteristics of altered differentiation and function [4]. These features include skewing toward T follicular helper cell (Tfh) function, a phenomenon seen in chronic LCMV clone 13 in mice [5], and HCV in humans [6]. Tfh cells are a subset of $CD4^+$ T cells that express CXCR5 and provide help for B cell maturation and development of high affinity antibody (Ab) responses in the germinal center (GC) of secondary lymphoid organs. $CXCR5^+$ cells can also be found in the peripheral blood as circulating memory cells (cTfh) [7], however, their origin is not fully understood. Although cTfh cells could originate from non-GC Tfh cells, recent studies highlight the clonal and phenotypic overlap between activated blood cTfh cells and GC Tfh cells during steady state or after vaccination [8,9], demonstrating that GC Tfh cells fuel at least in part the blood cTfh pool.

Tfh cell-dependant humoral responses are required for eventual viral control of chronic murine LCMV infection [10]. In chronic HIV infection, expansion of bulk GC Tfh cells occurs in lymph nodes [11–13]; while technical hurdles have thus far limited studies of the specificity of these cells, part of this expanded GC Tfh population appears to be HIV-specific [14]. This quantitative increase in GC Tfh in HIV infection correlates with markers of disease progression and qualitative defects in their capacity to provide help to B cells [15]. Studies of peripheral blood responses confirmed an Ag-driven component to these alterations: the transcriptome of blood HIV-specific $CD4^+$ T cells exhibits a Tfh-like signature that directly correlates with viral load [4]. In contrast to LCMV, however, in HIV infection, this Tfh skewing does not result in virus clearance, perhaps due to the remarkable capacity of HIV to generate escape mutations and elude autologous Ab neutralization.

While current antiretroviral therapy (ART) regimens are highly effective at suppressing viral replication, resulting in improved immunity against opportunistic infections and remarkable reduction in morbidity and mortality, they do not lead to the restoration of an effective HIV-specific immune response capable of suppressing virus. Consequently, ART interruption generally leads to a rapid viral rebound from a reservoir of latently infected cells [16].

Frequencies of total GC Tfh decrease in lymphoid tissue with ART initiation but can stay elevated compared to uninfected controls [11–13]. Bulk cTfh cells from ART-treated donors show a reduced

capacity to induce HIV antibody production and B cell differentiation in vitro when compared to uninfected controls [17,18]. We observed that cTfh constitute a readily detectable fraction of HIV-specific $CD4^+$ T cells in individuals prior to ART initiation, this irrespective of viral load [4]. ART decreased the marked Tfh gene signature present in viremic persons at the transcriptional level [4], however, the impact of ART on the differentiation and function of HIV-specific $CD4^+$ T cell has not yet been investigated. Whether immunological features of HIV-specific cTfh would be unique to this virus or shared with other Ag specificities in the same individual, remains to be determined.

Here, we used activation-induced marker (AIM) assays [4,19,20], and functional tests to define the frequency, phenotype and function of blood $CD4^+$ T cells, in particular cTfh, specific to HIV, CMV and HBV in ART-treated individuals. We longitudinally investigated participants pre- and post-ART initiation to delineate features of HIV-specific $CD4^+$ T cells that were modulated by therapeutic control of viral load from those that persisted despite suppressive ART. Finally, we identified features of these HIV-specific cTfh cells that correlated with the size of the translation-competent HIV reservoir.

2. Material and methods

2.1. Human sample collection and processing

Subject characteristics are summarized in Tables S1-3. HIV-infected, ART-treated participants were on ART for over 12 months with controlled viral load (<50 vRNA copies/ml) for at least 6 months. Donors on ART were not excluded when a single small viral blip (VL >50 but <200 vRNA copies/ml) occurred with below detection viral load on precedent and subsequent tests. Untreated participants were either treatment naive or untreated for at least 3 months. HIV-uninfected individuals were used as negative controls for HIV antibody and reservoir measurements. PBMCs were isolated from leukapheresis samples by the Ficoll-Hypaque density gradient centrifugation and cryo-preserved in liquid nitrogen until use.

2.2. CD69/CD40L AIM assay

Peripheral blood mononuclear cells (PBMCs) were thawed, washed and put in culture at a concentration of 10 million cells/ml in RPMI 1640 medium (Gibco by Life Technologies, Cat# 11-875-093) supplemented with 0.5% penicillin/streptomycin (Gibco by Life Technologies, Cat# 15140122) and 10% human serum (Sigma). After a rest of 3 h at 37 °C, a CD40 blocking antibody (Miltenyi Biotec, Cat# 130-094-133, RRID: AB_10839704) was added to the culture to prevent the interaction of CD40L with CD40 and its subsequent downregulation. In addition, antibodies for chemokine receptors CXCR5, CXCR3 and CCR6 were added into the culture medium. After 15 min incubation at 37 °C, cells were stimulated with 0.5 µg/ml staphylococcal enterotoxin B (SEB) or 0.5 µg/ml of overlapping peptide pools for CMV pp65 (Cat# PM-PP65), HBV HBsAg (Cat# PM-HBV-IEP), HIV Gag (Cat# PM-HIV-GAG), HIV Env (Cat# PM-HIV-ENV) or HIV Nef (Cat# PM-HIV-NEF) (all JPT) for 9 h at 37 °C. An unstimulated condition served as a negative control. Cells were stained for viability dye (Aquavidid, Thermofisher, Cat# L34957), surface markers (30 min., 4 °C) and fixed using 2% paraformaldehyde (PFA) before acquisition at the flow cytometer (LSRII, BD) (see Table S4 for antibodies). Analysis was performed using FlowJo version 10 for Mac (Treestar, RRID: SCR_008520) and Spice version 5.3 (RRID: SCR_016603) [21]. For phenotypic analysis of Ag-specific $CD4^+$ T cells, only responses that were >2-fold over unstimulated condition were included to limit the impact of background staining. In contrast, for analysis of Ag-specific $CD4^+$ T cells subsets as percentage of total $CD4^+$ T cells, background-subtracted net values were used, which did not require excluding responses.

2.3. Standard intracellular cytokine staining

PBMCs were thawed, washed and put in culture at a concentration of 4 million cells/ml in RPMI 1640 medium (Gibco by Life Technologies, Cat# 11875-093) supplemented with penicillin/streptomycin (Gibco by Life Technologies, Cat# 15140122) and 10% fetal bovine serum (FBS) (Seradigm, Cat#1500-500). After a rest of 2 h, cells were stimulated with 0.5 µg/ml of overlapping peptide pools for CMVpp65, HBV HBsAg or HIV Gag for 6 h in presence of Brefeldin A (BD Biosciences, Cat# 555029) and monensin (BD Biosciences, Cat# 554724). For some experiments, anti-CD107A-BV785 (Biolegend, Cat#328644, RRID: AB_2565968) was added into culture. Cells were stained for viability marker, surface markers and intracellular cytokines using the IC Fixation/Permeabilization kit (eBioscience, Cat# 88-8824-00) before fixation with 2% PFA and acquisition on the flow cytometer (see Table S4 for antibodies). For the detection of CD107A, granzyme B and perforin within Ag-specific $CD4^+$ T cells, we identified AIM^+ cells by intracellular staining for CD69 and CD40L.

2.4. Delayed ICS assay

For the detection of some cytokines (IFNγ, IL-2, TNFα, IL-21, CXCL13) within AIM^+ Ag-specific $CD4^+$ T cells, cultured PBMCs were incubated with a CD40-blocking antibody, stimulated with peptide pools for 9 h as described above and further incubated for 12 h at 37 °C in the presence of Brefeldin A (BD Biosciences, Cat# 555029). Cells were surface stained, fixed and permeabilized using the IC Fixation/Permeabilization kit (Thermo Fisher, Cat# 88-8824-00) and incubated with antibodies against cytokines for 30 min at 4 °C (see Table S4 for antibodies).

2.5. Transcription factor staining

For the detection of transcription factors within AIM^+ Ag-specific $CD4^+$ T cells, cultured PBMCs were incubated with CD40-blocking antibodies and stimulated with peptide pools for 9 h as described above. Cells were stained for viability dye (Aquavidid, Thermofisher, Cat# L34957), surface markers (30 min., 4 °C), fixed (30 min, room temperature (RT)) and permeabilized using the Transcription Factor Staining Buffer Set (Invitrogen/ThermoFisher, Cat# 00–5523–00) before staining with antibodies against transcription factors for 1 h at RT (see Table S4 for antibodies).

2.6. HLA class II typing

Genomic DNA was extracted from PBMC using a QIAamp DNA blood kit (Qiagen, Cat# 51106). All subjects were typed for MHC class II alleles by sequence-based typing using kits from Atria

Genetics (South San Francisco, CA). Assign software was used to interpret sequence information for allele typing (Conexio Genetics, Perth, Australia).

2.7. MHCII tetramer staining

$CD4^+$ T cells were isolated from thawed PBMCs using a negative isolation kit (StemCell, Cat# 19052), rested for 2 h at 37 °C, washed and stained for 60 min at room temperature with PE-labeled MHC-II tetramers loaded with DV16 peptide (DRFYKTLRAEQASQEV) for the DRB1*01:01 allele or YV18 peptide (YVDRFYKTLRAEQASQEV) for the DRB1*11:01 allele (NIH Tetramer Core Facility at Emory University, Atlanta, GA). These sequences encompass an immunodominant, HLA Class II promiscuous epitope in Gag [22]. Control tetramers loaded with an irrelevant peptide (CLIP: PVSKMRMATPLLMQA) or HIV-uninfected donors with the same HLA-DRB1 genotype served as negative controls. $Tetramer^+$ $CD4^+$ T cells were column enriched using anti-PE beads (Miltenyi, Cat# 130-048-801). Cells were stained for viability marker (Aquavivid, Thermofisher, Cat# L34957), CXCR5 (45 min, 37 °C), surface markers (30 min, 4 °C) and fixed with 2% PFA before acquisition at the flow cytometer (LSRIIB, BD).

2.8. Quantification of total and integrated HIV DNA

Total and integrated HIV DNA were measured in $CD4^+$ T cells isolated from PBMCs by magnetic bead-based negative selection (Stem Cell Technologies, Cat# 19052) by real time nested polymerase chain reaction (PCR) as described previously [23].

2.9. Detection of translation-competent reservoir by RNA flow-FISH

$CD4^+$ T cells harbouring latent translation-competent reservoir were identified using the $HIV^{RNA/Gag}$ assay as previously described [24,25]. Briefly, $CD4^+$ T cells were isolated by magnetic bead negative selection (StemCell, Cat# 19052) from PBMCs from ART-treated individuals, rested for 3 h and stimulated with PMA (50 ng/ml, Sigma-Aldrich, Cat# P1585) and Ionomycin (0.5 µg/ml, Sigma-Aldrich, Cat# I9657) for 12 h. Unstimulated cells and cells from HIV-uninfected individuals served as controls. Cells were stained with surface markers, anti-Gag KC57 (Beckman Coulter) by intracellular staining and labeled for HIV *gag* RNA with Alexa Fluor 750-coupled probes (ThermoFisher) using the PrimeFlow RNA Assay (ThermoFisher, Cat# 88-18005-210) (see Table S4 for antibodies). Translation-competent $CD4^+$ T cells were identified as cells expressing both HIV Gag protein and *gag* RNA after PMA/Ionomycin stimulation.

2.10. Detection of p24-specific antibodies by ELISA

96 well plates (Thermo Scientific Nunc, FluoroNunc/LumiNunc, MaxiSorp Surface) were coated with 0.1 µg/ml of recombinant p24 (NIH AIDS Research and Reference Reagent Program, Cat# 12028) or bovine serum albumin (BSA) (Bioshop, Cat# ALB001.1) in PBS overnight at 4 °C. Plates were blocked for 90 min at RT with blocking buffer (TBS, Tween 0.1%, BSA 2%) and then washed 4 times with washing buffer (TBS, Tween 0.1%). Dilutions of human sera (1:3000) or rabbit anti-HIV p24 antiserum (NIH AIDS Reagent Program, Cat# 4250) in washing buffer containing 0.1% of BSA were incubated for 2 h at RT. Plates were washed 4 times with washing buffer before incubation for 90 min at RT with HRP-conjugated secondary Abs goat anti-human IgG HRP (Thermo Fisher Scientific Cat# 31410, RRID:AB_228269) or anti IgG rabbit HRP (Thermo Fisher Scientific Cat# 65-6120, RRID: AB_2533967). Plates were then washed 4 times with washing buffer before revealing with standard ECL (Perkin Elmer) with a TriStar luminometer (LB 941, Berthold Technologies).

2.11. Detection of gp120-specific antibodies

Gp120-specific antibodies were detected in plasma samples using a flow cytometry-based assay as described previously [26]. Briefly, CEM.NKr cells were coated with recombinant HIV-1YU2 gp120 (100 ng/ml) for 30 min at 37 °C and incubated with human plasma from HIV-infected ART-treated donors or uninfected controls (1:10,000 dilution) for 30 min at 37 °C. Cells were washed with PBS and stained with 1 µg/ml goat anti-human Alexa Fluor 647 (Thermo Fisher Scientific, Cat# A-21445, RRID: AB_2535862) secondary antibody for 15 min in PBS at room temperature. Cells were washed and fixed using 2% PFA before acquisition at the flow cytometer. The geometric mean of the Alexa Fluor 647 signal was used to express plasma gp120-antibody levels.

2.12. Statistics

Statistical analyses were done using GraphPad Prism version 8 using non-parametric tests. Two-group comparisons were performed using the Mann-Whitney and pairwise comparisons were performed using the Wilcoxon matched pair test. For comparisons between three or more groups, Kruskal–Wallis (for unpaired samples or when values were missing in paired samples) or Friedman one-way ANOVA (for paired samples) with Dunn's post-test was used. Permutation test (10,000 permutations) was applied for pie-chart comparison using the SPICE software. For correlations, Spearman's R correlation coefficient was applied. Statistical tests were two-sided and $p < 0.05$ was considered significant.

2.13. Ethic statement

Leukaphereses were obtained from study participants at the McGill University Health Centre, Montreal, Canada, and at the Centre Hospitalier de l'Université de Montréal (CHUM) in Montreal, Canada. The study was approved by the respective IRBs, written informed consent obtained from all participants prior to enrolment.

2.14. Data availability

Raw experimental data associated with the figures presented in the manuscript are available from the corresponding author upon reasonable request.

3. Results

3.1. AIM assay identifies HIV-specific CD4$^+$ responses with cTfh expansion in ART-treated individuals

To study Ag-specific CD4$^+$ T cells with diverse differentiation and functionality in HIV-infected ART-treated people, we used an approach based on the concurrent detection of activation-induced markers (AIM) on the cell surface after cognate Ag stimulation, as previously described [4,19,20]. PBMCs from a cohort of 27 HIV-infected individuals on ART (Participant characteristics: Table S1 (ART1-27)) were stimulated for 9 h with overlapping peptide pools spanning the sequence of the immunodominant HIV structural protein Gag (Fig. S1a). HIV Gag-specific T cells were identified by concurrent surface expression of AIM CD69 and CD40L (AIM$^+$ cells) (Fig. 1a, S1b). In addition, we examined within the same individual CD4$^+$ T cells specific for other Ags (CMV and HBV) to delineate characteristics that differentiate HIV-specific CD4$^+$ T cells. AIM$^+$ HIV Gag-specific responses were readily detectable in all ART-treated subjects examined, with low background in the absence of exogenous Ag (Fig. 1b, S1c) (responses were considered as positive when more than 2-fold over unstimulated condition). CMV-specific CD4$^+$ T cell responses were detectable in all individuals with positive CMV serology and absent for the 4 CMV-seronegative participants, demonstrating the high specificity of the assay (Fig. 1b, Table S1). Due to the low number of donors with a detectable HBV-specific CD4$^+$ T cell response (6 individuals of the 27 examined; 2 resolved infection, 4 vaccinated) (Fig. 1b, Table S1), we pooled responses elicited by infection or vaccination for further analysis, given the similarities of their profile.

The AIM assay identified significantly higher frequencies of virus-specific CD4$^+$ T cells compared to IFNγ intra-cellular staining (ICS) (Fig. S1d-e), demonstrating that ICS underestimates the frequency of Ag-specific CD4$^+$ T cell responses. This is particularly striking for HIV and HBV, but also apparent for known Th1-skewed responses such as CMV.

Ag-specific cTfh show limited cytokine production and are more likely to be missed by standard ICS, but are detectable by AIM assays [19,27]. Here, we broadly identified cTfh cells as memory (CD45RA$^-$) CD4$^+$ T cells expressing CXCR5 (Fig. S2a, 1c) to avoid the potential confounding factor of PD-1 upregulation in chronic infection [28,29]. Phenotypic analysis was only performed for donors with detectable AIM responses. Compared to CMV- and HBV-specific CD4$^+$ T cells, HIV-specific CD4$^+$ responses were characterized by a significantly higher proportion of CXCR5$^+$ memory cells (Fig. 1d) with comparable CXCR5 MFI for all specificities (Fig. S2b). This skewing was not due to in vitro stimulation, as a similar frequency was observed by staining with MHC

Class II tetramers loaded with an immunodominant HIV Gag epitope (Fig. S2c-e). To test whether the enrichment of cTfh cells was a general feature of HIV-specific $CD4^+$ T cell responses, we analyzed responses against the HIV envelope glycoprotein Env and the accessory protein Nef, which showed a lower magnitude compared to HIV Gag as described previously (Fig. 1e) [22]. Despite these lower frequencies, responses were detectable in 13/27 participants for Env and 18/27 participants for Nef. HIV Env- and Nef-specific $CD4^+$ T cell responses were characterized by a similar frequency of $CXCR5^+$ memory cells when compared to Gag-specific $CD4^+$ responses (Fig. 1f). Accordingly, due to the higher magnitude of HIV Gag-specific $CD4^+$ responses, HIV Gag-specific cTfh were more prevalent in the total $CD4^+$ populations compared to HIV Nef or Env (Fig. 1g). In conclusion, our results demonstrate the expansion of cTfh cells within HIV-specific $CD4^+$ T cell responses compared to other specificities in ART-treated individuals.

3.2. HIV-specific cTfh and non-cTfh cells express multiple co-inhibitory receptors despite viral suppression

IRs are key modulators of T cell signaling for both the regulation of physiologic responses to Ag stimulation and in the context of diseases characterized by persistent Ag exposure. Consistent with a requirement for tight functional control, Tfh cells frequently express IRs such as PD-1, TIGIT and CD200 [30,31]. On the other hand, upregulation of multiple IRs on $CD8^+$ and $CD4^+$ T cells also occurs in cancer or chronic infections including HIV and contribute to exhaustion (reviewed in [32]). Given this dual role of IRs, we next analyzed IR expression on Ag-specific $CD4^+$ responses in the context of the massive reduction in HIV Ag load due to viral suppression during ART.

HIV Gag-specific cTfh from ART-treated individuals were characterized by a significantly higher frequency of cells expressing the IRs TIGIT and CD200 compared to non-cTfh cells, while the frequency of PD-1^+ cells was similar between both subsets (Fig. S3a). When we compared cTfh IR expression between Ags, we observed a high frequency of $TIGIT^+$ for HIV-specific cTfh cells compared to CMV- and HBV-specific cTfh (Fig. 2a–b). In addition, high levels of CD200 and PD-1 characterized HIV- and HBV-specific cTfh cells (Fig. 2b). The frequency of cTfh cells specific for HIV co-expressing TIGIT, PD-1 and CD200 was significantly higher compared to CMV or HBV (Fig. 2c-d). The differences in IR expression observed for Ag-specific non-cTfh reflected those seen on cTfh, albeit at lower levels (Fig. S3b-c).

IR expression can be transiently induced by activation [33], and may thus be impacted by the 9 h stimulation required for the AIM assay. Therefore, we used MHC Class II tetramers to phenotype HIV-specific cTfh cells in 3 ART-treated donors (Fig. S2b). We detected similar frequencies of

TIGIT$^+$ and PD-1$^+$ cells on tetramer$^+$ as on AIM$^+$ Gag-specific cTfh cells, which were increased when compared to the total cTfh population (Fig. S3d). In contrast, more HIV Gag-specific cTfh cells expressed CD200 when the AIM assay was used. These findings show that a high frequency of HIV-specific cTfh cells in ART-treated donors pre-express multiple IRs, such as PD-1 and TIGIT, before stimulation with the cognate Ag. On the other hand, while a fraction of HIV-specific cTfh cells pre-expresses CD200, this molecule is further rapidly upregulated during stimulation, as shown previously [34]. Therefore, a higher capacity to upregulate CD200 after stimulation might contribute to its increased expression on HIV- vs HBV- and CMV-specific CD4$^+$ T cells.

In summary, our results demonstrate that despite viral suppression on ART, HIV-specific cTfh and non-cTfh CD4$^+$ T cells are characterized by a high frequency of cells expressing multiple IRs.

3.3. HIV-specific cTfh cells produce higher levels of Tfh cytokines than CMV-specific cTfh

To elucidate whether high expression of IRs on HIV-specific cTfh influences Tfh function, we assessed the production of the canonical Tfh-related cytokines CXCL13 and IL-21. IL-21 is an important cytokine for B cell help [7], and decreased IL-21 expression has been reported in HIV-specific CD4$^+$ T cells of HIV$^+$ individuals on and off ART [35,36]. Detection of CXCL13 and IL-21 at the protein level is challenging due to their limited expression upon Ag stimulation and unspecific background staining. To overcome this hurdle, we used a modified ICS assay ("delayed ICS"), which included an extended (9 h) stimulation prior to addition of Brefeldin A, thus allowing for upregulation of AIM markers on the cell surface before the phase of intracellular protein trapping (Fig. 3a). We analyzed cytokine expression by a sequential gating strategy: pre-gating on CD69$^+$CD40L$^+$ cTfh cells increased specificity for CXCL13 and IL-21 and enabled robust detection of rare cytokine-expressing cells (Fig. 3b). We detected a significantly higher frequency of CXCL13- and IL-21-producing cells in HIV-specific compared to CMV-specific cTfh cells (Fig. 3c-d). Consistent with the known role of IRs for Tfh function [37], Tfh-cytokine production was highest in cTfh cells expressing multiple IRs (Fig. 3e-f). Therefore, HIV-specific cTfh cells expressing multiple IRs demonstrate robust expression of Tfh-related functions.

3.4. HIV-specific cTfh cells show preferential Th1-like phenotype and function

Co-expression patterns of the chemokine receptors CXCR3 and CCR6 have been associated with T helper cell differentiation and function [38,39], and can also provide an indication of cTfh polarization and of their capacity to provide help to B cells [40]. We thus next examined CXCR3 and CCR6 expression on AIM$^+$ Ag-specific cTfh cells in ART-treated individuals (Fig. 4a). HIV- and CMV-specific cTfh predominantly had a Th1-like (CXCR3$^+$CCR6$^-$) phenotype, while HBV-

specific cTfh responses showed a mixed cTfh profile with Th2-like ($CXCR3^{-}CCR6^{-}$) and Th1-like polarizations (Fig. 4a, S4a). HIV-specific cTfh cells expressed in addition higher levels of Eomes and/or T-bet, whereas RORγt or GATA3 was rarely detected (Fig. S4bc), confirming their preferential Th1-like polarization. Importantly, the frequency of Th1-polarized cTfh was significantly higher for HIV than for both CMV and HBV (Fig. 4b).

In contrast, the proportion of $CXCR3^{+}CCR6^{-}$ Th1-like cells within the HIV-specific non-cTfh subset was comparable to CMV and HBV (Fig. S4d). In addition, HIV-specific non-cTfh cells included a high frequency of $CCR6^{+}$ Th1Th17-like ($CCR6^{+}CXCR3^{+}$) and Th17-like ($CCR6^{+}CXCR3^{-}$) (Fig. S4d). Accordingly, we identified subsets of HIV-specific non-cTfh cells characterized by Eomes/T-bet and RORγt expression (Fig. S4e). Eomes and/or T-bet expression was significantly lower in HIV-specific cTfh than non-cTfh (Fig. S4f). These data suggest that the distinctive Th1-like phenotype skewing of HIV-specific cTfh compared to other specificities might correspond to a mixed differentiation pattern that does not reach the full acquisition of all Th1-related features seen in non-cTfh cells.

We next investigated whether the phenotypic polarization of HIV-specific cTfh correlated with function. We analyzed expression of classical Th1-cytokines in HIV- or CMV-specific cTfh cells (Fig. 4c). We detected a significantly higher frequency of IFNγ, TNFα and IL-2-expressing cells in HIV- vs CMV-specific cTfh (Fig. 4c-d). This profile of elevated Th1-cytokine expression was not seen for non-cTfh cells; indeed, IFNγ secretion was significantly reduced in HIV-specific non-cTfh compared to CMV-specific, while IL-2 production was increased (Fig. S4g). Consistent with previous findings at the bulk cTfh level [30], $CXCR3^{+}$ HIV-specific cTfh populations ($CXCR3^{+}CCR6^{-}$ Th1-like, and to a lesser extent $CXCR3^{+}CCR6^{+}$ Th1/Th17-like) produced IFNγ following stimulation (Fig. 4e). However, a large fraction of Ag-specific $CXCR3^{+}$ cTfh cells also produced the Tfh-cytokines CXCL13 and IL-21. Thus, co-expression analyses revealed increased CXCL13 and IL-21 single-positive in addition to Tfh-cytokines/IFNγ co-expressing HIV-specific cTfh cells, compared to their CMV-specific counterparts (Fig. 4f).

We next compared the frequency of $cytokine^{+}$ cells within Th1-like Ag-specific cTfh and found comparable levels for IFNγ but a significantly higher CXCL13 and IL-21 expression in HIV vs CMV (Fig. S4h). These findings suggest that the elevated production of Th1-cytokines in HIV-specific cTfh cells may be related to their predominant Th1-like polarization compared to CMV, but that polarization alone is not responsible for the elevated production of Tfh cytokines.

In contrast and as shown previously [41], cTfh cells, independent of their specificity, rarely expressed cytolytic markers such as CD107A, granzyme B or perforin (Fig. S5ab). These functions were, however, detectable in Ag-specific non-cTfh cells, especially for CMV (Fig. S5ab).

Collectively, these observations demonstrate a preferential Th1-associated phenotype and function of HIV-specific cTfh cells in ART-treated individuals, contrasting with lack of cytotoxic molecule expression.

3.5. Suppression of HIV viremia by ART does not reverse the phenotype of HIV-specific cTfh cells

Having identified several distinct features of HIV-specific $CD4^+$ T cell responses in ART-treated individuals, we next investigated whether these characteristics were present prior to ART initiation, and if they were modulated by therapeutic control of Ag load. For this, we examined samples from 7 HIV-infected donors obtained during the chronic phase of untreated infection before ART initiation and after 1 to 3.2 years of therapy (Participant characteristics: Table S2). We first determined the magnitude of HIV-specific $CD4^+$ T cell responses and detected little change after starting therapy using the AIM assay, contrasting with a clear contraction of the HIV-specific $CD4^+$ T cell response when the $IFN\gamma^+$ ICS was used (Fig. 5a).

In a transcriptional analysis of HIV-specific $CD4^+$ T cells, we recently demonstrated that ART decreased the Tfh gene signature present in viremic individuals off therapy [4]. As this analysis was performed at the RNA level on total AIM^+ HIV-specific $CD4^+$ cells, we next investigated whether HIV-specific cTfh and non-cTfh were affected differentially at the phenotypic level by ART.

Although the frequency of cTfh cells within the total memory $CD4^+$ T cell pool did not change following ART initiation, we observed an increase in the frequency of cTfh cells within the HIV-specific $CD4^+$ T cell population (Fig. 5b). We detected a significant decrease in $ICOS^+$ HIV-specific cTfh and non-cTfh cells (Fig. 5c), consistent with a general reduction of activation of HIV-specific $CD4^+$ T cells. In addition, we detected a significant decrease in the frequencies of $PD\text{-}1^+$, $CD200^+$ and $PD\text{-}1^+TIGIT^+CD200^+$ HIV-specific non-cTfh cells (Fig. 5d). In contrast, viral suppression on ART had a limited impact on expression and co-expression of IRs on HIV-specific cTfh cells (Fig. 5d). Similar to IR expression, we did not detect changes in the CXCR3/CCR6 phenotype of HIV-specific cTfh cells following ART initiation (Fig. 5e), contrasting with a significant decrease in Th1-polarization of HIV-specific non-cTfh cells.

In summary, our results demonstrate that the phenotype of cTfh, characterized by a preferential Th1-profile and high expression of multiple IRs, is established during chronic HIV infection and maintained despite suppressed viremia, this at least for the first three years after ART initiation.

3.6. Persistent levels of plasma HIV-specific antibodies in ART-treated individuals correlate with HIV-specific cTfh

Untreated HIV infection is associated with GC Tfh expansion and hypergammaglobulinemia [11]. Although HIV-specific Ab plasma levels decrease after ART initiation, they are detectable in the plasma of long-term treated individuals [42]. It has been suggested that ongoing Ag stimulation in lymphoid tissue may contribute to elevated HIV-specific plasma concentrations [43].

We therefore next assessed plasma levels of p24- and gp120-specific antibodies in our cohort of ART-treated individuals and how they relate to persistent Tfh responses. Despite their decrease after viral suppression on ART (Fig. 6a), HIV-specific Ab levels were detectable in nearly all ART-treated participants (Fig. 6b) and remained stable over time during ART (Fig. 6c). In addition, levels of p24- and gp120-specific Abs in plasma of ART-treated individuals were directly correlated (Fig. 6d). There was no association between total HIV-specific $CD4^+$ T cell or HIV-specific non-cTfh responses and HIV-specific Abs (Fig. 6e-f). However, we detected a significant correlation between HIV-specific cTfh and persistent plasma HIV-specific Ab levels in ART-treated donors (Fig. 6g). Thus, our results suggest ongoing stimulation of HIV-specific B and T cells, which is associated with augmented Ab responses in ART-treated people in vivo.

3.7. The translation-competent HIV reservoir correlates with Th1-like phenotype and function of HIV-specific cTfh

As the phenotypic profiles of HIV-specific cTfh cells during untreated infection and during ART were similar, we next explored possible links between these maintained features detected in our analyses and markers of HIV persistence during ART. We assessed the size of the HIV reservoir in $CD4^+$ T cells using PCR for total viral DNA (vDNA), PCR for integrated vDNA and by measuring the inducible translation-competent reservoir by an RNA flow cytometric fluorescent in situ hybridization (RNA flow-FISH) assay. With this method, the translation-competent reservoir is defined as $CD4^+$ T cells capable of co-expressing HIV *gag* RNA and Gag protein after in vitro stimulation (Fig. 7a) [24,25]. Translation-competent $HIV^{RNA+/Gag+}$ $CD4^+$ cells were undetectable in most ART-treated individuals in the absence of stimulation and in HIV-uninfected controls (Fig. 7b, Table S3), but could be identified in ART-treated donors after stimulation with PMA/Ionomycin with varying frequencies (Fig. 7b). DNA PCR-based methods detect defective viral genomes or

proviruses unable to express viral proteins, and as expected the two PCR assays gave much larger estimates than the RNA flow-FISH method (Fig S6a). As low Ag persistence might contribute to maintain the pool of virus-specific T cells on ART, we examined the relationship between reservoir size and magnitude of HIV-specific $CD4^+$ T cell responses. We observed no significant association between the frequency of HIV-specific $CD4^+$ T cells or cTfh responses and vDNA reservoir measurements but a non-significant correlation between the magnitude of the HIV-specific $CD4^+$ T cell response and the translation-competent reservoir (Fig. S6b).

We next explored potential relationships between the size of the total or integrated vDNA reservoir and phenotypic or functional features of HIV-specific cTfh or non-cTfh responses and found no significant association (Fig. 7c). In contrast, the size of the translation-competent HIV reservoir during ART was significantly positively associated with TIGIT, ICOS expression and the Th1-like phenotype and -function of HIV-specific cTfh (Fig. 7c, S6c-d). Of note, no association was detected between the size of the translation-competent reservoir and the phenotype or function of HIV-specific non-cTfh in ART-treated individuals (Fig. 7c). Therefore, our results indicate that the expression of IRs and Th1 functions of HIV Gag-specific cTfh cells correlate with a marker of the functional viral reservoir in individuals on ART. This suggests that the low but continuous levels of HIV Ag production may contribute to the maintenance of this population after prolonged therapy.

4. Discussion

Tfh cells are of high interest in HIV infection: at the total subset level, they serve as important sites of viral replication pre-ART [12] and reservoirs post-ART [13]. Studies of the total cTfh compartment show positive associations between memory Tfh cells and generation of HIV-specific broadly neutralizing antibodies (bNAbs) [30,44,45], but investigations of HIV-specific cTfh have been hampered by the lack of sensitive tools to assess them. It remained unclear whether frequencies of HIV-specific Tfh cells, and/or altered functions, set them apart from Tfh specific for other viruses. Here, we used cytokine-independent AIM assays, alone or in combination with functional readouts, to characterize HIV-specific cTfh. We found that compared to their CMV- and HBV-specific counterparts in the same donors, HIV-specific cTfh, defined as $CXCR5^+$ memory cells, were more abundant and that this difference was exacerbated after ART initiation. On suppressive therapy, HIV-specific cTfh maintained a distinct phenotype with high expression of IRs, high production of cytokines, and a Th1-like skewing. Positive correlations between the magnitude, phenotype and function of HIV-specific cTfh responses with HIV-specific antibody levels and with the size of the translation-competent reservoir suggest that persistent exposure to

viral products contribute to ongoing stimulation of HIV-specific Tfh despite undetectable HIV viremia on ART.

Our experimental approach gives a different picture of the impact of ART on HIV-specific $CD4^+$ T cell responses compared to traditional assays such as IFNγ ICS. HIV-specific $CD4^+$ T cell responses were detectable in all ART-treated individuals examined by the AIM assay, in contrast to IFNγ ICS. Matched samples obtained before and after ART initiation demonstrated a clear contraction of $IFN\gamma^+$ HIV-specific $CD4^+$ T cell responses, whereas AIM^+ responses were maintained. Therefore, the impact of ART on the magnitude of HIV-specific $CD4^+$ T cells may have been overestimated in previous reports using IFNγ as a readout [46]. Rather than massive attrition, smaller changes in frequency associated with more dramatic changes in polarization, differentiation and function of HIV-specific $CD4^+$ T cells occur after viral suppression.

Many studies suggest that Tfh cells and GC play a critical role in the ability of the immune system to generate bNAbs, which are uncommon, leading to the hypothesis that rarity and/or qualitative defects of HIV-specific Tfh could be limiting factors in the bNAb generation in infected humans [47]. Here, we demonstrate that, surprisingly, the median fraction of cTfh within the HIV-specific $CD4^+$ T cell population in ART-treated people is large, 3.7-fold greater than in CMV-specific and 2.8-fold greater than in HBV-specific $CD4^+$ T cells. The frequencies of HIV-specific cTfh observed by AIM assay were similar to the frequencies measured by tetramer staining in our experiments and to those reported by another group [18]. These results also confirm the capacity of the CD69/CD40L AIM assay to sensitively detect cTfh to chronic pathogens, besides its capacity to detect acute cTfh responses, as has been recently shown for the flu vaccine [20]. As these comparisons were made on an intra-individual basis, they control for the frequent persistence of an inflammatory environment despite suppressive ART and potential for bystander changes in T cell responses, therefore demonstrating actual virus-specific differences in cTfh responses. These expanded HIV-specific cTfh also present distinct phenotypic and functional features: they express higher levels of the IRs PD-1, TIGIT and CD200 compared to their CMV- and HBV-specific counterparts yet produce more cytokines. This augmented production includes not only the Tfh-cytokines CXCL13 and IL-21, but also the Th1 cytokines IFNγ, TNFα, and IL-2, consistent with the Th1-like phenotype of high CXCR3 expression. The production of Tfh-associated cytokines CXCL13 and IL-21 was highest in Ag-specific cTfh cells expressing multiple IRs. Previous studied demonstrated the importance of PD-1 for optimal Tfh cell positioning and function including IL-21 production in vivo [37].

In this manuscript, we compare our findings related to HIV-specific $CD4^+$ T cells to responses specific to CMV, which also causes a chronic infection albeit with some differences. The length of CMV infection in our cohort is likely greater when compared to HIV. However, CMV viral loads are usually undetectable in ART-treated non-immunocompromised individuals [48]. Life-long CMV Ag exposure can induce a particularly large T cell response, which is characterized by high Th1-related cytokine expression including cytolytic markers and expansion of senescent cells [49]. However, we detected these functions only in the CMV-specific non-cTfh population. No cTfh expansion nor preferential IR upregulation in CMV-specific $CD4^+$ T cell responses was detected in our cohort, similar to HBV-specific responses induced by vaccination or resolved infections. In contrast, other studies observed a Tfh expansion and Th1-phenotype in other chronic infections that share some features with HIV, such as LCMV clone 13 in mice [5], SIV in non-human primates [50], HCV [6], and malaria [51], in humans. The underlying mechanisms are poorly understood, but several studies suggested that increased duration of Ag exposure, high levels of Ag and inflammatory cytokines, common for these infections, favor this polarization (reviewed in [52]).

Two non-mutually exclusive mechanisms may be responsible for maintaining the characteristics of virus-specific $CD4^+$ T cell responses during viral suppression on ART. First, persistent low-level HIV Ag expression could continuously stimulate Tfh responses on ART and maintain HIV-specific cTfh phenotype and function. Importantly, such a mechanism does not imply residual replication of the full virus, as abortive expression of some viral genes or trapped Ag, for example on follicular DCs, may have similar consequences [53]. HIV Ags can be detected in lymphoid tissue of ART-treated donors [54,55]. In support of this hypothesis, we detected a significant correlation between the size of the translation-competent reservoir and expression of TIGIT, ICOS and Th1-like phenotype and function of HIV-specific cTfh but not non-cTfh cells. In contrast, HIV DNA measurements, which include a large fraction of defective genomes unable to produce viral Ags [56], were not associated. One possible explanation to our observations is that occasional reactivation of persistently infected cells leads to stochastic production of viral proteins within the GCs of lymphoid tissues and stimulation of HIV-specific Tfh cells. These cells eventually exit the GC when the burst of HIV products resolves, and subsequently become cTfh cells. A second possibility of persistent characteristics of HIV-specific $CD4^+$ T cells is permanent epigenetic programming. Previous studies demonstrated that during chronic viral exposure, virus-specific $CD8^+$ T cells in mice and humans are epigenetically altered so that PD-1 expression was persistently elevated even after Ag withdrawal [57–60]. Thus, maintenance of certain phenotypic profiles in HIV-specific cTfh cells during ART could be related to an epigenetic reprogramming due to high levels of chronic Ag exposure during untreated infection.

We recently showed that HIV-specific $CD4^+$ T cells in untreated HIV infection are characterized by an atypical Tfh signature in $CXCR5^-$ cells [4]. Longitudinal samples analyzed before and after ART initiation demonstrated a decrease of a Tfh transcriptional signature and a reduction of phenotypic markers including PD-1, TIGIT, CD200 and CXCR3 in HIV-specific $CD4^+$ T cells at the RNA level [4]. Here, we demonstrate that the proportion of $CXCR5^+$ cTfh cells within HIV-specific $CD4^+$ responses not only remains expanded, but increases on therapy. While the phenotype of HIV-specific cTfh cells does not change with ART, non-cTfh cells experience a decline in cells co-expressing multiple IRs and Th1-like phenotype. Taken together, these data suggest that some $CXCR5^-$ HIV-specific $CD4^+$ T cells with Tfh-like properties identified in viremic infection [61], might gain (or recover) the ability to express CXCR5; and that the previously observed reduction of Tfh-related gene expression and phenotypic markers in HIV-specific $CD4^+$ T cells on ART [4], is not due to a reduction of cTfh cells, but related to partial normalization of cTfh markers in HIV-specific non-cTfh responses.

This work raises questions that will need to be addressed in further studies. Our report focuses on the characterization of cTfh responses and the blood HIV reservoir. Studies on secondary lymphoid tissues could provide critical information regarding Ag persistence and its impact on HIV-specific Tfh alterations. Of note, HIV Gag-specific Tfh cells expressing Th1-like cytokines have been detected in lymphoid tissues of HIV-infected individuals [11,12,41], suggesting that some of the features we identified may be shared between the peripheral blood and secondary lymphoid tissue compartments. As these are very challenging to conduct in humans, investigations in non-human primates could prove powerful alternatives. Further detailed analyses on pre- vs post-ART samples will be essential to better understand subset-related changes in HIV-specific $CD4^+$ T cells and their ontogeny. Taking into account our observations into the advanced immunomonitoring of interventional studies will allow addressing a key question: what are the immunological consequences of the distinct characteristics of HIV-specific cTfh on ART? Our results show a direct correlation of these responses with anti-p24 and anti-gp120 Ab titers, whereas there is no such association between Ab levels and magnitude of non-cTfh HIV-specific $CD4^+$ T cell responses. This suggests that ongoing HIV Ag stimulation in lymphoid tissues leads to persistent induction and/or maintenance of HIV-specific B cell, Ab and cTfh expansion. As therapeutic vaccination to complement ART is an important strategy considered to achieve HIV cure, future studies should address how such pre-existing, expanded HIV-specific Tfh would impact development of new Thelper and/or B cell responses. Animal models suggest that overabundant Ag-specific Tfh, especially if qualitatively impaired, may be detrimental, leading to low affinity responses [62,63]. Such studies should address whether priming of new, effective Tfh responses

may be hampered by competition from the boosting of large pre-existing cell populations. Finally, the presence of marked quantitative and qualitative differences in the cTfh specific for different viruses has likely relevance beyond HIV vaccine development and therapy and may be important for other pathogens for which the human system frequently fails to develop high-quality immune responses.

Declaration of Competing Interest

The authors have declared that no conflict of interest exists.

Acknowledgments

We thank Josée Girouard, the clinical staff at the McGill University Health Centre in Montreal and all study participants for their invaluable role in this project; Dr. Dominique Gauchat, Philippe St-Onge and the CRCHUM Flow Cytometry Platform as well as Dr. Olfa Debbeche and the CRCHUM BSL3 platform for technical assistance. The following reagent was obtained through the NIH AIDS Reagent Program, Division of AIDS, NIAID, NIH: Anti-HIV-1 SF2 p24 Polyclonal and HIV-1 IIIB p24 Recombinant Protein from ImmunoDX, LLC. The following reagents were obtained through the NIH Tetramer Core Facility: HLA Class II tetramers DRB1*01:01 DRFYKTLRAEQASQEV-PE and DRB1*11:01-YVDRFYKTLRAEQASQEV-PE. Fig. S1A was prepared using images from Servier Medical Art by Servier, which is licensed under a Creative Commons Attribution 3.0 Unported License.

Funding Sources

This study was supported by the National Institutes of Health (no. HL092565 to D.E.K., no. AI100663 and no. AI144462 CHAVI-ID to D.E.K. (Consortium PI: Dennis Burton); the Canadian Institutes of Health Research grants (no. 137694 and no. 320721 to D.E.K.; foundation grant no. 352417 to A.F.; no. 36440 to N.C.); the Canada Foundation for Innovation Program Leader grant (no. 31756 to D.E.K.); and the FRQS AIDS and Infectious Diseases Network. D.E.K. is a FRQS Merit Research Scholar. N.C. is supported by a FRQS Research Scholar Career Award. J.N. is supported by scholarships from the FRQS, the Bavarian Research Alliance (BayFor) and the Department of Microbiology, Infectious Diseases and Immunology of the University of Montreal. A.E.B. is supported by a CIHR post-doctoral fellowship. J.R. is the recipient of a Mathilde Krim Fellowship in Basic Biomedical Research from AmfAR. I.T. is supported by a CIHR scholarship. J.P.R. is the holder of the Louis Lowenstain Chair in Hematology & Oncology, McGill University. A.F. is supported by a Canada Research Chair Award. The funding sources had no role in: study design; in the collection, analysis, and interpretation of data; in the writing of the report; and in the decision to submit the paper for publication.

References

[1] Matloubian M., Concepcion R.J., Ahmed R. CD4+ T cells are required to sustain CD8+ cytotoxic T-cell responses during chronic viral infection. J. Virol. 1994;68:8056–8063.

[2] Laidlaw B.J., Craft J.E., Kaech S.M. The multifaceted role of CD4(+) T cells in CD8(+) T cell memory. Nat Rev Immunol 2016;16:102–111.

[3] McLane L.M., Abdel-Hakeem M.S., Wherry E.J. CD8 T cell exhaustion during chronic viral infection and cancer. Annu Rev Immunol 2019;37:457–495.

[4] Morou A., Brunet-Ratnasingham E., Dubé M., et al. Altered differentiation is central to HIV-specific CD4(+) T cell dysfunction in progressive disease. Nat Immunol 2019;20:1059–1070.

[5] Fahey L.M., Wilson E.B., Elsaesser H., Fistonich C.D., McGavern D.B., Brooks D.G. Viral persistence redirects CD4 T cell differentiation toward T follicular helper cells. J Exp Med 2011;208:987–999.

[6] Raziorrouh B., Sacher K., Tawar R.G., et al. Virus-Specific CD4+ T cells have functional and phenotypic characteristics of follicular T-Helper cells in patients with acute and chronic HCV infections. Gastroenterology 2016;150:696–706.

[7] Crotty S. T follicular helper cell differentiation, function, and roles in disease. Immunity 2014;41:529–542.

[8] Vella L.A., Buggert M., Manne S., et al. T follicular helper cells in human efferent lymph retain lymphoid characteristics. J Clin Invest 2019;129:3185–3200.

[9] Heit A., Schmitz F., Gerdts S., et al. Vaccination establishes clonal relatives of germinal center T cells in the blood of humans. J Exp Med 2017;214:2139–2152.

[10] Greczmiel U., Krautler N.J., Pedrioli A., et al. Sustained T follicular helper cell response is essential for control of chronic viral infection. Sci Immunol 2017;2. doi:10.1126/sciimmunol.aam8686.

[11] Lindqvist M., van Lunzen J., Soghoian D.Z., et al. Expansion of HIV-specific T follicular helper cells in chronic HIV infection. J Clin Invest 2012;122:3271–3280.

[12] Perreau M., Savoye A.-.L., De Crignis E., et al. Follicular helper T cells serve as the major CD4 T cell compartment for HIV-1 infection, replication, and production. J Exp Med 2013;210:143–156.

[13] Banga R., Procopio F.A., Noto A., et al. PD-1+ and follicular helper T cells are responsible for persistent HIV-1 transcription in treated aviremic individuals. Nat. Med. 2016;22:754–761.

[14] Wendel B.S., del Alcazar D., He C., et al. The receptor repertoire and functional profile of follicular T cells in HIV-infected lymph nodes. Sci Immunol 2018;3. eaan8884.

[15] Cubas R.A., Mudd J.C., Savoye A.-.L., et al. Inadequate T follicular cell help impairs B cell immunity during HIV infection. Nat. Med. 2013;19:494–499.

[16] Fagard C., Oxenius A., Gunthard H., et al. A prospective trial of structured treatment interruptions in human immunodeficiency virus infection. Arch Intern Med 2003;163:1220–1226.

[17] Cubas R., van Grevenynghe J., Wills S., et al. Reversible reprogramming of circulating memory t follicular helper cell function during chronic HIV infection. J Immunol 2015;195:5625–5636.

[18] Claireaux M., Galperin M., Benati D., et al. A high frequency of HIV-specific circulating follicular helper T cells is associated with preserved memory B cell responses in HIV controllers. MBio 2018;9:e00317–e00318.

[19] Reiss S., Baxter A.E., Cirelli K.M., et al. Comparative analysis of activation induced marker (AIM) assays for sensitive identification of antigen-specific CD4 T cells. PLoS ONE 2017;12:e0186998.

[20] Pallikkuth S., de Armas L.R., Rinaldi S., et al. Dysfunctional peripheral t follicular helper cells dominate in people with impaired influenza vaccine responses: results from the Florah study. PLoS Biol. 2019;17:e3000257.

[21] Roederer M., Nozzi J., Nason M. SPICE: exploration and analysis of post-cytometric complex multivariate datasets. Cytometry 2011;79:167–174.

[22] Kaufmann D.E., Bailey P.M., Sidney J., et al. Comprehensive analysis of human immunodeficiency virus type 1-Specific CD4 responses reveals marked immunodominance of gag and nef and the presence of broadly recognized peptides. J. Virol. 2004;78:4463–4477.

[23] Vandergeeten C., Fromentin R., Merlini E., et al. Cross-clade ultrasensitive PCR-based assays to measure HIV persistence in large-cohort studies. J. Virol. 2014;88:12385–12396.

[24] Baxter A.E., Niessl J., Fromentin R., et al. Single-Cell characterization of viral translation-competent reservoirs in HIV-infected individuals. Cell Host Microbe 2016;20:368–380.

[25] Baxter A.E., Niessl J., Fromentin R., et al. Multiparametric characterization of rare HIV-I nfected cells using an RNA-flow FISH technique. Nat Protoc 2017;12:2029–2049.

[26] Richard J., Veillette M., Batraville L.-.A., et al. Flow cytometry-based assay to study HIV-1 gp120 specific antibody-dependent cellular cytotoxicity responses. J. Virol. Methods 2014;208:107–114.

[27] Dan J.M., Lindestam Arlehamn C.S., Weiskopf D., et al. A cytokine-independent approach to identify antigen-specific human germinal center T follicular helper cells and rare antigen-specific CD4+ T cells in blood. J Immunol 2016. doi:10.4049/jimmunol.1600318. published online June 24.

[28] Hokey D.A., Johnson F.B., Smith J., et al. Activation drives PD-1 expression during vaccine-specific proliferation and following lentiviral infection in macaques. Eur J Immunol 2008;38:1435–1445.

[29] Porichis F., Kwon D.S., Zupkosky J., et al. Responsiveness of HIV-specific CD4 T cells to PD-1 blockade. Blood 2011;118:965–974.

[30] Locci M., Havenar-Daughton C., Landais E., et al. Human circulating PD-1+CXCR3-CXCR5+ memory Tfh cells are highly functional and correlate with broadly neutralizing hiv antibody responses. Immunity 2013;39:758–769.

[31] Choi Y.S., Yang J.A., Yusuf I., et al. Bcl6 expressing follicular helper CD4 T cells are fate committed early and have the capacity to form memory. J Immunol 2013;190:4014–4026.

[32] Fuertes Marraco S.A., Neubert N.J., Verdeil G., Speiser D.E. Inhibitory receptors beyond T cell exhaustion. Front Immunol 2015;6:1–14.

[33] Attanasio J., Wherry E.J. Costimulatory and coinhibitory receptor pathways in infectious disease. Immunity 2016;44:1052–1068.

[34] Herati R.S., Muselman A., Vella L., et al. Successive annual influenza vaccination induces a recurrent oligoclonotypic memory response in circulating T follicular helper cells. Sci Immunol 2017;2. doi:10.1126/sciimmunol.aag2152.

[35] Chevalier N., Jarrossay D., Ho E., et al. CXCR5 expressing human central memory CD4 T cells and their relevance for humoral immune responses. J Immunol 2011;186:5556–5568.

[36] Iannello A., Boulassel M.-.R., Samarani S., et al. Dynamics and consequences of IL-21 production in HIV-Infected individuals: a longitudinal and cross-sectional study. J Immunol 2010;184:114.

[37] Shi J., Hou S., Fang Q., Liu X., Liu X., Qi H. PD-1 controls follicular T helper cell positioning and function. Immunity 2018;49:264–274.

[38] Bonecchi R., Bianchi G., Bordignon P.P., et al. Differential expression of chemokine receptors and chemotactic responsiveness of type 1 T helper cells (Th1s) and Th2s. J Exp Med 1998;187:129–134.

[39] Acosta-Rodriguez E.V., Rivino L., Geginat J., et al. Surface phenotype and antigenic specificity of human interleukin 17-producing T helper memory cells. Nat Immunol 2007;8:639–646.

[40] Schmitt N., Bentebibel S.-.E., Ueno H. Phenotype and functions of memory Tfh cells in human blood. Trends Immunol. 2014;35:436–442.

[41] Buggert M., Nguyen S., McLane L.M., et al. Limited immune surveillance in lymphoid tissue by cytolytic CD4+ T cells during health and HIV disease. PLoS Pathog 2018;14:e1006973.

[42] Gach J.S., Achenbach C.J., Chromikova V., et al. HIV-1 specific antibody titers and neutralization among chronically infected patients on long-term suppressive antiretroviral therapy (ART): a cross-sectional study. PLoS ONE 2014;9:e85371. –10.

[43] Binley J.M., Trkola A., Ketas T., et al. The effect of highly active antiretroviral therapy on binding and neutralizing antibody responses to human immunodeficiency virus type 1 infection. J Infect Dis 2000;182:945–949.

[44] Moody M.A., Pedroza-Pacheco I., Vandergrift N.A., et al. Immune perturbations in HIV-1-infected individuals who make broadly neutralizing antibodies. Sci Immunol 2016;1. aag0851.

[45] Cohen K., Altfeld M., Alter G., Stamatatos L. Early preservation of CXCR5+ PD-1+ helper T cells and B cell activation predict the breadth of neutralizing antibody responses in chronic HIV-1 infection. J. Virol. 2014;88:13310–13321.

[46] Pitcher C.J., Quittner C., Peterson D.M., et al. HIV-1-specific CD4+ T cells are detectable in most individuals with active HIV-1 infection, but decline with prolonged viral suppression. Nat. Med. 1999;5:518–525.

[47] Burton D.R., Ahmed R., Barouch D.H., et al. A blueprint for HIV vaccine discovery. Cell Host Microbe 2012;12:396–407.

[48] Goossens V.J., Wolffs P.F., van Loo I.H., Bruggeman C.A., Verbon A. CMV DNA levels and CMV gB subtypes in ART-naive HAART-treated patients: a 2-year follow-up study in The Netherlands. AIDS 2009;23:1425–1429.

[49] Casazza J.P., Brenchley J.M., Hill B.J., et al. Autocrine production of β-chemokines protects CMV-specific CD4+ T cells from HIV infection. PLoS Pathog 2009;5:e1000646.

[50] Velu V., Mylvaganam G.H., Gangadhara S., et al. Induction of Th1-biased T follicular helper (Tfh) cells in lymphoid tissues during chronic simian immunodeficiency virus infection defines functionally distinct germinal center Tfh cells. J Immunol 2016;197:1832–1842.

[51] Obeng-Adjei N., Portugal S., Tran T.M., et al. Circulating Th1 cell-type Tfh cells that exhibit impaired B cell help are preferentially activated during acute malaria in children. CellReports 2015;13:425–439.

[52] Vella L.A., Herati R.S., Wherry E.J. CD4(+) T cell differentiation in chronic viral infections: the Tfh perspective. Trends Mol Med 2017;23:1072–1087.

[53] Baxter A.E., O'Doherty U., Kaufmann D.E. Beyond the replication-competent HIV reservoir: transcription and translation-competent reservoirs. Retrovirology 2018;15:18.

[54] Estes J.D., Kityo C., Ssali F., et al. Defining total-body AIDS-virus burden with implications for curative strategies. Nat. Med. 2017;23:1271–1276.

[55] Stellbrink H.-J., van Lunzen J., Westby M., et al. Effects of interleukin-2 plus highly active antiretroviral therapy on HIV-1 replication and proviral DNA (COSMIC trial). AIDS 2002;16:1479–1487.

[56] Bruner K.M., Murray A.J., Pollack R.A., et al. Defective proviruses rapidly accumulate during acute HIV-1 infection. Nat. Med. 2016;22:1043–1049.

[57] Pauken K.E., Sammons M.A., Odorizzi P.M., et al. Epigenetic stability of exhausted T cells limits durability of reinvigoration by PD-1 blockade. Science 2016;354:1160–1165.

[58] Sen D.R., Kaminski J., Barnitz R.A., et al. The epigenetic landscape of T cell exhaustion. Science 2016;354:1165–1169.

[59] Youngblood B., Noto A., Porichis F., et al. Cutting edge: prolonged exposure to hiv reinforces a poised epigenetic program for PD-1 expression in virus-specific CD8 T cells. J Immunol 2013;191:540.

[60] Youngblood B., Oestreich K.J., Ha S.-.J., et al. Chronic virus infection enforces demethylation of the locus that encodes PD-1 in antigen-specific CD8(+) T cells. Immunity 2011;35:400–412.

[61] del Alcazar D., Wang Y., He C., et al. Mapping the lineage relationship between CXCR5(+) and CXCR5(-) CD4(+) T cells in HIV-Infected human lymph nodes. CellReports 2019;28:3047. –7.

[62] Recher M., Lang K.S., Hunziker L., et al. Deliberate removal of T cell help improves virus-neutralizing antibody production. Nat Immunol 2004;5:934–942.

[63] Preite S., Baumjohann D., Foglierini M., et al. Somatic mutations and affinity maturation are impaired by excessive numbers of T follicular helper cells and restored by Treg cells or memory T cells. Eur J Immunol 2015;45:3010–3021.

Figures

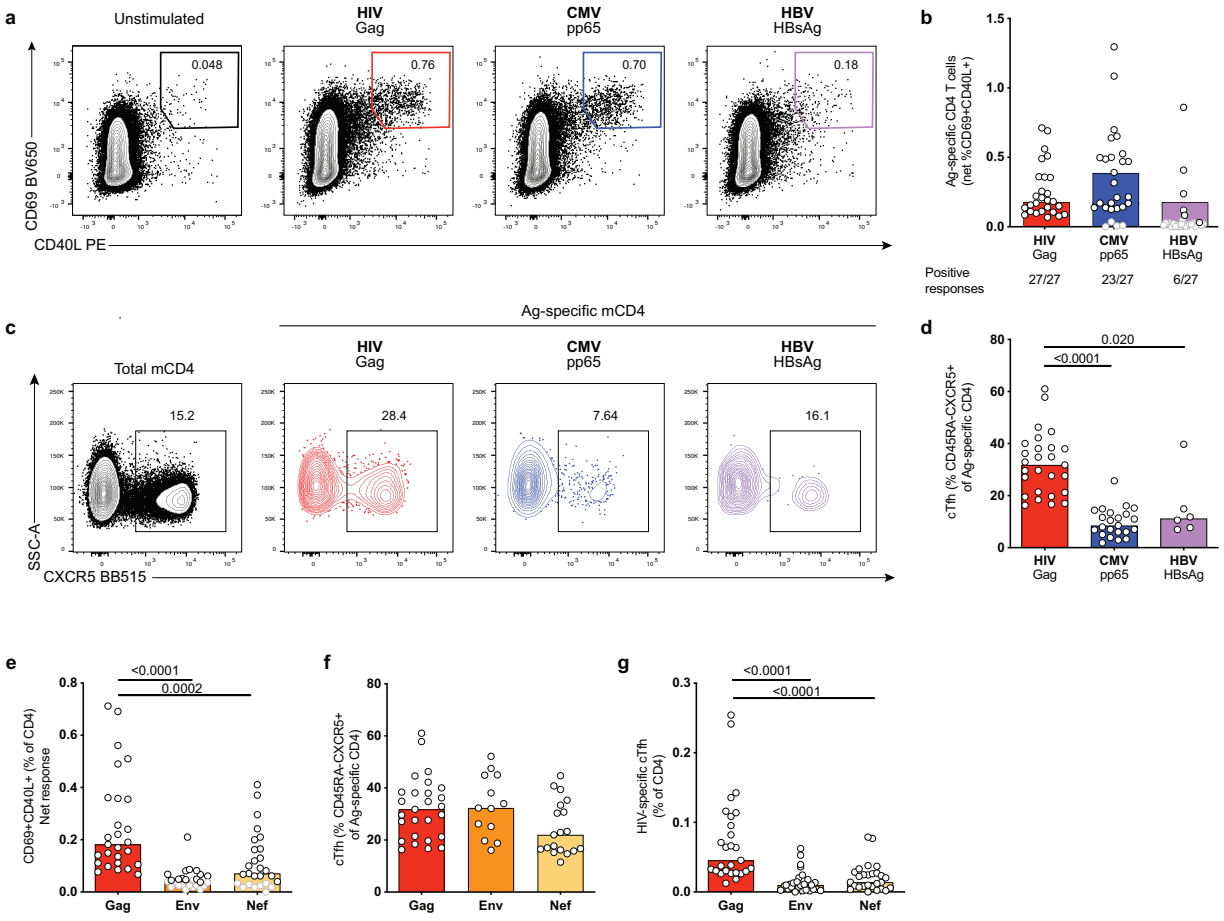

Figure 1 – **HIV-specific cTfh are expanded compared to CMV- and HBV-specific cTfh in ART-treated donors.**

PBMCs were stimulated for 9 h with peptide pools for HIV Gag, CMV pp65, HBV HBsAg or left unstimulated. Ag-specific CD4⁺ T cells were identified by the concurrent upregulation of CD40L and CD69 (AIM⁺ cells). (**a**) Example plots showing gating for CD69⁺CD40L⁺ for one representative donor (pre-gated on CD4⁺). (**b**) Net frequency of AIM⁺ Ag-specific CD4⁺ T cells. Responses greater than 2-fold over background are shown as black bordered circles, responses below this threshold are shown as gray-bordered symbols. Median values shown were calculated using responses greater than 2-fold over background only. Below each bar, numbers of individuals with positive responses for each antigen are shown. (**c**) Example plot showing gating of cTfh as memory CD4⁺ T cells expressing CXCR5. Left hand panel shows gating on total memory CD4⁺ (black). Ag-specific memory CD4⁺ T cells are shown as colored plots. (**d**) Quantification of results in (**c**). (**e**) Net frequency of HIV-specific CD4⁺ T cell responses identified using AIM assay. (**f**) Frequency of cTfh (CXCR5⁺) within HIV-specific CD4⁺ T cells (**g**) Frequency of HIV-specific cTfh of total CD4⁺ T cells. n = 27 for (**b**), (**e**) and (**g**); for (**d**): HIV Gag: n = 27, CMV pp65: n = 23, HBV HBsAg n = 6; for (**f**): HIV Gag: n = 27, Env: n = 13, Nef: n = 19. Bars represent median values. Only significant p-values are shown and were calculated by Kruskal–Wallis test with Dunn's post test. (For interpretation of the references to color in this figure legend, the reader is referred to the web version of this article.)

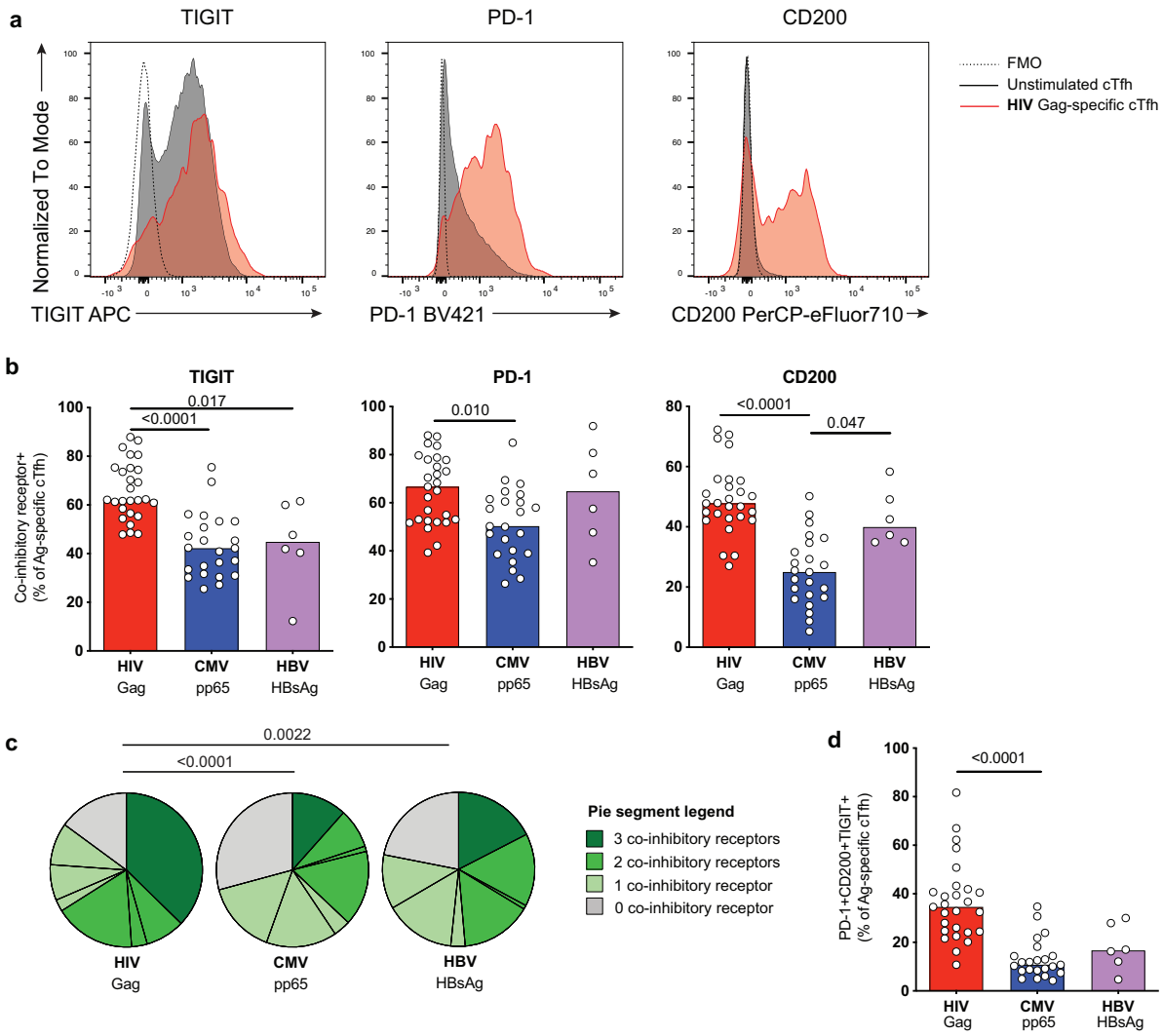

Figure 2 – **HIV-specific cTfh express multiple IRs despite viral suppression.**

cTfh specific for HIV, CMV and HBV were analyzed by flow cytometry for expression of the co-inhibitory receptors TIGIT, PD-1 and CD200. (**a**) Example plots showing expression of TIGIT, PD-1 or CD200 on unstimulated (black) or HIV-specific cTfh (red) from one representative donor. FMO controls are shown as dotted lines. (**b**) Frequency of TIGIT-, PD-1- or CD200-expressing Ag-specific cTfh. (**c**) Analysis of co-expression of TIGIT, PD-1 and CD200 on Ag-specific cTfh. (**d**) Comparison of frequency of $TIGIT^{+}CD200^{+}PD\text{-}1^{+}$ Ag-specific cTfh. n = 27 (HIV), n = 23 (CMV) or n = 6 (HBV) for (**b-d**). Significant p-values are shown in figure and were calculated by Kruskal–Wallis test with Dunn's post test (**b,d**) or permutation test (**c**). (For interpretation of the references to color in this figure legend, the reader is referred to the web version of this article.)

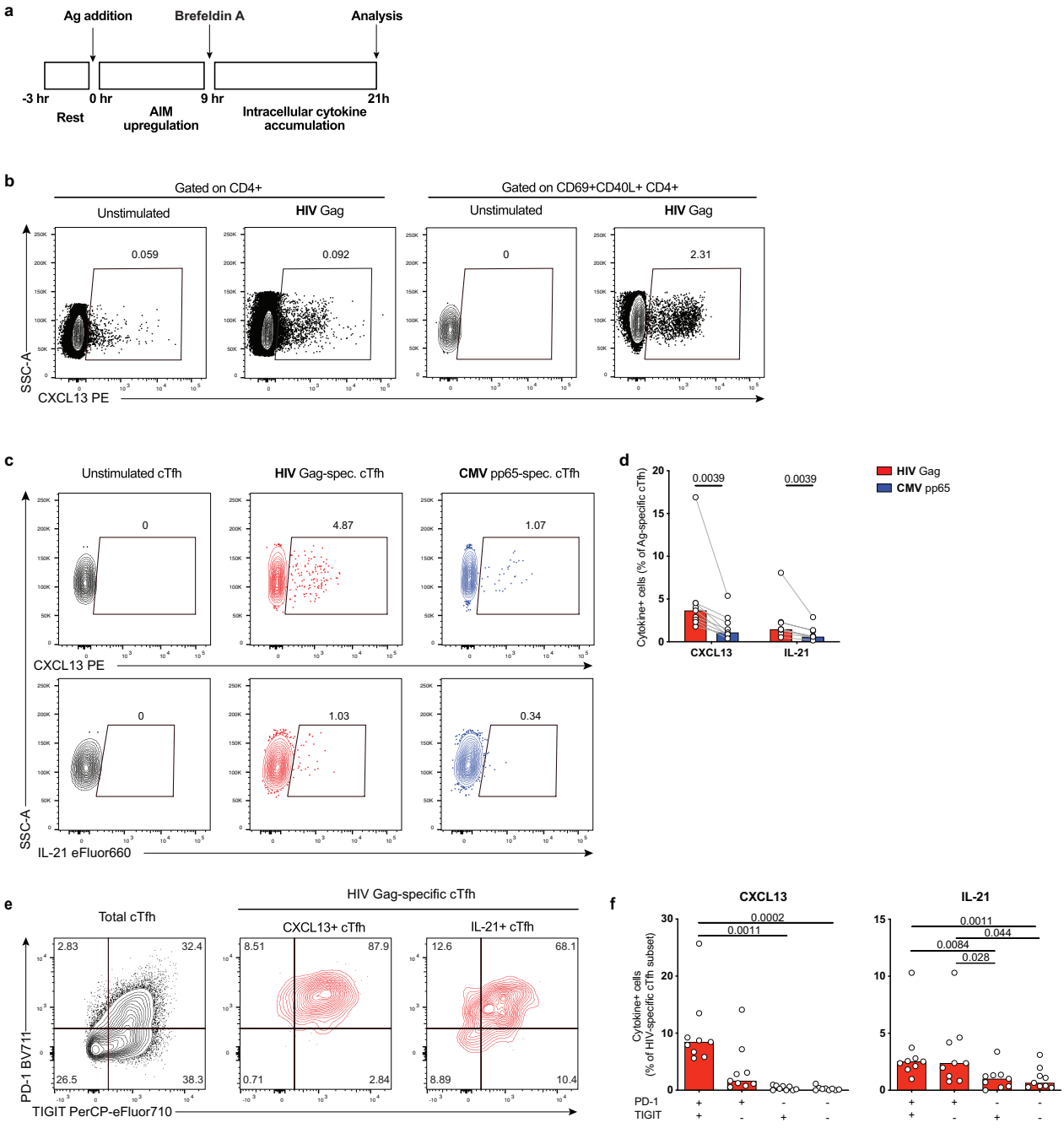

Figure 3 – **HIV-specific cTfh produce higher levels of Tfh cytokines than CMV-specific cTfh.**

Ag-specific cTfh responses were analyzed by flow cytometry for expression of CXCL13 and IL-21 using a delayed ICS assay. (**a**) Schematic representation of the delayed ICS assay. (**b**) Example plot showing CXCL13 expression in unstimulated or HIV-stimulated $CD4^+$ cells after gating on either total $CD4^+$ or $CD69^+CD40L^+$ Ag-specific $CD4^+$. Plots shown are from the same sample. (**c**) Example plot showing CXCL13 or IL-21 expression in $CD69^+CD40L^+$ cTfh. (**d**) Comparison of $cytokine^+$ HIV-specific vs CMV-specific cTfh. (**e**) Example plot showing phenotype of total cTfh cells (black) or HIV-specific $CXCL13^+$ or $IL\text{-}21^+$ cTfh (shown in red) based on PD-1 and TIGIT expression. (**f**) Frequency of $cytokine^+$ cells in cTfh subsets based on TIGIT/PD-1 expression. n = 9. Significant p-values shown were calculated by Wilcoxon test (**d**) or Friedman test with Dunn's post test (**f**). (For interpretation of the references to color in this figure legend, the reader is referred to the web version of this article.)

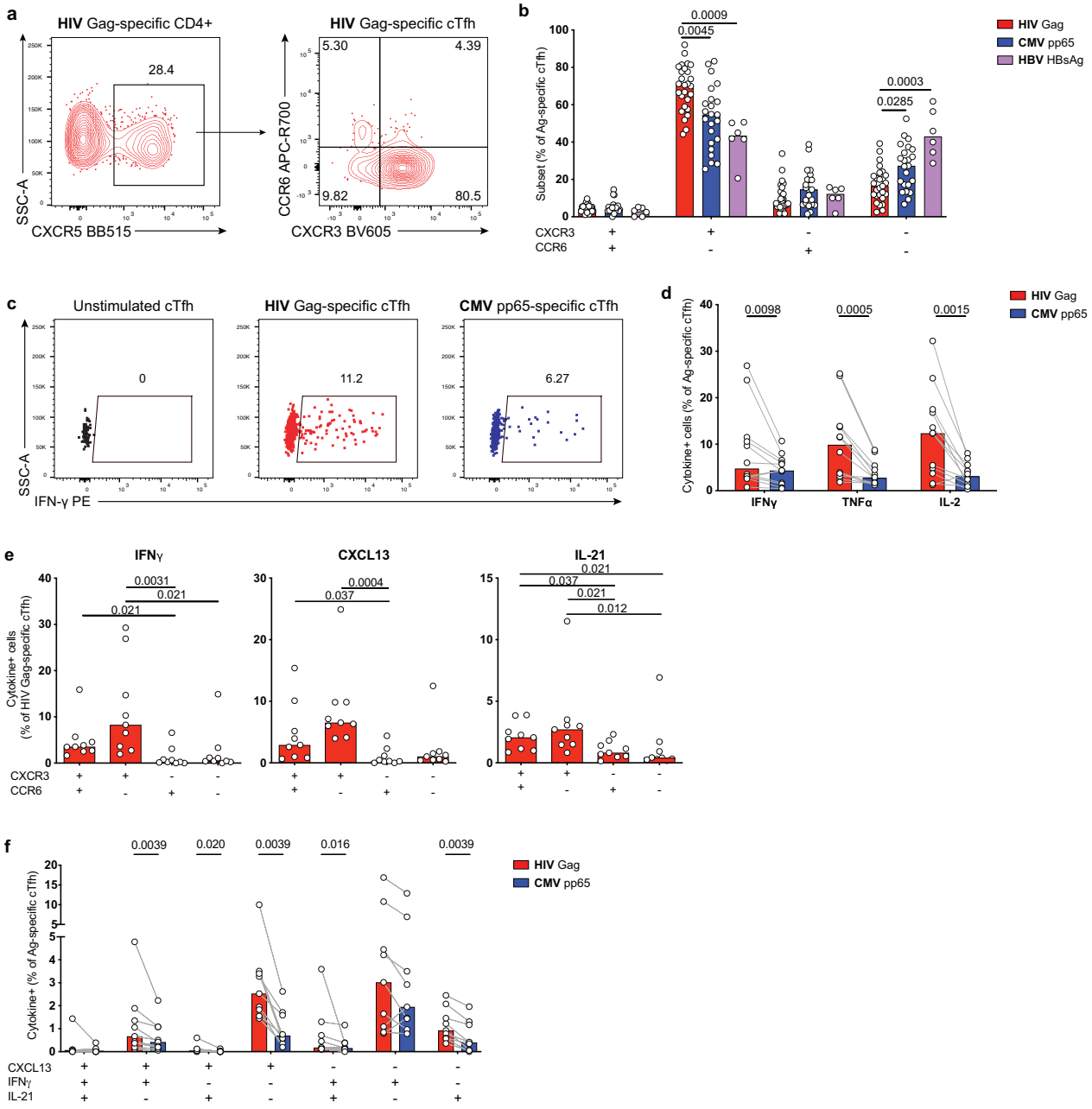

Figure 4 – **HIV-specific cTfh are predominantly Th1-polarized.**

(**a**) Example plot showing CXCR3/CCR6 expression on HIV-specific cTfh. (**b**) Comparison of Ag-specific cTfh subsets based on CXCR3/CCR6 coexpression. (**c**) Example plots showing expression of IFNγ in HIV- and CMV-specific cTfh. (**d**) Frequency of Th1-cytokine^{+} HIV- vs CMV-specific cTfh. (**e**) Frequency of HIV Gag-specific cTfh subsets expressing IFNγ, CXCL13 or IL-21. (**f**) Co-expression analysis of Ag-specific cTfh cells based on CXCL13, IFNγ and IL-21 expression. n = 27 (HIV), n = 23 (CMV) or n = 6 (HBV) for (**b**); n = 12 for (**d**), n = 9 for (**e,f**). P-values shown in figure were calculated by Kruskal–Wallis test with Dunn's post test (b), Wilcoxon test (d, f) or Friedman test with Dunn's post test (e).

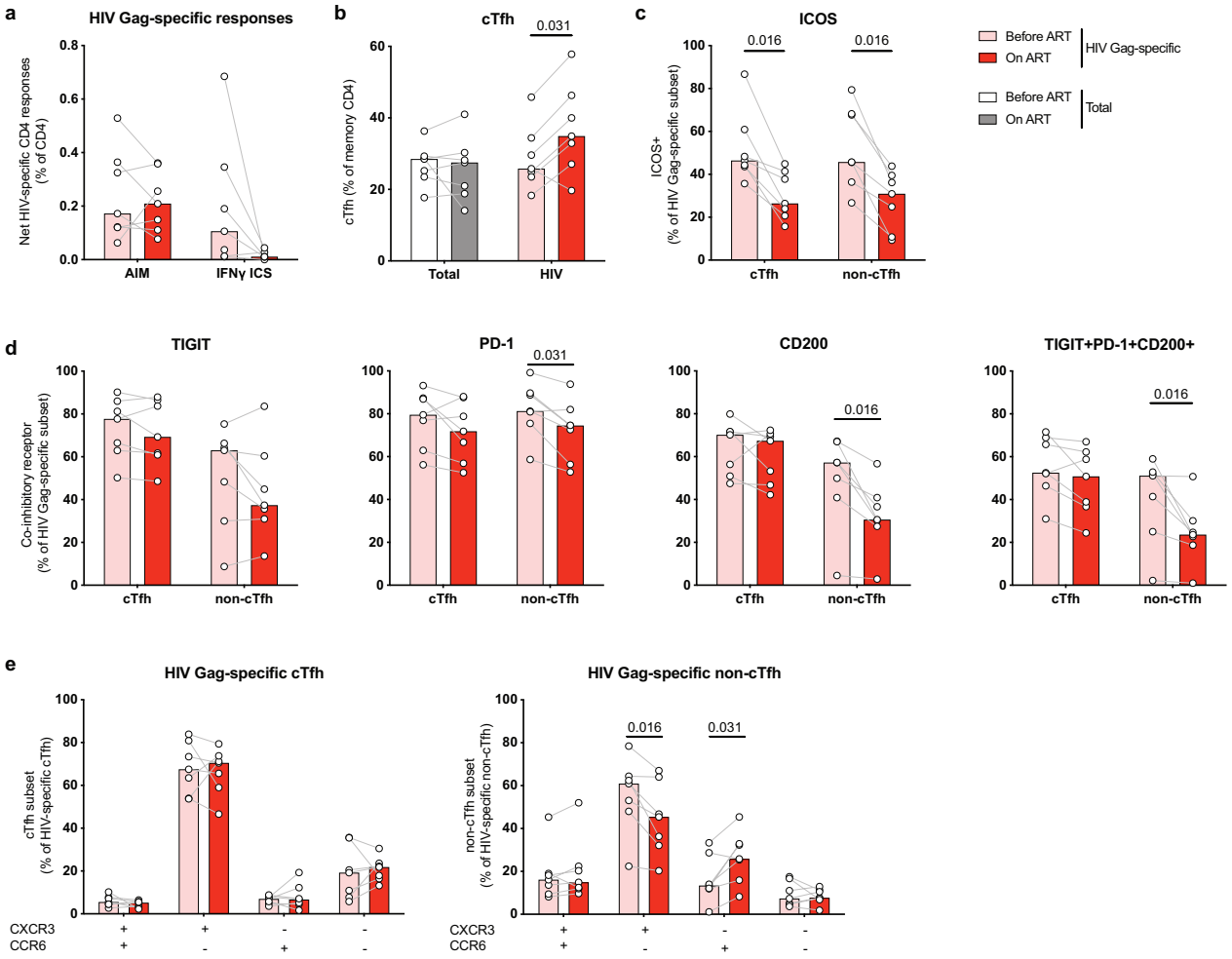

Figure 5 – **HIV-specific cTfh responses increase with initiation of ART and maintain expression of co-inhibitory receptors and a Th1-like phenotype.**

HIV-specific CD4⁺ responses were analyzed longitudinally using matched PBMCs samples obtained during chronic HIV infection (Before ART) or after 1.0–3.2 years of ART (On ART). (**a**) Net frequency of Ag-specific CD4⁺ responses identified by CD69/CD40L AIM assay or standard IFNγ ICS. (**b**) Frequency of total (left) or Ag-specific cells with cTfh phenotype (right), defined as CXCR5⁺ memory CD4⁺ T cells. (**c**) Frequency of Ag-specific CD4⁺ subsets expressing ICOS. (**d**) Single or co-expression analysis of IRs TIGIT, PD-1 or CD200 on HIV-specific cTfh or non-cTfh before vs after ART initiation. (**e**) Phenotypic analysis of HIV-specific cTfh (left) or non-cTfh (right) based on the expression of CXCR3 and CCR6 before and after ART initiation. n = 7 longitudinal pairs of untreated/treated HIV-infected donors. Significant p-values are shown in figure and were calculated by Wilcoxon test.

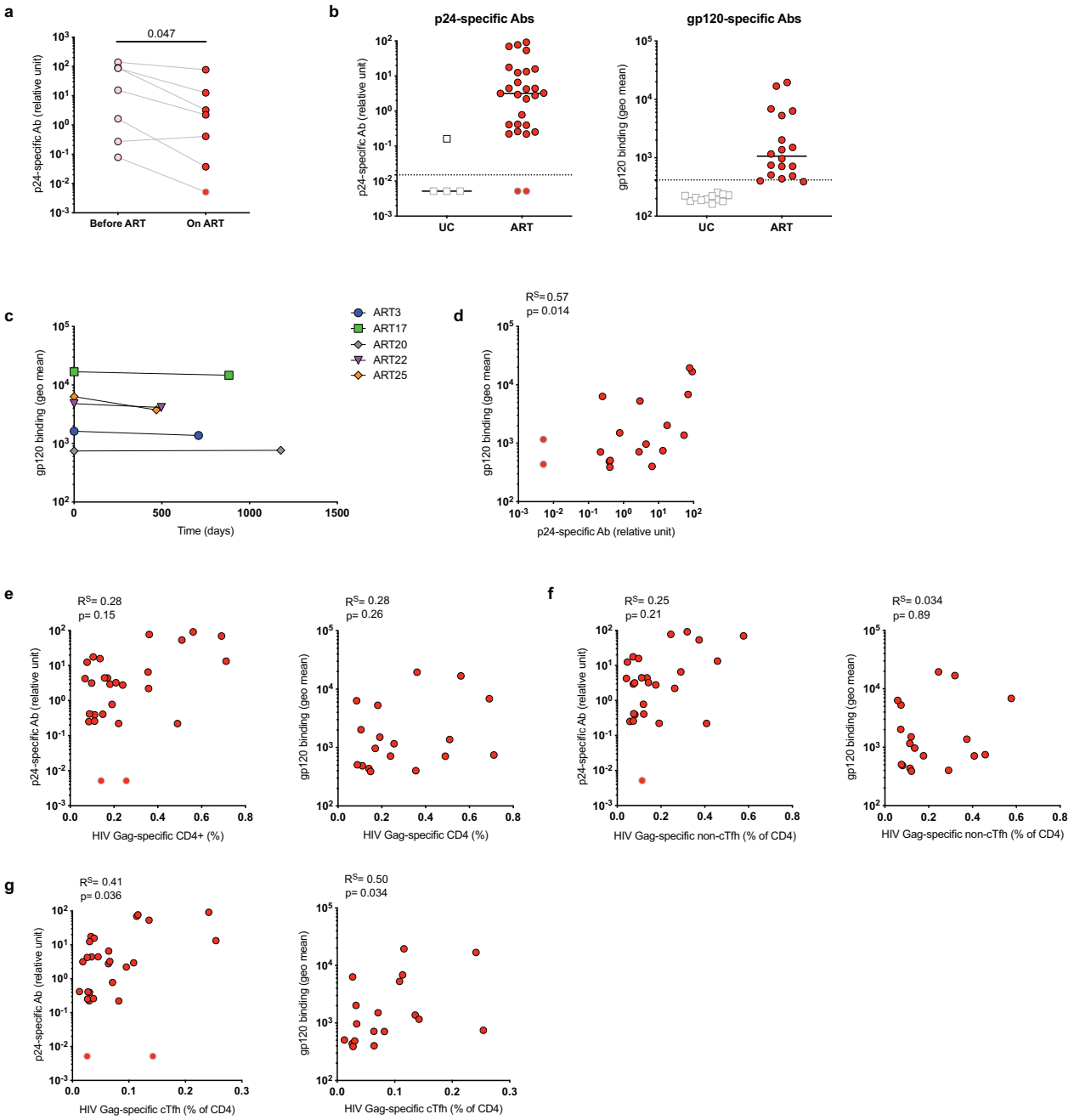

Figure 6 – **HIV-specific cTfh responses correlate with p24- and gp120-specific antibody levels in ART-treated donors.**

Plasma samples from HIV$^+$ donors were analyzed for HIV-specific Abs by ELISA (p24-Abs) or flow cytometry (gp120-Abs). (**a**) Longitudinal analysis of p24-specific Ab levels using matched plasma samples obtained during chronic untreated infection or during ART. (**b**) Level of p24- or gp120-specific Abs in ART-treated vs uninfected control (UC) donors. Dotted line represents limit of detection. (**c**) Longitudinal analysis of gp120-specific Abs using matched plasma samples from 2 different time points of long-term ART-treated subjects. (**d**) Correlation between p24- and gp120-specific Ab plasma levels. (**e-g**) Correlation between total HIV-specific CD4$^+$ T cells (**e**), HIV-specific non-cTfh (**f**) or HIV-specific cTfh (**g**) and levels of p24- or gp120-specific Abs, respectively. n = 7 for (**a**); p24-Abs: n = 4 UC and n = 27 ART, gp120-Abs: n = 12 UC and n = 18 ART for (**b**); n = 5 for (c); n = 18 for (**d**); p24-Abs: n = 27, gp120-Abs: n = 18 for (**e-g**). Gray-bordered symbols represent values below limit of detection. P values were calculated by Wilcoxon test (**a**) or Spearman correlation (**d-g**).

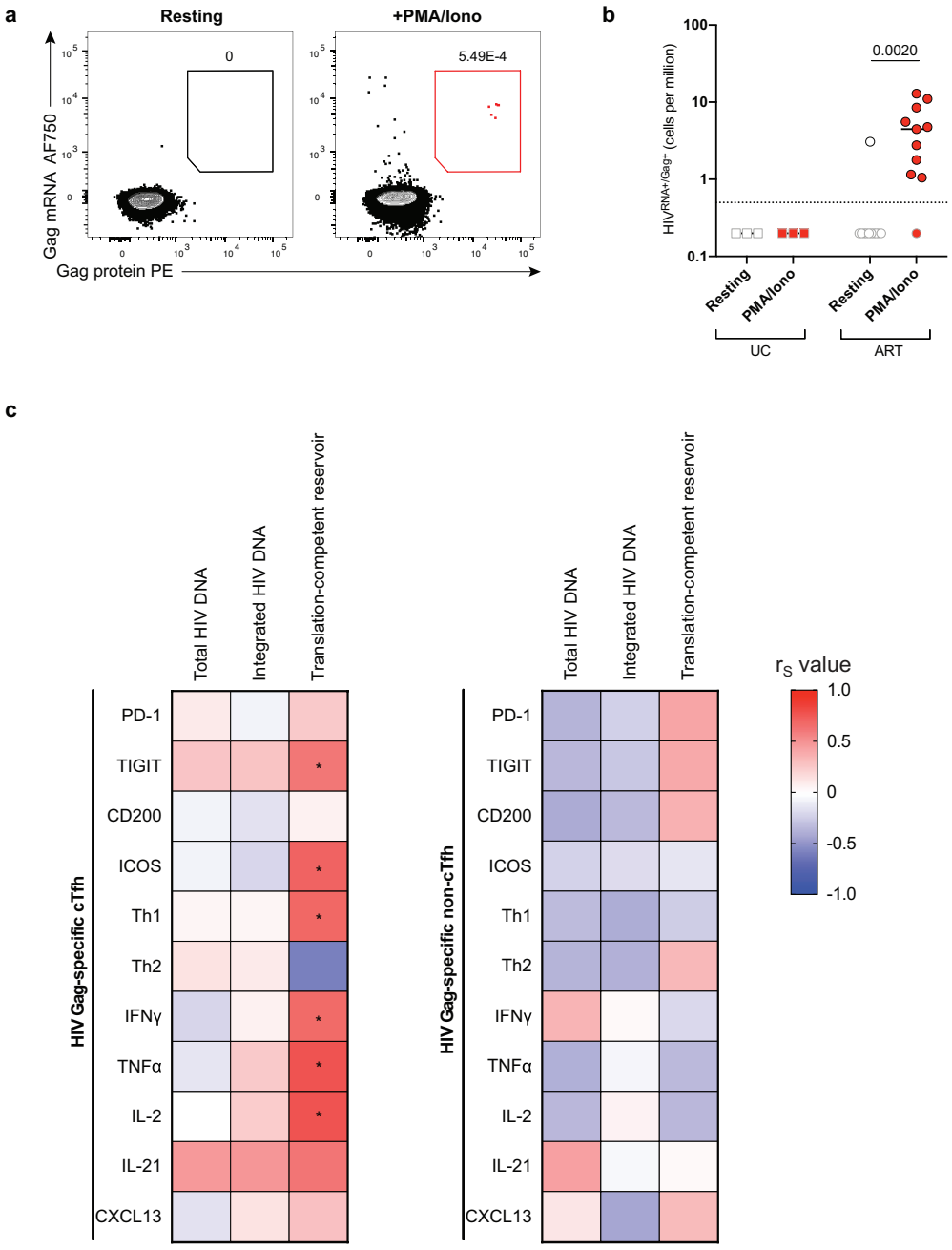

Figure 7 – **Th1-like phenotype and function of HIV-specific cTfh correlates with size of the translation-competent reservoir.**

(**a**) Example plot showing CD4⁺ T cells from one representative ART-treated donor expressing HIV *gag* mRNA and HIV Gag protein after resting or stimulation with PMA/Ionomycin. (**b**) Frequency of $HIV^{RNA+/Gag+}$ CD4⁺ T cells in uninfected control (UC) or ART-treated individuals in resting CD4⁺ or after PMA/Ionomycin stimulation. Gray-bordered symbols are below limit of detection (dotted line). Lines represent median values. (**c**) Heatmap showing associations between phenotype and function of HIV-specific cTfh (left graph) or HIV-specific non-cTfh (right graph) with total HIV DNA, integrated HIV DNA and translation-competent reservoir. Color represents R value for each association calculated and *p < 0.05 indicates significant correlations (Spearman correlation). n = 3 UC (uninfected control donors), n = 11 ART for (**b**); n = 23 ART for correlations with total or integrated HIV DNA, n = 11 for correlations with translation-competent reservoir (**c**). (For interpretation of the references to color in this figure legend, the reader is referred to the web version of this article.)

Supplementary Materials

Supplementary Figures

Supplementary Tables

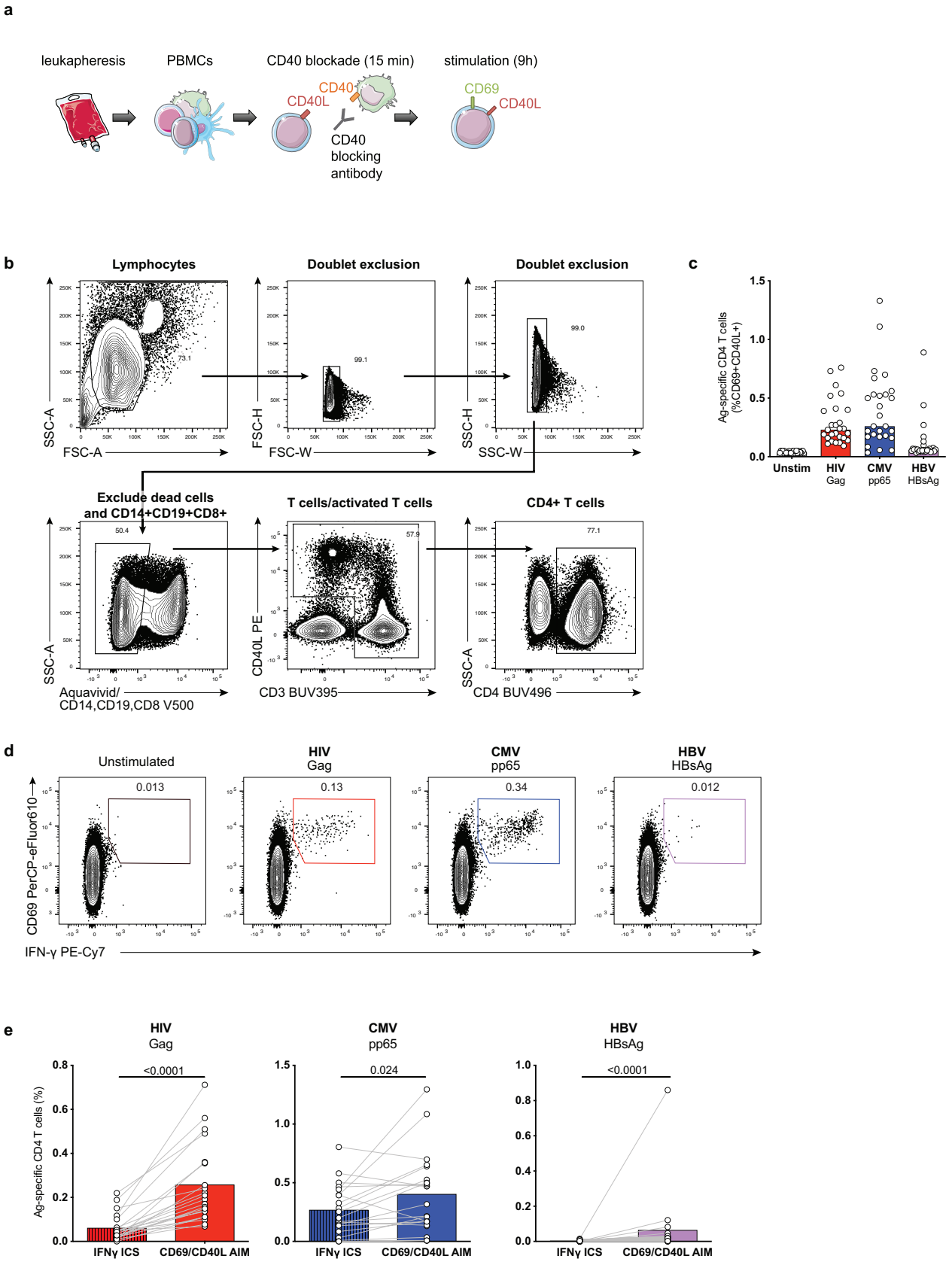
a
leukapheresis
PBMCs
CD40 blockade (15 min)
stimulation (9h)
CD40
CD40L
CD40 blocking antibody
CD69
CD40L
b
Lymphocytes
Doublet exclusion
Doublet exclusion
SSC-A
FSC-A
FSC-H
FSC-W
SSC-H
SSC-W
73.1
99.1
99.0
Exclude dead cells and CD14+CD19+CD8+
T cells/activated T cells
CD4+ T cells
50.4
57.9
77.1
Aquavivid/ CD14,CD19,CD8 V500
CD40L PE
CD3 BUV395
CD4 BUV496
c
Ag-specific CD4 T cells (%CD69+CD40L+)
Unstim
HIV Gag
CMV pp65
HBV HBsAg
d
Unstimulated
HIV Gag
CMV pp65
HBV HBsAg
0.013
0.13
0.34
0.012
CD69 PerCP-eFluor610
IFN-γ PE-Cy7
e
HIV Gag
CMV pp65
HBV HBsAg
<0.0001
0.024
<0.0001
Ag-specific CD4 T cells (%)
IFNγ ICS
CD69/CD40L AIM

Figure S1 **– CD69/CD40L assay identifies higher frequency of Ag-specific $CD4^+$ T cells compared to IFNγ ICS.**

(**a**) Protocol for AIM assay using peptide pool stimulation. (**b**) Gating strategy to identify $CD4^+$ T cells after 9h antigen stimulation. Due to CD3 downregulation on stimulated T cells, $CD3^-CD40L^+$ cells were included for analysis. (**c**) Frequency of $CD4^+$ T cell co-expressing CD69 and CD40L without stimulation (Unstim) or after Ag-stimulation. (**d**) Example plots showing $CD4^+$ T cells co-expressing CD69 and IFNγ without stimulation or after Ag-stimulation. (**e**) Paired comparison between Ag-specific $CD4^+$ T cell frequencies detected using the CD69/CD40L AIM assay or IFNγ ICS. n=27 for (**c**), n=23 for (**e**). Significant p values are shown in graph and were calculated by Wilcoxon test.

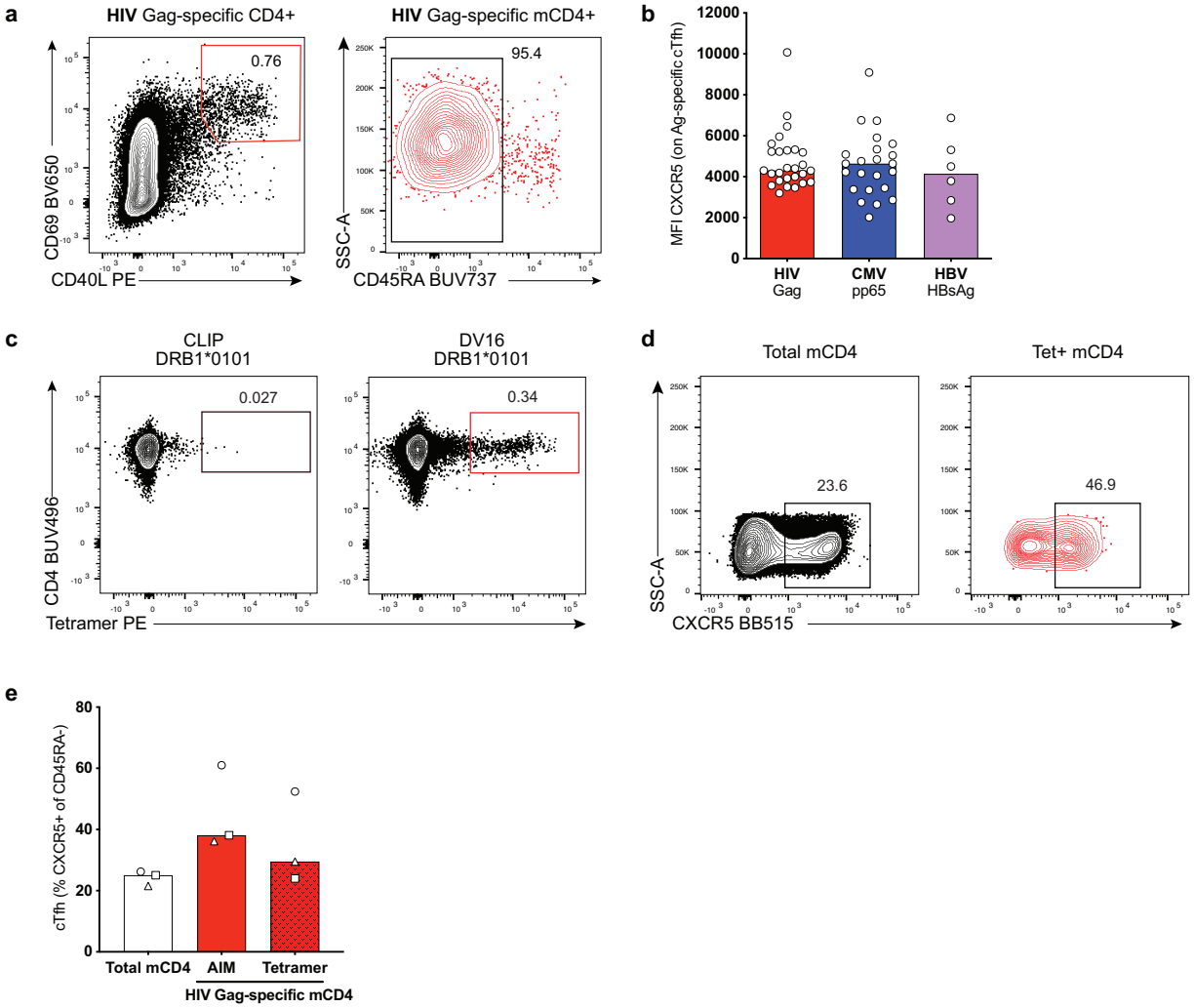

Figure S2 – **Tetramer staining confirms frequency of CXCR5⁺ within HIV Gag-specific CD4⁺ T cells.**

(**a**) Example plot showing gating strategy for identification of memory CD45RA⁻ cells within Ag-specific CD69⁺CD40L⁺ CD4⁺ T cells. (**b**) Comparison of CXCR5 MFI on Ag-specific cTfh cells. (**c**) Example tetramer staining showing identification of HIV Gag-specific CD4⁺ T cells using tetramer DV16 DRB1*0101. Left: CLIP control staining. (**d**) Example staining showing frequency of CXCR5⁺ in total memory CD4⁺ (mCD4) (left, black) or HIV-specific mCD4⁺ (right, red) identified by tetramer staining. (**e**) Comparison of frequency of cTfh cells in total mCD4 or HIV Gag-specific mCD4⁺ identified by either AIM assay or tetramer staining. Different symbols represent the three different individuals. n=27 (HIV), n=23 (CMV), n=6 (HBV) for (**b**), n=3 for (**e**).

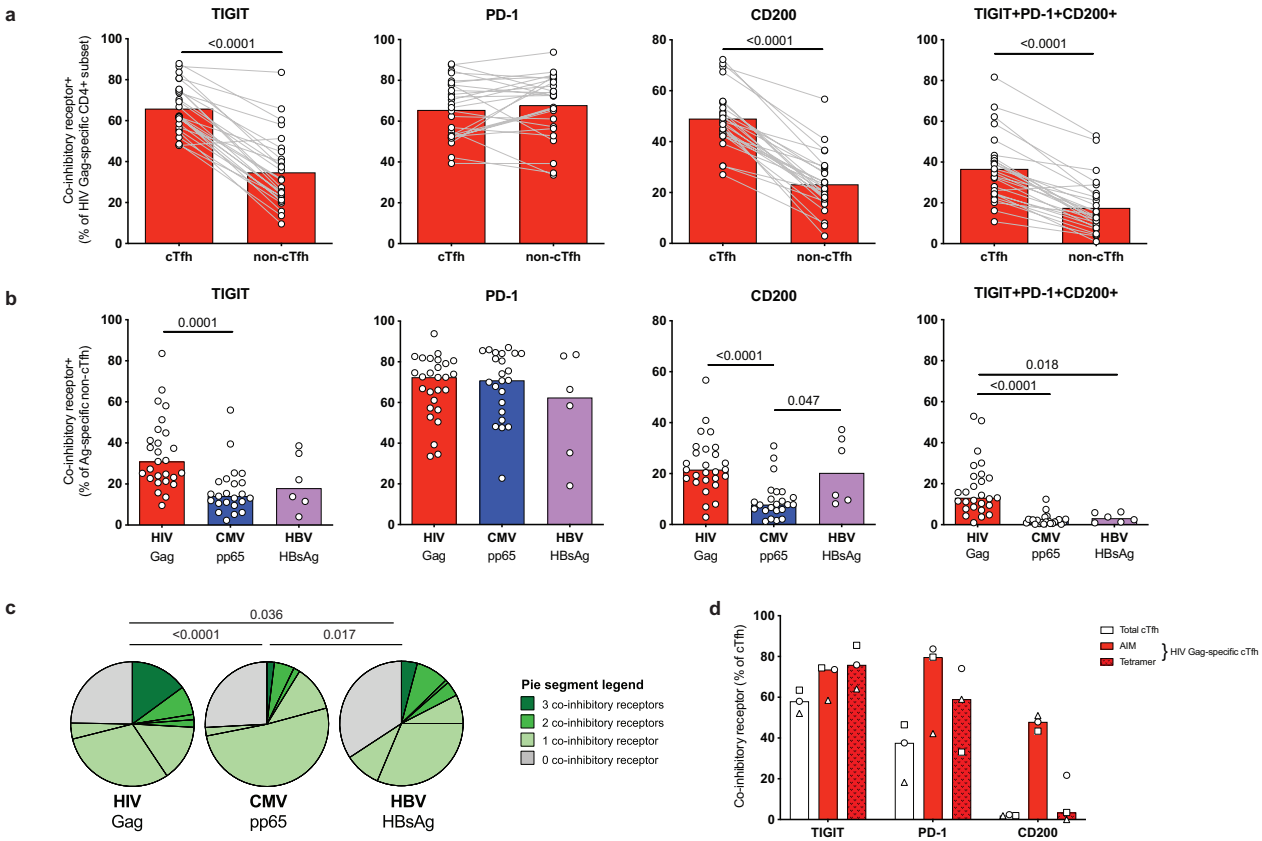

Figure S3 – **Elevated frequency of IR$^+$ cells in HIV-specific compared to CMV- or HBV-specific non-cTfh cells.**

(**a**) Frequency of TIGIT, PD-1 and CD200-expressing cells or triple-positive HIV-specific cTfh vs non-cTfh. (**b**) Comparison of frequency of TIGIT$^+$, PD-1$^+$, CD200$^+$ or TIGIT$^+$PD-1$^+$CD200$^+$ on Ag-specific non-cTfh. (**c**) Coexpression analysis of TIGIT, PD-1 and CD200 on Ag-specific non-cTfh cells. (**d**) Comparison of frequency of IR$^+$ cells in total (white) or HIV Gag-specific cTfh (red) identified by either AIM assay or tetramer staining. Different symbols represent the three different individuals. n=27 (HIV), n=23 (CMV), n=6 (HBV) except for (**d**) (n=3). Significant p values are shown in graphs and were calculated by Wilcoxon test (**a**), Kruskal-Wallis test with Dunn's multiple comparison post-test (**b**) or permutation test (**c**).

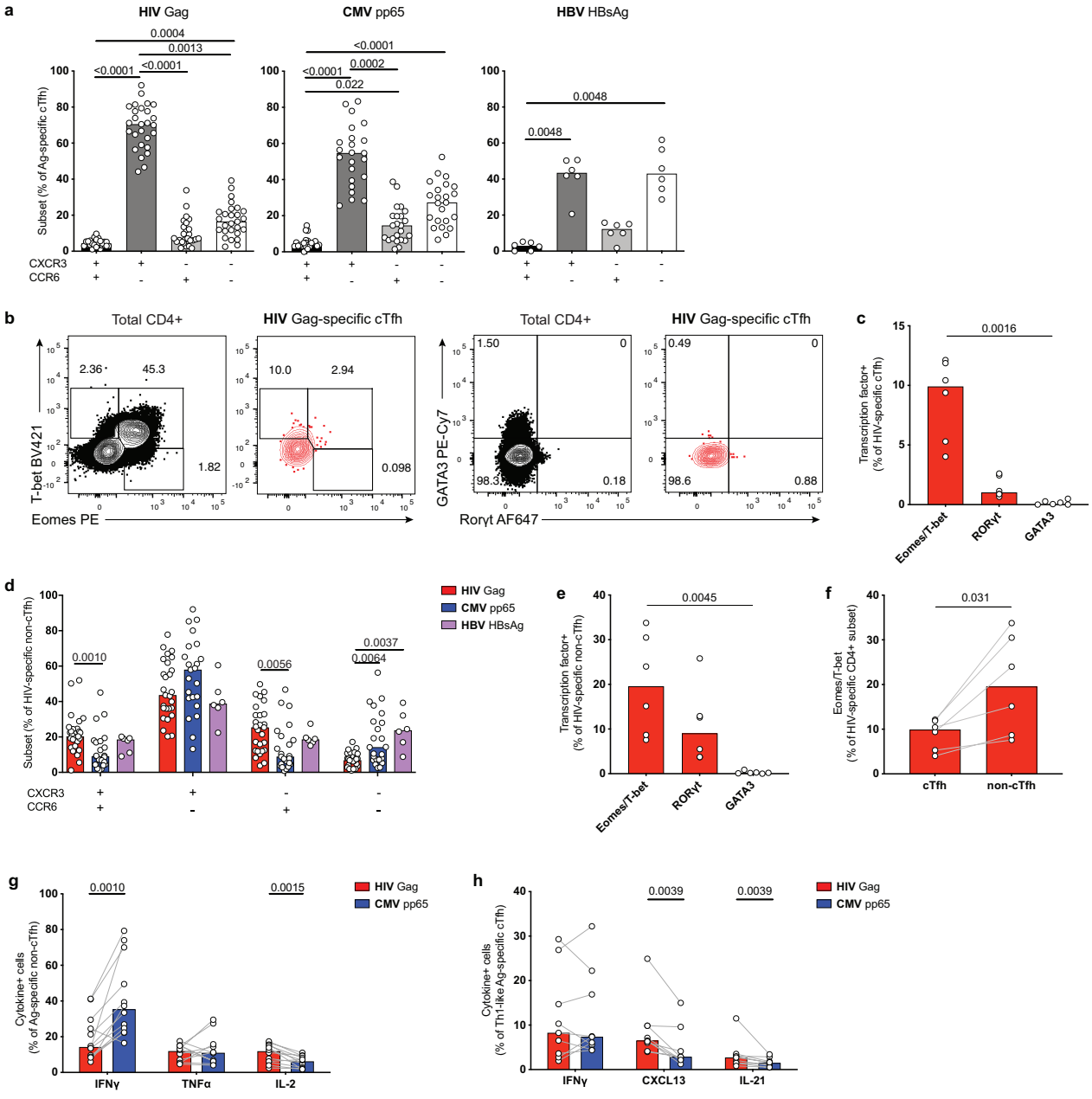

Figure S4 – **HIV-specific non-cTfh cells do not show preferential Th1-like polarization and function compared to CMV-specific non-cTfh cells.**

(**a**) Polarization profile of Ag-specific cTfh based on CXCR3/CCR6 expression. (**b**) Example plots showing the expression of Eomes and T-bet (left) or Rorγt and GATA3 (right) in total CD4$^+$ (black graphs) or HIV-specific cTfh cells (red graphs). (**c**) Frequency of HIV-specific cTfh cells expressing Eomes and/or T-bet (Eomes/Tbet) or Rorγt or GATA3. (**d**) Comparison of frequency of non-cTfh subsets identified by CXCR3 and CCR6 coexpression patterns. (**e**) Frequency of HIV-specific non-cTfh cells expressing Eomes and/or T-bet (Eomes/Tbet) or Rorγt or GATA3. (**f**) Comparison of frequency of Eomes$^+$ and/or T-bet$^+$ HIV-specific cTfh versus non-cTfh. (**g**) Comparison of cytokine$^+$ cells in HIV- vs CMV-specific non-cTfh responses. (**h**) Frequency of Ag-specific Th1-like cTfh expressing IFNγ, CXCL13 or IL-21. n=27 (HIV), n=23 (CMV), n=6 (HBV) for (**a,d**), n=6 for (**c,e,f**), n=12 for (**g**), n=9 for (**h**). Significant p values are shown in graphs and were calculated by Friedman test with Dunn's post test (**a,c,e**), Kruskal-Wallis test with Dunn's post test (**d**) or Wilcoxon test (**f,g,h**).

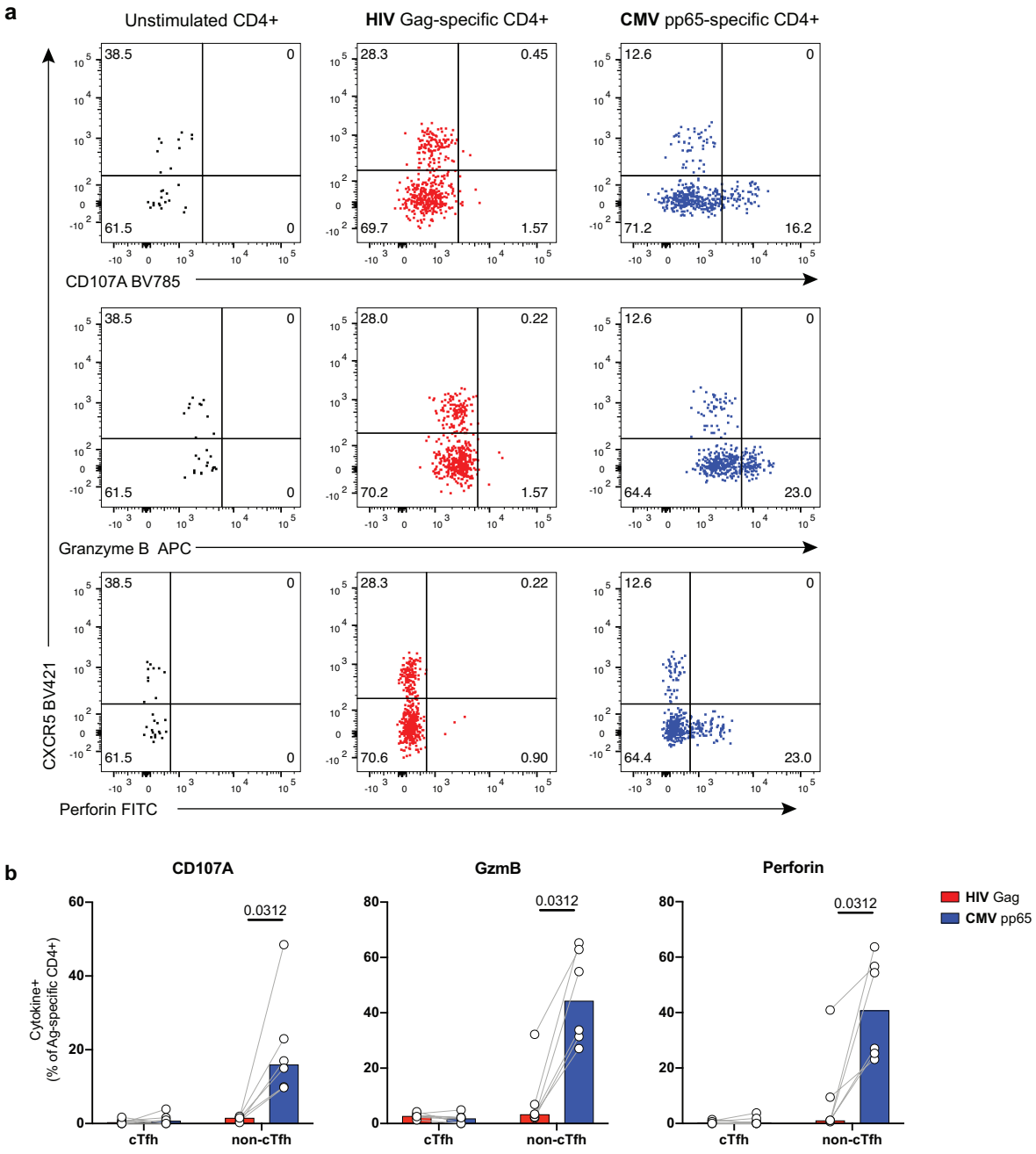

Figure S5 – **Ag-specific cTfh cells rarely express cytolytic markers**

Ag-specific CD4⁺ responses were analyzed by flow cytometry for expression of CD107A, granzyme B (GzmB) or perforin using standard ICS. (**a**) Example plot showing CD107A, GzmB or perforin expression in unstimulated, HIV- or CMV-stimulated CD4⁺ cells after gating on CD69⁺CD40L⁺ CD4⁺. Plots shown are from the same sample. (**b**) Frequency of cytokine⁺ cells in HIV- or CMV-specific cTfh or non-cTfh. n=6. Significant p-values shown were calculated by Wilcoxon test (**b**).

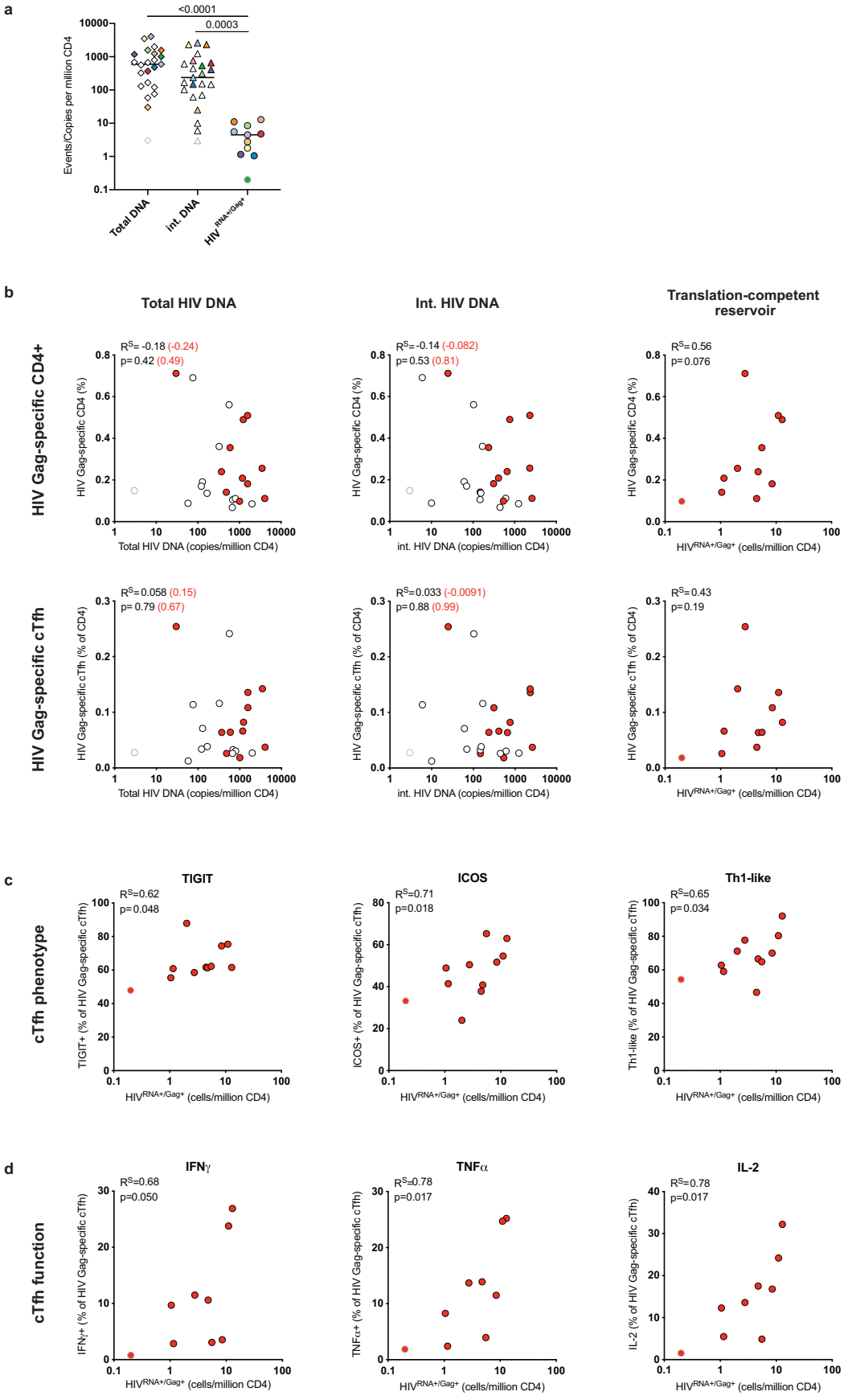
a
<0.0001
0.0003
Events/Copies per million CD4
Total DNA
Int. DNA
HIV RNA+/Gag+
b
Total HIV DNA
Int. HIV DNA
Translation-competent reservoir
HIV Gag-specific CD4+
HIV Gag-specific CD4 (%)
RS= -0.18 (-0.24)
p= 0.42 (0.49)
Total HIV DNA (copies/million CD4)
RS= -0.14 (-0.082)
p= 0.53 (0.81)
int. HIV DNA (copies/million CD4)
RS= 0.56
p= 0.076
HIVRNA+/Gag+ (cells/million CD4)
HIV Gag-specific cTfh
HIV Gag-specific cTfh (% of CD4)
RS= 0.058 (0.15)
p= 0.79 (0.67)
RS= 0.033 (-0.0091)
p= 0.88 (0.99)
RS= 0.43
p= 0.19
c
cTfh phenotype
TIGIT
ICOS
Th1-like
TIGIT+ (% of HIV Gag-specific cTfh)
RS=0.62
p=0.048
ICOS+ (% of HIV Gag-specific cTfh)
RS=0.71
p=0.018
Th1-like (% of HIV Gag-specific cTfh)
RS=0.65
p=0.034
d
cTfh function
IFNγ
TNFα
IL-2
IFNγ+ (% of HIV Gag-specific cTfh)
RS=0.68
p=0.050
TNFα+ (% of HIV Gag-specific cTfh)
RS=0.78
p=0.017
IL-2 (% of HIV Gag-specific cTfh)
RS=0.78
p=0.017

Figure S6 – **Associations between HIV reservoir measurements and HIV-specific CD4$^+$ T cell responses.**

(**a**) Comparison of HIV reservoir measured by different techniques; total HIV DNA PCR (Total DNA), integrated HIV DNA PCR (int. DNA) and HIV$^{RNA/Gag}$ assay with PMA/iono stimulation. Individuals measured with all 3 techniques are color-coded. (**b**) Associations between size of the HIV reservoir measured by different techniques and frequency of HIV-specific CD4$^+$ T cell or HIV-specific cTfh responses. Red symbols represent individuals measured with all 3 techniques. For associations with total and int. HIV DNA: Black R^S and p values were calculated using all individuals, red values were calculated using the 11 individuals measured by HIV$^{RNA/Gag}$ assay. (**c-d**) Association between the translation-competent reservoir (HIV$^{RNA+/Gag+}$ CD4$^+$ T cells) and phenotypic (**c**) or Th1-associated functional markers (**d**) of HIV-specific cTfh cells. n=23 for total and int. HIV DNA (**a-b**); n=11 for HIV$^{RNA/Gag}$ assay (**a-d**). P values shown in graphs were calculated by Kruskal-Wallis test with Dunn's post test (**a**), R^S and p values shown in (**b-d**) were calculated using Spearman correlation.

Table S1 – **Clinical data ART-treated individuals**

Donor ID	Age	Sex	Time on ART (months)	Plasma HIV RNA (copies/ml)	CD4 count	CD8 count	CD4/CD8 ratio	CMV IgG	CMV IgM	HBsAg	HBS (IU/L)	HBC
ART1	51	M	181	< 40	533	416	1.28	123.5 POS	0.06 NEG	Neg	0.57	Neg
ART2	28	M	15	< 40	694	585	1.20	176.5 POS	0.21 NEG	Neg	1.57	Pos
ART3	52	M	303	< 40	194	729	0.27	> 250 POS	0.18 NEG	Neg	333.3	Pos
ART4	23	M	28	< 40	762	255	2.99	0 NEG	0.05 NEG	Neg	5	Neg
ART5	44	M	30	< 40	403	915	0.44	227.2 POS	0.37 NEG	Neg	14.28	Pos
ART6	61	M	41	< 40	499	255	1.96	0 NEG	0.41 NEG	Neg	55.03	Neg
ART7	48	M	120	< 40	101	191	0.53	249 POS	0.05 NEG	Neg	28.67	Pos
ART8	50	M	15	< 40	700	872	0.80	198.1 POS	0.06 NEG	Neg	36.09	Pos
ART9	43	M	12	< 40	482	788	0.6	182.6 POS	0.10 NEG	Neg	5.04	Neg
ART10	43	M	53	< 40	793	570	1.4	> 250 POS	0.15 NEG	Neg	48.2	pos
ART11	19	M	121	< 40	708	700	1.01	145.7 POS	0.13 NEG	Neg	55.31	Neg
ART12	58	M	106	< 40	619	553	1.12	127.3 POS	0.70 NEG	Neg	131.33	Neg
ART13	51	M	86	<40	630	560	1.14	> 250 POS	0.42 NEG	Neg	3.09	Neg
ART14	51	M	130	< 40	941	576	1.63	> 250 POS	0.08 NEG	Neg	5.02	Neg
ART15	56	M	114	< 40	677	504	1.34	170.8 POS	0.11 NEG	Neg	6.75	Pos
ART16	38	M	15	< 40	1091	462	2.4	> 250 POS	0.89 NEG	Neg	1.01	Neg
ART17	58	M	84	<40	278	493	0.61	> 250 POS	0.44 NEG	Neg	20.02	Neg
ART18	23	M	15	< 40	738	642	1.2	135.9 POS	0.10 NEG	Neg	>1000	Neg
ART19	36	M	14	< 40	729	5663	0.13	> 250 POS	1.04 POS	Neg	0	Neg
ART20	55	M	190	74	398	1301	0.31	1.3 NEG	0.11 NEG	Neg	49.39	Pos
ART21	59	M	238	< 40	843	398	2.12	197.6 POS	0.41 NEG	Neg	94.5	Pos
ART22	52	M	297	< 40	333	1018	0.33	> 250 POS	0.60 NEG	Neg	137.28	Pos
ART23	24	M	19	< 40	394	725	0.54	110.6 POS	0.82 NEG	Neg	> 1000	Neg
ART24	58	M	20	< 40	728	202	3.6	0.1 NEG	0.07 NEG	Neg	0.04	Neg
ART25	47	M	52	< 40	356	807	0.44	101.6 POS	0.28 NEG	Neg	973.08	Pos
ART26	40	M	17	< 40	940	804	1.20	> 250 POS	NA	Neg	0	Neg
ART27	70	M	210	< 40	381	953	0.4	> 250 POS	0.18 NEG	Neg	227.02	Pos
ART28	40	M	14	< 40	616	1245	0.49	180.4 POS	0.15 NEG	Neg	39.51	Neg

Table S2 – **Clinical data untreated chronic HIV-infected individuals for longitudinal pre-/post-ART analysis**

Donor ID	Corresponding treated donor ID	Age	Sex	Plasma HIV RNA (copies/ml)	CD4 count	CD8 count	CD4/CD8 ratio
UNT1	ART2	26	M	2700	597	539	1.11
UNT2	ART8	48	M	15250	416	1198	0.35
UNT3	ART9	41	M	6671	406	914	0.44
UNT4	ART18	22	M	35859	597	1920	0.3
UNT5	ART19	34	M	1000000	300	4372	0.07
UNT6	ART26	38	M	6235	1036	1162	0.9
UNT7	ART28	38	M	132886	320	1372	0.23

Table S3 – **Clinical data HIV-uninfected control individuals**

Donor ID	Age	Sex	CD4 count	CD8 count	CD4/CD8 ratio
UC1	37	F	705	441	1.56
UC2	50	M	1758	426	4.10
UC3	64	M	552	310	1.78
UC4	39	F	717	349	2.05
UC5	70	M	771	451	1.71
UC6	66	M	599	171	3.50
UC7	39	M	1400	678	2.06
UC8	60	F	670	460	1.46
UC9	44	F	754	319	2.36
UC10	55	M	518	245	2.11
UC11	43	M	1053	353	2.98
UC12	59	M	882	257	3.43
UC13	51	M	922	322	2.86
UC14	62	M	482	466	1.03
UC15	45	M	550	113	4.80

Table S4 – **Antibodies, tetramer and RNA probe used for flow cytometry staining.**

Target	Fluorochrome	Clone	Supplier	Detection	Catalogue number	RRID
CCR6	APC-R700	11A9	BD Biosciences	In culture	565173	AB_2739092
CCR6	BUV737	11A9	BD Biosciences	In culture	564377	AB_2738778
CD14	V500	M5E2	BD Biosciences	Surface	562693	AB_2737727
CD14	BV510	M5E2	Biolegend	Surface	367124	AB_2716229
CD16	BV510	3G8	BD Biosciences	Surface	302048	AB_2562085
CD19	V500	H1B19	BD Biosciences	Surface	561121	AB_10562391
CD19	BV510	H1B19	Biolegend	Surface	302241	AB_2561381
CD200	PerCP-eFluor710	OX-104	ThermoFisher	Surface	46-5200-82	AB_10598213
CD3	BUV395	UCHT1	BD Biosciences	Surface	563548	AB_2744387
CD3	BV650	UCHT1	BD Biosciences	Surface	563852	AB_2744391
CD3	APC-Fire750	UCHT1	Biolegend	Surface	300470	AB_2629689
CD3	BB700	HIT1a	BD Biosciences	Surface	742207	-
CD4	BUV496	SK3	BD Biosciences	Surface	564652	AB_2744422
CD4	BV605	RPA-T4	BD Biosciences	Surface	562658	AB_2744420
CD40L	PE	TRAP1	BD Biosciences	Surface/intracellular	555700	AB_396050
CD40L	BV421	TRAP1	BD Biosciences	Surface	563886	AB_2738466
CD40L	BV711	24-31	Biolegend	Surface	310838	AB_2563845
CD45RA	BUV737	HI100	BD Biosciences	Surface	564442	AB_2738810
CD45RA	PE-Dazzle594	HI100	Biolegend	Surface	304145	AB_2564078
CD56	BV510	NCAM16.2	BD Biosciences	Surface	563041	AB_2732786
CD69	BV650	FN50	Biolegend	Surface	310934	AB_2563158
CD69	PerCP-eFluor710	FN50	ThermoFisher	Intracellular	46-0699-42	AB_2573694
CD69	BUV395	FN50	BD Biosciences	Surface	564364	AB_2738770
CD8	V500	RPA-T8	BD Biosciences	Surface	561617	AB_10896281
CD8	APC-Fire750	SK1	Biolegend	Surface	344745	AB_2572094
CD8	BV510	SK1	Biolegend	Surface	344732	AB_2564624
CD107A	BV785	H4A3	Biolegend	In culture	328644	AB_2565968
CXCL13	PE	53610	R&D	Intracellular	IC801P	AB_2086047
CXCR3	BV605	G025H7	Biolegend	In culture	353728	AB_2563157
CXCR5	BB515	RF8B2	BD Biosciences	In culture	564624	AB_2738871
CXCR5	BV421	J252D8	Biolegend	In culture	356920	AB_2562303
CXCR5	BV605	J252D4	Biolegend	In culture	356929	AB_2566226
EOMES	PE	WD1928	ThermoFisher	Intranuclear	12-4877-41	AB_2572614
GATA3	PE-Cy7	TWAJ	ThermoFisher	Intranuclear	25-9966-41	AB_2573567
Granzyme B	APC	QA16A02	Biolegend	Intracellular	372203	AB_2687027
HIV Gag	RD1	KC57	Beckman Coulter	Intracellular	6604667	AB_1575989
HIV Gag RNA	Alexa Fluor 750	-	ThermoFisher	Intracellular	VF6-6000975	-
ICOS	PE-Cy7	ISA-3	ThermoFisher	Surface	25-9948-41	AB_1518755
IFNγ	PE-Cy7	B27	BD Biosciences	Intracellular	557643	AB_396760
IFNγ	PE	B27	Biolegend	Intracellular	506506	AB_315439
IL-2	Alexa Fluor 488	MQ1-17H12	Biolegend	Intracellular	500314	AB_493368
IL-21	eFluor660	eBio3A3-n2	ThermoFisher	Intracellular	50-7219-42	AB_10598202
PD-1	BV421	EH12.2H7	Biolegend	Surface	329920	AB_10960742
PD-1	BV711	EH12.2H7	Biolegend	Surface	329928	AB_2562911
Perforin	FITC	B-D48	Biolegend	Intracellular	353310	AB_2571967
RORγt	Alexa Fluor 647	Q21-559	BD Biosciences	Intranuclear	563620	AB_2738324
T-bet	BV421	O4-46	BD Biosciences	Intranuclear	563318	AB_2687543
Tetramer	PE	-	NIH Tetramer Core Facility-Emory University	Surface	-	-
TIGIT	APC	MBSA43	ThermoFisher	Surface	17-9500-41	AB_2573305
TIGIT	PerCP-eFluor710	MBSA43	ThermoFisher	Surface	46-9500-42	AB_10853679
TIGIT	PE-Cy7	MBSA43	ThermoFisher	Surface	25-9500-41	AB_2573547
TNFα	APC	MAb11	BD Biosciences	Intracellular	562084	AB_10893226

Chapter 4 Manuscript 2: Combination anti-HIV-1 antibody therapy is associated with increased virus-specific T cell immunity

Status: This research article was published in *Nature Medicine,* February 3, 2020; https://doi.org/10.1038/s41591-019-0747-1

Author contribution: Julia Niessl, Amy E. Baxter, Michel C. Nussenzweig and Daniel E. Kaufmann designed the immunological studies. Marina Caskey, Florian Klein and Michel C. Nussenzweig designed the trial from which the samples were obtained. Julia Niessl performed ICS, AIM, ELISpot and HIV inhibition assays and analyzed the data. Amy E. Baxter contributed to AIM assay design and assisted with the AIM experiments. Pilar Mendoza, Mila Jankovic and Ching-Lan Lu performed HIV DNA sequencing experiments. Mathieu Dubé provided input on manuscript content and data representation. Henning Gruell, Yehuda Z. Cohen and Allison L. Butler contributed to recruitment and clinical assessments. Irina Shimeliovich coordinated and performed sample processing. Julia Niessl, Michel C. Nussenzweig and Daniel E. Kaufmann interpreted the data and wrote the paper with all co-authors' assistance. Michel C. Nussenzweig and Daniel E. Kaufmann provided supervision.

Combination anti-HIV-1 antibody therapy is associated with increased virus-specific T cell immunity

Julia Niessl[1,2,3], Amy E. Baxter[1,2,3,9], Pilar Mendoza[4], Mila Jankovic[4], Yehuda Z. Cohen[4], Allison L. Butler[4], Ching-Lan Lu[4,10], Mathieu Dubé[1], Irina Shimeliovich[4], Henning Gruell[5,6,7], Florian Klein[5,7,8], Marina Caskey[4], Michel C. Nussenzweig[4,11*] and Daniel E. Kaufmann[1,2,3,11*]

[1]Research Centre of the Centre Hospitalier de l'Université de Montréal (CRCHUM), Montréal, Montreal, QC, Canada

[2]Université de Montréal, Montreal, QC, Canada

[3]Consortium for HIV/AIDS Vaccine Development (CHAVD), La Jolla, CA USA

[4]Laboratory of Molecular Immunology, The Rockefeller University, New York, NY, USA

[5]Laboratory of Experimental Immunology, Institute of Virology, Faculty of Medicine and University Hospital Cologne, University of Cologne, Cologne, Germany

[6]Department I of Internal Medicine, Faculty of Medicine and University Hospital Cologne, University of Cologne, Cologne, Germany

[7]German Center for Infection Research (DZIF), Partner Site Bonn-Cologne, Cologne, Germany

[8]Center for Molecular Medicine Cologne, University of Cologne, Cologne, Germany

[9]Present address: Perelman School of Medicine, University of Pennsylvania, Philadelphia, PA, USA

[10]Present address: Department of Internal Medicine, Columbia University Medical Center, New York, NY, USA

[11]These authors contributed equally: Michel C. Nussenzweig, Daniel E. Kaufmann

*email: nussen@mail.rockefeller.edu; daniel.kaufmann@umontreal.ca

Abstract

Combination antiretroviral therapy (ART) is highly effective in controlling human immunodeficiency virus (HIV)-1 but requires lifelong medication due to the existence of a latent viral reservoir[1,2]. Potent broadly neutralizing antibodies (bNAbs) represent a potential alternative or adjuvant to ART. In addition to suppressing viremia, bNAbs may have T cell immunomodulatory effects as seen for other forms of immunotherapy[3]. However, this has not been established in individuals who are infected with HIV-1. Here, we document increased HIV-1 Gag-specific $CD8^+$ T cell responses in the peripheral blood of all nine study participants who were infected with HIV-1 with suppressed blood viremia, while receiving bNAb therapy during ART interruption[4]. Increased $CD4^+$ T cell responses were detected in eight individuals. The increased T cell responses were due both to newly detectable reactivity to HIV-1 Gag epitopes and the expansion of pre-existing measurable responses. These data demonstrate that bNAb therapy during ART interruption is associated with enhanced HIV-1-specific T cell responses. Whether these augmented T cell responses can contribute to bNAb-mediated viral control remains to be determined.

HIV-1 infection is characterized by high initial levels of plasma viremia that are variably controlled by virus-specific $CD8^+$ T cell responses[5,6]. Individuals who fail to control viremia, rapidly develop immunodeficiency. In contrast, strong, broad HIV-specific $CD8^+$ and $CD4^+$ T cell responses have been associated with spontaneous viral control (that is, elite controllers, viral load <50 copies per ml) and delayed progression to AIDS[7–9]. ART is highly effective in maintaining viral suppression but does not boost host antiviral immunity because it limits antigen availability. In contrast, antibodies do not prevent virus replication or production and, unlike small molecule drugs, they have dual functionality; variable domains neutralize the virus and constant domains (Fc) engage the host immune system[3]. In humanized mice, Fc interactions lead to accelerated clearance of viruses and infected cells[10]. bNAb administration to macaques infected with chimeric simian and human immunodeficiency viruses (SHIV) is associated with $CD8^+$ T cell-dependent lasting control in a fraction of the treated animals[11]. In humans, bNAb monotherapy was associated with increased T cell responses in 9 of 12 individuals; however, this occurred after rebound viremia in all but 3 individuals[12]. Whether bNAb therapy has a positive impact on HIV-1-specific T cell immune responses in infected humans with prolonged suppression during ART interruption has not been determined. In a phase 1b clinical trial, individuals who were infected with HIV-1 and on ART were infused with a combination of two bNAbs, 3BNC117 and 10-1074, at 0, 3 and 6 weeks (Fig. 1a)[4]. ART was interrupted 2 d after the first antibody infusion. Nine bNAb-infused individuals harboring viruses sensitive to both bNAbs maintained viral suppression for at least 15 weeks following analytical treatment interruption (ATI) (Extended Data Fig. 1a,b)[4]. Individuals who were infected with HIV-1 and on ART show stable or decreasing levels of HIV-1-specific $CD8^+$ and $CD4^+$ T cell responses over time[13–15]. To determine whether the combination of bNAb treatment and ATI was associated with alterations of $CD8^+$ and $CD4^+$ T cell responses to HIV-1, we analyzed the peripheral blood of the nine individuals on bNAb+ATI at baseline (week −2) and during bNAb-mediated suppression (weeks 6/7, 12 and 18; Extended Data Fig. 1b; week 18 samples were limited to seven individuals). Peripheral blood mononuclear cells (PBMCs) were stimulated with an HIV-1 Consensus B Gag peptide pool. $CD8^+$ T cells were analyzed for expression of interferon (IFN)-γ, tumor necrosis factor (TNF)-α, macrophage inflammatory protein (MIP)1-β and the degranulation marker CD107A; $CD4^+$ T cells were analyzed for expression of IFN-γ, TNF-α, interleukin (IL)-2 and CD40L (Supplementary Table 1 and Supplementary Fig. 1a–c). In line with previous reports[13–15], anti-HIV-1 T cell responses in individuals on long-term viral suppression by ART alone remained stable over time (Extended Data Fig. 2a,b). In contrast, the frequency of antigen-specific $CD8^+$ T cells expressing IFN-γ, TNF-α, MIP1-β and/or CD107A increased significantly in all nine individuals receiving bNAbs during ATI after 6/7 weeks (Fig. 1b and

Extended Data Fig. 3a). Of note, bNAb plasma levels were highest at this time point[4] (Extended Data Fig. 1b). $CD8^+$ T cell responses decreased by week 12 in six individuals but remained significantly elevated for IFN-γ, TNF-α and MIP1-β when compared to baseline. At week 18, when antibody levels were 2–3 orders of magnitude below the week 6/7 peak, $CD8^+$ T cell responses were similar to week 12, but interpretation of these data was limited by the small sample size (Fig. 1b). $CD4^+$ T cells expressing IFN-γ, CD40L, TNF-α and/or IL-2 in response to Gag also increased significantly between baseline and week 6/7 in eight bNAb+ATI individuals (Fig. 1c). When measured individually, only CD40L and TNF-α remained significantly elevated at week 12 and no responses were significantly elevated at week 18. However, the total frequency of $cytokine^+$ $CD4^+$ T cells (percentage of cells positive for one or more cytokines or functional markers) was above baseline at all time points tested (Fig. 1c). In contrast, cytomegalovirus (CMV) pp65-specific T cell responses remained unchanged (Extended Data Fig. 4a,b), suggesting that the increased T cell immunity in bNAb+ATI individuals was specific to HIV-1. In summary, $CD8^+$ and $CD4^+$ T cell responses to Gag were most prominent at week 6/7 but remained elevated for weeks after the last antibody dose in individuals who remained suppressed while receiving bNAbs during ATI.

Two additional individuals recruited to the study harbored antibody-resistant viruses and showed early rebound after ATI (9245 and 9251, Extended Data Fig. 5a,b)[4]. Gag-specific T cell responses in both participants were analyzed at baseline, week 6/7 and week 11 or 12 after reinitiation of ART. Where the frequency of $cytokine^+$ cells for $CD8^+$ and $CD4^+$ increased for individual 9245, the responses decreased for 9251 (Extended Data Fig. 5c), consistently with rebound viremia being sufficient to increase $CD8^+$ T cell responses in some individuals[16]. Polyfunctional HIV-1-specific $CD8^+$ T cells have been associated with enhanced HIV-1 control[9,17], whereas other studies reported superior antiviral functions of MIP1-β monofunctional cells[18]. To examine Gag-specific T cells in bNAb+ATI individuals for poly-functional responses, we performed coexpression analysis using Boolean gating. Gag-specific $CD8^+$ T cells coexpressing IFN-γ, TNF-α, MIP1-β and CD107A were significantly increased at weeks 6/7 and 12 after receiving bNAb therapy (Fig. 2a). However, the greatest absolute increase in $CD8^+$ T cell responses to Gag was associated with expansion of $MIP1\text{-}\beta^+$ single-positive cells (Fig. 2a). In addition, the frequency of $CD4^+$ T cells expressing IFN-γ or CD40L alone or in combination with other functions and IL-2/TNF-α-double positive cells was also increased (Fig. 2b). Thus, several subsets of Gag-specific mono- or polyfunctional $CD8^+$ and $CD4^+$ T cells were augmented at weeks 6/7 and 12 compared to baseline for bNAb-treated individuals (Fig. 2a,b).

Activation-induced marker (AIM) assays give a broader overview of the total peptide-reactive T cell response and identify cells without cytokine expression or expressing cytokines that are challenging to detect by intracellular cytokine staining (ICS)[19,20]. We therefore used the AIM assay as an alternative, cytokine-independent method to confirm our findings obtained by ICS. $CD4^+$ or $CD8^+AIM^+$ cells were identified as $CD69^+$ programmed death ligand (PD-L)1^+ or $CD69^+4\text{-}1BB^+$ or $PD\text{-}L1^+4\text{-}1BB^+$ after Gag peptide pool stimulation (Supplementary Fig. 2 and Supplementary Table 2). Similarly to ICS, we found increased Gag-specific T cell responses in seven ($CD8^+$) or six ($CD4^+$) out of nine bNAb+ATI individuals at week 12 compared to baseline (Fig. 3a,b). As expected[19], the frequency of Gag-specific $CD4^+$ and $CD8^+$ T cells was higher in the AIM assay but correlated with ICS (Fig. 3c,d, $r = 0.64$). We did not detect changes in human leukocyte antigen (HLA)-DR^+CD38^+ or programmed cell death (PD)-1^+ cells within AIM^+ Gag-specific T cell responses at week 12 versus baseline (Extended Data Fig. 6). We further used the AIM assay to investigate responses to less immunodominant HIV-1 antigens with expected lower frequencies than Gag. In contrast to Gag, we did not find a significant increase in HIV-1-specific T cell responses directed against HIV-1 Pol, Nef, gp120 or gp41 at the cohort level (Fig. 3e). Nevertheless, enhanced $CD8^+$ and/or $CD4^+$ T cell responses to these HIV-1 proteins were noted in several individuals at week 12 compared to week −2, including against gp120 and gp41 (Extended Data Fig. 7a,b). Specifically, the two individuals with controlled viremia beyond 30 weeks showed increased $CD8^+$ and $CD4^+$ responses to nearly all HIV-1 antigens tested at week 12 (Extended Data Fig. 7a–c, participants 9254 and 9255). This was not seen in individuals who rebounded before week 26 after ATI (Extended Data Fig. 7a–c, participants 9241, 9242, 9243, 9244, 9246, 9247 and 9252). However, the association between prolonged control and breadth in these two individuals is anecdotal. Larger studies will be required to understand the precise relationship between prolonged control, bNAb therapy and enhanced breadth of T cell immunity.

To determine whether the increased HIV-1 Gag-specific T cell responses were directed against pre-existing or new peptide epitopes, we stimulated PBMCs with a peptide library spanning the entire HIV Gag protein Consensus B sequence (Supplementary Table 3) and compared IFN-γ responses before and after ATI for the nine bNAb+ATI individuals. IFN-γ ELISpot responses were detectable for six study participants (Fig. 4a–d, Extended Data Fig. 8 and Supplementary Table 4). Four individuals from these six (9244, 9246, 9252 and 9255) broadened the IFN-γ ELISpot response to Gag during ATI (Fig. 4a–d and Extended Data Fig. 8f). Overall, 41% (9 of 22) of the detectable responses in these six individuals at week 12 were directed against Gag epitopes that did not induce a detectable response at baseline (new responses: red dots and section, Fig. 4e,f). In contrast, none of the Gag responses detected at baseline were lost by week 12. Finally, several

individuals with detectable responses at week 12 had IFN-γ ELISpot responses against the major homology region (peptide 69-76, Gag285-304; Fig. 4g), a highly conserved motif in the gag gene of all retroviruses[21]. Thus, the increased IFN-γ responses that developed during bNAb therapy result from increased breadth and magnitude of detectable peptide-specific responses.

To determine whether the increased HIV-1-specific T cell response could eliminate HIV-1-infected cells in vitro, we performed HIV-1 viral inhibition assays[22]. $CD4^+$ T cells from participants 9246 and 9252 at baseline were infected with $HIV\text{-}1_{BaL}$ and cultured either alone or in the presence of $CD8^+$ T cells isolated from the same individuals before and after ATI (Extended Data Fig. 9a and Supplementary Table 5). Participant 9252 showed increased suppression of $HIV\text{-}1_{BaL}$ in vitro at week 12 compared to baseline (Extended Data Fig. 9b). However, 9246 was uninformative with no detectable impact on $HIV\text{-}1_{BaL}$ outgrowth at baseline or week 12 (Extended Data Fig. 9b). Given the importance of HIV-1-specific $CD8^+$ T cells in controlling viral replication, we also examined rebound viruses for mutations in HIV-1 *gag* in the seven individuals who rebounded before week 30. When compared to week −2 or 12, HIV-1 *gag* DNA from rebound plasma showed no consistent evidence for cytotoxic lymphocyte escape (Extended Data Fig. 10).

HIV-1-specific T cell responses likely play a key role in spontaneous control of HIV-1 viremia in elite controllers[7–9]. However, most individuals exhibit partial control of viral replication as evidenced by suppression of initial peak viremia by 1–2 orders of magnitude for prolonged periods of time before developing AIDS-defining clinical complications[23]. ART is highly effective in further suppressing viremia but fails to enhance virus-specific immunity possibly because of decreased viral antigen availability. In contrast, bNAb therapy in SHIV-infected rhesus macaques induces long-lasting $CD8^+$ T cell-mediated viral suppression in a subset of the animals[11,24]. Our data indicate that individuals who are infected with HIV-1, receiving bNAb therapy during ATI, show increased T cell immunity to HIV-1, including reactivity to Gag epitopes that were undetectable before bNAb administration. Specifically, we identified increased frequencies of MIP1-β-expressing $CD8^+$ T cells, which have been associated with control of viremia[18]. However, notably, the observational nature of this trial does not allow the determination of whether the observed expansion of HIV-1-specific T cell responses in bNAb-treated humans contributes to viral control. Previous clinical trials in individuals who are infected with HIV-1, who underwent ATI in the absence of immune intervention, showed increased HIV-1-specific T cell responses that coincided with plasma viral rebound, suggesting that this boost in antiviral immunity was induced by increased viral replication[16,25]. The increased T cell responses in individual 9245 are consistent with these observations (Extended Data Fig. 5). In contrast, our results demonstrate increased

HIV-1 Gag-specific $CD8^+$ and $CD4^+$ T cell immunity in bNAb+ATI individuals at a time when bNAbs maintained viral suppression. At least two mechanisms could account for the association of bNAb treatment with increased T cell responses. One possibility is that ART interruption in the presence of antibodies results in production of bNAb-HIV-1 immune complexes that activate antigen-presenting dendritic cells and enhance their antigen-presenting and cross-presenting capabilities to produce a vaccinal effect[3,26]. A second nonexclusive possibility is that the augmented $CD8^+$ T cell response is driven by increased low-grade viral replication and antigen availability in tissues that we have not been able to assay during overt viremia suppression by bNAbs. While the underlying mechanism of the observed increased T cell immunity remains to be determined, a potentially important advantage of bNAb+ATI treatment compared to ATI alone, standard ART or T cell vaccination is that the immune system is stimulated with the individual's own virus while circulating viremia is suppressed. Whether the same effects will be seen in individuals who receive bNAbs during ART and whether the increased T cell responses are sufficient to help control infection remains to be determined.

References

1. Chun, T. W. et al. Presence of an inducible HIV-1 latent reservoir during highly active antiretroviral therapy. Proc Natl Acad Sci U S A 94, 13193–13197 (1997).

2. Finzi, D. et al. Identification of a reservoir for HIV-1 in patients on highly active antiretroviral therapy. Science 278, 1295–1300 (1997).

3. Caskey, M., Klein, F. & Nussenzweig, M. C. Broadly neutralizing anti-HIV-1 monoclonal antibodies in the clinic. Nature Medicine 25, 547–553 (2019).

4. Mendoza, P. et al. Combination therapy with anti-HIV-1 antibodies maintains viral suppression. Nature Publishing Group 561, 479–484 (2018).

5. Koup, R. A. et al. Temporal association of cellular immune responses with the initial control of viremia in primary human immunodeficiency virus type 1 syndrome. Journal of Virology 68, 4650–4655 (1994).

6. Goonetilleke, N. et al. The first T cell response to transmitted/founder virus contributes to the control of acute viremia in HIV-1 infection. J Exp Med 206, 1253 (2009).

7. Rosenberg, E. S. et al. Vigorous HIV-1-specific CD4+ T cell responses associated with control of viremia. Science 278, 1447–1450 (1997).

8. Pereyra, F. et al. Genetic and immunologic heterogeneity among persons who control HIV infection in the absence of therapy. Journal of Infectious Diseases 197, 563–571 (2008).

9. Betts, M. R. et al. HIV nonprogressors preferentially maintain highly functional HIV-specific CD8+ T cells. Blood 107, 4781–4789 (2006).

10. Lu, C.-L. et al. Enhanced clearance of HIV-1-infected cells by broadly neutralizing antibodies against HIV-1 in vivo. Science 352, 1001–1004 (2016).

11. Nishimura, Y. et al. Early antibody therapy can induce long-lasting immunity to SHIV. Nature 543, 559–563 (2017).

12. Scheid, J. F. et al. HIV-1 antibody 3BNC117 suppresses viral rebound in humans during treatment interruption. Nature 535, 556–560 (2016).

13. Achenbach, C. J. et al. Effect of therapeutic intensification followed by HIV DNA prime and rAd5 boost vaccination on HIV-specific immunity and HIV reservoir (EraMune 02): a multicentre randomised clinical trial. Lancet HIV 2, e82–91 (2015).

14. Prebensen, C. et al. Immune activation and HIV-specific T cell responses are modulated by a cyclooxygenase-2 inhibitor in untreated HIV-infected individuals: An exploratory clinical trial. PLoS ONE 12, e0176527 (2017).

15. Gray, C. M. et al. Frequency of Class I HLA-Restricted Anti-HIV CD8+ T Cells in Individuals Receiving Highly Active Antiretroviral Therapy (HAART). J. Immunol. 162, 1780 (1999).

16. Oxenius, A. et al. Stimulation of HIV-specific cellular immunity by structured treatment interruption fails to enhance viral control in chronic HIV infection. Proc Natl Acad Sci USA 99, 13747–13752 (2002).

17. Almeida, J. R. et al. Superior control of HIV-1 replication by CD8+ T cells is reflected by their avidity, polyfunctionality, and clonal turnover. J Exp Med 204, 2473–2485 (2007).

18. Freel, S. A. et al. Phenotypic and functional profile of HIV-inhibitory CD8 T cells elicited by natural infection and heterologous prime/boost vaccination. Journal of Virology 84, 4998–5006 (2010).

19. Reiss, S. et al. Comparative analysis of activation induced marker (AIM) assays for sensitive identification of antigen-specific CD4 T cells. PLoS ONE 12, e0186998 (2017).

20. Morou, A. et al. Altered differentiation is central to HIV-specific CD4+ T cell dysfunction in progressive disease. Nat Immunol 20, 1059–1070 (2019).

21. Patarca, R. & Haseltine, W. A. Similarities among retrovirus proteins. Nature 312, 496 (1984).

22. Saez-Cirion, A., Shin, S. Y., Versmisse, P., Barre-Sinoussi, F. & Pancino, G. Ex vivo T cell-based HIV suppression assay to evaluate HIV-specific CD8+ T-cell responses. Nat Protoc 5, 1033–1041 (2010).

23. Piatak, M. J. et al. High levels of HIV-1 in plasma during all stages of infection determined by competitive PCR. Science 259, 1749–1754 (1993).

24. Borducchi, E. N. et al. Antibody and TLR7 agonist delay viral rebound in SHIV-infected monkeys. Nature Publishing Group 563, 360–364 (2018).

25. Fagard, C. et al. A prospective trial of structured treatment interruptions in human immunodeficiency virus infection. Arch Intern Med 163, 1220–1226 (2003).

26. Bournazos, S. & Ravetch, J. V. Fcgamma receptor pathways during active and passive immunization. Immunol Rev 268, 88–103 (2015).

Methods

All information regarding material and methods can be found in the Life Sciences Reporting Summary.

Study design and participants.

BNAb study participants were enrolled in an open-label phase 1b clinical trial at the Rockefeller University and University of Cologne and received three infusions with a combination of two bNAbs, 3BNC117 and 10-1074. ART was interrupted at day 2 after the first antibody infusion[4] (ClinicalTrials.gov identifier: NCT02825797). Viral load was assessed every 1–2 weeks and ART was reinitiated when two consecutive measurements showed viral load of >200 copies per ml. All individuals were infected with clade B HIV-1(ref. [4]). Clinical data of all participants are shown in Extended Data Figs. 1a and 5a. Individuals on continuous ART were enrolled in an observational study at the Rockefeller University. Clinical data of all ART individuals are shown in Extended Data Fig. 2a. The studies were approved by the Rockefeller University and the University of Cologne Institutional Review Boards and written informed consent was obtained from all participants before study enrollment. Secondary use of samples was approved by the University of Montréal Hospital Institutional Review Board.

Intracellular cytokine staining.

PBMCs were thawed and rested for 2 h in RPMI 1640 medium (Gibco by Life Technologies) supplemented with 10% FBS (Seradigm), penicillin and streptomycin (Gibco by Life Technologies) and HEPES (Gibco by Life Technologies) and stimulated with a HIV-1 Consensus B Gag peptide pool (0.5 μg ml−1 per peptide; NIH AIDS Reagent Program) or CMV pp65 peptide pool (0.5 μg ml−1 per peptide; JPT Peptide Technologies) for 6 h in the presence of anti-CD107A-BV786 (BD Biosciences), Brefeldin A (BD Biosciences) and monensin (BD Biosciences) at 37 °C and 5% CO2. DMSO-treated cells served as a negative control. Cells were stained for aquavivid viability marker (Life Technologies) for 20 min at 4 °C and surface markers (30 min, 4 °C), followed by intracellular detection of cytokines using the IC Fixation/Permeabilization kit (eBioscience) according to the manufacturer's protocol before acquisition at an LSRFortessa flow cytometer (BD Biosciences) (see Supplementary Table 1 for antibody staining panel).

Activation-induced marker assay.

PBMCs were thawed, washed and cultured in 24-well plates at a concentration of 10×10^6 cells per ml in RPMI 1640 supplemented with HEPES, penicillin and streptomycin and 10% human

serum (Sigma). Cells were rested for 3 h and stimulated with 0.5 μg ml−1 per peptide of HIV-1 Consensus B peptide pools spanning the entire protein for Gag, Nef, Pol, gp120 or gp41 (NIH AIDS Reagent Program) for 18 h at 37 °C and 5% CO2. Pools for gp120 and gp41 were obtained by combining single Env peptides 1–123 (gp120) and 124–211 (gp41) (HIV-1 Consensus B Env Peptide Set). A DMSO-treated condition served as a negative control. Cells were stained for viability dye (aquavivid, Life Technologies) and surface markers (30 min, 4 °C) and cells were fixed using 2% paraformaldehyde before acquisition at a LSRII flow cytometer (BD Biosciences) (see Supplementary Table 2 for antibody staining panel). DMSO-treated cells served as negative controls and were used together with fluorescence minus one controls to set gates for analysis.

IFN-γ ELISpot.

HIV Gag-specific IFN-γ responses were measured using an IFN-γ ELISpot assay as previously described[27]. The 96-well hydrophobic polyvinylidene difluoride membrane-backed plates (Millipore) were pre-wetted with 35% ethanol for 45 s, washed with PBS and coated overnight at 4 °C with anti-IFN-γ capture antibody (3 μg ml−1 in PBS, clone NIB42, BD Biosciences). PBMCs were thawed, rested for 2 h and seeded into plates at 1–2 × 10^5 PBMCs per well in RPMI with 10% FBS supplemented with HEPES and penicillin and streptomycin. Cells were stimulated with 123 peptides spanning the entire HIV-1 Consensus B Gag protein (10 μg ml−1, NIH AIDS Reagent Program; see Supplementary Table 3 for all sequences) for 20 h at 37 °C and 5% CO2. Plates were washed with PBS-T (PBS and 0.05% Tween-20) and incubated with biotinylated anti-IFN-γ antibody (0.5 μg ml−1 in PBS and 0.5% BSA, clone 4S.B3; BD Biosciences) for 2 h at room temperature. Plates were washed with PBS-T and incubated with streptavidin-alkaline-phosphatase conjugate (Bio-Rad Laboratories) (1:1,000 dilution in PBS and 0.5% BSA) for 1 h at room temperature. Spots were developed using an alkaline phosphatase conjugate substrate kit (Bio-Rad Laboratories) for 4 min and the reaction was stopped with tap water. Spots were counted using an Immunospot Analyzer Instrument (Cellular Technology). PBMCs incubated with medium alone served as negative controls and staphylococcal enterotoxin B-stimulated PBMCs (0.5 μg ml−1) as a positive control. The s.f.u. were calculated as number of spots in test wells minus the mean number of spots in medium control wells and normalized to s.f.u. per 10^6 PBMCs. A response was considered positive if greater than 50 s.f.u. per 10^6 PBMCs. Week −2 and week 12 samples from the same individual were assayed together in the same experiment.

***In vitro* viral inhibition assay.**

The capacity of $CD8^+$ T cells to suppress HIV-1 infection of autologous $CD4^+$ T cells was evaluated using a previously described HIV-1 suppression assay[22] with minor modifications. $CD4^+$ T cells were isolated using negative magnetic bead selection (StemCell Technologies) from PBMCs, rested for 2 h and cultured in RPMI and 10% FBS supplemented with PHA-L (2 μg ml−1; Sigma-Aldrich) and IL-2 (100 U ml−1; StemCell Technologies) for 72 h. After 72 h, $CD8^+$ T cells were isolated from PBMCs using negative magnetic bead selection (StemCell Technologies), counted and rested for 2 h at 37 °C. Meanwhile, cultured $CD4^+$ T cells were washed, counted and plated in U-bottom 96-well plates for infection with HIV-1_{BaL} (NIH AIDS Reagent Program) using a multiplicity of infection of 0.015: plates were first centrifuged at 1,200g for 1 h at 22 °C and then incubated for an additional hour at 37 °C. After infection, $CD4^+$ T cells from different wells were pooled, washed three times and plated in U-bottom 96-well plates (50,000 cells per well) with $CD8^+$ T cells at a 1:1 ratio in RPMI with 10% FBS supplemented with IL-2 (100 U ml−1). Uninfected $CD4^+$ T cells were included as negative controls and infected $CD4^+$ T cells cultured without $CD8^+$ T cells served as 100% infectivity controls. At days 3, 5 and 7 after infection, cells were stained with a viability dye (aquavivid, Life Technologies) and surface markers (30 min, 4 °C), followed by intracellular detection of HIV-1 Gag (Beckman Coulter) using the IC Fixation/Permeabilization kit (eBioscience) according to the manufacturer's protocol (see Supplementary Table 5 for the antibody staining panel). All experiments were performed in duplicate or triplicate, depending on cell availability.

Sequencing and phylogenetic analysis.

Gag sequences from latent reservoir viruses were obtained from $CD4^+$ T cell genomic DNA by near-full length HIV-1 sequencing as previously described[28]. *Gag* sequences from rebound plasma were obtained by HIV-1 RNA extraction and single-genome amplification as previously described[29]. In brief, HIV-1 RNA was extracted from plasma samples using the MinElute Virus Spin kit (Qiagen) followed by first-strand cDNA synthesis using SuperScript III reverse transcriptase (Invitrogen). The cDNA synthesis for plasma-derived HIV-1 RNA was performed using the antisense primer B5R2 5′-CAATCATCACCTGCCATCTGTTTTCCATA-3′. *Gag* was then amplified using the primer Gag5out 5′-TTGACTAGCGGAGGCTAGAAGG-3′ and Gag3out 5′-GATAAAACCTCCAATTCCCCCTATC-3′ in the first round and in the second round with nested primers Gag5in 5′-GAGAGATGGGTGCGAGAGCGTC-3′ and Gag3in 5′-CTGCTCCTGTATCTAATAGAGC-3′. PCRs were performed using High Fidelity Platinum Taq (Invitrogen) and run at 94 °C for 2 min; 35 cycles of 94 °C for 15 s, 58 °C for 30 s and 68 °C for 3

min; and 68 °C for 15 min. Second-round PCR was performed with 1 µl of the PCR product from the first round as a template and High Fidelity Platinum Taq at 94 °C for 2 min; 45 cycles of 94 °C for 15 s, 58 °C for 30 s and 68 °C for 3 min; and 68 °C for 15 min. Amino acid alignments of intact gag sequences were obtained by using ClustalW v.2.1 (ref. [30]) under the BLOSUM cost matrix. Sequences with premature stop codons were excluded from all analyses. Maximum likelihood phylogenetic trees were then generated from these alignments using RAxML v.8.2.9 (ref. [31]) under the GTRGAMMA model with 1,000 bootstraps. To analyze changes between reservoir and rebound viruses, *gag* sequences were aligned at the amino-acid-level to a HXB2 reference using ClustalW v.2.1.

Data analysis.

Flow cytometric data were analyzed using FlowJo v.10.5.0 for Mac. Statistical analyses were performed using GraphPad Prism v.8.0.1 for Mac using nonparametric tests. Pairwise comparisons were performed using the two-sided Wilcoxon matched-pairs signed rank test.

Reporting Summary.

Further information on research design is available in the Nature Research Reporting Summary linked to this article.

Data availability

Sequences from all isolated viruses are available in GenBank, accession numbers MN750027 to MN750174. Other raw experimental data associated with the figures presented in the manuscript are available from the corresponding authors upon reasonable request. Study participant-related data not included in the paper may be subject to confidentiality obligations.

References

27. Pelletier, S. et al. Increased degranulation of natural killer cells during acute HCV correlates with the magnitude of virus-specific T cell responses. Journal of hepatology 53, 805–816 (2010).

28. Lu, C.-L. et al. Relationship between intact HIV-1 proviruses in circulating CD4(+) T cells and rebound viruses emerging during treatment interruption. Proc Natl Acad Sci USA 115, E11341–E11348 (2018).

29. Salazar-Gonzalez, J. F. et al. Deciphering human immunodeficiency virus type 1 transmission and early envelope diversification by single-genome amplification and sequencing. Journal of Virology 82, 3952–3970 (2008).

30. Larkin, M. A. et al. Clustal W and Clustal X version 2.0. Bioinformatics 23, 2947–2948 (2007).

31. Stamatakis, A. RAxML version 8: a tool for phylogenetic analysis and post-analysis of large phylogenies. Bioinformatics 30, 1312–1313 (2014).

32. Gartner, S. et al. The role of mononuclear phagocytes in HTLV-III/LAV infection. Science 233, 215–219 (1986).

Acknowledgements

We thank the clinical staff in the Laboratory of Molecular Immunology at the Rockefeller University and the Division of Infectious Diseases at the University Hospital Cologne, as well as all study participants for their invaluable role in this project; D. Gauchat, P. St-Onge and the CRCHUM Flow Cytometry Platform and O. Debbeche and the CRCHUM BSL3 platform for technical assistance. The following reagents were obtained through the NIH AIDS Reagent Program, Division of AIDS, NIAID, NIH: Consensus B peptide pools for Gag (cat. no.12425), Pol (cat. no. 12438), Nef (cat. no. 12545), gp120 and gp41 (pools made using HIV-1 Consensus B Env Peptide Set, cat. no. 9480), Consensus B Gag Peptide Set (cat. no. 8117) and HIV-1BaL (cat. no. 510) from S. Gartner, M. Popovic and R. Gallo32. This study was supported by the Canadian Institutes for Health Research (grant nos. 152977 and 154049 to D.E.K), a Canada Foundation for Innovation Program Leader grant (no. 31756 to D.E.K); the FRQS AIDS and Infectious Diseases Network; the National Institutes of Health UM1 AI-100663 (CHAVI-ID) and AI-144462 (CHAVD); R01AI-129795 (M.C.N.); the Einstein-Rockefeller-CUNY Center for AIDS Research (1P30AI124414-01A1); BEAT-HIV Delaney grant UM1 AI-126620 (M.C.); and the Robertson Fund. We acknowledge grants from the Bill and Melinda Gates Foundation Collaboration for AIDS Vaccine Discovery, nos. OPP1092074 and OPP1124068 (M.C.N.). J.N. is supported by scholarships from the Quebec Health Research Fund (FRQS) and the Department of Microbiology, Immunology and Infectious Diseases, Université de Montréal. A.E.B. is the recipient of a CIHR Fellowship Award no. 152536. D.E.K is supported by a Merit Award of the Quebec Health Research Fund (FRQS). M.C.N. is an HHMI Investigator.

Author contributions

J.N., A.E.B., M.C.N. and D.E.K. designed the immunological studies; M.C., F.K. and M.C.N. designed the trial from which the samples were obtained; J.N., A.E.B., P.M., M.J., C.-L.L. and H.G. performed experiments; M.D. provided input on manuscript content and data representation; Y.Z.C. and A.L.B. contributed to recruitment and clinical assessments; I.S. coordinated and performed sample processing; J.N., M.C.N. and D.E.K. interpreted the data and wrote the paper with all co-authors' assistance; M.C.N. and D.E.K. provided supervision.

Competing interests

There are patents on 3BNC117 (PTC/US2012/038400) and 10-1074 (PTC/US2013/ 065696) that list M.C.N. as an inventor. M.C.N. is a member of the Scientific Advisory Board of Frontier Bioscience. Gilead has the rights to develop the 3BNC117 and 10-1074 antibody combination for clinical use.

Figures

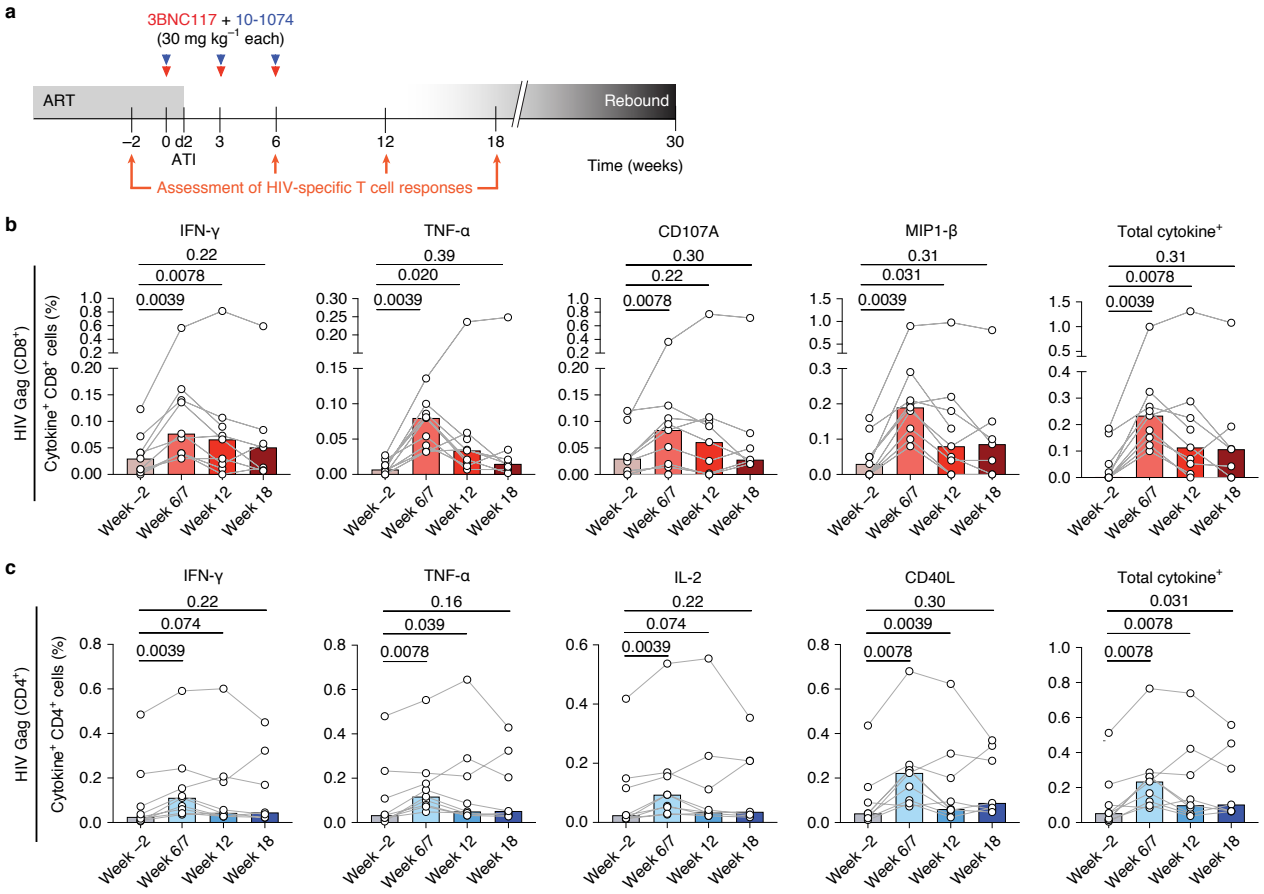

Figure 1 – **Increased frequency of Gag-specific T cells during ATI in bNAb-treated individuals**

a, Study design. **b,c**, Net frequency of cytokine+ CD8+ (**b**) or CD4+ cells (**c**) after Gag stimulation at weeks −2, 6/7, 12 and 18. Total cytokine+ cells include cells that express at least one cytokine and effector function upon Gag stimulation (CD107A, IFN-γ, MIP1-β and/or TNF-α for CD8+; CD40L, IFN-γ, IL-2 and/or TNF-α for CD4+). Net value was calculated by subtracting the frequency of cytokine+ cells detected in a DMSO control. Bars show median values. Symbols represent biologically independent samples from n = 9 (weeks –2, 6/7 and 12) and n = 7 (week 18) bNAb-treated individuals with suppressed viral load during ATI (week 18 sample was not available for individual 9244 and individual 9242 reinitiated ART after viral rebound at week 15). Lines connect data from the same donor. P values comparing responses at week 6/7, 12 or 18 versus baseline (week –2) were calculated using a paired two-tailed Wilcoxon test.

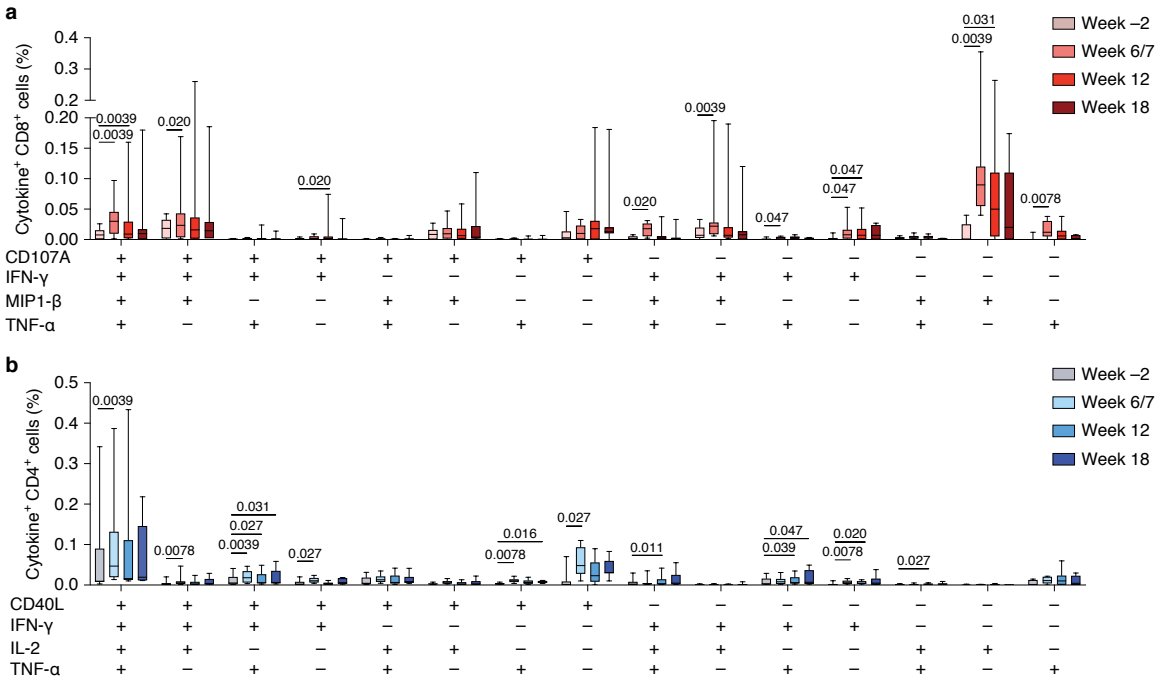

Figure 2 – **Polyfunctionality of Gag-specific T cells**

T cell cytokine coexpression after HIV-1 Gag peptide pool stimulation was evaluated in bNAb+ATI individuals by ICS and analyzed using combination gates. **a**, Coexpression of CD107A, IFN-γ, MIP1-β and TNF-α in $CD8^+$ T cells. **b**, Coexpression of CD40L, IFN-γ, IL-2 and TNF-α in $CD4^+$ T cells. Box-and-whisker plots show median values (line), 25th to 75th percentiles (box outline) and minimum and maximum values (whiskers); n = 9 (weeks −2, 6/7 and 12) and n = 7 (week 18) biologically independent samples from bNAb-treated individuals with suppressed viral load during ATI. P values comparing responses at week 6/7, 12 or 18 versus baseline (week −2) were calculated using a paired two-tailed Wilcoxon test.

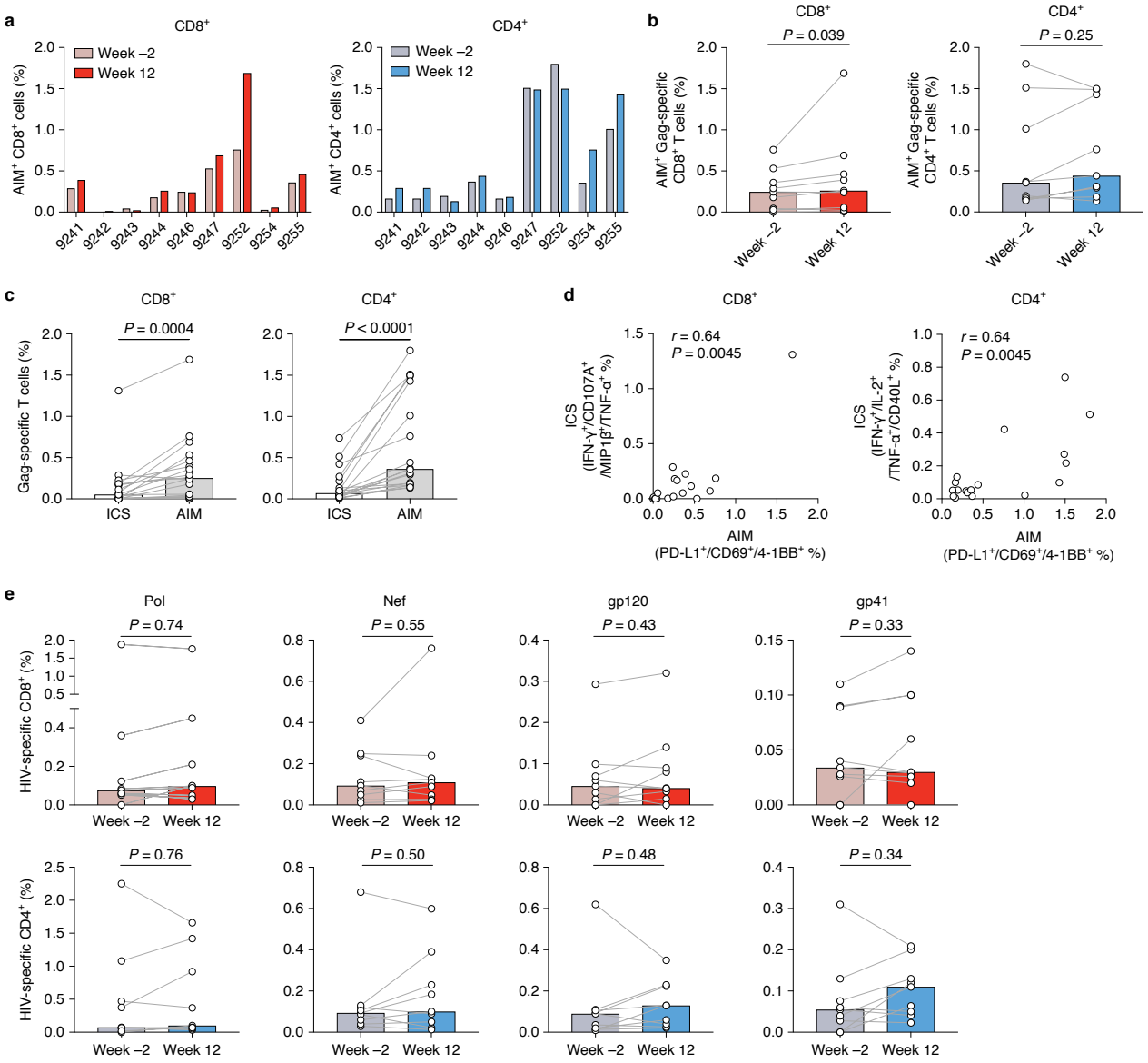

Figure 3 – **AIM assay evaluation of T cell responses to multiple HIV-1 antigens.**

AIM+ T cells include cells that were PD-L1+CD69+ or 4-1BB+CD69+ or PD-L1+4-1BB+. **a**, Net frequency of HIV-1 Gag-specific AIM+CD8+ (left, red) and CD4+ T cells (right, blue) for each bNAb+ATI individual. Net frequency of the Gag-stimulated condition was calculated by subtracting the frequency detected in a DMSO control. **b**, Comparison of net frequency HIV-1 Gag-specific AIM+CD8+ (left, blue) and CD4+ T cells (right, red) at week −2 and week 12. Symbols represent biologically independent samples from n = 9 bNAb+ATI individuals. Lines connect data from the same donor. Bars show median values. **c**, Comparison of the frequency of Gag-specific CD8+ or CD4+ T cells identified by AIM assay or ICS. The or-gate strategy was used for both assays. Symbols represent biologically independent samples from n = 9 bNAb+ATI individuals (samples obtained at week −2 and 12 for each individual were included for comparison). Lines connect data from the same donor and time point. **d**, Relationship between the frequency of Gag-specific CD8+ and CD4+ T cell responses identified either by AIM assay or ICS. Symbols represent biologically independent samples from n = 9 bNAb+ATI individuals (samples obtained at week −2 and 12 for each individual were included for comparison). Association was determined by Spearman correlation. **e**, Net frequency of HIV-1 Pol, Nef, gp120 or gp41-specific CD8+ (upper graphs) or CD4+ T cells (lower graphs) identified by AIM assay in bNAb+ATI individuals at week −2 and week 12. Symbols represent biologically independent samples from n = 9 bNAb+ATI individuals. Lines connect data from the same donor. Median values are shown as bars. P values indicated in **b,c,e** were calculated by a paired two-tailed Wilcoxon test.

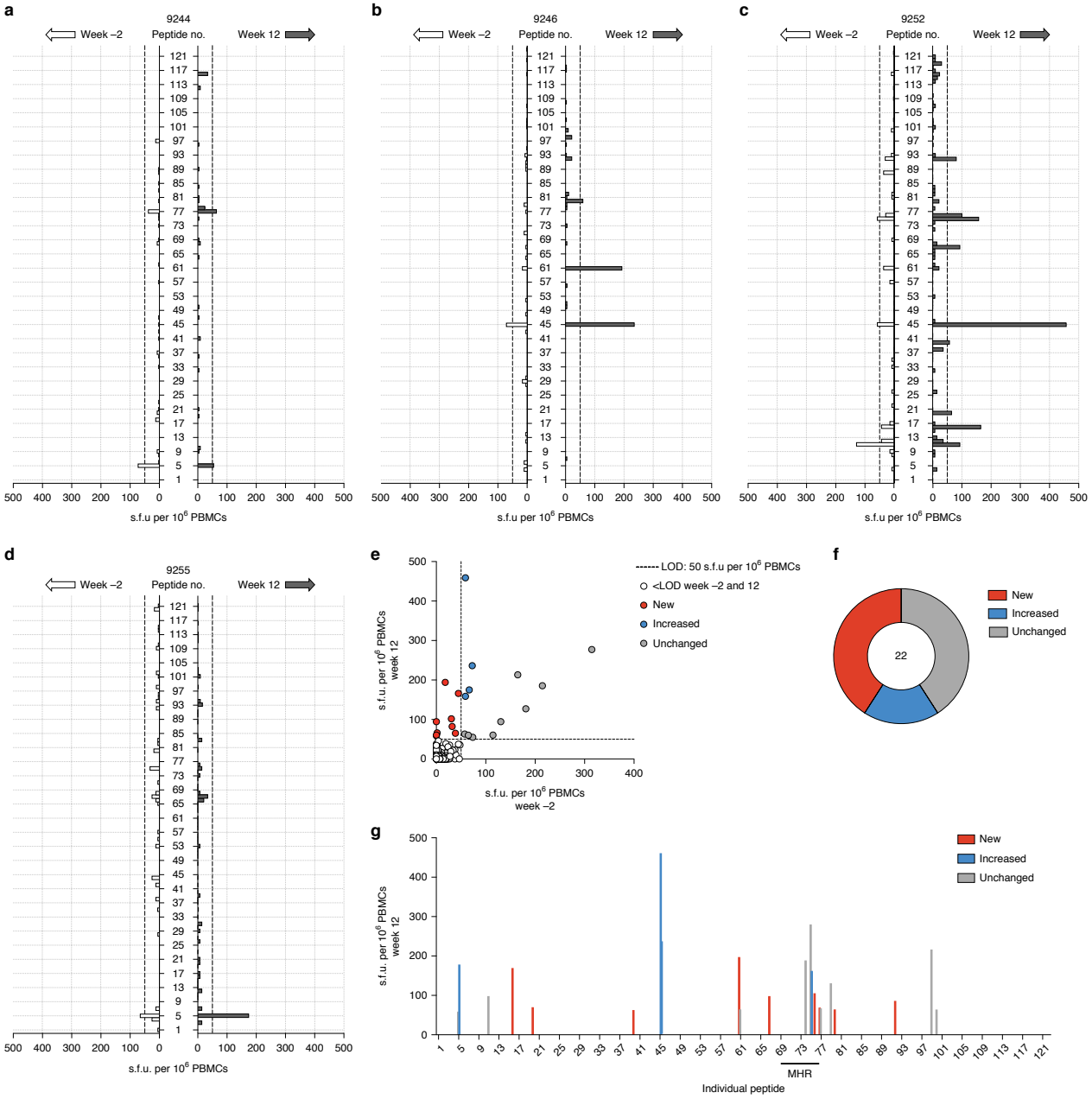

Figure 4 – **Responses to HIV-1 Gag epitopes.**

PBMCs obtained at week −2 and 12 were evaluated for IFN-γ ELISpot responses to 123 peptides spanning the entire HIV-1 Gag protein (Consensus Clade B sequence). **a–d**, Plots showing PBMC IFN-γ ELISpot response calculated as spot-forming units (s.f.u.) per 10^6 PBMCs for individuals with broadened IFN-γ ELISpot response at week 12 (dark gray bars) compared to week −2 (white bars): 9244, 9246, 9252 and 9255. **e**, PBMC IFN-γ ELISpot responses at week −2 were plotted against week 12 responses for all nine individuals in the bNAb+ATI group. White symbols represent responses that were below the limit of detection (LOD) for both time points. Responses were considered as new (red symbols) if responses were undetectable for week −2 and detectable for week 12. Responses were considered as unchanged (light gray symbols) if number of spots did not differ by more than twofold between both time points. Responses were considered as increased (blue symbols) if number of spots for week −2 were increased by more than twofold for week 12 versus week −2. **f**, Doughnut chart depicting proportion of new, increased or unchanged IFN-γ ELISpot responses within all detectable responses (n = 22) of the nine individuals at week 12. **g**, Summary of detectable IFN-γ ELISpot responses at week 12 for all nine bNAb study participants. The LOD of 50 s.f.u. per 10^6 PBMCs is indicated as a dashed line in **a–e**.

Additional information

a

ID	Age	Gender	Race	Years since HIV-1 dx	Years since first ART	Uninterr. ART before ATI (yrs)	ART at screening	Switched ART	Reported CD4 nadir	HLA alleles	CD4 count (d0)	HIV-1 RNA (cp/ml) Scr	HIV-1 RNA (cp/ml) Week -2	HIV-1 RNA (cp/ml) d0	Weeks to viral rebound
9241	40	M	White/Hisp	6	5	5	EVG/cobi/ TDF/FTC	-	500	A23,33; B14,44; C4,8	515	<20	<20	<20	21
9242	43	M	White/Hisp	3	3	2	EVG/cobi/ TDF/FTC	-	450	A24; B35,39; C4, 7	654	<20	<20	<20	15
9243	29	M	Amer Indian/Hisp	5	5	5	RPV/TDF/ FTC	DTG/ TDF/FTC	350	A24,30; B15,35; C2,15	350	<20	<20 D	<20 D	20
9244	36	M	Amer Indian/not Hisp	9	5	5	EVG/cobi/ TAF/FTC	-	730	A1,3; B44,51; C5,15	1,110	<20	<20	<20	21
9246	30	M	Black	5	5	5	EVG/cobi/ TAF/FTC	-	500	A29,68; B45,81; C16,18	745	<20	<20	<20 D	19
9247	31	M	Black	6	6	6	EVG/cobi/ TAF/FTC	-	600	A33,34; B44,78; C4,16	728	<20	<20	<20	26
9252	51	F	Black	11	11	11	EFV/TDF/ FTC	DTG/ TDF/FTC	270	A2,66; B39,78; C12,16	598	<20	<20	<20	22
9254	48	M	White	21	21	21	EVG/cobi/ TAF/FTC	-	590	A1,29 B38,44; C12,16	860	<20	<20	<20	>30
9255	30	M	White	5	4	4	EVG/cobi/ TAF/FTC	-	779	A3,25 B18,44; C7,12	1360	<20	<20 D	<20	>30

b

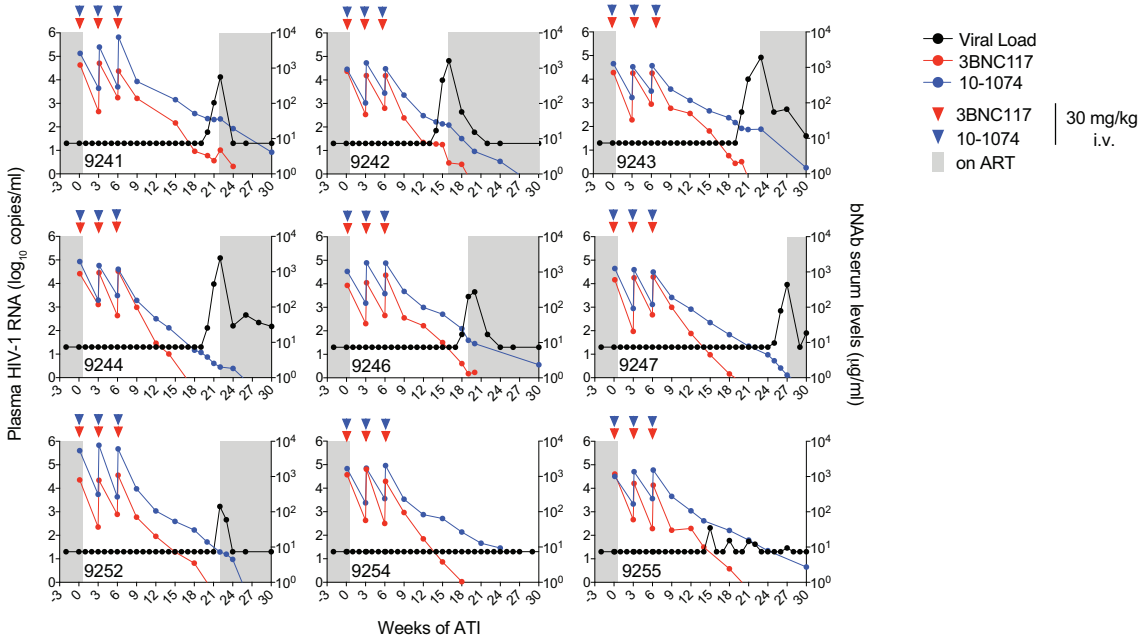

Extended Data Figure 1 – **Study participant clinical characteristics**

(**a**) Study participant demographics and baseline clinical data[4]. Amer Indian: American Indian; Hisp: Hispanic; cobi: cobicistat; DTG: dolutegravir; EFV: efavirenz; EVG: elvitegravir; FTC: emtricitabine; RPV: rilpivirine; TAF: tenofovir alafenamide fumarate; TDF: tenofovir disoproxil fumarate. NNRTI-based regimens were switched four weeks before ART interruption due to longer half-lives of NNRTIs. All participants harbored clade B viruses. Viral load <20D: plasma HIV-1 RNA detected but not quantifiable by clinical assays. d0: day 0; dx: diagnosis; Scr: screening. (**b**) Levels of plasma HIV-1 RNA (black; left y axis) and serum concentration of 3BNC117 (red) and 10-1074 (blue, right y axis) in the 9 participants enrolled in the bNAb+ATI trial[4].

a

ID	Age	Gender	Race	Years since		Years on continuous ART	ART regimen	Reported CD4 nadir	CD4 count		HIV-1 RNA (cp/ml)	
				HIV-1 dx	first ART				week 0	week 12	week 0	week 12
1A17	58	F	Black	20	13	13	EVG/cobi/TAF/FTC	1,000	1,370	1,163	<20	<20
1A33	50	M	Black	4	4	4	EFV/TDF/FTC	100	467	429	<20 D	<20
1B50	48	M	Black	16	16	16	RPV/TAF/FTC	400	461	483	<20	<20 D
1B26	54	M	Black	25	16	16	RAL/SQV/rit/TDF	5	707	905	<20	<20
B531	25	M	Black	3	3	3	EVG/cobi/TDF/FTC	350	750	759	<20 D	<20
B533	59	M	Black	28	28	21	RAL/DRV/cobiTDF/FTC	50	715	n.d.	<20	<20
B535	51	M	Hispanic/ multiple	14	14	14	EFV/TDF/FTC	100	642	n.d.	<20	<20
B536	34	M	White	8	4	4	EVG/cobi/TAF/FTC	750	1,022	n.d.	<20	<20
B539	29	M	White	4	4	4	EVG/cobi/TAF/FTC	500	741	n.d.	<20	<20
B544	36	M	White	12	11	11	DTG/ABC/3TC	350	504	n.d.	<20	<20
B545	30	M	Black	4	4	4	DTG/ABC/3TC	238	559	n.d.	<20	<20
B550	48	F	Black	11	11	11	RPV/TAF/FTC	600	868	n.d.	40	<20
B554	49	M	Black	24	24	4	DGV/TDF/FTC	560	834	n.d.	<20	<20

b

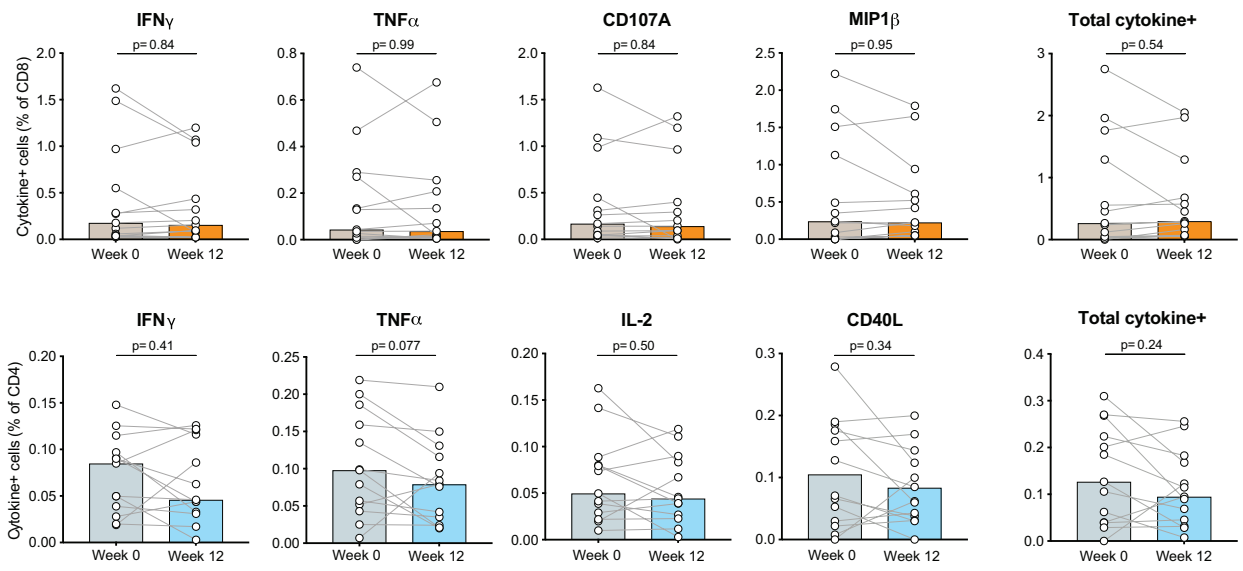

Extended Data Figure 2 – **Frequency of Gag-specific CD4⁺ and CD8⁺ unchanged in ART-treated individuals over time**

T cell cytokine co-expression after 6h HIV-1 Gag peptide pool stimulation was evaluated by intracellular cytokine staining (ICS) in individuals on continuous ART. (**a**) Demographics and clinical data of ART-treated individuals. 3TC: lamivudine; ABC: abacavir; cobi: cobicistat; DRV: darunavir; DTG: dolutegravir; EFV: efavirenz; EVG: elvitegravir; FTC: emtricitabine; RAL: raltegravir; rit: ritonavir; RPV: rilpivirine; SQV: saquinavir; TAF: tenofovir alafenamide fumarate; TDF: tenofovir disoproxil fumarate. Viral load <20D: plasma HIV-1 RNA detected but not quantifiable by clinical assays. n.d.: not determined. (**b**) Cytokine analysis of CD8⁺ and CD4⁺ after HIV-1 Gag peptide pool stimulation at week 0 and 12. Symbols represent biologically independent samples from n=13 individuals on continuous ART. Lines connect data from the same donor. Bars show median values. P values were calculated by paired two-tailed Wilcoxon test.

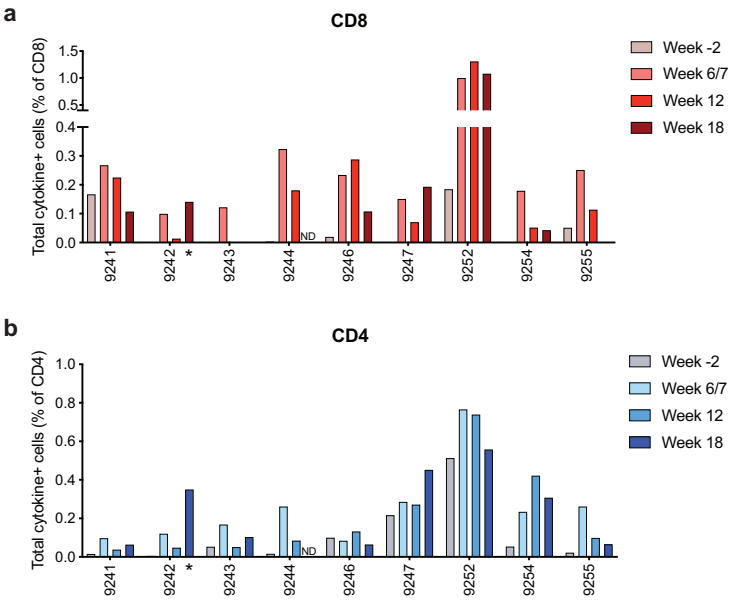

Extended Data Figure 3 – **Individual Gag-specific T cell responses measured by ICS**

(**ab**) Net frequency of total cytokine$^+$ CD8$^+$ (**a**) or CD4$^+$ cells (**b**) after Gag stimulation for each individual study participant. Total cytokine$^+$ cells include cells that express at least one cytokine/effector function upon Gag stimulation (CD107A, IFNγ, MIP1β and/or TNFα for CD8$^+$; CD40L, IFNγ, IL-2 and/or TNFα for CD4$^+$). Net value was calculated by subtracting frequency of total cytokine$^+$ cells detected in DMSO control. ND: Week 18 sample was not available for individual 9244. *9242 week 18 on ART after viral rebound at week 15.

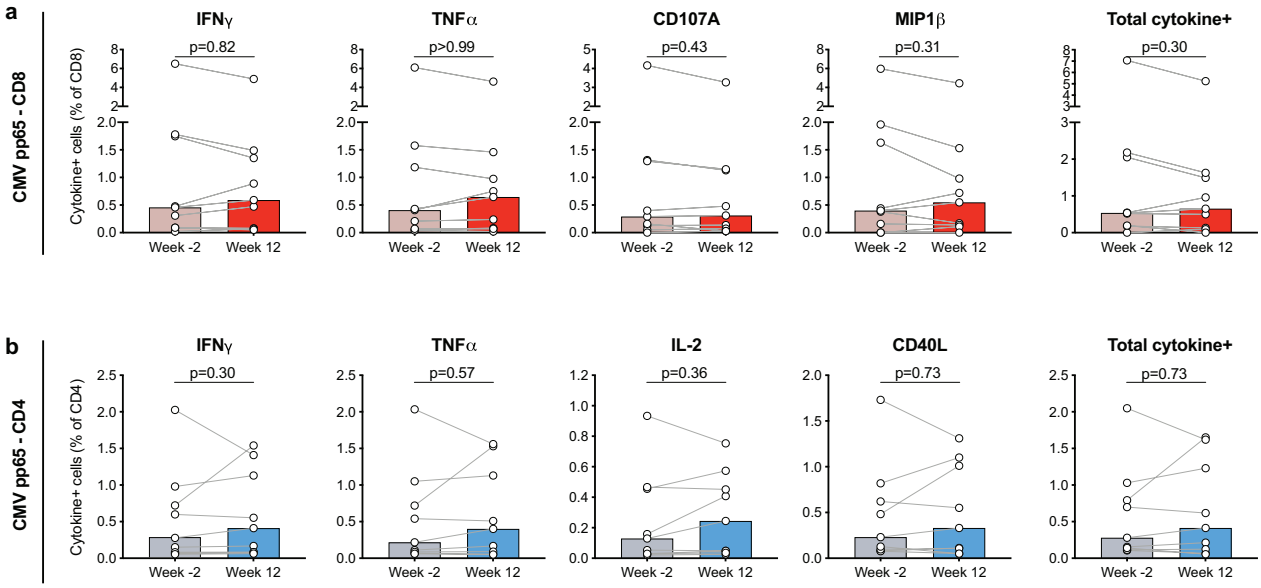

Extended Data Figure 4 – **Unchanged frequency of CMV-specific effector T cells detected by intracellular cytokine staining**

PBMCs were stimulated with CMV pp65 peptide pools for 6h and cytokine production was evaluated by ICS in bNAb+ATI individuals at week -2 and week 12. (**ab**) Cytokine analysis of $CD8^+$ (**a**) or $CD4^+$ T cells (**b**) at week -2 and week 12 after CMV pp65 stimulation. Net frequency of stimulated condition was calculated by subtracting frequency detected in DMSO control. Symbols represent biologically independent samples from n=9 bNAb+ATI individuals. Lines connect data from the same donor. Bars show median values. P values are indicated in graphs and were calculated by paired two-tailed Wilcoxon test.

a

ID	Age	Gender	Race	Years since HIV-1 dx	Years since first ART	Uninterr. ART before ATI (yrs)	ART at screening	Switched ART	Reported CD4 nadir	HLA alleles	CD4 count (d0)	HIV-1 RNA (cp/ml) Scr	HIV-1 RNA (cp/ml) Week -2	HIV-1 RNA (cp/ml) d0	Weeks to viral rebound
9245	22	M	White/Hisp	5	5	5	EVG/cobi/ TAF/FTC	-	360	A2,24; B15,15; C4,8	736	<20	<20	<20	5
9251	40	M	Black	6	2	2	EVG/cobi/ TDF/FTC	-	1,000	A2,34; B45,53; C4,16	672	<20	<20	<20	7

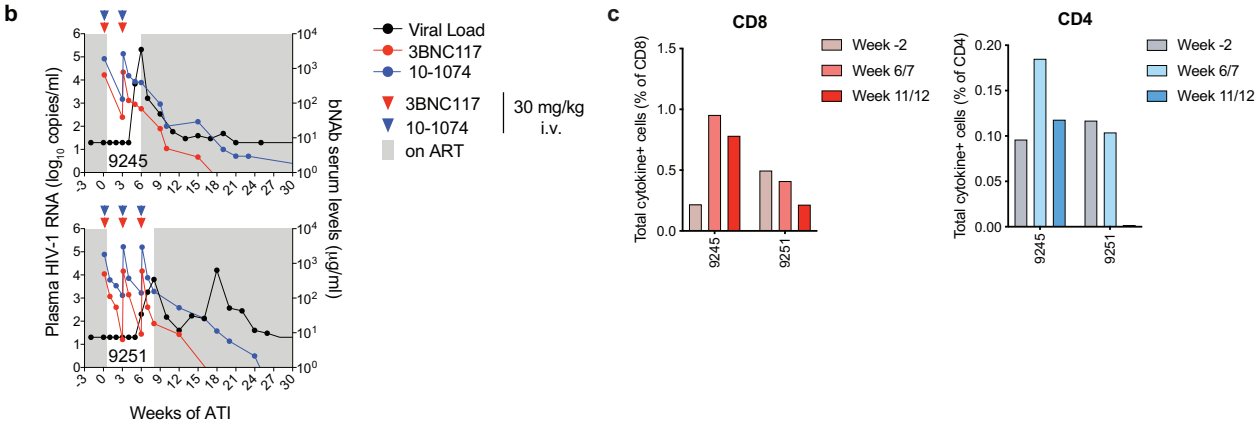

Extended Data Figure 5 – **HIV-1 Gag-specific T cell responses in early rebounders with bNAb-resistant reservoir**

(**a**) Study participant demographics and baseline clinical data[4]. Hisp: Hispanic; cobi: cobicistat; EVG: elvitegravir; FTC: emtricitabine; TAF: tenofovir alafenamide fumarate; TDF: tenofovir disoproxil fumarate. All participants harboured clade B viruses. d0: day 0; dx: diagnosis; Scr: screening. (**b**) Levels of plasma HIV-1 RNA (black; left y axis) and serum concentration of 3BNC117 (red) and 10-1074 (blue, right y axis) in the 2 participants enrolled in the bNAb+ATI trial with early rebound due to bNAb-resistant reservoir[4]. (**c**) Net frequency of total cytokine$^+$ CD8$^+$ or CD4$^+$ T cells after HIV-1 Gag stimulation in both individuals at weeks -2, 7 and 11 (9245), or weeks -2, 6 and 12 (9251).

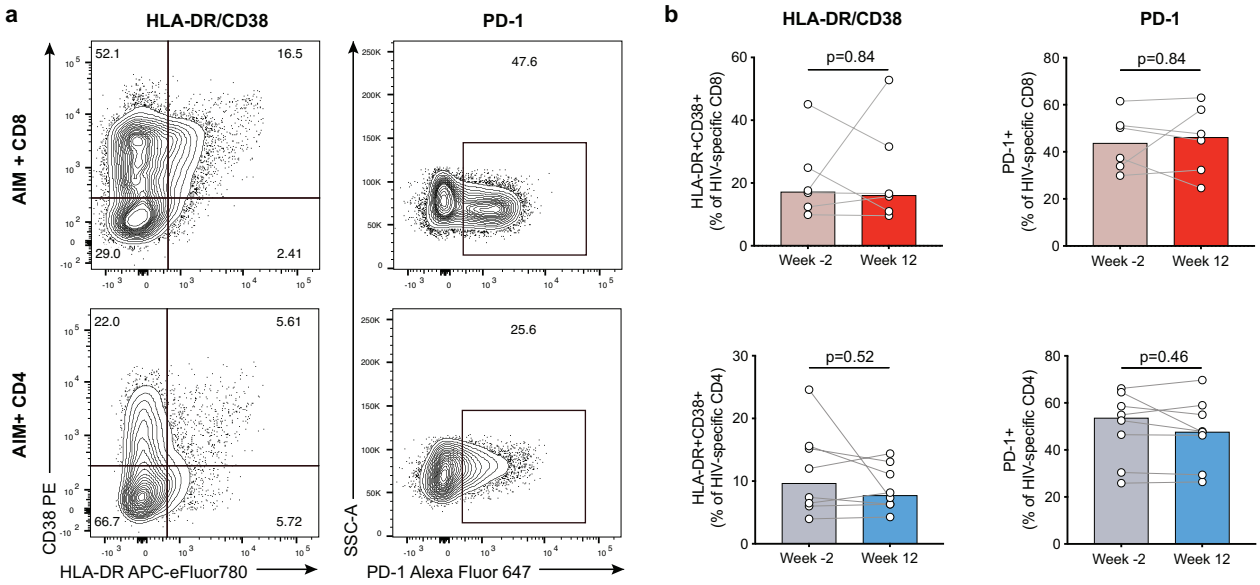

Extended Data Figure 6 – **No change in HLA-DR/CD38 and PD-1 expression of HIV-1-specific T cell responses**

HIV-1-specific T cell responses identified by PD-L1/CD69/4-1BB AIM assay were analyzed for surface expression of HLA-DR/CD38 and PD-1. (**a**) Representative plot showing expression of HLA-DR/CD38 and PD-1 on AIM$^+$ HIV-1-specific CD8$^+$ (upper graphs) and CD4$^+$ T cells (lower graphs). Flow panels are representative of n=6 (CD8$^+$) or n=8 (CD4$^+$) biologically independent bNAb+ATI individuals. (**b**) Frequency of HLA-DR$^+$CD38$^+$ or PD-1$^+$ of HIV-1-specific CD8$^+$ and CD4$^+$ T cell responses at week -2 or week 12. Symbols represent biologically independent samples from n=6 (CD8$^+$) and n=8 (CD4$^+$) bNAb+ATI individuals. Only samples with AIM-responses that are at least 2-fold over DMSO-stimulated control condition were analyzed for phenotype to limit the contribution of background events. Lines connect data from the same donor. Bars show median values. P values are indicated in graphs and were calculated by paired two-tailed Wilcoxon test.

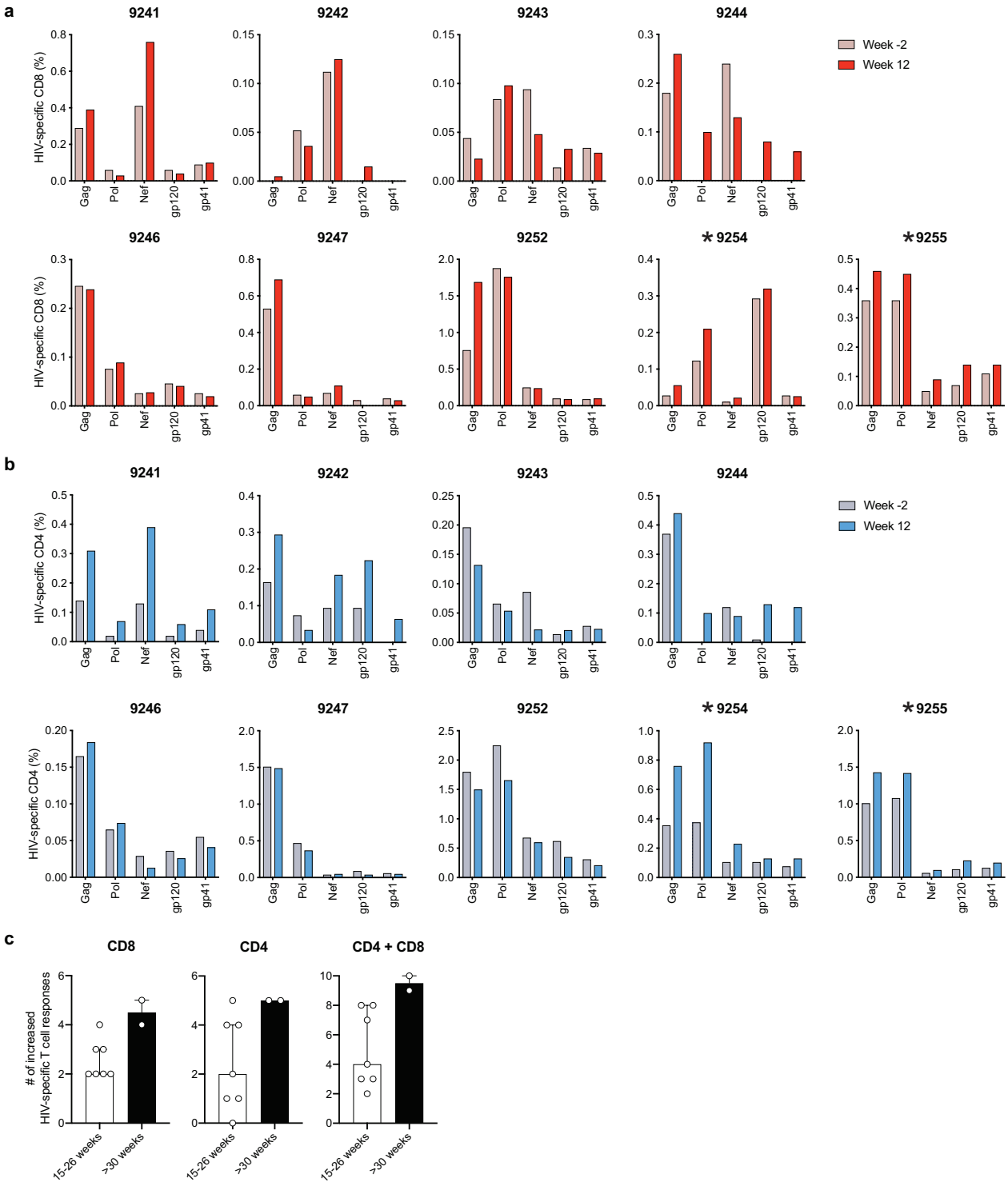
a
9241
9242
9243
9244
9246
9247
9252
*9254
*9255
HIV-specific CD8 (%)
Week -2
Week 12
Gag
Pol
Nef
gp120
gp41
b
HIV-specific CD4 (%)
c
CD8
CD4
CD4 + CD8
# of increased HIV-specific T cell responses
15-26 weeks
>30 weeks

Extended Data Figure 7 – **Dynamics of T cell responses to multiple HIV-1 antigens in bNAb+ATI individuals**

(**ab**) Frequency of $CD8^+$ (**a**) and $CD4^+$ T cells (**b**) specific to HIV-1 Pol, Nef, gp120 or gp41 were evaluated by CD69/PD-L1/4-1BB AIM assay at weeks -2 and 12. Individuals with viral suppression >30 weeks (9254, 9255) are marked with an asterisk (*). (**c**) Number of increased HIV-specific $CD4^+$ and $CD8^+$ T cell responses in n=7 biologically independent individuals with 15-26 weeks of viral control after ATI (15-26 weeks: 9241, 9242, 9243, 9244, 9246, 9247, 9252) versus n=2 biologically independent individuals with viral control beyond 30 weeks after ATI (>30 weeks: 9254 and 9255). Number of increased HIV-specific T cell responses was calculated as the sum of single HIV antigens (Gag, Pol, Nef, gp120, gp41) for which we observed an increase at week 12 versus week -2. Bars represent median values with IQR.

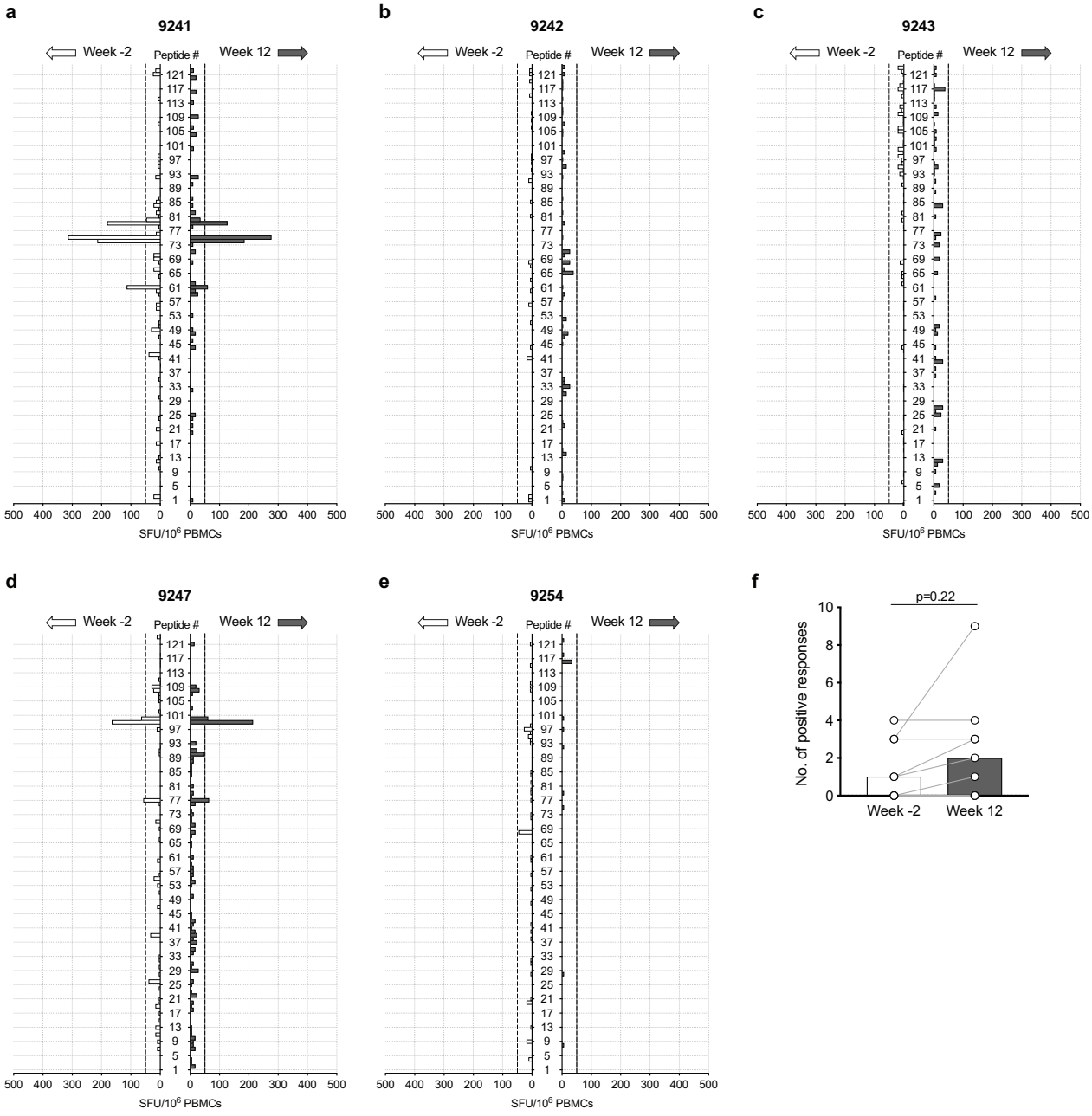

Extended Data Figure 8 – **PBMC IFNγ ELISpot responses were undetectable/not changed in 5 individuals**

PBMCs were evaluated for IFNγ ELISpot responses to 123 HIV-1 Gag peptides spanning the entire Gag protein. Spot forming units (SFU) were calculated as number of spots in test wells subtracted by mean number of spots in media control wells and normalized to SFU/10^6 PBMCs. A response was considered positive if greater than 50 SFU/10^6 PBMCs (=limit of detection, LOD, dashed line). (**a-e**) Graph representing IFNγ ELISpot responses for individuals with either undetectable (9242 (**b**), 9243 (**c**), 9254 (**e**)) or unchanged response (9241 (**a**), 9247 (**d**)) at week -2 (left axis, white bars) and week 12 (right axis, grey bars). (**f**) Number of responses above LOD for n=9 biologically independent bNAb+ATI individuals at week -2 and week 12. Lines connect data from the same donors, bars represent median values. P value was calculated by paired two-tailed Wilcoxon test.

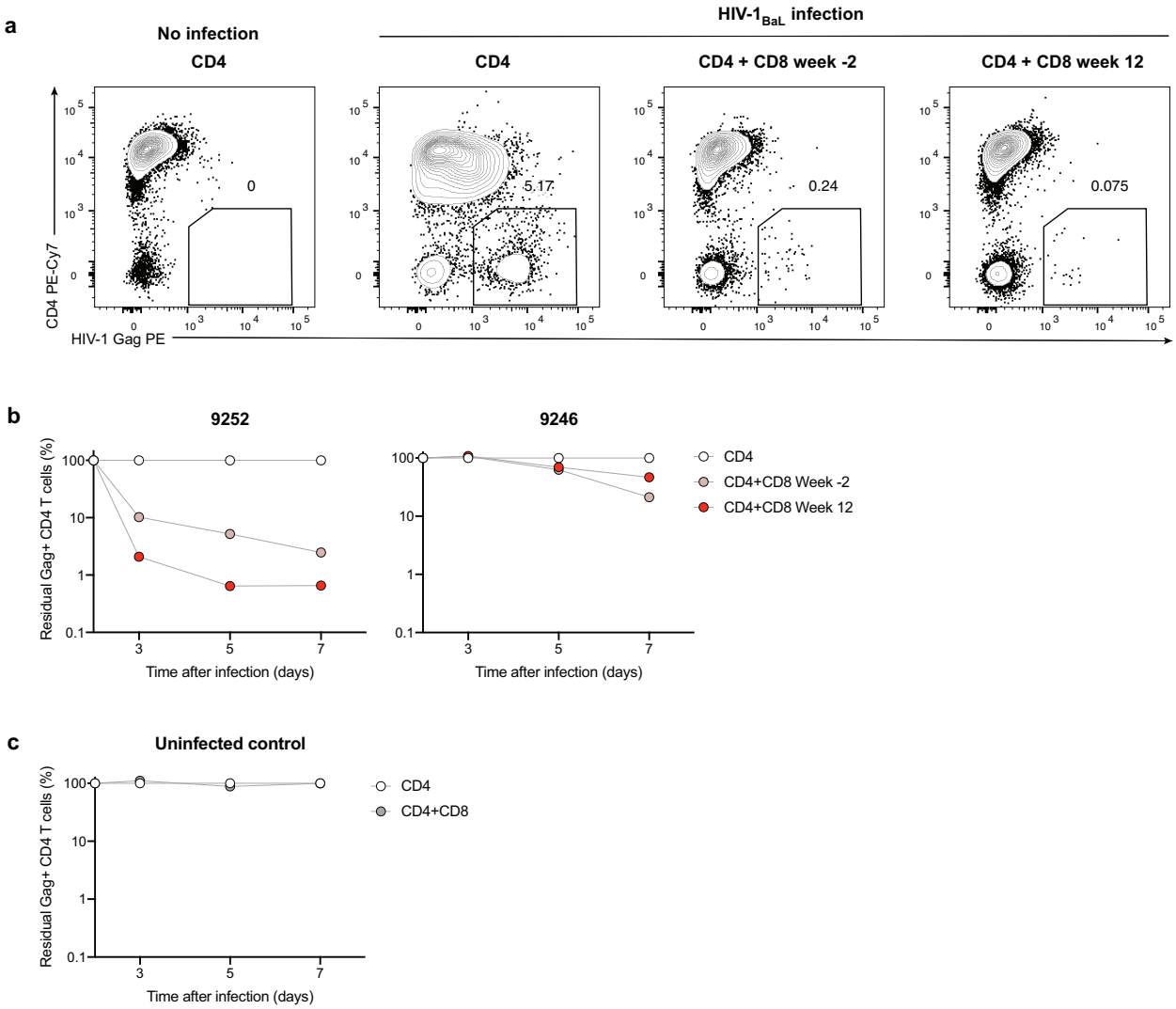

Extended Data Figure 9 – ***In vitro* HIV-1 inhibition assay for individuals 9252 and 9246**

PHA-activated CD4$^+$ T cells were infected *in vitro* with HIV-1$_{BaL}$, cultured alone or in presence with autologous CD8$^+$ T cells for 3, 5 and 7 days, and analyzed for infection using flow cytometry. (**a**) Example plot showing the frequency of infected CD4$^+$ T cells (HIV-1 Gag$^+$ cells with down-regulated surface CD4) for bNAb+ATI individual 9252. Flow panels are representative of n=3 technical replicates. (**b**) Fraction of residual HIV-1 Gag$^+$CD4$^-$ T cells after 3, 5 or 7 days of co-culture with CD8$^+$ T cells obtained at week -2 or week 12 for n=2 biologically independent individuals (9252 and 9246) normalized to infected CD4$^+$ T cells cultured without CD8$^+$ T cells. (**c**) Fraction of residual HIV-1 Gag$^+$CD4$^-$ T cells after 3, 5 or 7 days of co-culture with autologous CD8$^+$ T cells for one HIV-1-uninfected control individual. Each condition was done in technical duplicates or triplicates depending on cell availability and mean values are shown.

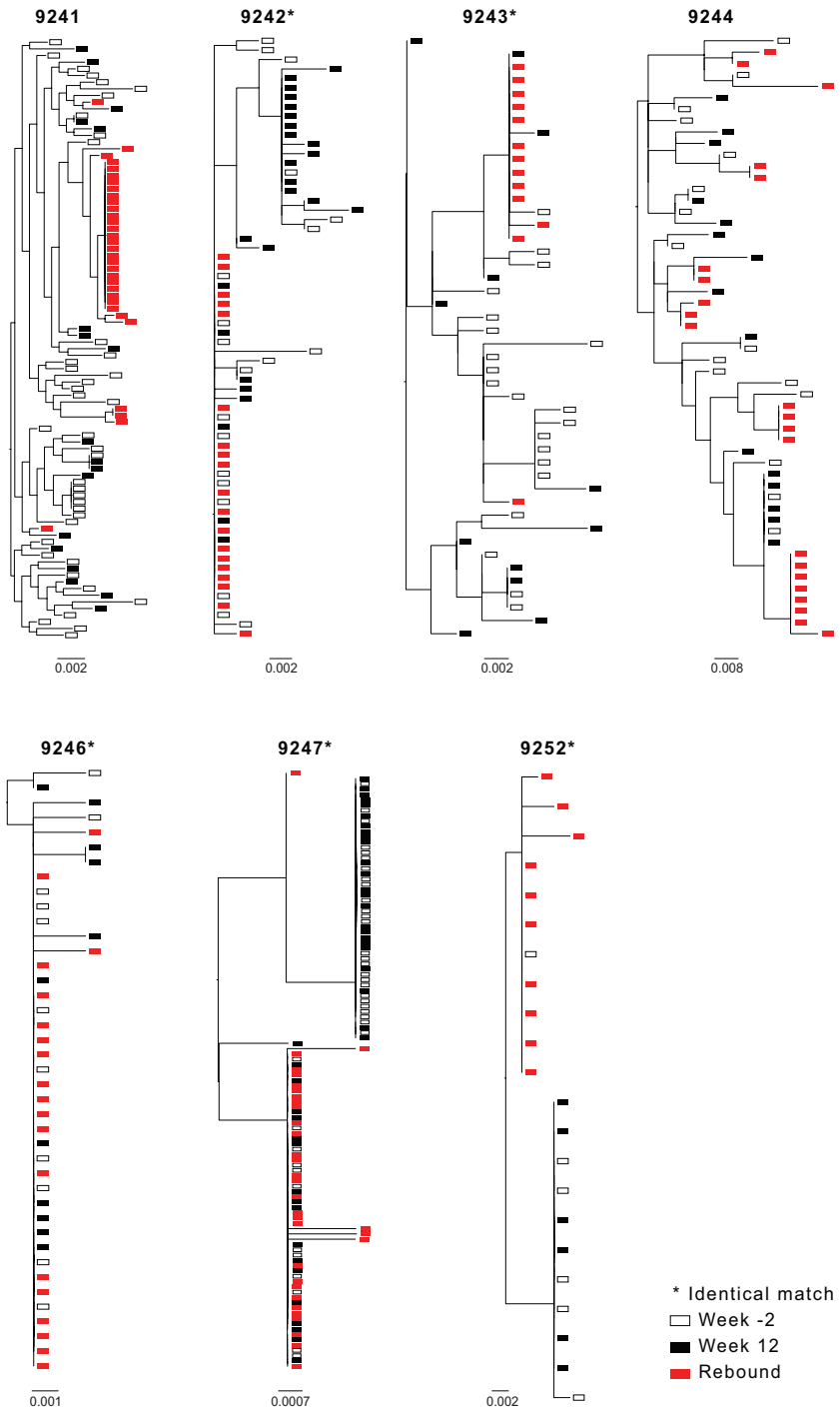

Extended Data Figure 10 – **Comparison of the circulating latent reservoir and rebound viruses**

Maximum likelihood phylogenetic trees of full-length *gag* sequences isolated from CD4⁺ T cell genomic near-full length (NFL) HIV-1 sequencing and rebound plasma SGA from participants 9241, 9242, 9243, 9244, 9246, 9247 and 9252. Open and closed black rectangles indicate NFL-derived viruses from pre-infusion (week -2) and week 12, respectively. Viruses obtained at the time of rebound are indicated by red rectangles (plasma SGA). Asterisks indicate individuals where there is at least one identical match between a *gag* sequence from the latent reservoir and the rebound viruses.

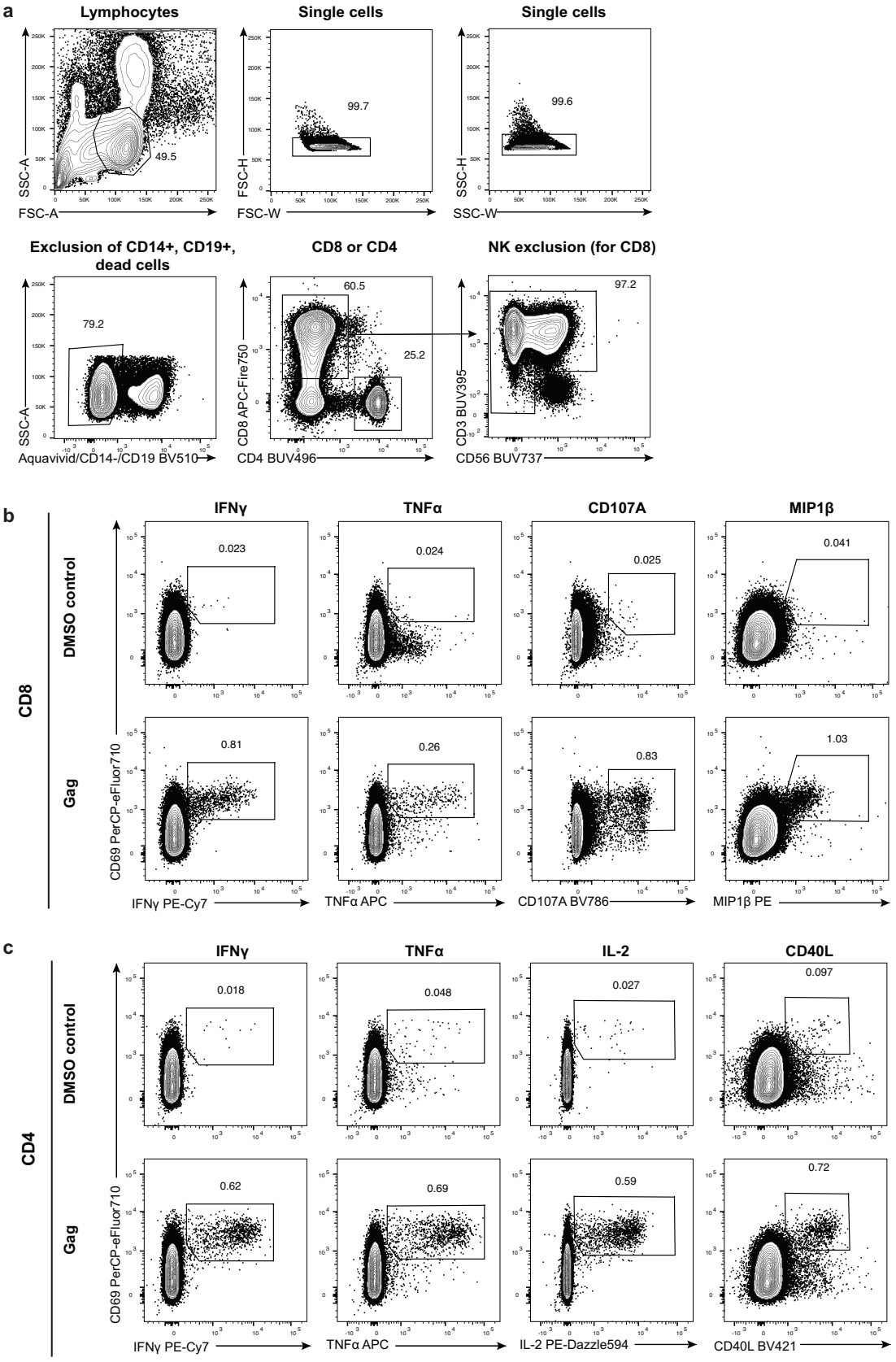
a
Lymphocytes
Single cells
Single cells
SSC-A
FSC-A
49.5
FSC-H
FSC-W
99.7
SSC-H
SSC-W
99.6
Exclusion of CD14+, CD19+, dead cells
CD8 or CD4
NK exclusion (for CD8)
79.2
Aquavivid/CD14-/CD19 BV510
60.5
25.2
CD8 APC-Fire750
CD4 BUV496
97.2
CD3 BUV395
CD56 BUV737
b
CD8
DMSO control
Gag
IFNγ
TNFα
CD107A
MIP1β
0.023
0.024
0.025
0.041
0.81
0.26
0.83
1.03
CD69 PerCP-eFluor710
IFNγ PE-Cy7
TNFα APC
CD107A BV786
MIP1β PE
c
CD4
DMSO control
Gag
IFNγ
TNFα
IL-2
CD40L
0.018
0.048
0.027
0.097
0.62
0.69
0.59
0.72
CD69 PerCP-eFluor710
IFNγ PE-Cy7
TNFα APC
IL-2 PE-Dazzle594
CD40L BV421

Supplementary Figure 1 – **Gating strategy for intracellular detection of cytokines in T cells after Gag peptide stimulation**

PBMCs were stimulated with HIV-1 Gag peptide pools for 6h and cytokine production was evaluated by ICS. (**a**) Gating strategy for identification of $CD8^+$ and $CD4^+$ T cells. For $CD8^+$ T cells, $CD8^+CD3^-CD56^+$ NK cells were excluded from analysis. $CD3^-CD56^-$ cells were included due to CD3 downregulation on T cells after stimulation. (**bc**) Representative plots showing respective cytokine staining in DMSO control or Gag-stimulated $CD8^+$ (**b**) or $CD4^+$ T cells (**c**). Flow panels in (**a-c**) are representative of n=24 biologically independent individuals analyzed (n=9 bNAb+ATI individuals with prolonged viral suppression, n=2 bNAb+ATI individuals with early rebound, and n=13 individuals on continuous ART).

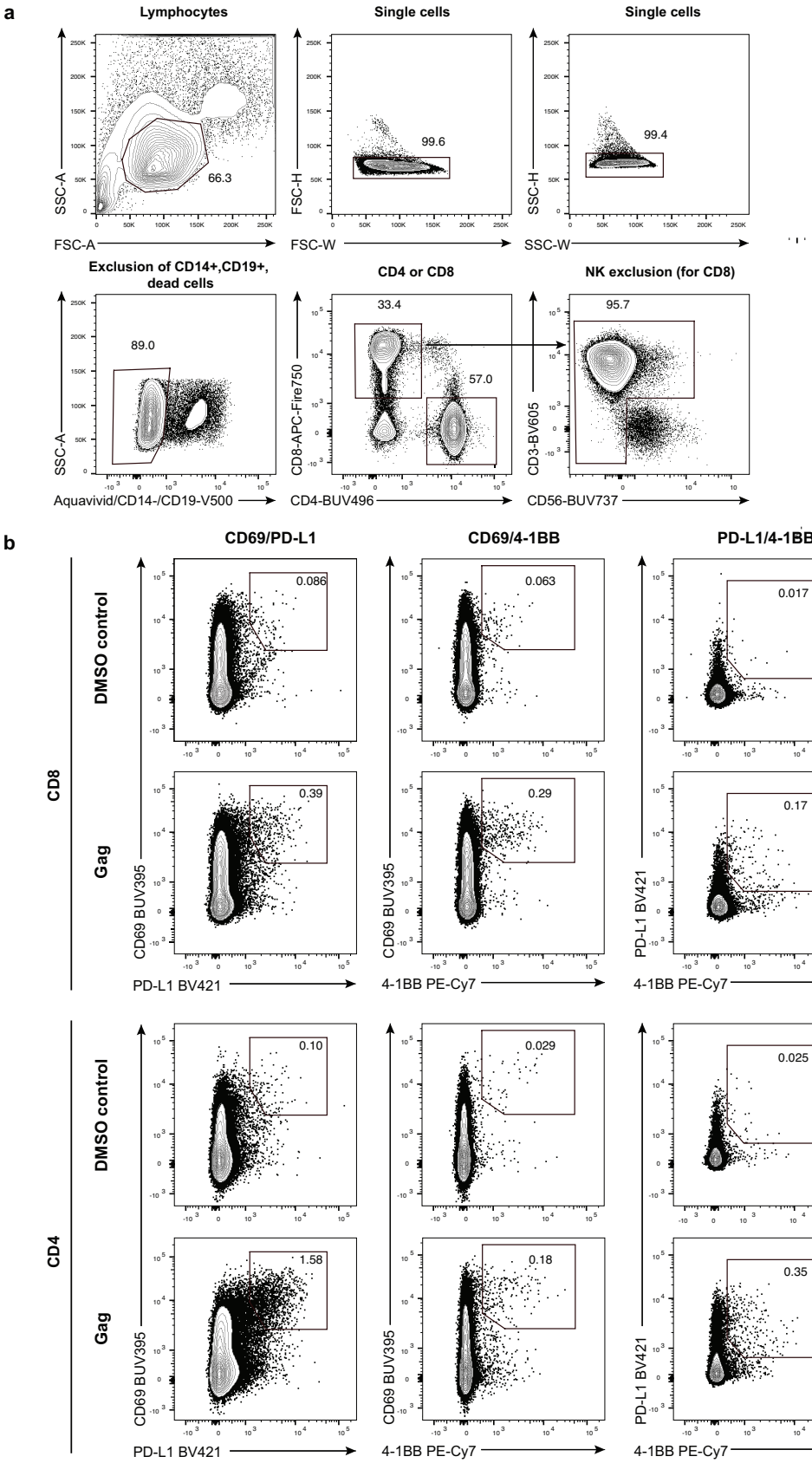
a
Lymphocytes
Single cells
Single cells
SSC-A
FSC-A
66.3
FSC-H
FSC-W
99.6
SSC-H
SSC-W
99.4
Exclusion of CD14+,CD19+, dead cells
CD4 or CD8
NK exclusion (for CD8)
89.0
Aquavivid/CD14-/CD19-V500
33.4
57.0
CD8-APC-Fire750
CD4-BUV496
95.7
CD3-BV605
CD56-BUV737
b
CD69/PD-L1
CD69/4-1BB
PD-L1/4-1BB
CD8
DMSO control
Gag
0.086
0.063
0.017
0.39
0.29
0.17
CD69 BUV395
PD-L1 BV421
4-1BB PE-Cy7
CD4
0.10
0.029
0.025
1.58
0.18
0.35

Supplementary Figure 2 – **Gating strategy for identification of HIV-1-specific T cell responses by AIM assay**

PBMCs were stimulated with HIV-1 peptide pools for 18h and surface expression of AIM molecules were analyzed on $CD8^+$ and $CD4^+$ T cells. DMSO-treated PBMCs served as negative control. (**a**) Gating strategy for identification of $CD8^+$ and $CD4^+$ T cells. For $CD8^+$ T cells, $CD8^+CD3^-CD56^+$ NK cells were excluded from analysis. $CD3^-CD56^-$ cells were included due to CD3 downregulation on T cells after stimulation. (**b**) Representative plot showing co-expression of PD-L1/CD69, 4-1BB/CD69 and PD-L1/4-1BB for $CD8^+$ (upper graphs) and $CD4^+$ T cells (lower graphs) after DMSO treatment or HIV-1 Gag stimulation. Flow panels in (**a-b**) are representative of n=9 biologically independent bNAb+ATI individuals.

Supplementary Table 1 – **Flow cytometry antibody staining panel for intracellular cytokine detection**

Target	Fluorochrome	Clone	Supplier	Detection	Catalog number	Lot number	Volume per test (µl)*
CD3	BUV395	UCHT1	BD Biosciences	Surface	563548	6343984	3
CD4	BUV496	SK3	BD Biosciences	Surface	564651	9080989	4
CD8	APC-Fire750	SK1	Biolegend	Surface	344745	B237278	0.5
CD14	BV510	M5E2	Biolegend	Surface	301842	B250901	3
CD19	BV510	H1B19	Biolegend	Surface	302242	B239285	3
CD40L	BV421	TRAP1	BD Biosciences	Intracellular	563886	6280762	5
CD56	BUV737	NCM16.2	BD Biosciences	Surface	564448	8288818	2.5
CD69	PerCP-eFluor710	FN50	eBioscience	Intracellular	46-0699-42	1920361	4
CD107A	BV786	H4A3	BD Biosciences	Staining during culture	563869	8144866	5
IFNγ	PE-Cy7	B27	BD Biosciences	Intracellular	557643	7202642	4
IL-2	PE-Dazzle594	MQ1-17H12	Biolegend	Intracellular	500344	B245312	3.5
MIP-1β	PE	D21-1351	BD Biosciences	Intracellular	550078	8176503	1
TNFα	APC	MAb11	BD Biosciences	Intracellular	562084	7163931	1.5

*One test: 2M PBMCs in 100µl staining buffer for surface and intracellular detection or 2M PBMCs in 500µl of media for staining during culture.

Supplementary Table 2 – **Flow cytometry antibody staining panel for PD-L1/CD69/4-1BB AIM assay**

Target	Fluorochrome	Clone	Supplier	Catalog number	Lot number	Volume per test (ul)*
CD3	PerCP-eFluor710	SK7	eBioscience	46-0036	1941534	3
CD4	BUV496	SK3	BD Biosciences	564651	9080989	4
CD8	BV711	RPA-T8	Biolegend	301044	B237121	2
CD14	BV510	M5E2	Biolegend	301842	B250901	3
CD19	BV510	H1B19	Biolegend	302242	B239285	3
CD38	PE	HB7	BD Biosicences	342371	8234511	10
CD56	BUV737	NCM16.2	BD Biosciences	564448	8288818	2.5
CD69	BUV395	FN50	BD Biosciences	564364	8242749	5
CD137 (4-1BB)	PE-Cy7	4B4-1	Biolegend	309818	B258325	5
HLA-DR	APC-eFluor780	LN3	eBioscience	47-9956	4312829	2.5
PD-1	Alexa Fluor 647	EH12.2H7	Biolegend	329910	B241533	2.5
PD-L1	BV421	29E2A3	Biolegend	329714	B258010	5

*One test: 5M PBMCs in 100µl staining buffer.

Supplementary Table 3 – **123 peptides covering entire consensus B Gag protein used for ELISpot epitope mapping**

Peptide #	Sequence
1	MGARASVLSGGELDR
2	ASVLSGGELDRWEKI
3	SGGELDRWEKIRLRP
4	LDRWEKIRLRPGGKK
5	EKIRLRPGGKKKYKL
6	LRPGGKKKYKLKHIV
7	GKKKYKLKHIVWASR
8	YKLKHIVWASRELER
9	HIVWASRELERFAVN
10	ASRELERFAVNPGLL
11	LERFAVNPGLLETSE
12	AVNPGLLETSEGCRQ
13	GLLETSEGCRQILGQ
14	TSEGCRQILGQLQPS
15	CRQILGQLQPSLQTG
16	LGQLQPSLQTGSEEL
17	QPSLQTGSEELRSLY
18	QTGSEELRSLYNTVA
19	EELRSLYNTVATLYC
20	SLYNTVATLYCVHQR
21	TVATLYCVHQRIEVK
22	LYCVHQRIEVKDTKE
23	HQRIEVKDTKEALEK
24	EVKDTKEALEKIEEE
25	TKEALEKIEEEQNKS
26	LEKIEEEQNKSKKKA
27	EEEQNKSKKKAQQAA
28	NKSKKKAQQAAADTG
29	KKAQQAAADTGNSSQ
30	QAAADTGNSSQVSQN
31	DTGNSSQVSQNYPIV
32	SSQVSQNYPIVQNLQ
33	SQNYPIVQNLQGQMV
34	PIVQNLQGQMVHQAI

Peptide #	Sequence
35	NLQGQMVHQAISPRT
36	QMVHQAISPRTLNAW
37	QAISPRTLNAWVKVV
38	PRTLNAWVKVVEEKA
39	NAWVKVVEEKAFSPE
40	KVVEEKAFSPEVIPM
41	EKAFSPEVIPMFSAL
42	SPEVIPMFSALSEGA
43	IPMFSALSEGATPQD
44	SALSEGATPQDLNTM
45	EGATPQDLNTMLNTV
46	PQDLNTMLNTVGGHQ
47	NTMLNTVGGHQAAMQ
48	NTVGGHQAAMQMLKE
49	GHQAAMQMLKETINE
50	AMQMLKETINEEAAE
51	LKETINEEAAEWDRL
52	INEEAAEWDRLHPVH
53	AAEWDRLHPVHAGPI
54	DRLHPVHAGPIAPGQ
55	PVHAGPIAPGQMREP
56	GPIAPGQMREPRGSD
57	PGQMREPRGSDIAGT
58	REPRGSDIAGTTSTL
59	GSDIAGTTSTLQEQI
60	AGTTSTLQEQIGWMT
61	STLQEQIGWMTNNPP
62	EQIGWMTNNPPIPVG
63	WMTNNPPIPVGEIYK
64	NPPIPVGEIYKRWII
65	PVGEIYKRWIILGLN
66	IYKRWIILGLNKIVR
67	WIILGLNKIVRMYSP
68	GLNKIVRMYSPTSIL

Peptide #	Sequence
69	IVRMYSPTSILDIRQ
70	YSPTSILDIRQGPKE
71	SILDIRQGPKEPFRD
72	IRQGPKEPFRDYVDR
73	PKEPFRDYVDRFYKT
74	FRDYVDRFYKTLRAE
75	VDRFYKTLRAEQASQ
76	YKTLRAEQASQEVKN
77	RAEQASQEVKNWMTE
78	ASQEVKNWMTETLLV
79	VKNWMTETLLVQNAN
80	MTETLLVQNANPDCK
81	LLVQNANPDCKTILK
82	NANPDCKTILKALGP
83	DCKTILKALGPAATL
84	ILKALGPAATLEEMM
85	LGPAATLEEMMTACQ
86	ATLEEMMTACQGVGG
87	EMMTACQGVGGPGHK
88	ACQGVGGPGHKARVL
89	VGGPGHKARVLAEAM
90	GHKARVLAEAMSQVT
91	RVLAEAMSQVTNSAT
92	EAMSQVTNSATIMMQ
93	QVTNSATIMMQRGNF
94	SATIMMQRGNFRNQR
95	MMQRGNFRNQRKTVK
96	GNFRNQRKTVKCFNC
97	NQRKTVKCFNCGKEG
98	TVKCFNCGKEGHIAK
99	FNCGKEGHIAKNCRA
100	KEGHIAKNCRAPRKK
101	IAKNCRAPRKKGCWK
102	CRAPRKKGCWKCGKE

Peptide #	Sequence
103	RKKGCWKCGKEGHQM
104	CWKCGKEGHQMKDCT
105	GKEGHQMKDCTERQA
106	HQMKDCTERQANFLG
107	DCTERQANFLGKIWP
108	RQANFLGKIWPSHKG
109	FLGKIWPSHKGRPGN
110	IWPSHKGRPGNFLQS
111	HKGRPGNFLQSRPEP
112	PGNFLQSRPEPTAPP
113	LQSRPEPTAPPEESF
114	PEPTAPPEESFRFGE
115	APPEESFRFGEETTT
116	ESFRFGEETTTPSQK
117	FGEETTTPSQKQEPI
118	TTTPSQKQEPIDKEL
119	SQKQEPIDKELYPLA
120	EPIDKELYPLASLRS
121	KELYPLASLRSLFGN
122	PLASLRSLFGNDPSS
123	LRSLFGNDPSSQ

Supplementary Table 4 – **HIV Gag sequence targeted at week 12**

ID	HIV Gag epitope targeted at week 12		
	Peptide #	**Sequence**	**Position in Consensus B sequence**
9241	61	STLQEQIGWMTNNPP	Gag(241-255)
	74	FRDYVDRFYKTLRAE	Gag(293-307)
	75	VDRFYKTLRAEQASQ	Gag(297-311)
	79	VKNWMTETLLVQNAN	Gag(313-327)
9244	5	EKIRLRPGGKKKYKL	Gag(17-31)
	77	RAEQASQEVKNWMTE	Gag(305-319)
9246	45	EGATPQDLNTMLNTV	Gag(177-191)
	61	STLQEQIGWMTNNPP	Gag(241-255)
	80	MTETLLVQNANPDCK	Gag(317-331)
9247	77	RAEQASQEVKNWMTE	Gag(305-319)
	99	FNCGKEGHIAKNCRA	Gag(393-407)
	100	KEGHIAKNCRAPRKK	Gag(397-411)
9252	11	LERFAVNPGLLETSE	Gag(41-55)
	16	LGQLQPSLQTGSEEL	Gag(61-75)
	20	SLYNTVATLYCVHQR	Gag(77-91)
	40	KVVEEKAFSPEVIPM	Gag(157-171)
	45	EGATPQDLNTMLNTV	Gag(177-191)
	67	WIILGLNKIVRMYSP	Gag(265-279)
	75	VDRFYKTLRAEQASQ	Gag(297-311)
	76	YKTLRAEQASQEVKN	Gag(301-315)
	92	EAMSQVTNSATIMMQ	Gag(365-379)
9255	5	EKIRLRPGGKKKYKL	Gag(17-31)

Supplementary Table 5 – **Flow cytometry antibody staining panel for HIV-1 suppression assay**

Target	Fluorochrome	Clone	Supplier	Detection	Catalog number	Lot number	Volume per test (µl)*
CD3	PerCP-eFluor710	SK7	eBioscience	Surface	460036	1941534	3
CD4	PE-Cy7	RPA-T4	BD Biosciences	Surface	560649	9086795	4
CD8	BV711	RPA-T8	Biolegend	Surface	301044	B237121	2
CD14	BUV737	M5E2	BD Biosciences	Surface	564444	7150893	3
CD19	BUV737	SJ25C1	BD Biosciences	Surface	564303	5100759	3
HIV-1 Gag	RD-1/PE	KC57	Beckman Coulter	Intracellular	6604667	7433072	1

*One test: 50,000-100,000 PBMCs in 100µl staining buffer.

nature research

Corresponding author(s): Daniel E. Kaufmann, Michel C. Nussenzweig

Last updated by author(s): 12/17/2019

Reporting Summary

Nature Research wishes to improve the reproducibility of the work that we publish. This form provides structure for consistency and transparency in reporting. For further information on Nature Research policies, see Authors & Referees and the Editorial Policy Checklist.

Statistics

For all statistical analyses, confirm that the following items are present in the figure legend, table legend, main text, or Methods section.

n/a	Confirmed	
☐	☒	The exact sample size (**n**) for each experimental group/condition, given as a discrete number and unit of measurement
☐	☒	A statement on whether measurements were taken from distinct samples or whether the same sample was measured repeatedly
☐	☒	The statistical test(s) used AND whether they are one- or two-sided **Only common tests should be described solely by name; describe more complex techniques in the Methods section.**
☒	☐	A description of all covariates tested
☒	☐	A description of any assumptions or corrections, such as tests of normality and adjustment for multiple comparisons
☐	☒	A full description of the statistical parameters including central tendency (e.g. means) or other basic estimates (e.g. regression coefficient) AND variation (e.g. standard deviation) or associated estimates of uncertainty (e.g. confidence intervals)
☐	☒	For null hypothesis testing, the test statistic (e.g. **F**, **t**, **r**) with confidence intervals, effect sizes, degrees of freedom and **P** value noted **Give P values as exact values whenever suitable.**
☒	☐	For Bayesian analysis, information on the choice of priors and Markov chain Monte Carlo settings
☒	☐	For hierarchical and complex designs, identification of the appropriate level for tests and full reporting of outcomes
☐	☒	Estimates of effect sizes (e.g. Cohen's **d**, Pearson's **r**), indicating how they were calculated

Our web collection on statistics for biologists contains articles on many of the points above.

Software and code

Policy information about availability of computer code

Data collection	DIVA 8.0.1 (cytometer), Immunospot 5.0 (ELISpot), MiSeq Control Software 2.6 2.1 (sequencing)
Data analysis	Flow cytometry data were analyzed with Flowjo v10 (Treestar) and statistical analyses were performed with Prism v8 for Mac (Graphpad Software Inc). Amino acid alignments of intact gag sequences were obtained by using ClustalW v.2.1 under the BLOSUM cost matrix. Sequences with premature stop codons were excluded from all analyses. Maximum likelihood phylogenetic trees were then generated from these alignments using RAxML v.8.2.9 under the GTRGAMMA model with 1,000 bootstraps. To analyze changes between reservoir and rebound viruses, gag sequences were aligned at the amino acid level to a HXB2 reference using ClustalW v.2.1.

For manuscripts utilizing custom algorithms or software that are central to the research but not yet described in published literature, software must be made available to editors/reviewers. We strongly encourage code deposition in a community repository (e.g. GitHub). See the Nature Research guidelines for submitting code & software for further information.

Data

Policy information about availability of data

All manuscripts must include a data availability statement. This statement should provide the following information, where applicable:

- Accession codes, unique identifiers, or web links for publicly available datasets
- A list of figures that have associated raw data
- A description of any restrictions on data availability

Sequences from all isolated viruses are available in GenBank, accession numbers MN750027 - MN750174. Additional datasets that support the findings of this study are available from the corresponding authors on reasonable request.

Field-specific reporting

Please select the one below that is the best fit for your research. If you are not sure, read the appropriate sections before making your selection.

☒ Life sciences ☐ Behavioural & social sciences ☐ Ecological, evolutionary & environmental sciences

For a reference copy of the document with all sections, see nature.com/documents/nr-reporting-summary-flat.pdf

Life sciences study design

All studies must disclose on these points even when the disclosure is negative.

Sample size	No sample size calculation was performed. Results obtained from the bNAb+ATI clinical trial (NCT02825797) have been previously published in Mendoza et al., Nature 561, 479–484 (2018). Nine of the 15 study participants who fulfilled the study eligibility criteria harbored latent reservoir that was sensitive to both bNAbs (10-1074 and 3BNC117) and maintained viral suppression for 15 to >30 weeks after ART discontinuation. We analyzed all available study participants (n=9) with prolonged viral suppression for this manuscript. In addition, two study participants who harbored latent reservoir that was resistant to one of the two bNAbs and who rebounded early after ATI (week 5 or 7) were analyzed (Extended Data Figure 5). The number of individuals included in the historical comparison group of people on continuous ART (n=13) was chosen to approximately match the number of participants enrolled into the Phase Ib trial.
Data exclusions	No participant fulfilling the criteria mentioned above was excluded from the analyses.
Replication	Samples analyzed in this study were obtained from participants of a clinical trial (bNAb+ATI) or an observational study (ART) and samples were analyzed on individual study participants. Experiments did not include replicates as all participants and data points are unique.
Randomization	The bNAb+ATI clinical trial was single arm.
Blinding	The bNAb+ATI clinical trial was open label.

Reporting for specific materials, systems and methods

We require information from authors about some types of materials, experimental systems and methods used in many studies. Here, indicate whether each material, system or method listed is relevant to your study. If you are not sure if a list item applies to your research, read the appropriate section before selecting a response.

Materials & experimental systems

n/a	Involved in the study
☐	☒ Antibodies
☒	☐ Eukaryotic cell lines
☒	☐ Palaeontology
☒	☐ Animals and other organisms
☐	☒ Human research participants
☐	☒ Clinical data

Methods

n/a	Involved in the study
☒	☐ ChIP-seq
☐	☒ Flow cytometry
☒	☐ MRI-based neuroimaging

Antibodies

Antibodies used	3BNC117 and 10-1074 are investigational anti-HIV-1 neutralizing antibodies manufactured for clinical use. They are being investigated under US FDA INDs 118225 and 123713. All antibodies used for flow cytometry are listed in supplementary tables 1, 2 and 5, which describe the specific panels used. 1. CD3 BUV395, UCHT1, BD Biosciences 563548, lot #6343984, 3 µl/test 2. CD4 BUV496, SK3, BD Biosciences 564651, lot #9080989, 4 µl/test 3. CD8 APC-Fire750 SK1, Biolegend 344745, lot#B237278, 0.5 µl/test 4.CD14 BV510 M5E2, Biolegend 301842, lot#B250901, 3 µl/test 5.CD19 BV510, M1B19, Biolegend 302242, lot#B239285, 3 µl/test 6. CD40L BV421, TRAP1, BD Biosciences 563886, lot#6280762, 5 µl/test 7. CD56 BUV737, NCM16.2, BD Biosciences 564448, lot#8288818, 2.5 µl/test 8. CD69 PerCP-eFluor710, FN50, eBioscience 46-0699-42, lot#1920361, 4 µl/test 9. CD107A BV786, H4A3, BD Biosciences 563869, lot#8144866, 5 µl/test 10. IFNγ PE-Cy7, B27, BD Biosciences 557643, lot#7202642, 4 µl/test 11. IL-2 PE-Dazzle594, MQ1-17H12, Biolegend 500344, lot#B245312, 3.5 µl/test 12. MIP1β PE, D21-1351, BD Biosciences 550078, lot#8176503, 1 µl/test

13. TNFα APC, Mab11, BD Biosciences 562084, lot#7163931, 1.5 µl/test
14. CD3 PerCP-eFluor710, SK7, eBioscience 46-0036, lot#1941534, 3 µl/test
15. CD8 BV711, RPA-T8, Biolegend 301044, lot#B237121, 2 µl/test
16. CD69 BUV395, FN50, BD Biosciences 564364, lot#8242749, 5 µl/test
17. CD137 (4-1BB) PE-Cy7, 4B4-1, Biolegend 309818, lot#B258325, 5 µl/test
18. PD-L1 BV421, 29E2A3, Biolegend 329714, lot#B258010, 5 µl/test
19. HLA-DR APC-eFluor780, LN3, eBioscience 47-9956, lot#4312829, 2.5 µl/test
20. CD38 PE, HB7, BD Biosciences 342371, lot# 8234511, 10 µl/test
21. PD-1 Alexa Fluor 647, EH12.2H7, Biolegend 329910, lot# B241533, 2.5 µl/test
22. CD4 PE-Cy7, RPA-T4, BD Biosciences 560649, lot#9086795, 4 µl/test
23. CD14 BUV737, M5E2, BD Biosciences 564444, lot# 7150893, 2 µl/test
24. CD19 BUV737, SJ25C1, BD Biosciences 564303, lot#5100759, 3 µl/test
25. HIV-1 Gag PE, KC57, Beckman Coulter 6604667, lot#7433072, 1 µl/test

Validation

3BNC117 and 10-1074 that were administered to the participants were manufactured by Celldex Therapeutics under Good Manufacturing Practice and have been fully characterized in terms of biophysical properties and potency (INDs 118225 and 123713). Both drug products are under long term stability monitoring.

3BNC117 and 10-1074 are investigational anti-HIV-1 neutralizing antibodies manufactured for clinical use. They are being investigated under US FDA INDs 118225 and 123713.

All antibodies used for flow cytometry were commercially available. Clones and companies are listed in the supplementary tables 1, 2 and 5.
1. CD3 BUV395, reactivity: human (QC testing, BD Biosciences), application: flow cytometry (routinely tested, BD Biosciences)
2. CD4 BUV496, reactivity: human (QC testing, BD Biosciences), application: flow cytometry (routinely tested, BD Biosciences)
3. CD8 APC-Fire750, reactivity: human (Biolegend), application: flow cytometry (quality tested, Biolegend)
4.CD14 BV510, reactivity: human (Biolegend), application: flow cytometry (quality tested, Biolegend)
5.CD19 BV510, reactivity: human (Biolegend), application: flow cytometry (quality tested, Biolegend)
6. CD40L BV421, reactivity: human (QC testing, BD Biosciences), application: flow cytometry (routinely tested, BD Biosciences)
7. CD56 BUV737, reactivity: human (QC testing, BD Biosciences), application: flow cytometry (routinely tested, BD Biosciences)
8. CD69 PerCP-eFluor710, reactivity: human (ThermoFisher), tested applications: flow cytometry (Thermofisher)
9. CD107A BV786, reactivity: human (QC testing, BD Biosciences), application: flow cytometry (routinely tested, BD Biosciences)
10. IFNγ PE-Cy7, reactivity: human (QC testing, BD Biosciences), application: flow cytometry (routinely tested, BD Biosciences)
11. IL-2 PE-Dazzle594, reactivity: human (Biolegend), application: flow cytometry (quality tested, Biolegend)
12. MIP1β PE, reactivity: human (QC testing, BD Biosciences), application: flow cytometry (routinely tested, BD Biosciences)
13. TNFα APC, reactivity: human (QC testing, BD Biosciences), application: flow cytometry (routinely tested, BD Biosciences)
14. CD3 PerCP-eFluor710, reactivity: human (ThermoFisher), tested applications: flow cytometry (Thermofisher)
15. CD8 BV711, reactivity: human (Biolegend), application: flow cytometry (quality tested, Biolegend)
16. CD69 BUV395, reactivity: human (QC testing, BD Biosciences), application: flow cytometry (routinely tested, BD Biosciences)
17. CD137 (4-1BB) PE-Cy7, reactivity: human (Biolegend), application: flow cytometry (quality tested, Biolegend)
18. PD-L1 BV421, reactivity: human (Biolegend), application: flow cytometry (quality tested, Biolegend)
19. HLA-DR APC-eFluor780, reactivity: human (ThermoFisher), tested applications: flow cytometry (Thermofisher)
20. CD38 PE, reactivity: human (QC testing, BD Biosciences), application: flow cytometry (routinely tested, BD Biosciences)
21. PD-1 Alexa Fluor 647, reactivity: human (Biolegend), application: flow cytometry (quality tested, Biolegend)
22. CD4 PE-Cy7, reactivity: human (QC testing, BD Biosciences), application: flow cytometry (routinely tested, BD Biosciences)
23. CD14 BUV737, reactivity: human (QC testing, BD Biosciences), application: flow cytometry (routinely tested, BD Biosciences)
24. CD19 BUV737, reactivity: human (QC testing, BD Biosciences), application: flow cytometry (routinely tested, BD Biosciences)
25. HIV-1 Gag PE, reactivity: HIV-1 core antigen (Beckman Coulter), listed under flow cytometry reagents (Beckman Coulter)

Human research participants

Policy information about studies involving human research participants

Population characteristics

Eligible participants for the bNAb clinical trial were adults aged 18-65 years, HIV-1-infected, on ART for a minimum of 24 months, with plasma HIV-1 RNA levels of 50 copies/ml for at least 18 months (one viral blip of >50 but <500 copies/ml during this 18-month period was allowed), plasma HIV-1 RNA levels of <20 copies/ml at the screening visit, and a current CD4+ T cell count >500 cells/µl. Clinical data are summarized in extended data figure 1 and 5.

To study HIV-specific T cell responses during ART suppression, individuals were recruited at Rockefeller University, that were on ART for at least 4 years. Clinical data for these individuals are shown in extended data figure 2.

Recruitment

Participants of the bNAb+ATI trial were pre-screened for sensitivity of latent proviruses against 3BNC117 and 10-1074 antibodies by bulk PBMC viral outgrowth. Sensitivity was defined as an IC50 < 2 µg/ml for both antibodies against outgrowth virus. Participants harboring sensitive viruses were invited for screening and were enrolled in the study sequentially. Participants were enrolled at the two clinical sites at the Rockefeller University (New York, USA) and Cologne University Hospital (Germany).

HIV-infected individuals on continuous ART were recruited at the Rockefeller University (New York, USA).

	No potential self-selection bias or other bias are known.
Ethics oversight	The clinical trial protocol was approved by the Federal Drug Administration in the USA, the Paul-Ehrlich-Institute in Germany, and the Institutional Review Boards (IRBs) at the Rockefeller University and the University of Cologne. The protocol for collection of samples from ART-suppressed participants was approved by the Rockefeller University IRB.

Note that full information on the approval of the study protocol must also be provided in the manuscript.

Clinical data

Policy information about clinical studies

All manuscripts should comply with the ICMJE guidelines for publication of clinical research and a completed CONSORT checklist must be included with all submissions.

Clinical trial registration	NCT02825797
Study protocol	https://clinicaltrials.gov/ct2/show/NCT02825797
Data collection	Results concerning this clinical trial have been previously published in Mendoza et al., Nature, 561, 479–484 (2018). For this study, we used PBMC samples collected at Rockefeller University or University of Cologne from enrolled HIV-infected trial participants at week -2, 6/7, 12 and 18 (see Extended Data Figures 1 and 5) for analysis.
Outcomes	All primary and secondary outcomes of the trial are described under https://clinicaltrials.gov/ct2/show/NCT02825797. For the immunological exploratory substudy presented here, we pre-selected participants with a specific outcome (maintained viral suppression for >12 weeks after analytical treatment interruption).

Flow Cytometry

Plots

Confirm that:

☒ The axis labels state the marker and fluorochrome used (e.g. CD4-FITC).

☒ The axis scales are clearly visible. Include numbers along axes only for bottom left plot of group (a 'group' is an analysis of identical markers).

☒ All plots are contour plots with outliers or pseudocolor plots.

☒ A numerical value for number of cells or percentage (with statistics) is provided.

Methodology

Sample preparation	Cryopreserved PBMCs were thawed, rested, stimulated, fixed, permeabilized and stained according to the demands on each experiment. All details are mentioned in the Methods section.
Instrument	LSRII (BD Biosciences) and LSR Fortessa (BD) for standard flow cytometry.
Software	Flow cytometry data were collected by DIVA 8.0.1 and analyzed with Flowjo v10 (Treestar).
Cell population abundance	For Flow Cytometry, we collected 0.1-15M events depending on the experiment. FMO controls and DMSO-treated controls were used as controls.
Gating strategy	The generic gating strategy is explained in supplementary figures 1&2 and extended data figures 6& 9.

☒ Tick this box to confirm that a figure exemplifying the gating strategy is provided in the Supplementary Information.

Chapter 5 Discussion

5.1 General conclusion

Despite the emergence of virus-specific T cell responses during HIV infection, the virus cannot be cleared, and virus replication remains detectable in the majority of individuals. Only a small fraction of people living with HIV are able to suppress HIV viremia to undetectable levels in the blood. This elite controller (EC) phenotype is frequently associated with very broad and potent HIV-specific T cell responses. In most cases, the HIV-specific T cell response becomes exhausted or dysfunctional. Most individuals rely on ART to suppress HIV replication, which does not restore effective HIV-specific immunity on its own. In addition, several attempts to improve it through therapeutic interventions have thus far failed.

Here, we studied the HIV-specific $CD4^+$ T cell response in individuals treated with standard ART to better understand its modulation (Manuscript 1). In addition, we analyzed changes in the HIV-specific $CD8^+$ and $CD4^+$ T cell responses in participants of a clinical trial that received a combination anti-HIV antibody therapy and performed an analytical interruption of ART (Manuscript 2).

In Manuscript 1, we examined a cohort of 27 ART-treated individuals recruited in Montreal to study HIV-specific $CD4^+$ T cell responses. We compared phenotype and functions to $CD4^+$ T cell responses specific to another chronic viral infection that is controlled by the immune system (CMV) and to an acute viral infection or vaccine response (HBV) within the same individual. We demonstrated that HIV-specific T cell responses show a persistent expansion of cTfh cells during ART, which were characterized by elevated IR expression, cytokine secretion and preferential Th1-like phenotype and function. These features were induced during chronic untreated HIV infection and persisted despite viral suppression by ART contrasting with a partial recovery of the non-cTfh response. Some persistent features of HIV-specific cTfh cell responses correlated with the translation-competent HIV reservoir suggesting that these might be maintained by continuous antigen stimulation during ART. However, in addition it is likely that other signs of dysfunction are maintained through epigenetic remodelling of T cell functions during chronic stimulation as can be seen for $CD8^+$ T cells in LCMV and cancer.

For Manuscript 2, we collaborated with the groups of Dr. Michel C. Nussenzweig at Rockefeller University, New York, USA and Dr. Florian Klein at the University of Cologne, Germany. They conducted a phase 1b clinical trial, during which recruited HIV-infected ART-treated study participants received repeated infusions with a combination of the anti-HIV bNAbs 10-1074 and 3BNC117 [316]. The study participants subsequently stopped ART and were able to suppress the

virus for at least 15 weeks. We demonstrated that during this period of viral suppression, the HIV-specific $CD8^+$ and $CD4^+$ T cell responses increased, which was not the case in individuals who maintained viral suppression with continuous ART. These increased responses peaked at week six after ATI, subsequently decreased but remained elevated even at later time points when compared to pre-infusion levels. Single epitope analyses revealed that the increased responses were due to both expansion of pre-existing responses and emergence of responses against new epitopes. Although the number of study participants was too small to associate changes in the HIV-specific T cell response with prolonged viral suppression, it provides a proof of concept that bNAb treatment and ATI allows the boosting of the HIV-specific immunity in a setting where $CD4^+$ T cells are protected from infection.

Together our results contribute to a better understanding of the modulation of HIV-specific T cell responses during standard ART and after immunotherapeutic intervention. They demonstrate that some features of HIV-specific $CD4^+$ T cell responses that were induced during untreated infection remain persistent after ART initiation. During continuous ART, this HIV-specific $CD4^+$ T cell response remained quite stable and did not change in magnitude. However, it could be modulated by immunotherapeutic bNAb treatment and ART interruption. Future studies will decipher whether this pre-existing pool of HIV-specific responses competes with the generation of new protective T cell responses after therapeutic vaccination, how HIV-specific responses can be further modulated using different bNAb-treatment strategies, and whether larger studies will find correlates of protective responses and sustained inhibition of HIV replication after the treatment.

5.2 Use of AIM assays to study antigen-specific T cells

In both studies presented, we used cytokine-independent AIM assays as one of the approaches to identify Ag-specific T cell responses. AIM assays identify a larger population of HIV-specific T cell responses when compared to cytokine-based assays as they include T cells that do not produce cytokines or that express functions that are difficult to detect by flow cytometry [21, 22]. Furthermore, AIM assays techniques are not restricted to defined epitopes or HLA types.

In the first manuscript, we used the combination of CD40L and CD69 to identify $CD4^+$ T cell responses after a 9h peptide pool stimulation as previously described by our group for the analysis of virus-specific T cell responses and described by others for the analysis of vaccine-specific T cell responses [23, 75, 222]. However, we detected a low expression of CD40L on activated $CD8^+$ T cells after peptide stimulation (not shown); it was therefore necessary to optimize an alternative AIM assay for the second manuscript to perform the concurrent analysis of HIV-specific $CD8^+$ and

$CD4^+$ T cell responses. After validation of several AIM molecules, we selected CD69, 4-1BB and PD-L1 that are expressed on the surface of antigen-specific cells of both antigen-specific $CD4^+$ and $CD8^+$ T cell responses. We considered T cells as antigen-specific when they expressed at least two of these molecules after peptide stimulation. While CD40L and CD69 are upregulated early after activation on $CD4^+$ T cells, 4-1BB and PD-L1 expression requires a longer stimulation period. Although both AIM strategies identify a larger population compared to standard IFN-γ ICS assay ([222] and Manuscript 1 and 2), they likely do not capture all virus-specific T cell responses. Depending on the combination used, AIM assays might in addition preferentially identify cells with certain functions or phenotypes. However, in Manuscript 1, we used the same AIM assay throughout the study and performed matched comparisons between HIV, CMV and HBV-specific responses. Furthermore, while there are some differences in the populations identified by different AIM markers, there is also a quite sizable overlap [23]. Therefore, it is highly likely that the difference regarding for example cTfh cell frequency between CMV, HBV and HIV-specific $CD4^+$ T cell responses would still be preserved using alternative techniques. As Manuscript 2 used an or-gate strategy and combined various combinations of AIM molecules, this strategy likely includes antigen-specific T cell responses of diverse polarizations and functions.

5.3 Magnitude of HIV-specific T cell responses

In both presented manuscripts, we analyzed the magnitude of HIV-specific T cell responses over time. In Manuscript 1, we detected a decrease of the HIV-specific $CD4^+$ T cell response with initiation of ART when the IFN-γ ICS assay was used as previously reported [325], whereas the responses remained stable when measured with the cytokine-independent AIM assay (Manuscript 1, Figure 5). This suggests that rather than a massive decline, responses undergo changes in polarization, differentiation and function after suppression of viremia, consistent with another study from our group [222]. Using the ICS assay, we did not detect changes in the HIV-specific $CD4^+$ and $CD8^+$ T cell responses over time in HIV-suppressed individuals on continuous ART (Manuscript 2, Extended Data Figure 4), suggesting that once established after ART initiation, the functional profile of these responses is maintained. In both studies, it was evident that HIV-specific T cell responses remain detectable in all HIV-infected individuals included in the studies even after long-term treatment.

In Manuscript 2, we analyzed HIV-specific T cell responses in individuals with suppressed viremia after combination bNAb-treatment and detected increased HIV Gag-specific $CD4^+$ and $CD8^+$ T cell responses after ATI compared to the baseline time point before the immunotherapeutic intervention using ICS and AIM assay. This demonstrates that the magnitude of virus-specific T

cell responses can be boosted after ATI when no viral load is detectable in the blood. Increased HIV Gag-specific T cell responses can also be detected in ART-treated individuals that received therapeutic T cell vaccinations [295, 296] or immune checkpoint blockade therapy [302, 303]. In previous studies that attempted ART interruption in the absence of adjuvant intervention, increased T cell responses against Gag did show no or modest effect on the timing and magnitude of the viral load after rebound [296]. Similarly, in the study presented in Manuscript 2, increased HIV-specific T cell responses did not protect from viral rebound in seven individuals. Furthermore, the two individuals with viral suppression after ART interruption beyond 30 weeks (9254, 9255) did not have the highest frequency of HIV Gag-specific T cell responses nor the biggest increase after the treatment. Together, these results suggest that determining magnitude of HIV Gag-specific T cell responses alone does not represent a reliable predictive marker of HIV control after treatment interruption.

5.4 Persistent expansion and maintained profile of HIV-specific cTfh responses during ART

5.4.1 Persistent cTfh expansion during ART

When we analyzed antigen-specific $CD4^+$ T cell responses in our cohort of ART-treated individuals, we detected a higher frequency of cTfh cells defined by CXCR5 expression that were specific for HIV when compared to CMV or HBV. This expansion of cTfh cells was not only detectable for HIV Gag but also for HIV Env and Nef, demonstrating a specific feature of HIV-specific compared to non-HIV-specific $CD4^+$ T cell responses. A high frequency of cTfh cells within HIV-specific $CD4^+$ T cell responses could already be detected in chronic untreated HIV infection (Manuscript 1, Figure 5 and [222]) and has also been observed in other setting of chronic antigen exposure and high levels of inflammation such as LCMV in mice or malaria or HCV infection in humans [240, 241, 326]. The generation of Tfh cells during chronic viral infection likely plays an important role in supporting humoral and $CD8^+$ T cell responses through IL-21 [327, 328]. Indeed, Tfh cell-dependent antibody responses are required for the eventual control of chronic LCMV infection in mice [240], but fail to control HIV due to escape mutations. In addition, abundant Tfh responses might have a detrimental effect on HIV-specific humoral responses by the selection of low affinity B cells [56]. Although the mechanism is unclear, preferential Tfh polarization has been associated with increased duration of antigen exposure and high levels of antigen and inflammatory cytokines (reviewed in [19]).

Interestingly, we detected an increase in CXCR5 expression upon initiation of therapy when we analyzed longitudinal HIV-specific $CD4^+$ T cell responses before and after starting ART (Manuscript 1, Figure 5). We recently detected an atypical Tfh signature in HIV-specific $CD4^+$ T cells lacking CXCR5 in the peripheral blood of viremic HIV-infected individuals [222]. This population can also be found in the LN and demonstrates a B cell helper capacity *in vitro* [242]. The increase of CXCR5 expression on HIV-specific $CD4^+$ T cells with initiation of antiviral therapy might therefore reflect a gain or recovery of the atypical cTfh cells to re-express CXCR5. An increase of cTfh cells can also be observed in HCV-specific $CD4^+$ T cell responses in the circulation after initiation of antiviral therapy [329]. In this study by Smits *et al.*, the authors concluded that this might represent an egress of Tfh responses from lymphoid or non-lymphoid tissues into the blood after viral clearance and decline of the GC activity [329], however analysis of matched tissue and blood samples would be necessary to confirm this.

Recently, studies in mice identified a subset of long-lived Tfh cells, that demonstrated a unique glycolytic signature, maintained stemness and a self-renewal gene expression profile [330]. In contrast to T_{CM} cells, long-lived Tfh cells were able to survive long-term in lymphoid tissues after clearance of an acute LCMV infection. Whether this population also exists in humans and whether long-lived Tfh cells contribute to the persistence of HIV-specific cTfh during ART remains to be determined.

Persistently expanded cTfh responses in ART-treated individuals might not only serve as a marker of a persistently modulated HIV-specific $CD4^+$ T cell response but could have important implications for therapeutic vaccination strategies. Generation of effective HIV-neutralizing antibodies require high level of maturation in the GC of LNs. Tfh help has to be limited in this context to allow the selection of high-affinity B cell responses. Overabundant pre-existing HIV-specific Tfh cells may therefore hamper the development of a protective B cell immunity.

5.4.2 Persistent cTfh profile during ART

Our results show that HIV-specific cTfh responses exhibited a predominant Th1-like phenotype and function during viremic infection that persisted during viral suppression with ART. This profile could also be observed in other chronic inflammatory infections or diseases including HCV, malaria and lupus [241, 326, 331]. Studies in mouse models demonstrated that during acute viral infection, this Th1-like phenotype of Tfh is induced via IL-12-dependent signal transducers and activators of transcription (STAT)4-signalling, which promotes expression of Bcl6 and T-bet and the generation of Th1-like Tfh cells that produce both IFN-γ and IL-21 [332]. IL-12 is necessary for

Tfh generation in humans [333, 334], and high levels can be detected in the LN of HIV-infected individuals [335]. *In vitro* culture of human $CD4^+$ with IL-12 induced the differentiation of Tfh cells with Th1-like phenotype and function [331]. Th1-like functions can be maintained in Tfh cells even in the absence of T-bet because a transient T-bet expression is sufficient to imprint the locus of Th1-functions epigenetically [336]. In lupus-prone mice and lupus patients, type I IFN and IL-12-dependent activation of STAT4 maintained this Th1-like phenotype of Tfh independent of T-bet expression (personal communication with Dr. Jason Weinstein). Indeed, we only detected a small fraction of T-bet^+ HIV-specific cTfh in ART-treated individuals despite the high frequency of cells expressing CXCR3 and Th1-associated cytokines (Manuscript 1, Figure S4 and 4).

A higher frequency of HIV-specific cTfh cells expressed multiple IRs when compared to other specificities during HIV infection, which was maintained during ART (Manuscript 1, Figure 2). IR expression on $CD8^+$ T cells is associated with a decreased proliferative capacity and effector functions [234], but IRs play an important role for Tfh cells. For example, PD-1 mediated Tfh positioning in the GC, secretion of IL-21 and proper B cell interaction in mouse models [60, 61]. In addition, IRs might regulate Tfh expansion and function in the GC, an environment with chronic antigen exposure [37]. However, despite viral suppression via ART, the frequency of IR^+ HIV-specific cTfh cells remained constantly high in our cohort, whereas it decreased for non-cTfh responses.

How the Th1-like phenotype and IR expression in HIV-specific cTfh during ART persists remains unknown. We speculated that constant antigen exposure in lymphoid tissues might maintain these features. Indeed, the frequency of $TIGIT^+$ and Th1-like phenotype and function of HIV-specific cTfh correlated with the size of the translation-competent HIV reservoir, whereas a correlation was absent with HIV-specific non-cTfh (Manuscript 1, Figure 7). Stochastic production of HIV antigens in lymphoid tissues or trapped antigen on FDCs might activate HIV-specific Tfh cells, which could eventually enter the blood circulation to become cTfh cells. In support of this hypothesis, HIV RNA and protein was detected in lymphoid tissues of successfully ART-treated individuals [175, 176]. A maintained frequency of PD-1 and TIGIT could also be observed in HCV-specific $CD4^+$ T cell responses in individuals that were treated and cleared the infection when compared to chronic infection [329]. However, despite the clearance of the virus with the antiviral treatment, HCV RNA can persist for years in treated individuals [337]. Further analyses are necessary to decipher whether persistent activation of virus-specific T cells possibly in the tissue during treated HIV or HCV infection maintains the dysfunctional response in the infected individuals.

An alternative non-exclusive explanation for the maintained profile of HIV-specific cTfh cell responses during ART might be its epigenetic imprinting during untreated infection with high levels of antigen and inflammation. $CD8^+$ T cells that undergo chronic antigen exposure during chronic viral infections or in the tumor environment do not differentiate into memory cells after the effector phase but become exhausted [234]. This state is characterized by the loss of effector functions and the expression of multiple IRs and limits their immunopathologic effects [234]. In addition, these exhausted $CD8^+$ T cells acquire a unique epigenetic state when compared to other $CD8^+$ T cell subsets that maintains a greater chromatic accessibility in exhaustion-specific regions, which is not reservable by immune-checkpoint blockade [338]. Recently, the HMG-box transcription factor TOX has been identified as a major regulator of $CD8^+$ T cell exhaustion as it induces and maintains the transcriptional and epigenetic programming of exhausted cells [339]. Whether epigenetic reprogramming plays a role in chronically stimulated $CD4^+$ T cells is less well understood. Complex analysis of assay for transposase-accessible chromatin using sequencing (ATAC-seq) data on primary tumor biopsies from patients that received anti-PD-1 immunotherapy revealed a shared program of Tfh and exhausted $CD8^+$ T cells [340]. In addition, TOX and TOX2 regulate chromatic accessibility of Tfh-associated sites and promote Tfh cell differentiation [341]. Therefore, overlapping programs, possibly regulated by TOX, might be responsible for the generation of exhausted cells for the $CD8^+$ T cell lineage and Tfh for the $CD4^+$ T cell lineage during chronic antigen stimulation in mice and humans, which could be maintained by the same mechanism once the antigen is removed. This finding has major implications for the field of therapeutic HIV vaccinations because it suggests that priming of new, effective $CD8^+$ and $CD4^+$ T cell responses instead of boosting pre-existing responses with an epigenetically imprinted profile may be necessary to generate a protective immunity in HIV-infected individuals.

5.5 Possible implications of HIV-specific cTfh profile for B cell immunity

GC responses have to be strictly regulated to allow competition of B cells for limited Tfh help for the selection of high-affinity clones against invading pathogens. This is ensured by keeping Tfh cells a minor population in the GC by limiting their proliferation and function. Regulatory mechanisms of the Tfh population include high expression of multiple IRs and by suppressor functions mediated via Tfr cells [59, 62, 68]. In Manuscript 1, we detected an expansion of cTfh cells within HIV-specific $CD4^+$ T cell responses that were able to express high levels of Tfh- and Th1-related cytokines upon *in vitro* re-stimulation. Tfh expansion and elevated production of effector molecules might therefore contribute to the dysregulated B cell response in HIV-infected

individuals by selecting low-affinity B cell clones for proliferation and differentiation. Indeed, stochastic models suggested that enhanced GC Tfh cell numbers leads to increased antibody responses, which were, however, of lower affinity [342]. This could be confirmed *in vivo* using mouse models [56, 57]. While these antibody responses seem to be beneficial against some viruses [240], HIV has the capacity to escape the humoral immune response.

In addition to expansion, we detected a preferential Th1-like phenotype and function of HIV-specific cTfh cells. Th1 cytokines play an important role during a functional GC response. IL-2 signalling in human cycling B cells induces a PC differentiation-committed transcriptional program [343, 344]. In addition, IL-2 inhibits Tfh differentiation [345]. In mice, IFN-γ is important for the induction of T-bet$^+$ B cells that are able to switch to IgG2a and contribute to viral clearance [346]. This population also increases in the blood of humans after vaccination or acute viral infections and is associated with IgG1 responses [347]. However, this B cell subset has also been associated with various inflammatory immunopathologies. Excessive IFN-γ expression induced T-bet$^+$ B cells in systemic lupus erythematosus and malaria patients, which demonstrate abnormal humoral responses [326, 348]. During untreated HIV-infection, T-bet$^+$ B cell frequency increased in the blood, remained persistently high and almost all Env-specific B cell responses presented this phenotype [347]. A recent study by Austin *et al.* reported a low BCR mutation frequency of T-bet$^+$ B cells and their localization outside the GC in LN samples from HIV-infected individuals, suggesting low affinity maturation [349]. Although Tfh cells were not examined in this study, *in vitro* stimulation of B cells from uninfected tonsil samples with CD40L and IL-21 and especially with IFN-γ induced differentiation into T-bet$^+$ B cells that closely resembled the population observed in tissues of HIV$^+$ individuals [349]. Therefore, the expansion of HIV-specific Tfh cells with preferential Th1-like functions might contribute to the differentiation of dysfunctional B cell responses in HIV-infected individuals, but this requires further investigation.

5.6 Possible mechanisms of increased T cell responses after bNAb treatment and ATI

In Manuscript 2, we detected increased HIV-specific T cell responses in bNAb-treated individuals while viral load was suppressed at undetectable levels after ART interruption, whereas responses remained stable in individuals on continuous ART. This could be due to the different modes of action of ART and bNAbs. Both were effective in suppressing viremia in the studied individuals. However, in contrast to ART, bNAbs do not block the generation of viral particles but inhibit new infections by neutralizing the virus. Increased HIV-specific T cell responses during maintained viral

suppression after bNAb-treatment could therefore be related to at least two mechanisms (Figure 15). First, bNAbs could form immune complexes with HIV antigens that activate APCs such as DCs to stimulate their antigen-presenting and cross-presenting activities [350, 351]. This so-called “vaccinal effect” has been observed in other settings; previous studies reported the development of anti-tumor adaptive T cell responses after tumor-specific monoclonal antibody-treatment in animals and humans [352]. The vaccinal effect was dependent on antigen release from dying tumor cells and antigen-antibody complex binding to FcyR-expressing DCs to induce maturation, antigen presentation and cross-presentation [352]. FcR-dependent induction of virus-specific $CD8^+$ and $CD4^+$ T cells via antigen-antibody complexes has also been reported in the context of SIV infection [353, 354].

An alternative non-exclusive explanation for increased T cell responses is that low-grade viral replication and antigen release, possibly in tissues, stimulates antiviral immunity while overt viremia is suppressed by bNAbs. Although in all individuals used for this study, plasma viral load was below the limit of detection using standard assays at this time point, tissues were not analyzed during this study. Indeed, in a study by Nishimura *et al.*, early combination bNAb treatment of $SHIV_{AD8}$-infected rhesus macaques induced a long-lasting viral suppression that was dependent on $CD8^+$ T cell responses [323]. Despite undetectable plasma viral load using standard assays, ultrasensitive techniques revealed low level replication in bNAb-treated animals [323].

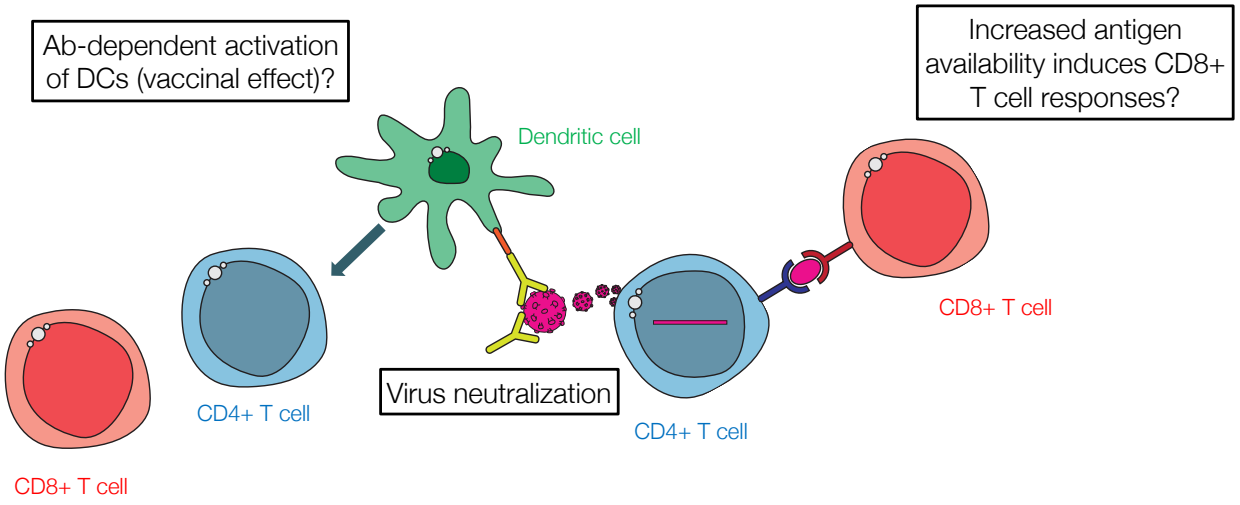

Figure 15 – **Model for mechanism of increased HIV-specific T cell responses in bNAb-treated individuals during ATI**

During analytical treatment interruption, HIV reactivates sporadically from infected $CD4^+$ T cells. The broadly neutralizing antibodies 10-1074 and 3BNC117 (yellow) neutralize reactivated viral particles (pink) and inhibits new infections. Antibody-HIV antigen immune complexes might bind FcRs (orange) expressed on antigen-presenting dendritic cells via their Fc portion. This leads to their activation and induces presentation and cross-presentation to generate HIV-specific $CD8^+$ and $CD4^+$ T cell responses. Alternatively, increased HIV availability of antigen in tissues might induce $CD8^+$ T cell responses. Ab: antibodies, DC: dendritic cell.

Longitudinal sampling at multiple time points after ATI revealed that the HIV-specific T cell responses were highest at week 6, decreased for the later time points of week 12 and 18, but remained elevated compared to baseline. Out of all time points analyzed, bNAb-concentrations were highest at week 6 in all study participants. Therefore, bNAb stimulation of T cell responses via FcR-dependent activation of APCs might be more pronounced at this time point. Alternatively, T cell responses might peak transiently in blood early after stimulation but could be sustained in tissues. T cells responding to blockade of the PD-1 immune-checkpoint in cancer therapy declined after an initial increase at week 3 and 6 post-treatment in the blood, contrasting with a long-lasting reset of the tumor/immune response equilibrium in tissues [355]. Similarly, vaccine-specific $CD4^+$ T cell reflective of GC responses may only be transiently detected in blood [52]. Thus, longitudinal analyses are necessary to capture dynamic changes in the HIV-specific T cell responses after immunotherapeutic intervention.

5.7 Emergence of T cell responses against new epitopes in bNAb+ATI individuals

As mentioned above, the priming of new HIV-specific T cell responses might be important to generate a protective antiviral immunity as during ART, a dysfunctional profile of HIV-specific $CD8^+$ and $CD4^+$ T cell responses persists. In support of the generation of new T cell responses in bNAb-treated individuals, single Gag epitope mapping by IFN-γ ELISpot assay demonstrated an increased breadth in some individuals and the appearance of T cell responses directed against previously untargeted peptides, while epitope recognition patterns remained stable in other subjects (Manuscript 2, Figure 4 & Extended Data Figure 8). We did not observe a clear immunodominance pattern of the new or increased immune responses, although the major homology region of p24 was targeted in several study participants. The IFN-γ ELISpot assay might, however, underestimate changes in the dynamics of HIV Gag-specific T cell responses: increased responses were not limited to IFN-γ-producing cells, as shown by the ICS and AIM results, and we used peptide sets based on consensus clade B sequences (http://www.hiv.lanl.gov/). Therefore, new T cell responses generated against autologous sequences and/or escape variants may have been missed by this approach and would require further analysis, especially as each individual's immune system was stimulated with the autologous virus.

5.8 Capacity to suppress HIV *in vitro* in bNAb-treated individuals

To test whether the increase in HIV-specific $CD8^+$ T cell responses in bNAb-treated individuals correlated with an increased capacity of these cells to block HIV infection, we performed an *in vitro* HIV suppression assay. The greatest absolute increase in the HIV-specific $CD8^+$ T cell responses in the study participants was associated with an expansion of MIP1-β single-positive cells. MIP1-β expression represents one mechanism of $CD8^+$ T cells to inhibit HIV infection because it binds to its receptor CCR5 causing its internalization or blocking its binding to HIV Env [221]. Based on these results, we decided to use the laboratory-adapted CCR5-tropic HIV_{BaL} strain for $CD4^+$ T cell infection for this experiment. While we detected an increased ability of $CD8^+$ T cells isolated from PBMCs obtained after bNAb+ATI treatment compared to baseline for one donor (9252), there was no detectable impact of $CD8^+$ T cells on HIV outgrowth for both time points for the other individual tested (9246). Although these results suggest that the improvement of $CD8^+$

T cells to suppress HIV infection after bNAb treatment might be donor-dependent, they might also underestimate the suppressive capacity of $CD8^+$ T cells against the patient's virus: In a study published by Saez-Cirion *et al.*, CD8-mediated viral suppression *in vitro* was higher against autologous versus laboratory-adapted viral strains in some individuals [356]. Viral suppression studies with each individual's autologous strain obtained by primary culture might therefore be a better estimate of $CD8^+$ T cell function but requires a large number of cells.

5.9 Two individuals with long-term viral suppression after bNAb treatment

Two individuals maintained long-term HIV control for more than 30 weeks after ATI (9254, 9255), even when bNAb antibody levels became undetectable in plasma [316]. Neither individual carried the B*27 and B*57 HLA Class I alleles, which are associated with HIV control [215, 216]. Although potent Gag-specific $CD8^+$ T cells have been linked to control of HIV replication [219], we did not find stronger Gag-specific responses in the long-term controllers compared to individuals who rebounded after the decrease of plasma bNAb concentration. However, we noticed an increase in virus-specific $CD8^+$ and $CD4^+$ responses to nearly all HIV antigens tested, which could not be observed in individuals who rebounded earlier. Although these findings have to be evaluated carefully due to the small sample size and will require assessment in larger trials, they suggest that rather than magnitude, qualitative characteristics might delineate protective versus inefficient HIV-specific T cell responses and/or facilitate long-term responses to bNAb therapy. This finding is consistent with previous therapeutic vaccine studies, which demonstrated that the induction of HIV-specific T cell responses against multiple HIV proteins led to a better control of the viral load when compared to the induction of responses against HIV Gag alone [297]. However, our results are based on a relatively small cohort. Evaluating the modulation of HIV-specific T cell responses in follow-up trials over time with a larger number of study participants will be of great interest to decipher, whether T cell responses can be further modulated in overall size and quality, whether these responses can be maintained long-term, and whether there are T cell immune correlates of prolonged viral suppression in absence of ART.

Chapter 6 Limitations and perspectives

6.1 Blood versus tissue

Both studies described here are based on the analysis of antigen-specific T cell responses in the peripheral blood. In Manuscript 1, we mainly focused on antigen-specific cTfh responses. Several studies highlighted the connection between cTfh cells detected in the peripheral blood and Tfh or GC Tfh responses in lymphoid tissue in humans: Activated cTfh from the blood were clonally related to GC Tfh after vaccination [52], and Tfh cells that demonstrate an intermediate population of GC Tfh in lymphoid tissues and cTfh in blood can be found in the thoracic duct lymph connecting the lymph to the blood system [357]. Therefore, the analysis of blood cTfh responses likely represents an estimate of Tfh responses in lymphoid tissues. Based on the correlation between the size of the translation-competent HIV reservoir and the maintained profile of HIV-specific cTfh responses during ART (Manuscript 1, Figure 7), we suspected a persistent HIV antigen stimulation of Tfh responses in lymphoid tissues. To confirm this assumption, studies would have to be performed on matched blood and tissue samples, which are difficult to obtain in humans. Similarly, in Manuscript 2, tissue studies on HIV antigen expression after ATI and kinetics of HIV-specific T cell responses, which might be different when compared to blood as described above, may be necessary to better understand the effect of bNAb-treatment on the HIV-specific immune system. As an alternative to surgical LN biopsies, fine needle aspirates (FNA) represent a minimally method to sample lymphoid tissues in humans. This technique, which was described around 100 years ago, is currently frequently used in the clinic to assess tumor metastasis, but can be applied to study GC Tfh responses in HIV-infected individuals [358]. Importantly, FNAs isolate a representative fraction of total LN immune cells and the same LN can be targeted repeatedly for longitudinal analyses [358]. To study certain LN resident immune populations, such as FDCs for example, or cell/antigen localization in the LN, excisional biopsies are indispensable and may be required to be done in NHP studies.

6.2 Bystander effect on non-HIV-specific T cell responses

In Manuscript 1, we compared HIV-specific $CD4^+$ T cell responses to control antigens CMV and HBV. However, HIV-infected individuals show a dysregulation of non-HIV-specific T cell immune responses that are only partially restored with ART. For example, IRs are highly upregulated on total $CD4^+$ and $CD8^+$ T cells in viremic HIV-infected individuals and remain higher during ART when compared to uninfected controls [204]. HIV-infected individuals are less likely to respond to vaccination compared to HIV^- individuals [359]. This suggests a general modulation of the adaptive

immune system that cannot be explained by a direct persistent HIV antigen stimulation. IRs and activation marker expression can be induced in an antigen-independent manner by common γ-chain cytokines that are generally elevated during HIV infection [204, 206]. Similarly, Tfh cell development and/or function against non-HIV antigens could be altered by the inflammatory milieu in HIV-infected LNs even during ART [359]. Future in-depth studies comparing CMV-, HBV- or other non-HIV-specific T cell responses in groups of HIV-infected individuals to uninfected controls will be important to decipher this mechanism of bystander T cell dysregulation during HIV infection.

6.3 Delineating increase in number and functional change of HIV-specific T cells after bNAb therapy

The increased HIV-specific $CD8^+$ and $CD4^+$ T cell responses in bNAb-treated individuals were evident by both ICS and AIM assay, although the fold change was less pronounced when the size of HIV-specific T cell responses was measured by AIM assay (Manuscript 2, Figure 1 & 3). Similar to what we observed in Manuscript 1, where ART initiation caused a contraction of the HIV-specific $CD4^+$ T cell response by ICS but not AIM assay, the increased responses measured by ICS in Manuscript 2 could be related to both an increase in number and a change in the T cell polarization and/or function. To delineate both, tetramer staining, which identifies antigen-specific T cells independent of their functional state, would be necessary to confirm an increased number of HIV-specific $CD8^+$ and $CD4^+$ T cell responses with bNAb treatment during ATI.

6.4 Tracing lineages of HIV-specific T cell responses longitudinally

The longitudinal profiling of the HIV-specific $CD8^+$ and $CD4^+$ T cell responses in both studies presented was done at the bulk level measuring the average magnitude and phenotype/function of the antigen-specific cell population. For example, although we detected no change in the overall frequency of the HIV-specific $CD4^+$ T cell response in HIV-infected individuals who started ART and over time in individuals on continuous ART, we cannot exclude that certain T cell lineages wax and wane dynamically with ART initiation. Therefore, tracing T cell lineages at the single-cell level using TCR sequencing techniques would allow a deeper understanding of HIV-specific T cell dynamics over time. This will be of specific importance to confirm the expansion of pre-treatment T cell responses or development of new responses in the bNAb-study participants study participants.

6.5 Mechanism of increased HIV-specific T cell responses in bNAb-treated individuals

Deciphering the mechanism of increased HIV-specific T cell immunity in bNAb-treated individuals during ATI is likely not possible in humans. Instead, NHP models could represent a good alternative. The FcR-dependent aspect of DC activation and T cell stimulation could be studied using bNAbs lacking the Fc portion or conversely using bNAbs with Fc portions that have a higher binding affinity to FcR [317]. This would, however, also interfere with NK-dependent antibody-dependent viral inhibition mechanisms.

6.6 Contribution of $CD8^+$ T cells to viral suppression during ATI in bNAb-treated individuals

Whether $CD8^+$ T cell responses contribute to HIV suppression during ATI in the bNAb-treated individuals remains known. Analysis of the HIV *gag* sequence from rebound plasma did not show any evidence for CTL escape in the seven individuals who rebounded between weeks 15 and 26 after ATI. However, as the viral rebound in these individuals was associated with clearance of the infused bNAbs from the body and/or occurrence of bNAb-resistance mutations, it is likely that viral suppression was mainly mediated by the antibodies. However, similar to studies in NHPs, where bNAb-treatment induced an effective $CD8^+$ T cell response that was able to control HIV even in the absence of bNAbs [323], HIV-specific T cell immunity could play an important role especially in the two individuals with long-term control of more than 30 weeks after ATI. Phenotypic and functional analyses of HIV-specific T cell responses beyond week 18 could provide important information on the long-term effect of bNAb-treatment and ATI in these individuals. In addition, it would be interesting to determine whether $CD8^+$ T cells exerted immune pressure on the virus by sequencing analysis once the two individuals should rebound.

6.7 Future clinical trials using bNAb and ATI as HIV therapy strategy

Several clinical trials are currently ongoing or recruiting study participants to follow up on the phase Ib study that used 3BNC117 and 10-1074 for treatment of HIV-infected individuals who underwent ATI [316]. These include trials that aim to study the effect of

1. 3BNC117 and 10-1074 in larger cohorts and with a placebo-treated control group (ClinicalTrials.gov identifier: NCT03571204),

2. different combinations of bNAbs (e.g. 10-1074 + VRC01; ClinicalTrials.gov identifier: NCT03831945),
3. modified versions of 3BNC117 and 10-1074 to extend their half-lives (ClinicalTrials.gov identifier: NCT04250636),
4. increased number of infusions (NCT03526848), and
5. the combination of bNAb-treatment with immunomodulators (e.g. TLR9 agonists, IFN-α2b or the IL-15 superagonist N-803 (ClinicalTrials.gov identifier: NCT03837756, NCT03588715, NCT04340596)

to maintain long-term viral suppression in HIV-infected individuals after ART interruption, reactivate and decrease the reservoir, and stimulate antiviral immune responses.

Chapter 7 Significance

Our results contribute to a better understanding of HIV-specific T cell responses during standard ART and immunotherapeutic bNAb therapy. Findings from both manuscripts may help to develop more effective HIV treatment strategies to improve the host's immune system so that HIV can be controlled without the need for ART.

Qualitatively impaired and overabundant antigen-specific Tfh responses were shown to be detrimental for effective humoral responses as they can lead to the selection of low affinity B cells. Our findings suggest that therapeutic vaccine strategies that aim to induce an effective antiviral humoral response likely need to induce new Tfh responses that exhibit an effective B helper cell profile instead of further boosting the pre-existing pool. In addition, our findings may be relevant for other infections, which are characterized by low-quality antibody responses.

It was known that bNAb treatment can act as an alternative strategy to ART to maintain suppressed viral loads in HIV-infected individuals. Our results added a new effect of this alternative treatment strategy, namely, to increase HIV-specific T cell responses. Increasing the HIV-specific T cell immunity via bNAb+ATI treatment has the advantage, when compared to ATI alone, standard ART or T cell vaccination strategies, to stimulate the immune system with each individual's own autologous virus while viremia is suppressed. Our findings related to the two long-term controllers, who were able to suppress viremia for more than 30 weeks even after the bNAbs were cleared, suggest that an increased breadth rather than augmented magnitude might be associated with prolonged suppression. Our results are highly relevant to ongoing and future trials using bNAb infusion alone or in combination with other immunomodulators, and to additional trials investigating antibody infusion to treat other viral infections or diseases.

Chapter 8 References

1. Yan, N. and Z.J. Chen, *Intrinsic antiviral immunity.* Nature immunology, 2012. **13**(3): p. 214-222.
2. Adams, N.M. and J.C. Sun, *Spatial and temporal coordination of antiviral responses by group 1 ILCs.* Immunological reviews, 2018. **286**(1): p. 23-36.
3. Mogensen, T.H., *Pathogen recognition and inflammatory signaling in innate immune defenses.* Clinical microbiology reviews, 2009. **22**(2): p. 240-273.
4. Hirosue, S. and J. Dubrot, *Modes of Antigen Presentation by Lymph Node Stromal Cells and Their Immunological Implications.* Frontiers in Immunology, 2015. **6**(446).
5. Demers, K.R., et al., *Temporal Dynamics of CD8+ T Cell Effector Responses during Primary HIV Infection.* PLOS Pathogens, 2016. **12**(8): p. e1005805.
6. Wherry, E.J. and R. Ahmed, *Memory CD8 T-cell differentiation during viral infection.* Journal of virology, 2004. **78**(11): p. 5535-5545.
7. Russ, B., et al., *T cell immunity as a tool for studying epigenetic regulation of cellular differentiation.* Frontiers in Genetics, 2013. **4**(218).
8. Andersen, M.H., et al., *Cytotoxic T Cells.* Journal of Investigative Dermatology, 2006. **126**(1): p. 32-41.
9. Nurieva, R.I. and Y. Chung, *Understanding the development and function of T follicular helper cells.* Cellular & Molecular Immunology, 2010. **7**(3): p. 190-197.
10. Buggert, M., et al., *Limited immune surveillance in lymphoid tissue by cytolytic CD4+ T cells during health and HIV disease.* PLOS Pathogens, 2018. **14**(4): p. e1006973.
11. Castro, G., et al., *RORgammat and RORalpha signature genes in human Th17 cells.* PLoS One, 2017. **12**(8): p. e0181868.
12. Plank, M.W., et al., *Th22 Cells Form a Distinct Th Lineage from Th17 Cells In Vitro with Unique Transcriptional Properties and Tbet-Dependent Th1 Plasticity.* Journal of immunology (Baltimore, Md. : 1950), 2017. **198**(5): p. 2182-2190.
13. Prlic, M. and M.J. Bevan, *Exploring regulatory mechanisms of CD8⁺ T cell contraction.* Proceedings of the National Academy of Sciences, 2008. **105**(43): p. 16689-16694.
14. Gasper, D.J., M.M. Tejera, and M. Suresh, *CD4 T-cell memory generation and maintenance.* Critical reviews in immunology, 2014. **34**(2): p. 121-146.
15. Sallusto, F., et al., *Two subsets of memory T lymphocytes with distinct homing potentials and effector functions.* Nature, 1999. **401**(6754): p. 708-12.
16. Mueller, S.N. and L.K. Mackay, *Tissue-resident memory T cells: local specialists in immune defence.* Nat Rev Immunol, 2016. **16**(2): p. 79-89.
17. Thome, J.J. and D.L. Farber, *Emerging concepts in tissue-resident T cells: lessons from humans.* Trends Immunol, 2015. **36**(7): p. 428-35.
18. Schenkel, J.M., et al., *IL-15-Independent Maintenance of Tissue-Resident and Boosted Effector Memory CD8 T Cells.* J Immunol, 2016. **196**(9): p. 3920-6.
19. Vella, L.A., R.S. Herati, and E.J. Wherry, *CD4+ T Cell Differentiation in Chronic Viral Infections: The Tfh Perspective.* Trends in Molecular Medicine, 2017. **23**(12): p. 1072-1087.
20. Hale, J.S., et al., *Distinct memory CD4+ T cells with commitment to T follicular helper- and T helper 1-cell lineages are generated after acute viral infection.* Immunity, 2013. **38**(4): p. 805-17.
21. Dan, J.M., et al., *A Cytokine-Independent Approach To Identify Antigen-Specific Human Germinal Center T Follicular Helper Cells and Rare Antigen-Specific CD4+ T Cells in Blood.* J Immunol, 2016. **197**(3): p. 983-93.
22. Havenar-Daughton, C., et al., *Cytokine-Independent Detection of Antigen-Specific Germinal Center T Follicular Helper Cells in Immunized Nonhuman Primates Using a Live Cell Activation-Induced Marker Technique.* J Immunol, 2016. **197**(3): p. 994-1002.

23. Reiss, S., et al., *Comparative analysis of activation induced marker (AIM) assays for sensitive identification of antigen-specific CD4 T cells.* PLOS ONE, 2017. **12**(10): p. e0186998.
24. Breitfeld, D., et al., *Follicular B helper T cells express CXC chemokine receptor 5, localize to B cell follicles, and support immunoglobulin production.* J Exp Med, 2000. **192**(11): p. 1545-52.
25. Schaerli, P., et al., *CXC chemokine receptor 5 expression defines follicular homing T cells with B cell helper function.* J Exp Med, 2000. **192**(11): p. 1553-62.
26. Choi, Y.S., et al., *LEF-1 and TCF-1 orchestrate TFH differentiation by regulating differentiation circuits upstream of the transcriptional repressor Bcl6.* Nature Immunology, 2015. **16**(9): p. 980-990.
27. Xu, L., et al., *The transcription factor TCF-1 initiates the differentiation of T(FH) cells during acute viral infection.* Nat Immunol, 2015. **16**(9): p. 991-9.
28. Johnston, R.J., et al., *Bcl6 and Blimp-1 are reciprocal and antagonistic regulators of T follicular helper cell differentiation.* Science, 2009. **325**(5943): p. 1006-10.
29. Nurieva, R.I., et al., *Bcl6 mediates the development of T follicular helper cells.* Science, 2009. **325**(5943): p. 1001-5.
30. Yu, D., et al., *The transcriptional repressor Bcl-6 directs T follicular helper cell lineage commitment.* Immunity, 2009. **31**(3): p. 457-68.
31. Kroenke, M.A., et al., *Bcl6 and Maf cooperate to instruct human follicular helper CD4 T cell differentiation.* J Immunol, 2012. **188**(8): p. 3734-44.
32. Liu, X., et al., *Transcription factor achaete-scute homologue 2 initiates follicular T-helper-cell development.* Nature, 2014. **507**(7493): p. 513-8.
33. Hardtke, S., L. Ohl, and R. Forster, *Balanced expression of CXCR5 and CCR7 on follicular T helper cells determines their transient positioning to lymph node follicles and is essential for efficient B-cell help.* Blood, 2005. **106**(6): p. 1924-31.
34. Tahiliani, V., et al., *OX40 Cooperates with ICOS To Amplify Follicular Th Cell Development and Germinal Center Reactions during Infection.* J Immunol, 2017. **198**(1): p. 218-228.
35. Kerfoot, S.M., et al., *Germinal center B cell and T follicular helper cell development initiates in the interfollicular zone.* Immunity, 2011. **34**(6): p. 947-60.
36. Baumjohann, D., et al., *Persistent antigen and germinal center B cells sustain T follicular helper cell responses and phenotype.* Immunity, 2013. **38**(3): p. 596-605.
37. Niessl, J. and D.E. Kaufmann, *Harnessing T Follicular Helper Cell Responses for HIV Vaccine Development.* Viruses, 2018. **10**(6).
38. Keck, S., et al., *Antigen affinity and antigen dose exert distinct influences on CD4 T-cell differentiation.* Proc Natl Acad Sci U S A, 2014. **111**(41): p. 14852-7.
39. MacLennan, I.C., et al., *Extrafollicular antibody responses.* Immunol Rev, 2003. **194**: p. 8-18.
40. Schwickert, T.A., et al., *A dynamic T cell-limited checkpoint regulates affinity-dependent B cell entry into the germinal center.* J Exp Med, 2011. **208**(6): p. 1243-52.
41. Victora, G.D., et al., *Germinal center dynamics revealed by multiphoton microscopy with a photoactivatable fluorescent reporter.* Cell, 2010. **143**(4): p. 592-605.
42. Gitlin, A.D., Z. Shulman, and M.C. Nussenzweig, *Clonal selection in the germinal centre by regulated proliferation and hypermutation.* Nature, 2014. **509**(7502): p. 637-40.
43. Moens, L. and S.G. Tangye, *Cytokine-Mediated Regulation of Plasma Cell Generation: IL-21 Takes Center Stage.* Front Immunol, 2014. **5**: p. 65.
44. Krautler, N.J., et al., *Differentiation of germinal center B cells into plasma cells is initiated by high-affinity antigen and completed by Tfh cells.* J Exp Med, 2017. **214**(5): p. 1259-1267.
45. Zhang, Y., et al., *Plasma cell output from germinal centers is regulated by signals from Tfh and stromal cells.* J Exp Med, 2018. **215**(4): p. 1227-1243.

46. Forthal, D.N. and C. Moog, *Fc receptor-mediated antiviral antibodies.* Current opinion in HIV and AIDS, 2009. **4**(5): p. 388-393.
47. Fazilleau, N., et al., *Lymphoid reservoirs of antigen-specific memory T helper cells.* Nat Immunol, 2007. **8**(7): p. 753-61.
48. Morita, R., et al., *Human blood CXCR5(+)CD4(+) T cells are counterparts of T follicular cells and contain specific subsets that differentially support antibody secretion.* Immunity, 2011. **34**(1): p. 108-21.
49. Locci, M., et al., *Human circulating PD-1+CXCR3-CXCR5+ memory Tfh cells are highly functional and correlate with broadly neutralizing HIV antibody responses.* Immunity, 2013. **39**(4): p. 758-69.
50. Simpson, N., et al., *Expansion of circulating T cells resembling follicular helper T cells is a fixed phenotype that identifies a subset of severe systemic lupus erythematosus.* Arthritis Rheum, 2010. **62**(1): p. 234-44.
51. Sage, P.T., et al., *Circulating T follicular regulatory and helper cells have memory-like properties.* J Clin Invest, 2014. **124**(12): p. 5191-204.
52. Heit, A., et al., *Vaccination establishes clonal relatives of germinal center T cells in the blood of humans.* J Exp Med, 2017. **214**(7): p. 2139-2152.
53. Bentebibel, S.E., et al., *Induction of ICOS+CXCR3+CXCR5+ TH cells correlates with antibody responses to influenza vaccination.* Sci Transl Med, 2013. **5**(176): p. 176ra32.
54. Velu, V., et al., *Induction of Th1-Biased T Follicular Helper (Tfh) Cells in Lymphoid Tissues during Chronic Simian Immunodeficiency Virus Infection Defines Functionally Distinct Germinal Center Tfh Cells.* J Immunol, 2016. **197**(5): p. 1832-42.
55. Nance, J.P., et al., *Bcl6 middle domain repressor function is required for T follicular helper cell differentiation and utilizes the corepressor MTA3.* Proc Natl Acad Sci U S A, 2015. **112**(43): p. 13324-9.
56. Preite, S., et al., *Somatic mutations and affinity maturation are impaired by excessive numbers of T follicular helper cells and restored by Treg cells or memory T cells.* Eur J Immunol, 2015. **45**(11): p. 3010-21.
57. Vinuesa, C.G., et al., *A RING-type ubiquitin ligase family member required to repress follicular helper T cells and autoimmunity.* Nature, 2005. **435**(7041): p. 452-8.
58. Choi, Y.S., et al., *Bcl6 expressing follicular helper CD4 T cells are fate committed early and have the capacity to form memory.* J Immunol, 2013. **190**(8): p. 4014-26.
59. Sage, P.T., et al., *The receptor PD-1 controls follicular regulatory T cells in the lymph nodes and blood.* Nat Immunol, 2013. **14**(2): p. 152-61.
60. Good-Jacobson, K.L., et al., *PD-1 regulates germinal center B cell survival and the formation and affinity of long-lived plasma cells.* Nat Immunol, 2010. **11**(6): p. 535-42.
61. Shi, J., et al., *PD-1 Controls Follicular T Helper Cell Positioning and Function.* Immunity, 2018. **49**(2): p. 264-274.e4.
62. Sage, P.T., et al., *The coinhibitory receptor CTLA-4 controls B cell responses by modulating T follicular helper, T follicular regulatory, and T regulatory cells.* Immunity, 2014. **41**(6): p. 1026-39.
63. Butler, N.S., et al., *Therapeutic blockade of PD-L1 and LAG-3 rapidly clears established blood-stage Plasmodium infection.* Nat Immunol, 2011. **13**(2): p. 188-95.
64. Hams, E., et al., *Blockade of B7-H1 (programmed death ligand 1) enhances humoral immunity by positively regulating the generation of T follicular helper cells.* J Immunol, 2011. **186**(10): p. 5648-55.
65. Linterman, M.A., et al., *Foxp3+ follicular regulatory T cells control the germinal center response.* Nat Med, 2011. **17**(8): p. 975-82.
66. Wollenberg, I., et al., *Regulation of the germinal center reaction by Foxp3+ follicular regulatory T cells.* J Immunol, 2011. **187**(9): p. 4553-60.

67. Chung, Y., et al., *Follicular regulatory T cells expressing Foxp3 and Bcl-6 suppress germinal center reactions.* Nat Med, 2011. **17**(8): p. 983-8.
68. Sage, P.T. and A.H. Sharpe, *T follicular regulatory cells in the regulation of B cell responses.* Trends Immunol, 2015. **36**(7): p. 410-8.
69. Clem, A.S., *Fundamentals of vaccine immunology.* Journal of global infectious diseases, 2011. **3**(1): p. 73-78.
70. Lee, S. and M.T. Nguyen, *Recent advances of vaccine adjuvants for infectious diseases.* Immune network, 2015. **15**(2): p. 51-57.
71. Pulendran, B. and R. Ahmed, *Immunological mechanisms of vaccination.* Nature immunology, 2011. **12**(6): p. 509-517.
72. Amanna, I.J. and M.K. Slifka, *Contributions of humoral and cellular immunity to vaccine-induced protection in humans.* Virology, 2011. **411**(2): p. 206-15.
73. Ueno, H., *Tfh cell response in influenza vaccines in humans: what is visible and what is invisible.* Curr Opin Immunol, 2019. **59**: p. 9-14.
74. Crotty, S., *T Follicular Helper Cell Biology: A Decade of Discovery and Diseases.* Immunity, 2019. **50**(5): p. 1132-1148.
75. Pallikkuth, S., et al., *Dysfunctional peripheral T follicular helper cells dominate in people with impaired influenza vaccine responses: Results from the FLORAH study.* PLOS Biology, 2019. **17**(5): p. e3000257.
76. Virgin, H.W., E.J. Wherry, and R. Ahmed, *Redefining Chronic Viral Infection.* Cell, 2009. **138**(1): p. 30-50.
77. Ribbert, H., *Uber protozoenartige Zellen in der Niere eines syphilitischen Neugeborenen und in der Parotis von Kindern.* Zbl Allg Pathol., 1904. **15**: p. 945-948.
78. Ho, M., *The history of cytomegalovirus and its diseases.* Medical Microbiology and Immunology, 2008. **197**(2): p. 65-73.
79. Pardieck, I.N., et al., *Cytomegalovirus infection and progressive differentiation of effector-memory T cells.* F1000Research, 2018. **7**: p. F1000 Faculty Rev-1554.
80. Hosie, L., et al., *Cytomegalovirus-Specific T Cells Restricted by HLA-Cw*0702 Increase Markedly with Age and Dominate the CD8+ T-Cell Repertoire in Older People.* Frontiers in Immunology, 2017. **8**(1776).
81. Zuhair, M., et al., *Estimation of the worldwide seroprevalence of cytomegalovirus: A systematic review and meta-analysis.* Rev Med Virol, 2019. **29**(3): p. e2034.
82. Barrett, L., et al., *Immune resilience in HIV-infected individuals seronegative for cytomegalovirus.* Aids, 2014. **28**(14): p. 2045-9.
83. Kalejta, R.F., *Tegument proteins of human cytomegalovirus.* Microbiology and molecular biology reviews : MMBR, 2008. **72**(2): p. 249-265.
84. Fuhrmann, S., et al., *T Cell Response to the Cytomegalovirus Major Capsid Protein (UL86) Is Dominated by Helper Cells with a Large Polyfunctional Component and Diverse Epitope Recognition.* The Journal of Infectious Diseases, 2008. **197**(10): p. 1455-1458.
85. Dolan, A., et al., *Genetic content of wild-type human cytomegalovirus.* Journal of General Virology, 2004. **85**(5): p. 1301-1312.
86. Sinzger, C., M. Digel, and G. Jahn, *Cytomegalovirus cell tropism.* Curr Top Microbiol Immunol, 2008. **325**: p. 63-83.
87. Jean Beltran, P.M. and I.M. Cristea, *The life cycle and pathogenesis of human cytomegalovirus infection: lessons from proteomics.* Expert review of proteomics, 2014. **11**(6): p. 697-711.
88. Sinclair, J., *Human cytomegalovirus: Latency and reactivation in the myeloid lineage.* J Clin Virol, 2008. **41**(3): p. 180-5.
89. Zdziarski, P., *CMV-Specific Immune Response-New Patients, New Insight: Central Role of Specific IgG during Infancy and Long-Lasting Immune Deficiency after Allogenic Stem Cell Transplantation.* Int J Mol Sci, 2019. **20**(2).

90. Sylwester, A.W., et al., *Broadly targeted human cytomegalovirus-specific CD4+ and CD8+ T cells dominate the memory compartments of exposed subjects.* The Journal of experimental medicine, 2005. **202**(5): p. 673-685.
91. Chen, S.F., et al., *Antiviral CD8 T Cells in the Control of Primary Human Cytomegalovirus Infection in Early Childhood.* The Journal of Infectious Diseases, 2004. **189**(9): p. 1619-1627.
92. Khan, N., et al., *Cytomegalovirus Seropositivity Drives the CD8 T Cell Repertoire Toward Greater Clonality in Healthy Elderly Individuals.* The Journal of Immunology, 2002. **169**(4): p. 1984-1992.
93. Pourgheysari, B., et al., *The Cytomegalovirus-Specific CD4⁺ T-Cell Response Expands with Age and Markedly Alters the CD4⁺ T-Cell Repertoire.* Journal of Virology, 2007. **81**(14): p. 7759-7765.
94. van den Berg, S.P.H., et al., *The hallmarks of CMV-specific CD8 T-cell differentiation.* Med Microbiol Immunol, 2019. **208**(3-4): p. 365-373.
95. Chiu, Y.-L., et al., *Cytotoxic polyfunctionality maturation of cytomegalovirus-pp65-specific CD4 + and CD8 + T-cell responses in older adults positively correlates with response size.* Scientific Reports, 2016. **6**(1): p. 19227.
96. Gerna, G., et al., *Human cytomegalovirus serum neutralizing antibodies block virus infection of endothelial/epithelial cells, but not fibroblasts, early during primary infection.* Journal of General Virology, 2008. **89**(4): p. 853-865.
97. Bruno, F., et al., *Follicular helper T-cells and virus-specific antibody response in primary and reactivated human cytomegalovirus infections of the immunocompetent and immunocompromised transplant patients.* Journal of General Virology, 2016. **97**(8): p. 1928-1941.
98. Sissons, J.G.P. and M.R. Wills, *How understanding immunology contributes to managing CMV disease in immunosuppressed patients: now and in future.* Medical Microbiology and Immunology, 2015. **204**(3): p. 307-316.
99. Jabs, D.A., et al., *Course of cytomegalovirus retinitis in the era of highly active antiretroviral therapy: 2. Second eye involvement and retinal detachment.* Ophthalmology, 2004. **111**(12): p. 2232-2239.
100. Bronke, C., et al., *Dynamics of Cytomegalovirus (CMV)–Specific T Cells in HIV-1–Infected Individuals Progressing to AIDS with CMV End-Organ Disease.* The Journal of Infectious Diseases, 2005. **191**(6): p. 873-880.
101. Goossens, V.J., et al., *CMV DNA levels and CMV gB subtypes in ART-naive HAART-treated patients: a 2-year follow-up study in The Netherlands.* Aids, 2009. **23**(11): p. 1425-9.
102. Masur, H., et al., *An Outbreak of Community-Acquired Pneumocystis carinii Pneumonia.* New England Journal of Medicine, 1981. **305**(24): p. 1431-1438.
103. CDC, *Pneumocystis pneumonia--Los Angeles.* MMWR Morb Mortal Wkly Rep, 1981. **30**(21): p. 250-2.
104. CDC, *Acquired immune deficiency syndrome (AIDS): precautions for clinical and laboratory staffs.* MMWR. Morbidity and mortality weekly report, 1982. **31**(43): p. 577-580.
105. Barre-Sinoussi, F., et al., *Isolation of a T-lymphotropic retrovirus from a patient at risk for acquired immune deficiency syndrome (AIDS).* Science, 1983. **220**(4599): p. 868-71.
106. Gallo, R.C., et al., *Isolation of human T-cell leukemia virus in acquired immune deficiency syndrome (AIDS).* Science, 1983. **220**(4599): p. 865-7.
107. Campbell-Yesufu, O.T. and R.T. Gandhi, *Update on human immunodeficiency virus (HIV)-2 infection.* Clinical infectious diseases : an official publication of the Infectious Diseases Society of America, 2011. **52**(6): p. 780-787.
108. Lemey, P., et al., *Tracing the origin and history of the HIV-2 epidemic.* Proceedings of the National Academy of Sciences, 2003. **100**(11): p. 6588-6592.

109. Gao, F., et al., *Origin of HIV-1 in the chimpanzee Pan troglodytes troglodytes.* Nature, 1999. **397**(6718): p. 436-441.
110. D'Arc, M., et al., *Origin of the HIV-1 group O epidemic in western lowland gorillas.* Proceedings of the National Academy of Sciences of the United States of America, 2015. **112**(11): p. E1343-E1352.
111. Keele, B.F., et al., *Chimpanzee reservoirs of pandemic and nonpandemic HIV-1.* Science (New York, N.Y.), 2006. **313**(5786): p. 523-526.
112. Robertson, D.L., et al., *HIV-1 nomenclature proposal.* Science (New York, N.Y.), 2000. **288**(5463): p. 55-56.
113. Bbosa, N., P. Kaleebu, and D. Ssemwanga, *HIV subtype diversity worldwide.* Current Opinion in HIV and AIDS, 2019. **14**(3): p. 153-160.
114. UNAIDS. *Global HIV & AIDS statistics - 2019 fact sheet*. 2019 25.05.2020]; Available from: https://www.unaids.org/sites/default/files/media_asset/UNAIDS_FactSheet_en.pdf.
115. German Advisory Committee Blood, S.A.o.P.T.b.B., *Human Immunodeficiency Virus (HIV).* Transfusion medicine and hemotherapy : offizielles Organ der Deutschen Gesellschaft fur Transfusionsmedizin und Immunhamatologie, 2016. **43**(3): p. 203-222.
116. Robinson, H.L., *New hope for an aids vaccine.* Nature Reviews Immunology, 2002. **2**(4): p. 239-250.
117. Hu, W.-S. and S.H. Hughes, *HIV-1 reverse transcription.* Cold Spring Harbor perspectives in medicine, 2012. **2**(10): p. a006882.
118. Watts, J.M., et al., *Architecture and secondary structure of an entire HIV-1 RNA genome.* Nature, 2009. **460**(7256): p. 711-716.
119. Kwong, P.D., et al., *Structure of an HIV gp120 envelope glycoprotein in complex with the CD4 receptor and a neutralizing human antibody.* Nature, 1998. **393**(6686): p. 648-659.
120. Wilen, C.B., J.C. Tilton, and R.W. Doms, *HIV: cell binding and entry.* Cold Spring Harbor perspectives in medicine, 2012. **2**(8): p. a006866.
121. Lusic, M. and R.F. Siliciano, *Nuclear landscape of HIV-1 infection and integration.* Nature Reviews Microbiology, 2017. **15**(2): p. 69-82.
122. Fassati, A. and S.P. Goff, *Characterization of intracellular reverse transcription complexes of human immunodeficiency virus type 1.* J Virol, 2001. **75**(8): p. 3626-35.
123. Roberts, J.D., K. Bebenek, and T.A. Kunkel, *The accuracy of reverse transcriptase from HIV-1.* Science (New York, N.Y.), 1988. **242**(4882): p. 1171-1173.
124. Mangeat, B., et al., *Broad antiretroviral defence by human APOBEC3G through lethal editing of nascent reverse transcripts.* Nature, 2003. **424**(6944): p. 99-103.
125. Dismuke, D.J. and C. Aiken, *Evidence for a functional link between uncoating of the human immunodeficiency virus type 1 core and nuclear import of the viral preintegration complex.* J Virol, 2006. **80**(8): p. 3712-20.
126. Lewis, P., M. Hensel, and M. Emerman, *Human immunodeficiency virus infection of cells arrested in the cell cycle.* EMBO J, 1992. **11**(8): p. 3053-8.
127. Craigie, R. and F.D. Bushman, *HIV DNA integration.* Cold Spring Harbor perspectives in medicine, 2012. **2**(7): p. a006890-a006890.
128. Delelis, O., et al., *Integrase and integration: biochemical activities of HIV-1 integrase.* Retrovirology, 2008. **5**: p. 114.
129. Pereira, L.A., et al., *A compilation of cellular transcription factor interactions with the HIV-1 LTR promoter.* Nucleic Acids Res, 2000. **28**(3): p. 663-8.
130. Das, A.T., A. Harwig, and B. Berkhout, *The HIV-1 Tat protein has a versatile role in activating viral transcription.* J Virol, 2011. **85**(18): p. 9506-16.
131. Romani, B., S. Engelbrecht, and R.H. Glashoff, *Functions of Tat: the versatile protein of human immunodeficiency virus type 1.* J Gen Virol, 2010. **91**(Pt 1): p. 1-12.
132. Tazi, J., et al., *Alternative splicing: regulation of HIV-1 multiplication as a target for therapeutic action.* FEBS Journal, 2010. **277**(4): p. 867-876.

133. Gheysen, D., et al., *Assembly and release of HIV-1 precursor Pr55gag virus-like particles from recombinant baculovirus-infected insect cells.* Cell, 1989. **59**(1): p. 103-112.
134. Sundquist, W.I. and H.G. Krausslich, *HIV-1 assembly, budding, and maturation.* Cold Spring Harb Perspect Med, 2012. **2**(7): p. a006924.
135. Göttlinger, H.G., et al., *Effect of mutations affecting the p6 gag protein on human immunodeficiency virus particle release.* Proceedings of the National Academy of Sciences of the United States of America, 1991. **88**(8): p. 3195-3199.
136. Engelman, A. and P. Cherepanov, *The structural biology of HIV-1: mechanistic and therapeutic insights.* Nat Rev Micro, 2012. **10**(4): p. 279-290.
137. Poropatich, K. and D.J. Sullivan, *Human immunodeficiency virus type 1 long-term non-progressors: the viral, genetic and immunological basis for disease non-progression.* Journal of General Virology, 2011. **92**(2): p. 247-268.
138. Grossman, Z., et al., *Pathogenesis of HIV infection: what the virus spares is as important as what it destroys.* Nature Medicine, 2006. **12**(3): p. 289-295.
139. Cohen, M.S., *Preventing Sexual Transmission of HIV.* Clinical Infectious Diseases, 2007. **45**(Supplement_4): p. S287-S292.
140. Joseph, S.B., et al., *Bottlenecks in HIV-1 transmission: insights from the study of founder viruses.* Nature reviews. Microbiology, 2015. **13**(7): p. 414-425.
141. Stieh, D.J., et al., *Th17 Cells Are Preferentially Infected Very Early after Vaginal Transmission of SIV in Macaques.* Cell host & microbe, 2016. **19**(4): p. 529-540.
142. Saba, E., et al., *HIV-1 sexual transmission: early events of HIV-1 infection of human cervico-vaginal tissue in an optimized ex vivo model.* Mucosal Immunology, 2010. **3**(3): p. 280-290.
143. Perez-Zsolt, D., et al., *Dendritic Cells From the Cervical Mucosa Capture and Transfer HIV-1 via Siglec-1.* Frontiers in Immunology, 2019. **10**(825).
144. Cohen, M.S., et al., *Acute HIV-1 Infection.* The New England journal of medicine, 2011. **364**(20): p. 1943-1954.
145. McMichael, A.J., et al., *The immune response during acute HIV-1 infection: clues for vaccine development.* Nat Rev Immunol, 2010. **10**(1): p. 11-23.
146. Grossman, Z., et al., *CD4+ T-cell depletion in HIV infection: Are we closer to understanding the cause?* Nat Med, 2002. **8**(4): p. 319-323.
147. Ostrowski, S.R., *Immune activation in chronic HIV infection.* Dan Med Bull, 2010. **57**(3): p. B4122.
148. Koup, R.A., et al., *Temporal association of cellular immune responses with the initial control of viremia in primary human immunodeficiency virus type 1 syndrome.* Journal of virology, 1994. **68**(7): p. 4650-4655.
149. Doitsh, G. and W.C. Greene, *Dissecting How CD4 T Cells Are Lost During HIV Infection.* Cell Host Microbe, 2016. **19**(3): p. 280-91.
150. Doitsh, G., et al., *Cell death by pyroptosis drives CD4 T-cell depletion in HIV-1 infection.* Nature, 2014. **505**.
151. Cummins, N.W. and A.D. Badley, *Mechanisms of HIV-associated lymphocyte apoptosis: 2010.* Cell death & disease, 2010. **1**(11): p. e99-e99.
152. CDC, *1993 revised classification system for HIV infection and expanded surveillance case definition for AIDS among adolescents and adults.* MMWR Recomm Rep, 1992. **41**(Rr-17): p. 1-19.
153. Fischl, M.A., et al., *The efficacy of azidothymidine (AZT) in the treatment of patients with AIDS and AIDS-related complex. A double-blind, placebo-controlled trial.* N Engl J Med, 1987. **317**(4): p. 185-91.
154. Larder, B.A. and S.D. Kemp, *Multiple mutations in HIV-1 reverse transcriptase confer high-level resistance to zidovudine (AZT).* Science, 1989. **246**(4934): p. 1155-8.

155. Barry, M., F. Mulcahy, and D.J. Back, *Antiretroviral therapy for patients with HIV disease.* Br J Clin Pharmacol, 1998. **45**(3): p. 221-8.
156. Atta, M.G., S. De Seigneux, and G.M. Lucas, *Clinical Pharmacology in HIV Therapy.* Clinical Journal of the American Society of Nephrology, 2019. **14**(3): p. 435-444.
157. Cihlar, T. and A.S. Ray, *Nucleoside and nucleotide HIV reverse transcriptase inhibitors: 25 years after zidovudine.* Antiviral Res, 2010. **85**(1): p. 39-58.
158. Pau, A.K. and J.M. George, *Antiretroviral therapy: current drugs.* Infectious disease clinics of North America, 2014. **28**(3): p. 371-402.
159. Arts, E.J. and D.J. Hazuda, *HIV-1 Antiretroviral Drug Therapy.* Cold Spring Harbor Perspectives in Medicine, 2012. **2**(4).
160. Moore, J.P., et al., *A monoclonal antibody to CD4 domain 2 blocks soluble CD4-induced conformational changes in the envelope glycoproteins of human immunodeficiency virus type 1 (HIV-1) and HIV-1 infection of CD4+ cells.* Journal of virology, 1992. **66**(8): p. 4784-4793.
161. FDA, U. *FDA approves new HIV treatment for patients who have limited treatment options [media release]*. 6 Mar 2018 [cited 2019 Dec 10]; Available from: https://www.fda.gov/newsevents/newsroom/pressannouncements/ucm599657.htm.
162. WHO. *HIV drug resistance report 2019*. 2019 Dec 10, 2019]; WHO/CDS/HIV/19.21]. Available from: https://www.who.int/hiv/pub/drugresistance/hivdr-report-2019/en/.
163. Harrigana, P.R., M. Whaley, and J.S.G. Montaner, *Rate of HIV-1 RNA rebound upon stopping antiretroviral therapy.* AIDS, 1999. **13**(8): p. F59-F62.
164. Ledford, H., *HIV rebound dashes hope of 'Mississippi baby'cure.* Nature News, 2014.
165. Whitney, J.B., et al., *Rapid seeding of the viral reservoir prior to SIV viraemia in rhesus monkeys.* Nature, 2014. **advance online publication**.
166. Van Lint, C., S. Bouchat, and A. Marcello, *HIV-1 transcription and latency: an update.* Retrovirology, 2013. **10**(1): p. 67.
167. Darcis, G., B. Berkhout, and A.O. Pasternak, *The Quest for Cellular Markers of HIV Reservoirs: Any Color You Like.* Frontiers in Immunology, 2019. **10**(2251).
168. Trepel, F., *Number and distribution of lymphocytes in man. A critical analysis.* Klinische Wochenschrift, 1974. **52**(11): p. 511-515.
169. Wong, J.K. and S.A. Yukl, *Tissue reservoirs of HIV.* Current opinion in HIV and AIDS, 2016. **11**(4): p. 362-370.
170. Perreau, M., et al., *Follicular helper T cells serve as the major CD4 T cell compartment for HIV-1 infection, replication, and production.* J Exp Med, 2013. **210**(1): p. 143-56.
171. Xu, Y., et al., *Simian immunodeficiency virus infects follicular helper CD4 T cells in lymphoid tissues during pathogenic infection of pigtail macaques.* J Virol, 2013. **87**(7): p. 3760-73.
172. Kohler, S.L., et al., *Germinal Center T Follicular Helper Cells Are Highly Permissive to HIV-1 and Alter Their Phenotype during Virus Replication.* J Immunol, 2016. **196**(6): p. 2711-22.
173. El Hed, A., et al., *Susceptibility of human Th17 cells to human immunodeficiency virus and their perturbation during infection.* J Infect Dis, 2010. **201**(6): p. 843-54.
174. Petrovas, C., et al., *Follicular CD8 T cells accumulate in HIV infection and can kill infected cells in vitro via bispecific antibodies.* Science Translational Medicine, 2017. **9**(373): p. eaag2285.
175. Fletcher, C.V., et al., *Persistent HIV-1 replication is associated with lower antiretroviral drug concentrations in lymphatic tissues.* Proc. Natl. Acad. Sci. U. S. A., 2014. **111**(6): p. 2307-2312.
176. Estes, J.D., et al., *Defining total-body AIDS-virus burden with implications for curative strategies.* Nat. Med., 2017.

177. Banga, R., et al., *PD-1(+) and follicular helper T cells are responsible for persistent HIV-1 transcription in treated aviremic individuals.* Nat Med, 2016. **22**(7): p. 754-61.
178. Kearney, M.F., et al., *Lack of detectable HIV-1 molecular evolution during suppressive antiretroviral therapy.* PLoS Pathog, 2014. **10**(3): p. e1004010.
179. Kearney, M.F., et al., *Origin of Rebound Plasma HIV Includes Cells with Identical Proviruses That Are Transcriptionally Active before Stopping of Antiretroviral Therapy.* J Virol, 2016. **90**(3): p. 1369-76.
180. Lorenzo-Redondo, R., et al., *Persistent HIV-1 replication maintains the tissue reservoir during therapy.* Nature, 2016. **530**(7588): p. 51-56.
181. Kuo, H.-H. and M. Lichterfeld, *Recent progress in understanding HIV reservoirs.* Current opinion in HIV and AIDS, 2018. **13**(2): p. 137-142.
182. Siliciano, J.D., et al., *Long-term follow-up studies confirm the stability of the latent reservoir for HIV-1 in resting CD4+ T cells.* Nature medicine, 2003. **9**(6): p. 727-728.
183. Crooks, A.M., et al., *Precise Quantitation of the Latent HIV-1 Reservoir: Implications for Eradication Strategies.* The Journal of Infectious Diseases, 2015. **212**(9): p. 1361-1365.
184. Hiener, B., et al., *Identification of Genetically Intact HIV-1 Proviruses in Specific CD4(+) T Cells from Effectively Treated Participants.* Cell Rep., 2017. **21**(3): p. 813-822.
185. O'Doherty, U., et al., *A sensitive, quantitative assay for human immunodeficiency virus type 1 integration.* J. Virol., 2002. **76**(21): p. 10942-10950.
186. Brady, T., et al., *Quantitation of HIV DNA integration: effects of differential integration site distributions on Alu-PCR assays.* J. Virol. Methods, 2013. **189**(1): p. 53-57.
187. Mexas, A.M., et al., *Concurrent measures of total and integrated HIV DNA monitor reservoirs and ongoing replication in eradication trials.* AIDS, 2012. **26**(18): p. 2295-2306.
188. Chomont, N., et al., *HIV reservoir size and persistence are driven by T cell survival and homeostatic proliferation.* Nat Med, 2009. **15**.
189. Vandergeeten, C., et al., *Cross-clade ultrasensitive PCR-based assays to measure HIV persistence in large-cohort studies.* J Virol, 2014. **88**(21): p. 12385-96.
190. Margolis, D.M., et al., *Latency reversal and viral clearance to cure HIV-1.* Science, 2016. **353**(6297): p. aaf6517.
191. Eriksson, S., et al., *Comparative analysis of measures of viral reservoirs in HIV-1 eradication studies.* PLoS Pathog., 2013. **9**(2): p. e1003174.
192. Ho, Y.-C., et al., *Replication-competent noninduced proviruses in the latent reservoir increase barrier to HIV-1 cure.* Cell, 2013. **155**(3): p. 540-551.
193. Morón-López, S., et al., *Sensitive quantification of the HIV-1 reservoir in gut-associated lymphoid tissue.* PLoS One, 2017. **12**(4): p. e0175899.
194. Soriano-Sarabia, N., et al., *Quantitation of Replication-Competent HIV-1 in Populations of Resting CD4 T Cells.* J. Virol., 2014. **88**(24): p. 14070-14077.
195. Baxter, A.E., et al., *Single-Cell Characterization of Viral Translation-Competent Reservoirs in HIV-Infected Individuals.* Cell Host Microbe, 2016. **20**(3): p. 368-380.
196. Baxter, A.E., et al., *Multiparametric characterization of rare HIV-infected cells using an RNA-flow FISH technique.* Nat. Protoc., 2017. **12**(10): p. 2029-2049.
197. Altfeld, M. and M. Gale, Jr., *Innate immunity against HIV-1 infection.* Nat Immunol, 2015. **16**(6): p. 554-62.
198. Baldauf, H.M., et al., *SAMHD1 restricts HIV-1 infection in resting CD4(+) T cells.* Nat Med, 2012. **18**(11): p. 1682-7.
199. Stopak, K., et al., *HIV-1 Vif blocks the antiviral activity of APOBEC3G by impairing both its translation and intracellular stability.* Mol Cell, 2003. **12**(3): p. 591-601.
200. Sowrirajan, B. and E. Barker, *The natural killer cell cytotoxic function is modulated by HIV-1 accessory proteins.* Viruses, 2011. **3**(7): p. 1091-111.
201. Brenchley, J.M., et al., *Microbial translocation is a cause of systemic immune activation in chronic HIV infection.* Nat Med, 2006. **12**.

202. Soper, A., et al., *Type I Interferon Responses by HIV-1 Infection: Association with Disease Progression and Control.* Frontiers in immunology, 2018. **8**: p. 1823-1823.
203. Boasso, A., et al., *PDL-1 upregulation on monocytes and T cells by HIV via type I interferon: restricted expression of type I interferon receptor by CCR5-expressing leukocytes.* Clinical immunology (Orlando, Fla.), 2008. **129**(1): p. 132-144.
204. Chew, G.M., et al., *TIGIT Marks Exhausted T Cells, Correlates with Disease Progression, and Serves as a Target for Immune Restoration in HIV and SIV Infection.* PLOS Pathogens, 2016. **12**(1): p. e1005349.
205. Mujib, S., et al., *Antigen-independent induction of Tim-3 expression on human T cells by the common γ-chain cytokines IL-2, IL-7, IL-15, and IL-21 is associated with proliferation and is dependent on the phosphoinositide 3-kinase pathway.* J Immunol, 2012. **188**(8): p. 3745-56.
206. Kinter, A.L., et al., *The common gamma-chain cytokines IL-2, IL-7, IL-15, and IL-21 induce the expression of programmed death-1 and its ligands.* J Immunol, 2008. **181**(10): p. 6738-46.
207. Zicari, S., et al., *Immune Activation, Inflammation, and Non-AIDS Co-Morbidities in HIV-Infected Patients under Long-Term ART.* Viruses, 2019. **11**(3): p. 200.
208. Lederman, M.M., et al., *Residual immune dysregulation syndrome in treated HIV infection.* Advances in immunology, 2013. **119**: p. 51-83.
209. Takata, H., et al., *Delayed differentiation of potent effector CD8(+) T cells reducing viremia and reservoir seeding in acute HIV infection.* Science translational medicine, 2017. **9**(377): p. eaag1809.
210. Altfeld, M., et al., *Expansion of pre-existing, lymph node-localized CD8+ T cells during supervised treatment interruptions in chronic HIV-1 infection.* The Journal of clinical investigation, 2002. **109**(6): p. 837-843.
211. Goonetilleke, N., et al., *The first T cell response to transmitted/founder virus contributes to the control of acute viremia in HIV-1 infection.* J Exp Med, 2009. **206**(6): p. 1253-72.
212. Soghoian, D.Z., et al., *HIV-specific cytolytic CD4 T cell responses during acute HIV infection predict disease outcome.* Sci Transl Med, 2012. **4**(123): p. 123ra25.
213. Lichterfeld, M., et al., *Selective depletion of high-avidity human immunodeficiency virus type 1 (HIV-1)-specific CD8+ T cells after early HIV-1 infection.* J Virol, 2007. **81**(8): p. 4199-214.
214. Kim, A.Y. and R.T. Chung, *Coinfection with HIV-1 and HCV--a one-two punch.* Gastroenterology, 2009. **137**(3): p. 795-814.
215. Altfeld, M., et al., *Influence of HLA-B57 on clinical presentation and viral control during acute HIV-1 infection.* Aids, 2003. **17**(18): p. 2581-91.
216. Kaslow, R.A., et al., *Influence of combinations of human major histocompatibility complex genes on the course of HIV-1 infection.* Nat Med, 1996. **2**(4): p. 405-11.
217. Martinez-Picado, J., et al., *Fitness cost of escape mutations in p24 Gag in association with control of human immunodeficiency virus type 1.* Journal of virology, 2006. **80**(7): p. 3617-3623.
218. Schneidewind, A., et al., *Escape from the Dominant HLA-B27-Restricted Cytotoxic T-Lymphocyte Response in Gag Is Associated with a Dramatic Reduction in Human Immunodeficiency Virus Type 1 Replication.* Journal of Virology, 2007. **81**(22): p. 12382-12393.
219. Genovese, L., M. Nebuloni, and M. Alfano, *Cell-Mediated Immunity in Elite Controllers Naturally Controlling HIV Viral Load.* Frontiers in immunology, 2013. **4**: p. 86-86.
220. Cocchi, F., et al., *Identification of RANTES, MIP-1 alpha, and MIP-1 beta as the major HIV-suppressive factors produced by CD8+ T cells.* Science, 1995. **270**(5243): p. 1811-5.

221. Walker, W.E., et al., *Increased Levels of Macrophage Inflammatory Proteins Result in Resistance to R5-Tropic HIV-1 in a Subset of Elite Controllers.* Journal of Virology, 2015. **89**(10): p. 5502-5514.
222. Morou, A., et al., *Altered differentiation is central to HIV-specific CD4(+) T cell dysfunction in progressive disease.* Nat Immunol, 2019. **20**(8): p. 1059-1070.
223. Morou, A., B.E. Palmer, and D.E. Kaufmann, *Distinctive features of CD4+ T cell dysfunction in chronic viral infections.* Current opinion in HIV and AIDS, 2014. **9**(5): p. 446-451.
224. Collins, D.R., G.D. Gaiha, and B.D. Walker, *CD8+ T cells in HIV control, cure and prevention.* Nature Reviews Immunology, 2020. **20**(8): p. 471-482.
225. Leong, Y.A., et al., *CXCR5(+) follicular cytotoxic T cells control viral infection in B cell follicles.* Nature immunology, 2016. **17**(10): p. 1187-1196.
226. He, R., et al., *Follicular CXCR5- expressing CD8(+) T cells curtail chronic viral infection.* Nature, 2016. **537**(7620): p. 412-428.
227. Lugli, E., et al., *Stem, Effector, and Hybrid States of Memory CD8⁺ T Cells.* Trends in Immunology, 2020. **41**(1): p. 17-28.
228. Im, S.J., et al., *Defining CD8+ T cells that provide the proliferative burst after PD-1 therapy.* Nature, 2016. **537**(7620): p. 417-421.
229. Reuter, M.A., et al., *HIV-Specific CD8⁺ T Cells Exhibit Reduced and Differentially Regulated Cytolytic Activity in Lymphoid Tissue.* Cell Reports, 2017. **21**(12): p. 3458-3470.
230. Ferrando-Martinez, S., et al., *Accumulation of follicular CD8+ T cells in pathogenic SIV infection.* The Journal of Clinical Investigation, 2018. **128**(5): p. 2089-2103.
231. Rahman, M.A., et al., *Associations of Simian Immunodeficiency Virus (SIV)-Specific Follicular CD8⁺ T Cells with Other Follicular T Cells Suggest Complex Contributions to SIV Viremia Control.* The Journal of Immunology, 2018. **200**(8): p. 2714-2726.
232. Ganusov, V.V., et al., *Fitness costs and diversity of the cytotoxic T lymphocyte (CTL) response determine the rate of CTL escape during acute and chronic phases of HIV infection.* Journal of virology, 2011. **85**(20): p. 10518-10528.
233. Jones, R.B. and B.D. Walker, *HIV-specific CD8$^+$ T cells and HIV eradication.* The Journal of clinical investigation, 2016. **126**(2): p. 455-463.
234. Wherry, E.J., *T cell exhaustion.* Nature Immunology, 2011. **12**(6): p. 492-499.
235. Perdomo-Celis, F., N.A. Taborda, and M.T. Rugeles, *CD8+ T-Cell Response to HIV Infection in the Era of Antiretroviral Therapy.* Frontiers in Immunology, 2019. **10**(1896).
236. Kaufmann, D.E., et al., *Upregulation of CTLA-4 by HIV-specific CD4+ T cells correlates with disease progression and defines a reversible immune dysfunction.* Nat Immunol, 2007. **8**(11): p. 1246-54.
237. D'Souza, M., et al., *Programmed Death 1 Expression on HIV-Specific CD4⁺ T Cells Is Driven by Viral Replication and Associated with T Cell Dysfunction.* The Journal of Immunology, 2007. **179**(3): p. 1979-1987.
238. Lindqvist, M., et al., *Expansion of HIV-specific T follicular helper cells in chronic HIV infection.* J Clin Invest, 2012. **122**(9): p. 3271-80.
239. Wendel, B.S., et al., *The receptor repertoire and functional profile of follicular T cells in HIV-infected lymph nodes.* Sci Immunol, 2018. **3**(22).
240. Fahey, L.M., et al., *Viral persistence redirects CD4 T cell differentiation toward T follicular helper cells.* J Exp Med, 2011. **208**(5): p. 987-99.
241. Raziorrouh, B., et al., *Virus-Specific CD4+ T Cells Have Functional and Phenotypic Characteristics of Follicular T-Helper Cells in Patients With Acute and Chronic HCV Infections.* Gastroenterology, 2016. **150**(3): p. 696-706.e3.

242. Del Alcazar, D., et al., *Mapping the Lineage Relationship between CXCR5(+) and CXCR5(-) CD4(+) T Cells in HIV-Infected Human Lymph Nodes.* Cell Rep, 2019. **28**(12): p. 3047-3060.e7.
243. Pallikkuth, S., et al., *T Follicular Helper Cells and B Cell Dysfunction in Aging and HIV-1 Infection.* Frontiers in Immunology, 2017. **8**(1380).
244. Rehr, M., et al., *Emergence of Polyfunctional CD8⁺ T Cells after Prolonged Suppression of Human Immunodeficiency Virus Replication by Antiretroviral Therapy.* Journal of Virology, 2008. **82**(7): p. 3391-3404.
245. Youngblood, B., et al., *Cutting edge: Prolonged exposure to HIV reinforces a poised epigenetic program for PD-1 expression in virus-specific CD8 T cells.* Journal of immunology (Baltimore, Md. : 1950), 2013. **191**(2): p. 540-544.
246. Tomaras, G.D., et al., *Initial B-cell responses to transmitted human immunodeficiency virus type 1: virion-binding immunoglobulin M (IgM) and IgG antibodies followed by plasma anti-gp41 antibodies with ineffective control of initial viremia.* J Virol, 2008. **82**(24): p. 12449-63.
247. Davis, K.L., et al., *High titer HIV-1 V3-specific antibodies with broad reactivity but low neutralizing potency in acute infection and following vaccination.* Virology, 2009. **387**(2): p. 414-26.
248. Frost, S.D., et al., *Neutralizing antibody responses drive the evolution of human immunodeficiency virus type 1 envelope during recent HIV infection.* Proc Natl Acad Sci U S A, 2005. **102**(51): p. 18514-9.
249. Wei, X., et al., *Antibody neutralization and escape by HIV-1.* Nature, 2003. **422**(6929): p. 307-12.
250. Moir, S. and A.S. Fauci, *B-cell responses to HIV infection.* Immunological reviews, 2017. **275**(1): p. 33-48.
251. Sok, D. and D.R. Burton, *Recent progress in broadly neutralizing antibodies to HIV.* Nat Immunol, 2018. **19**(11): p. 1179-1188.
252. Burton, D.R. and L. Hangartner, *Broadly Neutralizing Antibodies to HIV and Their Role in Vaccine Design.* Annual review of immunology, 2016. **34**: p. 635-659.
253. Landais, E. and P.L. Moore, *Development of broadly neutralizing antibodies in HIV-1 infected elite neutralizers.* Retrovirology, 2018. **15**(1): p. 61.
254. Hraber, P., et al., *Prevalence of broadly neutralizing antibody responses during chronic HIV-1 infection.* Aids, 2014. **28**(2): p. 163-9.
255. Simek, M.D., et al., *Human immunodeficiency virus type 1 elite neutralizers: individuals with broad and potent neutralizing activity identified by using a high-throughput neutralization assay together with an analytical selection algorithm.* J Virol, 2009. **83**(14): p. 7337-48.
256. Gray, E.S., et al., *The neutralization breadth of HIV-1 develops incrementally over four years and is associated with CD4+ T cell decline and high viral load during acute infection.* J Virol, 2011. **85**(10): p. 4828-40.
257. Sather, D.N., et al., *Factors associated with the development of cross-reactive neutralizing antibodies during human immunodeficiency virus type 1 infection.* J Virol, 2009. **83**(2): p. 757-69.
258. Gruell, H. and F. Klein, *Opening Fronts in HIV Vaccine Development: Tracking the development of broadly neutralizing antibodies.* Nat Med, 2014. **20**(5): p. 478-9.
259. Burton, D.R., et al., *Efficient neutralization of primary isolates of HIV-1 by a recombinant human monoclonal antibody.* Science, 1994. **266**(5187): p. 1024-7.
260. Muster, T., et al., *A conserved neutralizing epitope on gp41 of human immunodeficiency virus type 1.* J Virol, 1993. **67**(11): p. 6642-7.
261. Mascola, J.R. and B.F. Haynes, *HIV-1 neutralizing antibodies: understanding nature's pathways.* Immunol Rev, 2013. **254**(1): p. 225-44.

262. Ugolini, S., et al., *Inhibition of virus attachment to CD4+ target cells is a major mechanism of T cell line-adapted HIV-1 neutralization.* J Exp Med, 1997. **186**(8): p. 1287-98.
263. Platt, E.J., M.M. Gomes, and D. Kabat, *Kinetic mechanism for HIV-1 neutralization by antibody 2G12 entails reversible glycan binding that slows cell entry.* Proc Natl Acad Sci U S A, 2012. **109**(20): p. 7829-34.
264. Frey, G., et al., *A fusion-intermediate state of HIV-1 gp41 targeted by broadly neutralizing antibodies.* Proc Natl Acad Sci U S A, 2008. **105**(10): p. 3739-44.
265. Blattner, C., et al., *Structural delineation of a quaternary, cleavage-dependent epitope at the gp41-gp120 interface on intact HIV-1 Env trimers.* Immunity, 2014. **40**(5): p. 669-80.
266. McLellan, J.S., et al., *Structure of HIV-1 gp120 V1/V2 domain with broadly neutralizing antibody PG9.* Nature, 2011. **480**(7377): p. 336-43.
267. Zhou, T., et al., *A Neutralizing Antibody Recognizing Primarily N-Linked Glycan Targets the Silent Face of the HIV Envelope.* Immunity, 2018. **48**(3): p. 500-513.e6.
268. Subbaraman, H., M. Schanz, and A. Trkola, *Broadly neutralizing antibodies: What is needed to move from a rare event in HIV-1 infection to vaccine efficacy?* Retrovirology, 2018. **15**(1): p. 52.
269. Fauci, A.S., *An HIV Vaccine Is Essential for Ending the HIV/AIDS Pandemic.* JAMA, 2017. **318**(16): p. 1535-1536.
270. Gruell, H. and F. Klein, *Antibody-mediated prevention and treatment of HIV-1 infection.* Retrovirology, 2018. **15**(1): p. 73.
271. Gautam, R., et al., *A single injection of anti-HIV-1 antibodies protects against repeated SHIV challenges.* Nature, 2016. **533**(7601): p. 105-109.
272. Ko, S.Y., et al., *Enhanced neonatal Fc receptor function improves protection against primate SHIV infection.* Nature, 2014. **514**(7524): p. 642-5.
273. Mingozzi, F. and K.A. High, *Therapeutic in vivo gene transfer for genetic disease using AAV: progress and challenges.* Nat Rev Genet, 2011. **12**(5): p. 341-55.
274. Pollara, J., D. Easterhoff, and G.G. Fouda, *Lessons learned from human HIV vaccine trials.* Curr Opin HIV AIDS, 2017. **12**(3): p. 216-221.
275. Haynes, B.F., et al., *Cardiolipin polyspecific autoreactivity in two broadly neutralizing HIV-1 antibodies.* Science, 2005. **308**(5730): p. 1906-8.
276. Bonsignori, M., et al., *Maturation Pathway from Germline to Broad HIV-1 Neutralizer of a CD4-Mimic Antibody.* Cell, 2016. **165**(2): p. 449-63.
277. Pauthner, M., et al., *Elicitation of Robust Tier 2 Neutralizing Antibody Responses in Nonhuman Primates by HIV Envelope Trimer Immunization Using Optimized Approaches.* Immunity, 2017. **46**(6): p. 1073-1088.e6.
278. Sanders, R.W., et al., *HIV-1 neutralizing antibodies induced by native-like envelope trimers.* Science, 2015. **349**(6244): p. aac4223.
279. Landais, E., et al., *Broadly Neutralizing Antibody Responses in a Large Longitudinal Sub-Saharan HIV Primary Infection Cohort.* PLoS Pathog, 2016. **12**(1): p. e1005369.
280. Yamamoto, T., et al., *Quality and quantity of TFH cells are critical for broad antibody development in SHIVAD8 infection.* Sci Transl Med, 2015. **7**(298): p. 298ra120.
281. Moody, M.A., et al., *Immune perturbations in HIV-1-infected individuals who make broadly neutralizing antibodies.* Sci Immunol, 2016. **1**(1): p. aag0851.
282. Havenar-Daughton, C., et al., *CXCL13 is a plasma biomarker of germinal center activity.* Proc Natl Acad Sci U S A, 2016. **113**(10): p. 2702-7.
283. Cohen, K., et al., *Early preservation of CXCR5+ PD-1+ helper T cells and B cell activation predict the breadth of neutralizing antibody responses in chronic HIV-1 infection.* J Virol, 2014. **88**(22): p. 13310-21.
284. Mabuka, J.M., et al., *Plasma CXCL13 but Not B Cell Frequencies in Acute HIV Infection Predicts Emergence of Cross-Neutralizing Antibodies.* Front Immunol, 2017. **8**: p. 1104.

285. Chun, T.W., et al., *Quantification of latent tissue reservoirs and total body viral load in HIV-1 infection.* Nature, 1997. **387**(6629): p. 183-188.
286. Finzi, D., et al., *Latent infection of CD4+ T cells provides a mechanism for lifelong persistence of HIV-1, even in patients on effective combination therapy.* Nat. Med., 1999. **5**(5): p. 512-517.
287. Finzi, D., et al., *Identification of a reservoir for HIV-1 in patients on highly active antiretroviral therapy.* Science, 1997. **278**(5341): p. 1295-1300.
288. Dahabieh, M.S., E. Battivelli, and E. Verdin, *Understanding HIV latency: the road to an HIV cure.* Annu Rev Med, 2015. **66**: p. 407-21.
289. Hütter, G., et al., *Long-Term Control of HIV by CCR5 Delta32/Delta32 Stem-Cell Transplantation.* New England Journal of Medicine, 2009. **360**(7): p. 692-698.
290. Gupta, R.K., et al., *HIV-1 remission following CCR5Δ32/Δ32 haematopoietic stem-cell transplantation.* Nature, 2019. **568**(7751): p. 244-248.
291. Shan, L., et al., *Stimulation of HIV-1-specific cytolytic T lymphocytes facilitates elimination of latent viral reservoir after virus reactivation.* Immunity, 2012. **36**(3): p. 491-501.
292. Fagard, C., et al., *A prospective trial of structured treatment interruptions in human immunodeficiency virus infection.* Arch Intern Med, 2003. **163**(10): p. 1220-6.
293. Oxenius, A., et al., *Stimulation of HIV-specific cellular immunity by structured treatment interruption fails to enhance viral control in chronic HIV infection.* Proc Natl Acad Sci U S A, 2002. **99**(21): p. 13747-52.
294. Warren, J.A., G. Clutton, and N. Goonetilleke, *Harnessing CD8(+) T Cells Under HIV Antiretroviral Therapy.* Frontiers in immunology, 2019. **10**: p. 291-291.
295. Hancock, G., et al., *Evaluation of the immunogenicity and impact on the latent HIV-1 reservoir of a conserved region vaccine, MVA.HIVconsv, in antiretroviral therapy-treated subjects.* J Int AIDS Soc, 2017. **20**(1): p. 21171.
296. Schooley, R.T., et al., *AIDS clinical trials group 5197: a placebo-controlled trial of immunization of HIV-1-infected persons with a replication-deficient adenovirus type 5 vaccine expressing the HIV-1 core protein.* J Infect Dis, 2010. **202**(5): p. 705-16.
297. Lévy, Y., et al., *Dendritic cell-based therapeutic vaccine elicits polyfunctional HIV-specific T-cell immunity associated with control of viral load.* European Journal of Immunology, 2014. **44**(9): p. 2802-2810.
298. Mothe, B., et al., *Therapeutic Vaccination Refocuses T-cell Responses Towards Conserved Regions of HIV-1 in Early Treated Individuals (BCN 01 study).* EClinicalMedicine, 2019. **11**: p. 65-80.
299. Watson, D.C., et al., *Treatment with native heterodimeric IL-15 increases cytotoxic lymphocytes and reduces SHIV RNA in lymph nodes.* PLoS pathogens, 2018. **14**(2): p. e1006902-e1006902.
300. Webb, G.M., et al., *The human IL-15 superagonist ALT-803 directs SIV-specific CD8(+) T cells into B-cell follicles.* Blood advances, 2018. **2**(2): p. 76-84.
301. Fromentin, R., et al., *PD-1 blockade potentiates HIV latency reversal ex vivo in CD4+ T cells from ART-suppressed individuals.* Nature Communications, 2019. **10**(1): p. 814.
302. Gay, C.L., et al., *Clinical Trial of the Anti-PD-L1 Antibody BMS-936559 in HIV-1 Infected Participants on Suppressive Antiretroviral Therapy.* The Journal of infectious diseases, 2017. **215**(11): p. 1725-1733.
303. Guihot, A., et al., *Drastic decrease of the HIV reservoir in a patient treated with nivolumab for lung cancer.* Ann Oncol, 2018. **29**(2): p. 517-518.
304. Ha, S.-J., et al., *Enhancing therapeutic vaccination by blocking PD-1-mediated inhibitory signals during chronic infection.* The Journal of experimental medicine, 2008. **205**(3): p. 543-555.
305. Filaci, G., et al., *Rationale for an Association Between PD1 Checkpoint Inhibition and Therapeutic Vaccination Against HIV.* Frontiers in Immunology, 2018. **9**(2447).

306. Cavacini, L.A., et al., *Phase I study of a human monoclonal antibody directed against the CD4-binding site of HIV type 1 glycoprotein 120.* AIDS Res Hum Retroviruses, 1998. **14**(7): p. 545-50.
307. Günthard, H.F., et al., *A Phase I/IIA Clinical Study With A Chimeric Mouse-Human Monoclonal Antibody To The V3 Loop Of Human Immunodeficiency Virus Type 1 Gp120.* The Journal of Infectious Diseases, 1994. **170**(6): p. 1384-1393.
308. Klein, F., et al., *HIV therapy by a combination of broadly neutralizing antibodies in humanized mice.* Nature, 2012. **492**(7427): p. 118-122.
309. Barouch, D.H., et al., *Therapeutic efficacy of potent neutralizing HIV-1-specific monoclonal antibodies in SHIV-infected rhesus monkeys.* Nature, 2013. **503**(7475): p. 224-8.
310. Shingai, M., et al., *Antibody-mediated immunotherapy of macaques chronically infected with SHIV suppresses viraemia.* Nature, 2013. **503**(7475): p. 277-80.
311. Caskey, M., et al., *Viraemia suppressed in HIV-1-infected humans by broadly neutralizing antibody 3BNC117.* Nature, 2015. **522**(7557): p. 487-491.
312. Lynch, R.M., et al., *Virologic effects of broadly neutralizing antibody VRC01 administration during chronic HIV-1 infection.* Science Translational Medicine, 2015. **7**(319): p. 319ra206-319ra206.
313. Caskey, M., et al., *Antibody 10-1074 suppresses viremia in HIV-1-infected individuals.* Nat Med, 2017. **23**(2): p. 185-191.
314. Bar-On, Y., et al., *Safety and antiviral activity of combination HIV-1 broadly neutralizing antibodies in viremic individuals.* Nat Med, 2018. **24**(11): p. 1701-1707.
315. Horwitz, J.A., et al., *HIV-1 suppression and durable control by combining single broadly neutralizing antibodies and antiretroviral drugs in humanized mice.* Proceedings of the National Academy of Sciences, 2013. **110**(41): p. 16538-16543.
316. Mendoza, P., et al., *Combination therapy with anti-HIV-1 antibodies maintains viral suppression.* Nature, 2018. **561**(7724): p. 479-484.
317. Bournazos, S., et al., *Broadly neutralizing anti-HIV-1 antibodies require Fc effector functions for in vivo activity.* Cell, 2014. **158**(6): p. 1243-1253.
318. Lu, C.L., et al., *Enhanced clearance of HIV-1-infected cells by broadly neutralizing antibodies against HIV-1 in vivo.* Science, 2016. **352**(6288): p. 1001-4.
319. Halper-Stromberg, A., et al., *Broadly neutralizing antibodies and viral inducers decrease rebound from HIV-1 latent reservoirs in humanized mice.* Cell, 2014. **158**(5): p. 989-999.
320. Parsons, M.S., et al., *Fc-dependent functions are redundant to efficacy of anti-HIV antibody PGT121 in macaques.* The Journal of Clinical Investigation, 2019. **129**(1): p. 182-191.
321. Stagg, J., et al., *Anti–ErbB-2 mAb therapy requires type I and II interferons and synergizes with anti–PD-1 or anti-CD137 mAb therapy.* Proceedings of the National Academy of Sciences, 2011. **108**(17): p. 7142-7147.
322. León, B., et al., *Prolonged antigen presentation by immune complex–binding dendritic cells programs the proliferative capacity of memory CD8 T cells.* Journal of Experimental Medicine, 2014. **211**(8): p. 1637-1655.
323. Nishimura, Y., et al., *Early antibody therapy can induce long-lasting immunity to SHIV.* Nature, 2017. **543**(7646): p. 559-563.
324. Schoofs, T., et al., *HIV-1 therapy with monoclonal antibody 3BNC117 elicits host immune responses against HIV-1.* Science, 2016. **352**(6288): p. 997-1001.
325. Pitcher, C.J., et al., *HIV-1-specific CD4+ T cells are detectable in most individuals with active HIV-1 infection, but decline with prolonged viral suppression.* Nat Med, 1999. **5**(5): p. 518-25.
326. Obeng-Adjei, N., et al., *Circulating Th1-Cell-type Tfh Cells that Exhibit Impaired B Cell Help Are Preferentially Activated during Acute Malaria in Children.* Cell Rep, 2015. **13**(2): p. 425-39.

327. Elsaesser, H., K. Sauer, and D.G. Brooks, *IL-21 is required to control chronic viral infection.* Science, 2009. **324**(5934): p. 1569-72.
328. Pallikkuth, S., A. Parmigiani, and S. Pahwa, *Role of IL-21 and IL-21 receptor on B cells in HIV infection.* Critical reviews in immunology, 2012. **32**(2): p. 173-195.
329. Smits, M., et al., *Follicular T helper cells shape the HCV-specific CD4+ T cell repertoire after virus elimination.* The Journal of Clinical Investigation, 2020. **130**(2): p. 998-1009.
330. Künzli, M., et al., *Long-lived T follicular helper cells retain plasticity and help sustain humoral immunity.* Science Immunology, 2020. **5**(45): p. eaay5552.
331. Ma, X., et al., *Expansion of T follicular helper-T helper 1 like cells through epigenetic regulation by signal transducer and activator of transcription factors.* Ann Rheum Dis, 2018. **77**(9): p. 1354-1361.
332. Weinstein, J.S., et al., *STAT4 and T-bet control follicular helper T cell development in viral infections.* The Journal of experimental medicine, 2018. **215**(1): p. 337-355.
333. Schmitt, N., et al., *Human dendritic cells induce the differentiation of interleukin-21-producing T follicular helper-like cells through interleukin-12.* Immunity, 2009. **31**(1): p. 158-69.
334. Ma, C.S., et al., *Early commitment of naive human CD4(+) T cells to the T follicular helper (T(FH)) cell lineage is induced by IL-12.* Immunol Cell Biol, 2009. **87**(8): p. 590-600.
335. Biancotto, A., et al., *Abnormal activation and cytokine spectra in lymph nodes of people chronically infected with HIV-1.* Blood, 2007. **109**(10): p. 4272-4279.
336. Fang, D., et al., *Transient T-bet expression functionally specifies a distinct T follicular helper subset.* J Exp Med, 2018. **215**(11): p. 2705-2714.
337. Radkowski, M., et al., *Persistence of hepatitis C virus in patients successfully treated for chronic hepatitis C.* Hepatology, 2005. **41**(1): p. 106-14.
338. Sen, D.R., et al., *The epigenetic landscape of T cell exhaustion.* Science (New York, N.Y.), 2016. **354**(6316): p. 1165-1169.
339. Khan, O., et al., *TOX transcriptionally and epigenetically programs CD8(+) T cell exhaustion.* Nature, 2019. **571**(7764): p. 211-218.
340. Satpathy, A.T., et al., *Massively parallel single-cell chromatin landscapes of human immune cell development and intratumoral T cell exhaustion.* Nature Biotechnology, 2019. **37**(8): p. 925-936.
341. Xu, W., et al., *The Transcription Factor Tox2 Drives T Follicular Helper Cell Development via Regulating Chromatin Accessibility.* Immunity, 2019. **51**(5): p. 826-839.e5.
342. Wang, P., et al., *A Stochastic Model of the Germinal Center Integrating Local Antigen Competition, Individualistic T–B Interactions, and B Cell Receptor Signaling.* The Journal of Immunology, 2016. **197**(4): p. 1169-1182.
343. Hipp, N., et al., *IL-2 imprints human naive B cell fate towards plasma cell through ERK/ELK1-mediated BACH2 repression.* Nature Communications, 2017. **8**(1): p. 1443.
344. Le Gallou, S., et al., *IL-2 Requirement for Human Plasma Cell Generation: Coupling Differentiation and Proliferation by Enhancing MAPK–ERK Signaling.* The Journal of Immunology, 2012. **189**(1): p. 161-173.
345. Ballesteros-Tato, A., et al., *Interleukin-2 Inhibits Germinal Center Formation by Limiting T Follicular Helper Cell Differentiation.* Immunity, 2012. **36**(5): p. 847-856.
346. Rubtsova, K., et al., *T-box transcription factor T-bet, a key player in a unique type of B-cell activation essential for effective viral clearance.* Proceedings of the National Academy of Sciences, 2013. **110**(34): p. E3216-E3224.
347. Knox, J.J., et al., *T-bet+ B cells are induced by human viral infections and dominate the HIV gp140 response.* JCI insight, 2017. **2**(8): p. e92943.
348. Zumaquero, E., et al., *IFNgamma induces epigenetic programming of human T-bet(hi) B cells and promotes TLR7/8 and IL-21 induced differentiation.* Elife, 2019. **8**.

349. Austin, J.W., et al., *Overexpression of T-bet in HIV infection is associated with accumulation of B cells outside germinal centers and poor affinity maturation.* Science Translational Medicine, 2019. **11**(520): p. eaax0904.
350. Caskey, M., F. Klein, and M.C. Nussenzweig, *Broadly neutralizing anti-HIV-1 monoclonal antibodies in the clinic.* Nature Medicine, 2019. **25**(4): p. 547-553.
351. Bournazos, S. and J.V. Ravetch, *Fcgamma receptor pathways during active and passive immunization.* Immunol Rev, 2015. **268**(1): p. 88-103.
352. DiLillo, D.J. and J.V. Ravetch, *Differential Fc-Receptor Engagement Drives an Anti-tumor Vaccinal Effect.* Cell, 2015. **161**(5): p. 1035-1045.
353. Villinger, F., et al., *Evidence for antibody-mediated enhancement of simian immunodeficiency virus (SIV) Gag antigen processing and cross presentation in SIV-infected rhesus macaques.* J Virol, 2003. **77**(1): p. 10-24.
354. Yamamoto, T., et al., *Polyfunctional CD4⁺ T-Cell Induction in Neutralizing Antibody-Triggered Control of Simian Immunodeficiency Virus Infection.* Journal of Virology, 2009. **83**(11): p. 5514-5524.
355. Huang, A.C., et al., *T-cell invigoration to tumour burden ratio associated with anti-PD-1 response.* Nature, 2017. **545**(7652): p. 60-65.
356. Saez-Cirion, A., et al., *Heterogeneity in HIV suppression by CD8 T cells from HIV controllers: association with Gag-specific CD8 T cell responses.* J Immunol, 2009. **182**(12): p. 7828-37.
357. Vella, L.A., et al., *T follicular helper cells in human efferent lymph retain lymphoid characteristics.* The Journal of Clinical Investigation, 2019. **129**(8): p. 3185-3200.
358. Havenar-Daughton, C., J.H. Lee, and S. Crotty, *Tfh cells and HIV bnAbs, an immunodominance model of the HIV neutralizing antibody generation problem.* Immunological Reviews, 2017. **275**(1): p. 49-61.
359. Parmigiani, A., et al., *Impaired Antibody Response to Influenza Vaccine in HIV-Infected and Uninfected Aging Women Is Associated with Immune Activation and Inflammation.* PLOS ONE, 2013. **8**(11): p. e79816.

Chapter 9 Appendices

Appendix I: The candidate's contribution to additional manuscripts

Author's contribution to the first additional manuscript «Single-Cell Characterization of Viral Translation-Competent Reservoirs in HIV-Infected Individuals»

Amy E. Baxter, Julia Niessl, Filippos Porichis, Andrés Finzi, Nicholas Chomont and Daniel E. Kaufmann designed the studies. Amy E. Baxter, Julia Niessl, Rémi Fromentin, Jonathan Richard, Roxanne Charlebois, Nathalie Brassard, Gloria-Gabrielle Delgado, Marta Massanella, and Nirmin Alsahafi performed experiments. Jean-Pierre Routy obtained IRB approval and recruited participants. Bruce D. Walker provided input on study design. Amy E. Baxter and Daniel E. Kaufmann interpreted the data and wrote the paper with all co-authors' assistance.

Author's contribution to the second additional manuscript «Multiparametric characterization of rare HIV-infected cells using an RNA-flow FISH technique»

Amy E. Baxter, Filippos Porichis and Daniel E. Kaufmann conceived and developed the $HIV^{RNA/Gag}$ assay, with input from Andrés Finzi and Nicholas Chomont. Amy E. Baxter, Julia Niessl, Rémi Fromentin, Jonathan Richard, Nathalie Brassard, Marta Massanella and Nirmin Alsahafi modified the protocol, designed specific experiments and provided reagents. Jean-Pierre Routy obtained IRB approval and recruited participants to provide primary samples. Daniel E. Kaufmann provided supervision. Amy E. Baxter and Daniel E. Kaufmann wrote the manuscript and all authors approved the final version.

Author's contribution to the first review «Harnessing T follicular helper cell responses for HIV Vaccine Development»

Julia Niessl performed the literature review and wrote the manuscript, with contributions from Daniel E. Kaufmann, who also edited structure and content.

Author's contribution to the second review «Tools for visualizing HIV in cure research»

Julia Niessl performed the literature review and wrote the manuscript with input from Amy E. Baxter and Daniel E. Kaufmann.

Appendix II: Additional manuscripts

Single-Cell Characterization of Viral Translation-Competent Reservoirs in HIV-Infected Individuals

Cell, Host & Microbe, 2016

Article

Cell Host & Microbe

Single-Cell Characterization of Viral Translation-Competent Reservoirs in HIV-Infected Individuals

Graphical Abstract

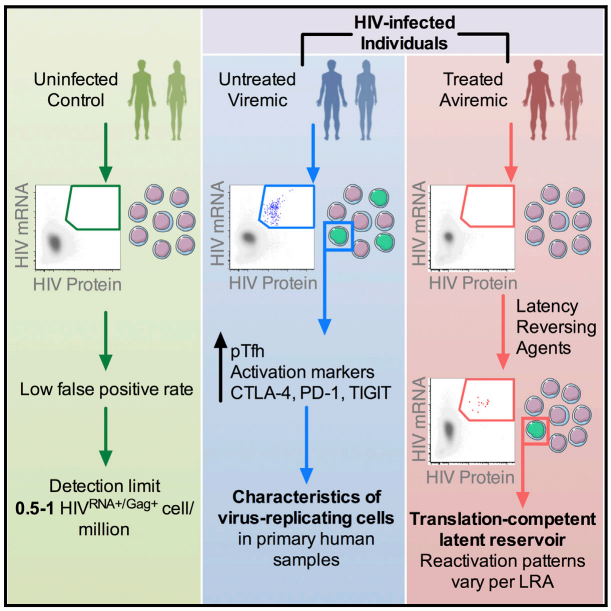

Highlights

- HIV RNA and protein co-expression allows ex vivo characterization of patient CD4 T cells
- HIV-infected CD4s show markers of exhaustion and peripheral follicular helper cells
- Translation-competent latent reservoir can be detected in most ART-treated patients
- PKC agonist Bryostatin preferentially reactivates HIV from effector memory CD4s

Authors

Amy E. Baxter, Julia Niessl, Rémi Fromentin, ..., Andrés Finzi, Nicolas Chomont, Daniel E. Kaufmann

Correspondence

daniel.kaufmann@umontreal.ca

In Brief

Technological limitations hamper characterization of CD4 T cells supporting ongoing HIV infection and quantification of the latent reservoir. Baxter et al. (2016) use simultaneous detection of viral protein and mRNA to quantify and phenotype both the ongoing infection during viremia and the translation-competent inducible reservoir in virally supressed, treated patients.

Baxter et al., 2016, Cell Host & Microbe *20*, 368–380
September 14, 2016
http://dx.doi.org/10.1016/j.chom.2016.07.015

CellPress

Cell Host & Microbe
Article

Single-Cell Characterization of Viral Translation-Competent Reservoirs in HIV-Infected Individuals

Amy E. Baxter,[1,2] Julia Niessl,[1,2] Rémi Fromentin,[1] Jonathan Richard,[1] Filippos Porichis,[2,3] Roxanne Charlebois,[1] Marta Massanella,[1] Nathalie Brassard,[1] Nirmin Alsahafi,[1,6] Gloria-Gabrielle Delgado,[1] Jean-Pierre Routy,[4] Bruce D. Walker,[2,3,5] Andrés Finzi,[1,6] Nicolas Chomont,[1] and Daniel E. Kaufmann[1,2,3,*]
[1]Research Centre of the Centre Hospitalier de l'Université de Montréal (CRCHUM) and Université de Montréal, Montreal, QC H2X 0A9, Canada
[2]Center for HIV/AIDS Vaccine Immunology and Immunogen Discovery (CHAVI-ID), La Jolla, CA 92037, USA
[3]Ragon Institute of Massachusetts General Hospital, Massachusetts Institute of Technology and Harvard University, Cambridge, MA 02139, USA
[4]Chronic Viral Illnesses Service and Division of Hematology, McGill University Health Centre, Montreal, QC H4A 3J1, Canada
[5]Howard Hughes Medical Institute, Chevy Chase, MD 20815, USA
[6]Department of Microbiology and Immunology, McGill University, Montreal, QC H3A 2B4, Canada
*Correspondence: daniel.kaufmann@umontreal.ca
http://dx.doi.org/10.1016/j.chom.2016.07.015

SUMMARY

HIV cure efforts are hampered by limited characterization of the cells supporting HIV replication in vivo and inadequate methods for quantifying the latent viral reservoir in patients receiving antiretroviral therapy. We combine fluorescent in situ RNA hybridization with detection of HIV protein and flow cytometry, enabling detection of 0.5–1 *gag-pol* mRNA$^+$/Gag protein$^+$-infected cells per million. In the peripheral blood of untreated persons, active HIV replication correlated with viremia and occurred in CD4 T cells expressing T follicular helper cell markers and inhibitory co-receptors. In virally suppressed subjects, the approach identified latently infected cells capable of producing HIV mRNA and protein after stimulation with PMA/ionomycin and latency-reversing agents (LRAs). While ingenol-induced reactivation mirrored the effector and central/transitional memory CD4 T cell contribution to the pool of integrated HIV DNA, bryostatin-induced reactivation occurred predominantly in cells expressing effector memory markers. This indicates that CD4 T cell differentiation status differentially affects LRA effectiveness.

INTRODUCTION

More than three decades after the identification of CD4 T lymphocytes as the main target of human immunodeficiency virus (HIV) infection, surprisingly little is still known about the characteristics of cells that support HIV replication in vivo (Swanstrom and Coffin, 2012) and serve as long-lived viral reservoirs in ART-treated individuals (Kulpa and Chomont, 2015). A deeper understanding of the frequency, phenotype, and regulation of these cells is critical for the development of targeted HIV cure strategies and vaccines eliciting immune responses capable of eliminating early foci of infection (Burton et al., 2012). Furthermore, determination of the tissue and cellular sources of persistent virus and the development of high-throughput scalable assays to measure the latent reservoir in patients have both been identified as key priorities in HIV eradication research (Deeks et al., 2012). This critical need is demonstrated by the focusing of cure efforts on latency-reversing agents (LRAs) even though their relative ability to induce latently infected cells of different phenotypes and differentiation states is not known.

To accurately measure in vivo the frequency and phenotype of CD4 T cells producing viral proteins, we developed a highly sensitive flow cytometry assay enabling simultaneous assessment of HIV RNA and Gag proteins, along with quantitation of phenotypic CD4 T cell molecules. We applied this technology to perform single-cell analysis of CD4 T cells harboring spontaneously produced and activation-inducible virus in treated and untreated individuals, quantitate viral reservoirs, and define the frequency and phenotype of primary CD4 T cells from patient blood that could be induced from latency.

RESULTS

Detection of HIV-Infected CD4 T Cells by mRNA Flow-FISH

Current flow cytometry methods are not sensitive or specific enough to assess HIV-infected cells in patient samples. We thus explored the capacity of fluorescent in situ hybridization for gene-specific mRNA (mRNA flow-FISH) to detect HIV transcription in infected CD4 T cells (Porichis et al., 2014). In this approach, multiple oligomeric probes and branched DNA signal amplification enhance detection sensitivity (see Figure S1 available online). We selected combined probe sets against the *gag* and *pol* genes, as their sequences are well conserved across clinical isolates and they are the most abundant viral transcripts in samples from both treated and untreated patients

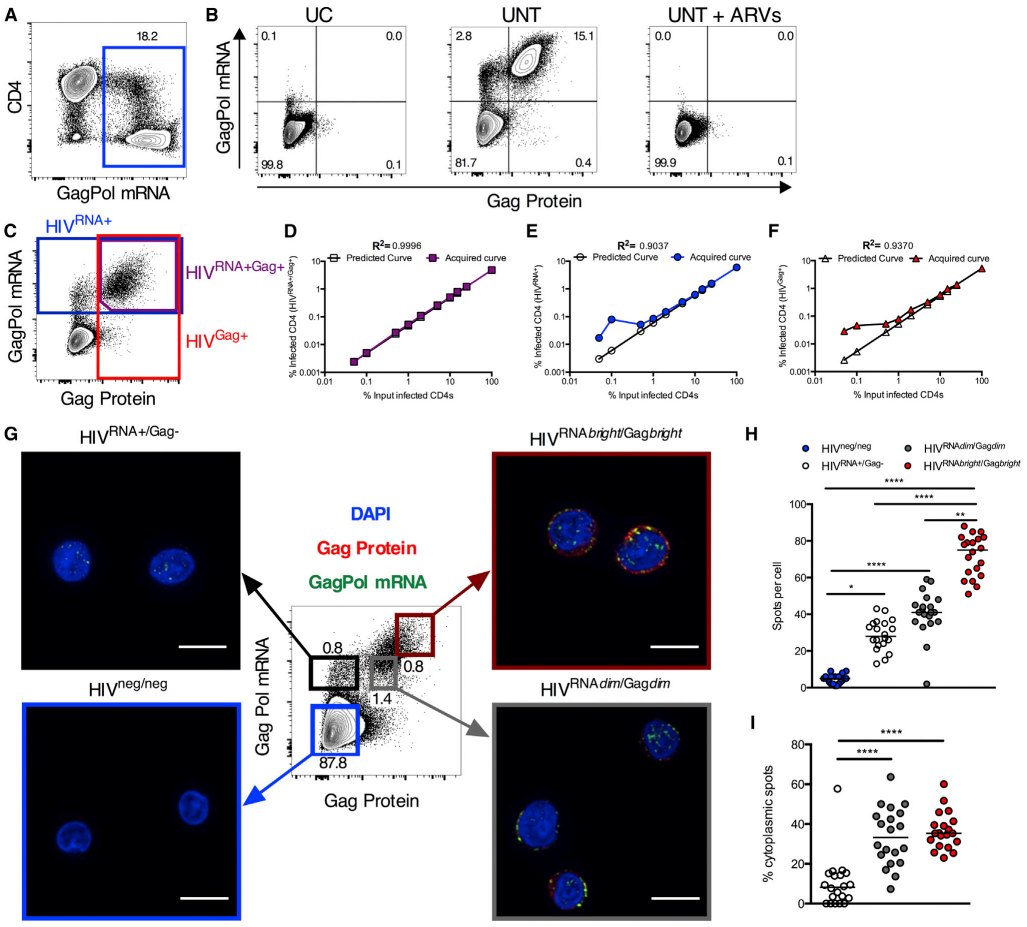

Figure 1. Dual Staining for mRNA and Protein Allows Highly Sensitive, Flow-Based Detection and Microscopy Analysis of HIV-Infected CD4

Peripheral CD4 from HIV-1-infected patients were activated in vitro and a spreading infection with endogenous virus established.

(A) Example plot showing GagPol mRNA staining.

(B) Example concurrent Gag protein and GagPol mRNA staining for an uninfected control (UC); a viremic patient (UNT) or UNT CD4 cultured with ARVs (UNT + ARVs).

(C–F) HIV-infected CD4 were "spiked" into uninfected CD4 at different ratios. (C) Example gating of CD4 expressing GagPol mRNA and protein (purple), GagPol mRNA (blue), or Gag protein (red). Quantification of predicted (clear symbols) versus acquired result (colored symbols) using (D) double mRNA and protein expression, or single (E) mRNA or (F) protein stain. R^2 calculated on log-transformed data.

(G–I) Reactivated, HIV-infected CD4 were sorted into four populations based on Gag protein and GagPol mRNA expression (indicated by colored boxes, G), and imaged by confocal microscopy. In example images from sorted populations, DAPI is in blue, GagPol mRNA in green, and Gag protein in red. Scale bars represent 10 μm. (H and I) GagPol mRNA spot analysis for sorted populations from (G). (H) GagPol mRNA spots per cell in sorted populations. (I) Frequency of cytoplasmic mRNA spots. Each symbol represents a cell. n = 20 cells, representative data from one donor. *p < 0.05, **p < 0.01, ***p < 0.001 by Kruskal-Wallis ANOVA with Dunn's post-test. See also Figures S1, S2, and S3; Table S1; and Movie S1 and Movie S2.

(Bagnarelli et al., 1996; see Table S1 for sequences used in probe design). Robust mRNA staining was detected in a primary CD4 T cell culture from an HIV-infected individual after expansion of endogenous virus (Figure 1A). Combining this method with staining for HIV protein using the Gag-specific KC57 antibody allowed for concurrent detection of HIV transcription and translation products. We could readily detect double-positive ($HIV^{RNA+/Gag+}$) cells in the expanded culture. This population was abrogated by addition of antiviral drugs to the culture and was not present in T cells from uninfected control (UC) donors

cultured and processed in parallel (Figure 1B). We define this population of HIV$^{RNA+/Gag+}$ cells as viral translation competent, as the cells detected contain virus capable of producing HIV mRNA and proteins.

To determine the specificity and linearity of this HIV$^{RNA/Gag}$ assay, we spiked expanded HIV-replicating primary CD4 T cells into uninfected CD4. HIV RNA/protein co-staining showed excellent consistency down to the lowest dilutions tested (23/million, R^2 = 0.9996, Figures 1C and 1D; 1/million, R^2 = 0.9856, Figures S2A and S2B). In contrast, background staining prevented reliable identification of infected cells for frequencies below 0.05%–0.1%, the equivalent of 500–1,000 HIV^{Gag+} or HIV^{RNA+} T cells per million CD4, when we assessed a single marker (Figures 1E, 1F, S2C, and S2D).

To verify that HIV$^{RNA+/Gag+}$ cells were HIV infected, we sorted expanded HIV-infected CD4 T cells into HIV mRNA-negative/Gag protein-negative (HIV$^{neg/neg}$) and HIV$^{RNA+/Gag+}$ populations (Figure S2E) and subsequently measured integrated HIV DNA. The HIV$^{RNA+/Gag+}$ subset was enriched for HIV DNA as compared to the HIV$^{neg/neg}$ population (Figure S2F), confirming that the HIV$^{RNA/Gag}$ assay identifies HIV-infected cells.

We next used confocal microscopy to determine whether this approach could provide semiquantitative information about viral replication (Figures 1G–1I). We expanded primary CD4 T cells isolated from one UC subject and two HIV-infected individuals (one untreated, one ART treated). We then sorted cell subsets defined by HIV mRNA/protein expression patterns for imaging (Figures 1G, S2G, and S3A–S3C). Spot counting for *gag-pol* mRNA FISH signals revealed a low background in both the UC subject and the HIV$^{neg/neg}$ subset and clear signals in the three HIV^{RNA+} populations (Figures 1H and S2H). Based on the false-positive rate observed in the UC patient (Figure S2H), we determined a conservative detection limit to minimize false-positive events (assuming Gaussian distribution, mean+3SD) of 20 gag-pol mRNA spots per cell. This accounts for 93% of all HIV^{RNA+} cells (Figure S2H). The hierarchy of total *gag-pol* mRNA spot counts was consistent with flow cytometry MFIs of the sorted populations, with the HIV$^{RNA\textit{bright}/Gag\textit{bright}}$ cells harboring most spots (Figure 1H). As the intensity of individual spots will contribute to the global signal intensity of a given cell, we examined the total intensity of *gag-pol* mRNA signal for individual cells using corrected total cell fluorescence (CTCF) (Burgess et al., 2010). Again, we found a direct relationship to flow cytometry data (Figures S3D–S3H).

We measured the relative distribution of *gag-pol* RNA spots in the nuclear and cytoplasmic compartments among the sorted subsets. In HIV$^{RNA+/Gag-}$ cells, the vast majority of the *gag-pol* RNA spots were located in the nucleus and only a small fraction (median 5.1%) in the cytoplasm, whereas this proportion reached 30%–40% in subsets also expressing Gag protein (Figure 1I). Such differences in localization were confirmed by z stack imaging (Movie S1 and Movie S2). This is consistent with data suggesting that viral transcription leads to accumulation of *gag-pol* mRNA in the nucleus before its egress to the cytoplasm is enabled by Rev-mediated export (Karn and Stoltzfus, 2012). Although this assay is not designed for single-molecule FISH, we demonstrate that it can be used semi-quantitatively to assess HIV transcription at the single-cell level. When used sequentially in flow sorting and confocal microscopy, it can greatly facilitate FISH studies of rare cell subsets of interest in heterogeneous populations.

Frequencies of HIV-Producing CD4 T Cells in the Blood of Untreated Patients

Having validated the assay on infected CD4 T cells expanded in vitro, we next sought to determine the frequency of cells that produce HIV at a given time in the peripheral blood of subjects with untreated HIV infection (UNT), compared to UC donors (subject characteristics and number of cells analyzed, Table S2). We quantified in parallel the population that spontaneously produces viral mRNA and proteins and the additional cells that can be induced to express such viral markers after short-term 12 hr PMA/ionomycin (PMA/iono) stimulation. Whereas false-positive events were very rare in UC (one HIV$^{RNA+/Gag+}$ cell detected from eight samples/7.7 million cells), we readily detected HIV$^{RNA+/Gag+}$ CD4 in UNT subjects (median[range] = 123[1.5–230]/per million CD4) (Figures 2A and 2B), which were further increased upon stimulation with PMA/iono (median[range] = 311[3.6–768]/million). The impact of PMA/iono was similar among subjects (Figures 2C and S4A). This suggested that, besides CD4 T cells spontaneously producing viral proteins, an additional larger pool of infected lymphocytes appeared poised for rapid induction of viral transcription and translation upon stimulation in UNT individuals. The superiority of the RNA/protein co-staining method over single marker use was clear when we compared unstimulated, primary samples of UC to UNT donors (Figure 2D). The limit of HIV$^{RNA+/Gag+}$ cell detection based on the UC false-positive detection rate was 0.5–1 cells/million, whereas high background staining rendered single KC57 Gag or mRNA staining alone non-interpretable in the 0–1,000 cells/million range, the frequency bracket that contained all UNT subjects examined. This represents a gain in detection of 1,000-fold over standard protein staining for HIV Gag.

We next assessed the correlation of HIV$^{RNA+/Gag+}$ frequencies with markers of disease progression. There was a strong correlation with viral load in both the resting and PMA/iono stimulated conditions (Figures 2E and S4C) and non-significant inverse correlations with CD4 count (Figures 2F and S4B). Interestingly, we found the strongest correlations between the absolute number of HIV-infected cells per μL and viral load (Figure 2G). We also observed an increase in the *gag-pol* mRNA and Gag protein MFI on HIV$^{RNA+/Gag+}$ cells following stimulation, suggesting increased viral production per cell when compared to spontaneous viral production (Figures S4D and S4E). We confirmed the reproducibility of the assay across different experiments, flow panels, and operators, even at lower frequencies of HIV$^{RNA+/Gag+}$ CD4 (Figure S4F). Therefore, CD4 T cells that produce HIV RNAs and protein, either spontaneously ex vivo or after stimulation, can be reliably identified and quantified in primary clinical samples from subjects with progressive HIV infection.

HIV-Infected CD4 T Cells Preferentially Express a Central/Transitional Memory Phenotype

The features of cells harboring replicating virus have thus far been largely inferred from in vitro infection or amplification of autologous virus, due to an inability to detect infected cells ex vivo using previously applied methods. To address this, we assessed the phenotype of HIV$^{RNA+/Gag+}$ CD4 T cells in primary

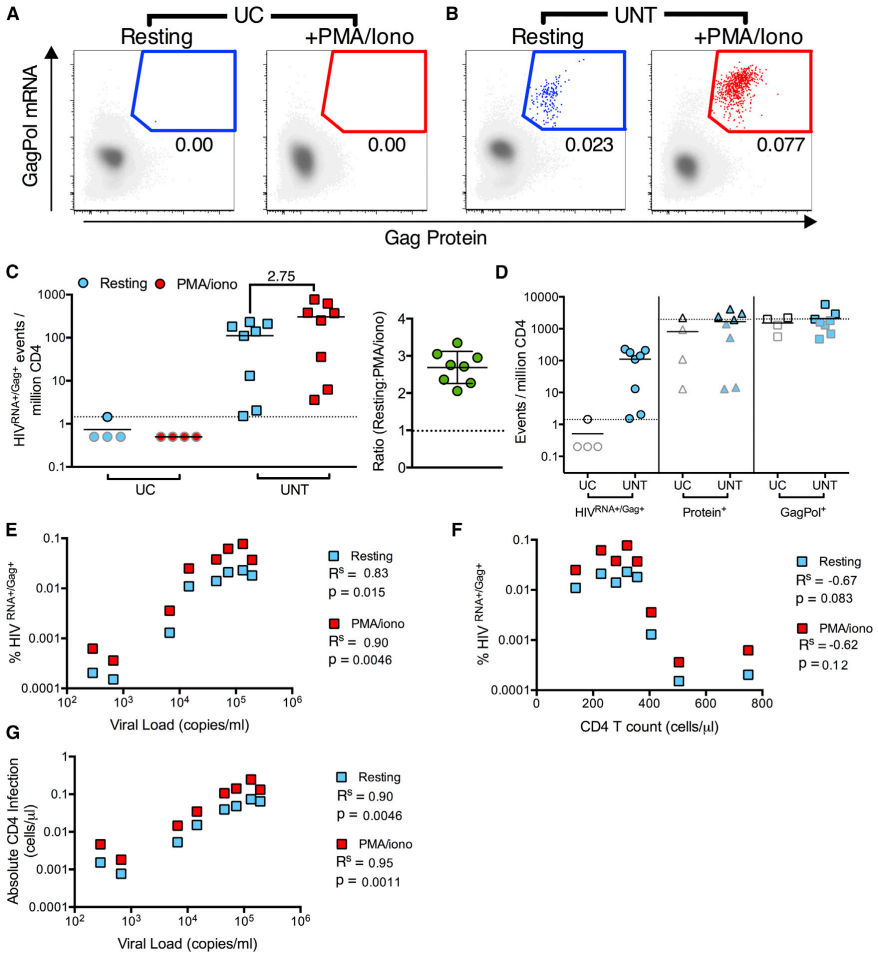

Figure 2. Detection of CD4 T Cells Supporting Ongoing and Activation-Inducible HIV Infection in Viremic Patients

$HIV^{RNA+/Gag+}$ CD4 were detected in uninfected controls (UC) or viremic patients (UNT) directly ex vivo (resting, blue symbols) or following 12 hr stimulation (PMA/iono, red symbols).

(A and B) Example plots and gating of $HIV^{RNA+Gag+}$ CD4 for an UC (A) and an UNT (B). $HIV^{RNA+/Gag+}$ events in red/blue are overlaid onto $HIV^{neg/neg}$ events in gray.

(C and D) Quantification of data in (A) and (B), shown as $HIV^{RNA+/Gag+}$ events per million CD4 (n = 4 UC, 8 UNT). On right, the fold change in frequency of $HIV^{RNA+Gag+}$ CD4 in resting versus stimulated infection is shown. n = 8 UNT. (D) Data as in (C) for unstimulated, resting CD4, except gated using only protein ($Protein^+$) or mRNA ($GagPol^+$) staining, compared to $HIV^{RNA+/Gag+}$ staining. Limit of detection (LOD) based on frequency of UC false positive events is indicated with a dotted line. Grey-bordered symbols are below LOD.

(E–G) Correlations of resting or stimulated infection with patient characteristics, (E) viral load, (F) CD4 count, or (G) absolute number of infected CD4 (CD4 count [cells/µl] × % $HIV^{RNA+/Gag+}$). R^s represents Spearman's non-parametric correlation with associated p values where $p < 0.05$ is significant. See also Figure S4 and Table S2.

UNT samples, analyzed directly from leukapheresis donation and without additional ex vivo stimulation. Such cells are defined here as in vivo-infected. CD4 downregulation is a hallmark of HIV infection in vitro, facilitating Env incorporation and viral replication (Argañaraz et al., 2003). We found that CD4 expression was profoundly diminished on in vivo-infected $HIV^{RNA+/Gag+}$ cells (Figures 3A–3C), consistent with previous data (DeMaster et al., 2016). HLA-class I downregulation, another well-known effect of Nef protein (Schwartz et al., 1996), was also observed in primary samples (Figure 3D), albeit at a more modest level than after

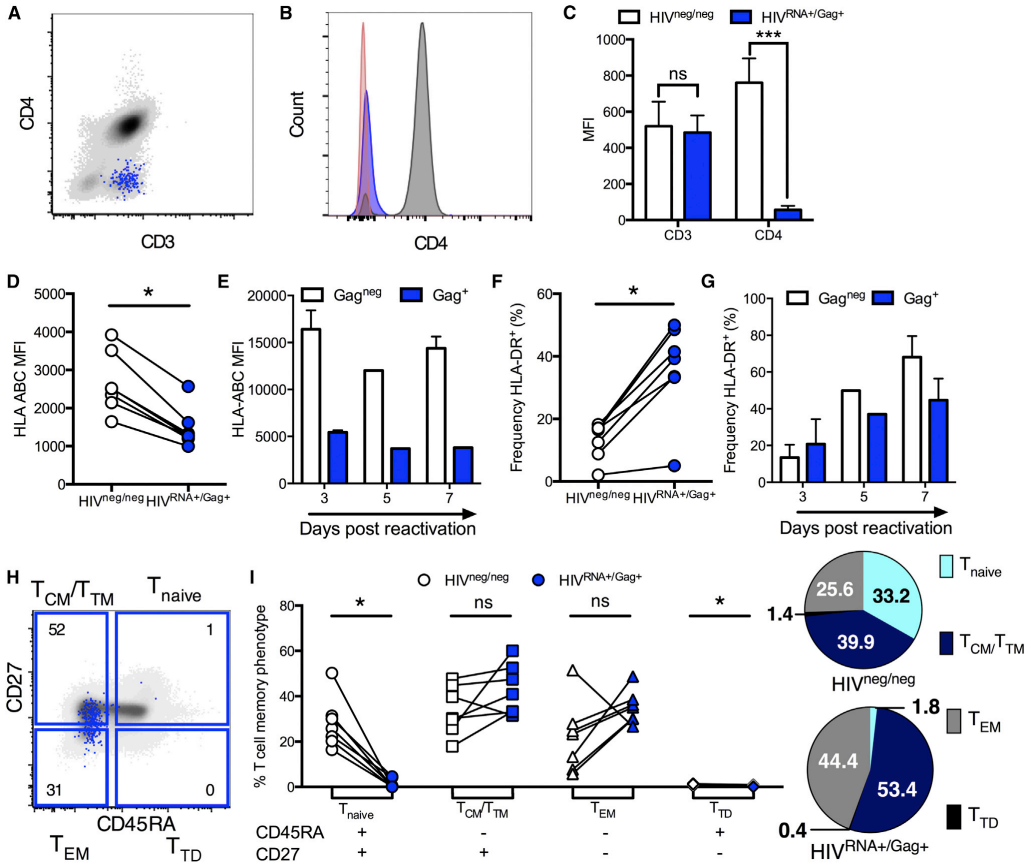

Figure 3. Dissociated Expression Patterns of CD4 Co-receptors and Memory Phenotype of CD4 Cells Maintaining Ongoing Infection in Viremic Individuals

Peripheral CD4 from viremic, untreated (UNT) patients were analyzed directly ex vivo without stimulation for phenotype. White symbols/bars represent $HIV^{neg/neg}$ CD4, and blue represents $HIV^{RNA+/Gag+}$ CD4 from the same patient sample.

(A–C) $HIV^{RNA+/Gag+}$ T cells downregulate CD4. (A) Example plot overlaying $HIV^{RNA+/Gag+}$ (blue) onto $HIV^{neg/neg}$ (gray) CD4. (B) Histogram of staining in (A) with negative control (red). (C) Quantification of results in (A) and (B). n = 5 UNT. ***$p < 0.001$ by Friedman ANOVA with Dunn's post-test.

(D–G) HLA-ABC expression (D and E) and $HLA\text{-}DR^+$ frequency (F and G) on HIV-infected versus uninfected CD4. For (D) and (F), infected cells were defined by dual mRNA/protein stain on unstimulated UNT CD4 analyzed directly ex vivo. For (E) and (G), infected CD4 were defined by standard Gag protein staining only at time points post-reactivation for an endogenous, spreading infection.

(H and I) Comparison of memory phenotype between $HIV^{RNA+/Gag+}$ CD4 in UNT compared to $HIV^{neg/neg}$ CD4. (H) Example plot and gating with $HIV^{RNA+/Gag+}$ CD4 (blue) overlaid onto total T cell population (gray). Numbers represent frequency of $HIV^{RNA+/Gag+}$ CD4 with specific phenotype. (I) Quantification of data in (H). Numbers shown in pie charts represent normalized mean. n = 7 UNT, except in (E and G), where n = 2. ns signifies $p > 0.05$, *$p < 0.05$ by Wilcoxon signed rank test. See also Figure S5.

stimulation and virus propagation ex vivo (Figure 3E). In contrast, HLA-class II expression on in vivo-infected cells differed from in vitro data; consistent with an activated state, HLA-DR was preferentially expressed on $HIV^{RNA+/Gag+}$ compared to $HIV^{RNA-/Gag-}$ cells in primary samples (Figure 3F), whereas no enrichment for HIV-infected cells in the HLA-DR+ population was observed at days 5 and 7 of endogenous viral reactivation (Figure 3G). Differences were also observed for PD-L1 expression on $HIV^{RNA+/Gag+}$ (Figures S5A and S5B). Whereas PD-L1 was highly expressed on stimulated HIV-infected and non-infected cells early after initiation (e.g., day 3) of T cell cultures, suggesting a potential mechanism of functional immune escape similar to that described for cancer cells, PD-L1 expression was low on in vivo-infected $HIV^{RNA+/Gag+}$ CD4. The latter was

surprising, given the same cells preferentially expressed HLA-DR, another marker of activation. Thus, the phenotype of HIV-replicating cells in vivo cannot be reliably inferred from in vitro expansion models.

Central memory cells are major long-lived viral reservoirs in ART-treated subjects (Chomont et al., 2009). However, whether viral replication during viremia preferentially occurs in this subset remains to be defined. We analyzed the differentiation of $HIV^{RNA+/Gag+}$ CD4 T cells according to CD45RA and CD27 expression (Figure 3H), described here as naive (T_{naive}, $CD27^+$ $CD45RA^+$), central/transitional memory ($T_{CM/TM}$, $CD27^+$ $CD45RA^-$), effector memory (T_{EM}, $CD27^-$ $CD45RA^-$), and terminally differentiated (T_{TD}, $CD27^-$ $CD45RA^+$) cells (Sallusto et al., 2004). The $T_{CM/TM}$ phenotype was dominant among $HIV^{RNA+/Gag+}$ cells (median[range] = 40.90%[31.5–60], normalized mean = 53.4%), in keeping with observations made for HIV DNA content in ART-treated patients (Figures 3I, S5C, S5D, and S6G). Compared to the $HIV^{neg/neg}$ population, HIV-infected cells contained few T_{naive} or T_{TD} CD4 and were enriched in both $T_{CM/TM}$ and T_{EM}. Thus, HIV-infected cells do not appear to shift toward a more differentiated phenotype in UNT individuals, in spite of high activation.

HIV-Infected Cells in Blood Preferentially Express T Follicular Helper Cell Markers and Inhibitory Co-receptors

Germinal center Tfh are critical for B cell help. Studies using viral outgrowth assays (VOAs; Finzi et al., 1997) and/or PCR quantitation have shown that Tfh serve as preferential sites of viral replication in lymph nodes in the absence of therapy (Perreau et al., 2013) and may represent a viral reservoir in controlled viremia (Banga et al., 2016). A peripheral blood equivalent of Tfh (pTfh) corresponding to a memory population has recently been identified (Morita et al., 2011) and predicts development of broadly neutralizing antibodies against HIV (Locci et al., 2013). We thus sought to define whether pTfh are preferentially infected. Indeed, pTfh, defined as $CD45RA^-$ memory CD4 T cells co-expressing PD-1 and CXCR5, were enriched in $HIV^{RNA+/Gag+}$ cells (Figures 4A and 4B). Expression of ICOS, a critical co-stimulator for Tfh function, was also highly enriched in $HIV^{RNA+/Gag+}$, suggesting recent activation (Figure 4C). However, there was no significant difference in expression of CXCR3, a classical Th1 marker whose co-expression identifies a less functional subset of Tfh but can also be induced by activation (Figure S5E). Thus, preferential replication of HIV in activated Tfh cells is not restricted to germinal centers but can also be detected in the periphery.

Blockade of inhibitory co-receptors of TCR signaling is considered a potential means of viral reactivation in "shock and kill" strategies (Deeks, 2012). Besides mediating CD4 T cell exhaustion (Kaufmann et al., 2007), molecules such as PD-1 may contribute to the maintenance of the quiescent state of viral latency in HIV-infected CD4 T cells; the $PD\text{-}1^+$ subset is a preferential viral reservoir in ART-treated subjects (Chomont et al., 2009). Expression of multiple inhibitory receptors on CD4 T cells prior to ART was shown to be a predictive biomarker of viral rebound post treatment interruption, suggesting that they may identify those latently infected cells with a higher proclivity to viral transcription (Hurst et al., 2015). However, this link between inhibitory co-receptor expression and spontaneous production of viral mRNA and protein has not been demonstrated in untreated infection. We therefore determined the expression patterns of the receptors PD-1, CTLA-4, and TIGIT on HIV-infected cells, molecules that are all either already targeted by cancer immunotherapies in clinical care or the subject of active drug development (Figures 4D–4F and S5F–S5H). Analysis of individual receptors showed that the $PD\text{-}1^+$, $TIGIT^+$, and $CTLA\text{-}4^+$ populations were all enriched for $HIV^{RNA+/Gag+}$ T cells. Indeed, the majority (median = 70%) of $HIV^{RNA+/Gag+}$ CD4 T cells expressed at least one inhibitory receptor, while even in UNT patients a minority of the uninfected, $HIV^{neg/neg}$ CD4 T cells (median = 35%) expressed such exhaustion markers (Figures 4G and 4H). The majority of $HIV^{RNA+/Gag+}$ CD4 T cells expressed PD-1 (median = 63%), in agreement with observations made on HIV DNA content in ART-treated patients, whereas a somewhat smaller fraction expressed TIGIT (median = 42%). By analyzing patterns of inhibitory receptor co-expression, we observed that half of the $PD\text{-}1^+$ cells also expressed TIGIT, while $TIGIT^+$-only cells were less frequent. The same trends were observed for $HIV^{neg/neg}$ CD4. While the frequency of $CTLA\text{-}4^+$ T cells was the lowest for the coreceptors studied, the relative enrichment of $HIV^{RNA+/Gag+}$ T cells compared to uninfected T cells was greatest for these populations. In particular, while $PD\text{-}1^+$ $CTLA\text{-}4^+$ and the triple positive ($CTLA\text{-}4^+$ $PD\text{-}1^+$ $TIGIT^+$) populations represented small subsets (<1%) in the uninfected T cell population, both of these populations were detectable at higher frequencies (~4%) in the $HIV^{RNA+/Gag+}$-infected T cells. These data show that robust viral replication occurs in blood lymphocytes in spite of high levels of inhibitory receptor co-expression.

Quantitation of Latent Reservoirs from Virally Suppressed Individuals and Correlation with PCR-Based Assays

Strategies to reduce the latent reservoirs are now being tested in clinical trials (Archin et al., 2012). There is an urgent need for high-throughput assays able to reliably quantify these cells in subjects, but their low frequency makes this challenging. Furthermore, estimation of reservoir size varies widely depending on the assay used (Eriksson et al., 2013), with the VOA giving a minimal value for the replication-competent reservoir and DNA PCR-based assays overestimating its size due to defective viral genomes. Here, we examined ART-treated subjects (Tx, characteristics and cells analyzed, Table S3) to assess the ability of the $HIV^{RNA/Gag}$ assay to quantify latently infected CD4 T cells harboring inducible virus capable of translating Gag and compared it to alternative measurements of reservoir size. As previously, we define this population as the viral translation-competent latent reservoir. In the absence of stimulation, $HIV^{RNA+/Gag+}$ events were very rare or absent (median[range] = 0.55[0–2.6]; Figures 5A and 5B), in keeping with published data utilizing HIV Gag protein staining alone, where rare HIV^{Gag+} cells were detected in ART-treated patients (Graf et al., 2013). In contrast, PMA/iono stimulation induced $HIV^{RNA+/Gag+}$ cells in all but one Tx subject, with frequencies ranging from 1.2 to 660/million (median = 3.56; Figures 5A, 5B, and S6C). Reactivation of the translation-competent latent reservoir measured by our assay showed a strong trend ($p = 0.061$) toward inverse correlation with CD4/CD8 ratio (Figure 5C) and a weaker inverse correlation with CD4 T cell count (Figure S6A). We next

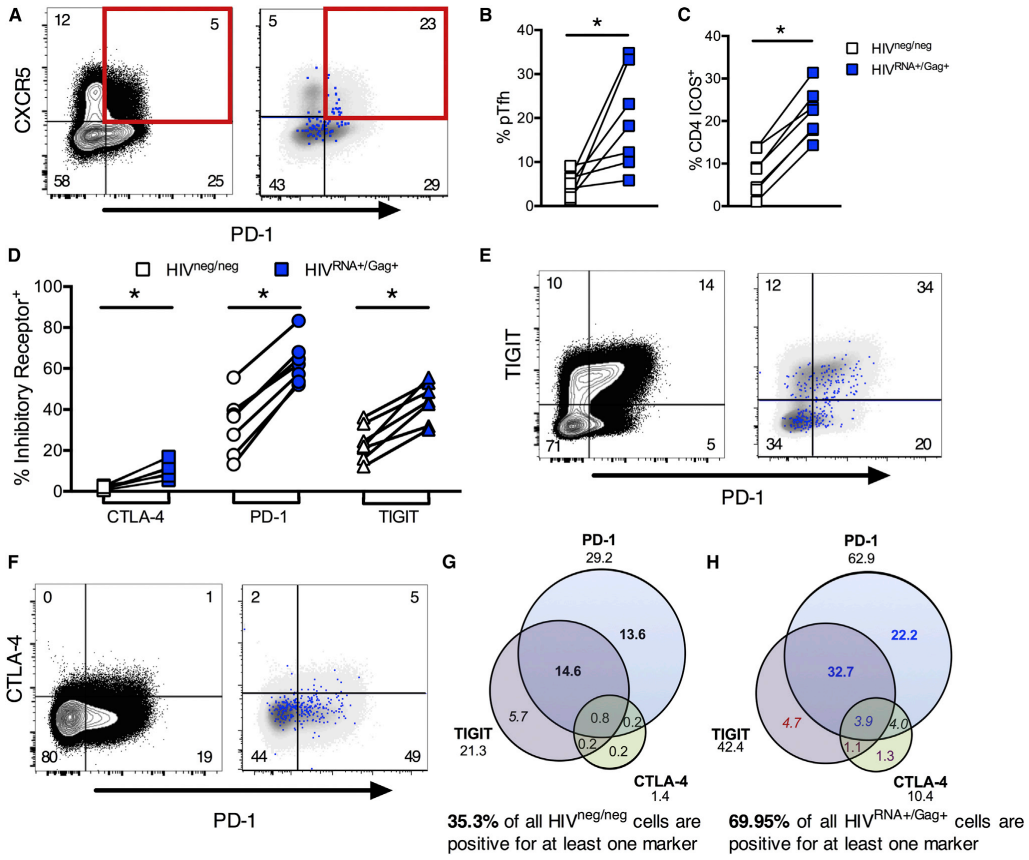

Figure 4. CD4 T Cells Maintaining Ongoing Replication during Viremia Show Markers of Activation, Exhaustion, and Peripheral T Follicular Helper Cells

Peripheral CD4 from viremic patients (UNT) were analyzed without stimulation for phenotype directly ex vivo. For example plots in (A), (E), and (F), left-hand panel shows gating on total CD4 T cells with frequencies of each population indicated. Right-hand panel shows $HIV^{RNA+/Gag+}$ CD4 events in blue, overlaid onto $HIV^{neg/neg}$ events (gray) for the same markers. Frequencies shown represent the $HIV^{RNA+/Gag+}$ population.

(A) Example plots of pTfh phenotype (pre-gated on CD45RA− memory CD4).

(B) Quantification of results in (A), shown as frequency of memory CD4.

(C) Frequency of ICOS expression on $HIV^{RNA+/Gag+}$ versus $HIV^{neg/neg}$ CD4.

(D) Relative expression of coinhibitory receptors CTLA-4, PD-1, and TIGIT on $HIV^{RNA+/Gag+}$ compared to $HIV^{neg/neg}$ CD4.

(E and F) Example plots of coexpression; TIGIT and PD-1 (E), CTLA-4 and PD-1 (F).

(G and H) Boolean analysis of inhibitory receptor coexpression on $HIV^{neg/neg}$ (G) versus $HIV^{RNA+/Gag+}$ (H) CD4 from the same patients. Numbers under inhibitory receptor name indicate total frequency of positive events (e.g., all PD-1^+) and correspond to data in (E) and (F). Red text indicates populations under represented in $HIV^{RNA+Gag+}$ versus $HIV^{neg/neg}$. Populations were enriched in $HIV^{RNA+Gag+}$ by 1- to 5-fold (blue), 5- to 10-fold (purple), or over 10-fold (black). Populations contributing more than 2% or 10% are in italics or bold, respectively. Data represent medians. n = 7 UNT. *$p < 0.05$ by Wilcoxon signed rank test. See also Figure S5.

compared the frequency of $HIV^{RNA+/Gag+}$ events to the estimated size of the reservoir based on integrated or total HIV DNA (Figure 5D). While the size of the reservoir determined by these assays correlated well (Figures 5E and S6B), the median reservoir size as measured by integrated DNA was ~800 copies/million compared to 3.56 cells/million by the $HIV^{RNA/Gag}$ assay. The median ratio between these two measures was 204, which is comparable to the differences detected between integrated DNA and the VOA (Bruner et al., 2015). Factors that may contribute to these differences include the inability of standard DNA assays to distinguish between replication-competent and defective integrated viral genomes (while the $HIV^{RNA/Gag}$ assay detects

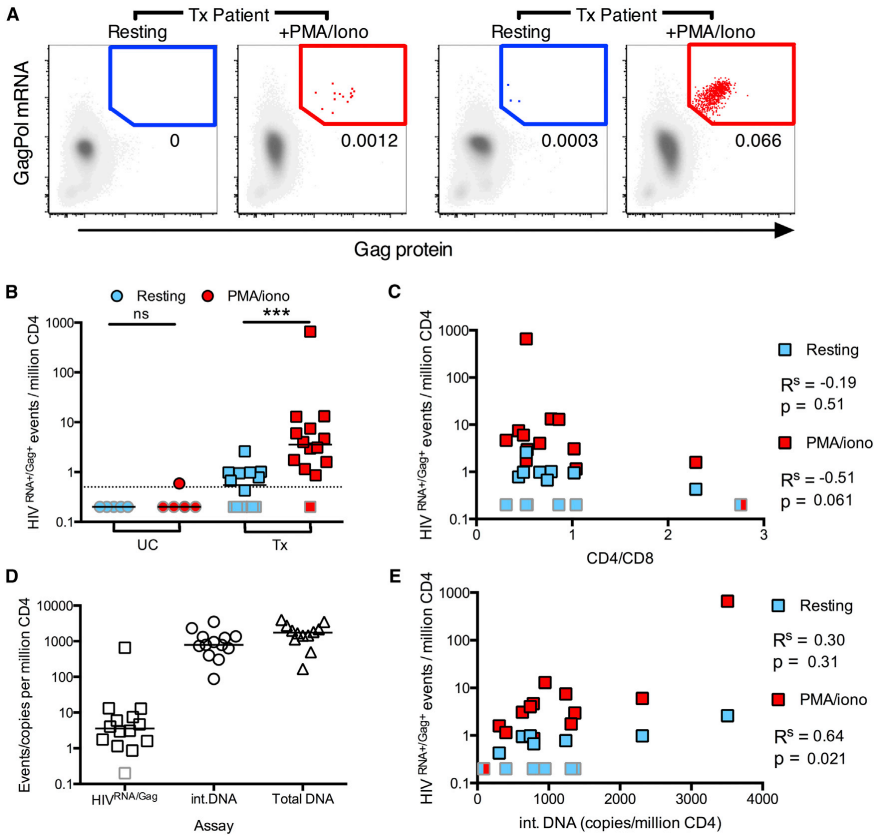

Figure 5. Detection of Latently HIV-Infected CD4 T Cells from ART-Treated Patients

Peripheral $HIV^{RNA+Gag+}$ CD4 were detected in treated, aviremic patients (Tx) directly ex vivo (resting, light blue) or following stimulation (PMA/iono, red).

(A) Example plots of a representative patient (left) or a patient with a large inducible reservoir (right).

(B) Quantification of data in (A) for Tx and uninfected controls (UC). Dotted line represents limit of detection (LOD). ns signifies $p > 0.05$, ***$p < 0.001$ by Wilcoxon signed rank test.

(C) Correlation between reactivation and CD4/CD8 T cell ratio. Where result is the same between two conditions, a split box is shown.

(D) Comparison of reservoir measured by different techniques; $HIV^{RNA/Gag}$ assay (with PMA/iono stimulation, data as in B), integrated HIV DNA PCR (int.DNA), and total HIV DNA PCR. Line shown at median.

(E) Correlation between reservoir as measured by integrated DNA and $HIV^{RNA/Gag}$ assays. Gray bordered symbols are below LOD. In all experiments, n = 5 UC and 14 Tx (13 for Figures 5D and 5E). Statistics shown are Spearman's correlation coefficient (R^s) with associated p values. See also Figure S6 and Tables S3 and S4.

only cells infected with virus capable of producing viral RNA and protein, thus narrowing estimates of the functional reservoir) and the possibility of multiple integration events in a cell. In addition, the stimulus used may play a role, as not all competent virus may be reactivated by a single round of potent stimulation (Ho et al., 2013), and detection of reactivated virus is limited to those proviruses able to produce Gag protein within the time frame of the assay.

We then compared the $HIV^{RNA/Gag}$ assay to the VOA in a subset of 11 patients (Figure S6D and S6E; Table S4). The $HIV^{RNA/Gag}$ assay and VOA detected a median[range] of 4.65 [0–110.4] $HIV^{RNA+/Gag+}$ translation-competent and 1.43[0.06–32.23] replication-competent HIV-infected cells/million CD4, respectively. In comparison, the median int.DNA copies/million CD4 for these patients was 648. Thus, while the relative frequencies measured by the VOA and $HIV^{RNA/Gag}$ assay varied and did not correlate in this group of patients, they were much closer in magnitude than the PCR-based measure.

We next tested the ability of the protein kinase C modulators bryostatin, an antineoplastic drug currently in clinical cancer trials, and ingenol, currently approved to topically treat actinic keratosis, to induce production of viral mRNA and proteins.

Bryostatin, ingenol, and their analogs have potent HIV LRA activity in vitro (DeChristopher et al., 2012; Jiang et al., 2014). We detected HIV reactivation in all Tx and UNT subjects examined although at varying degrees (Figures 6A–6C). In the majority of Tx patients, induction of the reservoir by both LRAs bryostatin (median[range] = 1.2[0.91–37.9]) and ingenol (median[range] = 1.38[1.01–3.63]) was lower than that of PMA/iono (median [range] = 7.5[0.86–660]). However, response to all stimuli varied considerably between donors. In contrast, in UNT subjects the response to bryostatin was close (68%–79%) to that of PMA/iono, likely reflecting the major difference in regulation of HIV gene expression in these two contexts. Finally, we examined the phenotype of latently infected cells reactivated with bryostatin and ingenol, as surface markers are much better preserved with these LRAs than with PMA/iono treatment.

In UNT patients, HIV-infected CD4 were predominantly T_{CM}/T_{TM} and T_{EM} in both ongoing and bryostatin-reactivated infection (Figures 6D and 6E). Concordantly, integrated HIV DNA was localized to these compartments (Figure S6F). Though the number of $HIV^{RNA+/Gag+}$ CD4 more than doubled (Figure 6C) following bryostatin reactivation, the proportion of HIV-infected T_{CM}/T_{TM} compared to T_{EM} was not significantly changed (Figure 6E). This suggests that, in individuals with ongoing viremia, bryostatin is able to reactivate a viral translation-competent reservoir from both the $T_{CM/TM}$ and T_{EM} compartments.

In comparison, in Tx subjects, the majority of bryostatin-reactivated $HIV^{RNA+/Gag+}$ cells were T_{EM} (Figures 6F and 6G), with T_{CM} contributing a minority fraction to the reactivated population. Indeed, over 90% of bryostatin-reactivated $HIV^{RNA+Gag+}$ cells were detected in the $T_{EM.}$ In contrast, in a subset of the same patients, ingenol reactivated $HIV^{RNA+/Gag+}$ cells from both T_{CM}/T_{TM} and T_{EM} in proportions comparable to those in the $HIV^{neg/neg}$ population (Figures 6H and 6I). Interestingly, when the frequency of cells harboring integrated HIV DNA was assessed, both T_{CM}/T_{TM} and T_{EM} contributed to the persistent reservoir (Figures S6G and S6H). Therefore, despite the presence of integrated DNA in both memory subsets, bryostatin-induced reactivation as measured with the $HIV^{RNA/Gag}$ assay was mostly limited to the T_{EM} compartment, while ingenol-induced reactivation was not. This suggests that the differentiation status of CD4 T cells may not affect all LRAs equally, even those from the same class.

DISCUSSION

Here, we establish and validate a flow-based RNA FISH assay to assess ongoing viral replication and the size of the inducible latent reservoir in HIV-infected individuals, and additionally demonstrate its ability to determine the efficacy of LRAs and the phenotype of the induced latently infected cells. The accurate detection of cells harboring virus able to produce HIV RNA and protein down to frequencies of 0.5–1/million CD4 T cells, combined with the power of single-cell analysis by polychromatic flow cytometry, enabled quantitative and phenotypic characterization of HIV-infected cells directly sampled from patient blood. While previous reports have utilized FISH-based techniques to identify HIV-infected cells (Patterson et al., 2001), the use of concurrent protein staining to identify the translation-competent reservoir allows increased specificity. Our data pinpoint markers of CD4 T cells supporting HIV replication in progressive disease, including features that cannot easily be inferred from in vitro infection, such as enrichment in the pTfh compartment and in the HLA-DR+ subset. Consistent with published data using integrated DNA as a measure of infection (Brenchley et al., 2004), we observe the localization of HIV-infected CD4 in the memory compartment, with limited infection of naive CD4. We also show that HIV-infected cells are more likely to express markers of exhaustion (PD-1, CTLA-4, and TIGIT) than uninfected CD4 in the context of ongoing viremia. The role for exhaustion markers in the context of CD4 infection remains to be determined—for example, are cells expressing such markers more likely to be infected in vivo, or is expression a consequence of infection itself? As multiple exhaustion markers (including PD-1) are also upregulated as negative feedback mechanisms following activation, an increased susceptibility of these cells to infection is in line with the observations made here and previously (Stevenson et al., 1990) that activated cells are more amenable to HIV infection. In the context of latency, it has been suggested that the expression of multiple inhibitory receptors may identify those CD4 with a higher proclivity to viral transcription (Hurst et al., 2015). The work presented here focuses on CD4 T cells as the major source of infectious virus during chronic infection and the major reservoir in patients receiving therapy. However, additional cell types have been reported as permissive to HIV in vivo, including macrophages and dendritic cells. Previous work has demonstrated that monocytes can be assessed (Porichis et al., 2014); thus, these subsets could be evaluated by applying the $HIV^{RNA/Gag}$ technique to tissues.

We also narrow down estimates for the size of the inducible reservoir (median 3.56 cells/million CD4 following 12 hr PMA/ionomycin activation, median 204-fold lower than integrated DNA) while demonstrating wide differences among subjects with suppressed viral load on therapy. When compared with alternative measurements of reservoir size, the $HIV^{RNA/Gag}$ assay most closely mirrors findings using the VOA, where the minimum size of the replication-competent reservoir is estimated to be 1 per million resting CD4 (1.4 in our cohort), 100- to 1,000-fold less than that measured by integrated DNA. In addition, both the reservoir size as measured by the $HIV^{RNA/Gag}$ assay here and the VOA, shown previously (Kiselinova et al., 2016), correlate with the reservoir measured by integrated HIV DNA. The advantage of the $HIV^{RNA/Gag}$ assay is the direct detection of HIV-infected cells, allowing phenotyping, which is not possible with the VOA. Both assays have the limitation that they may not detect all intact proviruses, due to the stochastic nature of reactivation and the stimuli used. Furthermore, while the VOA detects replication-competent virus (defined by the ability of secreted virus to establish a spreading infection in vitro), the $HIV^{RNA/Gag}$ assay detects cells containing virus able to produce HIV RNA and Gag protein (viral translation-competent virus). Therefore, one potential caveat for the $HIV^{RNA/Gag}$ assay is that not all of the reactivated virus is infectious and so the size of the replication-competent reservoir may be slightly overestimated. In contrast, the VOA may underestimate the size of the replication-competent reservoir as virus may be released but may not establish an in vitro infection and remain undetectable. These differences may explain the lack of correlation observed

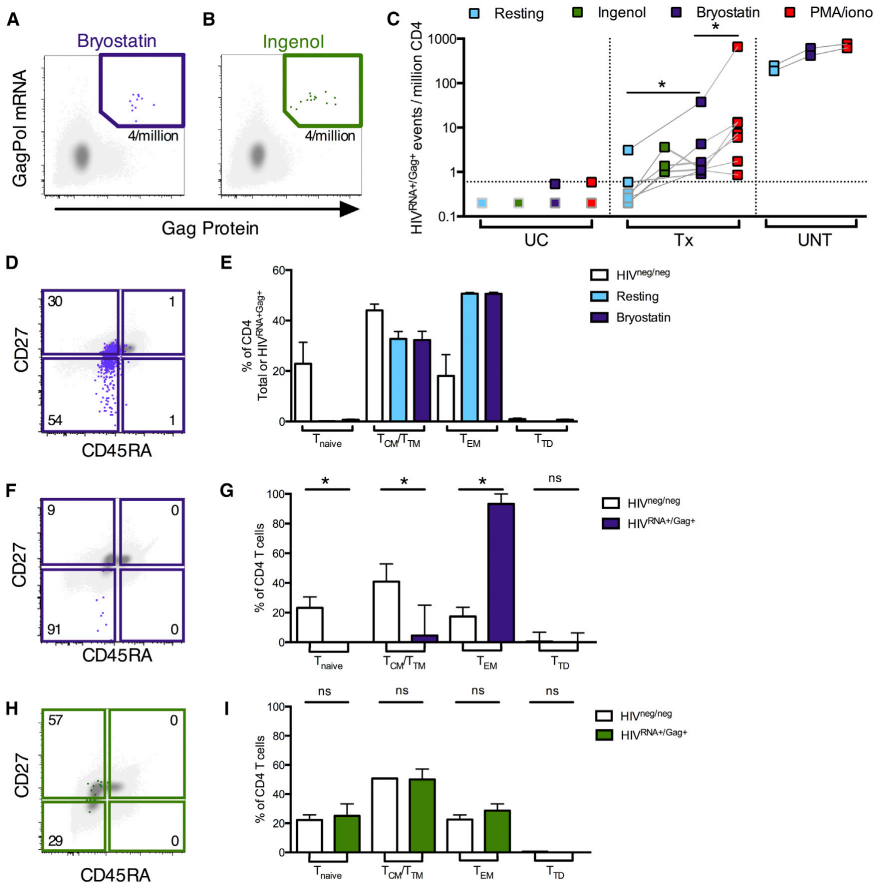

Figure 6. Quantification and Phenotyping of LRA-Reactivated Infected CD4 Cells in Patients On or Off ART

$HIV^{RNA+/Gag+}$ CD4 from UC, UNT, or Tx patients were detected directly ex vivo (resting, light blue symbols/bars) or following reactivation with ingenol (green), bryostatin (purple), or PMA/iono (red). In example plots, reactivated $HIV^{RNA+/Gag+}$ events (green/purple) are overlaid onto $HIV^{neg/neg}$ events (gray). Frequencies of $HIV^{RNA+/Gag+}$ CD4 are indicated in each gate.

(A and B) Example plots for Tx patients following bryostatin (A) or ingenol reactivation (B).

(C) Summary data of $HIV^{RNA+/Gag+}$ CD4 frequencies in unstimulated versus stimulated CD4. n = 4 UC, 2 UNT, and 3–7 Tx. Dotted line indicates LOD. Grey-bordered symbols are below LOD.

(D) Example plot showing memory phenotype of bryostatin-reactivated $HIV^{RNA+/Gag+}$ CD4 for an example UNT.

(E) Quantification of data in (D) for n = 2 UNT, comparing $HIV^{neg/neg}$ with $HIV^{RNA+/Gag+}$ CD4, unstimulated or after bryostatin stimulation. $HIV^{neg/neg}$ CD4 are shown in white. Bars represent mean ± SEM.

(F) Example plot showing memory phenotype of bryostatin-reactivated $HIV^{RNA+/Gag+}$ CD4 for a Tx patient.

(G) Quantification of data in (F). n = 7 Tx.

(H) Example plot showing memory phenotype of ingenol-reactivated $HIV^{RNA+/Gag+}$ CD4 for a Tx patient.

(I) Quantification of data in (H). n = 3 Tx patients. ns indicates $p > 0.05$, *$p < 0.05$ by Wilcoxon signed rank test. For (G) and (I), bars median ± interquartile range. See also Figure S6 and Table S3.

between these two assays and the larger reservoir size detected using the $HIV^{RNA/Gag}$ assay when compared to the VOA.

An additional factor in the detection of rare cells is the probability of detecting events due to Poisson distribution and sampling differences. To increase the probability of accurately detecting rare cells, increasing cell numbers must be analyzed. In the current study, 2–3 million CD4 T cells per patient per condition were usually acquired on the flow cytometer. The

requirement for high cell numbers may be a limiting factor for latency studies; however, a similar restriction exists for known techniques to measure latent reservoirs.

Finally, we show that this approach can be used to assess the efficiency of LRAs such as bryostatin and ingenol, drugs currently in clinical trials, and importantly determine the susceptibility of distinct CD4 cells to LRA-induced reactivation. The need for such primary cell assays is highlighted by the wide variability of results obtained in in vitro latency models (Spina et al., 2013). The phenotypic analysis of LRA-induced cells has important potential implications for the function of LRAs. First, while both the T_{EM} and T_{CM} CD4 pools contain integrated pro-virus, the relative frequencies of functional versus defective pro-viral DNA have been suggested to differ between subsets (Soriano-Sarabia et al., 2014). Alternatively, CD4 subsets may vary in their sensitivity to individual LRAs. While these two mechanisms are not mutually exclusive, our data suggest a differential sensitivity of CD4 populations to individual LRAs: bryostatin readily induced the T_{EM} reservoir but had limited effect on the T_{CM} compartment, contrasting with the more even effect observed with ingenol. An effective LRA must induce HIV protein expression in all latently infected cells regardless of phenotype to enable recognition and elimination by host immune responses, and as such ingenol may represent a promising candidate. Combinations of LRAs need to be assessed, to increase potency but also to recruit additional subsets of latently infected cells that may not be amenable to reactivation with a single drug. This technology and the results obtained may have important implications for HIV pathogenesis studies, including investigation of early transmission events, testing of LRAs, and monitoring of cure strategies.

EXPERIMENTAL PROCEDURES

Participants and Samples

Leukaphereses were obtained from study participants at the Montreal General Hospital, Montreal, Canada, and at Martin Memorial Health Systems, Florida, USA. The study was approved by the respective IRBs and written informed consent obtained from all participants prior to enrolment. See Supplemental Experimental Procedures for details. Untreated, viremic participants (UNT) were either treatment naive or untreated for at least 6 months. Treated subjects (Tx) were on ART for over 12 months with controlled viral load (<50 vRNA copies/mL) for at least 6 months. Patient characteristics are summarized in Tables S2–S4. In rare cases, due to limited sample availability, sequential leukaphereses were used for individual subjects. PBMCs isolated by Ficoll density gradient were stored in liquid nitrogen.

In Vitro Reactivation and Spreading Infection

CD4 T cells were isolated from PBMCs by negative magnetic bead selection (StemCell), resulting in an untouched population defined as CD3+CD4+/−CD8-CD14-CD19- (purity routinely over 95%). Cells were stimulated for 36–40 hr in RPMI with PHA-L (10 μg/ml, Sigma) and IL-2 (50U/ml), then washed and maintained for 6–7 days in RPMI with IL-2 (100 U/ml). In some experiments, ARVs (T20 [7.5 μg/ml] + AZT [1 μM]) were added. Enfuvirtide (T-20), Zidovudine (AZT), and IL-2 (Lahm and Stein, 1985) were obtained through NIH AIDS Reagent Program, Division of AIDS, NIAID, NIH, human rIL-2 from Dr. Maurice Gately, Hoffmann–La Roche Inc.

Reactivation of Latent Infection with PMA/Ionomycin or LRAs

CD4 T cells were isolated as above, resuspended at 2×10^6/ml media with ARVs (T20 + AZT, as before), and rested for 3–5 hr. Cells were either unstimulated, stimulated for 12 hr with PMA (50 ng/ml) and ionomycin (0.5 μg/ml), or stimulated for 18 hr with Bryostatin-1 (10 nM, Enzo Life Sciences) or Ingenol-3-angelate (25 nM, Sigma). A total of 5–12 × 10^6 purified CD4 was required per patient/condition.

$HIV^{RNA/Gag}$ Assay

See Figure S1 for the workflow schematic. Samples were subjected to the PrimeFlow RNA assay (Affymetrix/eBioscience) as per manufacturer's instructions. See Supplemental Experimental Procedures for protocol details and antibody panels. Cells were stained for viability, surface stained for phenotypic markers, and stained intracellulary for HIV Gag protein prior to mRNA detection. Samples were acquired on an LSRII (BD Bioscience). Analysis was performed using FlowJo (Treestar, V10).

Linearity and Specificity Experiment

Reactivated, HIV-replicating CD4 T cells from an untreated patient were spiked into uninfected cells at different ratios to set up a dilution series. The predicted frequency of $HIV^{RNA+/Gag+}$ (or HIV^{RNA+} or HIV^{Gag+}) was compared to the detected frequency. See Supplemental Experimental Procedures for details.

Microscopy on Sorted CD4 following $HIV^{RNA+/Gag+}$ Assay

Patient-reactivated CD4 T cells were sorted according to expression of Gag protein and GagPol mRNA. The number of nuclear and total *gag-pol* mRNA spots and CTCF were determined by confocal microscopy. See Supplemental Experimental Procedures for details.

HIV DNA Quantification

Quantifications of total and integrated HIV DNA were determined as previously described (Vandergeeten et al., 2014).

QVOA

Quantifications of replication-competent virus were performed as previously described (Siliciano and Siliciano, 2005).

Statistics

All statistical analyses were performed in Prism (V6, GraphPad). Data were tested for normality using the D'Augustino-Pearson Omnibus normality test. Where appropriate, parametric tests were applied. Statistical tests were two sided, and repeated measures were used for comparisons within subjects. For comparisons between groups, Kruskal-Wallis or Friedman one-way ANOVA with Dunn's post-test was used. For correlations, Spearman's R (R^s) correlation coefficient was used. For pairwise analysis of non-normally distributed data, Wilcoxon Signed Rank t tests were used. $p < 0.05$ was considered significant.

SUPPLEMENTAL INFORMATION

Supplemental Information includes six figures, four tables, two movies, and Supplemental Experimental Procedures and can be found with this article at http://dx.doi.org/10.1016/j.chom.2016.07.015.

AUTHOR CONTRIBUTIONS

A.E.B., J.N., F.P, A.F., N.C., and D.E.K. designed the studies; A.E.B., J.N., R.F., J.R., R.C., N.B., G.-G.D., M.M, and N.A. performed experiments; J.P.R. obtained IRB approval and recruited participants; B.D.W. provided input on study design; A.E.B. and D.E.K. interpreted the data and wrote the paper with all co-authors' assistance.

ACKNOWLEDGMENTS

We thank Josée Girouard, the clinical staff at McGill University Health Centre, and all study participants; Dr. Dominique Gauchat and the CRCHUM Flow Cytometry Platform, and Daniel Zenklusen and Chunfai Lai for technical assistance; Dylan Malayter for reagents and Drs. Shane Crotty and Naglaa Shoukry for their input on this manuscript. This study was supported by the National Institutes of Health (HL-092565, AI100663 CHAVI-ID, AI113096, AI118544, and the Delaney AIDS Research Enterprise [DARE] 1U19AI096109), the Canadian Institutes for Health Research (grant #137694; Canadian HIV Cure Enterprise),

a Canada Foundation for Innovation grant, the FRQS AIDS and Infectious Diseases Network, and the Foundation for AIDS Research (108928-56-RGRL). D.E.K. and N.C. are supported by FRQS Research Scholar Awards. A.F. is the recipient of a Canada Research Chair. J.P.R is the holder of Louis Lowenstein Chair, McGill University. J.R. is the recipient of CIHR Fellowship Award #135349. N.A. is the recipient of a King Abdullah scholarship from the Saudi Government.

Received: March 13, 2016
Revised: June 7, 2016
Accepted: July 13, 2016
Published: August 18, 2016

REFERENCES

Archin, N.M., Liberty, A.L., Kashuba, A.D., Choudhary, S.K., Kuruc, J.D., Crooks, A.M., Parker, D.C., Anderson, E.M., Kearney, M.F., Strain, M.C., et al. (2012). Administration of vorinostat disrupts HIV-1 latency in patients on antiretroviral therapy. Nature *487*, 482–485.

Argañaraz, E.R., Schindler, M., Kirchhoff, F., Cortes, M.J., and Lama, J. (2003). Enhanced CD4 down-modulation by late stage HIV-1 nef alleles is associated with increased Env incorporation and viral replication. J. Biol. Chem. *278*, 33912–33919.

Bagnarelli, P., Valenza, A., Menzo, S., Sampaolesi, R., Varaldo, P.E., Butini, L., Montroni, M., Perno, C.F., Aquaro, S., Mathez, D., et al. (1996). Dynamics and modulation of human immunodeficiency virus type 1 transcripts in vitro and in vivo. J. Virol. *70*, 7603–7613.

Banga, R., Procopio, F.A., Noto, A., Pollakis, G., Cavassini, M., Ohmiti, K., Corpataux, J.M., de Leval, L., Pantaleo, G., and Perreau, M. (2016). PD-1(+) and follicular helper T cells are responsible for persistent HIV-1 transcription in treated aviremic individuals. Nat. Med. *22*, 754–761.

Brenchley, J.M., Hill, B.J., Ambrozak, D.R., Price, D.A., Guenaga, F.J., Casazza, J.P., Kuruppu, J., Yazdani, J., Migueles, S.A., Connors, M., et al. (2004). T-cell subsets that harbor human immunodeficiency virus (HIV) in vivo: implications for HIV pathogenesis. J. Virol. *78*, 1160–1168.

Bruner, K.M., Hosmane, N.N., and Siliciano, R.F. (2015). Towards an HIV-1 cure: measuring the latent reservoir. Trends Microbiol. *23*, 192–203.

Burgess, A., Vigneron, S., Brioudes, E., Labbé, J.C., Lorca, T., and Castro, A. (2010). Loss of human Greatwall results in G2 arrest and multiple mitotic defects due to deregulation of the cyclin B-Cdc2/PP2A balance. Proc. Natl. Acad. Sci. USA *107*, 12564–12569.

Burton, D.R., Ahmed, R., Barouch, D.H., Butera, S.T., Crotty, S., Godzik, A., Kaufmann, D.E., McElrath, M.J., Nussenzweig, M.C., Pulendran, B., et al. (2012). A blueprint for HIV vaccine discovery. Cell Host Microbe *12*, 396–407.

Chomont, N., El-Far, M., Ancuta, P., Trautmann, L., Procopio, F.A., Yassine-Diab, B., Boucher, G., Boulassel, M.R., Ghattas, G., Brenchley, J.M., et al. (2009). HIV reservoir size and persistence are driven by T cell survival and homeostatic proliferation. Nat. Med. *15*, 893–900.

DeChristopher, B.A., Loy, B.A., Marsden, M.D., Schrier, A.J., Zack, J.A., and Wender, P.A. (2012). Designed, synthetically accessible bryostatin analogues potently induce activation of latent HIV reservoirs in vitro. Nat. Chem. *4*, 705–710.

Deeks, S.G. (2012). HIV: Shock and kill. Nature *487*, 439–440.

Deeks, S.G., Autran, B., Berkhout, B., Benkirane, M., Cairns, S., Chomont, N., Chun, T.W., Churchill, M., Di Mascio, M., Katlama, C., et al.; International AIDS Society Scientific Working Group on HIV Cure (2012). Towards an HIV cure: a global scientific strategy. Nat. Rev. Immunol. *12*, 607–614.

DeMaster, L.K., Liu, X., VanBelzen, D.J., Trinité, B., Zheng, L., Agosto, L.M., Migueles, S.A., Connors, M., Sambucetti, L., Levy, D.N., et al. (2016). A subset of CD4/CD8 double-negative T cells expresses HIV proteins in patients on antiretroviral therapy. J. Virol. *90*, 2165–2179.

Eriksson, S., Graf, E.H., Dahl, V., Strain, M.C., Yukl, S.A., Lysenko, E.S., Bosch, R.J., Lai, J., Chioma, S., Emad, F., et al. (2013). Comparative analysis of measures of viral reservoirs in HIV-1 eradication studies. PLoS Pathog. *9*, e1003174.

Finzi, D., Hermankova, M., Pierson, T., Carruth, L.M., Buck, C., Chaisson, R.E., Quinn, T.C., Chadwick, K., Margolick, J., Brookmeyer, R., et al. (1997). Identification of a reservoir for HIV-1 in patients on highly active antiretroviral therapy. Science *278*, 1295–1300.

Graf, E.H., Pace, M.J., Peterson, B.A., Lynch, L.J., Chukwulebe, S.B., Mexas, A.M., Shaheen, F., Martin, J.N., Deeks, S.G., Connors, M., et al. (2013). Gag-positive reservoir cells are susceptible to HIV-specific cytotoxic T lymphocyte mediated clearance in vitro and can be detected in vivo [corrected]. PLoS ONE *8*, e71879.

Ho, Y.C., Shan, L., Hosmane, N.N., Wang, J., Laskey, S.B., Rosenbloom, D.I., Lai, J., Blankson, J.N., Siliciano, J.D., and Siliciano, R.F. (2013). Replication-competent noninduced proviruses in the latent reservoir increase barrier to HIV-1 cure. Cell *155*, 540–551.

Hurst, J., Hoffmann, M., Pace, M., Williams, J.P., Thornhill, J., Hamlyn, E., Meyerowitz, J., Willberg, C., Koelsch, K.K., Robinson, N., et al. (2015). Immunological biomarkers predict HIV-1 viral rebound after treatment interruption. Nat. Commun. *6*, 8495.

Jiang, G., Mendes, E.A., Kaiser, P., Sankaran-Walters, S., Tang, Y., Weber, M.G., Melcher, G.P., Thompson, G.R., 3rd, Tanuri, A., Pianowski, L.F., et al. (2014). Reactivation of HIV latency by a newly modified Ingenol derivative via protein kinase Cδ-NF-κB signaling. AIDS *28*, 1555–1566.

Karn, J., and Stoltzfus, C.M. (2012). Transcriptional and posttranscriptional regulation of HIV-1 gene expression. Cold Spring Harb. Perspect. Med. *2*, a006916.

Kaufmann, D.E., Kavanagh, D.G., Pereyra, F., Zaunders, J.J., Mackey, E.W., Miura, T., Palmer, S., Brockman, M., Rathod, A., Piechocka-Trocha, A., et al. (2007). Upregulation of CTLA-4 by HIV-specific CD4+ T cells correlates with disease progression and defines a reversible immune dysfunction. Nat. Immunol. *8*, 1246–1254.

Kiselinova, M., De Spiegelaere, W., Buzon, M.J., Malatinkova, E., Lichterfeld, M., and Vandekerckhove, L. (2016). Integrated and Total HIV-1 DNA Predict Ex Vivo Viral Outgrowth. PLoS Pathog. *12*, e1005472.

Kulpa, D.A., and Chomont, N. (2015). HIV persistence in the setting of antiretroviral therapy: when, where and how does HIV hide? J. Virus Erad. *1*, 59–66.

Lahm, H.W., and Stein, S. (1985). Characterization of recombinant human interleukin-2 with micromethods. J. Chromatogr. A *326*, 357–361.

Locci, M., Havenar-Daughton, C., Landais, E., Wu, J., Kroenke, M.A., Arlehamn, C.L., Su, L.F., Cubas, R., Davis, M.M., Sette, A., et al.; International AIDS Vaccine Initiative Protocol C Principal Investigators (2013). Human circulating PD-1+CXCR3-CXCR5+ memory Tfh cells are highly functional and correlate with broadly neutralizing HIV antibody responses. Immunity *39*, 758–769.

Morita, R., Schmitt, N., Bentebibel, S.E., Ranganathan, R., Bourdery, L., Zurawski, G., Foucat, E., Dullaers, M., Oh, S., Sabzghabaei, N., et al. (2011). Human blood CXCR5(+)CD4(+) T cells are counterparts of T follicular cells and contain specific subsets that differentially support antibody secretion. Immunity *34*, 108–121.

Patterson, B.K., McCallister, S., Schutz, M., Siegel, J.N., Shults, K., Flener, Z., and Landay, A. (2001). Persistence of intracellular HIV-1 mRNA correlates with HIV-1-specific immune responses in infected subjects on stable HAART. AIDS *15*, 1635–1641.

Perreau, M., Savoye, A.L., De Crignis, E., Corpataux, J.M., Cubas, R., Haddad, E.K., De Leval, L., Graziosi, C., and Pantaleo, G. (2013). Follicular helper T cells serve as the major CD4 T cell compartment for HIV-1 infection, replication, and production. J. Exp. Med. *210*, 143–156.

Porichis, F., Hart, M.G., Griesbeck, M., Everett, H.L., Hassan, M., Baxter, A.E., Lindqvist, M., Miller, S.M., Soghoian, D.Z., Kavanagh, D.G., et al. (2014). High-throughput detection of miRNAs and gene-specific mRNA at the single-cell level by flow cytometry. Nat. Commun. *5*, 5641.

Sallusto, F., Geginat, J., and Lanzavecchia, A. (2004). Central memory and effector memory T cell subsets: function, generation, and maintenance. Annu. Rev. Immunol. *22*, 745–763.

Schwartz, O., Maréchal, V., Le Gall, S., Lemonnier, F., and Heard, J.M. (1996). Endocytosis of major histocompatibility complex class I molecules is induced by the HIV-1 Nef protein. Nat. Med. *2*, 338–342.

Siliciano, J.D., and Siliciano, R.F. (2005). Enhanced culture assay for detection and quantitation of latently infected, resting CD4+ T-cells carrying replication-competent virus in HIV-1-infected individuals. Methods Mol. Biol. *304*, 3–15.

Soriano-Sarabia, N., Bateson, R.E., Dahl, N.P., Crooks, A.M., Kuruc, J.D., Margolis, D.M., and Archin, N.M. (2014). Quantitation of replication-competent HIV-1 in populations of resting CD4+ T cells. J. Virol. *88*, 14070–14077.

Spina, C.A., Anderson, J., Archin, N.M., Bosque, A., Chan, J., Famiglietti, M., Greene, W.C., Kashuba, A., Lewin, S.R., Margolis, D.M., et al. (2013). An in-depth comparison of latent HIV-1 reactivation in multiple cell model systems and resting CD4+ T cells from aviremic patients. PLoS Pathog. *9*, e1003834.

Stevenson, M., Stanwick, T.L., Dempsey, M.P., and Lamonica, C.A. (1990). HIV-1 replication is controlled at the level of T cell activation and proviral integration. EMBO J. *9*, 1551–1560.

Swanstrom, R., and Coffin, J. (2012). HIV-1 pathogenesis: the virus. Cold Spring Harb. Perspect. Med. *2*, a007443.

Vandergeeten, C., Fromentin, R., Merlini, E., Lawani, M.B., DaFonseca, S., Bakeman, W., McNulty, A., Ramgopal, M., Michael, N., Kim, J.H., et al. (2014). Cross-clade ultrasensitive PCR-based assays to measure HIV persistence in large-cohort studies. J. Virol. *88*, 12385–12396.

Multiparametric characterization of rare HIV-infected cells using an RNA-flow FISH technique

Nature Protocols, 2017

Multiparametric characterization of rare HIV-infected cells using an RNA-flow FISH technique

Amy E Baxter[1,2], Julia Niessl[1,2], Rémi Fromentin[1], Jonathan Richard[1], Filippos Porichis[3,6], Marta Massanella[1], Nathalie Brassard[1], Nirmin Alsahafi[1,4], Jean-Pierre Routy[5], Andrés Finzi[1,4], Nicolas Chomont[1] & Daniel E Kaufmann[1,2]

[1]Research Centre of the Centre Hospitalier de l'Université de Montréal (CRCHUM) and Université de Montréal, Montreal, Quebec, Canada. [2]Center for HIV/AIDS Vaccine Immunology and Immunogen Discovery (CHAVI-ID), La Jolla, California, USA. [3]Ragon Institute of Massachusetts General Hospital, Massachusetts Institute of Technology and Harvard University, Cambridge, Massachusetts, USA. [4]Department of Microbiology and Immunology, McGill University, Montreal, Quebec, Canada. [5]Chronic Viral Illnesses Service and Division of Hematology, McGill University Health Centre, Montreal, Quebec, Canada. [6]Current address: EMD Serono-Merck, Billerica, Massachusetts, USA. Correspondence should be addressed to D.E.K. (daniel.kaufmann@umontreal.ca).

Published online 7 September 2017; doi:10.1038/nprot.2017.079

Efforts to cure HIV are hampered by limited characterization of the cells supporting HIV replication *in vivo* and inadequate methods for quantifying the latent viral reservoir in individuals receiving antiretroviral therapy (ART). We describe a protocol for flow cytometric identification of viral reservoirs, based on concurrent detection of cellular HIV *Gagpol* mRNA by *in situ* RNA hybridization combined with antibody staining for the HIV Gag protein. By simultaneously detecting both HIV RNA and protein, the CD4 T cells harboring translation-competent virus can be identified. The HIV$^{RNA/Gag}$ method is 1,000-fold more sensitive than Gag protein staining alone, with a detection limit of 0.5–1 *Gagpol* mRNA$^+$/Gag protein$^+$ cells per million CD4 T cells. Uniquely, the HIV$^{RNA/Gag}$ assay also allows parallel phenotyping of viral reservoirs, including reactivated latent reservoirs in clinical samples. The assay takes 2 d, and requires antibody labeling for surface and intracellular markers, followed by mRNA labeling and multiple signal amplification steps.

INTRODUCTION

In spite of the tremendous success of ART in controlling HIV replication and limiting progression to AIDS, current drug regimens do not lead to cure. No current scalable treatment can eradicate the virus from an HIV-infected person[1] or generate protective HIV-specific immunity[2]. The major barrier to HIV cure is the latent viral reservoir, a cell population primarily consisting of resting memory CD4 T lymphocytes that contain a stably integrated copy of the DNA provirus. HIV is able to rebound from this reservoir, usually within days or weeks, when a patient discontinues therapy; therefore, long-term adherence to ART is required. Although modern regimens are generally well tolerated, the long-term effects of ART remain unknown; individuals on suppressive ART remain at increased risk for a range of non-AIDS defining events[3,4]. Therefore, the requirement for a life-long treatment, particularly in the context of limited access to ART and social stigma, remains a key issue driving the need for a cure.

Different strategies, alone or in combination, are currently under investigation to achieve an HIV cure[5], such as preferential killing of viral reservoir cells; repopulation of the immune system by genetically engineered, infection-resistant cells; induction of deep latency; or generation of effective anti-HIV responses by therapeutic vaccines. A major strategy proposed for HIV cure is the 'shock and kill'[6] approach, whereby latency-reversing agents (LRAs) 'shock' the latent viral reservoir into reactivating. Cells containing reactivated HIV would either be killed by the pathogenic effects of the virus itself or targeted by the host's immune system, which may have to be vaccine-adjuvanted. Although this strategy has already been tested in limited clinical trials[7], the relative ability of LRAs to induce different cellular reservoirs remains poorly understood. The latent HIV reservoir is formed early in acute infection[8,9] and is inherently stable[10,11]; at present, no cellular markers have been identified that are capable of distinguishing the very rare CD4 T cells containing latent replication-competent proviruses (on the order of 1 per million resting CD4 T cells[12–15]) from uninfected, bystander cells. These factors have made both studying and targeting the latent viral reservoir for elimination highly challenging. The CD4 lineage presents tremendous heterogeneity *in vivo*, as do other cell types that might contribute to viral reservoirs (such as some myeloid cells[16]). Regardless of the strategy pursued to achieve a HIV cure, a deeper understanding of the cells that support HIV replication *in vivo* and serve as long-lived latent viral reservoirs in ART-treated subjects is required both to eliminate residual virus and to inform the development of a vaccine capable of eliminating HIV-infected cells.

Development of the protocol and comparisons with other methods

Research into HIV reservoirs has been limited by the sensitivity, specificity and caveats of available strategies used to detect and phenotype such cells. Standard techniques include, but are not limited to, the following: the use of *in vitro* cell lines and lab-adapted viruses to model infection; measurements of viral DNA by PCR for total or integrated viral genomes[13,17,18]; and the quantitative viral outgrowth assay (QVOA)[12,19]. Work performed using *in vitro* infections has provided a wealth of information, but is limited by the requirement of many models for cellular activation to enable efficient infection and/or the propagation of cells *in vitro*, both of which alter cell characteristics, and the substantial differences between lab-adapted viruses and the transmitted/founder or chronic viruses circulating in the population. Not all integrated HIV proviruses are replication-competent—i.e., able to produce fully infectious virus; indeed, over 90% of integrated HIV proviruses may contain deletions or mutations that preclude replication competence[20,21]. Because of the prevalence and rapid accumulation of these defective/dysfunctional HIV genomes, PCR-based estimates represent the maximal viral

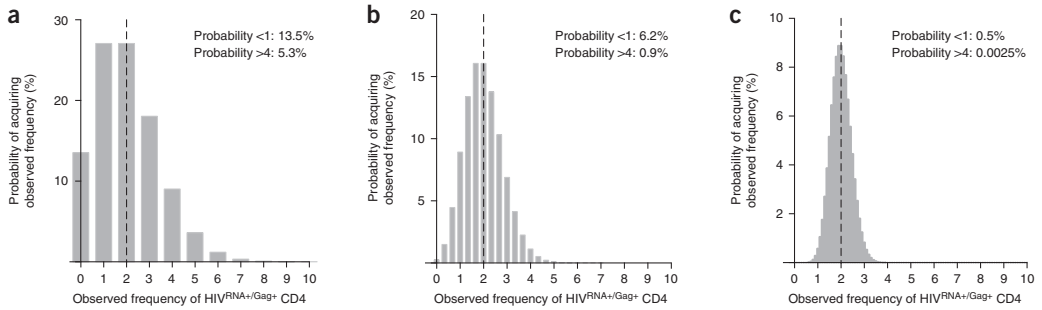

Figure 1 | Impact of Poisson distribution on the detection of rare $HIV^{RNA+/Gag+}$ events. (**a**–**c**) Models are based on an actual frequency of 2 $HIV^{RNA+/Gag+}$ events (dashed line) per 10^6 CD4 T cells and demonstrate the Poisson distribution of possible readings when (**a**) 1×10^6, (**b**) 3×10^6 or (**c**) 10×10^6 CD4 T-cell events are acquired.

reservoir size, even in individuals who initiated ART during acute infection[21,22]. At the opposite end of the spectrum, the QVOA represents a minimal estimate, as not all replication-competent viruses are reactivated following a single round of stimulation[20]. Recent work has resulted in additional mRNA-based techniques, such as the Tat/Rev induced limiting dilution assay (TILDA)[23], which have begun to close the gap between these two sets of measures. However, the above techniques rely either on population-level, rather than single-cell, analysis to detect viral reservoirs, resulting in a loss of critical information, or on limiting dilution strategy assays in which cell phenotypes cannot be determined retrospectively.

We thus sought to develop a flow-cytometry-based protocol for the single-cell identification and characterization of HIV viral reservoirs in primary samples from HIV-infected individuals[15]. Antibodies against HIV Gag proteins have been used previously to study *in vitro* infection, but are limited by high nonspecific binding, which prevents sensitive identification of HIV-infected cells at frequencies lower than 1,000 events per million[15]. By combining classic HIV Gag protein detection with RNA fluorescent *in situ* hybridization for HIV *Gag* and *Pol* mRNAs (mRNA Flow-FISH), we developed the $HIV^{RNA/Gag}$ assay, with which we are able to identify $HIV^{RNA+/Gag+}$ CD4 T cells in the range of 0.5–1 events per million. This gain in specificity markedly changes the scope of questions that can be addressed; it allows identification of HIV-infected CD4 T cells directly *ex vivo* in primary clinical samples from HIV-infected individuals, which was simply not possible with previous techniques.

To be identified by the $HIV^{RNA/Gag}$ assay, cells must contain virus that is able to transcribe viral mRNAs and translate viral protein. Therefore, we define this population as the translation-competent reservoir in HIV-infected subjects with ongoing viral replication. In ART-treated, virally suppressed individuals, the assay identifies the translation-competent latent reservoir in cells following latency reversal. This assay effectively narrows the gap between the maximal and minimal estimates of the reservoir size mentioned above, although the characteristics of the reservoirs measured are distinct.

A key advantage and novel feature of the $HIV^{RNA/Gag}$ assay is that it enables concurrent phenotyping of both the HIV-infected CD4 T cells that are maintaining infection in viremic individuals and of the CD4 T cells, which reactivate the virus in response to LRAs, at a single-cell level. This type of information has previously been inferred only at a population level, for example, by sorting subsets of CD4 T cells and determining the relative reservoir size.

Limitations

Identification of latent HIV reservoirs in primary samples is limited by the rarity of these cells in ART-treated individuals (on the order of 1 per million resting CD4 T cells). We have observed that the application of the Poisson distribution to the detection of these rare events can be a key source of variability and dictates the starting number of cells required. In the hypothetical examples in **Figure 1**, the true frequency of $HIV^{RNA+/Gag+}$ events is 2 per million CD4 T cells (the median size of the latent translation-competent reservoir detected following phorbol myristate acetate (PMA)/ionomycin stimulation in our cohort[15]). However, if 1×10^6 events are acquired on a flow cytometer, the probability of observing a frequency that differs by more than twofold from the true value (e.g., <1 or >4 $HIV^{RNA+/Gag+}$ events per million CD4 T cells) is 18.8% (**Fig. 1a**). When 3×10^6 events are collected, the probability of detecting a frequency of $HIV^{RNA+/Gag+}$ events outside of this bracket falls to 7.1% (**Fig 1b**), and at 10×10^6 events collected, it is 0.5% (**Fig. 1c**). Thus, the more events acquired, the higher the accuracy of the assay. Although it is in principle possible to acquire 10×10^6 or more events by setting up several tubes per condition and merging the FACS data files, this is frequently impractical in terms of cell numbers, operating time and costs. Therefore, we routinely acquire between 2 and 4×10^6 CD4 T cells per subject, per condition.

To enable the collection of $2–4 \times 10^6$ CD4 T cells at the final step of acquisition on the flow cytometer, we begin with $100–200 \times 10^6$ peripheral blood mononuclear cells (PBMCs), depending on the individual's CD4 T-cell count and the number of conditions to be tested. We aim to put into culture, for each donor and condition, at least 15×10^6 CD4 T cells to take into account the cell loss associated with an overnight culture and the effects of the agents required for latency reversal. Following this culture, we then start each $HIV^{RNA/Gag}$ assay with 10×10^6 CD4 T cells to account for an observed ~70% cell loss throughout the protocol. This cell number requirement may be a substantial limitation for studies in which leukapheresis or large blood draws are not obtained. It should be noted that this requirement for high cell numbers is not specific to this assay but a reflection of the mathematical

Box 1 | Adaptation to a 96-well-plate format

The version of the protocol described here and validated extensively in our laboratory uses a 1.5-ml-tube version of the assay. However, the approach can be modified to a 96-well-plate format. We note that this version of the assay has not been validated by our group to the same extent as the tube-based protocol. The key steps are the same between assays. However, the plate-based assay is adapted to work with lower volumes and with a dry pellet (rather than a 100-µl residual volume). For example, in Step 33, samples should be resuspended at 10–50 × 10^6 per ml, such that plating 200 µl in each well of a v-bottom plate provides 2–10 × 10^6 cells per well. All wash steps should be performed with 200 µl per well; an additional wash is required to take into account any incomplete first washes (i.e., 100-µl wash for 100-µl residual volume) and pellets are resuspended in a fresh 100 µl of the appropriate buffer. When using an antibody stain, the dry pellets can be resuspended either in 100 µl of buffer (and then proceeding as though this is the residual volume) or in an antibody mix pre-prepared in 100 µl of the appropriate buffer. Spins are performed at 500*g* (1,000*g* after fixation) for 4 min at 4 °C or RT, depending on the step. Following spins, samples can be decanted by pipetting of the residual liquid or carefully flicking the plate.

When deciding between the tube or plate versions of the assay, multiple factors must be considered. We have observed that cell loss may be greater, and more variable, when samples are processed in a plate as compared with tubes. Therefore, for precious samples, working with tubes may be preferable. There may also be sample transfer between adjacent wells; therefore, separation of samples on a plate is important to limit background. We have also observed that autofluorescent/nonspecific background in mRNA channels may be greater in plates as compared with tubes, which can negatively affect the signal/noise ratio. The major advantages of the plate-based assay are operator ease of use and by extension an increase in the maximum number of samples that can be processed per day. The protocol is substantially shortened by the flicking of plates to wash, rather than aspiration of individual tubes. Given the potential advantages and disadvantages, we therefore strongly recommend that investigators compare the tube and plate protocols in parallel, in their laboratories and for their specific purposes, to determine the version best suited to their studies.

Poisson law. Thus, any other assay aiming at detection of very rare events, such as the QVOA, has similar requirements for high starting numbers of cells.

Where cell numbers are not limiting, we recommend that each user determine the number of events that must be analyzed on the basis of the expected frequency of their population of interest and taking into account Poisson distribution, as well as the expected losses indicated above.

The probe sets indicated here against HIV *Gag* and *Pol* ('Reagents') and used by our group[15] were designed against the Clade B isolate JR-CSF. Each probe set contains 20 individual probes, for a total of 40 when the probe sets against HIV *Gag* and *Pol* are combined; these recognize regions along the whole length of the target mRNA. This provides redundancy and tolerance for sequence variation, as not all probes need to bind to generate a signal. However, the more probes that bind, the brighter the signal (higher mean fluorescence intensity (MFI)). Therefore, when adapting the assay to detect alternative, shorter or more variable mRNAs, the number of probes may have a substantial impact on the sensitivity of the assay. In our North American cohorts, where the majority of individuals are infected with Clade B isolates, the redundancy in the $HIV^{RNA/Gag}$ assay has been sufficient to account for inter-donor variability. However, for studies on samples from outside of North America and Europe, we would recommend designing a probe set against the consensus sequence for the circulating clade.

As discussed previously, the $HIV^{RNA/Gag}$ assay narrows the gap between the maximal and minimal estimates of the reservoir size inferred by alternative methods. However, some caveats remain. As mentioned, the QVOA is limited to detection of latently infected cells that reactivate the virus upon a single round of stimulation, and therefore may underestimate the size of the latent reservoir[20]. As a similar stimulation technique is applied in the $HIV^{RNA/Gag}$ assay, the same applies here. Furthermore, it should be noted that the detection of a provirus by the $HIV^{RNA/Gag}$ assay does not guarantee that this virus is replication competent. Detection is dependent on the production of Gag protein and *GagPol* mRNA, defining a 'translation-competent reservoir'; however, a provirus with a deletion outside of *GagPol* would be detected with this assay but could be unable to initiate a productive infection. This translation-competent reservoir is likely to contain a lower proportion of defective proviruses (and thus a higher frequency of replication-competent proviruses) than alternative PCR-based measurements such as integrated HIV DNA and TILDA. However, it probably still represents an overestimate of the true replication-competent reservoir size.

Applications of the protocol

The version of the $HIV^{RNA/Gag}$ assay described[15] could be applied to questions involving the HIV replication cycle, restriction factor, viral pathogenesis or effectiveness of intervention/cure therapies. Regarding the HIV cure/latency field, the detection of the translation-competent viral reservoir has substantial implications for (i) quantification of latent reservoir size; (ii) the efficacy assessment of cure strategies that rely on a reduction in the size of the latent reservoir, rather than complete eradication of latent proviruses; (iii) phenotyping of the viral reservoir; and (iv) the definition of HIV-infected CD4 cells as expressing HIV proteins, thus having the potential of being efficiently recognized by the adaptive immune system.

For the $HIV^{RNA/Gag}$ assay described here, we chose to use probes against both HIV *Gag* and *Pol* for the following reasons: (i) these regions have been shown to be relatively well conserved between clinical isolates; (ii) the length of these mRNAs allows for a relatively high number of mRNA-specific probes (40 total), which increases the redundancy in the system for intersubject sequence variability; and (iii) using a high number of probes amplifies the potential low copy number of HIV mRNAs per cell and increases the signal-to-noise ratio, thus increasing the detection limit in terms of RNA copy number. However, a key advantage of the $HIV^{RNA/Gag}$ technique is its versatility: it can easily be adapted to detect other HIV genes and proteins, including multiplexing different genes; flow panels can be adapted to quantify vast numbers of surface and intracellular markers—albeit with careful optimization; and—importantly—easy

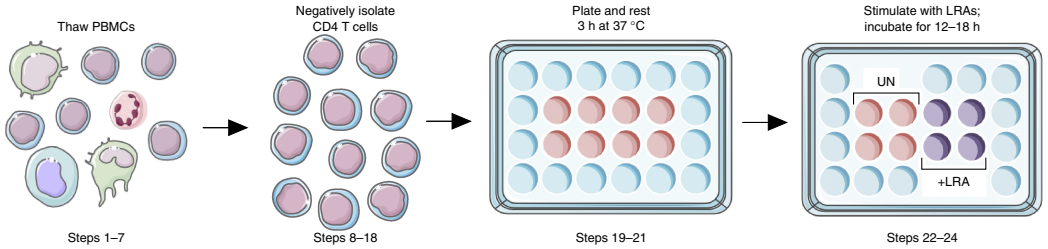

Figure 2 | Part I of the protocol. Schematic of CD4 T-cell isolation and stimulation. PBMCs are thawed and CD4 T cells are negatively isolated by magnetic isolation. Cells are counted, resuspended in RPMI + 10% (vol/vol) FBS + 50 U/ml penicillin–streptomycin (R10) with the antiretrovirals T20 and AZT, plated onto 24-well plates and rested for 3 h at 37 °C. LRAs are added to appropriate wells, with some wells left unstimulated (UN) as negative controls, and cells are incubated for a further 12–18 h at 37 °C.

translation to other tissues/cell types (e.g., lymphoid tissues) and/or other species/viruses (e.g., SIV detection in rhesus macaques). This type of mRNA Flow-FISH assay can also be used to detect cytokines[24], host factors and/or other pathogen-related RNAs. Last, the assay could be transferred to alternative cell types; the protocol here focuses on the CD4 T-cell reservoir. However, cells of the myeloid lineage (including macrophages) have been proposed as important cellular reservoirs[25] and these subsets could in principle be investigated by the same technique, provided that the user undertakes careful validation of the protocol. Therefore, it represents a powerful tool that can be applied to address a broad range of experimental questions, both within the HIV field and in immunological studies in general.

The version of the HIV$^{RNA/Gag}$ assay described here focuses on the use of a commercially available RNA Flow-FISH assay (Human PrimeFlow, Affymetrix/eBioscience; see 'Reagents') to detect HIV reservoirs *ex vivo*. However, alternative Flow-FISH techniques have previously been used to identify HIV-infected alveolar macrophages[26], study HIV-infected cell lines[27,28] and detect HIV reservoirs in primary samples[29]. These methods use single-mRNA staining only and thus have limited specificity and accuracy. Therefore, the lessons learned from the development of this assay could easily be translated to an alternative product or an in-house system.

Biohazardous materials

Samples from human peripheral blood represent a Class 2 material; therefore, appropriate precautions should be taken according to institutional and governmental guidelines when handling these materials. HIV-1 is a Class 2 human pathogen, so samples from HIV-1-infected individuals should be handled in at least a Biosafety Level (BSL)-2 facility. In the culture conditions used for the standard experiment, a spreading infection is restricted by the presence of anti-retrovirals. However, we use BSL-3 guidelines when working with such samples. Appropriate personal protective equipment, including double gloves and eye protection are worn at all times. All solid waste is inactivated by autoclave incineration; all liquid waste is inactivated with Virkon or similar and autoclaved.

Experimental design

The protocol to detect HIV viral-translation-competent reservoirs can be broken down into two major parts. Sample preparation, Part I, is highly adaptable and can be extensively modified according to the experimental question. Part II comprises the specific steps of the HIV$^{RNA/Gag}$ assay; Part IIA describes protein antigen detection and Part IIB describes gene-specific mRNA detection. Although the core steps in Part II are constant, the assay can be adapted for detection of different protein antigens or mRNAs.

The procedure described here is for the identification of latent translation-competent reservoirs from HIV-infected, ART-treated individuals. In the example described in the PROCEDURE and associated tables, there are a total of 12 samples: samples from three different donors (one HIV-uninfected, two HIV-infected), each of which is tested after stimulation with an LRA at two different doses or after no stimulation, plus three control tubes in which *in vitro*-infected CD4 T cells may be used. As controls, we recommend the following: control A, an HIV-Gag protein fluorescent-minus-one (FMO); control B, an mRNA negative control using an irrelevant or scrambled mRNA probe; and control C, a positive-control mRNA. Controls A and B can be used to confirm the gating strategy defined using the HIV-uninfected biological control; control C is useful to determine whether the assay worked, in the absence of *GagPol* mRNA staining.

This protocol uses a 1.5-ml-tube-based version of the assay. The assay can also be performed in a 96-well-plate format; however, our group has not validated this version of the assay to the same extent as the tube-based protocol. We therefore recommend using the 1.5-ml-tube version for initial implementation and careful side-by-side comparison before the investigator considers switching to a 96-well-plate-based assay. See **Box 1** for further discussion on the adaptation of the protocol to 96-well format.

Part I (4–6 h plus overnight incubation, fora standard experiment); sample preparation (Steps 1–24). Sample preparation is dependent on the experimental question to be addressed; however, in all cases the cells of interest must be in suspension to move into Part II (see **Fig. 2** for example experiment setup). It is important to ensure that the cell preparation is of good quality, with high viability, if possible, to ensure reasonable cell recovery throughout the protocol. For detection of translation-competent reservoirs in HIV-infected individuals *ex vivo*, or following reactivation, we isolate CD4 T cells from freeze-thawed PBMC samples isolated previously. CD4 T cells are either rested or stimulated overnight with an LRA of interest. Samples from uninfected donors, treated in parallel, are used as biological controls and to determine the flow cytometry gating strategy. For identification of the translation-competent latent reservoir following treatment with LRAs *in vitro*, it is important to include a donor-matched, untreated

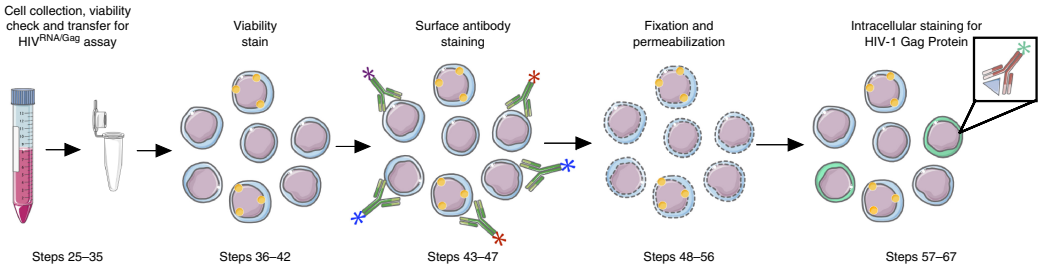

Figure 3 | Part IIA of the protocol. CD4 T cells are collected and washed, the viability is checked and they are resuspended for the $HIV^{RNA/Gag}$ assay. Cells are stained with a viability stain and surface antibody stain, and then fixed and permeabilized. CD4 T cells are then stained intracellularly for HIV Gag and fixed a final time.

condition. Additional relevant biological controls may be required depending on the experimental setup. See **Box 2** for an *ex vivo* autologous infection protocol that can be used to prepare HIV-positive-control samples.

Part IIA (0.5 d); protein antigen detection (Steps 25–67). Following stimulation/reactivation, CD4 T cells are collected, washed and divided into aliquots for staining (see **Fig. 3**). Samples are stained according to the experimental question with a mixture of surface antibody markers. As a minimum for primary cells, we recommend the inclusion of antibodies against basic phenotypic markers (CD3 and CD4) and an exclusion 'dump' channel (CD8, CD14, and CD19), as well as the addition of a viability dye to exclude dead cells and decrease background (see **Table 1** for reagent setup for this panel and **Table 2** for alternative panel options). Following fixation and permeabilization, samples are stained intracellularly for HIV-1 Gag protein as a minimum, but may also be stained for additional intracellular antigens concurrently. When staining for multiple markers, it is appropriate to include the same controls as for any multiparametric flow cytometry analysis, such as FMO controls. In FMO controls, the sample is stained for all markers (both mRNA and protein) except one and this is repeated for all markers. These controls can then be used to define the threshold of positivity when designing a gating strategy. Of note, for *GagPol* mRNA and Gag protein only, we recommend that gates be drawn using a biological control (e.g., an uninfected donor treated identically to the HIV-infected donors of interest) rather than FMOs. Following a second fixation, the protocol may be paused overnight. However, in general, for operator ease, we proceed to Part IIB and pause there at the second pause point.

Part IIB (1.5 d); mRNA detection, signal amplification, sample acquisition and analysis (Steps 68–109). Samples are labeled for

Box 2 | *Ex vivo* viral propagation for positive-control CD4 T cells ● TIMING 8.5 d

CD4 T cells infected with a lab-adapted virus (including vesicular stomatitis virus G glycoprotein (VSVG) pseudotyped viruses) using standard methods—e.g., Magnetofection[32]—can be used as a positive control for $HIV^{mRNA/Protein}$ assay. Alternatively, CD4 T cells infected with autologous virus following an *ex vivo* expansion, as described below, can be used.

Additional reagents

PHA-L (Sigma-Aldrich, cat. no. L4144)
IL-2 (NIH AIDS Reagent Program, cat. no. 136)

Procedure

1. Isolate CD4 T cells by negative selection as described in Steps 8–19 of the main PROTOCOL and resuspend at 2 × 10^6 per ml in R20 (RPMI 1640 with 20% (vol/vol) FBS).
2. Plate CD4 T cells into 24-well plates at a volume of 1 ml per well. Use only central wells; fill the wells at the edges with 1 ml of RT PBS.
3. Allow the cells to rest for 2 h at 37 °C.
4. Stimulate the CD4 T cells with PHA-L (10 µg/ml) and IL-2 (100 U/ml) for 36–40 h.
5. Collect activated CD4 T cells by gently pipetting the 1-ml volume up and down in the well to break up activation clumps. Transfer the 1 ml to a 15-ml conical tube. Repeat for all replicate wells. Wash out each well with 1 ml of warm R10 and combine with the CD4 T-cell suspension. Spin down the suspension (540*g*, 5 min, RT).
6. Wash the CD4 T cells twice in warm R10 to remove PHA.
7. Count cells using the method described in Step 6 of the main PROTOCOL.
8. Replate at 2 × 10^6 per ml in R20.
   ▲ **CRITICAL STEP** As cell clumping due to activation may limit counting accuracy, we assume no cell loss over the incubation in step 4 and replate CD4 T cells in the starting volume from step 1.
9. Maintain cells for 6–7 d at ~2 × 10^6 per ml, by splitting 1:2 as required (with a maximum of every other day). Maintain IL-2 at 100 U/ml throughout the culture.

TABLE 1 | Example reagent preparation.

Reagent	Preparation	For 1 tube	For 12 tubes[a]
Viability stain	1:500 in cold PBS (2× stock)	100 µl (99.8 µl of PBS + 0.2 µl of Viability Stain)	1,300 µl (1297.4 µl of PBS + 2.6 µl of Viability Stain)
Surface stain (use immediately)	Anti-CD3 BV605, anti-CD4 PE-Cy7, anti-CD8, CD14 and CD19 BV510	19 µl (anti-CD3 BV605 (5 µl), anti-CD4 PE-Cy7 (5 µl) anti-CD8, anti-CD14 and anti-CD19 BV510 (all 3 µl)	247 µl (anti-CD3 BV605 (65 µl), anti-CD4 PE-Cy7 (65 µl) anti-CD8, anti-CD14 and anti-CD19 BV510 (all 39 µl)
Fixation I (use immediately)	1 part Fixation Buffer 1A for 1 part Fixation Buffer 1B	1 ml (500 µl of Fixation Buffer 1A + 500 µl of 1B)	13 ml (6.5 ml of Fixation Buffer 1A + 6.5 ml of Fixation Buffer 1B)
Permeabilization Buffer (use immediately)	1:10 Permeabilization Buffer, 1:1,000 RNAsin I, 1:100 RNAsin II in H_2O	3 ml (300 µl of Permeabilization Buffer, 3 µl of RNAsin I, 30 µl of RNAsin II + 2.67 ml of H_2O)	39 ml (3.9 ml of Permeabilization Buffer, 39 µl of RNAsin I, 390 µl of RNAsin II + 34.71 of ml H_2O)
Fixation II (use immediately)	1:8 Fixation Buffer 2 in Wash Buffer	1 ml (125 µl of Fixation Buffer 2 + 875 µl of Wash Buffer)	13 ml (1.625 ml of Fixation Buffer 2 + 11.375 ml of Wash Buffer)
GagPol probes (warm to 40 °C)	1:20 Target mRNA probes in Target Probe Diluent	100 µl (5 µl of *Gag* probe + 5 µl of *Pol* probe + 90 µl of Target Probe Diluent)	1.3 ml (65 µl of *Gag* probe + 65 µl of *Pol* probe + 1.170 ml of Target Probe Diluent
Overnight storage buffer	1:1,000 RNAsin I in Wash Buffer	1 ml (1 µl of RNAsin I + 999 µl of wash buffer)	13 ml (13 µl of RNAsin I + 12.987 ml of Wash Buffer)
Label Probes (warm to 40 °C)	1:100 Label Probes in Label Probe Diluent	100 µl (1 µl + 99 µl)	1.3 ml (13 µl + 1.287 ml)

[a]Sufficient reagent for one spare test is prepared to take into account pipetting errors.

gene-specific mRNAs of interest, and then stored overnight; this is the second pause point (**Fig. 4**). The following day, the signal is amplified using a branched dsDNA system and the amplified signal is labeled with a fluorescent dye. For detection of translation-competent reservoirs, we use probes designed against the *GagPol* region of the HIV-1 strain JR-CSF. Additional controls that may be included

TABLE 2 | Panel options for 1-, 3/4-, or 5-laser flow cytometers.

Fluorochrome	Panel A (1 laser)	Panel B (3/4 lasers)	Panel C (5 lasers)
	Basic detection of HIV mRNA and protein—recommended for cell lines.	**Minimum panel for CD4 T-cell HIV translation-competent reservoir detection**	**Identification of memory phenotype of $HIV^{RNA+/Gag+}$ CD4**
BUV395			CD3
BUV496			CD4
AF488	*GagPol* mRNA (Type 4)		CXCR5[a]
PE	Gag protein	Gag protein	Gag protein
PE-Cy7		CD4	ICOS
BV421			PD-1
BV510/eF506		Exclusion	Exclusion + Viability Stain
BV605		CD3	CD27
BV711			CD45RA
AF647		*GagPol* mRNA (Type 1)	*GagPol* mRNA (Type 1)
eF780		Viability Stain	

See Reagents section for recommended clone and purchasing information.
[a]Stained during stimulation.

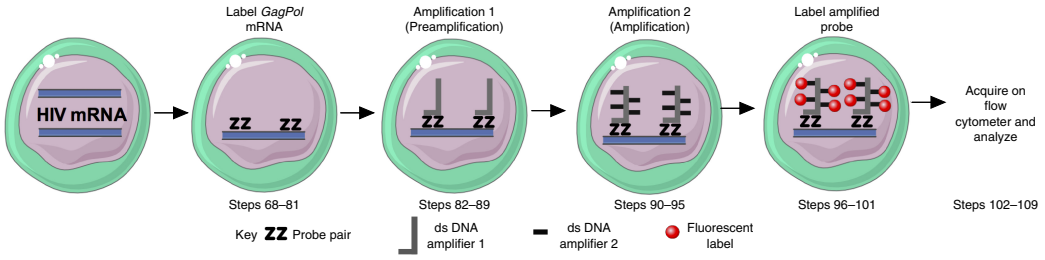

Figure 4 | Part IIB of the protocol. *GagPol* mRNA is labeled and amplified using a two-step dsDNA amplification system, and the amplified probe is labeled with a fluorescent marker. Samples can be stored short-term, or acquired by flow cytometry immediately, and then analyzed.

to monitor mRNA staining include a probe against a housekeeping gene (*RPL13A* is recommended). Negative-control probes (either scrambled or against an irrelevant mRNA such as bacterial *DapB*; see 'Reagents') can be used; however, we have found that for the HIV$^{RNA/Gag}$ assay HIV-uninfected samples treated identically to HIV-positive samples enable the most accurate gating. Samples are acquired on a flow cytometer according to standard operating procedures[30,31]. Correct compensation controls are essential and are discussed in **Box 3**. A 1-laser machine can be used to detect the HIV-1 Gag protein and *GagPol* mRNA without additional antibody stains (see **Table 2** for suggested panels/fluorochrome combinations), but this is not recommended for primary cells.

Box 3 | Effective compensation

As with general flow cytometry experiments, the correct compensation is key to accurate interpretation of the results. For surface and intracellular antibodies, we recommend the use of eBioscience OneComp Beads. All beads are stained at the same time as the intracellular antibody stain to mimic as closely as possible any change in fluorochrome signal or stability over time. As fixation is known to alter fluorochromes, the antibody-stained beads are fixed for 1 h at RT with a solution of 2% paraformaldehyde, washed with 2% (vol/vol) FBS/PBS and then stored at 4 °C until use. There are two options for the compensation of the mRNA stain. The first is to use cells from the experiment stained only with a positive-control mRNA that is highly expressed by the cells of interest, such as *RPL13A*. This has the advantage that the autofluorescence and background is most similar to those of the cells of interest. However, we have found that the signal from the *GagPol* mRNA probe set is consistently brighter than that of the positive control, leading to compensation issues. Therefore, we stain BD CompBeads Plus with an isotype control antibody conjugated to the same fluorochrome as the mRNA (AF647 for Type 1, AF488 for Type 4 and AF750 for Type 6). It is key that the same fluorochrome is used for compensation as is used for the mRNA probe type—i.e., APC is not an appropriate substitute for AF647. These beads have a larger size than eBioscience OneComp beads and we have found that this provides more accurate compensation.

MATERIALS

REAGENTS

- Peripheral CD4 T cells isolated from HIV-infected and uninfected donors
  ! CAUTION Any study protocols involving human subjects must conform to institutional and governmental ethical guidelines. **! CAUTION** HIV-1 is a Class 2 human pathogen and HIV-infected samples should be handled in a BSL-2 facility, in accordance with safe working practices. Gloves and protective eyewear should be worn.
- Human PrimeFlow 3-plex kit (Affymetrix eBioscience, cat. no. 88-18009, 40 or 100 tests). This kit includes the following: Fixation Buffers 1A + B, 10× Permeabilization Buffer, RNAsin I, RNAsin II, Fixation Buffer II, Wash Buffer, Target Probe Diluent, Preamplification and Amplification buffers, Label Probe Diluent, Label Probe Mix, and positive-control (*RPL13A*) mRNA probes **! CAUTION** Fixation buffers contain paraformaldehyde (PFA). PFA is an irritant; avoid exposure to skin or eyes.
- RPMI 1640 medium (500 ml; Gibco by Life Technologies, cat. no. 11875-093)
- HEPES (100 ml, 1 M; Life Technologies, cat. no. 15630-080)
- Penicillin–streptomycin (10,000 U/ml, 100 ml; Gibco by Life Technologies, cat. no. 15140-122)
- PBS, pH 7.4, no Ca^{2+}/Mg^{2+} (1×, 500 ml; Gibco by Life Technologies, cat. no. 14190-144)
- FBS (500 ml; Seradigm by VWR, cat. no. 1500-500)
- DMSO (Sigma-Aldrich, cat. no. D5879)
- Paraformaldehyde (Sigma-Aldrich, cat. no. P6148)
- EasySep Human CD4+ T-cell isolation kit (StemCell, cat. no. 19052, for 1×10^9 cells)
- The 'Big Easy' EasySep Magnet (StemCell, cat. no. 18001, for isolating 4×10^8 cells)
- EDTA, ultrapure (0.5 M, 100 ml; Invitrogen, cat. no. 15575-038)
- Trypan blue (0.4%, 100 ml; Gibco by Life Technologies, cat. no. 15250-061)
- S7 nuclease (15,000 U; Roche/Sigma-Aldrich, cat. no. 10107921001)
- Sterile RNase-free H_2O (500 ml; Wisent Bioproducts, cat. no. 809-115-CL)
- Zidovudine (AZT, 20 mg; NIH AIDS Reagent Program, cat. no. 8435)
- T20 (5 mg; Trimeris/Roche via NIH AIDS Reagent Program, cat. no. 9845)
- PMA (use at 50 ng/ml; Sigma-Aldrich, cat. no. P1585)
- Ionomycin (use at 0.5 µg/ml; Sigma-Aldrich, cat. no. I9657)
- Bryostatin 1 (10 µg; use at 10 nM; Enzo, cat. no. BML-ST103-0010)
- FcR block (2 ml; Miltenyi Biotec, cat. no. 130-059-901)
- BD CompBeads Plus (6 ml; BD Biosciences, cat. no. 560497)

• OneComp eBeads (eBioscience, cat. no. 01-1111-42)

Suggested antibodies, dyes and probes (see Table 2 for suggested panel information) for all panels

• Anti-HIV-1 Gag p24 (Beckman Coulter, clone KC57/FH190-1-1, RD-1 (PE), cat. no. 6604665)
• IgG Isotype control (BioLegend, clone MOPC-21; for Type 1 control, use AF467, cat. no. 400130, and for Type 4 control use AF488, cat. no. 400129)
• HIV-1 *Gag* mRNA probe set (Affymetrix eBioscience, JR-CSF target sequence, Type 1, cat. no. VF1-13962; Type 4 cat. no.VF4-18312, 20 pairs of branched DNA probes, probe length median[range] = 23[17–30] nt)
• HIV-1 *Pol* mRNA probe set (Affymetrix eBioscience, JR-CSF target sequence, Type 1, cat. no. VF1-13961; Type 4 cat. no. VF4-18314, 20 pairs of branched DNA probes, probe length median[range] = 25[18–30] nt)
• *RPL13A* positive-control mRNA probe set (provided with 3-plex version of Human PrimeFlow kit; can also be purchased from Affymetrix eBioscience as Type 1, cat. no. VA1-13100; Type 4, cat. no. VA4-13187)
• Scrambled negative-control mRNA (Affymetrix eBioscience, Type 1, cat. no. VF1-16506; Type 4, cat. no. VF4-19835)

Suggested antibodies, dyes and probes (see Table 2 for suggested panel information) for panel B

• Anti-CD3 (BioLegend, Clone OKT3, BV605, cat. no. 317322)
• Anti-CD4 (BD Biosciences, Clone RPA-T4, Pe-Cy7, cat. no. 560649)
• Anti-CD8 (BioLegend, Clone SK1, BV510, cat. no. 344732)
• Anti-CD14 (BioLegend, Clone M5E2, BV510, cat. no. 301842)
• Anti-CD19 (BioLegend, Clone H1B19, BV510, cat. no. 302242)
• Fixable Viability Dye (eBioscience, eFluor780, cat. no. 65-0865)

Suggested antibodies, dyes and probes (see Table 2 for suggested panel information) for panel C

• Anti-CD3 (BD Biosciences, Clone UCHT1, BUV395, cat. no. 563548)
• Anti-CD4 (BD Biosciences, Clone SK3, BUV496, cat. no. 564651)
• Anti-CD8 (BioLegend, Clone SK1, BV510, cat. no. 344732)
• Anti-CD14 (BioLegend, Clone M5E2, BV510, cat. no. 301842)
• Anti-CD19 (BioLegend, Clone H1B19, BV510, cat. no. 302242)
• Anti-CD27 (BD Biosciences, Clone L128, BV605, cat. no. 562655)
• Anti-CD45RA (BioLegend, Clone HI100, BV711, cat. no. 304138)
• Anti-CD278 (ICOS) (eBioscience, Clone ISA-3, PE-Cy7, cat. no. 25-9948)
• Anti-CD279 (PD-1) (BioLegend, Clone EH12.2H7, BV421, cat. no. 329920)
• Anti-CXCR5 (BD Biosciences, Clone RF8B2, BB515, cat. no. 564624, stain during culture)
• Fixable Viability Dye (eBioscience, eFluor506, cat. no. 65-0866)

EQUIPMENT

• Tissue culture facility (at least a BSL-2 facility is required)
• Centrifuge equipped with swinging-bucket rotor, able to cool to 4 °C (e.g., VWR Thermo Heraeus Multifuge Benchtop Centrifuge 1XR, cat. no. 97039-270) ▲ **CRITICAL** The use of a swinging-bucket centrifuge is key. Use of a fixed-angle rotor will result in poor cell recovery.
• Centrifuge adaptors for 15-ml Falcon tubes and 1.5-ml Eppendorf tubes
• Tissue culture incubator (37 °C, 5% CO_2; e.g., Sanyo Professional CO_2 incubator, model no. MCO19AICUVH)
• Aspirator (recommended: Mandel Vacusafe Comfort with Vacuboy, cat. no. TM-158310.
• Benchtop PCR hood (recommended: AirClean Systems PCR/RNA Workstation, model no. AC648DBC)
• Light microscope (suitable for cell counting and assessment of cell viability/activation; e.g., Fisher Scientific, model no. Wilovert 30)
• Hybridization oven, able to maintain 40 °C (e.g., Shel Lab Forced Air Oven, model no. 1330FM) ▲ **CRITICAL** Temperature stability is important. The oven used must be able to maintain a stable temperature with limited fluctuations.
• Flow cytometer with the capacity to detect at least two colors; see **Table 2** for example panels for setup of different laser numbers (e.g., BD Biosciences, model no. LSR II)
• Flow cytometry analysis software (e.g., Tree Star FlowJo, https://www.flowjo.com/solutions/flowjo/downloads)

Plasticware

• 15-ml Falcon tubes, sterile (Corning Falcon, cat. no. 353096)
• Plate, 24-well, sterile, tissue culture treated (Corning Falcon, cat. no. 353047)
• 14-ml FACS tubes, sterile (Corning Falcon, cat. no. 352057)
• Sterile, RNase-free, low-binding tips: p1000, p200, p20 (Ranin, cat. nos. 17007954, 17007961, 17007957)
• Sterile serological pipettes: 5 ml, 10 ml, 25 ml (Sarstedt, cat. nos. 86.1253.001, 86.1254.001, 86.1685.001)
• Kova Glastic SL 10W GRID (counting chambers; VWR, cat. no. CA36200-020)
• RNase-free, low-binding 1.5-ml tubes (provided with Human PrimeFlow Kit above) ▲ **CRITICAL** Low-binding RNase-free tubes greatly increase cell recovery and should be used throughout the protocol.
• 0.5-ml Tubes, sterile (Sarstedt, cat. no. 72.730.005)
• 1.5-ml Tubes, RNase-free, sterile (for reagent preparation; Sarstedt, cat. no. 72.692.405)

REAGENT SETUP

2% (wt/vol) PFA Add 4 g of PFA powder to 100 ml of PBS, then heat and stir until dissolved. Adjust the pH to 7.4. Prepare aliquots and store them at −20 °C. Dilute a thawed aliquot to a 2% (wt/vol) stock before use. The 2% (wt/vol) PFA stock is stable at 4 °C for 2 weeks.

Heat-inactivated FBS Complement-inactivate FBS by heating to 56 °C for 30 min in a water bath. Divide FBS into single-use aliquots and store them at −20 °C for up to 1 year.

Complete culture medium (R10) Prepare R10 by making up a solution of 10% (vol/vol) heat-inactivated FBS, 50 U/ml penicillin–streptomycin and 10 mM HEPES in RPMI 1640 medium with phenol red. Prepare the medium in advance and store it at 4 °C for up to 2 weeks.

R10 + antiretrovirals Prepare R10 as above. Add zidovudine (AZT) to a final concentration of 5 µM and T20 at a final concentration of 7.5 µg/ml. Freshly prepare this solution before use.

EasySep CD4 isolation buffer Prepare this buffer by combining 2% (vol/vol) heat-inactivated FBS and 1 mM EDTA in sterile PBS, pH 7.4. Prepare the buffer in advance and store it at 4 °C for up to 2 weeks.

S7 nuclease Add 3 ml of sterile PBS, pH 7.4, to a dried pellet of S7 nuclease. Store the solution at 4 °C for up to 1 month.

2% (vol/vol) FBS/PBS Prepare the solution by diluting heat-inactivated FBS to 2% (vol/vol) in PBS. Prepare in advance and store the solution at 4 °C for up to 2 weeks.

Zidovudine Reconstitute with DMSO to obtain a concentration of 50 mM. Prepare aliquots and store them at −20 °C for up to 1 year.

T20 Reconstitute with sterile PBS, pH 7.4, to obtain a concentration of 2 mg/ml. Prepare aliquots and store them at −20 °C for 1 year.

PMA Reconstitute with DMSO to obtain a concentration of 1 mg/ml. Prepare aliquots and store them at −80 °C for 1 year.

Ionomycin Reconstitute with DMSO to obtain a concentration of 0.5 mg/ml. Prepare aliquots and store them at −80 °C for 1 year.

Bryostatin 1 Reconstitute with DMSO to obtain a concentration of 25 µM. Prepare aliquots and store them at −80 °C for 1 year.

EQUIPMENT SETUP

Hybridization oven The hybridization oven should be calibrated to maintain a stable temperature of 40 °C. We recommend that the oven be turned on at least 24 h before use.

Flow cytometer The flow cytometer used should be routinely calibrated and cleaned. The 'CS&T' function should be run frequently. Quality assurance for multicolor flow cytometry is discussed elsewhere[30,31].

PROCEDURE

Part I: cell thawing, negative CD4 T-cell isolation and stimulation ● TIMING 4–6 h + overnight incubation

1| *Cell thawing*. Prepare cold, labeled, 15-ml conical tubes and precool the centrifuge to 4 °C. At least 1 conical tube is required for each donor sample to be thawed, with a maximum of 200 × 10^6 PBMCs per tube to avoid cell clumping. Work with a maximum of two donors at any time. Multiple cryovials of frozen PBMCs from one donor may be needed to meet cell number requirements (i.e., to start with 100 × 10^6 PBMCs, thaw two cryovials containing 50 × 10^6 PBMCs each). Work with a maximum of four cryovials at any point.

2| Thaw required donor sample cryovials by warming them in a 37 °C water bath, until floating ice is visible. Transfer the contents of each vial to a cold 15-ml conical tube prepared in Step 1. Wash the cryovial with 1 ml of cold FBS and add the contents to the 15-ml conical tube. Add Nuclease S7 to each conical tube (20 µl per ml of PBMC suspension; minimum 40 µl), mix by tapping the tube and incubate for 20 s. Add cold FBS to a final volume of 10 ml.

3| Centrifuge the conical tube at 420*g* for 10 min at 4 °C.

4| Discard the supernatant and gently resuspend the pellet in 1 ml of cold R10 and top up to 10 ml with R10. If there are multiple conical tubes for a single donor, resuspend each of the pellets in 1 ml of cold R10 and combine in a single conical tube. Top this tube up to 10 ml with R10, and then split the sample back out into the starting number of conical tubes. Top all conical tubes up to 10 ml with R10. This will ensure that the PBMCs are split evenly across all conical tubes, and thus only one conical tube will need to be counted per donor, while keeping the number of cells per conical tube under 200 × 10^6. Centrifuge the conical tubes at 420*g* for 10 min at 4 °C.

5| Discard the supernatant and gently resuspend the pellet in 1 ml of cold EasySep CD4 isolation buffer and top up to 10 ml with EasySep CD4 isolation buffer.

▲ **CRITICAL STEP** If you do not wish to isolate CD4 T cells—for example, for detection of HIV reservoirs in total PBMCs—perform Step 5 in cold R10, count cells as in Steps 6 and 7, and then proceed to Step 19. The presence of CD8 T cells in a reactivated culture may have an adverse effect on the detection of the reactivated latent viral reservoirs; therefore, we recommend performing a CD8 depletion (for example, using Dynabeads CD8 Positive Isolation Kit; Thermo Fisher Scientific, cat. no. 11333D) as a minimum.

6| *Cell counting*. Prepare a 0.5-ml tube with 90 µl of Trypan blue. Remove a 10-µl aliquot of cell suspension and add to the 0.5-ml tube containing Trypan blue. Mix by vortexing and transfer 10 µl to a Kova Glastic counting chamber. Count both the live cells (Trypan blue-negative) and any dead cells (Trypan blue-positive). Calculate total cell number and record the viability (given as %live cells) using the formula

$$100 - \left(\frac{\text{dead cells}}{\text{live cells} + \text{dead cells}} \times 100 \right)$$

? TROUBLESHOOTING

7| Centrifuge the conical tube at 420*g* for 10 min at 4 °C.

8| *CD4 T-cell isolation*. Discard the supernatant and gently resuspend the pellet in EasySep CD4 isolation buffer at a volume of 20 µl per 10^6 cells (i.e., at 50 × 10^6 per ml). Remove any clumps of dead cells with a pipette.

9| Transfer the cell suspension to a 14-ml FACS tube. PBMCs from multiple conical tubes from the same donor can be recombined into one 14-ml FACS tube. If total PBMC number is >400 × 10^6, prepare aliquots in multiple tubes.

10| Add 1 µl per 10^6 PBMCs of StemCell Biotinylated Antibody Cocktail from the EasySep CD4+ isolation kit. Mix well by pipetting. Incubate for 10 min at room temperature (RT; 20 °C).

11| Add 2 µl per 10^6 PBMCs of StemCell Bead Cocktail. Mix well by pipetting. Incubate for 5 min at RT.

12| Add EasySep CD4 isolation buffer to a final volume of 10 ml per 14-ml FACS tube.

13| Transfer the 14-ml FACS tube to a 'Big Easy' StemCell isolation magnet. Remove the cap. Incubate for 5 min at RT.

14| Prepare a fresh 15-ml conical tube with 2.5 ml of R10. Carefully pick up the magnet with the 14-ml FACS tube in place and slowly pour the unbound cell fraction into the fresh 15-ml conical tube containing R10.

© 2017 Macmillan Publishers Limited, part of Springer Nature. All rights reserved.

15| Centrifuge the conical tube at 540*g* for 5 min at 4 °C.

16| Discard the supernatant and gently resuspend the pellet in 1 ml of cold R10 and top up to 10 ml with R10.

17| Count the isolated CD4 T cells as in Step 6.
? TROUBLESHOOTING

18| Centrifuge the conical tube at 540*g* for 5 min at 4 °C.

19| *CD4 T-cell stimulation/reactivation of latent reservoirs.* Discard the supernatant and gently resuspend the pellet at 2 × 10^6 CD4 T cells/ml in R10 + antiretrovirals (Reagent Setup).

20| Plate onto a sterile, 24-well, tissue-culture-treated plate at a volume of 1 ml per well.
▲ **CRITICAL STEP** Use only the middle 8 wells and fill the outer wells with 1 ml of sterile PBS at RT to limit loss by evaporation
▲ **CRITICAL STEP** The number of CD4 T cells per donor per condition is critical to the accurate detection of latent translation-competent reservoirs. For detection of very rare events (~1 per 10^6), we recommend starting with at least 16 × 10^6 cells—i.e., 8 wells at 2 × 10^6 per ml.

21| Rest the cells at 37 °C with 5% CO_2 in a tissue culture incubator for 3 h.

22| Prepare the LRAs as desired. For example, for PMA/ionomycin stimulation, use concentrations of 50 ng/ml and 0.5 µg/ml, respectively. For Bryostatin-1 use a concentration of 10 nM.
▲ **CRITICAL STEP** We recommend titrating these reagents to maximize cell activation and minimize toxicity in the time frame studied.

23| Add LRAs to each well for the appropriate final concentration. Mix by pipetting gently, or swirling the plate.

24| Stimulate the cells overnight for 12–18 h at 37 °C with 5% CO_2.
▲ **CRITICAL STEP** The optimal length of incubation is dependent on the LRA used and should be determined by the user.

Part IIA: cell collection and preparation, viability staining, surface antibody staining and intracellular staining ● TIMING 4–11 h
25| *Cell collection and preparation*. As soon as incubation time ends, place all plates at 4 °C. Cool the centrifuge to 4 °C. Prepare cold 15-ml conical tubes for each donor/condition. We recommend checking the cultures under a microscope and taking note of any loss in viability and activation induced by any stimuli added.

26| Collect the cells by pipetting gently up and down to mix with a 1-ml pipette. Transfer the cells to a 15-ml conical tube. Identical wells can be combined.

27| Wash wells with cold R10. Add 1 ml to a well, pipette gently on the base of the well to lift any remaining cells and combine into 15-ml conical tubes. Repeat for all donors and conditions.
▲ **CRITICAL STEP** As soon as one 15-ml conical tube is full, place it at 4 °C to limit RNA degradation.

28| Centrifuge the conical tubes at 540*g* for 5 min at 4 °C.

29| Discard the supernatant and gently resuspend the pellet in 1 ml of cold R10 and top up to 10 ml with R10. Centrifuge the conical tubes at 540*g* for 5 min at 4 °C.

30| Discard the supernatant and gently resuspend the pellet in 1 ml of cold 2% (vol/vol) FBS/PBS.

31| Count the isolated CD4 T cells as in Step 6. In particular, take note of the cell viability. Samples with a low viability <50–60% may produce high background and show poor cell recovery throughout the protocol.
? TROUBLESHOOTING

32| Top up with 10 ml of cold 2% (vol/vol) FBS/PBS. Centrifuge the conical tubes at 540*g* for 5 min at 4 °C.

Box 4 | Antibody selection

As with general flow cytometry experiments, antibody selection (both in terms of the clone and fluorochrome) is critical to obtaining optimal results. First, with regard to monoclonal antibody selection, we have observed that some clones do not withstand the PrimeFlow procedure as well as others, resulting in a loss of signal. For example, the anti-CD4 clone RPA-T4 is more stable than SK3, but the latter can still be used. We recommend that each user test different clones against the antigen of interest before selection. Some fluorochromes are incompatible with the assay, including any peridinin chlorophyll protein (PerCP) or -Cy5 conjugates and Qdots. Signal from dim fluorochromes (such as V500 or FITC) may be masked by the increase in background associated with the assay. We have found that the BV dyes (BD, BioLegend) generally work well. However, we have observed degradation over time with some (BV650, in particular). Fluorochrome 'spreading' into other channels is also increased as compared with that observed in standard flow cytometry—for example, BV605 spreading into PE. These fluorochromes can be used, but only with careful antigen selection. We highly recommend the use of FMO (fluorescent minus one) controls to identify any potential issues. We have observed some limited interactions between specific BV dyes when multiple dyes are used in the same mix, as reported by BD Bioscience. This can be overcome by the addition of BD Horizon Brilliant Buffer (cat. no. 563794) to the antibody mix. We recommend that users determine the requirement of this buffer in their antibody panel of interest.

33| Discard the supernatant and resuspend the pellets at 10×10^6 per ml in cold sterile PBS. Prepare 1-ml aliquots in PrimeFlow 1.5-ml low-binding RNase-free tubes for viability staining as described in Steps 36–40.
▲ **CRITICAL STEP** If no viability staining is required, resuspend in cold 2% (vol/vol) FBS/PBS, rather than PBS, follow Steps 34 and 35 and then proceed to Step 40 for surface staining. We recommend that a viability stain be used for all primary cell samples.

34| Centrifuge the tubes (600*g*, 5 min, 4 °C).

35| Remove 900 µl with a pipette, or using an aspirator. The line on the tube at 100 µl can be used as a guide. Resuspend the cells in the residual volume either by pipetting gently or vortexing on a low speed.
▲ **CRITICAL STEP** We have observed that vortexing, particularly for samples from HIV-infected, untreated individuals, has a negative impact on cell viability. We recommend that for fragile samples resuspension be performed carefully and by gentle pipetting.

36| *Viability stain*. Prepare a stock of Fixable Viability stain. 100 µl of this stock is required per test. See **Table 1** for example calculations.

37| Add 100 µl of the Fixable Viability stain to the residual 100 µl left in each tube from Step 35, giving a volume of 200 µl per tube. Mix well by pipetting.

38| Incubate at 4 °C for 20 min in the dark.

39| Add 800 µl of cold 2% (vol/vol) FBS/PBS and invert the tubes three times to wash.

40| Centrifuge (600*g*, 5 min, 4 °C), discard the supernatant and resuspend the cells as in Steps 34 and 35.

41| *FcR block*. Add 1.4 µl of FcR block to the residual volume in each tube. If FcR block is not required, proceed to Step 43.
▲ **CRITICAL STEP** We recommend the use of FcR block, particularly when PBMCs are used as the starting cell population, to limit nonspecific antibody binding. If no surface stain is required, proceed to Step 48 for fixation.

42| Incubate at 4 °C for 10 min in the dark.

43| *Surface antibody stain*. During the incubation, prepare a mix of titrated antibodies for the surface stain.
▲ **CRITICAL STEP** Antibody selection will affect the quality of the cell staining. See **Box 4** for a detailed discussion.
▲ **CRITICAL STEP** Using the optimal antibody concentration to maximize the background/noise ratio is key. We advise titration of all antibodies used. As a minimum, we recommend antibody staining for basic phenotypic markers (e.g., CD3, CD4, exclusion) for cell identification.

▲ **CRITICAL STEP** If two or more Brilliant Violet (BV), Brilliant Ultra-violet (BUV) and Brilliant Blue (BB) fluorochromes are included in the panel, nonspecific interactions may be observed between these colors. Brilliant Stain Buffer (BD Bioscience, cat. no. 563794) can be used in preparation of the antibody mixes. We have not observed any issues when using this buffer with PrimeFlow; however, we highly recommend that investigators validate their specific antibody combinations with and without this buffer.

44| Add surface antibody mix directly to the residual 100 µl. Mix well by pipetting.

45| Incubate at 4 °C for 30 min in the dark.

46| Add 1 ml of cold 2% (vol/vol) FBS/PBS and invert the tubes three times to wash.

47| Centrifuge (600*g*, 5 min, 4 °C), discard the supernatant and resuspend the cells as in Steps 34 and 35, except here remove at least 1 ml to return to the 100-µl residual volume. This volume will now be used for all further steps.

48| *Fixation 1 and permeabilization*. Make up Fixation Buffer I by mixing equal parts of Fixation Buffer 1A and 1B. 1 ml is required per tube. See **Table 1** for example preparation calculations. Do not vortex—mix by gently inverting the tube. Freshly prepare and use the buffer. Store it at 4 °C until use.

49| Add 1 ml of Fixation Buffer I to the 100-µl residual volume. Invert to mix.

50| Incubate for 30 min at 4 °C in the dark.

51| Centrifuge at 800*g* for 5 min at 4 °C.
▲ **CRITICAL STEP** Note the increased spin speed after this fixation step. Failure to increase the spin speed will result in cell loss. Use 800*g* for all following steps.

52| Discard the supernatant and resuspend as in Step 35.

53| Prepare a stock of 1 × Permeabilization Buffer plus RNAsin. This buffer should be freshly prepared and stored at 4 °C before use. Do not vortex; mix by inverting. 3 ml is required per sample. See **Table 1** for example preparation calculations.

54| Add 1 ml of cold Permeabilization Buffer to the 100-µl residual volume in each tube. Invert to mix.

55| Spin (800*g*, 5 min, 4 °C), discard the supernatant and resuspend as in Steps 51 and 52.

56| Repeat Steps 54 and 55, such that each tube is washed twice in Permeabilization Buffer.

57| *Intracellular antibody stain*. Prepare intracellular antibody stains. If using additional intracellular stains, as well as the minimum anti-HIV-1 Gag antibody KC57 RD-1, prepare one mix for the additional stain excluding anti-HIV-1 Gag.
▲ **CRITICAL STEP** If you are not performing an intracellular stain, proceed to Step 65. This is not recommended for detection of translation-competent reservoirs.

58| Add 2 µl of anti-HIV-1 Gag antibody KC57 RD-1 directly to the residual 100 µl in each tube. Mix by pipetting gently.

59| Incubate at RT for 30 min in the dark.

60| If you are using additional intracellular antibody stains, add this mix directly to the residual 100-µl volume. If not, proceed to Step 61.

61| Incubate for a further 30 min at 4 °C in the dark, so that the samples are stained with anti-Gag KC57 for a total of 1 h.
▲ **CRITICAL STEP** Anti-Gag KC57-RD-1 requires a longer staining time as compared with most intracellular stain (ICS) antibodies. We have found that staining with anti-Gag KC57-RD-1 for 30 min at RT, before staining with additional intracellular antibodies, is optimal to maximize the anti-Gag signal while minimizing background for additional intracellular antibodies.

62| During this incubation, warm a 50-ml aliquot of Wash Buffer to RT.

TABLE 3 | Guidelines for preparation of target probes, amplification buffers and label probes.

Number of samples/tubes	Number of extra tests prepared
1	+0.2
2–3	+0.5
4–10	+1
10–20	+2

63| Add 1 ml of permeabilization buffer to the residual volume and invert three times to mix.

64| Spin, discard the supernatant and resuspend as in Steps 51 and 52.

65| *Fixation 2.* Prepare Fixation Buffer II by diluting the stock 8× Fixation Buffer II 1:8 in Wash Buffer at RT. 1 ml is required per sample. See **Table 1** for example calculations. Do not vortex; invert to mix.

66| Add 1 ml of RT Fixation Buffer II to the 100-µl residual volume and invert three times to mix.

67| Incubate for 1 h at RT in the dark.
■ **PAUSE POINT** As an alternative to this incubation, samples can be stored overnight in Fixation Buffer II at 4 °C. However, we have observed that longer-term storage in fixation buffers increases background and negatively affects fluorochrome stability. Therefore, we recommend continuing to a later Pause Point.

Part IIB: labeling of mRNA, amplification, labeling of amplified signal and data acquisition ● **TIMING 1.5 d**
▲ **CRITICAL** From this point forward, all buffers should be at RT or warmer; reagents and steps should be carried out at RT or above.

68| *Labeling mRNA.* During the incubation in Step 67, thaw mRNA target probes at RT and prepare mRNA Target Probe Mixes in Target Diluent. See **Table 1** for example calculations. Mixes should be warmed to 40 °C before use.
▲ **CRITICAL STEP** mRNA Target Probe Mix preparation is critical. The target probes should be added directly to the appropriate volume of Target Diluent; do not pipette down the sides. Mixes should be well-mixed by pipetting. The liquids are viscous and difficult to work with. We recommend using low-binding RNase-free tips where possible and preparing additional reagent to take into account pipetting error. The number of additional tests that we routinely prepare for is shown in **Table 3**.
▲ **CRITICAL STEP** PrimeFlow probes are available in three colors (types): Types 1 (AF647), 4 (AF488) and 6 (AF750). Types 1 and 4 are recommended for low-copy-number RNAs or RNAs for which the expression level is not known. Antibodies and mRNA probes cannot be used on fluorochromes with overlapping spectra (i.e., a FITC-tagged antibody cannot be used with a Type 4 AF488 probe set).

69| Centrifuge the cells in Fixation Buffer II at 800*g* for 5 min at RT.

70| Discard the supernatant and resuspend as in Step 35.

71| Add 1 ml of RT Wash Buffer to the residual 100-µl volume. Invert three times to mix.

72| Repeat Steps 69 and 70.

73| Repeat Steps 71 and 72 so that samples are washed twice in RT Wash Buffer.
■ **PAUSE POINT** To pause the protocol here, prepare Storage Wash Buffer as in the Reagent Setup (see **Table 1** for example calculations) and use in place of standard Wash Buffer in Step 73. Place samples at 4 °C for overnight storage. After overnight storage at 4 °C, warm samples to RT and pipette or gently vortex to resuspend pellets in the residual 100-µl volume before proceeding. Also warm the Wash Buffer required for Step 79 to RT.

74| Add 100 µl of the warm Target Probe Mix directly to the 100-µl residual volume; do not add down the sides of the tubes. Mix gently by pipetting until the two liquids no longer appear separate. Vortex briefly to mix, with two pulses on a low speed. Where possible, work in the dark.
▲ **CRITICAL STEP** Ensure that the cell pellets are well resuspended in the residual 100 µl before addition of the Target Probe Mix.

75| Place the samples into a metal heat block within an oven preheated to 40 °C.

76| Incubate for 1 h at 40 °C.
▲ **CRITICAL STEP** The correct temperature is very important. We recommend monitoring the temperature at all times. It should be 40 °C; a tolerance of ±1 °C is acceptable. The oven used should be well calibrated and the temperature stable.

77| Remove the metal heat block containing the tubes from the oven. Invert the whole heat block to mix, taking care to hold the tubes in place.

78| Incubate for a further 1 h at 40 °C.

79| Add 1 ml of RT Wash Buffer to the residual 200-µl volume. Invert three times to mix.

80| Centrifuge (800*g*, 5 min, RT), discard the supernatant and resuspend as in Steps 69 and 70.

81| Repeat Steps 79 and 80, so that the samples are washed twice.
■ **PAUSE POINT** To pause the protocol here, prepare Storage Wash Buffer per the Reagent Setup (see **Table 1** for example calculations) and use in place of standard Wash Buffer in Step 81. Place samples at 4 °C for overnight storage. After overnight storage at 4 °C, warm samples to RT and pipette or gently vortex to resuspend pellets in the residual 100-µl volume before proceeding. Also warm the Wash Buffer required for Step 87 to RT.

82| *Amplification*. Transfer the required volume of preamplification mix to a 1.5-ml RNase-free tube. Place in the heat block and warm to 40 °C.

83| Add 100 µl of the warm preamplification mix directly to the 100-µl residual volume; do not add down the sides of the tubes. Mix gently by pipetting until the two liquids no longer appear separate. Vortex briefly to mix, with two pulses on a low speed. Where possible, work in the dark.
▲ **CRITICAL STEP** Ensure that the cell pellets are well resuspended in the residual 100 µl and at RT before addition of the preamplification mix.

84| Place the samples into a metal heat block within an oven preheated to 40 °C.

85| Incubate for 1.5 h at 40 °C.

86| Add the required volume of amplification mix to a 1.5-ml RNase-free tube. Place the tube in the heat block and warm to 40 °C.

87| Add 1 ml of RT Wash Buffer to the 200-µl residual volume. Invert three times to mix.

88| Centrifuge (800*g*, 5 min, RT), discard the supernatant and resuspend as in Steps 69 and 70.

89| Repeat Steps 87 and 88 twice, so that the samples are washed three times.

90| Add 100 µl of the warm amplification mix directly to the 100-µl residual volume; do not add down the sides of the tubes. Mix gently by pipetting until the two liquids no longer appear separate. Vortex briefly to mix, with two pulses on a low speed. Where possible, work in the dark.

91| Incubate for 1.5 h at 40 °C.

92| During this incubation, transfer the required volume of Label Probe Diluent to a 1.5-ml RNase-free tube. See **Table 1** for example calculations. Place in the heat block and warm to 40 °C. Thaw the Label Probes mix in the dark on ice.

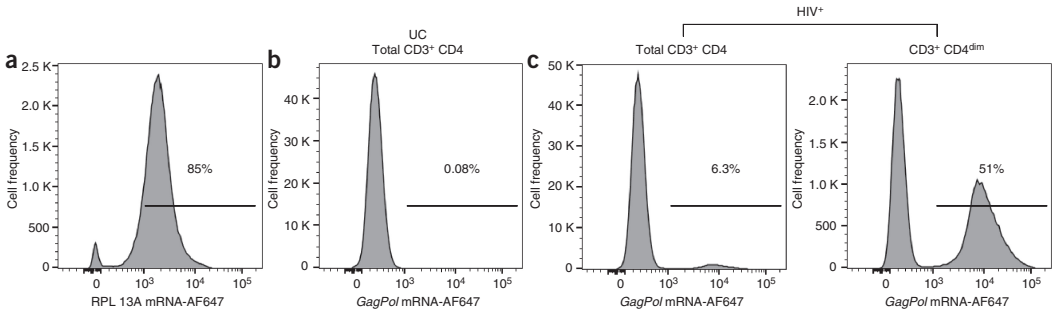

Figure 5 | Representative staining of mRNA-positive controls processed as described in the complete protocol, demonstrating the expected distribution of fluorescence intensities and frequencies of mRNA+ cells. The frequencies of mRNA+ CD4 T cells were determined using a histogram gate (represented by a black line) and are shown as a percentage of the parent population indicated above the plot. Gates were drawn using a negative control—here the uninfected donor (UC) control. Samples were acquired on a modified 5-laser BD LSRII and analyzed using FlowJo v9 and v10 for Mac. (**a**) CD4 T cells labeled for the housekeeping mRNA *RPL13A*. The majority of cells are positive for the housekeeping gene. (**b**,**c**) CD4 T cells from an uninfected control (UC, **b**) or an HIV-infected individual (HIV+, **c**) were cultured to establish a spreading infection *in vitro* as described in **Box 2** and labeled for *GagPol* mRNA. Low background staining is shown in **b** for the UC. In **c**, staining is shown for total $CD3^+$ CD4 T cells, or $CD3^+$ $CD4^{dim}$ T cells, demonstrating the increased frequency of HIV mRNA+ CD4 T cells in the $CD4^{dim}$ population.

93| Add 1 ml of RT Wash Buffer to the 200-µl residual volume. Invert three times to mix.

94| Centrifuge (800*g*, 5 min, RT), discard the supernatant and resuspend as in Steps 69 and 70.

95| Repeat Steps 93 and 94 twice, so that the samples are washed two times.

96| *Labeling amplified signal.* Prepare the Label Probe Mix as described in the Reagent Setup. See **Table 1** for example calculations. Ensure that the Label Probe diluent is at 40 °C before use and that the Label Probes have completely thawed. Mix by pipetting gently; do not vortex. We recommend limiting the number of freeze–thaw cycles for the label probe. If >5 freeze–thaw cycles are expected, aliquots should be prepared.

97| Add 100 µl of the warm Label Probe mix directly to the 100-µl residual volume; do not add down the sides of the tubes. Mix gently by pipetting. Vortex briefly, with two pulses on a low speed.

98| Incubate for 1 h at 40 °C.

99| Add 1 ml of RT Wash Buffer to the 200-µl residual volume. Invert three times to mix.

100| Centrifuge (800*g*, 5 min, RT), discard the supernatant and resuspend as in Steps 69 and 70.

101| Repeat the wash in Steps 99 and 100 with Wash Buffer.

102| *Acquisition.* For acquisition on a flow cytometer, complete a final wash with either Storage Buffer or 2% (vol/vol) FBS/PBS.
■ **PAUSE POINT** Samples can be stored overnight in 2% (vol/vol) FBS/PBS, or for 1 week in Storage Buffer, at 4 °C, depending on the fluorochromes used. We recommend acquiring the samples as soon as possible.

103| Acquire the samples on a flow cytometer equipped with the appropriate lasers and filter sets for the panel used. In the examples shown in Figures 5–8 and **Supplementary Figure 1**, samples were acquired on a modified 5-laser BD LSRII.
▲ **CRITICAL STEP** Ensure that the flow cytometer is clean before use; false-positive events will affect the limit of detection of the assay.
▲ **CRITICAL STEP** We recommend running samples slowly to decrease the electronic abort rate. In our experience, diluting samples to ~2,000 events per second and running at the lowest speed setting on a BD LSRII allows for maximal cell and event recovery.
▲ **CRITICAL STEP** Collecting a large number of events (2–4 million) takes up considerable memory and may cause issues with acquisition software; therefore, we recommend collecting data only within the 'Lymphocyte' or P1 gate to minimize data usage.
? TROUBLESHOOTING

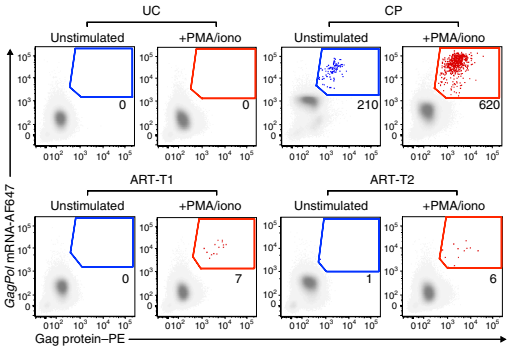

Figure 6 | Example flow cytometry plots from Steps 104 to 109 showing primary CD4 T-cell samples processed with the HIV$^{RNA/Gag}$ assay, demonstrating expected staining patterns and frequencies of HIV$^{RNA+/Gag+}$ cells. Samples were acquired on a modified 5-laser BD LSRII and analyzed using FlowJo v9 and v10 for Mac. Plots are shown for either unstimulated (blue) samples or samples following stimulation with PMA/ionomycin (PMA/iono, red). An HIV-uninfected negative-control donor (UC, 2 × 10^6 CD4 cells analyzed per condition) is used for gating, as described in Step 109, and illustrates expected low background. Detection of HIV$^{RNA+/Gag+}$ events in HIV-infected, untreated chronic progressor samples (CP, 4–8 × 10^5 CD4 cell analyzed per condition) define the CD4 T cells infected with translation-competent virus and maintaining an active *in vivo* infection. In HIV-infected, virally suppressed ART-treated donors (ART-T, 1–2 × 10^6 CD4 cells analyzed per condition), HIV$^{RNA+/Gag+}$ CD4 T cells detected following stimulation with PMA/iono represent the translation-competent latent reservoir. Numbers shown are events per 10^6 CD4 T cells.

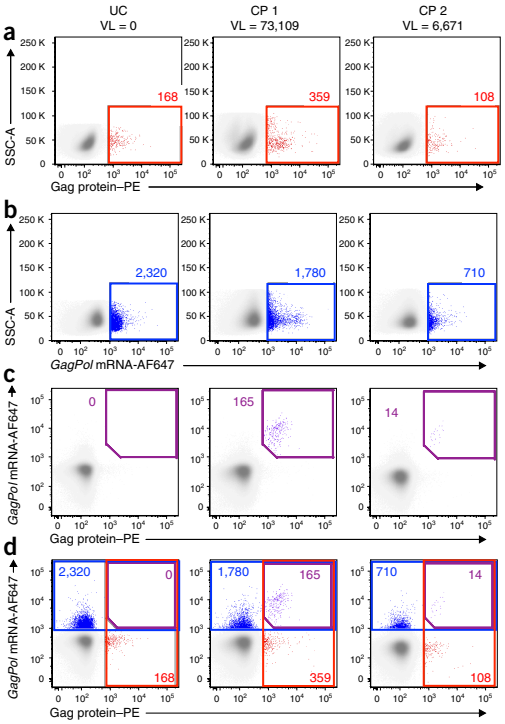

Figure 7 | Comparison of single mRNA, dual mRNA and protein staining on subject samples. Samples from one uninfected control (UC) and two chronic progressors (CPs) were processed as in the complete protocol. Events within gates are shown in color (*GagPol* mRNA$^+$ in red, Gag protein$^+$ in blue, GagPol mRNA$^+$ Gag protein$^+$ double positive in purple) and overlaid onto total events in gray. (**a**,**b**) Single stains for either Gag protein (**a**) or *GagPol* mRNA (**b**) result in a high background in the UC, which prevents accurate detection of low-frequency HIV^{Gag+} or HIV^{RNA+} events in CP samples. (**c**) In comparison, dual staining for Gag protein and *GagPol* mRNA enables identification of low frequencies of HIV$^{RNA+/Gag+}$ cells. This is summarized in **d**, where populations and gates from **a**–**c** are overlaid. Viral loads (VLs) are indicated as vRNA copies per ml. Numbers indicate positive events per million CD4 T cells. All gates were drawn based on the UC *GagPol* mRNA$^+$ Gag protein$^+$ gate in **c**. In all cases, 2 × 10^6 CD4 T cells were analyzed by flow cytometry. Samples were acquired on a modified 5-laser BD LSRII and analyzed using FlowJo v9 and v10 for Mac.

Data analysis ● **TIMING 1–4 h**

▲ **CRITICAL** Analyze the data using FlowJo v9 and v10 for Mac.

104| Gate on lymphocytes based on side scatter pulse area (SSC-A) versus forward scatter pulse area (FSC-A) using a restrictive gate, as shown in **Supplementary Figure 1a**.

▲ **CRITICAL STEP** A restrictive gate here helps eliminate autofluorescent cells.

105| Exclude doublets using side scatter pulse height/width (SSC-H/W) and forward scatter pulse height/width (FSC-H/W) as in **Supplementary Figure 1b**.

106| Exclude dead/dying cells using a viability stain, as shown in **Supplementary Figure 1c**.

107| For the identification of CD4 T cells, gate on exclusion channel–negative (e.g., CD8, CD14, CD19) events as in **Supplementary Figure 1d**. If a stimulation that may induce CD3 and/or CD4 downregulation (such as PMA/ionomycin) is used, proceed directly to Step 109.

▲ **CRITICAL STEP** We recommend the use of FMOs to guide gating of most phenotypic protein markers (except for HIV Gag protein—see Step 109). Autofluorescence is increased with the protocol, so FMOs must undergo the complete protocol.

108| Where CD3 is not downregulated by the conditions used, gate CD3$^+$ events as shown in **Supplementary Figure 1e**.

109| Gate *GagPol* mRNA$^+$ Gag Protein$^+$ double-positive cells (the HIV$^{RNA+/Gag+}$ population) using an HIV-uninfected control (UC) donor sample as a guide. See **Figures 5–7** for example gating using UC donor samples.

▲ **CRITICAL STEP** This sample should be treated identically and stained in parallel to the samples of interest. Cell number is also important—the same number of cells should be used for the UC as for the samples of interest.
? TROUBLESHOOTING

? TROUBLESHOOTING
Troubleshooting advice can be found in **Table 4**.

TABLE 4 | Troubleshooting table.

Step(s)	Problem	Possible reason	Solution
6, 17, 31, 103, 104–109	Poor cell recovery or high amounts of debris	Low viability of starting cells	Improve cell culture and preparation
		Incorrect spin speeds	Check spin speeds (note increased speed after fixation) in all centrifugations, particularly from Step 51 onward
		Low starting cell number	Increase cell starting number
		Harsh cell treatment	Limit vortexing of samples and handle them carefully throughout the protocol; see Step 35 for correct procedure
103, 104–109	Poor mRNA staining	Oven temperature was incorrect in Steps 76, 78, 85, 91 and 98	Recalibrate the oven
		Oven temperature was unstable in Steps 76, 78, 85, 91 and 98	Carefully monitor the oven temperature throughout the protocol
		Incorrect amount of mRNA Target Probes was used in Step 68	Use Target Probes at a 1:20 ratio
		Incorrect amount of Label Probes used in Step 96	Use Label Probes at a 1:100 ratio
		High residual volume in tubes following washes in Steps 73, 81, 89 and 95	Maintain residual volume at 100 µl
		mRNA degradation in Steps 1–64. See Step 27 for example	Ensure that cells are in the growth phase before use. Work at 4 °C before fixation
		Poor cell permeabilization and/or fixation in Steps 48, 53 and 65	Check Reagent Setup (**Table 1**). Use buffers prepared on the same day. Check incubation times and temperatures
		Poor washing in Steps 71–73, 79–81, 87–89, 93–95, 99–101	Ensure that all wash steps are followed, using the appropriate buffer at the required temperature
	High background in mRNA channel/ high mean fluorescence intensity (MFI) of mRNA-negative population	Low viability/number of starting cells in Steps 1–24 and 36–40. Check viability at Step 31	Improve cell culture and preparation. Use Viability Stain to exclude dead cells
		Incorrect amount of mRNA Target Probes used in Step 68	Use Target Probes at a 1:20 ratio
		Incorrect amount of Label Probes used in Step 96	Use Label Probes at a 1:100 ratio

(continued)

TABLE 4 | Troubleshooting table (Continued).

Step(s)	Problem	Possible reason	Solution
103, 104–109		Unclean flow machine/samples run too quickly	Clean the flow cytometer well before use. Run samples at ~2,000 events per s
		Low residual volume following washes in Steps 73, 81, 89 and 95	Residual volume should be 100 µl
		Incorrect fixation time in Steps 50 and 76	Check fixation time—longer fixations can increase the background
		Poor washing in Steps 71–73, 79–81, 87–89, 93–95 and 99–101	Ensure that all wash steps are followed, using the appropriate buffer at the required temperature
	No $HIV^{RNA+/Gag+}$ cells detected	Low starting cell number in Step 23	See 'Limitations' for discussion of starting cell number
		Poor mRNA staining	Run a positive-control sample to rule out assay issues
	Poor antibody staining	Clone was unstable during the protocol	Test new antibody clones. See **Box 4** for further information
		Fluorochrome was unstable during the protocol	Test additional fluorochromes. See **Box 4** for further information
		Incorrect incubation times/ temperatures in Steps 43 and 61	For anti-Gag KC57, stain for 1 h (30 min at RT, 30 min at 4 °C)
		Nonoptimal antibody concentration in Step 43	Titrate all antibodies before use
		Incorrect compensation	See **Box 4** for details
		Interactions between BV, BUV and BB polymer dyes	Prepare antibody mixes with BD Horizon Brilliant Stain Buffer (cat. no. 563794) and compare with the standard mix to determine whether this buffer is required

● **TIMING**

Steps 1–7, thawing of PBMC samples: 1–3 h, depending on sample number
Steps 8–18, CD4 T-cell isolation: 1–1.5 h, depending on sample number
Steps 19–24, reactivation of reservoirs: 15–21 h, depending on LRA used
Steps 25–35, sample collection and preparation: 0.5–3 h, depending on sample number
Steps 36–42, viability staining and FcR block: 1.5 h
Steps 43–47, surface antibody staining: 1 h
Steps 48–56, fixation 1 and permeabilization: 1.5 h
Steps 57–64, intracellular staining: 2 h
Steps 65–67, fixation 2: 2 h
Steps 68–81, mRNA labeling: 2 h
Steps 82–95, amplification of mRNA signal: 4 h
Steps 96–101, labeling of amplified signal: 2 h
Steps 102 and 103, sample acquisition: 2–6 h
Steps 104–109, data analysis: 1–4 h
Box 2, *ex vivo* viral propagation for positive-control CD4 T cells: 8.5 d
Box 5, sorting of $HIV^{RNA/Gag}$ assay samples for microscopy: 3.5 d for $HIV^{RNA/Gag}$ assay sorting and imaging

ANTICIPATED RESULTS

Positive-control samples can be used to optimize the HIV$^{RNA/Gag}$ assay in individual laboratories and are recommended for users unfamiliar with RNA Flow FISH or any of the steps within. Example staining for *RPL13A* housekeeping gene mRNA on expanded CD4 T cells, stained with a basic panel such as Panel A from **Table 2,** is shown in **Figure 5a**. *RPL13A* is stained with a Type 1 (AF647) probe here. As shown in the histogram, a majority of the cell population is clearly identified as positive for this mRNA. Example *GagPol* mRNA staining is shown in **Figure 5b,c**. Here, CD4 T cells from an HIV-uninfected negative-control donor (UC, **Fig. 5b**) or an HIV-infected donor (HIV$^+$, **Fig. 5c**) were activated *in vitro*, and then cultured to allow an autologous spreading infection to be established as detailed in **Box 2**. Samples were stained with stains from Panel B in **Table 2**. We expect very low background staining to be observed for the UC. For the HIV$^+$ sample, when gating on total CD3$^+$ CD4 T cells, 0.5–18% of cells can be expected to be HIV^{RNA+}, depending on the donor. When gating on CD3$^+$ CD4 dim cells, the frequency is increased; in the example shown, ~50% of the cells are HIV^{RNA+}. The mRNA$^+$ population is clear, at least one log above background, giving a distinct peak.

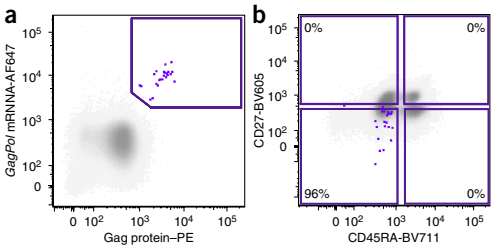

Figure 8 | Example HIV$^{RNA/Gag}$ assay staining and concurrent phenotyping of the translation-competent latent viral reservoir following LRA-induced reactivation for a virally suppressed, ART-treated individual. Such staining can be used to identify the phenotype of the CD4 T cells that are able to respond to LRA stimulation by production of HIV mRNAs and protein. Samples were processed as in the complete protocol, using Panel C from **Table 2**. (**a**) Example HIV$^{RNA/Gag}$ assay staining demonstrating detection of the translation-competent latent reservoir. (**b**) Example flow cytometry plot demonstrating the use of markers CD45RA and CD27 to phenotype the translation-competent latent viral reservoir. CD45RA$^-$CD27$^-$ cells are classified as effector memory cells; CD45RA$^-$CD27$^+$ as central/transitional memory cells; CD45RA$^+$CD27$^+$ as naive cells; and CD45RA$^+$CD27$^-$ as terminally differentiated cells. HIV$^{RNA+/Gag+}$ events in purple are overlaid onto total CD4 events in gray. 6 × 10^5 CD4 T cells were analyzed by flow cytometry. Samples were acquired on a modified 5-laser BD LSRII and analyzed using FlowJo v9 and v10 for Mac.

Example *GagPol* mRNA and Gag protein staining of CD4 T cells for a UC, HIV-infected, untreated, chronic progressing (CP) individuals and two HIV-infected, ART-treated participants (ART-T) is shown in **Figure 6**. Samples were gated as in **Supplementary Figure 1**, except that no gating was performed based on CD3, as this marker was downregulated with stimulation. The false-positive rate observed in UC is exceptionally low. We observed a total of 3 false-positive HIV$^{RNA+/Gag+}$ cells from a total of 30.5 × 10^6 UC donor CD4 T cells tested—an average of 0.1 false-positive HIV$^{RNA+/Gag+}$ events per 10^6 cells. The frequencies detected in HIV-infected primary samples vary considerably, depending on participant factors, including viral load and ART, as well as the stimulation used[15]. In samples from CP individuals, we readily detected HIV$^{RNA+/Gag+}$ CD4 T cells

Box 5 | Sorting of HIV$^{RNA/Gag}$ assay samples for microscopy ● TIMING 3.5 d

HIV mRNA and protein can be visualized in CD4 T cells from HIV-infected subjects by microscopy using the HIV$^{RNA/Gag}$ assay. In our case, isolated CD4 T cells infected with autologous virus after an *ex vivo* expansion for 7 d were used as in **Box 2**. This box continues from Step 102 of the main PROCEDURE. Process samples as described in the complete, detailed protocol. Samples should be stained with a minimal panel such as Panel B of **Table 2**, except that staining for CD3 and CD4 is not required.

Additional reagents/equipment

poly-L-lysine (0.01%, Sigma-Aldrich. cat. no. P8920)
DAPI (Sigma-Aldrich, cat. no. D9542)
μ-Slide VI 0.4 slides (Ibidi, cat. no. 80601)

Procedure

1. Follow Steps 1–102 of the main PROCEDURE and store the cells overnight in storage buffer if needed.
2. Coat μ-Slide VI 0.4 slides with poly-L-lysine (0.01%) for 30 min at RT. Aspirate poly-L-lysine solution and wash the slides with PBS. Dry them at RT overnight. Slides can be stored at 4 °C until use (for a maximum of 3 months).
3. Sort live, CD8$^-$CD14$^-$CD19$^-$ cells based on HIV$^{mRNA/Protein}$ expression pattern as desired (e.g., low/high-intensity mRNA staining[15]). Centrifuge (5 min, 800*g*, RT) and resuspend the cells in storage buffer. Cells can be stored at 4 °C for short-term (<1 week) storage or frozen at −20 °C for long-term storage (maximum 6 months). In the example shown in **Figure 9**, cells were sorted using a BD FACS Aria and BD DIVA.
4. Quench with glycine (100 nM, 10 min, RT) to decrease autofluoresence.
5. Wash the cells with PBS, centrifuge (800*g*, 5 min, RT), discard the supernatant and resuspend.
6. Stain the nucleus with DAPI (1–100 ng/ml, 2 min, RT). The optimal DAPI concentration may vary depending on cell type and microscope setup; therefore, we recommend that users titrate their own stock.
7. Wash the cells with PBS, centrifuge (5 min, 800*g*, RT), discard the supernatant and resuspend.
8. Plate cells onto poly-L-lysine-coated slides prepared in step 5.
9. Image the cells by confocal microscopy using appropriate filter sets (AF647 for HIV *GagPol* mRNA Type 1, PE for HIV Gag protein, DAPI for nuclear staining). We recommend using mRNA or Gag protein single-stained cells as controls.

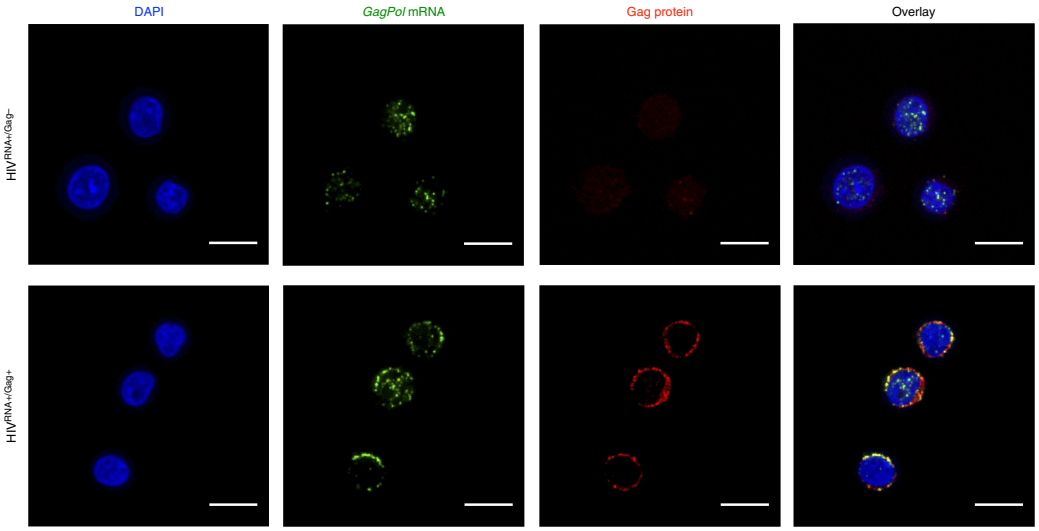

Figure 9 | The HIV$^{RNA/Gag}$ assay enables the microscopy analysis of rare populations of HIV-infected CD4 T cells, by sorting the rare populations of interest before microscopy. In the two examples shown here, CD4 T cells were processed with the full HIV$^{RNA/Gag}$ assay protocol from Steps 1 to 102, and then the rare HIV$^{RNA+/Gag+}$ CD4 T cells were sorted and imaged as described in **Box 5**. Two populations were sorted: CD4 T cells positive for HIV *GagPol* mRNA only (HIV$^{RNA+/Gag-}$, top panel) and CD4 T cells positive for both HIV *GagPol* mRNA and Gag protein (HIV$^{RNA+/Gag+}$, lower panel). Images are shown first as single channels (DAPI in blue, *GagPol* mRNA in green, Gag protein in red). Overlay analysis can be used to determine the cellular localization and colocalization of *GagPol* mRNAs and Gag protein. For example, in the HIV$^{RNA+/Gag-}$ population, *GagPol* mRNA expression is restricted to the nucleus. In comparison, in the HIV$^{RNA+/Gag+}$ population, *GagPol* mRNA is found in both the nucleus and the cytoplasm, with Gag protein found only in the cytoplasm. This suggests that the HIV$^{RNA+/Gag-}$ population may represent an early stage in the viral life cycle, or infection with defective viruses, whereas the HIV$^{RNA+/Gag+}$ population represents productively infected CD4 T cells. Scale bars, 10 μm.

in the absence of stimulation (median[range] = 123[1.5–230]/10^6 CD4 T cells). The size of this population was increased upon stimulation with PMA/ionomycin (median[range] = 311[3.6–768]/10^6). By contrast, in samples from ART-T individuals in the absence of stimulation, HIV$^{RNA+/Gag+}$ CD4 T cells were rare or absent (median[range] = 0.55[0–2.6]/10^6). However, following stimulation, the latent translation-competent reservoir could be detected in CD4 T cells from all but one of the 14 ART-T donors (median[range] = 3.56[1.52–660]/10^6)[15].

The marked gain in specificity with the HIV$^{RNA/Gag}$ assay as compared with standard flow-cytometry-based methods is due to the simultaneous detection of HIV mRNAs and proteins. As illustrated in **Figure 7**, high background staining is observed in the representative HIV-UC when analysis is performed using HIV Gag protein or *GagPol* mRNA staining alone (**Fig. 7a**,**b**). This background is sufficient to effectively mask the signal from two HIV-infected, untreated CP individuals, in particular for CP individual 2, who has a low viral load (<10,000 copies per ml). However, dual staining for both Gag protein and *GagPol* mRNA results in a decrease in background for the UC (0 events detected in 2 × 10^6 CD4 for this UC) and enables identification of rare HIV$^{RNA+/Gag+}$ CD4 T cells in both CP individuals at very low frequencies (13 per million for CP individual 2, **Fig. 7c**,**d**).

A major advantage of the HIV$^{RNA/Gag}$ assay is that it can be used to characterize and phenotype HIV reservoirs on a single-cell level. In **Figure 8**, example flow cytometry plots are shown for samples from an ART-T individual, in which isolated CD4 T cells were stimulated with the LRA Bryostatin-1 (10 nM, 18 h) and stained as in Panel C of **Table 2**. CD4 T cells were gated first as in **Supplementary Figure 1**, except that no gating was performed based on CD3, as this marker was downregulated with stimulation. HIV$^{RNA+/Gag+}$ events were then gated as in **Figure 8a**. These HIV$^{RNA+/Gag+}$ events, which represent the bryostatin-reactivated translation-competent reservoir, can then be analyzed for expression of additional phenotypic markers such as CD45RA and CD27, shown in **Figure 8b** as compared with the total CD4 phenotype.

Samples that have been processed with the HIV$^{RNA/Gag}$ assay can be used in downstream applications, including FACS and microscopy. This technique can be used to identify and sort very rare populations of cells, enabling microscopy analysis of a pure population of interest. Example images from HIV-infected CD4 T cells processed as in **Box 5**, and sorted and analyzed by microscopy are shown in **Figure 9**.

Note: Any Supplementary Information and Source Data files are available in the online version of the paper.

ACKNOWLEDGMENTS We thank J. Girouard, the clinical staff at McGill University Health Centre and all study participants; D. Gauchat, the CRCHUM Flow Cytometry Platform, O. Debbeche, the CRCHUM BSL3 Platform, D. Zenklusen and C. Lai for technical assistance; and D. Malayter for technical support. This study was supported by the National Institutes of Health (HL-092565, AI100663 CHAVI-ID, AI113096, AI118544), the Delaney AIDS Research Enterprise (DARE; 1U19AI096109), the Canadian Institutes for Health Research (137694; Canadian HIV Cure Enterprise), a Canada Foundation for Innovation grant, the FRQS AIDS and Infectious Diseases Network and the Foundation for AIDS Research (108928-56-RGRL). D.E.K. and N.C. are supported by FRQS Research Scholar Awards. A.F. is the recipient of a Canada Research Chair. J.-P.R. is the holder of the Louis Lowenstein Chair, McGill University. A.E.B. is the recipient of a CIHR Fellowship (award no. 152536). J.N. is the recipient of a scholarship from the Bavarian Research Alliance (BayFor). J.R. is the recipient of CIHR Fellowship Award no. 135349. N.A. is the recipient of a King Abdullah scholarship from the Saudi government.

AUTHOR CONTRIBUTIONS A.E.B., F.P. and D.E.K. conceived and developed the $HIV^{RNA/Gag}$ assay, with input from A.F. and N.C.; A.E.B., J.N., R.F., J.R., N.B., M.M. and N.A. modified the protocol, designed specific experiments and provided reagents; J.-P.R. obtained IRB approval and recruited participants to provide primary samples; D.E.K. provided supervision; A.E.B. and D.E.K. wrote the manuscript and all authors approved the final version.

COMPETING FINANCIAL INTERESTS The authors declare no competing financial interests.

1. Margolis, D.M., Garcia, J.V., Hazuda, D.J. & Haynes, B.F. Latency reversal and viral clearance to cure HIV-1. *Science* **353**, aaf6517 (2016).
2. Stephenson, K.E., D'Couto, H.T. & Barouch, D.H. New concepts in HIV-1 vaccine development. *Curr. Opin. Immunol.* **41**, 39–46 (2016).
3. Lederman, M.M., Funderburg, N.T., Sekaly, R.-P., Klatt, N.R. & Hunt, P.W. Residual immune dysregulation syndrome in treated HIV infection. *Adv. Immunol.* **119**, 51–83 (2013).
4. Klatt, N.R., Chomont, N., Douek, D.C. & Deeks, S.G. Immune activation and HIV persistence: implications for curative approaches to HIV infection. *Immunol. Rev.* **254**, 326–342 (2013).
5. Lederman, M.M. *et al.* A cure for HIV infection: 'Not in My Lifetime' or 'Just Around the Corner'? *Pathog. Immunol.* **1**, 154–164 (2016).
6. Deeks, S.G. HIV: shock and kill. *Nature* **487**, 439–440 (2012).
7. Rasmussen, T.A. & Lewin, S.R. Shocking HIV out of hiding: where are we with clinical trials of latency reversing agents? *Curr. Opin. HIV AIDS* **11**, 394–401 (2016).
8. Whitney, J.B. *et al.* Rapid seeding of the viral reservoir prior to SIV viraemia in rhesus monkeys. *Nature* **512**, 74–77 (2014).
9. Ananworanich, J. *et al.* HIV DNA set point is rapidly established in acute HIV infection and dramatically reduced by early ART. *EBioMedicine* **11**, 68–72 (2016).
10. Siliciano, J.D. *et al.* Long-term follow-up studies confirm the stability of the latent reservoir for HIV-1 in resting CD4+ T cells. *Nat. Med.* **9**, 727–728 (2003).
11. Crooks, A.M. *et al.* Precise quantitation of the latent HIV-1 reservoir: implications for eradication strategies. *J. Infect. Dis.* **212**, 1361–1365 (2015).
12. Finzi, D. *et al.* Identification of a reservoir for HIV-1 in patients on highly active antiretroviral therapy. *Science* **278**, 1295–1300 (1997).
13. Chun, T.W. *et al.* Presence of an inducible HIV-1 latent reservoir during highly active antiretroviral therapy. *Proc. Natl. Acad. Sci. USA* **94**, 13193–13197 (1997).
14. Eriksson, S. *et al.* Comparative analysis of measures of viral reservoirs in HIV-1 eradication studies. *PLoS Pathog.* **9**, e1003174 (2013).
15. Baxter, A.E. *et al.* Single-cell characterization of viral translation-competent reservoirs in HIV-infected individuals. *Cell Host Microbe* **20**, 368–380 (2016).
16. Sattentau, Q.J. & Stevenson, M. Macrophages and HIV-1: an unhealthy constellation. *Cell Host Microbe* **19**, 304–310 (2016).
17. Chun, T.W. *et al.* Quantification of latent tissue reservoirs and total body viral load in HIV-1 infection. *Nature* **387**, 183–188 (1997).
18. Vandergeeten, C. *et al.* Cross-clade ultrasensitive PCR-based assays to measure HIV persistence in large-cohort studies. *J. Virol.* **88**, 12385–12396 (2014).
19. Laird, G.M. *et al.* Rapid quantification of the latent reservoir for HIV-1 using a viral outgrowth assay. *PLoS Pathog.* **9**, e1003398 (2013).
20. Ho, Y.-C. *et al.* Replication-competent noninduced proviruses in the latent reservoir increase barrier to HIV-1 cure. *Cell* **155**, 540–551 (2013).
21. Bruner, K.M. *et al.* Defective proviruses rapidly accumulate during acute HIV-1 infection. *Nat. Med.* **22**, 1043–1049 (2016).
22. Bruner, K.M., Hosmane, N.N. & Siliciano, R.F. Towards an HIV-1 cure: measuring the latent reservoir. *Trends Microbiol.* **23**, 192–203 (2015).
23. Procopio, F.A. *et al.* A novel assay to measure the magnitude of the inducible viral reservoir in HIV-infected individuals. *EBioMedicine* **2**, 872–881 (2015).
24. Porichis, F. *et al.* High-throughput detection of miRNAs and gene-specific mRNA at the single-cell level by flow cytometry. *Nat. Commun.* **5**, 5641 (2014).
25. DiNapoli, S.R., Hirsch, V.M. & Brenchley, J.M. Macrophages in progressive human immunodeficiency virus/simian immunodeficiency virus infections. *J. Virol.* **90**, 7596–7606 (2016).
26. Jambo, K.C. *et al.* Small alveolar macrophages are infected preferentially by HIV and exhibit impaired phagocytic function. *Mucosal Immunol.* **7**, 1116–1126 (2014).
27. Borzì, R.M. *et al.* A fluorescent *in situ* hybridization method in flow cytometry to detect HIV-1 specific RNA. *J. Immunol. Methods* **193**, 167–176 (1996).
28. Wilburn, K.M. *et al.* Heterogeneous loss of HIV transcription and proviral DNA from 8E5/LAV lymphoblastic leukemia cells revealed by RNA FISH: FLOW analyses. *Retrovirology* **13**, 55 (2016).
29. Chargin, A. *et al.* Identification and characterization of HIV-1 latent viral reservoirs in peripheral blood. *J. Clin. Microbiol.* **53**, 60–66 (2014).
30. Perfetto, S.P., Ambrozak, D., Nguyen, R., Chattopadhyay, P. & Roederer, M. Quality assurance for polychromatic flow cytometry. *Nat. Protoc.* **1**, 1522–1530 (2006).
31. Perfetto, S.P., Ambrozak, D., Nguyen, R., Chattopadhyay, P.K. & Roederer, M. Quality assurance for polychromatic flow cytometry using a suite of calibration beads. *Nat. Protoc.* **7**, 2067–2079 (2012).
32. Sacha, J.B. & Watkins, D.I. Synchronous infection of SIV and HIV *in vitro* for virology, immunology and vaccine-related studies. *Nat. Protoc.* **5**, 239–246 (2010).

Harnessing T follicular helper cell responses for HIV Vaccine Development

Viruses, 2018

viruses

MDPI

Review

Harnessing T Follicular Helper Cell Responses for HIV Vaccine Development

Julia Niessl [1,2] and Daniel E. Kaufmann [1,2,*]

[1] Centre de Recherche du Centre Hospitalier de l'Université de Montréal (CRCHUM) and University of Montreal, Montreal, QC H2X 0A9, Canada; julia.niessl@umontreal.ca
[2] Scripps Center for HIV/AIDS Vaccine Immunology and Immunogen Discovery (CHAVI-ID), La Jolla, CA 92037, USA
* Correspondence: daniel.kaufmann@umontreal.ca; Tel.: +1-514-890-8000 (ext. 35261)

Received: 1 June 2018; Accepted: 16 June 2018; Published: 19 June 2018

Abstract: Passive administration of broadly neutralizing antibodies (bNAbs) capable of recognizing a broad range of viral strains to non-human primates has led to protection from infection with chimeric SIV/HIV virus (SHIV). This data suggests that generating protective antibody responses could be an effective strategy for an HIV vaccine. However, classic vaccine approaches have failed so far to induce such protective antibodies in HIV vaccine trials. HIV-specific bNAbs identified in natural infection show high levels of somatic hypermutations, demonstrating that they underwent extensive affinity maturation. It is likely that to gain ability to recognize diverse viral strains, vaccine-induced humoral responses will also require complex, iterative maturation. T follicular helper cells (Tfh) are a specialized CD4+ T cell subset that provides help to B cells in the germinal center for the generation of high-affinity and long-lasting humoral responses. It is therefore probable that the quality and quantity of Tfh responses upon vaccination will impact development of bNAbs. Here, we review studies that advanced our understanding of Tfh differentiation, function and regulation. We discuss correlates of Tfh responses and bNAb development in natural HIV infection. Finally, we highlight recent strategies to optimize Tfh responses upon vaccination and their impact on prophylactic HIV vaccine research.

Keywords: CD4 T cell help; T follicular helper cells (Tfh); B cells; antibody; broadly neutralizing antibody (bNAb); HIV; vaccine

1. Introduction

Most successful vaccines (e.g., against hepatitis B, yellow fever, and smallpox) work by inducing long-lasting neutralizing antibody responses that prevent infection of target cells [1]. Current human immunodeficiency virus (HIV) prevention strategies, including public awareness campaigns, condom use, and post-exposure prophylaxis, led to a decline of the annual number of new HIV infections to 1.8 million worldwide. In addition, full suppression of viral replication by antiretroviral therapy (ART) in HIV-infected individuals strongly reduces transmission rates. However, ending the pandemic without an effective vaccine seems unlikely [2].

Env is the only viral protein expressed on the surface of free, mature HIV virions. Broadly neutralizing antibodies (bNAbs) are able to recognize a variety of different HIV strains by targeting conserved regions of the HIV envelope protein. Passive administration of bNAbs has been shown to prevent infection in non-human primate (NHP) models [3–5]. In these studies, infused animals were challenged with Simian Human Immunodeficiency Virus (SHIV), a chimeric viral construct with an HIV envelope in an SIV backbone, which allows studying humoral responses against HIV in an animal model. These results suggest that vaccine-induced protective antibody responses

could also serve as a strategy for an HIV vaccine. However, the induction of long-lasting bNAbs responses remains a major challenge and has been unsuccessful in human HIV vaccine trials [6].

High quality and long-lived humoral immune responses require help from a specialized CD4+ T cell subset called T follicular helper cells (Tfh) [7]. Tfh cells differentiate from naïve CD4+ T cells upon interaction with antigen-presenting dendritic cells (DCs) and migrate to the germinal center (GC) of secondary lymphoid organs. There, they control B cell proliferation, affinity maturation, class-switch recombination (CSR), and long-lasting memory formation. They therefore play an important role in the generation of protective antibody responses [7]. HIV is characterized by exceptionally high mutation rates, and the human immune system lags behind the evolution of autologous strains: most circulating viruses are resistant to neutralizing antibodies in serum from the same time point. After years of infection, a minority of HIV individuals (in the range of 10–20%) develop potent antibodies capable of neutralizing diverse primary isolates [8]. In contrast to neutralizing antibodies against most other pathogens, these potent HIV-specific bNAbs usually exhibit high rate of somatic hypermutations (SHM), which are necessary for neutralizing potency and breath. This suggests that HIV-bNAbs must have undergone multiple rounds of affinity maturation in the GC [9]. It is therefore likely that, compared to conventional vaccine strategies, more efficient Tfh responses are required for the generation of HIV-specific bNAbs. In this review, we highlight recent findings on Tfh differentiation, function and regulation as well as correlates of Tfh responses and bNAb development during natural HIV infection. We report on strategies to optimize Tfh and GC responses for the induction of effective antibody responses, some of which have already shown some success in non-HIV-vaccines in humans or HIV-related vaccine studies in NHPs. These findings may guide future approaches for the development of a prophylactic HIV vaccine.

2. Tfh Differentiation

Tfh cells are a specialized CD4+ T helper subset, characterized by the expression of CXCR5, the ligand for the chemokine CXCL13, which allows their migration into the GC of secondary lymphoid organs [10,11]. There, they provide B cell help for the generation of high affinity antibody responses. Further phenotypic and functional markers include Bcl6, PD-1, ICOS, CD40L and IL-21, which are important for differentiation and function of Tfh cells and can be expressed at different levels depending on the differentiation status.

Tfh differentiation is a multifactorial and multistep process (see Overview, Figure 1). Initially, naïve CD4+ T cells are primed by antigen-presenting DCs in the T cell zone of secondary lymphoid organs. Early expression of the transcription factors Lef-1 and Tcf-1 primes naïve CD4+ T cells for further Tfh-promoting signals and leads to the upregulation of the transcriptional repressor Bcl6 [12,13], which is absolutely required for Tfh development [14–16]. Bcl6 acts together with other Tfh-related transcription factors (e.g., Maf and Ascl2) to repress non-Tfh related signature genes and induce key Tfh-associated genes such as PD-1 and CXCR5 [14,17,18]. Expression of CXCR5 and concomitant downregulation of CCR7 on the cell surface allows early Tfh cells to migrate to the T-B border [19]. There, Tfh cells interact with antigen-presenting B cells via ICOS-ICOSL [20], which leads to the reinforcement and persistence of the Tfh signature, and migration into the B cell follicle for the formation of GCs [21]. Further interactions between Tfh and antigen-presenting B cells in the GC are necessary to sustain Tfh commitment, demonstrating that continuous antigenic activation is important for their maintenance [22].

Signalling molecules involved in the positive or negative regulation of Tfh differentiation present some notable differences between mice and humans and are shown in Table 1. In addition, quantitative signals related to strong and prolonged interaction between the T cell receptor and the major histocompatibility complex class II (MHCII) molecule favours Tfh vs. non-Tfh commitment [23]. A better understanding of how Tfh differentiation can be regulated in humans is of great importance as these pathways might serve as target to induce and regulate Tfh responses for vaccine strategies.

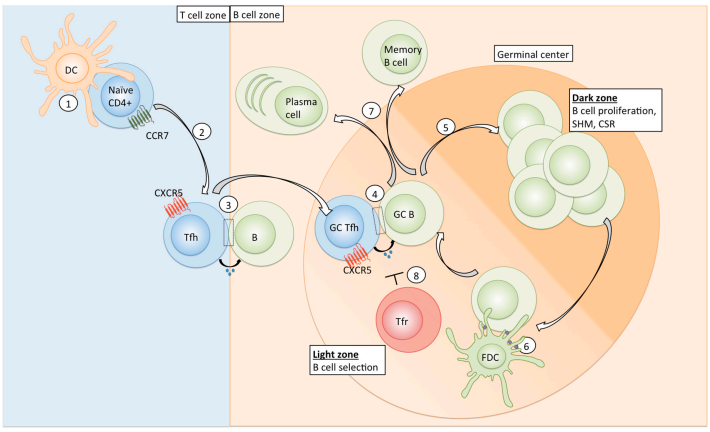

Figure 1. Overview of Tfh differentiation and function. Naïve CD4+ T cells are primed by antigen-presenting dendritic cells in the T cell zone of secondary lymphoid organs (1); Specific cytokines, co-signalling surface receptor molecules (see Table 1) and a prolonged DC-naïve CD4 interaction favour Tfh commitment. Tfh-polarized cells downregulate CCR7 and express CXCR5, the CXCL13 ligand, which allows their migration to the T-B-border (2); where first interaction with B cells occurs (3); Tfh cells then migrate into the germinal center, where further interaction with GC B cells sustains the GC Tfh polarization (4); In the dark zone of the GC, B cells undergo proliferation, affinity maturation via SHM, and CSR (5); B cells migrate to the light zone to receive survival and selection signals. They take up and process antigen (purple) from FDCs (6) and subsequently present it to GC Tfh cells (4). High affinity B cells are able to capture and present more antigen and therefore receive more Tfh cell help. Repeated circulation of B cells between DZ and LZ results in the acquisition of high levels of SHM and selection of high affinity clones. B cells eventually differentiate into antibody-producing plasma cells or memory B cells and enter the blood circulation (7); Tfr cells can inhibit GC Tfh and B cell responses via multiple mechanisms (8); DC: dendritic cell, Tfh: T follicular helper cell, SHM: somatic hypermutation, CSR: class switch recombination, FDC: follicular dendritic cell, DZ: dark zone; LZ: light zone; Tfr: follicular T regulatory cell.

Table 1. Signalling molecules regulating Tfh differentiation in mice and humans.

Signalling Molecule/Receptor Pair	Species	Role in Tfh Differentiation	Source/Interacting Cell Type	References
IL-6/IL-6R	Mouse	Promotion	DCs, B cells	[24,25]
IL-12/IL-12R	Mouse, human	Promotion	DCs	[26–28]
IL-21/Il-21R	Mouse	Promotion	T cells	[29,30]
IL-23/IL-23R	Human	Promotion	DCs	[31]
IL-27/IL-27R	Mouse	Promotion	DCs	[32,33]
IFN-γ/IFN-γR	Mouse	Promotion	T cells	[34]
TGF-β/TGF-βR	Mouse, human	Inhibition (mouse), Promotion (human)	DCs	[31,35,36]
Activin A/Activin-R	Human	Promotion	DCs	[37]
Ox40L/Ox40	Mouse, human	Promotion	DCs, B cells	[20,38]
ICOSL/ICOS	Mouse, human	Promotion	B cells	[39–41]
B7/CD28	Mouse	Promotion	DCs, B cells	[42,43]
SLAM family members	Mouse, human	Promotion	B cells	[44,45]
IL-2/IL-2R	Mouse, human	Inhibition	T cells	[37,46–48]
IL-7/IL-7R	Mouse	Inhibition	DCs	[49]
B7/CTLA-4	Mouse	Inhibition	-	[42,50]

3. T-Cell Dependent Antibody Responses

B cell differentiation and isotype switch can occur after initial T-B interaction and outside of the GC. This extrafollicular response emerges early after immunization and provides a first line of protective antibodies upon infection [51]. However, plasma cells generated following this type of interaction are usually short-lived and of low affinity due to only minimal affinity maturation [51]. For the efficient neutralization of viruses and other pathogens, high affinity antibodies are required. In addition, induction of long-lived memory B cell responses after infection or vaccination is desired to ensure long-term immunity. Both can be achieved in the GC reaction.

GC Tfh cells play a central role as they regulate multiple aspects of this process: B cell survival, proliferation, SHM, CSR, and differentiation. Tfh cells reside in the light zone of a mature GC. There, B cells take up antigen from follicular dendritic cells (FDCs), process it and present it to GC Tfh via MHCII. During this process, B cells compete for limited Tfh help: High affinity B cells, which were able to capture and therefore present more antigen compared to B cells with lower affinity, are more likely to receive Tfh signals [52,53]. Selected B cells enter the dark zone (DZ), where they proliferate and undergo SHM of the B cell receptor (BCR) V-region genes, the rate of which directly correlates with the Tfh help received in the light zone (LZ) [54]. During this process, mainly single nucleotide exchanges are introduced, resulting in a random modification of the BCR binding-affinity. GC B cell clones return to the LZ and are further selected by Tfh based on their antigen binding capacity. Repeated circulation between the LZ for selection for high-affinity and DZ for proliferation and affinity maturation results in the acquisition of elevated rates of somatic mutations and ensures the dominance of high-affinity B cell clones. Eventually, B cells differentiate into long-lived plasma cells or memory B cells and enter the circulation, thus allowing seeding of other anatomic locations.

Tfh help in the GC occurs via direct cell-cell interactions with B cells and secretion of cytokines. Some important mediators for B cell survival, proliferation, and differentiation are summarized in Table 2. In addition, B cell functions and differentiation can be complemented and modulated by a variety of other cytokines that regulate alone or in combination CSR and differentiation and thus outcome of antibody responses (reviewed in [55]). Signals regulating GC B cell differentiation to plasma cell vs. memory B cells are not well understood but recent studies suggested that high affinity B cell antigen interaction and IL-21 produced by Tfh cells favour plasma cell differentiation [56,57].

Table 2. Tfh mediators for B cell activation, differentiation and affinity maturation.

Tfh Functional Molecule	Effect on B Cells	References
IL-21	CSR, activation, proliferation, SHM, plasma cell differentiation	[57–59]
IL-4	Proliferation, CSR, SHM	[60,61]
IL-10	Proliferation, CSR, plasma cell differentiation	[62,63]
CD40L	Activation, proliferation, CSR	[64]

4. Memory and Circulating Tfh Cells

GC Tfh cells have been shown to form a pool of memory cells upon antigen clearance in both mice and humans. Memory Tfh cells localize together with antigen-specific memory B cells in the draining lymph node (LN) for the rapid induction of humoral responses upon re-exposure to antigen [65]. A subset of CD4 T cells in peripheral blood, termed circulating Tfh (cTfh) or peripheral Tfh (pTfh), shares several features with tissue Tfh [66]. cTfh cells have a memory phenotype and express CXCR5, although at lower levels compared to their GC counterparts [67]. In addition, certain phenotypic markers of GC Tfh, e.g., BCL6, are lost or downregulated [68]. Studies in mice showed that cTfh cells originate from GC Tfh cells that left the GC into the blood. Upon activation cTfh cells can migrate to the GC secondary lymphoid organs for the interaction with B cells [69]. In humans, matched samples from blood and tonsils revealed that after vaccination clonal relatives of GC Tfh enter the circulation [70]. Despite the phenotypic differences, functional properties of cTfh cells are partially preserved when compared to their tissue counterparts: cTfh cells express higher levels of Tfh-related cytokines such

as IL-21 and CXCL13 and show a superior capacity for B cell help in in vitro co-culture assays when compared to CXCR5- non-cTfh cells [66]. Of note, all cells identified by a given set of markers as cTfh in blood may not have the same potential to home to lymphoid tissue and become activated GC Tfh. While a better understanding of the relationships between quantitative and qualitative characteristics of cTfh responses and GC activity is thus necessary, monitoring of cTfh and antigen-specific cTfh responses in blood can represent an alternative investigational tool during infection or in vaccine trials when access to lymphoid tissue is limited or not possible.

cTfh represent a heterogeneous population that can be classified into multiple subsets based on polarization and activation status. Differential expression of the chemokine receptors CXCR3 and CCR6 allows the distinction of Th1-like (CXCR3+CCR6-), Th1Th17-like (CXCR3+CCR6+), Th17-like (CXCR3−CCR6+), and Th2-like (CXCR3−CCR6-) cTfh subsets. These cTfh subsets express transcription factors and can produce cytokines upon stimulation that are typically associated with Th1, Th2, Th17, and Th1Th17 CD4+ subsets [66]. Using these surface markers, several groups have identified a differential B cell helper capacity of cTfh subsets in in vitro culture assays: CXCR3- populations were able to provide help for naïve and memory B cells and induced proliferation, differentiation, and class-switched antibody production after stimulation with SEB [66,67,71]. In contrast, CXCR3+ cTfh cells were able to provide help to memory B cells in vitro [71], suggesting a role in promoting recall responses instead of priming primary antibody responses.

Tfh subsets based on the expression of CXCR3 and CCR6 can also be identified in the LN of macaques [72]. However, it remains to be determined whether the helper potential of different cTfh subsets can be translated into GC Tfh cells in tissues.

5. Regulation of GC Tfh Responses

Given the important role of Tfh cells for the generation of high-affinity antibody responses, it is not surprising that absence of or impaired Tfh responses hamper the generation of protective antibodies after infection or vaccination [73]. However, on the other hand, excessive accumulation of an overactive GC Tfh response correlated with the development of antibody-mediated autoimmunity or the generation of low affinity antibody responses by allowing the survival of B cells with self-reactivity or low binding capacity [74,75]. This shows that Tfh number and function in the GC needs to be regulated to ensure an efficient and targeted B cell help. Indeed, Tfh cells are only a minor population in the GC to allow competition of B cells for limited help and selection of only high-affinity clones. Tfh number can be regulated at the stage of differentiation as mentioned above. In addition, several mechanisms control Tfh number and function in the GC.

Tfh cells are characterized by the high expression of multiple co-inhibitory receptors including PD-1, TIGIT or CD200 [67,76,77]. While PD-1 and likely other of these molecules are required for interaction with B cells and additional cell types to ensure proper humoral responses [78], they might also be involved in the regulation of Tfh expansion and function in the context of chronic antigen exposure in the GC environment. For example, knockout or blocking of the immune checkpoints CTLA-4 or PD-1, alone or in combination with Lag-3, induced Tfh proliferation and enhanced cytokine production [50,79,80].

In addition, GC responses are controlled by the recently identified T follicular regulatory cells (Tfr) [81–83]. Tfr cells express similar phenotypic markers compared to Tfh cells including CXCR5, PD-1, Bcl6, and ICOS [77,81–83]. In contrast to Tfh cells, Tfr cells differentiate from natural Tregs and express Foxp3 and Helios [83]. The mechanism of Tfr-mediated GC regulation is-especially in humans-not well understood. Studies in mice demonstrated that Tfr cells inhibit proliferation and cytokine expression in Tfh cells as well as CSR and antibody production in B cells [69,84]. These effects were mediated via Tfr-induced changes in the cellular metabolism of Tfh and B cells that were long lasting but reversible and partially due to epigenetic modifications [84]. Additional Tfr-mediated suppressor mechanisms may include the physical inhibition of Tfh-B-interaction, induction of cell death via granzyme B, and the expression of inhibitory cytokines (reviewed in [85]). Negative regulators

of Tfh cell number and function might serve as additional target for the induction of high-affinity antibody responses during infection or vaccination.

6. Tfh Cells during HIV Infection and Correlates with bNAb Development

Tfh cell are highly permissive to HIV or SIV infection [86–88], yet GC Tfh cell number and frequency is increased in infected animals and subjects [86,87,89]. This is driven by clonal expansion of chronically stimulated HIV-specific GC Tfh cells [90], and a Tfh-favourable cytokine milieu that induces general non-HIV-specific Tfh differentiation. Virus-specific Tfh expansion occurs in the context of other chronic viral infections such as hepatitis C in humans or lymphocytic choriomeningitis in mice [91,92]. In addition to their accumulation, GC Tfh cells showed phenotypic and functional changes during HIV or SIV infection that correlated with dysregulated B cell responses: GC Tfh expansion was associated with an elevated number of GC B cells and plasma cells, accompanied by hypergammaglobulinaemia, whereas memory B cells were decreased in chronically infected individuals [89]. Transcriptional analysis of spleen GC Tfh from untreated HIV+ subjects revealed a decrease in molecules involved in Tfh-B interaction such as CD40L, Ox40, and signaling lymphocytic activation molecule (SLAM) members, and reduced levels of IL-10 and IL-4 [93]. In contrast, GC Tfh showed higher levels of CXCL13 and IL-21 mRNA [93]. Another recent study reported the shift of GC Tfh towards an IL-21 single-producing phenotype with reduced polyfunctionality that correlated with increased plasma cell but decreased switched memory B cell frequencies [90], consistent with the role of IL-21 to promote plasma cell differentiation. Cubas et al. also detected a tendency for higher IL-21-production in GC Tfh from untreated HIV+ individuals [94]. However, the elevated expression of PD-L1 on GC B cells from triggered PD-1 signalling on co-cultured Tfh cells, which led to a reduced Tfh activation, proliferation and B cell help. In this study, addition of IL-21 to co-cultures rescued the impaired B cell help of LN Tfh cells from HIV+ donors [94].

Although the increase of Tfh cell frequencies in lymphoid tissue is not mirrored in peripheral blood of HIV-infected individuals, cTfh cells present qualitative defects in viremic and ART-treated subjects compared to uninfected controls, with a decreased ability to induce B cell differentiation and antibody production in vitro [95,96]. These results demonstrate phenotypic and functional changes of Tfh cells during HIV infection that contribute to impaired HIV-related and general B cell responses.

In untreated HIV infection, bNAbs typically develop after a few years of chronic antigen exposure. Because of immune escape of the autologous strain, these humoral responses are not associated with viral control [8]. These findings show that in a subset of HIV+ individuals, the immunological environment allows acquisition of the extensive hypermutations necessary for bNAb generation. Several groups subsequently investigated Tfh responses in subjects with good vs. poor neutralization to find correlates of efficient help. Studies in SHIV-infected rhesus macaques demonstrated a positive correlation between IL-4+ Env-specific LN Tfh and the frequency of Env-specific IgG+ GC B cells as well as neutralization breadth [97]. Further transcriptional analysis of these Env-specific Tfh cells revealed that animals with greater neutralization activity showed a higher expression of Tfh-related (Bcl6, MAF, CXCL13, and IL-21) and Th2-related genes (GATA3), whereas Th1- and Treg-related signatures (TBX21, IFNγ, or FoxP3) were reduced [97].

Correlates between Tfh responses and development of bNAbs in humans have been largely restricted to the analysis of blood as access to lymphoid tissue is limited. Differences in the cTfh response between HIV+ subjects with high or low levels of neutralizing antibody activity were detected with a high frequency of CXCR3-PD-1+ cTfh being associated with the development of bNAbs [67,98]. During the early phase of infection, individuals who later developed broad neutralization already showed superior Tfh and B cell responses compared to study participants who remained low neutralizers [99–101]. They demonstrated an enhanced ability of cTfh cells to induce antibody class-switching in vitro, a preserved B cell activation profile comparable to uninfected controls, and elevated levels of plasma CXCL13, which is a marker of GC activity. Furthermore, HIV-infected donors with bNAbs showed a higher level of plasma autoantibodies and less functional

regulatory CD4+ T cells with elevated PD-1 expression, which limited their suppressive capacity [98]. Together, these results demonstrate that a high GC activity and Tfh quality seems to be important for the development of high-affinity antibody responses.

However, most studies mentioned rely on the analysis of the bulk Tfh population. Further studies are necessary to specifically investigate HIV-specific Tfh responses and the correlation of phenotype and function with protective antibody development, which might differ from observations made on total Tfh cells. Such investigations have been hampered by the limited tools available to study T cell antigen specificity independently of cytokine production. As Tfh show only limited cytokine production upon activation, they are more likely to be missed with standard assays such as intracellular cytokine staining or enzyme-linked immunospot (ELISPOT). Activation-induced marker (AIM) assays, recently developed by our group and others [102–104], overcome these limitations and allow the identification and study of antigen-specific Tfh responses in the tissue and blood during HIV infection and vaccination. These approaches, along with other tools such as Class II tetramers, will further help to decipher correlates of HIV-specific Tfh responses for the generation of protective antibody responses during HIV infection in humans, which will help guide strategies to induce such responses during vaccination.

7. Induction of Tfh Responses during Immunization

Classical vaccination strategies, while successful for the induction of protective antibodies against various pathogens, have failed to induce protective and long-lasting humoral responses against HIV. Given the importance of the quantity and quality of Tfh cells for the development of effective antibody responses in natural HIV infection several groups sought to determine how Tfh responses could be induced or modulated to improve humoral immunity (selected strategies are summarized in Table 3).

Table 3. Summary of strategies to enhance Tfh responses.

Vaccine Component	Strategy	Result	Effect on Tfh	Potential Caveat	References
Adjuvant	Alum + TLR agonists, MF59	Enhanced APC recruitment to infection site and elevated antigen delivery to LN	Tfh differentiation and maintenance	Increased immunogenicity might cause increased local and systemic adverse effects	[105]
	Various vaccine formulations containing TLR agonists	Induction of Tfh-promoting signals in DCs	Tfh differentiation		[106–112]
		Reduction of Tfr/Tfh ratio	Enhanced Tfh function		
Route of vaccination	Subcutaneous vs. intramuscular	Enhanced drainage of soluble antigen	Tfh differentiation and maintenance	Overabundant Tfh might lead to the selection of low affinity B cell clones (also applies to other strategies)	[113–116]
	Intradermal vs. intramuscular	Targeting of higher DC number	Tfh differentiation		
	Mucosal alone or in combination with systemic	Enhancing mucosal antibody responses	Direct site of humoral response		
Enhanced or extended antigen delivery	Increased antigen dose, prolonged antigen delivery using multiple injections, osmotic pumps or mRNA systems	Enhanced DC-naïve CD4 interaction that promotes Tfh differentiation, sustained availability of antigen on FDCs	Tfh differentiation and maintenance	Excessive long-term antigen persistence may be detrimental (exhaustion)	[22,113,117,118]
Inhibition of negative regulators of Tfh	CTLA-4 blockade	Limit suppressive function of Tfr, direct effect on Tfh	Enhanced Tfh function	Systemic blockade of immune checkpoints can have serious side effects-local blockade at site of delivery might be an alternative	[50,119]

TLR: toll-like receptor: APC: antigen-presenting cell; Tfr: follicular T regulatory cell; DC: dendritic cell.

7.1. Use of Adjuvants to Direct Tfh Formation

Adjuvants are used to promote or shape immune responses during vaccination as the vaccine antigen alone is in most cases of low immunogenicity. They can enhance immune cell infiltration and antigen uptake into antigen-presenting cells (APCs) as well as activate innate immune cells via binding to specific receptors (e.g., toll-like receptor (TLR) agonists). Based on their different effects, specific adjuvants therefore guide distinctive types of generated immune responses. Alum is the most widely used adjuvant for vaccinations (>80% of all licensed vaccines) and has shown great success in vaccinations against for example hepatitis A and B, human papilloma virus, diphtheria, or tetanus [120]. However, alum alone induces low Tfh responses when compared to other adjuvants or when alum is combined with TLR agonists. A recently published study demonstrated that the oil-in-water adjuvant MF59 or a combination of alum and a TLR7 agonist promoted higher GC Tfh responses in the draining LN compared to alum alone using an NHP immunization model [105]. This was associated with an enhanced ability of MF59 or alum/TLR7 agonist to induce APC recruitment to the infection site and subsequent antigen uptake and presentation in the LN [105]. MF59 is approved as vaccine adjuvant in humans and did not only promote the generation of high titer antibody responses after flu immunization in children and elderly [121,122], who usually experience low efficacy, but increased the quality of antibody responses via enhancing cross-clade neutralization and affinity [123,124]. Total and influenza-specific ICOS+ cTfh were detectable in the blood of MF59-adjuvanted flu vaccine recipients and correlated with protective antibody titers [125].

Given the success of MF59 to enhance protective antibody titers in vaccines against other pathogens, it is currently used in some HIV vaccine efficacy trials, such as the HVTN702 study (ALVAC + gp120), conducted in South Africa (https://clinicaltrials.gov/ct2/show/NCT02968849?term=HVTN702&rank=1, accessed 27 May 2018). This study is based on the RV144 trial (ALVAC/AIDSVAX), which demonstrated partial antibody-mediated protection [126]. Compared to unsuccessful HIV vaccine trials, e.g., using a DNA/rAd5 vaccine regimen, vaccinees of the RV144 trial demonstrated a higher frequency of HIV-specific IL-21+ cTfh cells [127], which may suggest better Tfh help. This finding deserves further investigation and needs to be confirmed in other trials. Studies in NHPs mimicking the HVTN702 vaccine trial demonstrated a lower efficacy and protection against SIV acquisition despite a higher immunogenicity of MF59 when compared to alum [128]. Whether this will also be the case in the human trial remains to be determined and suggests, that a better understanding of adjuvant-mediated humoral responses is still required.

Other adjuvants that demonstrated a strong induction of GC Tfh responses include agonists for TLR4 [106], TLR7/TLR8 [107], and TLR9 [108] alone or in combination [109]. TLRs are either expressed on the surface or on intracellular compartments of APCs, B cells, and T cells and induce, when triggered, a pro-inflammatory immune response characterized by the expression of cytokines, chemokines, and co-stimulatory molecules [110]. Activation of TLRs of DCs induces the upregulation of molecules important for the interaction with naïve CD4+ T cells in the LN and, depending on the type of TLR activated, a specific cytokine and signalling molecule profile that can direct T cell differentiation [110]. For example, TLR3, TLR8, or TLR9 activation in APCs leads to the secretion of Tfh-promoting cytokines that mediated Tfh differentiation such as IL-6 in mice in vivo [111] or IL-12 in human APCs in vitro [107]. TLR9-signalling can also directly act on B cells and regulate affinity maturation and class switch [108]. In addition, immunization with TLR4 and TLR9 agonist adjuvants reduced the Tfr/Tfh ratio in the GC [108,112], which could lead to enhanced Tfh and B cell function. Immunomodulatory adjuvants for the induction of Tfh responses have to be carefully evaluated as Tfh-promoting cytokines differ between humans and mice (see Table 1). Therefore, given the close similarities between the NHP and human immune systems, NHPs are likely to be the best animal model for preclinical studies involving the modulation of Tfh responses. In a recent NHP study, immunization with the adjuvant Iscomatrix or using poly(lactic-co-glycolic acid) (PGLA)-nanoparticle encapsulated TLR4 and TLR7/8 agonists led to the induction of high frequencies of HIV-vaccine-antigen-specific GC Tfh responses, which correlated with antibody responses, when compared to alum [129]. In this study, GC Tfh

responses could be followed longitudinally using fine needle aspiration (FNA) sampling of draining LNs. This technique involves inserting a needle, frequently under ultrasound guidance, that removes a small representative cell fraction of the total LN cell population [130]. FNA probing of LNs is well tolerated, minimally invasive and can serve as vaccine immune response monitoring system in future human vaccine trials.

In summary, these results demonstrate that multiple aspects of the GC responses can be modified by TLR agonists and their success in NHP studies suggest that they may also be beneficial for human vaccine development.

Given the importance of defined cytokines in promotion of Tfh responses, it is also possible that direct administration of these cytokines in combination with vaccination could enhance frequencies of GC Tfh cells as well.

7.2. Route of Vaccine Administration

Most vaccines are administered by intramuscular (i.m.) injection as this vaccination route demonstrated only minimal adverse effects [131]. However, subcutaneous (s.c.) or intradermal (i.d.) injection triggered an elevated differentiation of GC Tfh cells and increased antibody responses compared to i.m. vaccination in mice and NHPs [113,114]. This could be due to multiple factors. Soluble dye tracking in NHPs demonstrated superior drainage to local LNs after s.c. injection compared to the i.m. route [113].

Another factor is the differential distribution of DCs between tissue compartments. As mentioned before, DCs regulate CD4+ T cell differentiation. In a recent study, Krishnaswamy et al. identified migratory CD11b+ type 2 DCs as superior inducers of Tfh generation in mice due to their enhanced homing potential to the T-B border in secondary lymphoid organs [115]. These CD11b+ DCs and other APCs are located at high concentration in the skin but not in the muscle. In humans, i.d. immunization has shown better induction of antibody responses or similar responses using a lower dose upon vaccination against hepatitis B, influenza or human papilloma virus compared to i.m [131]. In a NHP study, GC Tfh frequency and HIV-neutralizing antibody titers were higher in animals that were immunized s.c. vs. i.m. [113]. In addition, animals were immunized s.c. at two different sites to ensure the engagement of more T and B cells into the GC. These results suggest that i.d. or s.c. injection could serve as favourable immunization route to enhance LN antigen delivery and increased systemic antibody responses in HIV vaccine studies. However, as mentioned before, i.m. and i.d. vaccination are associated with higher risks of adverse side effects compared to i.m. [131].

Since HIV is mainly transmitted across mucosal surfaces, an effective HIV vaccine likely depends on the generation of humoral responses in the mucosa. Mucosal antibody responses can be induced by systemic immunization routes, however, the exact mechanisms and how to specifically induce them via s.c., i.m., or i.d. immunization are not known [132]. Mucosal immunization routes (e.g., oral, intranasal, intratracheal, intrarectal, and intravaginal) have shown some success in NHP studies but have failed thus far in human HIV-vaccine trials (reviewed in [116]). Further studies will show whether mucosal vaccination alone or in combination with systemic immunization will serve as a strategy to induce protective immune responses against HIV in humans.

7.3. Enhanced or Extended Administration of Antigen to Induce and Maintain Tfh

As mentioned earlier, Tfh differentiation is promoted by prolonged DC-T interaction and Tfh maintenance is dependent on persistent antigen availability in the GC, suggesting that Tfh differentiation could be regulated by the amount of antigen given during vaccination. Indeed, GC Tfh and B cell responses are elevated when mice were immunized with higher doses of antigen [22]. Similarly, high dose immunization enhanced Tfh and antibody responses to influenza immunization in humans [133,134].

An alternative strategy to enhancing the dose of the single vaccine infections is the prolonged administration of antigen. Single injection of a vaccine antigen might not recapitulate the sustained

availability of antigen in the GC during the natural infection of replicating pathogens. This might be especially important for the generation of HIV-specific bNAbs as they require extensive SHM acquired during multiple rounds of GC reactions [9]. To manipulate the kinetics of antigen availability, Tam et al. compared multiple or constant antigen delivery vs. single bolus injection during the prime immunization in mice [117]. Prolonged antigen exposure during the prime led to sustained antigen retention on FDCs in the LN, increased GC Tfh and B cell responses and elevated antigen-specific antibody titers in the plasma compared to single injection [117]. This strategy also showed success in HIV-Env-immunized NHPs: Animals that received the antigen continuously with osmotic pumps showed higher titers of tier 2 neutralizing antibody responses when compared to single injected animals [113].

Continuous antigen delivery can also be achieved using immunization with mRNAs encoding for the antigen of interest (reviewed in [135]). Single intradermal injection of an mRNA-containing immunization system encoding for HIV envelope, influenza hemagglutinin, or zika virus premembrane and envelope proteins led to protein expression for a prolonged time period and induced strong GC Tfh responses in immunized mice and NHPs [118]. Such de novo synthesis of immunogen in vivo-or extended release of immunogens shielded from protein degradation-may also be beneficial for preservation of conformational epitopes, for example for Env trimeric constructs.

8. Inhibiting Negative Regulators of GC Responses

Tfr cells represent an interesting target for inhibition to enhance GC Tfh and B cell function. Besides influencing Tfr/Tfh ratio at the differentiation level using certain TLR-agonists as mentioned before, Tfr cell function was directly targeted in mice. CTLA-4 blockade or knockout led to a decreased suppressive capacity of Tfr cells and augmented Tfh cell frequency and function, GC responses, and antigen-specific antibody responses upon immunization [50,119]. However, generated antigen-specific antibody responses were of lower affinity and sustained suppression of Tfr led to the emergence of auto-reactive antibodies [50,119]. Thus, Tfr cell-dependent suppression of GCs might actually be beneficial for the generation of effective antibody responses: only high-affinity B cell clones, which receive more activation signals, might be able to overcome Tfr-mediated suppression to proliferate and survive [85]. More studies are therefore necessary to understand the role of Tfr cells in regulating GC responses and the development of high-affinity antibody responses.

9. Future Directions

Current HIV-related vaccine studies in NHP animal models demonstrate that several new vaccination strategies alone or in combination are able to enhance GC Tfh and B cell responses, which will serve as basic concept for future studies. These strategies aim to enhance GC Tfh responses by broadly augmenting Tfh frequency, yet the question remains whether more targeted approaches and the induction of specifically efficient Tfh cells might be favourable for the generation of bNAbs upon vaccination. For this, a better understanding of Tfh function in the GC is indispensable.

This review focuses on the development of strategies for a prophylactic HIV vaccine. However, enhancing antiviral responses also plays a role in HIV strategies of a functional cure that aims at inducing control of any residual viral replication by the host's own immune system in the absence of ART. Administration of bNAbs in ART-treated HIV+ subjects delayed viral rebound after analytic treatment interruption until viral resistance mutations occurred [136], suggesting that HIV-specific humoral responses might contribute to such control. A better understanding of quantitative and qualitative HIV-specific Tfh responses is necessary to evaluate whether active vaccination might serve as a strategy to induce more effective HIV-specific humoral responses in HIV+ individuals, or whether passive administration of bNAbs or long-acting antiretroviral drugs may be a more realistic approach.

10. Conclusions

Tfh responses have been shown to be involved in the generation of protective antibody responses in various infectious diseases and after vaccination. Induction of more potent Tfh responses represents an interesting strategy for vaccines that show limited efficacy, including HIV. Understanding Tfh biology has allowed developing alternative strategies that aim to induce more efficient Tfh responses, which have shown some success in NHP studies. However, further efforts are needed to determine whether these strategies can be successfully applied to HIV vaccine trials in humans.

Author Contributions: J.N. performed the literature review and wrote the manuscript, with contributions from D.E.K., who also edited structure and content.

Funding: J.N is supported by a scholarship of the department of microbiology, infectious diseases and immunology of the University of Montreal. D.E.K is supported by a FRQS Senior Research Scholar Award (# 31035), the National Institutes of Health (NIH) grant UM1AI100663 (CHAVI-ID) (D.E.K.; Dennis Burton, principal investigator); and the Canadian Institutes for Health Research (project grants #137694 and #320721: D.E.K.).

Acknowledgments: We thank Mathieu Dubé for his input on this manuscript and his help with figure design.

Conflicts of Interest: The authors have no conflict of interest to report.

References

1. Amanna, I.J.; Slifka, M.K. Contributions of humoral and cellular immunity to vaccine-induced protection in humans. *Virology* **2011**, *411*, 206–215. [CrossRef] [PubMed]
2. Fauci, A.S. An HIV Vaccine Is Essential for Ending the HIV/AIDS Pandemic. *JAMA* **2017**, *318*, 1535–1536. [CrossRef] [PubMed]
3. Moldt, B.; Rakasz, E.G.; Schultz, N.; Chan-Hui, P.Y.; Swiderek, K.; Weisgrau, K.L.; Piaskowski, S.M.; Bergman, Z.; Watkins, D.I.; Poignard, P.; et al. Highly potent HIV-specific antibody neutralization in vitro translates into effective protection against mucosal SHIV challenge in vivo. *Proc. Natl. Acad. Sci. USA* **2012**, *109*, 18921–18925. [CrossRef] [PubMed]
4. Gautam, R.; Nishimura, Y.; Pegu, A.; Nason, M.C.; Klein, F.; Gazumyan, A.; Golijanin, J.; Buckler-White, A.; Sadjadpour, R.; Wang, K.; et al. A single injection of anti-HIV-1 antibodies protects against repeated SHIV challenges. *Nature* **2016**, *533*, 105–109. [CrossRef] [PubMed]
5. Julg, B.; Liu, P.-T.; Wagh, K.; Fischer, W.M.; Abbink, P.; Mercado, N.B.; Whitney, J.B.; Nkolola, J.P.; McMahan, K.; Tartaglia, L.J.; et al. Protection Against a Mixed SHIV Challenge by a Broadly Neutralizing Antibody Cocktail. *Sci. Transl. Med.* **2017**, *9*, eaao4235. [CrossRef] [PubMed]
6. Pollara, J.; Easterhoff, D.; Fouda, G.G. Lessons Learned from Human HIV Vaccine Trials. *Curr. Opin. HIV AIDS* **2017**, *12*, 216–221. [CrossRef] [PubMed]
7. Crotty, S. T Follicular Helper Cell Differentiation, Function, and Roles in Disease. *Immunity* **2014**, *41*, 529–542. [CrossRef] [PubMed]
8. Landais, E.; Huang, X.; Havenar-Daughton, C.; Murrell, B.; Price, M.A.; Wickramasinghe, L.; Ramos, A.; Bian, C.B.; Simek, M.; Allen, S.; et al. Broadly Neutralizing Antibody Responses in a Large Longitudinal Sub-Saharan HIV Primary Infection Cohort. *PLoS Pathog.* **2016**, *12*, e1005369. [CrossRef] [PubMed]
9. Bonsignori, M.; Zhou, T.; Sheng, Z.; Chen, L.; Gao, F.; Joyce, M.G.; Ozorowski, G.; Chuang, G.Y.; Schramm, C.A.; Wiehe, K.; et al. Maturation Pathway from Germline to Broad HIV-1 Neutralizer of a CD4-Mimic Antibody. *Cell* **2016**, *165*, 449–463. [CrossRef] [PubMed]
10. Breitfeld, D.; Ohl, L.; Kremmer, E.; Ellwart, J.; Sallusto, F.; Lipp, M.; Förster, R. Follicular B Helper T Cells Express Cxc Chemokine Receptor 5, Localize to B Cell Follicles, and Support Immunoglobulin Production. *J. Exp. Med.* **2000**, *192*, 1545–1552. [CrossRef] [PubMed]
11. Schaerli, P.; Willimann, K.; Lang, A.B.; Lipp, M.; Loetscher, P.; Moser, B. Cxc Chemokine Receptor 5 Expression Defines Follicular Homing T Cells with B Cell Helper Function. *J. Exp. Med.* **2000**, *192*, 1553–1562. [CrossRef] [PubMed]
12. Choi, Y.S.; Gullicksrud, J.A.; Xing, S.; Zeng, Z.; Shan, Q.; Li, F.; Love, P.E.; Peng, W.; Xue, H.H.; Crotty, S. LEF-1 and TCF-1 orchestrate T_{FH} differentiation by regulating differentiation circuits upstream of the transcriptional repressor Bcl6. *Nat. Immunol.* **2015**, *16*, 980–990. [CrossRef] [PubMed]

13. Xu, L.; Cao, Y.; Xie, Z.; Huang, Q.; Bai, Q.; Yang, X.; He, R.; Hao, Y.; Wang, H.; Zhao, T.; et al. The transcription factor TCF-1 initiates the differentiation of T_{FH} cells during acute viral infection. *Nat. Immunol.* **2015**, *16*, 991–999. [CrossRef] [PubMed]
14. Johnston, R.J.; Poholek, A.C.; DiToro, D.; Yusuf, I.; Eto, D.; Barnett, B.; Dent, A.L.; Craft, J.; Crotty, S. Bcl6 and Blimp-1 are reciprocal and antagonistic regulators of T follicular helper cell differentiation. *Science* **2009**, *325*, 1006–1010. [CrossRef] [PubMed]
15. Nurieva, R.I.; Chung, Y.; Martinez, G.J.; Yang, X.O.; Tanaka, S.; Matskevitch, T.D.; Wang, Y.H.; Dong, C. Bcl6 mediates the development of T follicular helper cells. *Science* **2009**, *325*, 1001–1005. [CrossRef] [PubMed]
16. Yu, D.; Rao, S.; Tsai, L.M.; Lee, S.K.; He, Y.; Sutcliffe, E.L.; Srivastava, M.; Linterman, M.; Zheng, L.; Simpson, N.; et al. The transcriptional repressor Bcl-6 directs T follicular helper cell lineage commitment. *Immunity* **2009**, *31*, 457–468. [CrossRef] [PubMed]
17. Kroenke, M.A.; Eto, D.; Locci, M.; Cho, M.; Davidson, T.; Haddad, E.K.; Crotty, S. Bcl6 and Maf cooperate to instruct human follicular helper CD4 T cell differentiation. *J. Immunol.* **2012**, *188*, 3734–3744. [CrossRef] [PubMed]
18. Liu, X.; Chen, X.; Zhong, B.; Wang, A.; Wang, X.; Chu, F.; Nurieva, R.I.; Yan, X.; Chen, P.; van der Flier, L.G.; et al. Transcription factor achaete-scute homologue 2 initiates follicular T-helper-cell development. *Nature* **2014**, *507*, 513–518. [CrossRef] [PubMed]
19. Hardtke, S.; Ohl, L.; Forster, R. Balanced expression of CXCR5 and CCR7 on follicular T helper cells determines their transient positioning to lymph node follicles and is essential for efficient B-cell help. *Blood* **2005**, *106*, 1924–1931. [CrossRef] [PubMed]
20. Tahiliani, V.; Hutchinson, T.E.; Abboud, G.; Croft, M.; Salek-Ardakani, S. OX40 Cooperates with ICOS To Amplify Follicular Th Cell Development and Germinal Center Reactions during Infection. *J. Immunol.* **2017**, *198*, 218–228. [CrossRef] [PubMed]
21. Kerfoot, S.M.; Yaari, G.; Patel, J.R.; Johnson, K.L.; Gonzalez, D.G.; Kleinstein, S.H.; Haberman, A.M. Germinal center B cell and T follicular helper cell development initiates in the inter-follicular zone. *Immunity* **2011**, *34*, 947–960. [CrossRef] [PubMed]
22. Baumjohann, D.; Preite, S.; Reboldi, A.; Ronchi, F.; Ansel, K.M.; Lanzavecchia, A.; Sallusto, F. Persistent Antigen and Germinal Center B Cells Sustain T Follicular Helper Cell Responses and Phenotype. *Immunity* **2013**, *38*, 596–605. [CrossRef] [PubMed]
23. Keck, S.; Schmaler, M.; Ganter, S.; Wyss, L.; Oberle, S.; Huseby, E.S.; Zehn, D.; King, C.G. Antigen affinity and antigen dose exert distinct influences on CD4 T-cell differentiation. *Proc. Natl. Acad. Sci. USA* **2014**, *111*, 14852–14857. [CrossRef] [PubMed]
24. Choi, Y.S.; Eto, D.; Yang, J.A.; Lao, C.; Crotty, S. Cutting edge: STAT1 is required for IL-6-mediated Bcl6 induction for early follicular helper cell differentiation. *J. Immunol.* **2013**, *190*, 3049–3053. [CrossRef] [PubMed]
25. Eto, D.; Lao, C.; DiToro, D.; Barnett, B.; Escobar, T.C.; Kageyama, R.; Yusuf, I.; Crotty, S. IL-21 and IL-6 Are Critical for Different Aspects of B Cell Immunity and Redundantly Induce Optimal Follicular Helper CD4 T Cell (Tfh) Differentiation. *PLoS ONE* **2011**, *6*, e17739. [CrossRef] [PubMed]
26. Nakayamada, S.; Kanno, Y.; Takahashi, H.; Jankovic, D.; Lu, K.T.; Johnson, T.A.; Sun, H.W.; Vahedi, G.; Hakim, O.; Handon, R.; et al. Early Th1 cell differentiation is marked by a Tfh cell-like transition. *Immunity* **2011**, *35*, 919–931. [CrossRef] [PubMed]
27. Ma, C.S.; Suryani, S.; Avery, D.T.; Chan, A.; Nanan, R.; Santner-Nanan, B.; Deenick, E.K.; Tangye, S.G. Early commitment of naive human $CD4^+$ T cells to the T follicular helper (T_{FH}) cell lineage is induced by IL-12. *Immunol. Cell Biol.* **2009**, *87*, 590–600. [CrossRef] [PubMed]
28. Schmitt, N.; Morita, R.; Bourdery, L.; Bentebibel, S.-E.; Zurawski, S.M.; Banchereau, J.; Ueno, H. Human dendritic cells induce the differentiation of interleukin-21-producing T follicular helper-like cells through interleukin-12. *Immunity* **2009**, *31*, 158–169. [CrossRef] [PubMed]
29. Nurieva, R.I.; Chung, Y.; Hwang, D.; Yang, X.O.; Kang, H.S.; Ma, L.; Wang, Y.H.; Watowich, S.S.; Jetten, A.M.; Tian, Q.; et al. Generation of T follicular helper cells is mediated by interleukin-21 but independent of T helper 1, 2, or 17 cell lineages. *Immunity* **2008**, *29*, 138–149. [CrossRef] [PubMed]
30. Vogelzang, A.; McGuire, H.M.; Yu, D.; Sprent, J.; Mackay, C.R.; King, C. A Fundamental Role for Interleukin-21 in the Generation of T Follicular Helper Cells. *Immunity* **2008**, *29*, 127–137. [CrossRef] [PubMed]

31. Schmitt, N.; Liu, Y.; Bentebibel, S.-E.; Munagala, I.; Bourdery, L.; Venuprasad, K.; Banchereau, J.; Ueno, H. The cytokine TGF-beta co-opts signaling via STAT3-STAT4 to promote the differentiation of human TFH cells. *Nat. Immunol.* **2014**, *15*, 856–865. [CrossRef] [PubMed]
32. Harker, J.A.; Dolgoter, A.; Zuniga, E.I. Cell-intrinsic IL-27 and gp130 cytokine receptor signaling regulates virus-specific $CD4^+$ T cell responses and viral control during chronic infection. *Immunity* **2013**, *39*, 548–559. [CrossRef] [PubMed]
33. Batten, M.; Ramamoorthi, N.; Kljavin, N.M.; Ma, C.S.; Cox, J.H.; Dengler, H.S.; Danilenko, D.M.; Caplazi, P.; Wong, M.; Fulcher, D.A.; et al. IL-27 supports germinal center function by enhancing IL-21 production and the function of T follicular helper cells. *J. Exp. Med.* **2010**, *207*, 2895–2906. [CrossRef] [PubMed]
34. Lee, S.K.; Silva, D.G.; Martin, J.L.; Pratama, A.; Hu, X.; Chang, P.-P.; Walters, G.; Vinuesa, C.G. Interferon-γ Excess Leads to Pathogenic Accumulation of Follicular Helper T Cells and Germinal Centers. *Immunity* **2012**, *37*, 880–892. [CrossRef] [PubMed]
35. Suto, A.; Kashiwakuma, D.; Kagami, S.-I.; Hirose, K.; Watanabe, N.; Yokote, K.; Saito, Y.; Nakayama, T.; Grusby, M.J.; Iwamoto, I.; et al. Development and characterization of IL-21–producing $CD4^+$ T cells. *J. Exp. Med.* **2008**, *205*, 1369–1379. [CrossRef] [PubMed]
36. McCarron, M.J.; Marie, J.C. TGF-beta prevents T follicular helper cell accumulation and B cell autoreactivity. *J. Clin. Investig.* **2014**, *124*, 4375–4386. [CrossRef] [PubMed]
37. Locci, M.; Wu, J.E.; Arumemi, F.; Mikulski, Z.; Dahlberg, C.; Miller, A.T.; Crotty, S. Activin A programs the differentiation of human TFH cells. *Nat. Immunol.* **2016**, *17*, 976–984. [CrossRef] [PubMed]
38. Jacquemin, C.; Schmitt, N.; Contin-Bordes, C.; Liu, Y.; Narayanan, P.; Seneschal, J.; Maurouard, T.; Dougall, D.; Davizon, E.S.; Dumortier, H.; et al. OX40 Ligand Contributes to Human Lupus Pathogenesis by Promoting T Follicular Helper Response. *Immunity* **2015**, *42*, 1159–1170. [CrossRef] [PubMed]
39. Akiba, H.; Takeda, K.; Kojima, Y.; Usui, Y.; Harada, N.; Yamazaki, T.; Ma, J.; Tezuka, K.; Yagita, H.; Okumura, K. The Role of ICOS in the CXCR5+ Follicular B Helper T Cell Maintenance In Vivo. *J. Immunol.* **2005**, *175*, 2340–2348. [CrossRef] [PubMed]
40. Choi, Y.S.; Kageyama, R.; Eto, D.; Escobar, T.C.; Johnston, R.J.; Monticelli, L.; Lao, C.; Crotty, S. ICOS receptor instructs T follicular helper cell versus effector cell differentiation via induction of the transcriptional repressor Bcl6. *Immunity* **2011**, *34*, 932–946. [CrossRef] [PubMed]
41. Bossaller, L.; Burger, J.; Draeger, R.; Grimbacher, B.; Knoth, R.; Plebani, A.; Durandy, A.; Baumann, U.; Schlesier, M.; Welcher, A.A.; et al. ICOS deficiency is associated with a severe reduction of CXCR5+CD4 germinal center Th cells. *J. Immunol.* **2006**, *177*, 4927–4932. [CrossRef] [PubMed]
42. Wang, C.J.; Heuts, F.; Ovcinnikovs, V.; Wardzinski, L.; Bowers, C.; Schmidt, E.M.; Kogimtzis, A.; Kenefeck, R.; Sansom, D.M.; Walker, L.S. CTLA-4 controls follicular helper T-cell differentiation by regulating the strength of CD28 engagement. *Proc. Natl. Acad. Sci. USA* **2015**, *112*, 524–529. [CrossRef] [PubMed]
43. Weber, J.P.; Fuhrmann, F.; Feist, R.K.; Lahmann, A.; Baz Al, M.S.; Gentz, L.-J.; Vu Van, D.; Mages, H.W.; Haftmann, C.; Riedel, R.; et al. ICOS maintains the T follicular helper cell phenotype by down-regulating Krüppel-like factor 2. *J. Exp. Med.* **2015**, *212*, 217–233. [CrossRef] [PubMed]
44. Cannons, J.L.; Qi, H.; Lu, K.T.; Ghai, M.; Gomez-Rodriguez, J.; Cheng, J.; Wakeland, E.K.; Germain, R.N.; Schwartzberg, P.L. Optimal Germinal Center Responses Require A Multi-stage T:B Cell Adhesion Process Involving Integrins, SLAM-associated protein and CD84. *Immunity* **2010**, *32*, 253–265. [CrossRef] [PubMed]
45. Crotty, S.; Kersh, E.N.; Cannons, J.; Schwartzberg, P.L.; Ahmed, R. SAP is required for generating long-term humoral immunity. *Nature* **2003**, *421*, 282–287. [CrossRef] [PubMed]
46. Ballesteros-Tato, A.; León, B.; Graf, B.A.; Moquin, A.; Adams, P.S.; Lund, F.E.; Randall, T.D. Interleukin-2 inhibits germinal center formation by limiting T follicular helper differentiation. *Immunity* **2012**, *36*, 847–856. [CrossRef] [PubMed]
47. Johnston, R.J.; Choi, Y.S.; Diamond, J.A.; Yang, J.A.; Crotty, S. STAT5 is a potent negative regulator of T FHcell differentiation. *J. Exp. Med.* **2012**, *209*, 243–250. [CrossRef] [PubMed]
48. Oestreich, K.J.; Mohn, S.E.; Weinmann, A.S. Molecular mechanisms that control the expression and activity of Bcl-6 in TH1 cells to regulate flexibility with a TFH-like gene profile. *Nat. Immunol.* **2012**, *13*, 405–411. [CrossRef] [PubMed]
49. McDonald, P.W.; Read, K.A.; Baker, C.E.; Anderson, A.E.; Powell, M.D.; Ballesteros-Tato, A.; Oestreich, K.J. IL-7 signalling represses Bcl-6 and the TFH gene program. *Nat. Commun.* **2016**, *7*, 10285. [CrossRef] [PubMed]

50. Sage, P.T.; Paterson, A.M.; Lovitch, S.B.; Sharpe, A.H. The Coinhibitory Receptor CTLA-4 Controls B Cell Responses by Modulating T Follicular Helper, T Follicular Regulatory, and T Regulatory Cells. *Immunity* **2014**, *41*, 1026–1039. [CrossRef] [PubMed]
51. MacLennan, I.C.M.; Toellner, K.M.; Cunningham, A.F.; Serre, K.; Sze, D.M.Y.; Zúñiga, E.; Cook, M.C.; Vinuesa, C.G. Extrafollicular antibody responses. *Immunol. Rev.* **2003**, *194*, 8–18. [CrossRef] [PubMed]
52. Schwickert, T.A.; Victora, G.D.; Fooksman, D.R.; Kamphorst, A.O.; Mugnier, M.R.; Gitlin, A.D.; Dustin, M.L.; Nussenzweig, M.C. A dynamic T cell–limited checkpoint regulates affinity-dependent B cell entry into the germinal center. *J. Exp. Med.* **2011**, *208*, 1243–1252. [CrossRef] [PubMed]
53. Victora, G.D.; Schwickert, T.A.; Fooksman, D.R.; Kamphorst, A.O.; Meyer-Hermann, M.; Dustin, M.L.; Nussenzweig, M.C. Germinal center dynamics revealed by multiphoton microscopy with a photoactivatable fluorescent reporter. *Cell* **2010**, *143*, 592–605. [CrossRef] [PubMed]
54. Gitlin, A.D.; Shulman, Z.; Nussenzweig, M.C. Clonal selection in the germinal center by regulated proliferation and hypermutation. *Nature* **2014**, *509*, 637–640. [CrossRef] [PubMed]
55. Moens, L.; Tangye, S.G. Cytokine-Mediated Regulation of Plasma Cell Generation: IL-21 Takes Center Stage. *Front. Immunol.* **2014**, *5*, 65. [CrossRef] [PubMed]
56. Kräutler, N.J.; Suan, D.; Butt, D.; Bourne, K.; Hermes, J.R.; Chan, T.D.; Sundling, C.; Kaplan, W.; Schofield, P.; Jackson, J.; et al. Differentiation of germinal center B cells into plasma cells is initiated by high-affinity antigen and completed by Tfh cells. *J. Exp. Med.* **2017**, *214*, 1259–1267. [CrossRef] [PubMed]
57. Zhang, Y.; Tech, L.; George, L.A.; Acs, A.; Durrett, R.E.; Hess, H.; Walker, L.S.K.; Tarlinton, D.M.; Fletcher, A.L.; Hauser, A.E.; et al. Plasma cell output from germinal centers is regulated by signals from Tfh and stromal cells. *J. Exp. Med.* **2018**, *215*, 1227–1243. [CrossRef] [PubMed]
58. Zotos, D.; Coquet, J.M.; Zhang, Y.; Light, A.; D'Costa, K.; Kallies, A.; Corcoran, L.M.; Godfrey, D.I.; Toellner, K.M.; Smyth, M.J.; et al. IL-21 regulates germinal center B cell differentiation and proliferation through a B cell-intrinsic mechanism. *J. Exp. Med.* **2010**, *207*, 365–378. [CrossRef] [PubMed]
59. Linterman, M.A.; Beaton, L.; Yu, D.; Ramiscal, R.R.; Srivastava, M.; Hogan, J.J.; Verma, N.K.; Smyth, M.J.; Rigby, R.J.; Vinuesa, C.G. IL-21 acts directly on B cells to regulate Bcl-6 expression and germinal center responses. *J. Exp. Med.* **2010**, *207*, 353–363. [CrossRef] [PubMed]
60. Avery, D.T.; Bryant, V.L.; Ma, C.S.; de Waal Malefyt, R.; Tangye, S.G. IL-21-induced isotype switching to IgG and IgA by human naive B cells is differentially regulated by IL-4. *J. Immunol.* **2008**, *181*, 1767–1779. [CrossRef] [PubMed]
61. Reinhardt, R.L.; Liang, H.-E.; Locksley, R.M. Cytokine-secreting follicular T cells shape the antibody repertoire. *Nat. Immunol.* **2009**, *10*, 385–393. [CrossRef] [PubMed]
62. Rousset, F.; Garcia, E.; Defrance, T.; Péronne, C.; Vezzio, N.; Hsu, D.H.; Kastelein, R.; Moore, K.W.; Banchereau, J. Interleukin 10 is a potent growth and differentiation factor for activated human B lymphocytes. *Proc. Natl. Acad. Sci. USA* **1992**, *89*, 1890–1893. [CrossRef] [PubMed]
63. Choe, J.; Choi, Y.S. IL-10 interrupts memory B cell expansion in the germinal center by inducing differentiation into plasma cells. *Eur. J. Immunol.* **1998**, *28*, 508–515. [CrossRef]
64. Elgueta, R.; Benson, M.J.; de Vries, V.C.; Wasiuk, A.; Guo, Y.; Noelle, R.J. Molecular mechanism and function of CD40/CD40L engagement in the immune system. *Immunol. Rev.* **2009**, *229*. [CrossRef] [PubMed]
65. Fazilleau, N.; Eisenbraun, M.D.; Malherbe, L.; Ebright, J.N.; Pogue-Caley, R.R.; McHeyzer-Williams, L.J.; McHeyzer-Williams, M.G. Lymphoid reservoirs of antigen-specific memory T helper cells. *Nat. Immunol.* **2007**, *8*, 753. [CrossRef] [PubMed]
66. Morita, R.; Schmitt, N.; Bentebibel, S.-E.; Ranganathan, R.; Bourdery, L.; Zurawski, G.; Foucat, E.; Dullaers, M.; Oh, S.; Sabzghabaei, N.; et al. Human Blood CXCR5^{+}CD4^{+} T Cells Are Counterparts of T Follicular Cells and Contain Specific Subsets that Differentially Support Antibody Secretion. *Immunity* **2011**, *34*, 108–121. [CrossRef] [PubMed]
67. Locci, M.; Havenar-Daughton, C.; Landais, E.; Wu, J.; Kroenke, M.A.; Arlehamn, C.L.; Su, L.F.; Cubas, R.; Sette, A.; Haddad, E.K.; et al. Human Circulating PD-1+CXCR3-CXCR5^{+} Memory Tfh Cells Are Highly Functional and Correlate with Broadly Neutralizing HIV Antibody Responses. *Immunity* **2013**, *39*, 758–769. [CrossRef] [PubMed]
68. Simpson, N.; Gatenby, P.A.; Wilson, A.; Malik, S.; Fulcher, D.A.; Tangye, S.G.; Manku, H.; Vyse, T.J.; Roncador, G.; Huttley, G.A.; et al. Expansion of circulating T cells resembling follicular helper T cells is a fixed phenotype that identifies a subset of severe systemic lupus erythematosus. *Arthritis Rheum.* **2010**, *62*, 234–244. [PubMed]

69. Sage, P.T.; Alvarez, D.; Godec, J.; von Andrian, U.H.; Sharpe, A.H. Circulating T follicular regulatory and helper cells have memory-like properties. The Journal of Clinical Investigation. *Am. Soc. Clin. Investig.* **2014**, *124*, 5191–5204. [CrossRef] [PubMed]
70. Heit, A.; Schmitz, F.; Gerdts, S.; Flach, B.; Moore, M.S.; Perkins, J.A.; Harlan, S.R.; Aderem, A.; Spearman, P.; Tomaras, G.D.; et al. Vaccination establishes clonal relatives of germinal center T cells in the blood of humans. *J. Exp. Med.* **2017**, *214*, 2139–2152. [CrossRef] [PubMed]
71. Bentebibel, S.E.; Lopez, S.; Obermoser, G.; Schmitt, N.; Mueller, C.; Harrod, C.; Flano, E.; Mejias, A.; Albrecht, R.A.; Blankenship, D.; et al. Induction of ICOS+CXCR3^{+}CXCR5^{+} TH Cells Correlates with Antibody Responses to Influenza Vaccination. *Sci. Transl. Med.* **2013**, *5*, 176ra32-2. [CrossRef] [PubMed]
72. Velu, V.; Mylvaganam, G.H.; Gangadhara, S.; Hong, J.J.; Iyer, S.S.; Gumber, S.; Ibegbu, C.C.; Villinger, F.; Amara, R.R. Induction of Th1-Biased T Follicular Helper (Tfh) Cells in Lymphoid Tissues during Chronic Simian Immunodeficiency Virus Infection Defines Functionally Distinct Germinal Center Tfh Cells. *J. Immunol.* **2016**, *197*, 1832–1842. [CrossRef] [PubMed]
73. Nance, J.P.; Bélanger, S.; Johnston, R.J.; Hu, J.K.; Takemori, T.; Crotty, S. Bcl6 middle domain repressor function is required for T follicular helper cell differentiation and utilizes the corepressor MTA3. *Proc. Natl. Acad. Sci. USA* **2015**, *112*, 13324–13329. [CrossRef] [PubMed]
74. Preite, S.; Baumjohann, D.; Foglierini, M.; Basso, C.; Ronchi, F.; Fernandez Rodriguez, B.M.; Corti, D.; Lanzavecchia, A.; Sallusto, F. Somatic mutations and affinity maturation are impaired by excessive numbers of T follicular helper cells and restored by Treg cells or memory T cells. *Eur. J. Immunol.* **2015**, *45*, 3010–3021. [CrossRef] [PubMed]
75. Vinuesa, C.G.; Cook, M.C.; Angelucci, C.; Athanasopoulos, V.; Rui, L.; Hill, K.M.; Yu, D.; Domaschenz, H.; Whittle, B.; Lambe, T.; et al. A RING-type ubiquitin ligase family member required to repress follicular helper T cells and autoimmunity. *Nature* **2005**, *435*, 452–458. [CrossRef] [PubMed]
76. Choi, Y.S.; Yang, J.A.; Yusuf, I.; Johnston, R.J.; Greenbaum, J.; Peters, B.; Crotty, S. Bcl6 Expressing Follicular Helper CD4 T Cells Are Fate Committed Early and Have the Capacity To Form Memory. *J. Immunol.* **2013**, *190*, 4014–4026. [CrossRef] [PubMed]
77. Sage, P.T.; Francisco, L.M.; Carman, C.V.; Sharpe, A.H. PD-1 controls Lymph Node and Blood T Follicular Regulatory Cells. *Nat. Immunol.* **2013**, *14*, 152–161. [CrossRef] [PubMed]
78. Good-Jacobson, K.L.; Szumilas, C.G.; Chen, L.; Sharpe, A.H.; Tomayko, M.M.; Shlomchik, M.J. PD-1 regulates germinal center B cell survival and the formation and affinity of long-lived plasma cells. *Nat. Immunol.* **2010**, *11*, 535–542. [CrossRef] [PubMed]
79. Butler, N.S.; Moebius, J.; Pewe, L.L.; Traore, B.; Doumbo, O.K.; Tygrett, L.T.; Waldschmidt, T.J.; Crompton, P.D.; Harty, J.T. Therapeutic PD-L1 and LAG-3 blockade rapidly clears established blood-stage Plasmodium infection. *Nat. Immunol.* **2012**, *13*, 188–195. [CrossRef] [PubMed]
80. Hams, E.; McCarron, M.J.; Amu, S.; Yagita, H.; Azuma, M.; Chen, L.; Fallon, P.G. Blockade of B7-H1 (programmed death ligand 1) enhances humoral immunity by positively regulating the generation of T follicular helper cells. *J. Immunol.* **2011**, *186*, 5648–5655. [CrossRef] [PubMed]
81. Linterman, M.A.; Pierson, W.; Lee, S.K.; Kallies, A.; Kawamoto, S.; Rayner, T.F.; Srivastava, M.; Divekar, D.P.; Beaton, L.; Hogan, J.J.; et al. Foxp3^{+} follicular regulatory T cells control T follicular helper cells and the germinal center response. *Nat. Med.* **2011**, *17*, 975–982. [CrossRef] [PubMed]
82. Wollenberg, I.; Agua-Doce, A.; Hernandez, A.; Almeida, C.; Oliveira, V.G.; Faro, J.; Graca, L. Regulation of the germinal center reaction by Foxp3+ follicular regulatory T cells. *J. Immunol.* **2011**, *187*, 4553–4560. [CrossRef] [PubMed]
83. Chung, Y.; Tanaka, S.; Chu, F.; Nurieva, R.; Martinez, G.J.; Rawal, S.; Wang, Y.-H.; Lim, H.Y.; Reynolds, J.M.; Zhou, X.-H.; et al. Follicular regulatory T (Tfr) cells with dual Foxp3 and Bcl6 expression suppress germinal center reactions. *Nat. Med.* **2011**, *17*, 983–988. [CrossRef] [PubMed]
84. Sage, P.T.; Ron-Harel, N.; Juneja, V.R.; Sen, D.R.; Maleri, S.; Sungnak, W.; Kuchroo, V.K.; Haining, W.N.; Chevrier, N.; Haigis, M.; et al. Suppression by TFR cells leads to durable and selective inhibition of B cell effector function. *Nat. Immunol.* **2016**, *17*, 1436–1446. [CrossRef] [PubMed]
85. Sage, P.T.; Sharpe, A.H. T follicular regulatory cells in the regulation of B cell responses. *Trends Immunol.* **2015**, *36*, 410–418. [CrossRef] [PubMed]

86. Perreau, M.; Savoye, A.-L.; De Crignis, E.; Corpataux, J.-M.; Cubas, R.; Haddad, E.K.; De Leval, L.; Graziosi, C.; Pantaleo, G. Follicular helper T cells serve as the major CD4 T cell compartment for HIV-1 infection, replication, and production. *J. Exp. Med.* **2013**, *210*, 143–156. [CrossRef] [PubMed]
87. Xu, Y.; Weatherall, C.; Bailey, M.; Alcantara, S.; De Rose, R.; Estaquier, J.; Wilson, K.; Suzuki, K.; Corbeil, J.; Cooper, D.A.; et al. Simian Immunodeficiency Virus Infects Follicular Helper CD4 T Cells in Lymphoid Tissues during Pathogenic Infection of Pigtail Macaques. *J. Virol.* **2013**, *87*, 3760–3773. [CrossRef] [PubMed]
88. Kohler, S.L.; Pham, M.N.; Folkvord, J.M.; Arends, T.; Miller, S.M.; Miles, B.; Meditz, A.L.; McCarter, M.; Levy, D.N.; Connick, E. Germinal Center T Follicular Helper Cells Are Highly Permissive to HIV-1 and Alter Their Phenotype during Virus Replication. *J. Immunol.* **2016**, *196*, 2711–2722. [CrossRef] [PubMed]
89. Lindqvist, M.; van Lunzen, J.; Soghoian, D.Z.; Kuhl, B.D.; Ranasinghe, S.; Kranias, G.; Flanders, M.D.; Cutler, S.; Yudanin, N.; Muller, M.I.; et al. Expansion of HIV-specific T follicular helper cells in chronic HIV infection. *J. Clin. Investig.* **2012**, *122*, 3271–3280. [CrossRef] [PubMed]
90. Wendel, B.S.; del Alcazar, D.; He, C.; Del Río-Estrada, P.M.; Aiamkitsumrit, B.; Ablanedo-Terrazas, Y.; Hernandez, S.M.; Ma, K.-Y.; Betts, M.R.; Pulido, L.; et al. The receptor repertoire and functional profile of follicular T cells in HIV-infected lymph nodes. *Sci. Immunol.* **2018**, *3*, eaan8884. [CrossRef] [PubMed]
91. Fahey, L.M.; Wilson, E.B.; Elsaesser, H.; Fistonich, C.D.; McGavern, D.B.; Brooks, D.G. Viral persistence redirects CD4 T cell differentiation toward T follicular helper cells. *J. Exp. Med.* **2011**, *208*, 987–999. [CrossRef] [PubMed]
92. Raziorrouh, B.; Sacher, K.; Tawar, R.G.; Emmerich, F.; Neumann-Haefelin, C.; Baumert, T.F.; Thimme, R.; Boettler, T. Virus-Specific CD4+ T Cells Have Functional and Phenotypic Characteristics of Follicular T-Helper Cells in Patients with Acute and Chronic HCV Infections. *Gastroenterology* **2016**, *150*, 696–706. [CrossRef] [PubMed]
93. Colineau, L.; Rouers, A.; Yamamoto, T.; Xu, Y.; Urrutia, A.; Pham, H.-P.; Cardinaud, S.; Samri, a.; Dorgham, K.; Coulon, P.-G.; et al. HIV-Infected Spleens Present Altered Follicular Helper T Cell (Tfh) Subsets and Skewed B Cell Maturation. *PLoS ONE* **2015**, *10*, e0140978-19. [CrossRef] [PubMed]
94. Cubas, R.A.; Mudd, J.C.; Savoye, A.-L.; Perreau, M.; van Grevenynghe, J.; Metcalf, T.; Connick, E.; Meditz, A.; Freeman, G.J.; Abesada-Terk, G., Jr.; et al. Inadequate T follicular cell help impairs B cell immunity during HIV infection. *Nat. Med.* **2013**, *19*, 494–499. [CrossRef] [PubMed]
95. Boswell, K.L.; Paris, R.; Boritz, E.; Ambrozak, D.; Yamamoto, T.; Darko, S.; Wloka, K.; Wheatley, A.; Narpala, S.; McDermott, A.; et al. Loss of Circulating CD4 T Cells with B Cell Helper Function during Chronic HIV Infection. *PLoS Pathog.* **2014**, *10*, e1003853-14. [CrossRef] [PubMed]
96. Cubas, R.; van Grevenynghe, J.; Wills, S.; Kardava, L.; Santich, B.H.; Buckner, C.M.; Muir, R.; Tardif, V.; Nichols, C.; Procopio, F.; et al. Reversible Reprogramming of Circulating Memory T Follicular Helper Cell Function during Chronic HIV Infection. *J. Immunol.* **2015**, *195*, 5625–5636. [CrossRef] [PubMed]
97. Yamamoto, T.; Lynch, R.M.; Gautam, R.; Matus-Nicodemos, R.; Schmidt, S.D.; Boswell, K.L.; Darko, S.; Wong, P.; Sheng, Z.; Petrovas, C.; et al. Quality and quantity of TFH cells are critical for broad antibody development in SHIVAD8 infection. *Sci. Transl. Med.* **2015**, *7*, 298ra120-0. [CrossRef] [PubMed]
98. Moody, M.A.; Pedroza-Pacheco, I.; Vandergrift, N.A.; Chui, C.; Lloyd, K.E.; Parks, R.; Soderberg, K.A.; Ogbe, A.T.; Cohen, M.S.; Liao, H.-X.; et al. Immune perturbations in HIV-1-infected individuals who make broadly neutralizing antibodies. *Sci. Immunol.* **2016**, *1*, aag0851. [CrossRef] [PubMed]
99. Havenar-Daughton, C.; Lindqvist, M.; Heit, A.; Wu, J.E.; Reiss, S.M.; Kendric, K.; Bélanger, S.; Kasturi, S.P.; Landais, E.; Akondy, R.S.; et al. CXCL13 is a plasma biomarker of germinal center activity. *Proc. Natl. Acad. Sci. USA* **2016**, *113*, 2702–2707. [CrossRef] [PubMed]
100. Cohen, K.; Altfeld, M.; Alter, G.; Stamatatos, L. Early Preservation of CXCR5^{+} PD-1^{+} Helper T Cells and B Cell Activation Predict the Breadth of Neutralizing Antibody Responses in Chronic HIV-1 Infection. *J. Virol.* **2014**, *88*, 13310–13321. [CrossRef] [PubMed]
101. Mabuka, J.M.; Dugast, A.-S.; Muema, D.M.; Reddy, T.; Ramlakhan, Y.; Euler, Z.; Ismail, N.; Moodley, A.; Dong, K.L.; Morris, L.; et al. Plasma CXCL13 but Not B Cell Frequencies in Acute HIV Infection Predicts Emergence of Cross-Neutralizing Antibodies. *Front. Immunol.* **2017**, *8*, 1104. [CrossRef] [PubMed]
102. Dan, J.M.; Lindestam Arlehamn, C.S.; Weiskopf, D.; da Silva Antunes, R.; Havenar-Daughton, C.; Reiss, S.M.; Brigger, M.; Bothwell, M.; Sette, A.; Crotty, S. A Cytokine-Independent Approach To Identify Antigen-Specific Human Germinal Center T Follicular Helper Cells and Rare Antigen-Specific CD4^{+} T Cells in Blood. *J. Immunol.* **2016**, *197*, 983–993. [CrossRef] [PubMed]

103. Reiss, S.; Baxter, A.E.; Cirelli, K.M.; Dan, J.M.; Morou, A.; Daigneault, A.; Brassard, N.; Silvestri, G.; Routy, J.-P.; Havenar-Daughton, C.; et al. Comparative analysis of activation induced marker (AIM) assays for sensitive identification of antigen-specific CD4 T cells. *PLoS ONE* **2017**, *12*, e0186998. [CrossRef] [PubMed]
104. Havenar-Daughton, C.; Reiss, S.M.; Carnathan, D.G.; Wu, J.E.; Kendric, K.; Torrents de la Pena, A.; Pai Kasturi, S.; Dan, J.M.; Bothwell, M.; Sanders, R.W.; et al. Cytokine-Independent Detection of Antigen-Specific Germinal Center T Follicular Helper Cells in Immunized Nonhuman Primates Using a Live Cell Activation-Induced Marker Technique. *J. Immunol.* **2016**, *197*, 994–1002. [CrossRef] [PubMed]
105. Liang, F.; Lindgren, G.; Sandgren, K.J.; Thompson, E.A.; Francica, J.R.; Seubert, A.; De Gregorio, E.; Barnett, S.; O'Hagan, D.T.; Sullivan, N.J.; et al. Vaccine priming is restricted to draining lymph nodes and controlled by adjuvant-mediated antigen uptake. *Sci. Transl. Med.* **2017**, *9*, eaal2094. [CrossRef] [PubMed]
106. Desbien, A.L.; Dubois Cauwelaert, N.; Reed, S.J.; Bailor, H.R.; Liang, H.; Carter, D.; Duthie, M.S.; Fox, C.B.; Reed, S.G.; Orr, M.T. IL-18 and Subcapsular Lymph Node Macrophages are Essential for Enhanced B Cell Responses with TLR4 Agonist Adjuvants. *J. Immunol.* **2016**, *197*, 4351–4359. [CrossRef] [PubMed]
107. Ugolini, M.; Gerhard, J.; Burkert, S.; Jensen, K.J.; Georg, P.; Ebner, F.; Volkers, S.M.; Thada, S.; Dietert, K.; Bauer, L.; et al. Recognition of microbial viability via TLR8 drives TFH cell differentiation and vaccine responses. *Nat. Immunol.* **2018**, *19*, 386–396. [CrossRef] [PubMed]
108. Rookhuizen, D.C.; DeFranco, A.L. Toll-like receptor 9 signaling acts on multiple elements of the germinal center to enhance antibody responses. *Proc. Natl. Acad. Sci. USA* **2014**, *111*, E3224–E3233. [CrossRef] [PubMed]
109. Madan-Lala, R.; Pradhan, P.; Roy, K. Combinatorial Delivery of Dual and Triple TLR Agonists via Polymeric Pathogen-like Particles Synergistically Enhances Innate and Adaptive Immune Responses. *Sci. Rep.* **2017**, *7*, 2530. [CrossRef] [PubMed]
110. Dowling, J.K.; Mansell, A. Toll-like receptors: The swiss army knife of immunity and vaccine development. *Clin. Trans. Immunol.* **2016**, *5*, e85. [CrossRef] [PubMed]
111. Brahmakshatriya, V.; Kuang, Y.; Devarajan, P.; Xia, J.; Zhang, W.; Vong, A.M.; Swain, S.L. IL-6 Production by TLR-Activated APC Broadly Enhances Aged Cognate CD4 Helper and B Cell Antibody Responses In Vivo. *J. Immunol.* **2017**, *198*, 2819–2833. [CrossRef] [PubMed]
112. Radtke, A.J.; Anderson, C.F.; Riteau, N.; Rausch, K.; Scaria, P.; Kelnhofer, E.R.; Howard, R.F.; Sher, A.; Germain, R.N.; Duffy, P. Adjuvant and carrier protein-dependent T-cell priming promotes a robust antibody response against the Plasmodium falciparum Pfs25 vaccine candidate. *Sci. Rep.* **2017**, *7*, 40312. [CrossRef] [PubMed]
113. Pauthner, M.; Havenar-Daughton, C.; Sok, D.; Nkolola, J.P.; Bastidas, R.; Boopathy, A.V.; Carnathan, D.G.; Chandrashekar, A.; Cirelli, K.M.; Cottrell, C.A.; et al. Elicitation of Robust Tier 2 Neutralizing Antibody Responses in Nonhuman Primates by HIV Envelope Trimer Immunization Using Optimized Approaches. *Immunity* **2017**, *46*, 1073–1076. [CrossRef] [PubMed]
114. Koutsonanos, D.G.; Esser, E.S.; McMaster, S.R.; Kalluri, P.; Lee, J.-W.; Prausnitz, M.R.; Skountzou, I.; Denning, T.L.; Kohlmeier, J.E.; Compans, R.W. Enhanced immune responses by skin vaccination with influenza subunit vaccine in young hosts. *Vaccine* **2015**, *33*, 4675–4682. [CrossRef] [PubMed]
115. Krishnaswamy, J.K.; Gowthaman, U.; Zhang, B.; Mattsson, J.; Szeponik, L.; Liu, D.; Wu, R.; White, T.; Calabro, S.; Xu, L.; et al. Migratory CD11b +conventional dendritic cells induce T follicular helper cell–dependent antibody responses. *Sci. Immunol.* **2017**, *2*, eaam9169. [CrossRef] [PubMed]
116. Tuero, I.; Robert-Guroff, M. Challenges in Mucosal HIV Vaccine Development: Lessons from Non-Human Primate Models. *Viruses* **2014**, *6*, 3129–3158. [CrossRef] [PubMed]
117. Tam, H.H.; Melo, M.B.; Kang, M.; Pelet, J.M.; Ruda, V.M.; Foley, M.H.; Hu, J.K.; Kumari, S.; Crampton, J.; Baldeon, A.D.; et al. Sustained antigen availability during germinal center initiation enhances antibody responses to vaccination. *Proc. Natl. Acad. Sci. USA* **2016**, *113*, E6639–E6648. [CrossRef] [PubMed]
118. Pardi, N.; Hogan, M.J.; Naradikian, M.S.; Parkhouse, K.; Cain, D.W.; Jones, L.; Moody, M.A.; Verkerke, H.P.; Myles, A.; Willis, E.; et al. Nucleoside-modified mRNA vaccines induce potent T follicular helper and germinal center B cell responses. *J. Exp. Med.* **2018**, *136*, jem.20171450. [CrossRef] [PubMed]
119. Wing, J.B.; Ise, W.; Kurosaki, T.; Sakaguchi, S. Regulatory T Cells Control Antigen-Specific Expansion of Tfh Cell Number and Humoral Immune Responses via the Coreceptor CTLA-4. *Immunity* **2014**, *41*, 1013–1025. [CrossRef] [PubMed]

120. Lee, S.; Nguyen, M.T. Recent Advances of Vaccine Adjuvants for Infectious Diseases. *Immune Netw.* **2015**, *15*, 51–57. [CrossRef] [PubMed]
121. Vesikari, T.; Knuf, M.; Wutzler, P.; Karvonen, A.; Kieninger-Baum, D.; Schmitt, H.-J.; Baehner, F.A.; Borkowski, A.; Tsai, T.F.; Clemens, R. Oil-in-Water Emulsion Adjuvant with Influenza Vaccine in Young Children. *N. Engl. J. Med.* **2011**, *365*, 1406–1416. [CrossRef] [PubMed]
122. Domnich, A.; Arata, L.; Amicizia, D.; Puig-Barbera, J.; Gasparini, R.; Panatto, D. Effectiveness of MF59-adjuvanted seasonal influenza vaccine in the elderly: A systematic review and meta-analysis. *Vaccine* **2017**, *35*, 513–520. [CrossRef] [PubMed]
123. Galli, G.; Hancock, K.; Hoschler, K.; DeVos, J.; Praus, M.; Bardelli, M.; Malzone, C.; Castellino, F.; Gentile, C.; McNally, T.; et al. Fast rise of broadly cross-reactive antibodies after boosting long-lived human memory B cells primed by an MF59 adjuvanted prepandemic vaccine. *Proc. Natl. Acad. Sci. USA* **2009**, *106*, 7962–7967. [CrossRef] [PubMed]
124. Khurana, S.; Verma, N.; Yewdell, J.W.; Hilbert, A.K.; Castellino, F.; Lattanzi, M.; Del Giudice, G.; Rappuoli, R.; Golding, H. MF59 Adjuvant Enhances Diversity and Affinity of Antibody-Mediated Immune Response to Pandemic Influenza Vaccines. *Sci. Transl. Med.* **2011**, *3*, 85ra48-8. [CrossRef] [PubMed]
125. Spensieri, F.; Siena, E.; Borgogni, E.; Zedda, L.; Cantisani, R.; Chiappini, N.; Schiavetti, F.; Rosa, D.; Castellino, F.; Montomoli, E.; et al. Early Rise of Blood T Follicular Helper Cell Subsets and Baseline Immunity as Predictors of Persisting Late Functional Antibody Responses to Vaccination in Humans. *PLoS ONE* **2016**, *11*, e0157066. [CrossRef] [PubMed]
126. Rerks-Ngarm, S.; Pitisuttithum, P.; Nitayaphan, S.; Kaewkungwal, J.; Chiu, J.; Paris, R.; Premsri, N.; Namwat, C.; de Souza, M.; Adams, E.; et al. Vaccination with ALVAC and AIDSVAX to Prevent HIV-1 Infection in Thailand. *N. Engl. J. Med.* **2009**, *361*, 2209–2220. [CrossRef] [PubMed]
127. Schultz, B.T.; Teigler, J.E.; Pissani, F.; Oster, A.F.; Kranias, G.; Alter, G.; Marovich, M.; Eller, M.A.; Dittmer, U.; Robb, M.L.; et al. Circulating HIV-Specific Interleukin-21^{+}CD4^{+} T Cells Represent Peripheral Tfh Cells with Antigen-Dependent Helper Functions. *Immunity* **2016**, *44*, 167–178. [CrossRef] [PubMed]
128. Vaccari, M.; Gordon, S.N.; Fourati, S.; Schifanella, L.; Liyanage, N.P.M.; Cameron, M.; Keele, B.F.; Shen, X.; Tomaras, G.D.; Bilings, E.; et al. Adjuvant-dependent innate and adaptive immune signatures of risk of SIVmac251 acquisition. *Nat. Med.* **2016**, *22*, 762–770. [CrossRef] [PubMed]
129. Kasturi, S.P.; Kozlowski, P.A.; Nakaya, H.I.; Burger, M.C.; Russo, P.; Pham, M.; Kovalenkov, Y.; Silveira, E.L.V.; Havenar-Daughton, C.; Burton, S.L.; et al. Adjuvanting a Simian Immunodeficiency Virus Vaccine with Toll-Like Receptor Ligands Encapsulated in Nanoparticles Induces Persistent Antibody Responses and Enhanced Protection in TRIM5α Restrictive Macaques. *J. Virol.* **2017**, *91*, e01844-16. [CrossRef] [PubMed]
130. Xu, Y.; Fernandez, C.; Alcantara, S.; Bailey, M.; De Rose, R.; Kelleher, A.D.; Zaunders, J.; Kent, S.J. Serial study of lymph node cell subsets using fine needle aspiration in pigtail macaques. *J. Immunol. Methods* **2013**, *394*, 73–83. [CrossRef] [PubMed]
131. Zhang, L.; Wang, W.; Wang, S. Effect of Vaccine Administration Modality on Immunogenicity and Efficacy. *Expert Rev. Vaccines* **2015**, *14*, 1509–1523. [CrossRef] [PubMed]
132. Su, F.; Patel, G.B.; Hu, S.; Chen, W. Induction of mucosal immunity through systemic immunization: Phantom or reality? *Hum. Vaccines Immunother.* **2016**, *12*, 1070–1079. [CrossRef] [PubMed]
133. Remarque, E.J.; van Beek, W.C.; Ligthart, G.J.; Borst, R.J.; Nagelkerken, L.; Palache, A.M.; Sprenger, M.J.W.; Masurel, N. Improvement of the immunoglobulin subclass response to influenza vaccine in elderly nursing-home residents by the use of high-dose vaccines. *Vaccine* **1993**, *11*, 649–654. [CrossRef]
134. Pilkinton, M.A.; Nicholas, K.J.; Warren, C.M.; Smith, R.M.; Yoder, S.M.; Talbot, H.K.; Kalams, S.A. Greater activation of peripheral T follicular helper cells following high dose influenza vaccine in older adults forecasts seroconversion. *Vaccine* **2017**, *35*, 329–336. [CrossRef] [PubMed]
135. Pardi, N.; Hogan, M.J.; Porter, F.W.; Weissman, D. mRNA vaccines—A new era in vaccinology. *Nat. Rev. Drug Discov.* **2018**, *17*, 261–279. [CrossRef] [PubMed]
136. Nishimura, Y.; Martin, M.A. Of Mice, Macaques, and Men: Broadly Neutralizing Antibody Immunotherapy for HIV-1. *Cell Host Microbe* **2017**, *22*, 207–216. [CrossRef] [PubMed]

Tools for visualizing HIV in cure research

Current HIV/AIDS Reports, 2018

Current HIV/AIDS Reports
https://doi.org/10.1007/s11904-018-0376-1

HIV PATHOGENESIS AND TREATMENT (AL LANDAY AND N UTAY, SECTION EDITORS)

Tools for Visualizing HIV in Cure Research

Julia Niessl[1,2] · Amy E. Baxter[1,2] · Daniel E. Kaufmann[1,2]

Abstract

Purpose of Review The long-lived HIV reservoir remains a major obstacle for an HIV cure. Current techniques to analyze this reservoir are generally population-based. We highlight recent developments in methods visualizing HIV, which offer a different, complementary view, and provide indispensable information for cure strategy development.

Recent Findings Recent advances in fluorescence in situ hybridization techniques enabled key developments in reservoir visualization. Flow cytometric detection of HIV mRNAs, concurrently with proteins, provides a high-throughput approach to study the reservoir on a single-cell level. On a tissue level, key spatial information can be obtained detecting viral RNA and DNA in situ by fluorescence microscopy. At total-body level, advancements in non-invasive immuno-positron emission tomography (PET) detection of HIV proteins may allow an encompassing view of HIV reservoir sites.

Summary HIV imaging approaches provide important, complementary information regarding the size, phenotype, and localization of the HIV reservoir. Visualizing the reservoir may contribute to the design, assessment, and monitoring of HIV cure strategies in vitro and in vivo.

Keywords HIV cure · In situ hybridization (ISH) · Flow cytometry · Microscopy · RNA flow · Viral reservoir · Positron emission tomography (PET)

Introduction

Despite the tremendous success of antiretroviral therapy (ART), HIV persists in infected subjects predominantly in rare latently infected CD4+ T cells [1–3]. Life-long ART is necessary, as treatment interruption would allow virus to rebound from this pool of cells and plasma viral load to return to pre-ART levels [4]. Broadly, an HIV cure may be achieved by either complete eradication of the HIV reservoir from the body (known as a sterilizing cure) or a long-term control of HIV replication without ART (functional cure) [5]. Recent cure strategies have mainly focused on the "shock/kick and kill" strategy whereby HIV is reactivated from its latent state using latency-reversing agents (LRAs). This is followed by the death of the infected cell, due to the cytopathic effects of HIV itself or killing by the host's own immune system. However, despite initial promise, LRA-based strategies have shown limited success in clinical trials [6], suggesting that additional information regarding the HIV reservoir and alternative approaches are required to help rationally design effective cure strategies.

In this context, a more detailed understanding of such viral reservoirs is required. Firstly, a better understanding of the distribution of the HIV reservoir at both the cellular and anatomic level is essential. This will help guide treatment agents that can efficiently target the various cell types and penetrate the different organs that harbor HIV. Secondly, although a substantial fraction of CD4+ T cells of HIV-infected subjects on ART harbor integrated HIV DNA (~600 copies/million resting CD4+ T cells [7]), the majority of integrated proviral sequences (~90–95%) are defective and not able to produce infectious viral particles (defined as replication-competent virus) [8, 9]. Thus, the specific detection of the HIV-infected cells containing a provirus that is able to transcribe viral RNA (vRNA, transcription-competent reservoir), translate

This article is part of the Topical Collection on *HIV Pathogenesis and Treatment*

✉ Daniel E. Kaufmann
daniel.kaufmann@umontreal.ca

[1] Centre de Recherche du Centre Hospitalier de l'Université de Montréal (CRCHUM), 900, St-Denis Street, Room 09-456, Montreal, QC H2X 0A9, Canada

[2] Scripps Center for HIV/AIDS Vaccine Immunology and Immunogen Discovery (CHAVI-ID), La Jolla, CA, USA

Published online: 27 January 2018

proteins (translation-competent reservoir), and/or is replication-competent is of critical importance. Lastly, potential cure therapies need to be monitored for their effectiveness in decreasing the size of the viral reservoir in vitro and in vivo. Therefore, the size of these HIV reservoirs needs to be evaluated longitudinally by techniques that are scalable in the context of clinical trials for cure strategies.

Looking Beyond Classical Reservoir Measures

Multiple techniques have been developed to quantify and characterize the HIV reservoir. PCR-based approaches represent simple and rapid methods to measure, for example, the total and integrated forms of HIV DNA [10–13], and have been widely used to study both circulating cellular populations and also disrupted tissue biopsies [14, 15]. Such techniques have identified specific anatomic locations, including the gut-associated lymphoid tissues, and cell populations, such as transitional memory (TTM) and central memory (TCM) CD4+ T cells, as preferential sites of HIV integration [14, 15]. In contrast to measures of integrated DNA, inducible infectious virus was detected after reactivation from the TCM, but rarely the TTM, by the quantitative viral outgrowth assay (qVOA) [16]. While further studies are necessary, these apparent discrepancies may be explained by the nature of the reservoir measured by these different techniques. Assays quantifying HIV DNA, such as PCR, cannot discriminate between intact or defective proviral sequences and, therefore, may vastly overestimate the size of the replication-competent reservoir in these populations [17]. At the other end of the scale, results obtained using qVOA represents a minimal estimate, as multiple rounds of stimulations might be needed for reactivation [8] and replication-competent viruses in vivo may not be able to spread in vitro. For the evaluation of cure strategies, these techniques could thus either mask an achieved cure by detecting defective HIV sequences, or miss replication-competent reservoirs that could be reactivated in vivo, but may not respond to stimulation in vitro. These subtleties illustrate the need for tools that can identify and distinguish different forms of HIV reservoirs to better estimate replication competence.

To determine the contribution of different cell populations to the reservoir, the techniques described above require cell suspensions to be first sorted, based on phenotypic markers, before analysis. The measured HIV reservoir size therefore represents a population-level value; it does not provide information about the heterogeneity within the studied cell pool and the specific anatomic location. Furthermore, this requirement for sorting limits the number of populations that can be analyzed concurrently and is not practical for rare subsets. Therefore, approaches that can detect and characterize the HIV reservoir at a single-cell level, either in heterogeneous, mixed cell suspensions or in situ, are required.

Given these caveats, imaging techniques, including flow cytometric and microscopic approaches, have been pursued as powerful strategies for the detection and characterization of HIV reservoirs in the context of cure research. Here, we detail techniques that allow the visualization of HIV at the proviral DNA, RNA, or protein level in single cells, individual tissues, or throughout the body (see Fig. 1 and Table 1 for overview). Each of these approaches provides different and often complementary information on the size, type, and distribution of the viral reservoir. Much of the work discussed here illustrates the study of baseline expression of vRNAs and proteins in infected cells during ART without any further stimulation, in vitro or in vivo. Although this has revealed important information about phenotype and localization of

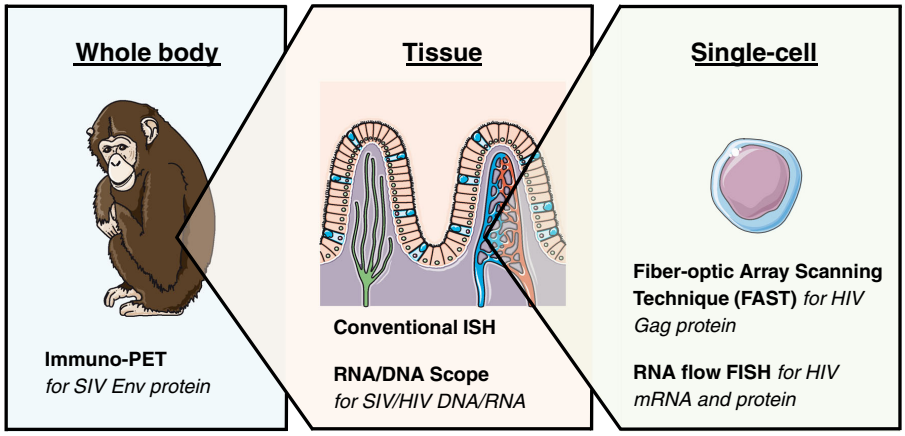

Fig. 1 Schematic representation of levels of HIV visualization including corresponding assays

Table 1 Overview of HIV imaging techniques

Level	Assay	Detection of	Assay overview	Advantages	Limitations	Key references
Single-cell	Fiber-Optic Array Scanning Technology (FAST)	HIV Gag protein	Microscopic detection of HIV Gag protein combined with CD4 downregulation, a cellular hallmark of HIV infection	Relatively high-throughput	Limited characterization possible, limited access to technology	[18•]
	RNA flow FISH	HIV RNA (with or without HIV Gag protein)	Flow cytometric detection of RNA using multiple probes for hybridization followed by signal amplification with branched DNA amplifiers	High-throughput, multiparametric characterization, flexible, and easily adaptable	Single-cell suspension required, large cell number requirement, 2–3-day assay	[19••, 20•, 21•, 22••]
Tissue	Conventional in situ hybridization	HIV/SIV RNA or DNA	Microscopic detection of RNA using radiolabeled probes for hybridization or enzymatic approaches, detection of DNA using prior sequence amplification (in situ PCR)	Detection and localization of HIV RNA/DNA in anatomically intact tissue sections	Long assay duration	[23, 24]
	DNA/RNAscope		Microscopic detection of RNA/DNA using multiple probes for hybridization followed by signal amplification with branched DNA amplifiers	Short assay duration, concurrent detection of HIV/SIV RNA and DNA	Limited multiparametric characterization of reservoir	[25••, 26••]
Whole body	Immuno-PET (positron emission tomography)	SIV Env protein	Detection of Env expression using radionucleotide-labeled gp120-specific antibodies followed by PET analysis	Non-invasive, in vivo imaging of SIV protein	Reduced sensitivity, bias towards tissues with higher antibody penetration	[27••]

transcription- and translation-competent reservoir cells that are spontaneously producing viral products in the absence of stimulation, this provides an understanding of only one aspect of the reservoir. Further studies must build upon this work to investigate latently infected cells, which are transcriptionally/translationally silent but are able to produce infectious viral particles upon stimulation. Understanding the reservoir on this level will help develop, evaluate, and monitor HIV cure strategies in vitro and in vivo.

Visualization of HIV at the Single-Cell Level

The detection of viral proteins, such as Gag, by specific antibody staining followed by flow cytometric analysis has been a valuable tool to study HIV infection at the single-cell level in vitro, where the frequencies of cells actively translating HIV protein is high. In contrast, HIV-infected cells in virally suppressed ART-treated subjects are exceedingly rare (minimal estimated frequency of one replication-competent cell in a million resting CD4+ T cells by qVOA [7]). Due to a high false-positive rate, Gag protein staining alone cannot be used to accurately quantify the translation-competent reservoir at frequencies lower than 1000 cells per million, masking the true HIV-infected cell pool [19••]. Indeed, proviral HIV DNA was detected in only 10% of HIV Gag protein^{+} cells sorted from ART-treated subjects [28]. Therefore, new approaches have been developed recently that combine the detection of Gag protein with a second marker for HIV infection, and thus can overcome this false-positive rate [18•, 19, 20•].

One such approach combines the detection of cells expressing Gag protein with the downregulation of CD4, a well-characterized feature of HIV infection [18•]. For this approach, the O'Doherty lab used a microscopy technique originally developed for the detection of rare circulating tumor cells [29, 30] known as FAST (Fiber-Optic Array Scanning Technology). Briefly, cells isolated from ART-treated HIV-infected individuals and analyzed directly ex vivo without stimulation are stained with antibodies, placed on microscopy slides, and automatically laser-scanned for Gag expression. Gag-expressing cells are then re-imaged by automated digital microscopy for CD4 internalization. This two-step process limits the false-positive detection rate [18•], and enabled the quantification of rare circulating cells (0.33 to 2.7 cells per million PBMCs) spontaneously producing Gag protein in the periphery of HIV-infected donors on ART [18•]. Further work is required to determine if this approach can be applied to the quantification of latent translation-competent HIV reservoir cells after LRA treatment in vitro and in vivo.

As CD4 downregulation requires the function of viral proteins Nef, Vpu, and Env [18•, 31–36], the loss of surface CD4 provides indirect information about the integrity of the infecting proviruses. Thus, this approach quantifies infected cells that are able to translate multiple HIV proteins. We suggest that such cells are substantially more likely to contain intact replication-competent proviruses, when compared to cells identified based on detection of integrated HIV DNA only. Therefore, results obtained with this technique will be—despite a slight overestimation—a closer estimate to the true HIV reservoir size. While powerful, this approach enables only a limited characterization of reservoir cells as a maximum of four markers (in addition to Gag and CD4) can be analyzed. Furthermore, access to the FAST microscopy technology is limited, which constrains the use of this technique.

Building on this concept of single-cell detection of the reservoir, flow cytometry-based approaches also allow single-cell analysis. However, the technology has the additional advantages of being widely available and of further enabling high-throughput, multiparametric characterization of the reservoir. One such flow cytometry-based approach utilizes Gag protein staining combined with the detection of vRNA by RNA flow FISH (fluorescent in situ hybridization) [19, 20•]. Original versions of this approach were able to identify cells containing HIV mRNAs by flow cytometry for the first time, but were limited by high false-positive detection rates [37–40]. A more recent iteration, developed by our group in collaboration with Affymetrix (commercially available as the PrimeFlow™ Assay from Thermo Fisher), attempts to overcome this by using multiple oligomeric probes that hybridize in pairs to the target RNA of interest [41]. Only two adjacently bound probes can be subsequently recognized by the branched-DNA amplification system, which reduces the probability of off-target binding. Finally, this amplified, branched scaffold is labeled with fluorescent probes. This approach was previously developed for the detection of cellular RNAs [42•], but is easily customizable for the identification of cells transcribing HIV mRNAs [19••, 20•, 21•, 22••]. In studies by our laboratory, GagPol vRNA was targeted because it is highly abundant within an infected cell and its sequence is relatively well conserved between primary isolates [43]. Furthermore, its length enables binding of a high number of probe pairs, increasing the probability of vRNA detection despite possible sequence variation that might prevent some pairs from recognition. The flow-cytometric detection of GagPol vRNA+ cells allowed HIV transcription in response to latency reversal to be studied in in vitro infection models [21•]. However, we and others found that the false-positive rate observed with GagPol probes precluded the identification of the low frequencies of events (< 1000 events/million), which would be predicted in clinical samples [19••, 21•]. In an attempt to overcome this, a recent study utilized a different probe set, with reported higher specificity than previously used sets [22••]; nevertheless, false-positive GagPol vRNA+ events were still identified in HIV-negative individuals. Therefore, in this study, the frequency of false-positive events detected in HIV-negative individuals was subtracted from the total number of GagPol

RNA+ events detected in HIV-infected subjects [22••]. Although this provided an estimate of the true frequency of the transcription-competent cells—assuming a constant background rate throughout all HIV-negative and HIV-infected donors tested—this approach limits the characterization of the infected cell population, due to the contamination with false-positive events.

As an alternative approach, we and others combined the detection of both HIV GagPol RNA and Gag protein. This dual staining reduced the number of false-positive events to one HIV GagPol RNA+/Gag protein+ ($HIV^{RNA+/Gag+}$) cell in eight million total analyzed CD4+ T cells from HIV-uninfected donors [19••]. The detection of $HIV^{RNA+/Gag+}$ cells was linear and specific down to 0.5–1 events per million CD4+ T cells and therefore did not require mathematical corrections in our hands [19••, 20•]. This strategy allowed the detection of rare circulating $HIV^{RNA+/Gag+}$ CD4+ T cells in samples from untreated and ART-treated HIV-infected donors without in vitro stimulation, but also enabled the study of both the size and cellular distribution of the latent, reactivated translation-competent reservoir in in vitro-stimulated CD4+ T cells from HIV-infected subjects on ART [19••]. Following in vitro PMA/ionomycin stimulation, ~4.7 $HIV^{RNA+/Gag+}$ per million CD4+ T cells were detected. This frequency is 2 log-fold lower than the reservoir size measured by PCR for HIV DNA in the same cohort, presumably as cells containing a provirus deficient for *GagPol* transcription and Gag translation would not be detected in the $HIV^{RNA/Gag}$ assay [19••]. However, it should be noted that the cellular reservoirs detected with the $HIV^{RNA/Gag}$ assay could include cells containing a provirus with point mutations/deletions in Gag that do not prevent translation, or defects in other viral proteins. Nevertheless, despite this possible overestimation, the frequency of $HIV^{RNA+/Gag+}$ cells was only slightly higher than that compared to the minimal estimate obtained with qVOA (~1.4 infectious units/million CD4+ T cells detected in the same cohort, a 3.6-fold difference) [19••]. Thus, the detection of the translation-competent reservoir through detection of both vRNA and HIV proteins provides an alternative approach to narrow down estimates of the true size of the reservoir.

Importantly, as these approaches are flow cytometry based, they can be used to identify and phenotype in detail single cells supporting viral replication or containing a translation-competent provirus that respond to LRA stimulation in vitro in clinical samples. Flow-based techniques were used to assess the ability of well-known LRAs such as romidepsin [22••] (a histone deacetylase inhibitor [44]) and bryostatin and ingenol [19••] (both protein kinase C (PKC) agonists [45, 46]) to reactivate the latent HIV reservoir in vitro. While both PKC agonists reactivated proviruses in similar frequency of CD4+ T cells, and in all donors tested, ingenol reactivated proviruses mainly in TCM/TTM CD4+ cells, while the majority of bryostatin-reactivated cells had a TEM phenotype. This suggests that cellular subsets might respond differently to distinct LRAs [19••]. Further studies are required to investigate whether combinations of multiple LRAs will be potent and broad enough in specificity to reactivate sufficient fraction of the latent HIV reservoir to make a cure achievable.

As the RNA flow FISH assay is highly adaptable to other viral RNAs, it provides a powerful tool to further study cure strategies at the single-cell level, in both Simian immunodeficiency virus (SIV)-infected non-human primate models and HIV-infected subjects. Notably, single-cell studies for viral reactivation thus far have focused on CD4+ T cells from peripheral blood. As the frequency of infected cells is thought to be higher in tissue [47], FAST and RNA flow FISH will be important tools for the evaluation of tissue reservoirs. Importantly, such studies will indicate if results obtained from peripheral blood CD4 T cells mirror latency reversal mechanisms in tissues. One limitation however is that for both of these approaches, samples need to be disrupted to obtain a single-cell suspension for analysis. Although this allows high-throughput investigations, important spatial information related to the anatomic localization of the viral reservoir within the tissue is lost. Thus, in situ microscopic techniques could act as complementary tools to comprehensively characterize tissue reservoir.

Visualization of HIV at the Tissue Level

Given these points, classical in situ hybridization (ISH) methods have been adapted to detect HIV or SIV in anatomically intact tissue samples from infected subjects or non-human primate models, respectively, as the access to human tissue samples is limited [23, 48, 49]. vRNA sequences are targeted by specific probes that can be radiolabeled for visualization. Alternatively, probes can be labeled with biotin or digoxigenin, and detected with a fluorescent or enzymatic approach to avoid the requirement for radioactive material [49]. However, these chromogenic detection methods have shown a lower sensitivity than radiolabeled probes. Combining this method with immunofluorescence or immunohistochemistry staining for cellular markers has allowed the phenotypic and spatial analysis of HIV/SIV-infected cells at the single-cell level directly within the tissue. Such studies thus contributed to important findings related to viral tissue dissemination, such as the spread and establishment of productive infection from vaginal tissue to lymph node over time during early infection [50], and identified principal anatomic sites of high-level replication such as the lymphoid tissue and gut [48, 51, 52]. Crucially, the majority of this work has been performed in the context of untreated viral infection.

During long-term ART, the frequency of actively transcribing vRNA+ cells in the lymphoid tissue is dramatically reduced compared with untreated infection (for example, by ~ 99% in lymphoid tissue after 6 months of ART) [23, 25••, 26••]. Nevertheless, rare vRNA+ cells can still be detected in tissue from ART-treated donors by ISH; such ongoing viral transcription has been correlated with low antiretroviral drug concentrations in these sites [24, 26••]. In addition to the classical CD4 T cell reservoir, in lymphoid tissues a proportion of these vRNA+ cells may represent virus persisting in different cell populations [24]. Indeed, during both untreated and ART-treated infection, trapped viral particles have been identified in the follicular dendritic cell (FDC) network [23, 48]. However, it remained unclear whether the FDCs in these networks were infected, and therefore contained viral DNA, or were acting as stores of free virus. As standard ISH approaches were not sensitive enough for the detection of proviral HIV DNA, PCR amplification of the target DNA sequences directly on the tissue section was combined with hybridization of the amplified sequences using radiolabeled probes (PCR-in situ or PCR-ISH) [53]. Using this approach, it was demonstrated that FDCs retain infectious virus but are not actually infected; they are positive for vRNA but negative for vDNA or spliced vRNA [48, 54]. Such findings would have been missed with single-cell techniques analyzing disrupted tissue samples, due to the challenges of isolating FDCs from lymphoid tissue [55].

Due to the marked decrease in viral burden on ART, many tissue sections need to be screened in order to quantify rare infected cells. Conventional ISH assays, as described above, are time-intensive as the detection of low copy numbers requires long exposure times or prior sequence amplification, thus limiting the application of this approach to cure studies. Recently, the RNAscope assay was developed to overcome these limitations. This approach uses the same principle as the RNA flow FISH technique described previously based on the recognition of pairs of target probes by branched DNA amplifiers, which was indeed originally developed for microscopy [41]. Adapted for the detection of SIV vRNA, this assay showed a sensitivity and specificity comparable to the techniques described above, with a false-positive detection rate of one vRNA+ cell per million cells analyzed [25••]. Importantly, the Scope technique enabled the detection of single vRNA sequences in a short time and could also be used to reliably identify single vDNA sequences with improved spatial resolution and without prior sequence amplification. In addition, both vRNA and vDNA can be visualized concurrently [25••]. It is important to note, however, that the detection of vDNA+ cells provides—similar to PCR methods described above—a maximal estimate of the HIV reservoir as defective sequences as well as unintegrated forms are included for detection. Regardless, this dual RNA/DNAscope technique confirmed the key role of the B cell follicles as a substantial tissue reservoir, due to the persistence of both HIV-infected mononuclear cells with or without active viral transcription and virus trapped in the FDC network [25••, 48, 56]. These findings highlight the need for drugs that can efficiently penetrate tissue sites, but also demonstrates that alternative strategies may be needed for the eradication of the virus trapped on FDCs in B cell follicles.

Although previous studies have focused on the detection of infected cells spontaneously transcribing vRNAs, Scope assays will be valuable tools to evaluate viral reactivation and eradication strategies in situ. Combined imaging of the viral reservoir together with virus-specific immune cells, for example, using in situ tetramer staining techniques [57], could provide valuable information about the effectivity of both HIV reservoir-targeting and immune system-enhancing strategies in vivo. As confocal microscopy is limited by the number of parameters that can be analyzed concurrently, Scope techniques could be used in combination with histocytometry for multiparametric analysis without losing spatial information [58].

Visualization of HIV at the Whole Organ/Body Level

The RNA/DNAscope technique provides important spatial information regarding the intra-tissue localization of HIV/SIV reservoirs, but can also be used to infer total tissue viral burdens [26••]. To achieve this, in a recent study, the frequency of vDNA+ or vRNA+ cells was determined per gram of analyzed tissue, then the number of total infected cells calculated from the weight of the analyzed organ [26••]. This approach confirmed lymphoid tissue as a main contributor to the whole-body SIV reservoir during ART, but also identified transcription-competent reservoirs in other organs such as brain, lung, and heart. Applying this strategy to HIV-infected donors on ART, this technique provided an estimate of $\sim 10^5$ vDNA+ cells per gram of lymphoid tissue and, based on the assumption that 5% of vDNA+ cells are replication-competent [8], a total body burden of $\sim 4 \times 10^8$ replication-competent HIV-infected cells [26••]. However, with this type of analysis, preselection of specific tissues of interest and the potential for sampling error may lead to biases. Furthermore, the invasive nature of tissue analysis prevents longitudinal imaging of the same subject, for example during a course of treatment. With these caveats in mind, non-invasive full body imaging methods could provide an unbiased and more encompassing view of HIV reservoir sites in the body, despite a limited anatomical spatial resolution.

Initial iterations of this approach utilized animal models infected with SIV or HIV constructs expressing reporter molecules detectable by body-scanning devices [59]. To apply this concept to HIV-infected humans and avoid the use of reporter viruses, the Villinger laboratory adapted a technique

developed for the monitoring of cancer therapies [60]. Whole-body Env expression was monitored in SIV-infected non-human primates, using radionucleotide-labeled SIV gp120-specific antibodies and detected by positron emission tomography (PET) [27••]. This approach enabled viral dissemination to be followed in untreated SIV infection, and importantly identified previously unconsidered or underestimated sanctuary sites in ART treatment, such as the nasal lymphoid tissue and lung. While this approach has not yet been applied to HIV-infected humans, its potential application for the non-invasive monitoring of cure strategies is clear. However, further work is required to determine if the PET-based approach is sensitive enough to detect the lower frequencies of translation-competent viral reservoirs in the context of HIV and ART. Importantly, and as expected, the antibodies used were not able to breach the blood-brain barrier; therefore, this approach cannot be used to study an important HIV reservoir site [61].

Future Directions

Recent developments in microscopic and flow cytometric assays have overcome technical limitations that previously prevented the sensitive and specific detection of HIV in cells and tissue. Further advancements will continue to build upon already existing techniques or develop new assays to study new or more detailed aspects of the viral reservoir. For example, BaseScope is a recent advancement based on the RNAscope technique, and may allow sensitive and specific detection of RNAs using only one probe pair (commercially available from ACD/Bio-Techne). Although this concept has not yet been tested in the context of HIV reservoir studies, this assay could potentially be used for the detection of multiply spliced vRNAs in situ as a surrogate marker for replication competence at baseline and after reactivation of the latent reservoir.

We have focused here on the flow cytometric advances that have enabled multiparametric, single-cell analysis of HIV-infected cells. However, small particle imaging, an emerging field, could visualize HIV at the single virus level. Previously, this approach required custom-made cytometers sensitive enough to capture small particles; however, the newly developed flow virometry technique overcomes this limitation [62]. HIV particles are detected with Env-specific antibodies coupled to magnetic nanoparticles. These nanoparticles can be detected by commercial flow cytometers, thus enabling quantification and phenotypic characterization of single viral particles in supernatants, body fluids, or tissues [62]. Importantly, this assay allows to distinguish between viral particles with non-functional or functional Envs [63]. This assay could provide additional complementary information to study viral reactivation after LRA stimulation at both the cellular, and viral, level.

Conclusion

Here, we highlight recently developed tools for the sensitive and specific visualization of the HIV reservoir at single-cell, tissue, and body levels. The majority of these techniques rely on the detection of vRNA and/or viral proteins, thereby providing a closer estimate for replication competence compared to classical reservoir measurements based on vDNA detection only. By providing a detailed insight into the phenotype and anatomic localization of single HIV-infected cells, such techniques support the development, evaluation, and monitoring of optimal HIV cure strategies in vitro and in vivo.

Acknowledgements Figure 1 has been adapted using images from Servier Medical Art (http://servier.com/Powerpoint-image-bank).

Funding Information This work was supported by National Institutes of Health (NIH) grants RO1 HL-092565 (D.E.K); NIAID UM1AI100663 (CHAVI-ID) (D.E.K; Dennis Burton, principal investigator), and the Canadian Institutes for Health Research (project grant # 377124: D.E.K). AEB is the recipient of a CIHR Postdoctoral Fellowship (award no. 152536); DEK is supported by a FRQS Senior Research Scholar Award (award no. 31035).

Compliance with Ethical Standards

Conflict of Interest The authors declare that they have no competing interests.

References

Papers of particular interest, published recently, have been highlighted as:
- • Of importance
- •• Of major importance

1. Finzi D, Hermankova M, Pierson T, Carruth LM, Buck C, Chaisson RE, et al. Identification of a reservoir for HIV-1 in patients on highly active antiretroviral therapy. Science. 1997;278(5341):1295–300. https://doi.org/10.1126/science.278.5341.1295.
2. Chun TW, Carruth L, Finzi D, Shen X, DiGiuseppe JA, Taylor H, et al. Quantification of latent tissue reservoirs and total body viral load in HIV-1 infection. Nature. 1997;387(6629):183–8. https://doi.org/10.1038/387183a0.
3. Finzi D, Blankson J, Siliciano JD, Margolick JB, Chadwick K, Pierson T, et al. Latent infection of CD4+ T cells provides a mechanism for lifelong persistence of HIV-1, even in patients on effective combination therapy. Nat Med. 1999;5(5):512–7. https://doi.org/10.1038/8394.
4. Harrigan PR, Whaley M, Montaner JS. Rate of HIV-1 RNA rebound upon stopping antiretroviral therapy. AIDS. 1999;13(8):F59–62. https://doi.org/10.1097/00002030-199905280-00001.

5. Dahabieh MS, Battivelli E, Verdin E. Understanding HIV latency: the road to an HIV cure. Annu Rev Med. 2015;66(1):407–21. https://doi.org/10.1146/annurev-med-092112-152941.
6. Margolis DM, Garcia JV, Hazuda DJ, Haynes BF. Latency reversal and viral clearance to cure HIV-1. Science. 2016;353(6297): aaf6517. https://doi.org/10.1126/science.aaf6517.
7. Eriksson S, Graf EH, Dahl V, Strain MC, Yukl SA, Lysenko ES, et al. Comparative analysis of measures of viral reservoirs in HIV-1 eradication studies. PLoS Pathog. 2013;9(2):e1003174. https://doi.org/10.1371/journal.ppat.1003174.
8. Ho Y-C, Shan L, Hosmane NN, Wang J, Laskey SB, Rosenbloom DIS, et al. Replication-competent noninduced proviruses in the latent reservoir increase barrier to HIV-1 cure. Cell. 2013;155(3): 540–51. https://doi.org/10.1016/j.cell.2013.09.020.
9. Hiener B, Horsburgh BA, Eden J-S, Barton K, Schlub TE, Lee E, et al. Identification of genetically intact HIV-1 proviruses in specific CD4(+) T cells from effectively treated participants. Cell Rep. 2017;21(3):813–22. https://doi.org/10.1016/j.celrep.2017.09.081.
10. O'Doherty U, Swiggard WJ, Jeyakumar D, McGain D, Malim MH. A sensitive, quantitative assay for human immunodeficiency virus type 1 integration. J Virol. 2002;76(21):10942–50. https://doi.org/10.1128/JVI.76.21.10942-10950.2002.
11. Brady T, Kelly BJ, Male F, Roth S, Bailey A, Malani N, et al. Quantitation of HIV DNA integration: effects of differential integration site distributions on Alu-PCR assays. J Virol Methods. 2013;189(1):53–7. https://doi.org/10.1016/j.jviromet.2013.01.004.
12. Mexas AM, Graf EH, Pace MJ, Yu JJ, Papasavvas E, Azzoni L, et al. Concurrent measures of total and integrated HIV DNA monitor reservoirs and ongoing replication in eradication trials. AIDS. 2012;26(18):2295–306. https://doi.org/10.1097/QAD.0b013e32835a5c2f.
13. Vandergeeten C, Fromentin R, Merlini E, Lawani MB, DaFonseca S, Bakeman W, et al. Cross-clade ultrasensitive PCR-based assays to measure HIV persistence in large-cohort studies. J Virol. 2014;88(21):12385–96. https://doi.org/10.1128/JVI.00609-14.
14. Chomont N, El-Far M, Ancuta P, Trautmann L, Procopio FA, Yassine-Diab B, et al. HIV reservoir size and persistence are driven by T cell survival and homeostatic proliferation. Nat Med. 2009;15(8):893–900. https://doi.org/10.1038/nm.1972.
15. Morón-López S, Puertas MC, Gálvez C, Navarro J, Carrasco A, Esteve M, et al. Sensitive quantification of the HIV-1 reservoir in gut-associated lymphoid tissue. PLoS One. 2017;12(4):e0175899. https://doi.org/10.1371/journal.pone.0175899.
16. Soriano-Sarabia N, Bateson RE, Dahl NP, Crooks AM, Kuruc JD, Margolis DM, et al. Quantitation of replication-competent HIV-1 in populations of resting CD4 T cells. J Virol. 2014;88(24):14070–7. https://doi.org/10.1128/JVI.01900-14.
17. Bruner KM, Hosmane NN, Siliciano RF. Towards an HIV-1 cure: measuring the latent reservoir. Trends Microbiol. 2015;23(4):192–203. https://doi.org/10.1016/j.tim.2015.01.013.
18.• De Master LK, Liu X, Van Belzen DJ, Trinité B, Zheng L, Agosto LM, et al. A subset of CD4/CD8 double-negative T cells expresses HIV proteins in patients on antiretroviral therapy. J Virol. 2015;90: 2165–79. **This study combined classical detection of HIV Gag protein with a cellular hallmark of HIV infection, CD4 downregulation, to reduce the false-positive rate associated with Gag staining alone. This enabled the identification of rare cells expressing HIV Gag directly ex vivo in samples from subjects on ART. The use of FAST (Fiber-optic Array Scanning Technology), enabled a relatively high-throughput for a microscopy-based technique.**
19.•• Baxter AE, Niessl J, Fromentin R, Richard J, Porichis F, Charlebois R, et al. Single-cell characterization of viral translation-competent reservoirs in HIV-infected individuals. Cell Host Microbe. 2016;20(3):368–80. **This study provided the initial demonstration of single-cell detection of translation-competent cellular HIV reservoirs by RNA flow cytometry, directly in samples from HIV-infected individuals. The RNA flow FISH approach used combines the detection of Gag protein with GagPol mRNA and enabled substantial advances in specificity. Importantly, the authors demonstrate that this technique enables the size and cellular distribution of the latent, translation-competent reservoir after latency reversal to be studied at the single-cell level.** https://doi.org/10.1016/j.chom.2016.07.015.
20.• Baxter AE, Niessl J, Fromentin R, Richard J, Porichis F, Massanella M, et al. Multiparametric characterization of rare HIV-infected cells using an RNA-flow FISH technique. Nat Protoc. 2017;12(10): 2029–49. **This paper provides a detailed protocol for the detection and characterization of translation-competent reservoir cells, identified by the concurrent expression of HIV Gag protein and vRNAs using the RNA flow FISH technique.** https://doi.org/10.1038/nprot.2017.079.
21.• Martrus G, Niehrs A, Cornelis R, Rechtien A, García-Beltran W, Lütgehetmann M, et al. Kinetics of HIV-1 latency reversal quantified on the single-cell level using a novel flow-based technique. J Virol. 2016;90(20):9018–28. **This study provided the demonstration that the RNA flow cytometry approach could be applied to in vitro models of HIV latency to detect and characterize cells expressing HIV mRNA and/or HIV protein.** https://doi.org/10.1128/JVI.01448-16.
22.•• Grau-Expósito J, Serra-Peinado C, Miguel L, Navarro J, Curran A, Burgos J, et al. A novel single-cell FISH-flow assay identifies effector memory CD4 T cells as a major niche for HIV-1 transcription in HIV-infected patients. MBio. 2017;8:e00876–17. **This work describes a key advance for the RNA flow FISH technique; the identification of GagPol vRNA+ cells directly in samples from HIV-infected individuals, without the requirement for concurrent Gag protein detection, thus identifying the transcription-competent reservoir. The authors demonstrate that this approach enables the identification of the transcription-competent reservoir after latency reversal.**
23. Cavert W, Notermans DW, Staskus K, Wietgrefe SW, Zupancic M, Gebhard K, et al. Kinetics of response in lymphoid tissues to antiretroviral therapy of HIV-1 infection. Science. 1997;276(5314): 960–4. https://doi.org/10.1126/science.276.5314.960.
24. Fletcher CV, Staskus K, Wietgrefe SW, Rothenberger M, Reilly C, Chipman JG, et al. Persistent HIV-1 replication is associated with lower antiretroviral drug concentrations in lymphatic tissues. Proc Natl Acad Sci U S A. 2014;111(6):2307–12. https://doi.org/10.1073/pnas.1318249111.
25.•• Deleage C, Wietgrefe SW, Del Prete G, Morcock DR, Hao XP, Piatak M Jr, et al. Defining HIV and SIV reservoirs in lymphoid tissues. Pathog Immun. 2016;1(1):68–106. **This study provided an initial demonstration of the in situ-hybridization Scope approach for the detection and localization of vRNA and vDNA in lymphoid tissues from SIV-infected non-human primates or HIV-infected subjects. Importantly, this assay shows greater speed compared to previous hybridization techniques and allows the concurrent detection of vRNA and vDNA on the same slide.** https://doi.org/10.20411/pai.v1i1.100.
26.•• Estes JD, Kityo C, Ssali F, Swainson L, Makamdop KN, Del Prete GQ, et al. Defining total-body AIDS-virus burden with implications for curative strategies. Nat. Med. [Internet]. 2017; https://doi.org/10.1038/nm.4411. **This study was the first to investigate how the in situ-hybridization DNA/RNAScope technique could be used to evaluate the contribution of various tissues to the SIV reservoir in ART-treated SIV-infected non-human primates. Based on these results, the authors use tissue biopsies from ART-treated HIV-infected subjects to estimate the total-body size of the replication-competent HIV reservoir.**
27.•• Santangelo PJ, Rogers KA, Zurla C, Blanchard EL, Gumber S, Strait K, et al. Whole-body immunoPET reveals active SIV

dynamics in viremic and antiretroviral therapy-treated macaques. Nat Methods. 2015;12(5):427–32. **This key method paper details the use of a non-invasive immuno-PET/CT approach to analyze the anatomic localization of viral protein-expressing cells throughout the whole body in untreated and ART-treated SIV-infected non-human primates.** https://doi.org/10.1038/nmeth.3320.

28. Graf EH, Pace MJ, Peterson BA, Lynch LJ, Chukwulebe SB, Mexas AM, et al. Gag-positive reservoir cells are susceptible to HIV-specific cytotoxic T lymphocyte mediated clearance in vitro and can be detected in vivo. PLoS One. 2013;8(8):e71879. https://doi.org/10.1371/journal.pone.0071879.
29. Krivacic RT, Ladanyi A, Curry DN, Hsieh HB, Kuhn P, Bergsrud DE, et al. A rare-cell detector for cancer. Proc Natl Acad Sci U S A. 2004;101(29):10501–4. https://doi.org/10.1073/pnas.0404036101.
30. Das M, Riess JW, Frankel P, Schwartz E, Bennis R, Hsieh HB, et al. ERCC1 expression in circulating tumor cells (CTCs) using a novel detection platform correlates with progression-free survival (PFS) in patients with metastatic non-small-cell lung cancer (NSCLC) receiving platinum chemotherapy. Lung Cancer. 2012;77(2):421–6. https://doi.org/10.1016/j.lungcan.2012.04.005.
31. Garcia JV, Miller AD. Serine phosphorylation-independent down-regulation of cell-surface CD4 by nef. Nature. 1991;350(6318):508–11. https://doi.org/10.1038/350508a0.
32. Willey RL, Maldarelli F, Martin MA, Strebel K. Human immunodeficiency virus type 1 Vpu protein induces rapid degradation of CD4. J Virol. 1992;66(12):7193–200.
33. Aiken C, Konner J, Landau NR, Lenburg ME, Trono D. Nef induces CD4 endocytosis: requirement for a critical dileucine motif in the membrane-proximal CD4 cytoplasmic domain. Cell. 1994;76(5):853–64. https://doi.org/10.1016/0092-8674(94)90360-3.
34. Geleziunas R, Bour S, Wainberg MA. Correlation between high level gp160 expression and reduced CD4 biosynthesis in clonal derivatives of human immunodeficiency virus type 1-infected U-937 cells. J Gen Virol. 1994;75(Pt 4):857–65. https://doi.org/10.1099/0022-1317-75-4-857.
35. Fujita K, Silver J, Omura S. Rapid degradation of CD4 in cells expressing human immunodeficiency virus type 1 Env and Vpu is blocked by proteasome inhibitors. J. Gen. Virol. 1997;78(3):619–25. https://doi.org/10.1099/0022-1317-78-3-619.
36. Wildum S, Schindler M, Munch J, Kirchhoff F. Contribution of Vpu, Env, and Nef to CD4 down-modulation and resistance of human immunodeficiency virus type 1-infected T cells to superinfection. J Virol. 2006;80(16):8047–59. https://doi.org/10.1128/JVI.00252-06.
37. Patterson BK, Till M, Otto P, Goolsby C, Furtado MR, McBride LJ, et al. Detection of HIV-1 DNA and messenger RNA in individual cells by PCR-driven in situ hybridization and flow cytometry. Science. 1993;260(5110):976–9. https://doi.org/10.1126/science.8493534.
38. Patterson BK, Mosiman VL, Cantarero L, Furtado M, Bhattacharya M, Goolsby C. Detection of HIV-RNA-positive monocytes in peripheral blood of HIV-positive patients by simultaneous flow cytometric analysis of intracellular HIV RNA and cellular immunophenotype. Cytometry. 1998;31(4):265–74. https://doi.org/10.1002/(SICI)1097-0320(19980401)31:4<265::AID-CYTO6>3.0.CO;2-I.
39. Patterson BK, Czerniewski MA, Pottage J, Agnoli M, Kessler H, Landay A. Monitoring HIV-1 treatment in immune-cell subsets with ultrasensitive fluorescence-in-situ hybridisation. Lancet. 1999;353(9148):211–2. https://doi.org/10.1016/S0140-6736(05)77222-6.
40. Chargin A, Yin F, Song M, Subramaniam S, Knutson G, Patterson BK. Identification and characterization of HIV-1 latent viral reservoirs in peripheral blood. J Clin Microbiol. 2015;53(1):60–6. https://doi.org/10.1128/JCM.02539-14.
41. Wang F, Flanagan J, Su N, Wang L-C, Bui S, Nielson A, et al. RNAscope: a novel in situ RNA analysis platform for formalin-fixed, paraffin-embedded tissues. J Mol Diagn. 2012;14(1):22–9. https://doi.org/10.1016/j.jmoldx.2011.08.002.
42.• Porichis F, Hart MG, Griesbeck M, Everett HL, Hassan M, Baxter AE, et al. High-throughput detection of miRNAs and gene-specific mRNA at the single-cell level by flow cytometry. Nat Commun. 2014;5:5641. **This paper provides the initial description of the commerical RNA flow cytometry approach discussed in this review. The authors demonstrated the high-throughput detection of cellular mRNAs using the RNA flow FISH assay based on a branched DNA labeling technique originally developed for microscopy. This study provided a framework for many of the RNA flow studies discussed here.** https://doi.org/10.1038/ncomms6641.
43. Bagnarelli P, Valenza A, Menzo S, Sampaolesi R, Varaldo PE, Butini L, et al. Dynamics and modulation of human immunodeficiency virus type 1 transcripts in vitro and in vivo. J Virol. 1996;70(11):7603–13.
44. Wei DG, Chiang V, Fyne E, Balakrishnan M, Barnes T, Graupe M, et al. Histone deacetylase inhibitor romidepsin induces HIV expression in CD4 T cells from patients on suppressive antiretroviral therapy at concentrations achieved by clinical dosing. PLoS Pathog. 2014;10(4):e1004071. https://doi.org/10.1371/journal.ppat.1004071.
45. Jiang G, Mendes EA, Kaiser P, Sankaran-Walters S, Tang Y, Weber MG, et al. Reactivation of HIV latency by a newly modified Ingenol derivative via protein kinase Cδ-NF-κB signaling. AIDS. 2014;28(11):1555–66. https://doi.org/10.1097/QAD.0000000000000289.
46. DeChristopher BA, Loy BA, Marsden MD, Schrier AJ, Zack JA, Wender PA. Designed, synthetically accessible bryostatin analogues potently induce activation of latent HIV reservoirs in vitro. Nat Chem. 2012;4(9):705–10. https://doi.org/10.1038/nchem.1395.
47. Barton K, Winckelmann A, Palmer S. HIV-1 reservoirs during suppressive therapy. Trends Microbiol. 2016;24(5):345–55. https://doi.org/10.1016/j.tim.2016.01.006.
48. Embretson J, Zupancic M, Ribas JL, Burke A, Racz P, Tenner-Racz K, et al. Massive covert infection of helper T lymphocytes and macrophages by HIV during the incubation period of AIDS. Nature. 1993;362(6418):359–62. https://doi.org/10.1038/362359a0.
49. Fox CH, Cottler-Fox M. In situ hybridization in HIV research. Microsc Res Tech. 1993;25(1):78–84. https://doi.org/10.1002/jemt.1070250111.
50. Miller CJ, Li Q, Abel K, Kim E-Y, Ma Z-M, Wietgrefe S, et al. Propagation and dissemination of infection after vaginal transmission of simian immunodeficiency virus. J Virol. 2005;79(14):9217–27. https://doi.org/10.1128/JVI.79.14.9217-9227.2005.
51. Li Q, Duan L, Estes JD, Ma Z-M, Rourke T, Wang Y, et al. Peak SIV replication in resting memory CD4+ T cells depletes gut lamina propria CD4+ T cells. Nature. 2005;434(7037):1148–52. https://doi.org/10.1038/nature03513.
52. Mehandru S, Poles MA, Tenner-Racz K, Horowitz A, Hurley A, Hogan C, et al. Primary HIV-1 infection is associated with preferential depletion of CD4+ T lymphocytes from effector sites in the gastrointestinal tract. J Exp Med. 2004;200(6):761–70. https://doi.org/10.1084/jem.20041196.
53. Haase AT, Retzel EF, Staskus KA. Amplification and detection of lentiviral DNA inside cells. Proc Natl Acad Sci U S A. 1990;87(13):4971–5. https://doi.org/10.1073/pnas.87.13.4971.
54. Reinhart TA, Rogan MJ, Viglianti GA, Rausch DM, Elden LE, Haase AT. A new approach to investigating the relationship

between productive infection and cytopathicity in vivo. Nat Med. 1997;3(2):218–21. https://doi.org/10.1038/nm0297-218.

55. Usui K, Honda S-I, Yoshizawa Y, Nakahashi-Oda C, Tahara-Hanaoka S, Shibuya K, et al. Isolation and characterization of naïve follicular dendritic cells. Mol Immunol. 2012;50(3):172–6. https://doi.org/10.1016/j.molimm.2011.11.010.
56. Fukazawa Y, Lum R, Okoye AA, Park H, Matsuda K, Bae JY, et al. B cell follicle sanctuary permits persistent productive simian immunodeficiency virus infection in elite controllers. Nat Med. 2015;21(2):132–9. https://doi.org/10.1038/nm.3781.
57. Li Q, Skinner PJ, Ha S-J, Duan L, Mattila TL, Hage A, et al. Visualizing antigen-specific and infected cells in situ predicts outcomes in early viral infection. Science. 2009;323(5922):1726–9. https://doi.org/10.1126/science.1168676.
58. Gerner MY, Kastenmuller W, Ifrim I, Kabat J, Germain RN. Histocytometry: a method for highly multiplex quantitative tissue imaging analysis applied to dendritic cell subset microanatomy in lymph nodes. Immunity. 2012;37(2):364–76. https://doi.org/10.1016/j.immuni.2012.07.011.
59. Song J, Cai Z, White AG, Jin T, Wang X, Kadayakkara D, et al. Visualization and quantification of simian immunodeficiency virus-infected cells using non-invasive molecular imaging. J. Gen. Virol. 2015;96(10):3131–42. https://doi.org/10.1099/jgv.0.000245.
60. Mestel *R.* Cancer: imaging with antibodies. Nature 2017;543:743–746, 7647, DOI: https://doi.org/10.1038/543743a.
61. Marban C, Forouzanfar F, Ait-Ammar A, Fahmi F, El Mekdad H, Daouad F, et al. Targeting the brain reservoirs: toward an HIV cure. Front. Immunol. [Internet]. 2016;7. Available from: https://doi.org/10.3389/fimmu.2016.00397
62. Arakelyan A, Fitzgerald W, Margolis L, Grivel J-C. Nanoparticle-based flow virometry for the analysis of individual virions. J Clin Invest. 2013;123(9):3716–27. https://doi.org/10.1172/JCI67042.
63. Arakelyan A, Fitzgerald W, King DF, Rogers P, Cheeseman HM, Grivel J-C, et al. Flow virometry analysis of envelope glycoprotein conformations on individual HIV virions. Sci Rep. 2017;7(1):948. https://doi.org/10.1038/s41598-017-00935-w.

Curriculum Vitae

Education

May 2015 – August 2020	**Ph.D. in Virology and Immunology** Faculté de Médecine Université de Montréal
October 2012 – March 2015	**M.Sc. with distinction in Molecular Medicine** Medizinische Fakultät Friedrich-Alexander-Universität Erlangen-Nürnberg
October 2009 – September 2012	**B.Sc. in Molecular Medicine** Medizinische Fakultät Friedrich-Alexander-Universität Erlangen-Nürnberg

Distinctions, awards and honors

Scholarships

2019 – 2020	FRQS Doctoral Scholarship	Fonds de Recherche en santé du Québec
2019	Bourse d'excellence, doctorat	CRCHUM
2017 – 2018	Bourse de doctorat	Département de Microbiologie, Infectiologie et Immunologie, Université de Montréal
2015	Bourse de formation, doctorat	CRCHUM
2015 – 2017	Scholarship for Quebec international student fees	BayFor (Bavarian Research Alliance)
2012 – 2013	Deutschlandstipendium	Friedrich-Alexander-Universität Erlangen-Nürnberg

Awards, Prizes and Honors

2020	Young Investigator Award	Scripps Consortium for HIV/AIDS Vaccine Development (CHAVD)
2019	Travel Award	CRCHUM
2018	Travel Award	Conference on Retroviruses and Opportunistic Infections (CROI)
2016	Best poster award	CRCHUM, Journée Scientifique
2016	2nd place poster award	FRQS-SIDA, Journée des étudiants
2014	3rd place presentation award	FRQS-SIDA, Journée des étudiants
2013	Travel award	Ilse & Dr. Alexander Mayer-Stiftung
2012 – 2014	Member of the Leonardo-Kolleg, honoring top 5% students	Friedrich-Alexander-Universität Erlangen-Nürnberg

Publications

First author publications:

J. Niessl, A.E. Baxter, P. Mendoza, M. Jankovic, Y.Z. Cohen, A.L. Butler, M. Dubé, I. Shimeliovich, H. Gruell, F. Klein, M. Caskey, M.C. Nussenzweig, D.E. Kaufmann
Combination anti-HIV-1 antibody therapy is associated with increased virus-specific T cell immunity.
Nature Medicine. 26, 222–227(2020). doi: 10.1038/s41591-019-0747-1

J. Niessl, A.E. Baxter, A. Morou, E. Brunet-Ratnasingham, G. Sannier, J. Richard, G. Gendron-Lepage, G.G. Delgado, N. Brassard, M. Dubé, J.P. Routy, A. Finzi, N. Chomont, D.E. Kaufmann
Persistent expansion and Th1-like polarization of HIV-specific circulating follicular helper T cells during antiretroviral therapy.
EBioMedicine. 2020 Apr;54:102727. doi: 10.1016/j.ebiom.2020.102727

J. Niessl, D.E. Kaufmann
Harnessing T Follicular Helper Cell Responses for HIV Vaccine Development.
Viruses. 2018 *10*(6), 336. doi: 10.3390/v10060336

J. Niessl, A.E. Baxter, D.E. Kaufmann
Tools for visualizing HIV in Cure research.
Current HIV/AIDS Reports. 2018 Feb;15(1):39-48. doi: 10.1007/s11904-018-0376-1

Co-author publications:

A. Morou, E. Brunet-Ratnasingham, M. Dubé, R. Charlebois, E. Mercier, S. Darko, N. Brassard, K. Nganou-Makamdop, S. Arumugam, G. Gendron-Lepage, L. Yang, **J. Niessl**, A.E. Baxter, J.M. Billingsley, P.A. Rajakumar, F. Lefebvre, R.P. Johnson, C. Tremblay, J.P. Routy, R.T. Wyatt, A. Finzi, D.C. Douek, D.E. Kaufmann
Altered differentiation is central to HIV-specific $CD4^+$ T cell dysfunction in progressive disease.
Nature Immunology. 2019 Aug;20(8):1059-1070. doi: 10.1038/s41590-019-0418-x

A.E. Baxter, **J. Niessl**, R. Fromentin, J. Richard, F. Porichis, N. Brassard, N. Alsahafi, J.P. Routy, B.D. Walker, A. Finzi, N. Chomont, D.E. Kaufmann
Multi-parametric characterization or rare HIV-infected cells using an RNA-flow FISH technique.
Nature Protocols. 2017 Oct;12(10):2029-2049. doi: 10.1038/nprot.2017.079

A.E. Baxter, **J.Niessl**, A. Morou, D.E. Kaufmann
RNAflow cytometry for investigations into HIV immunology, vaccination and cure strategies.
AIDS Research and Therapy. 2017 Sept 12;14:40, doi: 10.1186/s12981-017-0171-x

A.E. Baxter, **J. Niessl**, R. Fromentin, J. Richard, F. Porichis, N. Brassard, N. Alsahafi, J.P. Routy, B.D. Walker, A. Finzi, N. Chomont, D.E. Kaufmann
Single-cell characterization of viral translation-competent latent reservoirs in HIV-infected individuals.
Cell Host and Microbe. 2016 Sep 14;20(3):368-80. doi: 10.1016/j.chom.2016.07.015

S. DaFonseca, **J. Niessl**, S. Pouvreau, V.S. Wacleche, A. Gosselin, A. Cleret-Buhot, N. Bernard, C. Tremblay, M.A. Jenabian, J.P. Routy, P. Ancuta
Impaired Th17 polarization of phenotypically naive $CD4^+$ T-cells during chronic HIV-1 infection and potential restoration with early ART.
Retrovirology. 2015 Apr 30;12:38.doi:10.1186/s12977-015-0164-6

E. Brunet-Ratnasinham, A. Morou, M. Dubé, **J. Niessl**, A.E. Baxter, O. Tastet, N. Brassard, G.G. Delgado, R. Charlebois, G.J. Freeman, C. Tremblay, J.P. Routy, D.E. Kaufmann
Immune checkpoint expression and response to blockade are dependent on HIV-specific $CD4^+$ T cell lineage and function
In revision, *Science Advances*, August 2020

Presentations

Oral presentations:

J. Niessl, A.E. Baxter, P. Mendoza, M. Jankovic, Y.Z. Cohen, A.L. Butler, M. Dubé, I. Shimeliovich, H. Gruell, F. Klein, M. Caskey, M.C. Nussenzweig, D.E. Kaufmann
Combination bNAb-therapy is associated with increased virus-specific T cell immunity
Consortium For HIV/AIDS Vaccine Development (CHAVD), Annual Retreat, La Jolla (USA), 2020

J. Niessl, A.E. Baxter, P. Mendoza, M. Jankovic, Y.Z. Cohen, A.L. Butler, M. Dubé, I. Shimeliovich, H. Gruell, F. Klein, M. Caskey, M.C. Nussenzweig, D.E. Kaufmann
Combination anti-HIV antibody therapy is associated with increased virus-specific T cell immunity
17th International Congress of Immunology (IUIS), Beijing (China), 2019

J. Niessl, A.E. Baxter, D.E. Kaufmann
mRNA flow FISH assay: Technical considerations.
Invited speaker, McGill University Symposium: Cutting Edge Applications in Flow Cytometry, Montreal (Canada), 2017

J. Niessl, S. DaFonseca, J.P. Routy, P. Ancuta
Contribution des cellules T $CD4^+$ naïves à la persistance du VIH sous ART.
FRQS-SIDA Journée des étudiants, Montreal (Canada), 2014

Poster presentations:

J. Niessl, A.E. Baxter, A. Morou, E. Brunet-Ratnasingham, G. Sannier, G. Gendron-Lepage, J. Richard, M. Dubé, R. Fromentin, J.P. Routy, N. Chomont, A. Finzi, D.E. Kaufmann;
Persistent expansion and Th1-like skewing of HIV-specific cTfh during antiretroviral therapy.
Keystone Conference: T Cell Memory, Banff (Canada), 2020

J. Niessl, A.E. Baxter, P. Mendoza, M. Jankovic, Y.Z. Cohen, A.L. Butler, M. Dubé, I. Shimeliovich, H. Gruell, F. Klein, M. Caskey, M.C. Nussenzweig, D.E. Kaufmann
Combination anti-HIV antibody therapy is associated with increased virus-specific T cell immunity
Montreal Immunology Meetings, Montreal (Canada), 2019

J. Niessl, A.E. Baxter, A. Morou, E. Brunet-Ratnasingham, M. Lindqvist, P.A. Vagefi, E.P. Scully, J.P. Routy, D.E. Kaufmann; Persistent dysregulation of HIV-specific T follicular helper cells during ART.
CROI (Conference on Retroviruses and Opportunistic Infections), Boston (USA), 2018

J. Niessl, A.E. Baxter, A. Morou, E. Brunet-Ratnasingham, G. Gendron-Lepage, J. Richard, J.P. Routy, A. Finzi, D.E. Kaufmann; Persistent expansion of HIV-specific T follicular helper cells with altered features during antiretroviral therapy.
CRCHUM Journée des étudiants, Montreal (Canada), 2018

J. Niessl, A.E. Baxter, A. Morou, J. Richard, N. Brassard, G.G. Delgado, J.P. Routy, A. Finzi, D.E. Kaufmann; Identification and characterization of antigen-specific follicular helper T cells in HIV-infected subjects on antiretroviral therapy
Keystone conference: B Cells and T Follicular Helper Cells – Controlling Long-Lived Immunity, Whistler (Canada), 2017

J. Niessl, A.E. Baxter, A. Morou, J. Richard, N. Brassard, G.G. Delgado, J.P. Routy, A. Finzi, D.E. Kaufmann; Identification and characterization of antigen-specific follicular helper T cells in HIV-infected subjects on antiretroviral therapy
Canadian Conference on HIV/AIDS Research (CAHR), Montreal (Canada), 2017

J. Niessl, A.E. Baxter, A. Morou, J. Richard, N. Brassard, G.G. Delgado, J.P. Routy, A. Finzi, D.E. Kaufmann; Identification and characterization of antigen-specific follicular helper T cells in HIV-infected subjects on antiretroviral therapy
Annual CanCure Meeting, Montreal (Canada), 2017

J. Niessl, A.E. Baxter, A. Morou, J. Richard, N. Brassard, G.G. Delgado, J.P. Routy, A. Finzi, D.E. Kaufmann; Identification and characterization of antigen-specific follicular helper T cells in HIV-infected subjects on antiretroviral therapy
CRCHUM Journée Scientifique, Montreal (Canada), 2016

J. Niessl, A.E. Baxter, A. Morou, J. Richard, N. Brassard, G.G. Delgado, J.P. Routy, A. Finzi, D.E. Kaufmann; Identification and characterization of antigen-specific follicular helper T cells in HIV-infected subjects on antiretroviral therapy
Montreal Immunology Meetings, Montreal (Canada), 2016

J. Niessl, A.E. Baxter, A. Morou, J. Richard, N. Brassard, G.G. Delgado, J.P. Routy, A. Finzi, D.E. Kaufmann; Identification and characterization of antigen-specific follicular helper T cells in HIV-infected subjects on antiretroviral therapy
FRQS-SIDA Journée des étudiants, Montreal (Canada), 2016

J. Niessl, S. DaFonseca, J.P. Routy, P. Ancuta; Contribution of naïve $CD4^+$ T cells to the persistence of HIV during ART
Montreal Immunology Meetings, Montreal (Canada), 2014

Technical expertise and trainings

- **Immunological techniques:** Multiparameter flow cytometry for detection of surface protein, intracellular protein or mRNA (RNAflow FISH), proliferation assays (CFSE dilutions), enzyme linked immunospot (ELISpot), ELISA, immunofluorescence microscopy
- **Cell biology techniques:** Isolation and culture of T and B cells from human blood or tissue samples, work with infectious material in BSL2 and BSL3 conditions
- **Molecular biology techniques:** PCR, Real-time PCR
- **Virological techniques:** Virus production, culture of infectious viral particles, HIV suppression assay
- **Computer software:** FlowJo, GraphPad Prism, SPICE, Adobe Illustrator, Image J, R

- Certificate PH125.1x: Data Science: R Basics, Harvard University, 2019 https://courses.edx.org/certificates/57b4b0dbdd2848b689f8cf386df3165a
- Certificate PH125.2x: Data Science: R Data Visualization, Harvard University, 2019 https://courses.edx.org/certificates/15952ecde62c48839a2599321c429589
- Training flow cytometry, Dr. Dominique Gauchat, CRCHUM, 2013
- European certificate for animal experiments (FELASA B), Friedrich-Alexander-Universität Erlangen-Nürnberg, 2013
- Laboratory radiation science and radioprotection certificate, Friedrich-Alexander-Universität Erlangen-Nürnberg, 2012